

## Kinetics of Amylose Retrogradation

H. L. DOPPERT\* and A. J. STAVERMAN, *Laboratorium voor  
Anorganische en Fysische Chemie der Rijksuniversiteit Leiden, Leiden,  
Netherlands*

### Synopsis

This article deals with the kinetics of the retrogradation of amylose in aqueous solutions of pH 4.0, 9.2, and 11.9. The course of the retrogradation is followed by means of light-scattering measurements. From our interpretation of the light-scattering data we conclude that the retrogradation mechanism appears to be in qualitative agreement with von Smoluchowski's theory on coagulation. From the rate of retrogradation one may tentatively conclude that only a small fraction of the collisions between the amylose aggregates leads to permanent coagulation. In order to explain this phenomenon, additional conditions are suggested for permanent attachment of two colliding aggregates. The relevant fraction is smaller at pH 11.9 than at the lower pH's, a fact which is ascribed to the mutual repulsions of the aggregates due to their negative charges.

### INTRODUCTION

A well-known property of amylose is its instability in neutral aqueous solution. Although a slow flocculation process is found for many other polymers like poly(vinyl alcohol),<sup>1</sup> methylcellulose,<sup>2</sup> and poly(vinyl chloride),<sup>3</sup> the term retrogradation for this phenomenon appears to be used exclusively for the case of amylose.

The retrogradation of amylose has been studied by means of light scattering by several authors.<sup>4-7</sup> The results thus far found are rather inconsistent. Part of the disagreement may originate from differences in the fractionation procedures giving rise to differences in the number of helical configurations which may be partially preserved after dissolution. Experiments on the relation between molecular configuration and solubility properties have been reported by Sarko et al.<sup>8</sup>

Knowing from previous investigations<sup>9,10</sup> the polyelectrolytic nature of amylose, we made a study of the pH dependence of the retrogradation by means of light scattering. If the conditions are appropriately chosen, the growth of the aggregates is very slow compared to the time required to record the scattering intensity at a certain moment of time.

An interpolation procedure applied to the experimental data, made it even possible to construct Zimm plots for any desired moment of time during the retrogradation process. It turned out then, that the kinetics of the retrogradation could be described qualitatively with von Smoluchow-

\* Present address: Algemene Kunstzijde Unie N.V. AKU, Arnhem, Netherlands.

ski's<sup>11-13</sup> theory on coagulating systems. Electrostatic charges on the molecules lead to a considerable decrease of the rate of retrogradation.

### THEORY

The picture underlying von Smoluchowski's theory is that of spherical particles diffusing into each others' sphere of influence and then sticking together. It can be shown that all the particles have practically equal probability of sticking, provided the ratio between the diameters of the largest and the smallest particles does not exceed, say 1.3. By solving Fick's diffusion equation with appropriate boundary conditions, von Smoluchowski derived for the number of particles per unit of volume at time  $t$ :

$$\sum_{k=1}^{\infty} n_k = n_0 / (1 + 4\pi D_1 R_{11} n_0 t) \quad (1)$$

in which  $n_0$  is the number of particles at  $t = 0$ ,  $n_k$  is the number of aggregates consisting of  $k$  elementary particles,  $D_1$  is the diffusion constant, and  $R_{11}$  is the diameter of the elementary particles. It can further be derived, that for a weight-average molecular weight of the aggregates  $\bar{M}_w$ , the following relation holds

$$\bar{M}_w = M_1 [1 + (8\pi D_1 R_{11} n_0) t] \quad (2)$$

where  $M_1$  is the molecular weight of the elementary particle. On defining the rate constant  $\beta$  by

$$\beta = 8\pi D_1 R_{11} N \quad (3)$$

in which  $N$  denotes Avogadro's number, eq. (2) can be written as

$$\bar{M}_w = M_1 + \beta c t \quad (4)$$

where  $c$  is the concentration of the particles, for instance, in grams per milliliter. The applicability of this equation to the retrogradation of amylose can be verified experimentally by light scattering. From the scattering data,  $\bar{M}_w$  and the  $z$ -average radius of gyration  $s_z^2$  can be obtained according to the well-known equations

$$Kc/R_{(\theta)} = 1/\bar{M}_w P_{(\theta)} + 2A_2c + \dots \quad (5)$$

$$P_{(\theta)}^{-1} = 1 + (16\pi^2/3\lambda^2 \sin^2 \theta/2) s_z^2 + \dots \quad (6)$$

The symbols in these equations have their usual significance.<sup>14,15</sup> In the discussion we will examine the rate constant  $\beta$  with regard to its physical meaning as suggested by eq. (3).

### EXPERIMENTAL

#### Sample, Apparatus, and Preparation of Solutions

The amylose sample, bearing the code number A430, was supplied by the A.V.E.B.E., G.A, Veendam, Holland. The polymer was obtained by

fractionation of potato starch with a  $\text{MgSO}_4$  solution as described by Hiemstra et al.<sup>16</sup> The limiting viscosity number  $[\eta]$  for our sample dissolved in 1*N* KOH was 214 ml./g. The light-scattering apparatus was constructed at the Centraal Laboratorium T.N.O., Delft; this type of apparatus is now produced by Cenco Instrumenten Mij. The instrument was calibrated with the use of benzene as reference.<sup>17</sup> The weight-average molecular weight of the sample in dimethyl sulfoxide was found to be  $5.7 \times 10^5$ ; for the refractive index increment the value of Everett and Foster,<sup>18</sup>  $dn/dc = 0.0676$  ml./g., was taken.

Since we were dealing mainly with aqueous solutions of amylose we thought it necessary to determine  $dn/dc$  in this solvent medium and to compare the value with literature data. To this end the amylose was dissolved in 1*N* KOH and neutralized with HCl until the pH of the solution was 12.6, at which pH no retrogradation could be observed.

Finally  $dn/dc$  was measured at constant salt concentration (0.20*M* KCl) in a Brice-Phoenix differential refractometer. The value of 0.147 ml./g. at 4360 Å. we obtained is in good agreement with the data of Paschall and Foster<sup>4</sup> and Burchard,<sup>19</sup> who found 0.146 and 0.151 ml./g., respectively, for neutral amylose solutions. The agreement however is not self-evident. At pH 12.5 the amylose has a polyelectrolytic nature, so one may expect<sup>10</sup> a  $dn/dc$  value which deviates from those measured in neutral solutions in which the molecules do not carry electrostatic charges.

Amylose stock solutions were prepared by dissolving 0.875 g. of the sample in 25 ml. 1*N* KOH with vigorous stirring. To study the possible influence of the method of dissolution as well as of slight polymer degradation on the rate constant  $\beta$ , two solutions were prepared by heating the alkaline amylose solutions until they turned slightly yellow in color.

To prevent rapid retrogradation during neutralization the stock solutions were diluted with distilled water before they were neutralized with HCl. The solutions having a pH of 4 and 9 were buffered with potassium hydrogen phthalate and borax, respectively. The resulting amylose concentration in the stock solutions was  $1.75 \times 10^{-3}$  g./ml. The amylose solutions and the diluting agents of corresponding pH and salt compositions were centrifuged to remove dust. Cuvets were cleaned with acetone in a Thurmond<sup>20</sup> apparatus. It should be noted that traces of acetone will accelerate the retrogradation. From each amylose stock solution a dilution series was prepared in three cuvettes, the concentrations thus obtained were  $1.75 \times 10^{-3}$ ,  $1.17 \times 10^{-3}$ , and  $0.58 \times 10^{-3}$  g./ml. For convenience we will denote these concentrations by  $a$ ,  $2a/3$ , and  $a/3$ , respectively. In order to obtain comparable data within each dilution series, it was necessary to define the moment of time at which a series is prepared in the cuvettes as  $t = 0$  (at this specific time the value of  $\bar{M}_w$  in a series is equal in all three solutions), although the retrogradation starts immediately after or even during the neutralization of the stock solution.

The intensities of the scattered light at various angles was measured at intervals of 4–10 hr. at room temperature. The change of the scattering

intensity was small (less than 1%) during the time required to record the intensities at the chosen time.

### Construction of Zimm Plots

Figures 1-5 are the results of measurements performed on the dilution series denoted by A in Table I. Rather similar figures were obtained for the other series and are omitted. Figures 1, 2, and 3 are diagrams of plots of  $Kc/R_\theta$  against  $t \times 10^{-5}$  (sec.) +  $\sin^2 \theta/2$  for amylose concentrations  $a$ ,  $2a/3$ , and  $a/3$ , respectively. The values of  $\theta$  used were  $30^\circ$ ,  $37.5^\circ$ ,  $45^\circ$ ,  $60^\circ$ ,  $75^\circ$ ,  $90^\circ$ ,  $105^\circ$ ,  $120^\circ$ , and  $130^\circ$ . The heavy lines give the values of  $Kc/R_\theta$  as a function of  $\sin^2 \theta/2$  at a particular moment of time, i.e., at constant  $t$ . The thin lines represent  $Kc/R_\theta$  as a function of  $t$  at constant angle  $\theta$ . The open circles indicate  $\lim_{\theta \rightarrow 0} Kc/R_\theta = Kc/R_0$  at a particular moment of time.

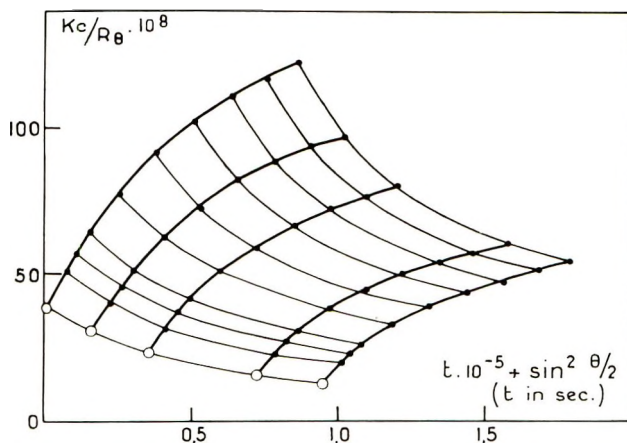


Fig. 1. Plot of  $Kc/R_\theta$  as a function of time and  $\sin^2 \theta/2$ . Amylose concentration  $1.75 \times 10^{-3}$  g./ml. (a). Dilution series A.

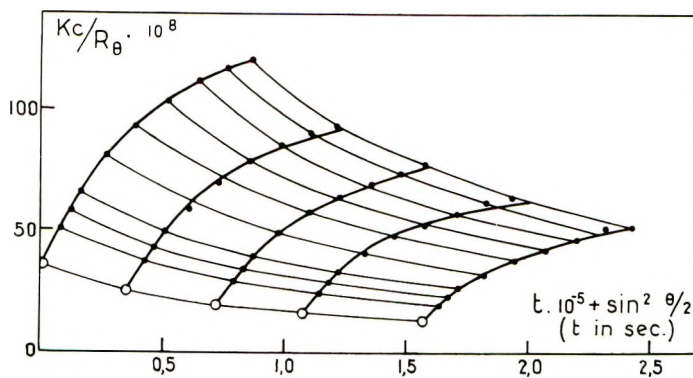


Fig. 2. Plot of  $Kc/R_\theta$  as a function of time and  $\sin^2 \theta/2$ . Amylose concentration  $1.17 \times 10^{-3}$  g./ml. ( $2a/3$ ). Dilution series A.

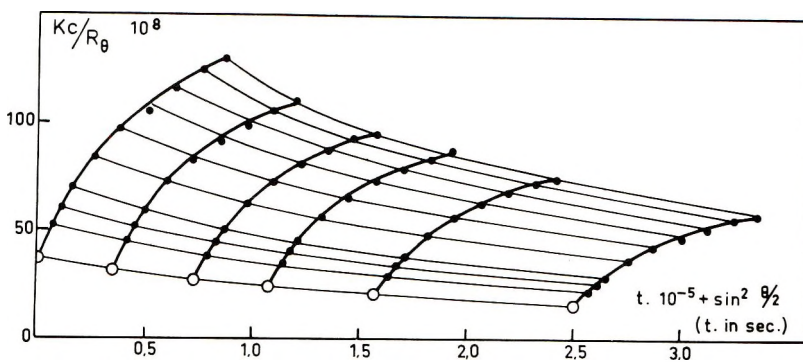


Fig. 3. Plot of  $Kc/R_\theta$  as a function of time and  $\sin^2 \theta/2$  Amylose concentration  $0.58 \times 10^{-3}$  g./ml. ( $a/3$ ). Dilution series A.

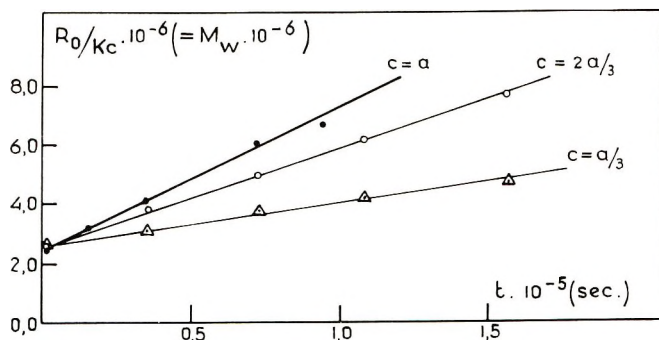


Fig. 4.  $R_0/Kc$  as a function of time for three amylose concentrations.  $a = 1.75 \times 10^{-3}$  g./ml. Dilution series A.

In accordance with eqs. (5) and (6)  $R_0/Kc \approx \bar{M}_w$ , we plotted  $R_0/Kc$  as a function of time in order to get tentative information about the relation between  $\bar{M}_w$  and  $t$ .

The plot is shown by Figure 4, and suggests a linear relationship between  $R_0/Kc$  and  $t$ . This indicates that the relation between  $\bar{M}_w$  and  $t$  is linear. If it is assumed that the second virial coefficient  $A_2$  is zero [see eq (5)], then  $R_0/Kc = \bar{M}_w$ , and then the change of the molecular weight with time  $d\bar{M}_w/dt$  and the parameter  $\beta$  in eq. (4) can be calculated. The results, collected in Table II, strongly support eq. (4), as for all these amylose concentrations  $\beta$  has practically the same value. In other words, the assumptions that the relation between  $\bar{M}_w$  and  $t$  is linear and that  $d\bar{M}/dt$  is directly proportional to the concentration appear to be justified. Provided one starts the kinetic experiments with a dilution series containing amylose aggregates of equal  $\bar{M}_w$ , the above-mentioned outcome leads to the application of an interpolation procedure to obtain Zimm plots for a specific concentration and time of the retrograding system. At time  $t$  the parameter  $\bar{M}_w$  of the amylose aggregates in a solution of amylose concentration  $a$  will be equal to the  $\bar{M}_w$  of solutions with concentrations  $2a/3$  and  $a/3$  at

TABLE I

Dilution series	Temp., °C.	Max. amylose concn. $\times 10^3$ , g./ml.	pH	Borax, $M$	KH phthalate, $M$	KCl, $M$	Ionic strength, g-ion/l.	$\beta \times 10^{-3}$ , ml./mole-sec.	$t \times 10^{-3}$ , sec.	$\bar{M}_w \times 10^{-6}$	$s_z^2 \times 10^{-6}$ , A. <sup>2</sup>
A <sup>a</sup> (Degraded amylose)	21 ± 1	1.75	9.19	0.005	—	0.05	0.06	25 ± 3	1.3	2.63	1.07
									15.7	3.23	0.99
									35.0	4.03	0.97
									72.4	5.88	1.16
									94.3	6.67	1.14
B <sup>b</sup>	21 ± 1	1.75	9.18	0.005	—	0.05	0.06	28 ± 3	1.0	3.13	1.11
									7.6	3.45	1.06
									22.8	4.08	0.97
									40.3	5.00	1.10
									63.7	6.45	1.51
C <sup>c</sup>	21 ± 1	1.75	3.95	—	0.01	0.05	0.06	28 ± 4	0.2	3.85	1.50
									14.9	4.52	1.44
									30.8	5.56	1.78
									77.3	7.14	1.84

D <sup>d</sup>	21 ± 1	1.75	3.95	—	0.01	0.05	0.06	23 ± 3	1.1	2.72	1.31
									15.7	3.34	1.25
									29.9	3.74	1.41
									78.6	5.71	1.49
E <sup>e</sup>	21 ± 1	1.75	4.00	—	0.01	0.05	0.06	26 ± 3	0.8	2.94	1.24
(Degraded amylose)									16.0	3.85	1.01
									33.9	4.55	1.20
									72.9	6.25	1.41
									87.4	6.67	1.42
F <sup>f</sup>	21 ± 1	1.75	11.9 ± 0.2	—	—	0.06	0.06	7 ± 1	1.7	1.91	1.05
									17.3	2.13	1.01
									40.1	2.50	1.16
									73.1	2.70	1.16
									82.1	2.94	1.20

<sup>a</sup> See Figs. 1-6.      <sup>d</sup> See Fig. 9.

<sup>b</sup> See Fig. 7.      <sup>e</sup> See Fig. 10.

<sup>c</sup> See Fig. 8.      <sup>f</sup> See Fig. 11.

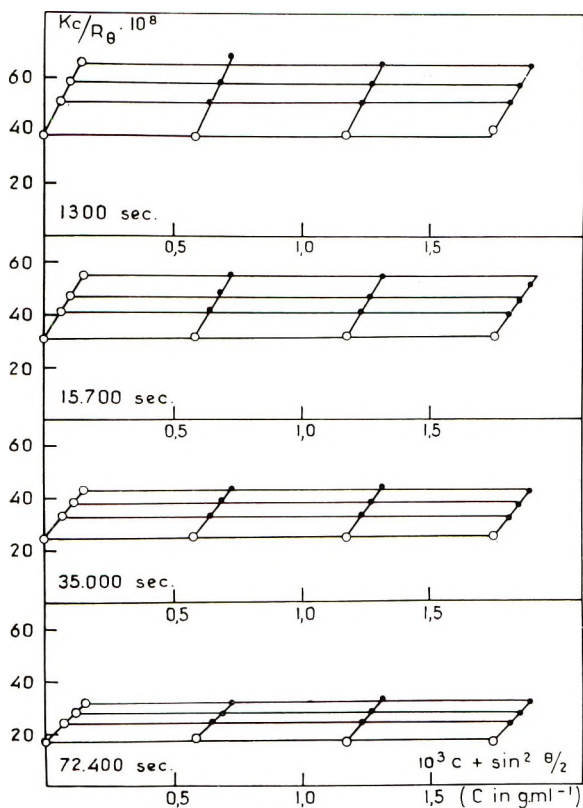


Fig. 5. Zimm plots made up from Figs. 1-3.

times  $3t/2$  and  $3t$ , respectively. By interpolation in the diagrams as shown by Figures 1-3 one can obtain the entity  $(Kc/R_\theta)_t$  for any value of  $\theta$  and  $t$ . This method affords the data to compose Zimm plots, which give information about  $\bar{M}_w$  and  $s_z^2$  at various times in a solution of a definite concentration, i.e., concentration  $a$ . Figure 5 is an example of a series of Zimm plots obtained from Figures 1-3; the diagrams are related to values of  $t$  as indicated in the figure.

$Kc/R_\theta$  is determined here for angles  $\theta$  of  $30^\circ$ ,  $37.5^\circ$ , and  $45^\circ$ , as at these angles only a linear extrapolation of  $Kc/R_\theta$  to  $\sin^2 \theta/2 = 0$  appeared to be possible.

TABLE II

Amylose concentration*	$dM_w/dt$ , g./mole-sec.	$\beta \times 10^{-3}$ , ml./mole-sec.
$a$	49	28
$2a/3$	33	28
$a/3$	15	25

\*  $a = 1.75 \times 10^{-3}$  g./ml.



It turned out then that the second virial coefficient  $A_2 = 0$ , which was also the case in the other series presented in Table I. This is in rather good agreement with the values of  $A_2$  found by Everett and Foster<sup>18</sup> and Husemann et al.<sup>7</sup> for neutral aqueous amylose solutions. According to these authors  $A_2$  is rather small, about  $0.3 \times 10^{-4}$  ml.-mole/g.<sup>2</sup>.

### DISCUSSION

In Table I the results are collected from various series of experiments. The change in the radius of gyration  $s_z^2$  is remarkably small compared to the change in  $\bar{M}_w$  with time.

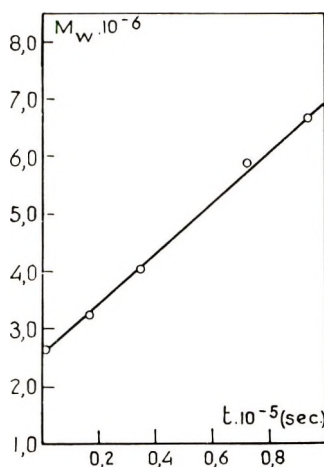


Fig. 6.  $\bar{M}_w$  as a function of time. Dilution series A. Degraded amylose, pH 9.19;  $\beta = (25 \pm 3) \times 10^3$  ml./mole-sec.

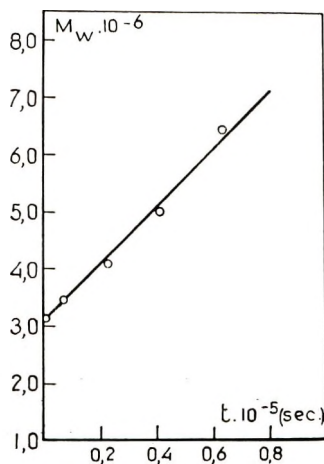


Fig. 7.  $\bar{M}_w$  as a function of time. Dilution series B. pH 9.18;  $\beta = (28 \pm 3) \times 10^3$  ml./mole-sec.

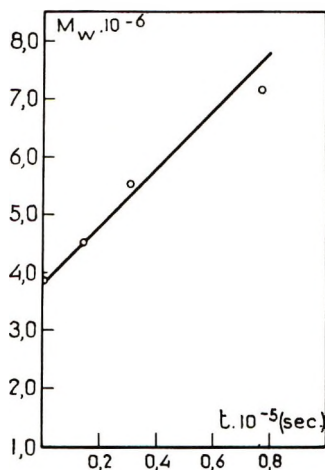


Fig. 8.  $\bar{M}_w$  as a function of time. Dilution series C. pH 3.95;  $\beta = (28 \pm 4) \times 10^3$  ml./mole-sec.

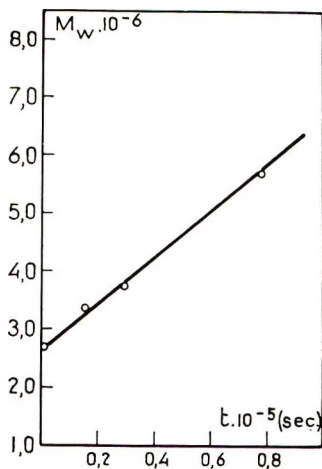


Fig. 9.  $\bar{M}_w$  as a function of time. Dilution series D. pH 3.95;  $\beta = (23 \pm 3) \times 10^3$  ml./mole-sec.

Preliminary viscosity determinations on the retrograding systems<sup>21</sup> showed a decrease in the viscosity with time, i.e., with increasing  $\bar{M}_w$ . Rather similar results were obtained by Neely<sup>2</sup> for methylcellulose aggregates in aqueous solutions. The difference in viscosity and radius of gyration were small compared to the differences in  $\bar{M}_w$  of methylcellulose at various degrees of aggregation. Our findings may provide additional support for Neely's view that the aggregates appear to be built up from molecules laid down side by side, as such associations give maximum contact leading to a greater stability.

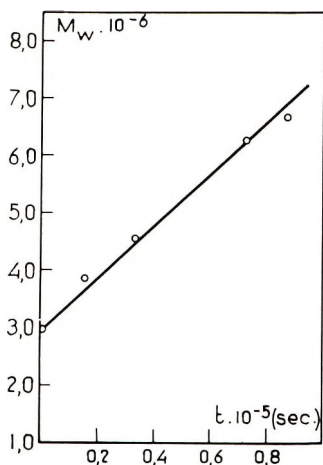


Fig. 10.  $\bar{M}_w$  as a function of time. Dilution series E. Degraded amylose, pH 4.00;  $\beta = (26 \pm 3) \times 10^3$  ml./mole-sec.

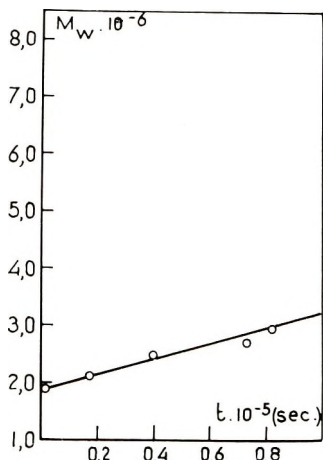


Fig. 11.  $\bar{M}_w$  as a function of time. Dilution series F. pH 11.9;  $\beta = (7 \pm 1) \times 10^3$  ml./mole-sec.

As was pointed out earlier, one of the conditions for a coagulation according to von Smoluchowski's theory is that the ratio between the radii of the colliding particles may not exceed a value of about 1.3. Regarding the small changes in  $s_z^2$  this condition appears to be fulfilled indeed by the retrograding amylose aggregates.

Figures 6-11 show plots of  $\bar{M}_w$  against the time related to amylose concentrations of 1.75 g./ml. (see also Table I). As previously mentioned in the description of the experiments, retrogradation sets in as soon as the alkaline amylose solutions are neutralized. For the various series this causes different values of  $\bar{M}_w$  at the time which is defined as  $t = 0$ .

Figures 6 and 7 show  $\bar{M}_w$  as a function of the time for the degraded and original sample. The pH's of the solutions were about 9.2. The course of the retrogradation in solutions of a pH of about 4.0 is demonstrated by Figures 8, 9, and 10, the last of which is for a degraded sample. In all these experiments the values for the rate constants  $\beta$  are practically equal, the differences being within experimental error. The rate constant does not appear to be much affected by a slight degradation of the amylose sample during the preceding heat treatment in alkaline solution, nor by the pH of the solution, provided the pH is low enough to prevent the molecules from assuming a negative charge.

As is shown by Figure 11, the rate of retrogradation is much smaller at pH 11.9. If a  $pK$  of dissociation of about 12.6 is assumed,<sup>9</sup> then the average number of negative electrostatic charges per monomer unit is 0.2. The electrostatic repulsion between the molecules appears to diminish the effective collisions, which leads to permanent sticking of the molecules.

It should be mentioned that the absolute values of the  $\bar{M}_w$  at this pH may be somewhat in error. As the molecules carry electrostatic charges, the value of  $dn/dc$  in this medium had to be measured at constant chemical potential of the salt<sup>22,23</sup> in order to obtain the correct molecular weight. The dialysis procedure, however, required to measure  $dn/dc$  according to these conditions, cannot be performed experimentally in the retrograding system. Dealing with changes of molecular weight rather than with the absolute values, we believe that the use of the incorrect refractive index increment will not affect the essence in our interpretation. With regard to the rate constant  $\beta$  at lower pH, one can try to verify its physical significance as stated by eq. (3). The theoretical value of  $\beta$  can be computed, if one assumes the diffusion constant  $D_1$  and the molecular diameter or radius of interaction to be related to the monomer unit, i.e., the glucose molecule. On taking the average diameter<sup>24</sup> of a glucose molecule to be about 4.4 Å. and the diffusion constant<sup>25</sup> to be  $7 \times 10^{-6}$  cm.<sup>2</sup>/sec., it turns out that the value of  $\beta$  has to be about  $46 \times 10^{11}$  instead of  $26 \times 10^3$  as found for amylose.

It is obviously senseless to correct the assumed values of  $D_1$  or  $R_{11}$  by a factor of  $0.6 \times 10^{-8}$  in order to get quantitative agreement between theory and experiment without having these parameters lose their physical meaning. Apparently we have to assume that in the lower pH region, where electrostatic repulsions cannot be expected, only a small fraction of the collisions lead to coagulation. This means that for an effective collision some conditions have to be fulfilled, which have not been taken into account. The conditions can be, for instance, a certain amount of kinetic energy and/or a specific mutual orientation of the colliding aggregates. It is difficult to see how these effects could be predicted quantitatively from theoretical considerations. However, if the fraction of effective collisions does not depend on the molecular weight and the concentration of amylose, then the principles of von Smoluchowski's coagulation theory remain valid.

## References

1. T. Matsuo and H. Inagaki, *Makromol. Chem.*, **53**, 130 (1962).
2. W. B. Neely, *J. Polymer Sci. A*, **1**, 311 (1963).
3. E. J. Mouton, Thesis, Leiden, 1959.
4. E. F. Paschall and J. F. Foster, *J. Polymer Sci.*, **9**, 73, 85 (1952).
5. J. F. Foster and M. D. Sterman, *J. Polymer Sci.*, **21**, 91 (1956).
6. M. Ceh and N. Vene, *Stärke*, **11**, 290 (1959).
7. E. Husemann, B. Pfannemüller, and W. Burchard, *Makromol. Chem.*, **59**, 1 (1963).
8. A. Sarko, F. J. Germino, B. R. Zeitlin, and P. F. Dupas, *J. Appl. Polymer Sci.*, **8**, 1343 (1964).
9. H. L. Doppert and A. J. Staverman, *J. Polymer Sci., A-1*, **4**, 2367 (1966).
10. H. L. Doppert, and A. J. Staverman, *J. Polymer Sci., A-1*, **4**, 2373 (1966).
11. M. von Smoluchowski, *Physik. Z.*, **17**, 557, 585 (1916); *Z. Physik. Chem.*, **72**, 129 (1918); *Kolloid Z.*, **21**, 90 (1917).
12. J. Th. G. Overbeek, in *Colloid Science*, Vol. 1, H. R. Kruyt, Ed., Elsevier, Amsterdam, 1952, p. 278.
13. J. Stauff, *Kolloidchemie*, Springer-Verlag, Berlin, 1960, p. 482.
14. B. H. Zimm, *J. Chem. Phys.*, **16**, 1093, 1099 (1948).
15. H. Benoit and P. Doty, *J. Phys. Chem.*, **57**, 958 (1953).
16. P. Hiemstra, W. C. Bus, and J. Muetgeert, *Stärke*, **8**, 235 (1956).
17. J. J. Hermans and S. Levinson, *J. Opt. Soc. Am.*, **41**, 460 (1951).
18. W. W. Everett and J. F. Foster, *J. Am. Chem. Soc.*, **81**, 3459 (1959).
19. W. Burchard, *Makromol. Chem.*, **59**, 16 (1963).
20. C. D. Thurmond, *J. Polymer Sci.*, **8**, 607 (1952).
21. H. L. Doppert, Thesis, Leiden, 1963.
22. A. Vry, Thesis, Utrecht, 1959.
23. P. Ander, *Kolloid Z.*, **185**, 102 (1962).
24. K. H. Meyer and L. Misch, *Helv. Chim. Acta*, **20**, 232 (1937).
25. M. C. Bourne, C. O. Chichester, and C. Sterling, *J. Polymer Sci. A*, **1**, 817 (1963).

## Résumé

Cet article traite de la cinétique de la rétrogradation de l'amylose en solutions aqueuses à des pH de 4,0, 9,2 et 11,9. On a suivi la rétrogradation au moyen de mesures de diffusion lumineuse. Au départ de notre interprétation des données de diffusion lumineuse nous admettons que le mécanisme de rétrogradation est en accord qualitatif avec la théorie de von Smoluchowski concernant la coagulation. Au départ de la vitesse de rétrogradation, on peut conclure qu'uniquement une faible fraction des collisions entre les agrégats d'amylose amène une coagulation permanente. En vue d'expliquer ce phénomène des conditions supplémentaires sont suggérées pour assurer l'aggrégation permanente de particules en collision. La fraction correspondante est plus petite à pH 11,9 qu'à des pH plus bas, ce fait étant attribué à des repulsions mutuelles des agrégats par suite de leurs charges négatives.

## Zusammenfassung

In der vorliegenden Arbeit wird die Kinetik der Retrogradierung von Amylose in wässriger Lösung bei den pH-Werten 4,0, 9,2 und 11,9 beschrieben. Der Verlauf der Retrogradierung wird durch Lichtstreuungsmessungen verfolgt. Die Interpretierung der Lichtstreuungsergebnisse führte zu dem Schluss, dass der Retrogradierungsmechanismus in qualitativer Übereinstimmung mit der Koagulationstheorie von Smoluchowski steht. Aus der Retrogradierungsgeschwindigkeit kommt man zu dem vorläufigen Schluss, dass nur ein kleiner Bruchteil der Zusammenstöße zwischen den Amyloseaggregaten zu einer permanenten Koagulation führt. Um dieses Phänomen zu er-

klären, werden zusätzliche Bedingungen für eine dauernde Verbindung zweier zusammenschlossender Aggregate angenommen. Der entsprechende Bruchteil ist bei pH 11,9 kleiner als bei den anderen pH-Werten und dieser Umstand wird auf die gegenseitige, durch ihre negative Ladung verursachte Abstossung der Aggregate zurückgeführt.

Received January 7, 1966

Prod. No. 5047A

## Polyelectrolytic Character of Amylose. I.

H. L. DOPPERT\* and A. J. STAVERMAN, *Laboratorium voor Fysische Chemie, Universiteit Leiden, Leiden, Netherlands*

### Synopsis

Electrophoresis and titration experiments on amylose solutions and gels are described. The experimental results clearly demonstrate the negative charge of the amylose molecules at pH values of 11 and higher. With the assumption that a monomer unit can carry one charge only,  $pK$ 's of amylose are calculated. The agreement between the  $pK$ 's of amylose and glucose forms an indication that hydroxyl groups dissociate in the above-mentioned pH range.

### INTRODUCTION

In the past years many controversial opinions have been expressed about the nature of the interaction of polysaccharides with hydroxyl ions. Well-known phenomena are the solubility of amylose and the partial solubility of cellulose in 1*N* sodium hydroxide solutions. The viscosity of amylose solutions as well as the swelling behavior of cellulose gels in dependence of the hydroxyl ion concentration is described in several papers. Everett and Foster<sup>1</sup> attribute the increase of the viscosity of amylose solutions with increasing hydroxyl ion concentration to electrolytic dissociation of hydroxyl groups. From studies of the change of the optical rotation of amylose as a function of the pH, Rao and Foster<sup>2</sup> suggest that the ionizing groups responsible for this effect must have a  $pK$  of 12 or slightly higher. Holló et al.,<sup>3</sup> on the other hand, ascribe this phenomenon to conformational changes of anhydroglucose units, as a consequence of their interaction with hydroxyl ions. They even reject the possibility of dissociation of hydroxyl groups. In considering the swelling behavior of cellulose, Neale<sup>4</sup> and Pennings and Prins<sup>5</sup> have the opinion that cellulose is a very weak polyacid; this is in contrast to the view of other authors,<sup>6-8</sup> who believe in the existence of a cellulose-NaOH addition complex which is responsible for the typical swelling phenomenon, which shows a maximum at about 9% NaOH. Recently Barry and Halsey<sup>9</sup> found convincing indications of the negative charge of a natural polysaccharide (extracted from locust bean) in alkali solutions with the aid of conductometric measurements.

In the present paper we will deal with some electrophoresis and titration experiments on amylose solutions and gels, respectively. It will be shown that at high pH amylose molecules bear negative charges, while an indica-

\* Present address: Algemene Kunstzijde Unie N.V. AKU, Arnhem, Netherlands.

tion is found that these charges are the consequence of dissociation of hydroxyl groups.

## EXPERIMENTAL

### General

The amylose, bearing the code number A430, was supplied by the AVEBE. G.A., Veendam, Netherlands. The polymer was obtained by fractionation of potato starch with a  $MgSO_4$  solution, as described previously by Hiemstra et al.<sup>10</sup> The limiting viscosity number  $[\eta]$  for our sample in 1*N* KOH was 214 ml./g.

Amylose solutions were prepared by dissolving the amylose in 1*N* KOH, followed by dilution with distilled water and neutralization with HCl until the desired pH and concentration were obtained.

### Electrophoresis

The electrophoretic mobilities of amylose in solutions of various pH's were determined at 25°C. with the aid of an L.K.B. 3023 Tiselius-Svenson apparatus. The boundaries were KOH, KCl/amylose, KOH, KCl/KOH KCl. In the measuring cell, obviously, the solutions all had equal pH's and salt concentrations. The amylose and salt concentration were  $0.3 \times 10^{-2}$  g./ml. and 0.05*M* (KOH + KCl), respectively. The velocities of the ascending and descending boundaries were determined by plotting graphically the covered distance against the time. Coagulation of amylose did not appear to have a noticeable influence on the linear relationship between these entities. The electrophoretic mobility  $U$  was calculated according to eq. (1),

$$U = VGS\kappa/i \quad (1)$$

where  $V$  is the velocity of the peak in the Schlieren diagram,  $G$  the enlargement factor of the optical system,  $S$  the cross-sectional area of the cell,  $\kappa$  the specific conductivity of the solution, and  $i$  the electric current.

### Potentiometric Titration of Amylose Gels

A 1-g. portion of the amylose sample (12½% moist) was put into a large weighing bottle, whereafter 25 ml. of a 0.05*M* (KOH + KCl) solution of the desired pH was pipetted on the amylose powder. An amylose gel formed on the bottom of the weighing bottle. Experiments were carried out at three pH values.

Reference solutions were prepared by the same procedure, in which 1 ml. purified water (pH 6.5) was added instead of amylose.

The experiments were carried out under  $N_2$  to prevent as much as possible a decrease of the pH of the solution by absorption of  $CO_2$ , from the air. To make sure that equilibrium was reached, the sealed bottles were stored under  $N_2$  in a desiccator for 14 and 26 days before the pH was finally determined again.



## RESULTS

## Electrophoresis

The values of the electrophoretic mobilities of amylose in aqueous solutions of various pH's are collected in Table I. In all cases the amylose molecules moved to the positive electrode which proves the negative charge of the molecules. The mobilities found at pH 4 and 10, however, are of the order of the experimental error. For comparison the electrophoretic data<sup>11,12</sup> for a Na-carboxymethylcellulose sample (NaCMC) is also given in Table I. The sample was kindly supplied by the Algemene Kunstzijde Unie, Arnhem. The pH of the NaCMC solution was about 8, a pH at which practically all carboxymethyl groups are dissociated.

One may wonder whether the negative charge is due to association of hydroxyl ions with amylose molecules or dissociation of protons from the hydroxyl groups of the polymer. From the experimental data one can calculate either an association or a dissociation constant. Our preference for the assumption of dissociation of hydroxyl groups will be justified at the end of the subsequent discussion. To calculate a  $pK$  for dissociation the following assumptions have to be made. (a) Only one hydroxyl group per monomer unit is able to dissociate under the given experimental conditions, i.e.,  $pH < 13$ . (b) The electrophoretic mobilities of NaCMC and amylose do not depend on their molecular weights. (c) The ratio between the average electrostatic charge per monomer unit and the mobility  $U$  is a constant. In other words, if the degree of dissociation of amylose and the degree of substitution of NaCMC are given by  $\alpha$  and  $s$ , respectively, then it will be assumed that

$$\alpha/U_{\alpha} = C_1$$

and

$$s/U_s = C_2$$

(d) The constants  $C_1$  and  $C_2$  have the same value. This leads to the simple relation:

$$\alpha/U_{\alpha} = s/U_s \quad (2)$$

TABLE I  
Electrophoretic Mobilities of NaCMC and Amylose Samples at Various pH's

	pH	$U \times 10^3$ , cm. <sup>2</sup> /v.- sec.	$s$	$\alpha$	$pK^a$
NaCMC-73	8	39	0.56	—	—
Amylose	4.0 ± 0.2	0.6	—	—	—
Amylose	10.0 ± 0.2	0.5	—	—	—
Amylose	11.2 ± 0.1	3.5	—	0.05	12.5 ± 0.2
Amylose	12.5 ± 0.1	18.4	—	0.26	13.0 ± 0.1

<sup>a</sup>  $pK$ 's of amylose determined according to eqs. (2) and (3) based on the data for NaCMC-73.

TABLE II  
pH's of Solutions Above the Amylose Gels and Their Corresponding Reference Solutions,  
as Measured at Different Times After Their Preparation<sup>a</sup>

1st day		After 14 days				After 26 days			
Refer- ence pH	Amy- lose pH	Refer- ence pH	Amy- lose pH	$\alpha \times$ $10^2$	pK	Refer- ence pH	Amy- lose pH	$\alpha \times$ $10^2$	pK
11.00	11.00	10.90	10.00	0.2	12.6	10.49	9.60	0.08	12.7
11.50	11.50	11.48	10.78	0.8	12.9	11.32	10.34	0.5	12.7
11.80	11.80	11.80	10.88	1.8	12.6	11.52	10.52	1.0	12.5

<sup>a</sup> Degree of dissociation  $\alpha$  and pK of amylose calculated according to description in text.

Thus  $\alpha$  can be found from the experimental data, and one is able to calculate the pK according to the Henderson-Hasselbach relation:

$$pK = pH - \log[\alpha/(1 - \alpha)] \quad (3)$$

provided that pK thus calculated does not depend strongly on  $\alpha$  (see Tables I and II). In the last column of Table I the pK's are found with the aid of the data for NaCMC-73.<sup>11,12</sup>

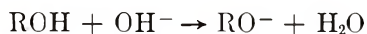
### Potentiometric Titration

The results of the potentiometric titrations are given in Table II. After equilibrium was reached, the solutions above the amylose gels all had a lower pH than their corresponding reference solutions, indicating an OH<sup>-</sup> consumption. Starting again from the hypothesis that we are dealing here with the dissociation of weakly acidic hydroxyl groups on the amylose, we also calculated the pK of amylose from these experiments. Equation (3) is now written in the form:

$$pK = pH - \log\left\{\frac{[RO^-]}{[ROH]}(f_{RO^-}/f_{ROH})\right\} \quad (4)$$

where [ROH] and [RO<sup>-</sup>] are the concentrations of the undissociated and dissociated anhydroglucose units, respectively, and  $f_{ROH}$  and  $f_{RO^-}$  are the corresponding activity coefficients. The activity coefficients of the OH<sup>-</sup> ions in the reference solution and in the solution above the amylose gel are  $f_{OH^-}$  and  $f_{OH^-}^0$ .

From the pH drop of the solution above the amylose gel one can determine (after correction for CO<sub>2</sub> absorption) the decrease in OH<sup>-</sup> ion activity as a consequence of the neutralization reaction:



The CO<sub>2</sub> correction can be carried out by assuming the quantity of CO<sub>2</sub> absorbed by the solution above the gel and the corresponding reference solution to be exactly the same. (The influence of CO<sub>2</sub> absorption is shown by the decrease of the pH's of the reference solution in the course of time.)

To calculate  $pK$ 's from the experimental data one has to assume that  $f_{ROH} = 1$  and  $f_{RO^-} = f_{OH^-} = f_{OH^-}^0$ . Furthermore, the decrease in  $OH^-$  ion activity after neutralization has to be equated to  $[RO^-]/f_{RO^-}$ .

The  $pK$  determined by this method is found to lie between 12.5 and 12.9, as is shown in Table II.

## DISCUSSION

The movement of the amylose molecules to the anode unequivocally proves the presence of negative charges of amylose at high pH. As is well known,<sup>13</sup> the  $pK$  of polyelectrolytes is not a constant, but increases with increasing degree of dissociation. As is shown by Table I, we indeed find a higher  $pK$  with increasing  $\alpha$ . We do not, however, know to what extent the values of the  $pK$ 's are influenced by the numerous assumptions we had to make in the calculation. In spite of the rather great experimental errors, the  $pK$ 's found from titration of amylose gels (Table II) confirm very well those obtained from the electrophoresis experiments.

Thamsen<sup>14</sup> estimated the  $pK$  of glucose by potentiometric titration. He started from the assumption that only one hydroxyl group per glucose molecule dissociates, a working hypothesis which is the same as our assumption that one hydroxyl group per monomer unit dissociates at  $pH < 13$ . The  $pK$ 's he found had the values of 12.43 at 18°C. and 12.92 at 0°C. At low degrees of dissociation, the  $pK$  of poly(methacrylic acid)<sup>15</sup> is about 4.5; this is of the same order of magnitude as the  $pK$  value of 4.8 for isobutyric acid. So it is not unreasonable to compare the  $pK$  of amylose at low degree of dissociation with the  $pK$  of glucose. The agreement between the  $pK$ 's of amylose and glucose is excellent. Moreover Hine and Hine<sup>16</sup> have demonstrated that isopropanol is able to split off a proton in the absence of  $OH^-$  ions. This provides a strong argument for the hypothesis of dissociation of alcohols and amylose as opposed to that of association of  $OH^-$  groups at high pH.

## References

1. W. W. Everett and J. F. Foster, *J. Am. Chem. Soc.*, **81**, 3459, 3464 (1959).
2. V. S. R. Rao and J. F. Foster, *Biopolymers*, **1**, 527 (1963).
3. J. Holló, J. Szejtli, and M. Toth, *Stärke*, **13**, 222 (1961).
4. S. M. Neale, *J. Textile Inst.*, **20**, T373 (1929); *ibid.*, **21**, T225 (1930); *ibid.*, **22**, T320, T349 (1931).
5. A. J. Pennings and W. Prins, *J. Polymer Sci.*, **58**, 229 (1962).
6. E. Ott, H. M. Spurlin, and M. W. Grafflin, Eds., *Cellulose and Cellulose Derivatives*, Part I, Interscience, New York, 1954, p. 328.
7. G. Denoyelle, *Svensk Papperstidn.*, **62**, 390 (1959).
8. J. Chédin and A. Marsaudon, *Makromol. Chem.*, **15**, 115 (1954); *ibid.*, **20**, 57 (1956); *ibid.*, **33**, 195 (1959).
9. J. A. Barry and G. D. Halsey, *J. Phys. Chem.*, **67**, 1698 (1963).
10. P. Hiemstra, W. C. Bus, and J. Muetgeert, *Stärke*, **8**, 235 (1956).
11. P. J. Napjus, Thesis, Leiden, 1958.
12. P. J. Napjus and J. J. Hermans, *J. Colloid Sci.*, **14**, 252 (1959).
13. A. Katchalsky and J. Gillis, *Rec. Trav. Chim.*, **68**, 879 (1949).

14. J. Thamsen, *Acta Chem. Scand.*, **6**, 270 (1952).
15. J. C. Leyte, Thesis, Leiden, 1961.
16. J. Hine and M. Hine, *J. Am. Chem. Soc.*, **74**, 5266 (1952).

### Résumé

On décrit des expériences électrophorétiques et de titration sur des solutions et des gels d'amylose. Les résultats expérimentaux démontrent clairement la charge négative des molécules d'amylose à des valeurs de pH de 11 et supérieures. En admettant qu'une unité monomérique peut uniquement porter une seule charge on a calculé les pK de l'amylose. L'accord entre les pK de l'amylose et du glucose forme une indication que les groupes hydroxyles se dissocient dans le domaine des pH mentionnés ci-dessus.

### Zusammenfassung

Elektrophorese- und Titrationsversuche an Amyloselösungen und gellen werden beschrieben. Die Versuchsergebnisse beweisen das Vorhandensein einer negativen Ladung der Amylosemoleküle bei pH-Werten von 11 und höher. Unter der Annahme, dass eine Monomereinheit nur eine Ladung tragen kann, werden die pK-Werte von Amylose berechnet. Die Übereinstimmung zwischen den pK-Werten von Amylose und Glukose bildet einen Hinweis dafür, dass im oben erwähnten pH-Bereich die Hydroxylgruppen dissoziieren.

Received August 27, 1965

Revised December 8, 1965

Prod. No. 5042A

## Polyelectrolytic Character of Amylose. II.

H. L. DOPPERT\* and A. J. STAVERMAN, *Laboratorium voor Fysische Chemie, Universiteit Leiden, Leiden, The Netherlands*

### Synopsis

Viscometric titrations of amylose are described. The curves confirm the earlier results of Rao and Foster. A more quantitative consideration is given concerning the changes of the electrostatic charge of the amylose molecules in the pH range of 11-12, where a minimum in the titration curve is found. A viscometric titration performed in solutions containing urea shows a considerably higher viscosity, especially at lower pH's; the curve, however, still shows a minimum between pH 11 and 12. Experiments on the dependence of  $[\eta]$  on the ionic strength at pH 12.7 also demonstrate the typical polyelectrolytic nature of amylose.

### Introduction

In a previous paper<sup>1</sup> some electrophoresis and titration experiments on amylose solutions and gels were reported, which demonstrated the negative charge of the amylose molecules at pH's higher than 11. This discovery induced us to investigate dimensional changes of the molecules in relation to their electrostatic charge. The present paper thus deals with experiments on the viscosity behavior of amylose solutions as a function of the pH and the ionic strength.

Our viscometric titrations confirm the experimental data of Foster and Rao.<sup>2</sup> We believe, however, it may be interesting to publish our results, as in these titration experiments we accounted for the polyelectrolyte nature of amylose by keeping the ionic strength constant. Moreover, one of our viscometric titrations, performed in a solution which was 6*M* in urea, gives additional insight into the mechanism of the conformational changes, as proposed<sup>2</sup> by these authors, at pH 11-12.

### Experimental

To obtain aqueous amylose solutions of rather low pH we made use of the following procedure: The amylose was dissolved in 1*N* KOH, then diluted with distilled water to avoid retrogradation (flocculation) as much as possible during the subsequent neutralization with HCl. At last the solution was again diluted with a salt solution (KCl) and water until the desired amylose concentration and ionic strength were obtained.

Vigorous stirring during the neutralization and the addition of salt solutions appeared to retard the retrogradation process. The pH of the solu-

\* Present address: Algemene Kunstzijde Unie N.V. AKU, Arnhem, the Netherlands.

tions were controlled with a Pye Dynacap pH-meter. The viscometric measurements were performed at  $25 \pm 0.02^\circ\text{C}$ . with an Ubbelohde dilution viscometer mounted in a Vitatron thermostat. The flow time for water in the viscometer was  $249.8 \pm 0.1$  sec. The limiting viscosity number  $[\eta]$  can be obtained from the experimental data according to one of the two Huggins relations:

$$\eta_{sp}/c = [\eta] + k_1[\eta]^2c \quad (1)$$

$$(\ln \eta_{rel})/c = [\eta] - k_2[\eta]^2c \quad (2)$$

The data from the viscometric titrations are expressed in the logarithmic viscosity number  $(\ln \eta_{rel}/c)$ , as it was found that these values were less than 5% lower than the limiting viscosity number  $[\eta]$  for an amylose concentration  $c = 0.16 \times 10^{-2}$  g./ml. A plot of  $\ln \eta_{rel}/c$  against  $c$ , however, did not give a straight line. So for an exact determination of  $[\eta]$  we preferred a plot of  $\eta_{sp}/c$  against  $c$  according to eq. (1) as, in this case a linear relation was found.

Preliminary measurements also showed that the decrease in the viscosity number as a consequence of retrogradation of the amylose was not more than 1%/hr. To control the reproducibility of the experimental data, the viscometric titrations were performed as follows.

Two solutions were prepared, of equal amylose concentrations ( $0.16 \times 10^{-2}$  g./ml.), equal ionic strengths (0.05 or 0.1*M*) but different pH's (4.0 and 12.7, respectively). (In the case of solutions containing urea, the urea concentrations in both solutions were equal.) By adding small amounts of the solutions with a high pH to the solution with pH 4 the viscometric titration was carried out from low to high pH. In the same way these measurements were also performed in the direction from high to low pH. The pH dependence of the viscosity appeared to be a completely reversible phenomenon. The measured viscosity changes cannot therefore be attributed to retrogradation, as the latter is an irreversible effect.

At pH 12.7 the values of  $[\eta]$  were determined at various ionic strengths and salt species. Any value of  $[\eta]$  was obtained by measuring the viscosities of a series of solutions of different amylose concentrations having the same ionic strength and salt species.

## Results and Discussion

Figures 1 and 2 are the results of the viscometric titrations at ionic strengths of 0.05*M* and 0.1*M*. The curves are essentially the same as those presented by Rao and Foster.<sup>2</sup> These authors suggest that the minimum in the curve between pH 11 and 12 is a consequence of a conformational change caused by interactions of electrostatic charges on the molecules. These charges originate from the dissociation of protons from the hydroxyl groups.

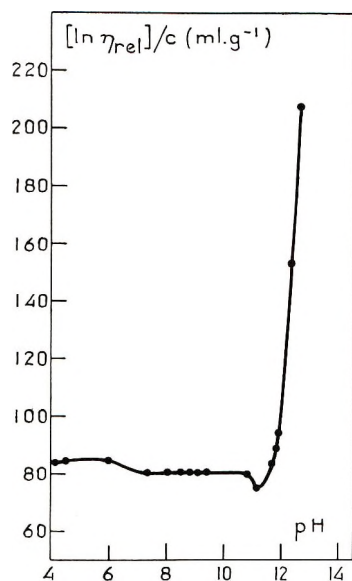


Fig. 1. Viscometric titration of amylose. Ionic strength 0.05*M*.

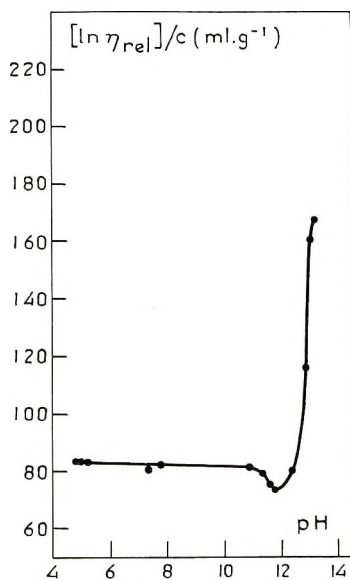


Fig. 2. Viscometric titration of amylose. Ionic strength 0.10*M*.

At higher pH's the increase of the degree of dissociation results in an increasing expansion of the polyelectrolyte, which is responsible for the steep rise of the curve. In a way similar to Holló and Szejli<sup>3</sup> they further propose that in neutral solutions the polymer has the conformation of a nearly Gaussian, but rather stiff coil, with a backbone structure which is essentially helical.

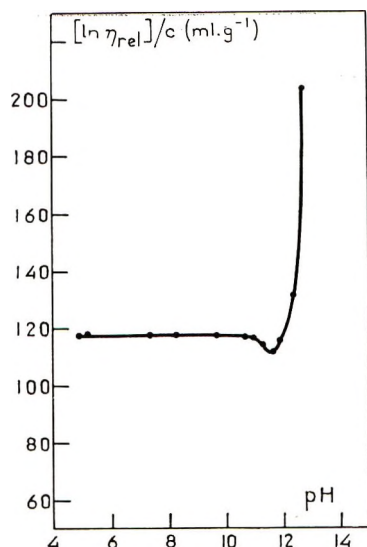


Fig. 3. Viscometric titration of amylose. Ionic strength  $0.05M$ ; urea concentration  $6M$  (36%).

As mentioned earlier, we described<sup>1</sup> some titration and electrophoresis experiments which showed the negative charge of amylose molecules at pH higher than 11. We calculated a  $pK$  for amylose which turned out to be about 12.7. Assuming this to be correct, it can be calculated that from pH 11 to 12 the average elementary charge per monomer unit increases from 0.02 to 0.2. The change of the negative charges in this pH interval made the hypothesis of Rao and Foster on the conformational change fairly acceptable.

The denaturation of ovalbumin by urea was studied extensively by Kauzmann and co-workers.<sup>4,5</sup> The action of urea consists of an unfolding followed by a slow aggregation of the protein. If at low pH the amylose molecules possess a helical conformation stabilized by hydrogen bondings, as is suggested by Foster and Sterman,<sup>6</sup> one might expect some conformational change, i.e., unfolding of the molecules by the action of urea.

Figure 3 shows the results for a viscometric titration of an aqueous amylose solution which was  $6M$  (36%) in urea and had an ionic strength of  $0.05M$ . There is a considerable elevation of the logarithmic viscosity number in the pH region from 4 to 12. This is even such a great effect that in two earlier experiments (Figs. 1 and 2) values for  $(\ln \eta_{rel})/c$  of this order of magnitude are found only at pH greater than 12, i.e., beyond the observed minimum. In spite of the molecular expansion caused by the interaction with urea, a minimum still appears in the curve. Thus it seems that interactions of electrostatic nature are an essential condition for this conformational change of amylose molecules in aqueous solutions. Although the results of this experiment throws some doubt on Foster and Sterman's hypothesis, it does not form a strong argument against their



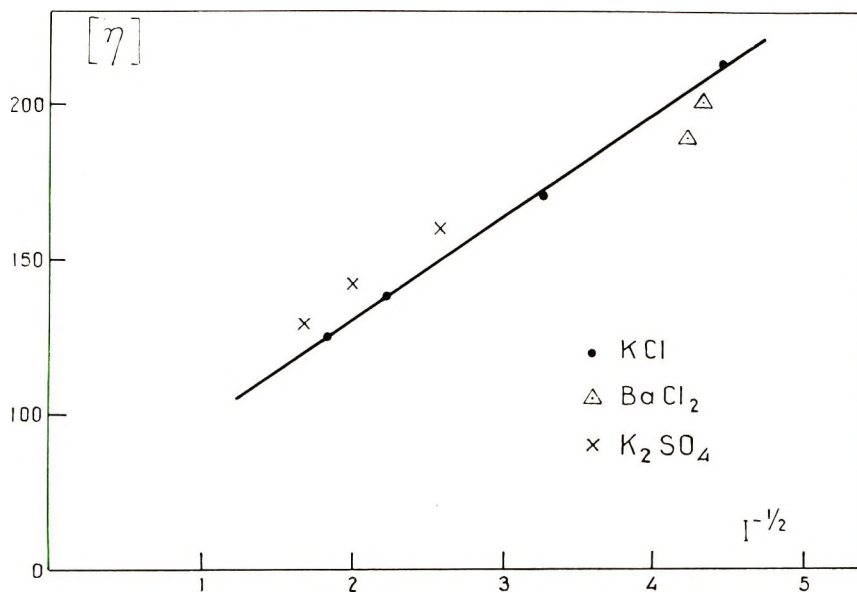


Fig. 4. Dependence of  $[\eta]$  of amylose on  $I^{-1/2}$  at pH 12.7 (0.05N KOH).

statement, as it might be possible that the specific hydrogen bonds responsible for the stabilization of the helical conformation have not reacted with urea.

A relation between the limiting viscosity number determined from isoionic dilution series, and the ionic strength is given by Pals and Hermans<sup>7</sup> on the basis of the theory of Hermans and Overbeek.<sup>8</sup> Their equation is as follows:

$$[\eta] = \frac{1.55}{2} [\eta_0] + \frac{0.53}{2} [\eta_0] a \left( \frac{8\pi e^2 N I}{1000 \epsilon k T} \right)^{-1/2} \quad (3)$$

in which

$$a^2 = (36/5 h_0^2)^{3/2} 3 Z^2 e^2 / 2 \epsilon k T$$

where  $[\eta_0]$  is the reference viscosity of the uncharged polymer,  $e$  is the elementary charge,  $N$  is Avogadro's number,  $I$  is ionic strength,  $\epsilon$  is the dielectric constant of the solution,  $K$  is Boltzmann's constant,  $T$  is the absolute temperature,  $h_0^2$  is the mean-square end-to-end distance of the molecule if it does not carry electrostatic charges, and  $Z$  is the number of ionized groups per polymer chain. The factor in parentheses on the right-hand side of eq. (3) is known as the Debye radius.

A linear relationship between  $[\eta]$  and  $I^{-1/2}$  should be found for a free-draining spherical symmetric polyelectrolyte molecule, in which all ionizable groups are dissociated. If dissociation is not completed, the degree of dissociation, and thus the electrostatic charge  $Ze$ , at constant  $H^+$  ion

concentration will depend upon the activity coefficient of the  $H^+$  ions, i.e., the ionic strength. Although for amylose at pH 12.7 (0.05*N* KOH) the dissociation of the ionizable OH groups is far from complete, the relation holds at least qualitatively if KCl is the added electrolyte. This is shown by Figure 4, where  $[\eta]$  is plotted against  $I^{-1/2}$ . It must be noted, that we obviously accounted for the contribution of the  $OH^-$  ions to the ionic strength. The qualitative interpretation of this phenomenon is that increasing ionic strength will increase the shielding of the charged groups of the polyelectrolyte by the counterions.

The shielding will decrease the mutual electrostatic interactions, which results in a decrease of the polyelectrolyte dimensions and consequently decrease of the viscosity. Thus, the dependence on  $[\eta]$  from the ionic strength may serve as an indication for the presence of charged groups on very weak polyacids or bases.

Figure 4 also demonstrates the specific nature of the ion species. A higher value for  $[\eta]$  is obtained for equal ionic strength if KCl is replaced by  $K_2SO_4$  as added electrolyte. On replacing KCl by a salt of a bivalent cation, for instance,  $BaCl_2$ , a lower value of  $[\eta]$  is found than one might predict on the basis of the results with KCl. Reliable determinations of  $[\eta]$  in the presence of  $Ba^{++}$  ions were possible only at very low concentrations of these ions. A rapid retrogradation sets in at a  $BaCl_2$  concentration as low as  $3 \times 10^{-3}M$  in a solution which is 0.05*N* in KOH (pH 12.7). It is a very well-known phenomenon in colloid science that solutions of charged colloidal particles soon lose their stability and flocculate on the addition of a small amount of oppositely charged multivalent ions.<sup>9</sup>

The flocculation of amylose at relatively low  $BaCl_2$  concentration can very well be understood, in view of the negative charge of amylose at pH 12.7.

### References

1. H. L. Doppert and A. J. Staverman, *J. Polymer, Sci. A-1*, **4**, 2367 (1966).
2. V. S. R. Rao and J. F. Foster, *Biopolymers*, **1**, 527 (1963).
3. J. Holló and J. Szejtli, *Stärke*, **10**, 49 (1958).
4. R. B. Simpson and W. Kauzmann, *J. Am. Chem. Soc.*, **75**, 5139 (1953).
5. H. H. Fiensdorff, M. T. Watson, and W. Kauzmann, *J. Am. Chem. Soc.*, **75**, 5157 (1953).
6. J. F. Foster and M. D. Sterman, *J. Polymer Sci.*, **21**, 91 (1956).
7. D. T. F. Pals and J. J. Hermans, *Rec. Trav. Chim.*, **71**, 433 (1952).
8. J. J. Hermans and J. Th. G. Overbeek, *Rec. Trav. Chim.*, **67**, 761 (1948).
9. H. R. Kruyt, Ed., *Colloid Science*, Vol. I and II, Elsevier, Amsterdam, 1949, 1952.

### Résumé

Des titrations viscosimétriques de l'amylose ont été décrites. Les courbes confirment très bien les résultats antérieurs de Rao et Foster. On donne un examen plus quantitatif des variations de la charge électrostatique des molécules d'amylose dans le domaine de pH de 11 ou 12, où un minimum des courbes de titration est trouvé. La titration viscosimétrique, effectuée en solution contenant de l'urée, montre une viscosité considérablement plus élevée, particulièrement aux pH plus bas; cette courbe toutefois, montre

encore un minimum entre pH 11 et 12. Les expériences relatives à la dépendance de la viscosité en fonction de la force ionique à pH 12.7 montrent également la nature typiquement polyélectronique de l'amylose.

### Zusammenfassung

Die viskosimetrische Amylosetitration wird beschrieben. Die erhaltenen Kurven bestätigen die früheren Ergebnisse von Rao und Foster sehr gut. Eine mehr quantitative Betrachtung der Änderung der elektrostatischen Ladung der Amylosemoleküle im pH-Bereich von 11–12, wo ein Minimum in der Titationskurve auftrat, wird gegeben. Eine in Harnstoffhaltigen Lösungen ausgeführte viskosimetrische Titration zeigt besonders bei niedrigerem pH eine beträchtlich höhere Viskosität; die Kurve besitzt jedoch immer noch zwischen pH 11 und 12 ein Minimum. Versuche über die Abhängigkeit von  $[\eta]$  von der Ionenstärke bei pH 12,7 bestätigen die typische Polyelektrolytnatur von Amylose.

Received August 27, 1965

Prod. No. 4992A

## Photolysis of Poly(*tert*-butyl Acrylate) in the Region of the Glass Transition Temperature

ALAN R. MONAHAN, *Xerox Corporation, Rochester, New York 14603*

### Synopsis

The thin film ( $1 \times 10^{-5}$  cm.) photolysis (2537 Å.) of poly(*tert*-butyl acrylate) under 1 atm. helium pressure has been investigated in detail. Isobutene was the only significant volatile product in the temperature range 20–110°C. The reaction was demonstrated to be initially a first-order decomposition with an energy of activation of 3.3 kcal./mole in the glassy state. Above the glass transition temperature a value of 1.8 kcal./mole was found. The rate of isobutene formation is autoaccelerated when a minimum of one acrylic acid unit is generated per chain. The initial quantum yield for the formation of isobutene varies from 0.083 to 0.17 over the temperature range studied. There was no dependence of quantum yield on the exciting wavelength using sources of 1849, 2537, and 3660 Å. The intensity exponent was found to be unity, consistent with first-order decomposition kinetics.

### INTRODUCTION

Although polymer degradation studies are receiving considerable attention, little is known about the kinetics and activation energies of decomposition in the region of the glass transition temperature ( $T_g$ ). Stokes and Fox<sup>1</sup> have photolyzed poly- $\alpha$ -methylstyrene at 25°C. and above the  $T_g$  at 115°C. A fourfold increase in kinetic chain length was found above the  $T_g$ . However, many complicating factors, such as thick films and large temperature variations, prevented a clear mechanistic interpretation.

A polymer suited for a study of this type is poly(*tert*-butyl acrylate) (PTBA). PTBA on photolysis in the temperature range 20–110°C. gives isobutene and poly(acrylic acid). No significant complicating side reactions, including depolymerization, are found. Therefore, the study of the kinetics of this ester decomposition, over a temperature range encompassing the  $T_g$ , was undertaken in an attempt to compare the factors altering the mechanical and electrical properties of polymers, i.e., elasticity, viscosity, resistivity, etc. with those affecting the chemical properties. The effects on the decomposition rates of variations of wavelength, light intensity, and polymer molecular weight were studied under thin film conditions to elucidate the reaction mechanism.

### EXPERIMENTAL

*tert*-Butyl acrylate monomer (Borden Chemical Co.) was washed with dilute sodium hydroxide, dried with anhydrous sodium sulfate, and vacuum-

TABLE I  
Polymerization and Properties of Poly(*tert*-butyl Acrylate)

Initiator	Initiation concn., mole-%	Temperature, °C.	Conversion, mole-%	$\bar{M}_w \times 10^{-3}$	$T_g$ , °C.	$\rho$ , g./cc.
Benzoyl peroxide	1.55	93.0	~10	4.48	69 ± 1	1.07 ± 0.02
Azobisisobutyronitrile	2.14	51.3	~20	8.80	72	
Azobisisobutyronitrile	1.03	53.2	~20	16.0	73	

distilled to remove the 0.1% *p*-hydroxyanisole inhibitor. By vapor-phase chromatography it was found to be free from water and other possible impurities. The monomer was then degassed three times to a vacuum of  $2 \times 10^{-6}$  mm. and distilled into 50 cm.<sup>3</sup> Pyrex reactors. The reactors were sealed under vacuum. Benzoyl peroxide (Eastman Organic) or azobisisobutyronitrile (Borden Chemical Co.) were used as polymerization initiators under the conditions presented in Table I. After reaction, the mixture was dissolved in acetone and the polymer precipitated and reprecipitated with methanol. The powder was then dried under vacuum at 50°C. for ~24 hr. Measurements of solution viscosity in chloroform at 30.0°C. were made utilizing an Ubbelohde viscometer and weight-average molecular weights obtained from the expression:<sup>2</sup>

$$\eta = 2 \times 10^{-6} \bar{M}_w^{1.0}$$

Glass transition temperatures were obtained on a Dupont differential thermal analyzer. Reproducible temperatures were obtained by using 10-mg. samples and a heating rate of 20°C./min.

Uniform film thicknesses of from  $6 \times 10^{-6}$  to  $6 \times 10^{-5}$  cm. could be obtained by dip-coating from solutions containing 0.5–5 g. of polymer per 100 cm.<sup>3</sup> of toluene. Quartz slides measuring 3 cm. × 10 cm. × 1 mm. were used for substrates. The films were dried under vacuum at 50°C. for 24 hr. Average coatings weighed from 0.2 to 2.0 mg. Residual toluene was determined by dissolving the coatings in 100  $\mu$ l. of acetone and analyzing 2- $\mu$ l. aliquots by gas chromatography. It was found that the maximum thickness films ( $6 \times 10^{-5}$  cm.) contained approximately 0.1% toluene by weight. This can be taken as the upper limit of solvent content in the films. Thickness measurements were obtained by use of a Reichert microscope fitted with a Watson 16-mm. interference objective. Absorption properties of the polymer on Suprasil quartz were determined at 1700–3700 Å. by using a Tropel Model N-2 far ultraviolet monochromator and a Cary 14 spectrophotometer.

Rates of decomposition were carried out in a previously described<sup>3</sup> square cross-section fused quartz cell, infrared heating of graphite being used to maintain polymer film temperature ( $\pm 1^\circ\text{C}$ ). Products were

sampled continuously in stainless steel traps frozen with a 2-methylpentane-liquid N<sub>2</sub> mixture (-154°C.). A 5-psig helium-1% methane mixture was used as carrier. The products were sampled at 10-20 min. intervals and analyzed with a Barber-Coleman Series 5000 gas chromatograph operated isothermally at 50°C. A 6-ft., 3-mm. glass column of 15% Apiezon L on 80/100 mesh Chromosorb W allowed total analysis of products in 10 min. A micro cross-section detector was used and gave a calibration of products which was linear down to  $1 \times 10^{-12}$  mole/sec.

Volatile products were obtained in pure form by standard microcollection techniques and identified by use of a Perkin-Elmer Infracord spectrophotometer and a quadrupole mass spectrometer.<sup>4</sup> Poly(acrylic acid) was identified by its characteristic OH absorption at  $\sim 3500$  cm.<sup>-1</sup>

The light sources used are listed in Table II. Lamp outputs were calibrated with an Eppley Thermopile. Spectrophotometric traces of the

TABLE II  
Light Sources and Measured Outputs

Lamp	Filter	Arc-film distance, in.	$\lambda$ , A.	Peak half width, A.	Output, $\times 10^{-15}$ quanta/sec.-cm. <sup>2</sup>
Hanovia 83A-1	Quartz, air, Corning 7-54 Filter	5	2537	0.6	1.33
Hanovia 93A-1	Quartz, N <sub>2</sub>	5	1849	$\sim 1$	0.300
G.E. S-4	Quartz, air, Corning 7-51 Filter	4	3660	350	4.00

mercury lamps at 1800-4000 A. were taken with a No. 1700-11 Czerny-Turner spectrometer. The 2537-A. line from the Hanovia 83A-1 lamp was found to be a factor of 60 times more intense than the sum of all other ultraviolet lines. The most significant lines in decreasing order of intensity were 3650, 3125, 3132, 3655, and 3664 A. The Hanovia 93A-1 was calibrated with and without a nitrogen flush. The increase in output with the use of N<sub>2</sub> was taken to be the contribution due to 1849-A. emission. Correction was made for isobutene formation from the 2537 A. radiation. Other lines, as in the 83A-1, were not significant. A Corning 7-51 filter and G.E. S-4 mercury lamp were found to be satisfactory for near-ultraviolet photolysis. The 350-A. band pass of the filter is justified when the broad and very weak absorption of PTBA in the 2900-3700 A. region is considered.

Blackened Lektromesh copper screens were used to vary the intensity of 2537-A. radiation from  $6.8 \times 10^{14}$  to  $1.3 \times 10^{15}$  quanta/sec.-cm.<sup>2</sup>

## RESULTS

### Products

The major products of the PTBA photolysis were found to be isobutene and poly(acrylic acid). Hydrogen, methane, propylene, isobutane, carbon dioxide, water, *tert*-butyl acrylate, and acrylic acid were also identified in trace amounts during exploratory experiments with large sample weights (0.02 g.). In the least representative photolysis, i.e., 110°C., the total amount of products other than isobutene never exceeded 5%. Also, in this same experiment, 2% of the total products were found to be caused by the thermal decomposition.

### Kinetics

The photochemical rate of formation of isobutene from 20 to 110°C. is represented in the plots in Figure 1. The tabulated temperatures, rates and rate constants are shown in Table III. Initial integral rates were found to be independent of molecular weight and initiator.

The data of Figure 1 are successfully represented by a first-order rate law:

$$\ln (C/C_0) = -k_1 t$$

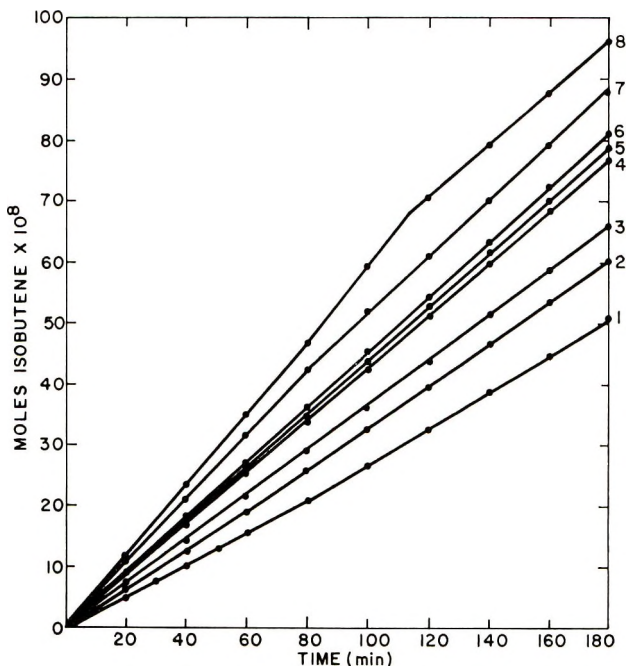


Fig. 1. Photochemical rate of formation of isobutene from poly(*tert*-butyl acrylate): (1) 23.0°C.; (2) 28.4°C.; (3) 34.8°C.; (4) 53.8°C.; (5) 61.4°C.;  $T_0$ ; (6) 71.6°C.; (7) 85.9°C.; (8) 109.9°C.

TABLE III  
Rate of Formation of Isobutene<sup>a</sup>

Temperature, °C.	Rate $\times 10^3$ , mole/min.	$k_1 \times 10^4$ , min. <sup>-1</sup>
23.0	2.86	1.76
28.4	3.24	1.99
34.8	3.59	2.21
53.0	4.25	2.61
61.4	4.44	2.73
69 <sup>b</sup>		
71.6	4.55	2.80
85.9	5.33	3.28
109.9	5.88	3.61

<sup>a</sup> All kinetic runs normalized to 2.0 mg. of  $\bar{M}_w = 4,480$ ,  $\lambda = 2537$  Å.

<sup>b</sup>  $T_g$ .

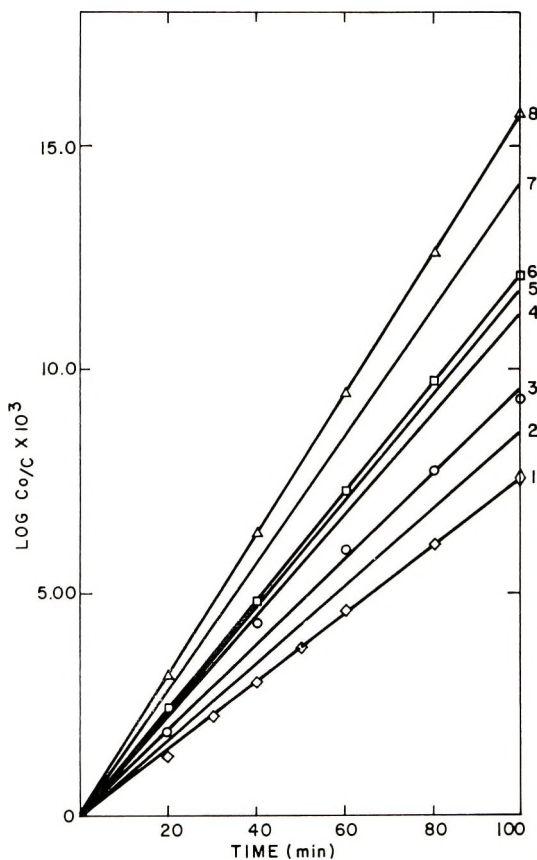


Fig. 2. First-order rate plots for poly(*tert*-butyl acrylate) photolysis: (1) 23.0°C.; (2) 28.4°C.; (3) 34.8°C.; (4) 53.8°C.; (5) 61.4°C.;  $T_g$ ; (6) 71.6°C.; (7) 85.9°C.; (8) 109.9°C. Points are shown only on a few of these lines.



where  $C/C_0$  is the molar fraction of unreacted *tert*-butyl groups in the film at time  $t$ . Plots of  $\log C_0/C$  against time are linear and are shown in Figure 2.

### Effect of Exciting Wavelength and Intensity

The absorption spectrum for a  $1.08 \mu$  film is shown in Figure 3. A double beam experiment was run with a film thickness of  $2\text{-}\mu$  in the sample beam and a  $1\text{-}\mu$  film in the reference compartment. From this measurement, Fresnel reflection was found to be approximately 1% of the total incident intensity.

From the rate of production of isobutene, the light source outputs, and the extinction coefficients, quantum yields were calculated. In the  $23\text{--}110^\circ\text{C}$ . temperature range studied, the quantum yield for initial formation of isobutene was found to vary from  $8.3 \times 10^{-2}$  to  $17 \times 10^{-2}$ , respectively. The results in Table IV indicate that the quantum yield for the initial formation of isobutene is independent of exciting wavelength.

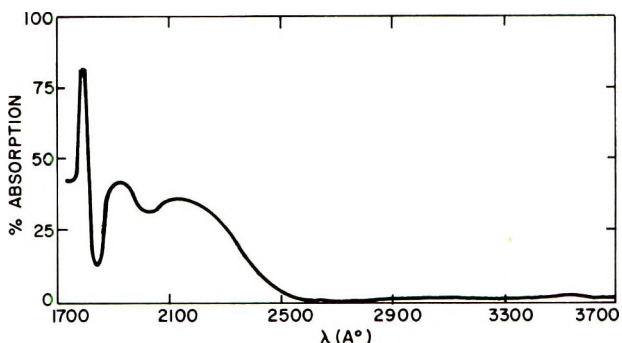


Fig. 3. Absorption spectrum of a  $1.08\text{-}\mu$  poly(*tert*-butyl acrylate) film.

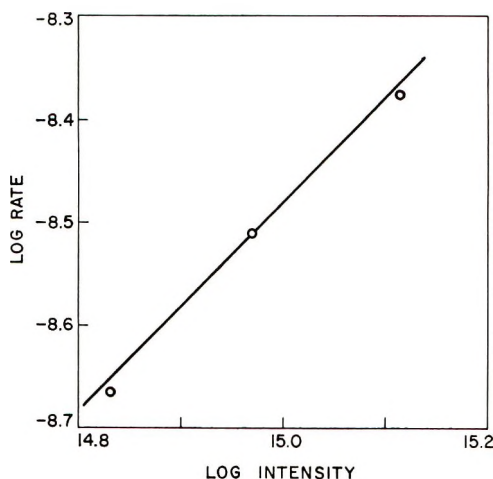


Fig. 4. Intensity exponent of photolysis of poly(*tert*-butyl acrylate) at  $53^\circ\text{C}$ .

TABLE IV  
Effect of Exciting Wavelength on Quantum Yield  
for Initial Formation of Isobutene

$\lambda$ , A.	$\epsilon$ , cm. <sup>-1</sup>	Film thickness, $\mu$	Temperature, °C.	Rate $\times 10^9$ , mole/min.	$\Phi$
1849	590	0.39	21.3	4.87	0.076
2537	73	0.40	24.5	2.86	0.083
3660	45	0.40	24.5	4.62	0.073

Blackened Lektromesh copper screens were used to vary the intensity of 2537-A. radiation. The intensity exponent of the reaction from Figure 4 was found to be unity at a film temperature of 53°C.

## DISCUSSION

### Kinetics in the $T_g$ Region

An Arrhenius plot of the rate data is shown in Figure 5. From the slope of the linear portion of the  $\log R$  versus  $1/T$  graph corresponding to the interval from 23 to 35°C., a value of 3.3 kcal./mole is obtained. The activation energy in the glassy region is to be regarded as a minimum value due to the increasing slope of this line toward lower temperatures. This is to be compared with 1.8 kcal./mole for the higher temperature region from 69°C. ( $T_g$ ) to 110°C. The continuous decrease in slope as the temperature increases in the direction of the  $T_g$  is interpreted as being caused by a gradual reduction in van der Waals bonding. The 1.5 kcal./mole change in overall activation energy is consistent with this analysis. In this same connection, consideration of the nature of molecular bonding in the polymer solid state presented by Andrews et al.<sup>5,6</sup> is helpful. Many polymers may be regarded as consisting of a doubly bonded single phase with the intermolecular bonding comprised of van der Waals matrix forces and dipole-dipole association forces. Birefringence measurements show

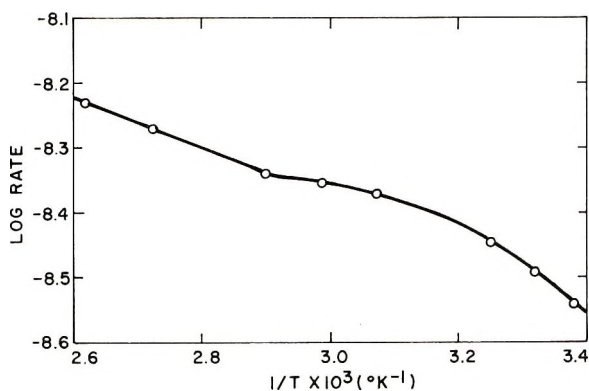
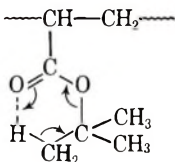


Fig. 5. Arrhenius plot for the formation isobutene from poly(*tert*-butyl acrylate).

that a polymer upon heating through the transition region varies continuously from a state of high disorder to one of higher order. This is supported in this work by the constant activation energy above the  $70^{\circ}\text{C}$ .  $T_g$ . In accordance with Andrews interpretation of the transition regions a second loss peak is observed in the DTA curve in the  $185\text{--}187^{\circ}\text{C}$ . region. The melting point of PTBA was found to be  $261\text{--}262^{\circ}\text{C}$ . Since x-ray diffraction measurements show no trace of polymer crystallinity within 1%, the second transition region ( $185\text{--}187^{\circ}\text{C}$ .) is attributed to the breakdown of dipole-dipole association forces. This region is presently under study.

### Mechanism

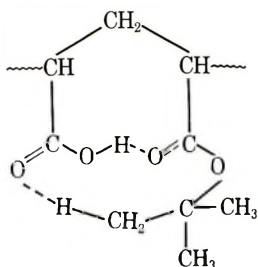
The first-order kinetics of the polymer photolysis, the unity intensity exponent, and product analyses confirm a unimolecular first-order decomposition. The transition state may be described as six-membered:



and is comparable to the general class of Chugaev type reactions.<sup>7</sup> This concerted movement of electrons has also been proposed by Grant and Grassie<sup>8</sup> in polymer systems, e.g., in the thermal decompositions of poly(vinyl acetate) and poly(*tert*-butyl methacrylate). Disproportionation of the *tert*-butyl radical to isobutene and isobutane was found to be negligible. This further supports a molecular, rather than a radical mechanism. Further evidence was gained from a study of the thermal decomposition of PTBA over the range  $90\text{--}170^{\circ}\text{C}$ . The details of this study will be reported in the near future. However, it should be noted here that bond energetics and the observed activation energy are in excellent agreement with the proposed intramolecular six-membered transition state.

This type of molecular decomposition may be general for acrylate ester polymers containing  $\beta$  hydrogens. A study of the effect of hydrogen acidity on olefin quantum yield would be helpful in confirming this viewpoint.

From Figure 1, it is seen that a slight acceleration in the rate of formation of isobutene occurs with time. For example, at  $23$  and  $28^{\circ}\text{C}$ . the plot deviates from initial linearity at rates corresponding to  $2\text{--}3 \times 10^{16}$  molecules/sec. of isobutene. It is calculated that  $2.7 \times 10^{16}$  PTBA chains are available on the average for the standard 2-mg. polymer sample. The nature of the acid-catalyzed mechanism is not yet clear. However, a cooperative mechanism between acid and ester,<sup>8</sup> i.e.,



is ruled out in the lower temperature range because of the fact that rotational sites of the polymer are not mutually accessible below the  $T_g$ . For example, in poly(methyl methacrylate) the methyl-ester group may be found either *cis* or *trans* to the carbonyl group. The ratio of the integrated intensities for the two skeletal vibrations has been found<sup>9</sup> to be independent of temperature below the  $T_g$ . Also, the intensity ratio below the  $T_g$  was dependent of the conditions of sample annealing.

Above the  $T_g$ , the population in the two isomeric states is controlled by Maxwell-Boltzmann statistics. Formation of a ten-membered transition state may be the rate-determining step in this region. This is in contrast to the glassy region. However, in the photolyses at 86 and 110°C., negative deviations from linearity are observed in the rate plots. This is consistent with a high-temperature destabilization of the transition state. In solution, intermolecular bonding is absent, and a temperature dependence of the population is observed below the  $T_g$ . It would be interesting to obtain a single activation energy for isobutene formation over the entire temperature range when poly(*tert*-butyl acrylate) is photolyzed in solution.

### Quantum Yield and Exciting Wavelength

The results from Table V show that exciting wavelength has no effect on the quantum yield for production of isobutene. The electronic absorption spectrum of the polymer (Fig. 3) indicates an  $n \rightarrow \pi^*$  transition at 2150 Å. and a  $\pi \rightarrow \pi^*$  at 1800 Å. The one at 1925 Å. is  $n \rightarrow \sigma^*$ . This assignment is consistent with work on other carbonyl polymers.<sup>10</sup> The broad 2900–3700 Å. absorption is probably due to an impurity. Products caused by the inhibitor and/or initiator with polymer are possible origins of this transition. The fact that the quantum yield for isobutene formation is the same at 1849, 2537, and 3660 Å. may indicate that energy transfer can occur between this impurity and the poly(*tert*-butyl acrylate) and that the product is formed via some low-lying triplet in the polymer. Experiments are now in progress with organics which produce a high triplet population in order to investigate the detailed energy transfer. Phosphorescence yields of the dopants, along with simultaneous isobutene rate measurements, are being used to determine whether the photolytic degradation of poly(*tert*-butyl acrylate) occurs via a singlet or triplet.

The author would like to sincerely thank the referee for numerous suggestions which led to an improvement in the manuscript.

This paper is dedicated to Catherine Block (deceased August 2, 1965) who made many contributions during its initial stages.

### References

1. S. Stokes and R. B. Fox, *J. Polymer Sci.*, **56**, 507 (1962).
2. M. L. Miller and C. E. Rauhut, *J. Polymer Sci.*, **38**, 63 (1959).
3. A. R. Monahan, *J. Polymer Sci. A-1*, **4**, 2381 (1966).
4. M. M. Shahin, *J. Chem. Phys.*, **43**, 1798 (1965).
5. R. D. Andrews and R. M. Kimmel, *J. Polymer Sci.*, **3**, 167 (1965).
6. T. J. Hammack and R. D. Andrews, *J. Appl. Phys.*, **36**, 3574 (1965).
7. W. J. Bailey and J. J. Hewitt, *J. Org. Chem.*, **21**, 543 (1956).
8. D. H. Grant and N. Grassie, *Polymer*, **1**, 445 (1960).
9. S. Havriliak paper presented at American Chemical Society Winter Meeting, January 1966.
10. W. M. Pasika and R. Brandon, *Polymer*, **6**, 503 (1965).

### Résumé

On a étudié en détail la photolyse (2537 Å) d'un film fin ( $1 \times 10^{-5}$  cm) de polyacrylate de *t*-butyle sous une atmosphère d'hélium. Le seul produit volatil significatif formé entre 20 et 110°C, était l'isobutène. La réaction était initialement une décomposition de premier ordre avec une énergie d'activation de 3.3 Kcal/mole à l'état vitreux. Au-dessus de la température de transition vitreuse, une valeur de 1.8 Kcal/mole a été trouvée. La vitesse de formation de l'isobutène est auto-accelérée lorsqu'un minimum d'unités d'acide acrylique est engendré par chaîne. Le rendement quantique initial pour la formation d'isobutène varie de 0.083 à 0.17 dans la gamme de température étudiée. Il n'y avait pas de dépendance du rendement quantique en fonction de la longueur d'ondes excitatrice utilisant des sources de 1849, 2537 et 3660 Å. L'exposant affectant l'intensité lumineuse est égale à unité ce qui est en accord avec un cinétique de décomposition de premier ordre.

### Zusammenfassung

Die Photolyse (2537 Å) von dünnen ( $1 \cdot 10^{-5}$  cm) Poly-*t*-butylacrylatfilmen unter dem Heliumdruck von 1 Atmosphäre wurde im Detail untersucht. Im Temperaturbereich von 20–110°C war Isobuten das einzige signifikante flüchtige Produkt. Im Anfangsteil ist die Reaktion eine Zersetzung erster Ordnung mit einer Aktivierungsenergie von 3,3 kcal/Mol im Glaszustand. Oberhalb der Glasumwandlungstemperatur wurde ein Wert von 1,8 kcal/Mol gefunden. Die Geschwindigkeit der Isobutenbildung beschleunigt sich bei einem Minimum der Entstehung von einer Acrylsäureeinheit pro Kette selbst. Die Anfangsquantenausbeute für die Bildung von Isobuten liegt im untersuchten Temperaturbereich zwischen 0,083 und 0,17. Bei Lichtquellen mit 1849, 2537 und 3660 Å trat keine Abhängigkeit der Quantenausbeute von der Wellenlänge auf. Der Intensitätsexponent betrug in Übereinstimmung mit der Zersetzungs kinetik erster Ordnung 1.

Received March 1, 1966

Revised March 28, 1966

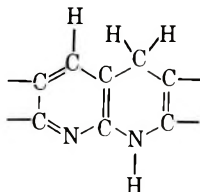
Prod. No. 5135A

## Thermal Degradation of Polyacrylonitrile in the Temperature Range 280–450°C.

ALAN R. MONAHAN, *Xerox Corporation, Rochester, New York 14603*

### Synopsis

This paper presents a study of the thermal degradation of polyacrylonitrile of 13,000 to 43,000 number-average molecular weight in vacuum over the temperature range 280–450°C. Sixteen products of the decomposition were identified by chromatographic and infrared analytical techniques. The five major products, i.e., cyanogen, hydrogen cyanide, acrylonitrile, acetonitrile, and vinylacetonitrile, were monitored at intervals during the decomposition using gas chromatography. Activation energies of 15 and 23 kcal./mole were calculated from initial rates of formation of HCN and cyanogen, respectively. The overall activation energy of the polymer degradation was found to be 3.6 kcal./mole. The residue of the decomposition in the temperature region 280–450°C. was suggested by infrared absorption measurements and elemental analysis to be a polymer of the structure



The rate of production of vinylacetonitrile was found to be proportional to the production of the residual black poly-1,4,4-trihydronaphthyridine. A new photothermal degradation cell is also presented.

### INTRODUCTION

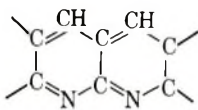
The thermal degradation of polyacrylonitrile (PAN) has been studied extensively. However, there still remains uncertainty about the analysis of reaction products, a detailed pyrolytic mechanism, and the structure of the residual black polymer.

Kern and Fernow<sup>1</sup> first found that HCN was formed when PAN was heated at 400°C. Burlant and Parsons<sup>2</sup> degraded the polymer in the temperature range 200–320°C. and found H<sub>2</sub>, NH<sub>3</sub>, and a trace of HCN. In contrast to this work, Nagao<sup>3</sup> and co-workers found HCN evolution high in the 200–350°C. range. Takayama,<sup>4</sup> by mass spectrometry, has shown the decomposition products after heating in the region 250–300°C. to be methacrylonitrile, HCN, and N<sub>2</sub>.

The most extensive study has been carried out at the National Bureau of Standards by Straus and Madorsky.<sup>5,6</sup> Pyrolyses were made by using

a tungsten spring balance under high vacuum in the temperature range 250–800°C. An overall activation energy of 31 kcal./mole was reported for the temperature range 240–260°C. High purity PAN of number-average molecular weight  $4 \times 10^4$  was used, giving the products hydrogen, hydrogen cyanide, acrylonitrile, vinylacetonitrile, pyrrole, acetonitrile, butyronitrile, and propionitrile. No ammonia was observed. The black powder residue was analyzed as a C,H,N polymer of lower H and N content than the original PAN.

The structure of the black polymer has been assumed<sup>7</sup> to be that shown as I.



I

In the present paper the 280–450°C. high vacuum pyrolytic degradation of polyacrylonitrile having a number-average molecular weight of 13,000 to 43,000 is described. The volatile products were fed directly into a vapor-phase chromatograph and monitored continuously. The kinetics were complex, owing to the large number of products. However, activation energies corresponding to initial stages of the reaction were obtained from the rates of formation of hydrogen cyanide and cyanogen. An overall activation energy was also measured.

An effort was also made to identify the black polymeric residue. The probable structure of this compound and the mechanism of its formation are inferred from the evidence obtained.

## EXPERIMENTAL

### Monomer and Initiators

Acrylonitrile obtained from American Cyanamid and Borden Chemical Co. was washed with concentrated NaOH and then five times with distilled water. It was subsequently distilled and dried over anhydrous sodium sulfate and stored at  $-10^{\circ}\text{C}$ . Vapor-phase chromatography showed the monomer to be free from water.

Benzoyl peroxide from Eastman Organic Chemicals and 15.2% *n*-butyllithium in hexane obtained from Foote Mineral Company were used as polymerization catalysts without further purification.

### Preparation of Polymers

Monomer was degassed three times to a vacuum of  $2 \times 10^{-6}$  mm. and distilled into 50-cm.<sup>3</sup> Pyrex reactors fitted with West-Glass Teflon stopcocks, silicon septa, and glass-encased stirring rods. Conditions of the polymerization reactions are presented in Table I. Polymers were purified by reprecipitation from *N,N'*-dimethylformamide and dried under vacuum at 50°C.

TABLE I  
Polymerization of Acrylonitrile and PAN Properties

Initiator	[Initiator], mole-%	Reaction temperature, °C.	Reaction time, min.	$T_g$ , °C.	$\bar{M}_n \times 10^{-3}$
BuLi	2.0	-50	70	79	16
BuLi	1.1	-50	30	75	13
BuLi	0.35	-50	30	90	43
Bz <sub>2</sub> O	1.0	90	28	84	22

Reproducible glass transition temperatures were obtained on a Dupont differential thermal analyzer, and molecular weights were calculated from the relation:<sup>8</sup>

$$\bar{M}_n = 2.8 \times 10^5 / (96.5 - T_g)$$

No evidence was found for polymer crystallinity by using x-ray powder diffraction. Also, spectrophotometric techniques proved the absence of crosslinking and conjugated C=N sequences. Thus, it is assumed that reasonable approximations of molecular weights were obtained from glass transition temperatures. Tacticity of the polymer samples were not determined.

### Degradation Experiments

Degradation of polyacrylonitrile was carried out in an all-quartz vacuum cell. Polymer film temperature was controlled to  $\pm 1^\circ\text{C}$ . by utilizing infrared heating of a quartz-encased graphite block. The cell is presented in Figure 1.

Polymer films, 0.5-7  $\mu$ , were dip-coated on a reaction boat which had quartz-encased iron rods. Using a magnet, the film was transferred to the

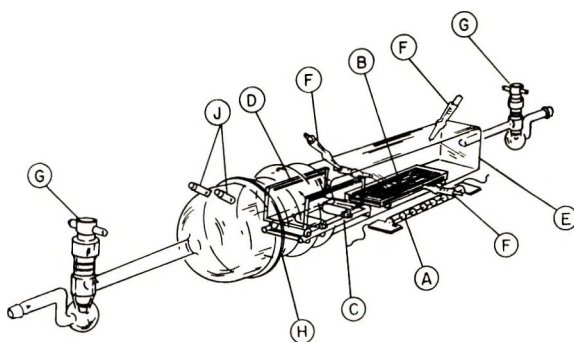


Fig. 1. All-quartz photothermal degradation cell: (A) lamps (500-w. G.E. infrared lamps, 2 req.); (B) 10.5-in.<sup>2</sup> quartz-encased UT-31 graphite block (Ultra Carbon Corp.); (C) quartz conveyor; (D) quartz reaction boat; (E) 2-in.<sup>2</sup> quartz cell, 15 in. long; (F) 10/30 quartz thermocouple wells; Teflon stopcocks (West Glass); (H) 60/50 quartz joint; (J) thermocouple wells.



graphite heater. Film thicknesses were measured by means of a Reichert microscope fitted with a Watson 16-mm. interference objective.

The volatile products resulting from the experiments were frozen into sampling valves and fed at 5-min. intervals into a Barber-Colman Series 5000 vapor-phase chromatograph. For the separations, 6-ft., 3-mm. glass columns of 15% ethylene glycol succinate on 80/100 mesh Johns-Manville Gas-Chrom P and 15% Apiezon L on 80/100 mesh Chromosorb W were used. Temperature programming of the columns allowed a total analysis of the products in 5 min. Detection was achieved by using a Lovelock<sup>9</sup> micro cross-section detector made of Teflon and brass. A linear calibration of products was obtained down to  $1 \times 10^{-12}$  mole/sec. by use of a 1%  $\text{CH}_4$ -helium carrier mixture.

Degradation products were also trapped in  $1/16$ -in. o.d. stainless steel traps and transferred to a micro gas infrared cell. Infrared and ultraviolet absorption spectra were measured with a Perkin-Elmer 337 grating Infra-ord and Cary 14 spectrophotometers, respectively. Trace amounts of relatively nonvolatile liquids were condensed on Millipore matched thickness filters ( $25 \mu$ ) for infrared spectral measurements.<sup>10</sup>

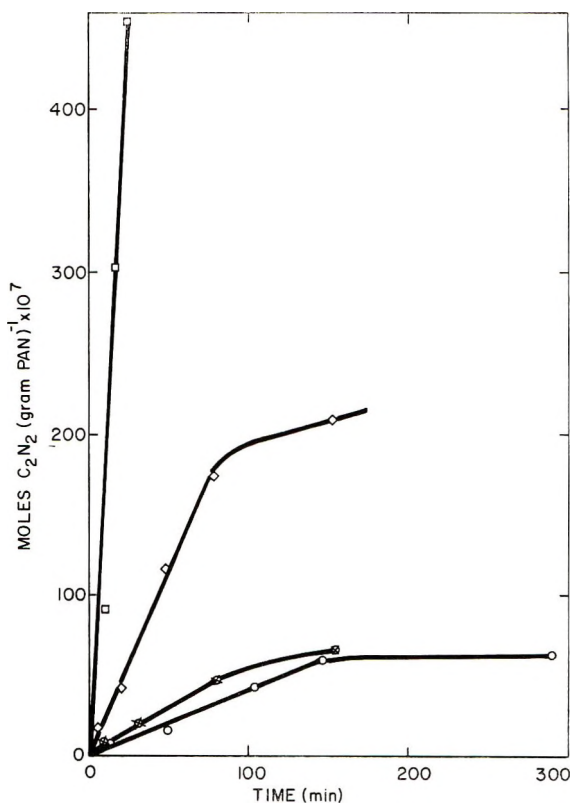
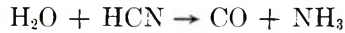


Fig. 2. Rate of formation of  $\text{C}_2\text{N}_2$  at various temperatures: (○) 286°C.; (⊗) 327°C.; (◇) 379°C.; (□) 456°C.

## RESULTS

The major volatile products of the degradation were found to be cyanogen, hydrogen cyanide, acrylonitrile, acetonitrile, and vinylacetonitrile. Eleven other minor products were identified and agree with the work of Straus and Madorsky.<sup>6</sup> Cyanogen, benzene, toluene, pyridine, 3- and 4-methylpyridines, and 1,3,5-triazine were previously unreported. 3,6-Dimethyl-1,8-naphthyridine was also isolated and identified by its infrared and ultraviolet spectra.

Ammonia was found only when trace amounts of water were present in the film. The concentration of ammonia was found to be directly proportional to the amount of water present, and inversely proportional to the HCN formed during the decomposition. The following room temperature, gas-phase reaction has been demonstrated in our laboratory:<sup>11</sup>



This is probably responsible for the production of ammonia at the expense of the product hydrogen cyanide.

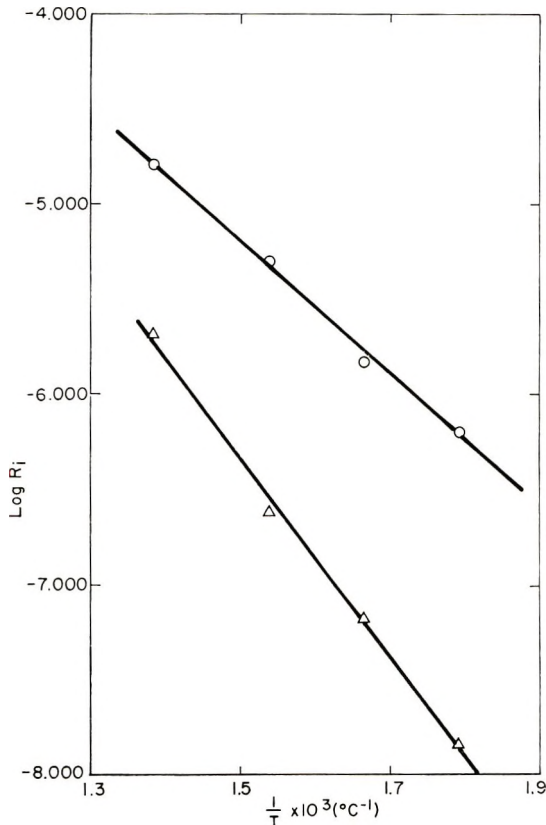


Fig. 3. Arrhenius plots for initial rates of formation of HCN and  $\text{C}_2\text{N}_2$ : ( $\odot$ ) HCN; ( $\triangle$ )  $\text{C}_2\text{N}_2$ .

TABLE II  
Product Distribution from Pyrolysis of PAN

	Product, mole-% after 30 min. pyrolysis at various temperatures			
	286°C.	327°C.	379°C.	456°C.
Cyanogen	0.01	0.02	0.01	0.46
Hydrogen cyanide	0.03	1.54	0.49	20.97
Acetonitrile	5.23	5.86	1.02	2.42
Acrylonitrile	94.73	90.90	59.28	3.85
Vinylacetonitrile	0.01	1.68	39.20	72.30

TABLE III  
Rates of PAN Degradation

Temperature, °C.	Duration of pyrolysis, min.	Initial overall rate, mole/min./g. PAN $\times 10^4$
286	290	2.12
327	152	3.46
379	95	3.63
456	102	4.47

The distribution of major products as a function of temperature is shown in Table II.

The overall rate of degradation, as measured by total moles of volatiles formed, was found to be independent of the molecular weight range studied, i.e., 13,000–43,000. It was also independent of the polymerization initiator used.

The initial overall rates of degradation are presented in Table III.

Figure 2 shows the rate plots for cyanogen. In the early stages of the degradation, hydrogen cyanide and cyanogen were the only products formed. Therefore, from the initial rates of formation of these products, activation energies were determined.

The pyrolysis residue was a brownish-black powder. Microelemental analysis of the product gave the following result: C, 75.4%; N, 21.4%; H, 3.2%. Infrared spectral analyses of the powder residue revealed a strong absorption at 1560–1600  $\text{cm}^{-1}$  which is attributed to a conjugated  $-(\text{C}=\text{N})_x-$  group.<sup>12</sup> Weak amine absorptions at 3400, 3230, and 1620  $\text{cm}^{-1}$  along with aromatic C=C vibrations at 1150, 965, and 810  $\text{cm}^{-1}$  were also found. The ultraviolet spectrum of the residue showed broad absorption maxima at 205, 268, and 315  $\text{m}\mu$ .

## DISCUSSION

An activation energy of 3.6 kcal./mole was obtained from the overall rate data in Table III. No significance is placed on this value due to the large number of products present in the degradation. However, activation

energies based on the initial rates of formation of cyanogen and hydrogen cyanide were found to be 23 and 15 kcal./mole, respectively. The Arrhenius plots are shown in Figure 3. The 8 kcal./mole difference in the activation energies is virtually identical to the difference between the C—H and C—CN bond energies<sup>13,14</sup> in the polyacrylonitrile. This is based on the assumption that the endothermicity associated with each bond rupture is the same.

Determination of the overall reaction order was not possible because of the large number of products formed in this decomposition. However, during the initial stages of reaction, when hydrogen cyanide and cyanogen

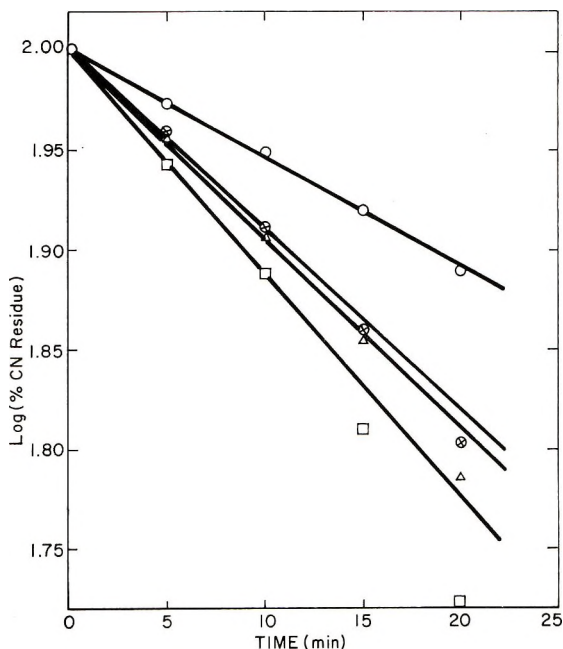
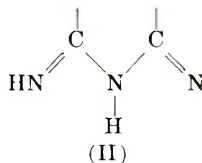


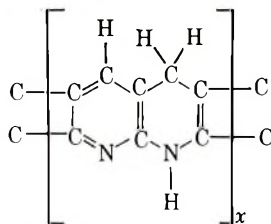
Fig. 4. Dependence of the molar concentration of undegraded nitrile units upon time at various temperatures: (○) 286°C.; (⊗) 327°C.; (△) 379°C.; (□) 456°C.

are the only products, the logarithm of percentage residue of CN versus time yields a straight line, indicating that the initiation approaches first order in CN concentration. This is shown in Figure 4 for a series of temperatures.

The elemental microanalysis supports a residue with a C:H:N atom ratio of 4:2:1. In addition, the infrared spectrum of this material contains bonds corresponding to conjugated C=N and C=C vibrations.<sup>15</sup> The 1620-cm.<sup>-1</sup> absorption has been assigned by others<sup>2</sup> to C=N conjugated with an amine. The 1540–1570 cm.<sup>-1</sup> band is associated with the glutarimidine structure<sup>15</sup> (II).

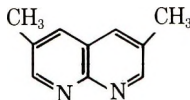


as is a 208-210  $m\mu$  electronic absorption. Also, substituted naphthyridines have absorption maxima in the 300-330  $m\mu$  region. The residue absorbs at 315  $m\mu$ . A poly-1,4,4-trihydronaphthyridine III



III

is the only structure that supports all the microelemental and spectrophotometric data. 3,6-Dimethyl-1,8-naphthyridine (IV)



IV

isolated in the reaction crude is further support for naphthyridine formation in this degradation.

An interesting result is shown in Table IV. That is, the weight per cent of black polymer in the total residue increased in proportion to the rate of

TABLE IV  
Rates of Formation of Vinylacetonitrile (VAN)

Temperature, °C.	Rate of VAN, mole/min./g. PAN	Black polymer in residue, wt.-%
286	$1.10 \times 10^{-8}$	0
327	$5.83 \times 10^{-6}$	20
379	$1.25 \times 10^{-4}$	87
456	$3.23 \times 10^{-4}$	100

formation of vinylacetonitrile (VAN). This apparent correlation suggests that the VAN could be mechanistically involved in the formation of the polynaphthyridine.

The author would like to express his thanks to Drs. J. V. Martinez, W. Roth, and M. M. Shahin for numerous helpful discussions. The help of Dr. E. L. Lind in the design of the degradation cell is acknowledged.

### References

1. L. W. Kern and H. Fernow, *Rubber Chem. Technol.*, **17**, 356 (1944).
2. W. J. Burlant and J. L. Parsons, *J. Polymer Sci.*, **22**, 249 (1956).
3. H. Nagao, M. Uchida, and T. Yamaguchi, *Kogyo Kagaku Zasshi*, **59**, 698 (1958).
4. Y. Takayama, *Kogyo Kagaku Zasshi*, **61**, 1021 (1958).
5. S. Straus and S. L. Madorsky, *J. Res. Natl. Bur. Std.*, **61**, 77 (1958).
6. S. L. Madorsky and S. Straus, *J. Res. Natl. Bur. Std.*, **63A**, 261 (1959).
7. M. Becher and H. F. Mark, *Angew. Chem.*, **73**, 641 (1961).
8. R. B. Beevers, *J. Polymer Sci. A*, **2**, 5257 (1964).
9. J. E. Lovelock, G. R. Shoemake, and A. Zlatkis, *Anal. Chem.*, **35**, 461 (1963).
10. P. J. Thomas and J. L. Dwyer, *J. Chromatog.*, **13**, 366 (1964).
11. J. V. Martinez, private communication, June 1965.
12. N. Grassie and J. N. Hay, *J. Polymer Sci.*, **56**, 189 (1962).
13. N. Grassie and N. A. Weir, *J. Appl. Polymer Sci.*, **9**, 975 (1965).
14. N. Grassie and J. R. MacCallum, *J. Polymer Sci. B*, **1**, 551 (1963).
15. T. Takata, I. Hiroi, and M. Taniyana, *J. Polymer Sci. A*, **2**, 1567 (1964).

### Résumé

Ce manuscrit présente une étude de la dégradation thermique du polyacrylonitrile sous vide sur une gamme de température de 280 à 450°C; leur poids moléculaire variait de 13.000 à 43.000 comme poids moléculaire moyen en nombre. 16 produits de décomposition ont été identifiés par chromatographie et par analyse infra-rouge. Les cinq produits principaux, à savoir, le cyanogène, l'acide cyanhydrique, l'acrylonitrile, l'acétonitrile et le vinylacétonitrile ont été trouvés à des intervalles courts de décomposition par chromatographie gazeuse. Les énergies d'activation de 15 Kcal/mole et de 23 Kcal/mole ont été calculées au départ des vitesses initiales de formation de l'acide cyanhydrique et du cyanogène respectivement. L'énergie d'activation globale de la dégradation polymérique était de 3,6 Kcal/mole. Le résultat des décompositions dans la région de température de 280 à 450°C a été suggéré par les mesures d'absorption infra-rouge et l'analyse élémentaire suggère un polymère de structure indiquée dans le résumé anglais. La vitesse de production du vinylacétonitrile était proportionnelle à la production du poly-1,4,4-trihydronaphthridine noir résiduel. Une nouvelle cellule de dégradation photo-thermique est également présentée.

### Zusammenfassung

In der vorliegenden Mitteilung wird eine Untersuchung des thermischen Abbaues von Polyacrylnitril mit einem Zahlenmittelmolekulargewicht von 13.000 bis 43.000 im Vakuum im Temperaturbereich von 280–450°C beschrieben. 16 Zersetzungsprodukte wurden chromatographisch und infrarotspektroskopisch identifiziert. Die fünf Hauptprodukte, nämlich Cyanogen, Cyanwasserstoff, Acrylnitril, Acetonitril und Vinylacetonitril wurden in gewissen Intervallen während der Zersetzung gaschromatographisch aufgezeichnet. Für die Anfangsbildungsgeschwindigkeit von HCN und Cyanogen wurden Aktivierungsenergien von 15 kcal/Mol bzw. 23 kcal/Mol berechnet. Die Bruttoaktivierungsenergie des Polymerabbaues betrug 3,6 kcal/Mol. Der Zersetzungszustand scheint im Temperaturbereich von 280–450°C nach IR-Absorptionsmessungen und Elementaranalyse ein Polymeres mit der in der englischen Zusammenfassung angegebenen Struktur zu sein. Die Bildungsgeschwindigkeit von Vinylacetonitril war der Bildung des schwarzen Rückstands von Poly-1,4,4-trihydronaphthridin proportional. Schliesslich wird eine neuartige Zelle für den photothermischen Abbau angegeben.

Received November 3, 1965

Revised April 20, 1966

Prod. No. 5152A

## Flow Rates of Polymer Solutions through Porous Disks as a Function of Solute. II. Thickness and Structure of Adsorbed Polymer Films

FRED W. ROWLAND\* and FREDERICK R. EIRICH, *Polytechnic Institute of Brooklyn, Brooklyn, New York 11201*

### Synopsis

The thickness of films of poly(methyl methacrylate) (PMMA), poly(vinyl acetate) (PVAc), and polystyrene (PS) adsorbed on Pyrex glass was studied by measuring the flow rates of polymer solutions and the corresponding pure solvents through sintered filter disks. Adsorption isotherms were in agreement with those reported by other workers and showed saturation adsorption equivalent to 2-8 condensed monolayers of monomer units. Film thicknesses were of the order of magnitude of the free coil diameters in solution and were directly proportional to the intrinsic viscosity of the polymer, except for PS in benzene where the thicknesses leveled off as molecular weight increased. It was concluded that polymers adsorb from solution in monolayers of compressed or interpenetrating coils; that below some critical molecular weight which varies with polymer and solvent, a much larger fraction of the segments lies directly in the interface; that adsorbed films may consist of a dense layer immediately adjacent to the surface and a deep layer of loops extending into the solvent; and that it is the segment-solvent interaction rather than the segment-surface interaction which dominates the conformation of the adsorbed chain.

A number of theoretical treatments of the physical state of macromolecules adsorbed from solution have appeared in the literature.<sup>1-7</sup> Structures are predicted ranging from highly swollen coils which contact the surface at only a few points to chains which lie almost entirely in the interface, with only a few short bridges extending into the solution. Experimental data are available which are compatible with thin<sup>8-10</sup> and with thick films<sup>11-15</sup> of adsorbed polymers, but most of these studies have either been very limited in scope or are subject to the objection that the method of measurement of the film thickness probably produced gross distortions of the polymer films. This paper presents the results of a study of film thicknesses in which the adsorbent surface was at all times in contact with the equilibrium solution of the adsorbate, and in which this equilibrium solution acted as the examining probe.

Although starting originally from a different experimental arrangement, i.e., the settling of beads in adsorption equilibrium through the solution,

\* Present address: Carothers Research Laboratory, E. I. du Pont de Nemours and Company, Inc., Wilmington, Delaware.

this arrangement was abandoned because of difficulties presented by hydrodynamic instabilities due to density differences. Flow of the solution through a disk of sintered beads was used instead. Thus our technique became basically the same as that explored by Öhrn<sup>11</sup> and by Hermans and Tuijnman.<sup>12</sup> The adsorption of polymer on the interior of a capillary reduces its effective diameter, and this causes a reduction in the rate of flow of a polymer solution relative to that of pure solvent through the sintered glass disk in excess of that due to viscosity differences between solvent and solution alone (see Figure 1, Part I<sup>16</sup>). From the size of this difference and a knowledge of the average capillary radius in the disk, an average hydrodynamic film thickness can be calculated. Full details of the experimental technique, calibration methods, and calculations have been given in Part I.<sup>16</sup> A single adsorbent, Pyrex glass No. 7740, was chosen for reproducibility and ease of cleaning. The variables studied include the chemical nature and molecular weight of the polymer, the solvent, the temperature, and the concentration of the solutions.

## EXPERIMENTAL

### Materials

Six fractions of a bulk-polymerized poly(vinyl acetate) (PVAc) and six fractions of a commercial polystyrene (PS) were used. Properties are given in Table I, where numbers designate primary fractions and letters subfractions, obtained by refractionating the primary fractions. Poly(methyl methacrylate) (PMMA) samples were found to contain small amounts of insoluble gel. This was removed by precipitation fractionation, where the first two high molecular weight fractions were discarded and a large third fraction was retained after filtering through an ultrafine sintered glass filter. These are also included in Table I. All solvents were of reagent or spectro grade and were stored over molecular sieves, except for cyclohexane, which was percolated through silica gel immediately before use, and 2-butanone, which was distilled from calcium chloride and stored over sodium chloride. The Pyrex No. 7740 glass used as an adsorbent was in the form of either a 325 mesh powder or an ultrafine sintered disk. Both were cleaned with a mixture of hot nitric acid-sulfuric acid, rinsed thoroughly with distilled water, and stored over molecular sieves.

### Adsorption and Desorption Isotherms

The isotherms were determined by using the method of Koral et al.<sup>17</sup> and of Ellerstein and Ullman,<sup>9</sup> which consists of shaking the adsorbent overnight with the polymer solution and measuring the change in concentration of the supernatant. For the desorption curves, one-half of the supernatant was removed and replaced with fresh solvent. The container was then returned to the shaker for reequilibration.

Infrared absorption at  $7.5 \mu$  was used to analyze the benzene solutions of PVAc and PMMA. PS in cyclohexane was determined by ultraviolet



TABLE I  
Characterization of Polymer Fractions

Polymer	Fraction	$M \times 10^{-3}$	Radius of gyration at 30°C., A.
Poly(vinyl acetate)	PVAc 2	1190 <sup>a</sup>	443 <sup>a</sup>
	" 3B	958	396
	" 4B	838	359
	" 5A	619	305
	" 5B	382	236
	" 6	76.5	92.8
Polystyrene	PS 1	1400, <sup>b</sup> 1820 <sup>c</sup>	462 <sup>c</sup>
	" 2	950, 1200	379
	" 3B	500	
	" 4	260, 280	190
	" 7	110, 120	122
	" 9	60	
Poly(methyl methacrylate)	PMMA 897	1430 <sup>a</sup>	
	" 739	830	
	" 871	710	
	" 259	230	

<sup>a</sup> By light scattering in 2-butanone.

<sup>b</sup> Viscosity-average in toluene.

<sup>c</sup> By light scattering in benzene.

absorption at 260.5  $\mu$ . PS in benzene was measured by two methods, turbidimetric titration and interferometry. The latter was used only for relatively high concentrations (>0.1 g./100 ml.) and was always checked by titration of at least one sample. Solutions of PVAc in 2-butanone and PS in benzene-cyclohexane mixtures were analyzed by removing the solvent under vacuum and taking up the dried polymer in a known amount of benzene. Great care was required in this process, and blanks and standards were always run concurrently to ensure complete removal of the original solvent.

### Characterization of Disks

The sintered disks used to measure adsorbed film thicknesses were characterized by the methods described in Part I.<sup>16</sup> Nine disks were selected from an original group of twenty on the basis of uniform thickness, absence of oversized "pin holes" as revealed by injection of dye at the upstream face of the disk under steady-flow conditions, and a convenient range of solvent permeability values. The properties of the selected disks are summarized in Table II.

The agreement between the last two columns, in which the internal surface of the disks was calculated by two independent methods, demonstrates the consistency of the entire technique and justifies the use of the compromise value, 1 m.<sup>2</sup>/g. for the specific surface of the powdered Pyrex

TABLE II  
Properties of Sintered Pyrex Disks

Disk	Porosity <sup>a</sup>	Area, cm. <sup>2</sup>	Thickness, cm.	$\ r\ , \mu^b$	$r_{\max}, \mu^c$	$a, \mu^{-1d}$	Tortuosity <sup>e</sup>	Internal surface, cm. <sup>2</sup> $\times 10^{-4}$	
								Method A <sup>f</sup>	Method B <sup>g</sup>
1	0.204	4.00	0.186	0.31				0.98	1.32
2	0.206	4.55	0.150	0.37	0.450	14.05	1.61	0.76	1.21
4	0.205	5.40	0.165	0.31	0.416	15.82	1.58	1.18	1.58
9	0.207	5.24	0.183	0.33	0.408	16.70	1.56	1.20	1.69
10	0.237	5.45	0.151	0.39				1.00	1.40
12	0.206	4.20	0.194	0.32				1.05	1.44
13	0.203	4.37	0.192	0.315				1.08	1.49
15	0.235	5.03	0.191	0.355	0.421	15.73	1.64	1.27	1.64
B.D	0.238	5.09	0.182	0.385	0.462	13.59	1.64	1.14	1.57

<sup>a</sup> Void volume/disk volume.

<sup>b</sup> Root-mean-fourth average pore radius;  $\|r\| = [(1/N) \sum_1^N r_i^4]^{1/4}$ .

<sup>c</sup> By extrapolation of cumulative pore size distribution to 100% (see Fig. 1).

<sup>d</sup> From cumulative pore size distribution,  $F(r) = C \exp \{ar\}$ , where  $C = N/[\exp \{ar_{\max}\} - 1]$  and  $N$  is the total number of pores (see Fig. 1).

<sup>e</sup> Fluid path length/disk thickness.

<sup>f</sup> Internal surface =  $2 \times \text{area} \times \text{thickness} \times \text{porosity} / \|r\|$ .

<sup>g</sup> Internal surface =  $\text{area} \times \text{thickness} \times (1 - \text{porosity}) \times \text{density of Pyrex} \times \text{specific area } S \text{ of Pyrex powder}$ . The "compromise" value of  $S = 1 \text{ m.}^2/\text{g.}$  was used.

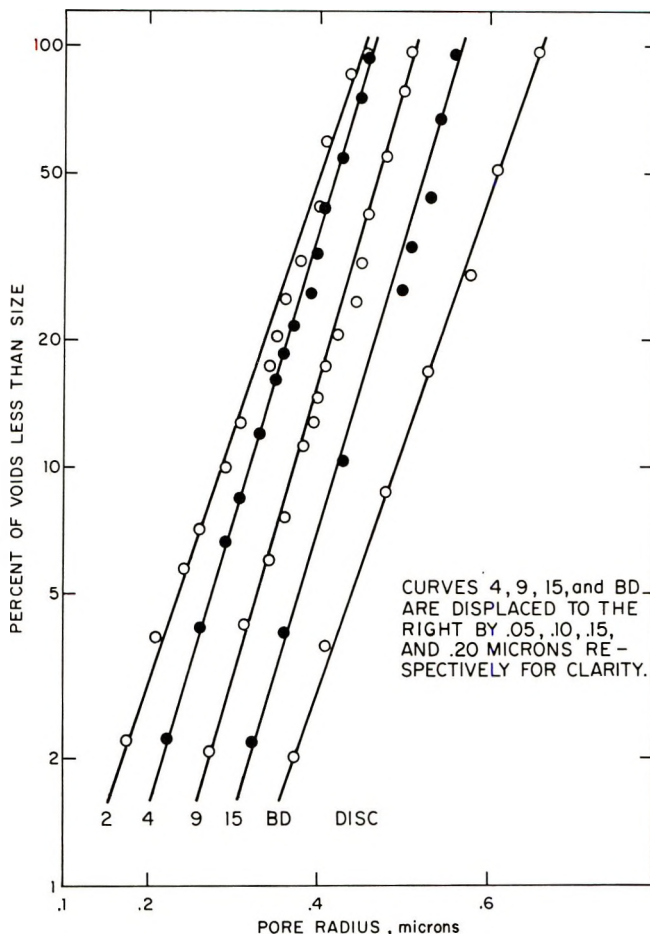


Fig. 1. Distribution of pore sizes in ultrafine Pyrex filters.

adsorbent. This value was originally selected independent of the comparison in Table II, as a reasonable choice between the nitrogen adsorption value of  $2 \text{ m.}^2/\text{g.}$  and the stearic acid figure of  $0.24 \text{ m.}^2/\text{g.}$

## RESULTS AND DISCUSSION

The adsorption isotherms of PMMA and PVAc, shown in Figures 2-6, are quite similar to and agree with those reported by Ellerstein<sup>9</sup> and Koral,<sup>17</sup> respectively. They are characterized by a rapid initial rise to a plateau, an inverse relationship between solvent power and amount adsorbed, and the absence of detectable desorption upon dilution of the supernatant solution. Temperature effects are negligible in good solvents but appreciable in poor ones, e.g., there is about a 20% increase in the amount of PVAc adsorbed from 2-butanone upon raising the temperature from 30 to 50°C. The reason for this behavior will be discussed later.

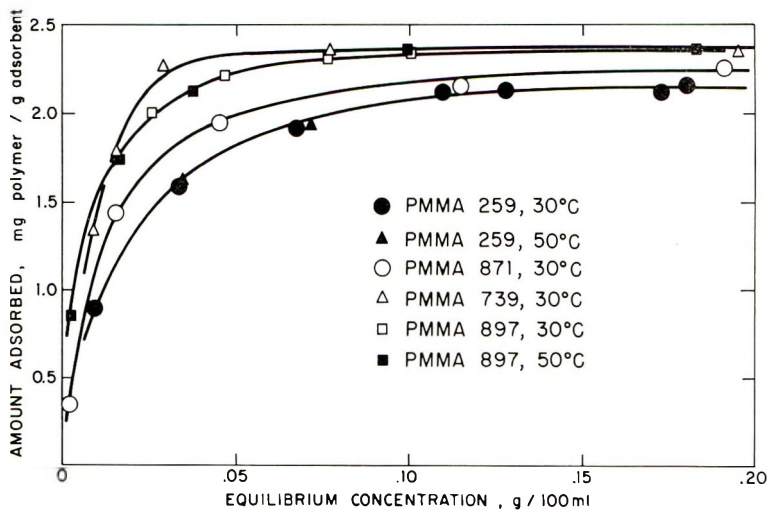


Fig. 2. Adsorption of poly(methyl methacrylate) from benzene onto Pyrex.

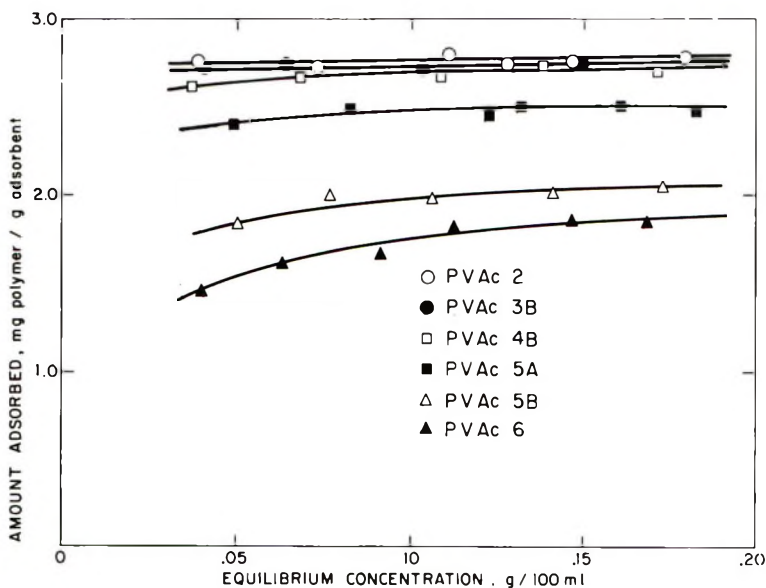


Fig. 3. Adsorption of poly(vinyl acetate) from 2-butanone onto Pyrex at 30°C.

The PS isotherms (Figs. 7-9) are quite different, showing a slow rise toward saturation with the high molecular weight fractions rising most rapidly, and an appreciable degree of reversibility. This is not surprising, since bonding with the surface can involve only van der Waal's forces ( $\pi$ -electron polarization), instead of the stronger polar or hydrogen bonding which can be expected between the glass and the other two polymers. Plots of  $\log$  (solution concentration) of PS in benzene against  $1/T$  at con-

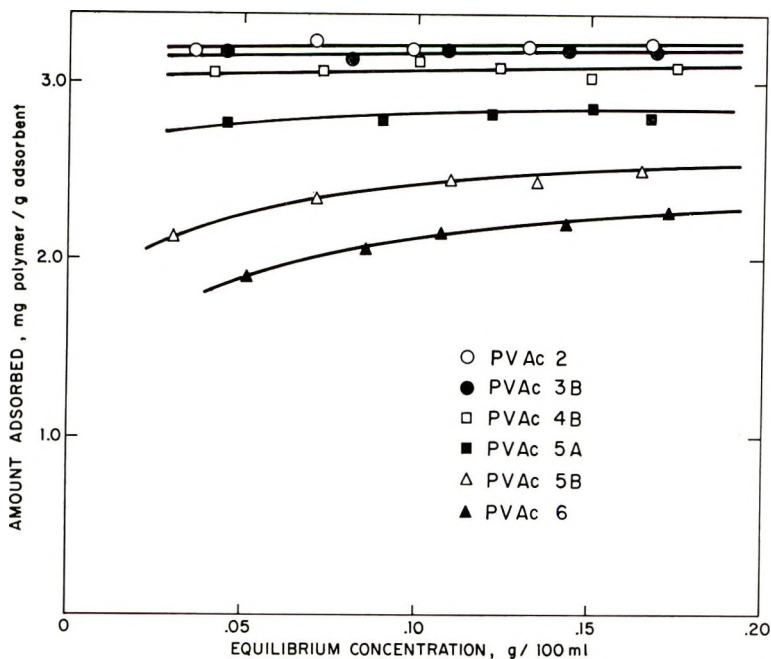


Fig. 4. Adsorption of poly(vinyl acetate) from 2-butanone onto Pyrex at 50°C.

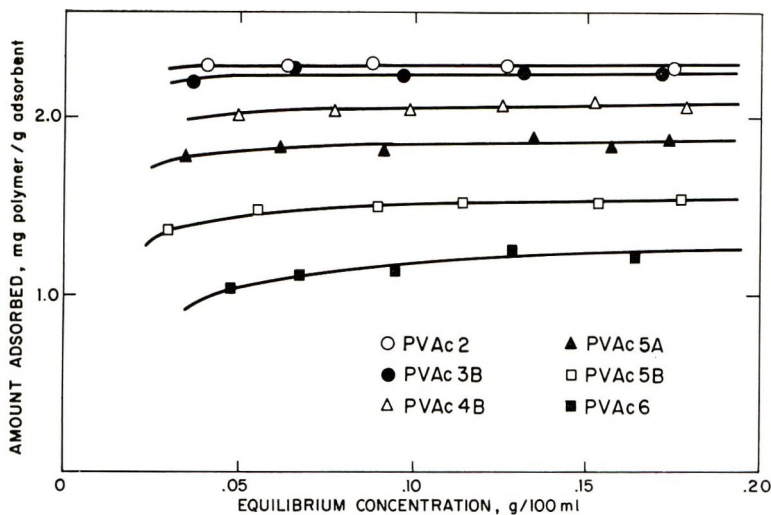


Fig. 5. Adsorption of poly(vinyl acetate) from benzene onto Pyrex at 30°C.

stant (high) surface coverage yield heats of adsorption ranging from +2.2 kcal./mole for the highest molecular weight to +1.8 kcal./mole for the lowest. This implies a positive entropy of adsorption, presumably due to the release of solvent molecules from the adsorbent and/or the adsorbate. In the  $\theta$  solvent, cyclohexane at 34.2°C., the isotherm (Fig. 9) resembles

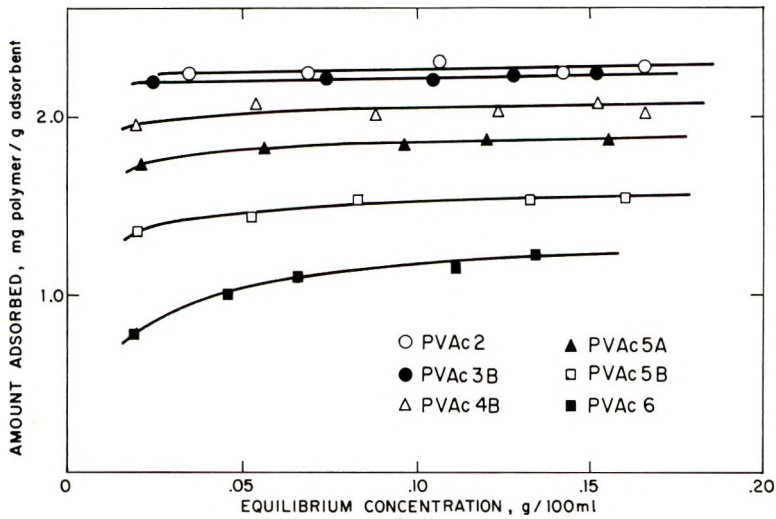


Fig. 6. Adsorption of poly(vinyl acetate) from benzene onto Pyrex at 50°C.

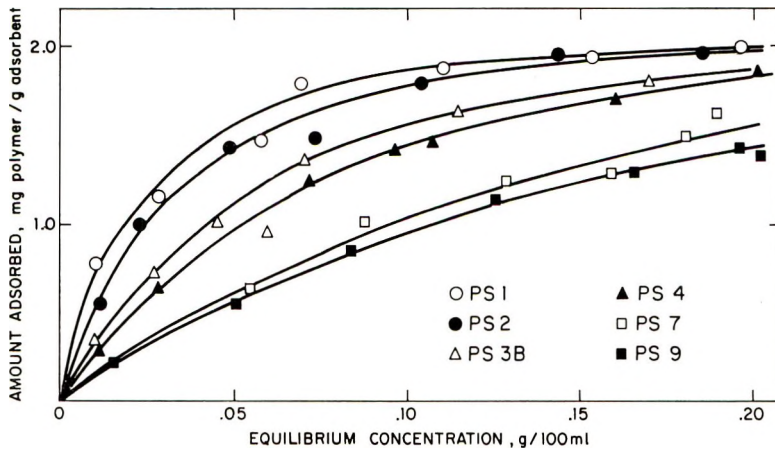


Fig. 7. Adsorption of polystyrene from benzene onto Pyrex at 30°C.

those of the two polar polymers. Even small amounts of benzene added to cyclohexane reduce the slopes of the isotherms, i.e., the affinities of adsorption of the polymer, as well as the adsorption capacity markedly, showing a lesser tendency for the polymer to leave the solution and/or a more effective competition by the solvent for the available surface sites.

For the carbonyl-containing polymers, the thicknesses were measured at surface saturation, while for polystyrene at the highest solution concentration used (0.1 g./100 ml.) the lower molecular weight fractions had not reached saturation. Thus the  $\Delta r$  data are, in part, not compatible but useful conclusions may be drawn from their main features. If one considers as a very primitive model of the adsorption process the sticking of rigid

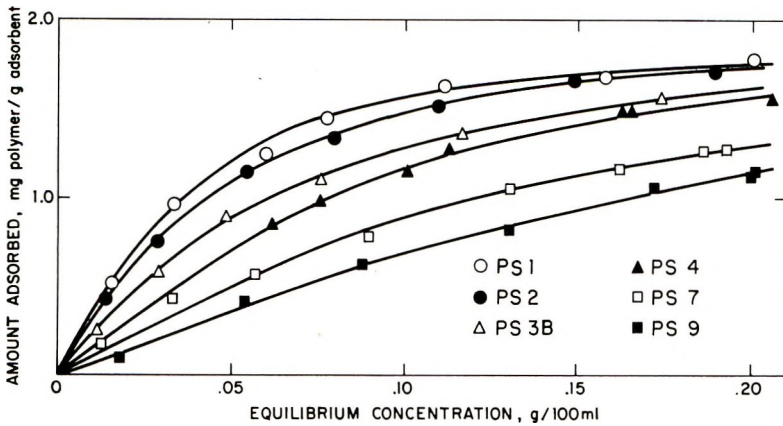


Fig. 8. Adsorption of polystyrene from benzene onto Pyrex at 50°C.

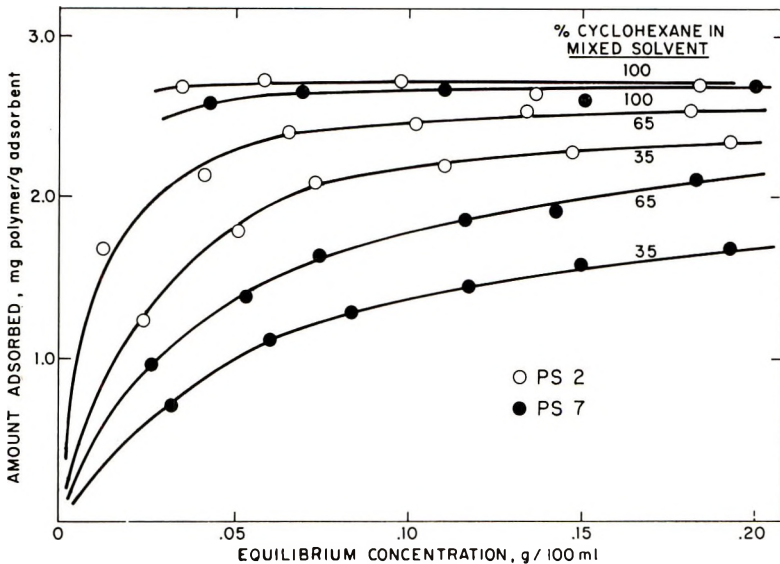


Fig. 9. Adsorption of polystyrene from cyclohexane and benzene-cyclohexane mixtures onto Pyrex at 34.2°C.

spheres to a flat surface, it is evident that above some particular, but still incomplete, extent of surface coverage the addition of more spheres only smooths out the film without increasing the hydrodynamic thickness. A curve of thickness versus concentration of the equilibrium solution would then reach a plateau at a lower concentration than the corresponding plot of surface coverage versus concentration. If, on the other hand, the film builds up by the steady accumulation of thin layers of material, the two curves should flatten out at nearly the same concentration when saturation occurs. An inspection of Figures 7 and 10 shows that the former model permits a better description, at least for polystyrene adsorption.

According to most theories, adsorption by formation of hydrogen bonds or strong dipole interaction should lead to conformations in which most of the polymer segments lie directly on the surface. Such a largely collapsed film would have a much lower dependence of thickness on molecular weight ( $\Delta r \propto M^0$  power, if all segments were on the surface) than would one in which the chains looped or coiled away from the surface ( $\Delta r \propto M^{1/4}$  to  $\Delta r \propto M^1$ ). Comparison of our data (Figs. 11 and 12) shows much

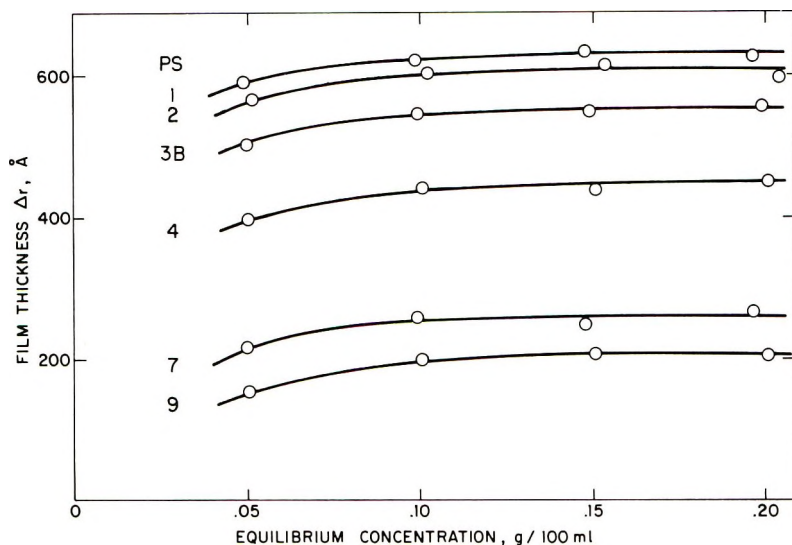


Fig. 10. Adsorbed film thickness and solution concentration for polystyrene in benzene at 30°C.

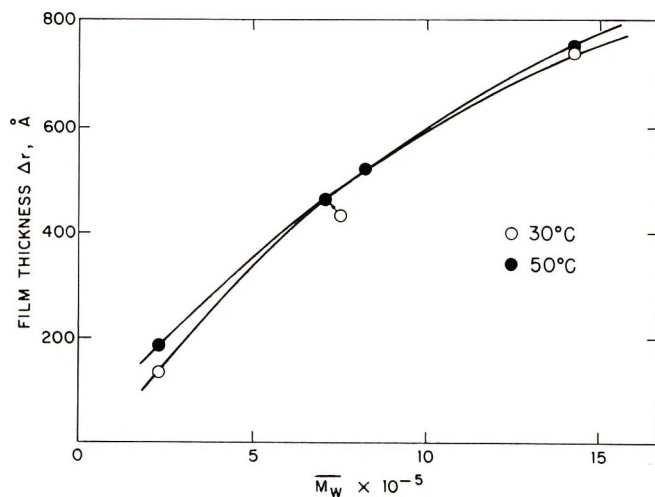


Fig. 11. Film thickness at high surface coverage as a function of molecular weight of poly(methyl methacrylate) in benzene.



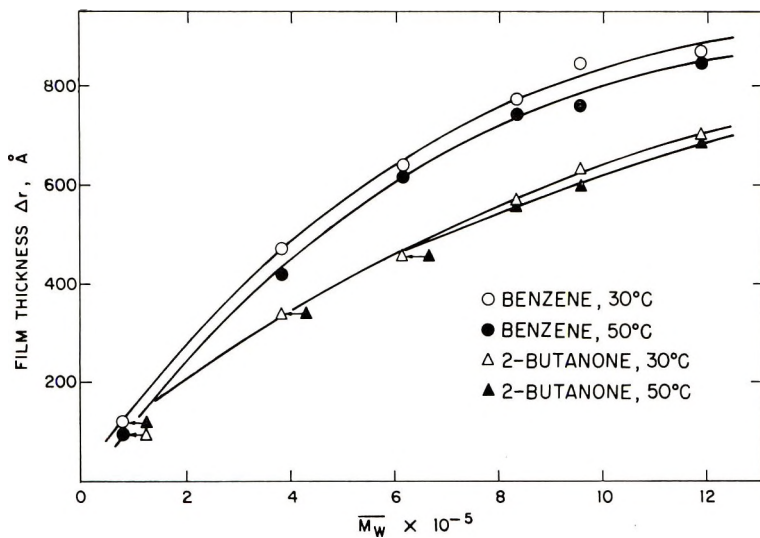


Fig. 12. Film thickness at high surface coverage as a function of molecular weight of poly(vinyl acetate) in benzene and 2-butanone.

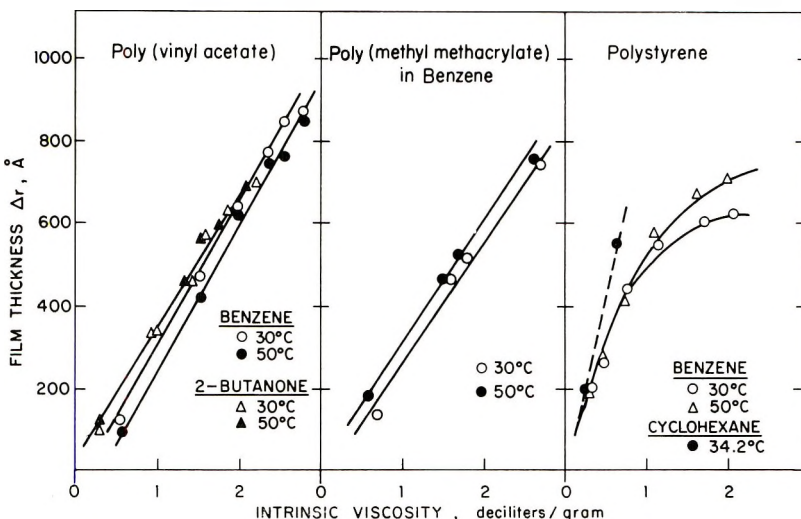


Fig. 13. Film thickness at high surface coverage as a function of intrinsic viscosity.

smaller differences in  $\Delta r$  between the polar and nonpolar polymers than might have been expected. The nature of the existing differences will become more apparent below.

In contrast to the lesser importance of the polymer-surface interaction, the polymer-solvent interaction has a major influence on film thicknesses. These decrease steadily, e.g., for the PS fractions 2 and 7, as one goes at constant temperature from benzene as a good solvent to the  $\theta$  solvent. For PVAc the thickness is greater in benzene, a good solvent, than in 2-

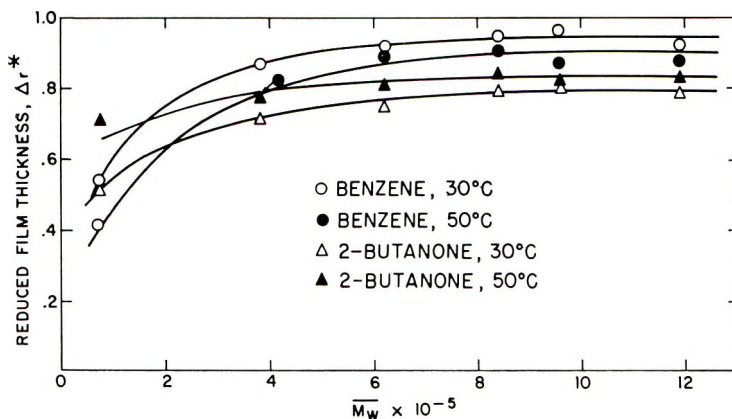


Fig. 14. Reduced film thickness at high surface coverage of poly(vinyl acetate) in benzene and 2-butanone.

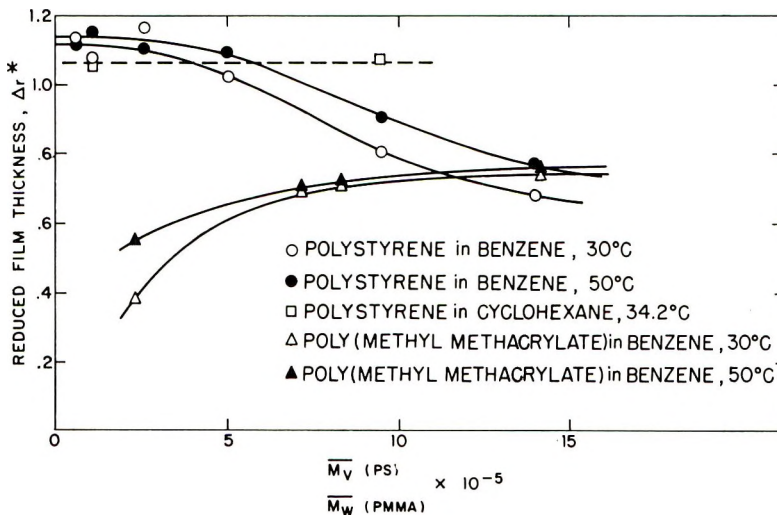


Fig. 15. Reduced film thickness at high surface coverage of polystyrene in benzene and cyclohexane and poly(methyl methacrylate) in benzene.

butanone, a fair solvent, even though less polymer is adsorbed. This indicates very strongly that the chains are not collapsed at the interface but are sufficiently extended so that the segment-solvent interaction rather than the segment-surface interaction dominates their conformation. If so, there should be some simple relationship for a given polymer between the film thickness and the intrinsic viscosity, since the latter is also a measure of solvent power and coil volume. Figure 13 shows strikingly that this is the case, and that the relationship is linear for the polar polymers, while PS in a good solvent shows thicknesses less than those predicted on the basis of the  $\theta$ -solvent line.

Support for the correctness of the trend of  $\Delta r$  found in the present work

comes from at least three other studies. Bulas,<sup>18</sup> in a viscosity study where  $\Delta r$  values were obtained from the increase of the dispersed volume after adsorbing PMMA (the same parent material as that of Table I) on calcium carbonate powder in toluene, has obtained very similar results, and Rothstein<sup>19</sup> also found  $\Delta r$  proportional to intrinsic viscosity for alkyd resins on three different pigments using the same method. In a study at the National Bureau of Standards, Stromberg et al.<sup>14,15</sup> have determined the thicknesses of adsorbed polystyrene of  $\bar{M}_w = 76,000$  on chromium surfaces in cyclohexane at 30°C., i.e., under near  $\theta$ -solvent conditions. Their value from ellipsometry is 115 Å., as compared to our 200 Å. for a closely similar PS, an agreement which can be considered good in view of the differences in adsorbent, temperature, sharpness of the fractions, and especially of techniques which must lead to different effective thicknesses of the layers.

While under our conditions polymer chains tend to adsorb in extended looplike conformations, an inspection of Figures 14 and 15 shows that there is also deformation or compression of the coils. A convenient measure of such deformation is the ratio of the film thickness to twice the average radius of gyration of the free coils in solution, which we call the reduced film thickness  $\Delta r^*$ . For a coil which adsorbs without distortion, this ratio should be about 0.9. Figure 15 shows values somewhat greater than this for low molecular weight PS, but in view of the errors undoubtedly present in the measurement of our film thicknesses this is not unreasonable. Thus the PS coils of low molecular weight seem to fit on the surface almost undeformed, and therefore presumably weakly adsorbed with only a few segments held at any one time. As the molecular weight increases and the chemical potential, and therefore solubility, of the molecules decreases, the coils become compressed toward the surface,  $\Delta r^*$  falls, and the number of adsorbed segments per weight will rise. This effect would be still greater were it not that in good solvents the coil dimensions resist reduction to the density of  $\theta$  coils; most likely this is the factor which eventually leads to the leveling off of the  $\Delta r^*$  versus  $M$  plots at very high molecular weights.

Comparison of the PS curves with the data for PMMA and PVAc (Figs. 14 and 15) shows characteristic differences in line with those found between the intrinsic viscosity plots of Figure 13. Again, this difference can be explained as that between strongly held polar chains and weakly bound nonpolar chains. The polar monomeric units of PVAc and PMMA will be more adsorbed on glass as part of the interface than will the styrene unit. This difference is readily apparent for low molecular weights. At higher molecular weights restrictions on chain conformation play an increasingly important part and lead to the more extended loops shown by PVAc and PMMA. In the case of polystyrene in benzene, short chains are very extended, so that the normal decrease of solubility with increasing molecular weight causes an approach (relative) of the segments toward the interface, reducing  $\Delta r^*$ .

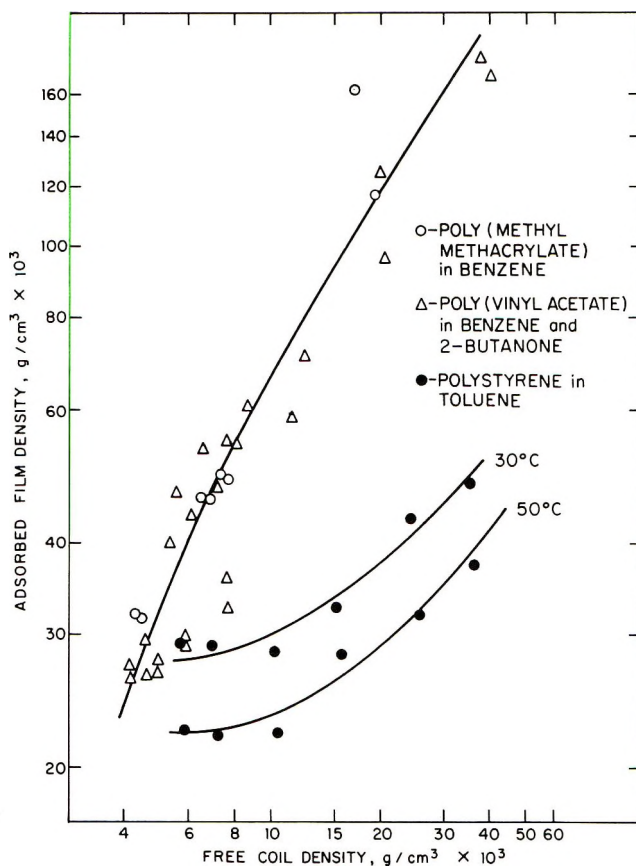


Fig. 16. Relative densities of free coils and adsorbed films.

It must also be kept in mind that the amounts adsorbed are not simply equivalent to complete monolayers of undeformed coils. The area occupied by spheres of radius  $r$  in two-dimensional hexagonal close packing is  $3.5 r^2$ , and the radius of gyration of a random walk coil is  $1/6 N l^2$ , where  $l^2$  is an overestimate of the area per segment. Thus, a complete monolayer of  $\theta$  coils should be approximately equivalent in amount of material adsorbed to a monolayer of segments lying flat on the surface. Instead, amounts adsorbed equivalent to 2 to 8 monomer monolayers were found in similar studies.<sup>17</sup> In our work, a value for the specific surface area of the glass adsorbent of  $1 \text{ m.}^2/\text{g.}$ , intermediate between the value from fatty acid adsorption of  $0.24 \text{ m.}^2/\text{g.}$  and the BET value of  $2 \text{ m.}^2/\text{g.}$  leads, in terms of segments to adsorbed amounts, equivalent to about 6 monolayers. These, as we have seen, are laid down in adsorbed layers of thicknesses comparable to free coil diameters. It follows that appreciable interpenetration and/or lateral compression must occur, which is feasible in view of the very low absolute segment densities involved (of the order of 0.1%) (see Fig. 16). In order to reduce the density to that in the free coil,

the polymer would have to see a surface area three times that available for nitrogen adsorption, which is unlikely. The fact that the segment density of the adsorbed film changes with molecular weight in about the same way as the segment density in the free coils demonstrates that the expansion coefficient  $\alpha$  is comparable for free and adsorbed polymer, in the polar or  $\theta$ -coil cases.

These same data are presented in a different form in Figure 17, where thicknesses are plotted versus the amounts adsorbed for either changing solvent or molecular weight. The two nearly horizontal lines (Fig. 17a) show the effect of solvent power on  $\Delta r$  for PS-2 (of molecular weight

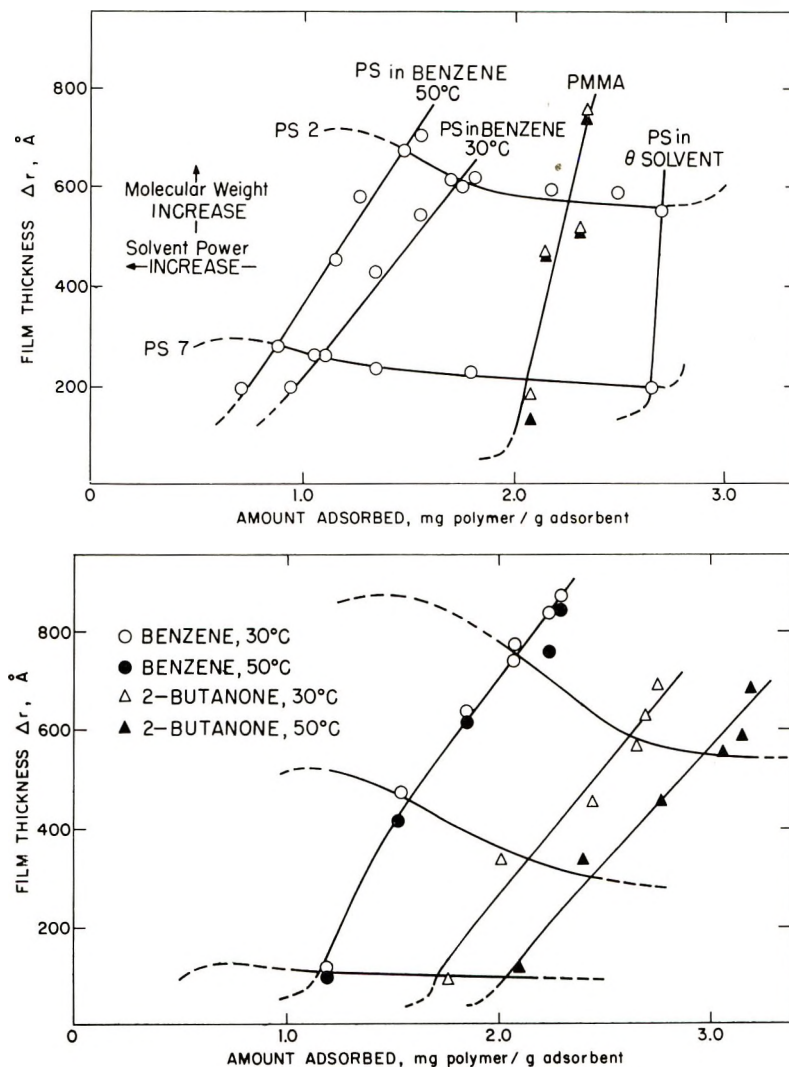


Fig. 17. Film thickness and amount adsorbed: (a) polystyrene and poly(methyl methacrylate) (b) poly(vinyl acetate).

950,000) and PS-7 (molecular weight 110,000). As the solvent power decreases from left to right, the amounts adsorbed increase while the film thicknesses diminish slightly, so that the adsorbed layers become much denser. Extrapolating to the left, the lines must pass through a maximum in the region of very good solvents, since eventually the increased solubilities must reduce the adsorbed amounts, lead to a breakup of the condensed layer, and both adsorption and  $\Delta r$  must vanish.

The sloping lines in Figure 17 show the trend with changing molecular weight. For PS, these extrapolate reasonably well to the origin. For the polar polymers, a sharp kink toward the origin must be assumed. This indicates in another fashion that the lower molecular weight PMMA and PVAc polymers, in contrast to the corresponding PS polymer, are relatively tightly bound to the surface even at low surface coverage. The steep rise of these lines is probably due to the stiffness of doubly anchored loops such that from a certain molecular weight on, relatively few additional segments form loops which greatly increase the hydrodynamically effective thickness  $\Delta r$ .

The two PS fractions in the  $\theta$  solvent deserve special consideration. Since the film thickness is approximately equal to the average diameter of the free coils while the amounts adsorbed are equivalent to certainly more than one segmental monolayer, the layer density must be appreciably greater than that of the free  $\theta$  coils. The dimensions parallel to the surface must then be compressed relative to the free coil value. In solution this would lead, of course, to further collapse and to precipitation. A possible explanation of the stability of the dimensions of conformations denser than  $\theta$  coils in the interface may be as follows. First, the site density for accommodation of segments will hardly be sufficient to permit very close packing and second, collapse will be resisted by osmotic pressure which must tend to keep coil dimensions not far below  $\theta$  values.

Concerning the question whether the data reported here represent true adsorption equilibria, a recent paper by Stromberg et al.<sup>15</sup> has shown by tracer methods that polymer exchanges at interfaces are reasonably fast. The large desorption hysteresis often quoted as a mark of irreversibility (though this interpretation has already been disproved by using displacing solvents) is then in fact merely an experimental artifact, in that the ordinary method of replacing the supernatant by solvent removes those polymer molecules which would adsorb at the sites vacated by the desorbing ones, i.e., which would block the sites for re-adsorption of the original chains. The increases in amounts adsorbed with temperature may be attributed to the reduction of rotation barriers which permit a more rapid approach to equilibrium and to a real increase due to reduction of the number of adsorption sites blocked by solvent molecules. Upon cooling the system, the raising of the rotation barriers and the slowing of exchange rates will produce a delay in reaching the equilibrium appropriate to the lower temperature.

The increase of polymer adsorption with rising temperature has tradi-

tionally been attributed to a decrease in the overall free energy due to a positive entropy contribution from the desorbing solvent. An alternative possibility is that the number of segments adsorbed actually decreases but that the number of segments per pendant loop becomes greater. Since adsorption experiments by concentration differences do not permit separation of the number of sites occupied and the number of segments associated with each occupied site, such measurements cannot decide this question. Simultaneous determinations of the amounts adsorbed and either the number of sites occupied or the length of the pendant loops is necessary. Our data, though not specifically directed toward this problem, do indicate that loop size increases with increasing temperature.

A comparison of our findings with existing theories is difficult because most of them deal only with low degrees of surface coverage.<sup>5</sup> Also, many of the parameters used by these theories, such as effective chain flexibility, coordination numbers, segmental dimensions, number of contact points, surface uniformity, and the like, are either very hard to determine experimentally or are too loosely defined to allow fruitful experimental comparison. The situation is aggravated by the fact that the experimentalist is very hard put to achieve high precision. Finally, many of the essential features of polymer adsorption were not known at the time the theories were developed, so that the latter were designed to explain the then-known results, including the conflict between the monolayer-type isotherms and the excessive amounts adsorbed, the strong solvent and weak molecular weight and temperature dependence, and the slowness of desorption. Therefore these aspects require no additional discussion. However, very little was known until quite recently about the thickness of the adsorbed layers and even presently available data are open to criticism. The theories differ widely, therefore, in this point. The theory of Frisch, Simha, and Eirich<sup>1,2</sup> assigns to the polymer a conformation in the solvent which is based on reflection from the adsorbing surface. Adherence occurs at a number of reflection points when the free energy of the total system of surface, polymer with all its segments (free and held), and solvent can be decreased thereby. The number of adherence points will rise, and the polymer loop size decrease, as segment-surface attraction rises or segment-solvent attraction falls. In a given system where solubility changes slowly with polymer molecular weight, the number of contact points is proportional to  $M^{1/2}$ . On the other hand, as full surface coverage is approached, as is the case in this study, the contact number will decline at constant molecular weight while the loop length increases. The already adsorbed molecules, with a hydrodynamic thickness  $\propto$  (loop length)<sup>1/2</sup> and therefore to  $M^{1/4}$ , act as temporary barriers for newcomers. Since we find a dependence close to  $M^{1/2}$  for the polar polymers and polystyrene in the  $\theta$  solvent, this could be construed as a failure of the theory, but another possibility can be envisioned. The molecular layer is not being probed by an agent approaching perpendicularly to the capillary walls, but the clearance is measured as the solution flows parallel

to the walls. Thus, the whole loop length and not just its perpendicular projection participates in offering hydrodynamic resistance and, since it is the latter which is measured, this resistance is likely to be the same as that of the loop in free coils, i.e., proportional to the intrinsic viscosity.

Silberberg<sup>4</sup> has criticized the reflection model employed by Frisch-Simha-Eirich<sup>1,2</sup> (FSE) as inappropriate for a process which does not constitute a Markov chain, a point reiterated by DiMarzio<sup>5</sup> in a recent paper. Silberberg favors strong segment-surface interaction at the expense of segment-solvent interaction, as a result of which his theory expects much of the chain to lie in the interface except for very weak adsorption. This result is contrary to our findings and to those of Bulas,<sup>18</sup> Rothstein,<sup>19</sup> and of Stromberg et al.<sup>14,15</sup>

DiMarzio et al.<sup>5</sup> also reject the model of the surface as a reflecting barrier and picture it as an adsorbing barrier. Like their predecessors, they consider the internal partition function of the segments in loops to be the same as for segments in free molecules, but in contrast to Silberberg (and in company with Frisch et al.) they introduce the degree of chain flexibility as an explicit parameter. This eliminates many of the on-surface positions and leads, especially for flexible chains, to a wide distribution of loop sizes with the number of adsorbed segments per chain proportional to the molecular weight. One could consider this result compatible with our tentative, but as yet unsubstantiated, extrapolated portions of Figure 17, but this theory does not explain the proportionality of  $\Delta r$  to intrinsic viscosity for the higher molecular weight polar (strongly attracted) polymers, nor does it agree in its prediction of very large loop sizes for weak interactions with our values for high molecular weight polystyrene. It is true that the theory of DiMarzio, Peysers, and Hoeve<sup>5</sup> extends so far only to low surface coverage, but our few data in this region do not indicate any substantial departure from the overall pattern. It appears then, that our data agree clearly with the more qualitative aspects of the FSE theory, and that theories and experiments stand in need of much further work.

In conclusion, the evidence obtained so far permits the following picture of the structure of layers of polymer adsorbed from organic solvents within the pores of sintered glass disks.

(1) The polymers adsorb in monolayers in the form of somewhat compressed or interpenetrating molecular coils; this follows from the shape of the isotherms, from the values found for the thickness of the adsorbed layers allowing even for wide margins of error, from the fact that curves of  $\Delta r$  versus the equilibrium concentration in solution reach limiting values much faster than the adsorption isotherms, and particularly from the proportionality between the calculated thickness and the intrinsic viscosities of the same polymers in solution.

(2) This conclusion must be modified for molecular weights below some critical extrapolated value, varying with polymer and solvent,



where a much larger fraction of segments appears to lie in or near the interface. This result might be considered an artifact arising from the bridging or blocking of pores were it not that the amounts adsorbed do not rise correspondingly above this critical molecular weight but show a very weak dependence on molecular weight over the entire experimental range. It follows, incidentally, that the almost universally found low dependence of amount adsorbed on  $M$  may not hold for low molecular weights. One is then drawn to the conclusion that the increase in amount adsorbed (above a limiting amount obtained by linear extrapolation of Figure 17 to the abscissas) is actually that contained in loops, and that the occurrence of loops is the result of an increasing elastic resistance to compression, increasing because the relative deformation of the molecular coils when they are drawn into the surface becomes greater with molecular weight. In thermodynamic terms, with rising molecular weight the loss of conformational entropy by flattening out of chains begins to balance  $\Delta H_{\text{adsorption}}$  and causes an increased equilibrium swelling of the adherent polymer layer.

(3) The same arguments can be applied to the dependence of  $\Delta r$  on  $M$  for a given polymer series and solvent, which is of the order of  $M^{1/2}$  for polar polymers and for polystyrene in a  $\theta$  solvent, i.e., in cases of rather extensive segmental adsorption. For lower affinities of adsorption, such as polystyrene in a good solvent on glass, extensive loop formation occurs even at low molecular weight, so that the plot of  $\Delta r$  versus intrinsic viscosity becomes concave toward the abscissa.

(4) The distribution of segmental density within the adsorbed layer is therefore likely to show two strata: a denser and lower one in or near the surface which, however, is still much below the density of a segmental monolayer because of steric hindrances, and a far layer of less density consisting of loops, i.e., of polymer whose segments are not accommodated in the interface; it is this layer which is responsible for the apparent "excess" adsorption. Whether or not these loops will contribute much to an effective hydrodynamic thickness will depend on the volume concentration of segments and on the loop stiffness, but the approximate proportionality of  $\Delta r$  to intrinsic viscosity indicates that the upper layer structure is similar to that of the free coils in solution. This model adds some detail to the previously postulated overall compression and interpenetration of adsorbed polymer coils, which must be extensive in the case of adsorption from a  $\theta$  solvent. The finding that the effects of solvent and temperature are very similar in the film and in the solution phase adds support to this picture. At the same time, the frequently observed increase of amount adsorbed with increasing temperature may be explained not only by a positive enthalpy and strongly positive entropy of polymer adsorption (due to solvent desorption), but also by an actually decreased occupancy of surface sites by polymer segments which is overcompensated by an increased number of segments pendant from each site.

Taken from a dissertation submitted by F. W. R. in partial fulfillment of the requirements for the degree of Doctor of Philosophy (Chemistry) at the Polytechnic Institute of Brooklyn.

Support by the United States Air Force Office of Scientific Research is gratefully acknowledged.

### References

1. R. Simha, H. L. Frisch, and F. R. Eirich, *J. Phys. Chem.*, **57**, 584 (1953).
2. H. L. Frisch and R. Simha, *J. Phys. Chem.*, **58**, 507 (1954).
3. H. L. Frisch and R. Simha, *J. Chem. Phys.*, **27**, 702 (1957).
4. A. Silberberg, *J. Phys. Chem.*, **66**, 1872, 1884 (1962).
5. E. A. Di Marzio, P. Peyser, and C. A. J. Hoeve, *J. Chem. Phys.*, **42**, 2558 (1965).
6. W. C. Forsman and R. E. Hughes, *J. Chem. Phys.*, **38**, 2123, 2130 (1963).
7. W. I. Higuchi, *J. Phys. Chem.*, **65**, 487 (1961).
8. B. J. Fontana and J. R. Thomas, *J. Phys. Chem.*, **65**, 480 (1961).
9. S. Ellerstein and R. Ullman, *J. Polymer Sci.*, **55**, 123 (1961).
10. M. H. Gottlieb, *J. Phys. Chem.*, **64**, 427 (1960).
11. O. E. Öhrn, *Arkiv Kemi*, **12**, 397 (1958).
12. C. A. F. Tuijnman and J. J. Hermans, *J. Polymer Sci.*, **25**, 385 (1957).
13. M. M. Huque, M. Fishman, and D. A. I. Goring, *J. Phys. Chem.*, **63**, 767 (1959).
14. R. R. Stromberg, E. Passaglia, and D. J. Tutas, *J. Res. Natl. Bur. Std.*, **67A**, 431 (1963).
15. R. R. Stromberg, D. J. Tutas, and E. Passaglia, *J. Phys. Chem.*, **69**, 3955 (1965).
16. F. W. Rowland and F. R. Eirich, *J. Polymer Sci. A-1*, **4**, 2033 (1966).
17. J. Koral, R. Ullman, and F. R. Eirich, *J. Phys. Chem.*, **62**, 541 (1958).
18. R. Bulas, thesis, Polytechnic Institute of Brooklyn, 1963.
19. E. Rothstein, thesis, Polytechnic Institute of Brooklyn, 1964.

### Résumé

L'épaisseur de films de polyméthacrylate de méthyle, d'acétate de polyvinyle, de polystyrène adsorbés sur du verre pyrex a été étudiée en mesurant les vitesses d'écoulement de solutions polymériques de même que celles des solvants purs correspondants à travers des disques filtrant en verre fritté. Les isothermes d'adsorption sont accord avec celles rapportées par d'autres auteurs en montrent une adsorption de saturation équivalente de 2 à 8 couches monomoléculaires d'unités monomériques. Les épaisseurs de films étaient de l'ordre de grandeur du diamètre de la pelote statistique en solution et étaient directement proportionnelles à la viscosité intrinsèque dupolymère sauf pour le polystyrène en solution benzénique où l'épaisseur diminuait lorsque le poids moléculaire augmentait. On en conclut que le polymère s'adsorbe au départ de leurs solutions sous forme de deux couches monomoléculaires de pelotes comprimées ou interpénétrées; que, en-dessous d'un poids moléculaire critique qui varie avec le polymère et le solvant, une beaucoup plus grande quantité de segments se trouvent directement à l'interface; que les films adsorbés peuvent consister en une couche dense immédiatement adjacente à la surface et en une couche profonde de boucles s'étendant jusque dans le solvant; et que ce sont ces interactions segment/solvant plutôt que l'interaction segment/surface qui dominent la conformation de la chaîne adsorbée.

### Zusammenfassung

Die Dicke von an Pyrexglas adsorbierten Poly(methylmethacrylat)-(PMMA)-, Poly(vinylacetat)-(PVAc)- und Polystyrol-(PS)-Filmen wurde durch Messung der Fließgeschwindigkeit von Polymerlösungen und der entsprechenden reinen Lösungsmittel durch Sinterfilterplatten untersucht. Die Adsorptionsisothermen stimmten mit

den von anderen Autoren angegebenen überein und zeigten einen Sättigungsbereich bei 2 bis 8 kondensierten monomolekularen Schichten von Monomereinheiten. Die Filmdickelage in der Grössenordnung der freien Knäueldurchmesser in Lösung und war der Viskositätszahl des Polymeren direkt proportional, mit Ausnahme von PS in Benzol, bei welchem die Dicke mit zunehmendem Molekulargewicht abflacht. Man kommt zu dem Schluss, dass das Polymere aus der Lösung in monomolekularen Schichten aus komprimierten oder einander durchdringenden Knäueln adsorbiert wird; dass unterhalb eines gewissen von Polymerem und Lösungsmittel abhängigen kritischen Molekulargewichts ein viel grösserer Bruchteil der Segmente direkt in der Grenzfläche liegt; dass adsorbierte Filme aus einer dichten, der Oberfläche unmittelbar anliegenden Schicht und einem tiefen, sich in das Lösungsmittel hinein erstreckenden Bereich von Schleifen bestehen können, und dass es die Segment-Lösungsmittelwechselwirkung und nicht die Segment-Oberflächenwechselwirkung ist, welche die Konformation der adsorbierten Kette bestimmt.

Received December 16, 1965

Prod. No. 5032A

## Crystalline Polymers of Bis( $\beta$ -chloroethyl) Vinylphosphonate

FRITZ MARKTSCHÉFFEL,\* A. F. TURBAK,† and Z. W.  
WILCHINSKY, *Esso Research and Engineering Company,*  
*Linden, New Jersey*

### Synopsis

The polymerization of bis( $\beta$ -chloroethyl) vinylphosphonate to a crystalline solid was carried out with a Ziegler-Natta catalyst. A confirmation of the crystalline nature of the polymers was carried out by x-ray diffraction. The polymers would not melt even at temperatures up to 620°C., but instead began to char. However, they were soluble in dimethylformamide and acrylonitrile.

The polymerization of unsaturated phosphorus compounds generally results in oily or semisolid products.<sup>1</sup> Recently the polymerization of phosphorus monomers to solid polymers in the presence of organometallic catalysts has been reported.<sup>2,3</sup> The polymerization of bis( $\beta$ -chloroethyl) vinylphosphonate (BCVP) to amorphous polymers has also been reported.<sup>3,4</sup> We do not know, however, of the existence of a crystalline polymer of BCVP. It is the purpose of this paper, to report the preparation and some properties of such a polymer.

### EXPERIMENTAL

#### Catalyst Preparation

A Ziegler-Natta type catalyst system was prepared from the following materials. The solid component consisted of either the  $\alpha$  form of  $\text{TiCl}_3$  or  $\text{TiCl}_3 \cdot 0.33 \text{ AlCl}_3$  prepared by reducing  $\text{TiCl}_4$  with triethylaluminum ( $\text{AlEt}_3$ ).<sup>5</sup> These solid components were activated by ball milling the dry powders for 6 days under a dry nitrogen atmosphere.

Triethylaluminum was used as the second component of the catalyst. For convenience, a 1M standard solution in xylene was prepared and stored in a nitrogen glovebox. In two of the catalyst preparations, hexamethylphosphoramide (HMPA) was used as a third component. This material and bis( $\beta$ -chloroethyl) vinylphosphonate (BCVP) were dried over  $\text{MgSO}_4$  for 24 hr. and then vacuum-distilled. Heart cuts were used in the experiments. For convenience, a 1M standard solution of HMPA in

\* Present address: Farbwerke Hoechst AG, Frankfurt-Höchst/Main, Germany.

† Present address: Tee-Pak, Inc., Danville, Illinois.

xylene was prepared. The xylene (nitration grade) was purified by percolation through Alcoa F-5 activated alumina and stored over sodium ribbon.

In the experiments where HMPA was used as a third catalyst component, 1M standard solutions of 2 mmole  $\text{AlEt}_3$  and 1 mmole HMPA were mixed and allowed to complex for 1 hr. at ambient temperature. To this solution, or, if no HMPA had been used, to a 1M standard solution of  $\text{AlEt}_3$  were added 2 mmole  $\alpha\text{-TiCl}_3$  and xylene to make up a slurry of the catalyst in 50 ml. xylene. Only 1.67 mmole  $\text{AlEt}_3$  was used, when 2 mmole  $\text{TiCl}_3 \cdot 0.33 \text{ AlCl}_3$  was added. The total catalysts were allowed to age for 15 min. at ambient temperature.

All catalyst preparations were carried out in a nitrogen glovebox. The nitrogen contained 1–10 ppm water and 0.1–1 ppm oxygen.

### Polymerizations

Four polymerization experiments were carried out according to the following procedures.

**Experiments 1–3.** The polymerizations were carried out in a four-necked round-bottomed flask equipped with stirrer, thermometer, dropping funnel, condenser with a Drierite drying tube, and nitrogen inlet and outlet.

Xylene (50 ml.) solvent was heated under a blanket of dry nitrogen to  $55^\circ\text{C}$ ., then a solution of 17.4 g. BCVP in 15 ml. xylene was added to the reactor, followed by the addition of the catalyst. The temperature was increased to  $85^\circ\text{C}$ . and kept for a total of 2–4 hr. as indicated in Table I. Shortly after increasing the temperature to  $85^\circ\text{C}$ ., a brownish solid precipitated at the walls of the reactor. After the total polymerization period it was cooled to room temperature and *n*-pentane ( $2\frac{1}{2}$  times the volume of the xylene solvent) was added with stirring to precipitate the polymer of BCVP formed. The liquid phase was decanted from the semisolid and the volatiles removed by evaporation under reduced pressure and at elevated temperatures, yielding 9.5 g. of a viscous, yellowish-brown oil. This oil is soluble in methanol but insoluble in benzene, acetone, and chloroform.

The semisolid was dried *in vacuo* at  $40^\circ\text{C}$ . to a brown, hard, powdery material. It was dissolved in 10 ml. hot dimethylformamide (DMF) and filtered into 50 ml. distilled water. This produced a white precipitate. The precipitate was collected and washed several times with water and finally with 50 ml. acetone and dried again for 24 hr. at  $40^\circ\text{C}$ . *in vacuo*. A white, sandlike powder (2.45 g., 14% monomer conversion) was obtained.

**Experiment 4.** The polymerization was carried out as described for experiments 1–3 but with 99 g. of BCVP in 575 ml. xylene. It was, however, polymerized for 4 hr. at  $85^\circ\text{C}$ . and the catalyst deactivated by adding 10 ml. acetylacetone in 75 ml. methanol at the end of this period. Then the reaction mixture was cooled to room temperature and allowed to stand overnight, during which period a heavy oil separated. Then one liter of *n*-heptane was added and the total mixture allowed to stand for an addi-

TABLE I  
 Polymerization of Bis( $\beta$ -chloroethyl) Vinylphosphonate in the Presence of  
 Ziegler-Natta Type Catalysts (Temperature 85°C.)

	Expt. 1	Expt. 2	Expt. 3	Expt. 4 <sup>a</sup>
Catalyst preparation				
AlEt <sub>3</sub> , mmole	2	2	1.67	10
Cocatalyst	$\alpha$ -TiCl <sub>3</sub>	$\alpha$ -TiCl <sub>3</sub>	TiCl <sub>3</sub> ·0.33 AlCl <sub>3</sub>	$\alpha$ -TiCl <sub>3</sub>
Cocatalyst, mmole	2	2	1	10
HMPA, mmole	1	—	—	5
Xylene, ml.	50	50	40	250
Monomer solution				
BCVP, g.	17.4	17.4	17.4	99
Xylene, ml.	15	15	20	75
Polymerization				
Xylene, ml.	50	50	40	250
Time, min.	120	120	120	240
Yield, g.	2.45	1.76	1.78	10
Monomer conversion, %	14	10	10	10
Polymer evaluation				
Inherent viscosity, dl./g.	0.06	0.05	0.05	0.2
Elemental analysis, <sup>b</sup> found, %				
C	28.05	27.06	28.4	28.6
H	4.64	4.50	4.55	4.4
P	14.86	13.9	14.67	15.3
Cl	—	—	—	22.8

<sup>a</sup> Deactivated with acetylacetone (see experimental part).

<sup>b</sup> Calculated: C, 30.9%; H, 4.75%; P, 13.31%; Cl, 30.45%.

tional 5 hr. During this period the amount of oil increased further. The supernatant liquid was decanted from the oil and the volatiles of the oil removed by heating the oil *in vacuo* for 100 hr. at 45°C., yielding 38 g. of a very viscous yellow oil containing some dispersed solids.

This oil formed a clear solution in 60 ml. hot DMF. The solution was filtered into 300 ml. methanol, and a white solid precipitated. This precipitated material was collected and washed twice with 50 ml. H<sub>2</sub>O and once with 50 ml. acetone, then dried *in vacuo* over P<sub>2</sub>O<sub>5</sub> for 24 hr., yielding 2 g. of white solid polymer powder (fraction A).

The filtrate of fraction A was poured into 500 ml. H<sub>2</sub>O. After filtration, washing, and drying, an additional 8 g. of a brown solid polymer powder was obtained. This polymer was reprecipitated from 50 ml. DMF into 500 ml. H<sub>2</sub>O, yielding, after drying over P<sub>2</sub>O<sub>5</sub> in a vacuum desiccator, 6.2 g. of a fine white powder.

### Polymer Properties and Analysis

The solution viscosities of these polymers were determined in DMF at 20°C. at concentrations of 0.5 g./100 ml.

For elemental analyses the polymers were reprecipitated twice from DMF-water.

X-ray diffraction examinations of the polymer was carried out with a Norelco diffractometer by using the symmetrical reflection method. The polymer, in powder form, was packed into a flat sample holder so that it presented a plane surface to the x-ray beam. Diffractometer scans were made in the range  $5^\circ < 2\theta < 60^\circ$  with  $\text{CuK}\alpha$  radiation.

## RESULTS AND DISCUSSION

The results of our experiments are summarized in Table I. In general, polymer yields are about 10% of the theoretical value. It appears that the molecular weight increases with increasing polymerization time.

These polymers of BCVP are obtained as hard, sandlike white powders after reprecipitation from  $\text{DMF-H}_2\text{O}$ . They dissolve in hot DMF and acrylonitrile but appear to be infusible. No melting was observed up to  $620^\circ\text{C}$ . (the limiting temperature of the melting point apparatus). However, during heating, the polymers started to char around  $350^\circ\text{C}$ ., changing in color from white to brown. As the temperature was raised, the color darkened, and at  $620^\circ\text{C}$ . a black but unmelted solid remained. This charring is probably due to splitting off of HCl.

The elemental analysis of these polymers indicate that some HCl has been split off during the course of polymerization. The failure to obtain close duplicate analyses may be due to the very high melting point of the polymers. It is known that the carbon analysis of phosphorus compounds tends to be low. Infrared spectra, however, support our conclusion that polymers of BCVP have been obtained. The monomer vinyl absorptions, normally at  $990\text{ cm}^{-1}$ , have been shifted to  $1020$  and  $985\text{ cm}^{-1}$ , respectively, because of the  $\text{P=O}$  environment. These bonds are absent in the spectrum of the polymer. Other spectral features of the monomer are retained in the polymer.

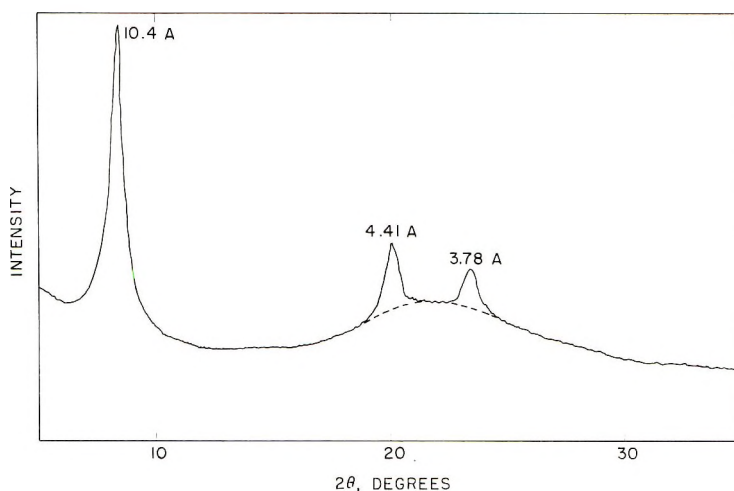


Fig. 1. Diffractometer pattern showing diffraction peaks of the crystalline polymer

Bonds that can be attributed to P=O (1250  $\text{cm}^{-1}$  in monomer) and P—O—C (1035  $\text{cm}^{-1}$  in monomer) are intact in the polymer. For the P=O band there is, however, a shift from 1250  $\text{cm}^{-1}$  to 1215  $\text{cm}^{-1}$  in the polymers.

The crystalline nature of the new polymer is evident from the diffractometer scan shown in Figure 1. Three peaks are present having interplanar spacings of 10.4, 4.41, and 3.78 Å. It can be noted that the last two peaks are superimposed on a diffuse band which is due to amorphous material. The pattern beyond  $2\theta \equiv 30^\circ$  (not shown) was devoid of crystalline peaks, consisting only of a background of slowly decreasing intensity.

For comparison, we prepared a polymer of BCVP in accordance with the preparation given by Coover and McCall,<sup>3</sup> using only  $\text{AlEt}_3$  as the catalyst. The diffractometer trace of this polymer did not show any crystalline peaks but only an amorphous halo that was observed in the preceding case having a maximum intensity at about  $2\theta = 21^\circ$  and a second halo having a maximum at about  $2\theta = 7.5^\circ$ .

We are indebted to Mr. E. Kreig, Jr., of the Chemicals Research Division for his skillful experiments and Mr. R. Hofstader, of the Analytical Research Division for carrying out the elemental analysis. We thank Dr. Erik Tornqvist, Chemicals Research Division, for his generous supply of the solid catalyst components,  $\text{TiCl}_3$  and  $\text{TiCl}_3 \cdot 0.33 \text{ AlCl}_3$ . The authors wish also to thank Esso Research & Engineering Company for permission to publish this paper.

### References

1. Ye. L. Gefter, *Organophosphorus Monomers and Polymers*, Pergamon, New York, 1962, pp. 147–192.
2. C. S. Marvel and D. M. Paisley, *J. Polymer Sci.*, **55**, 259 (1961).
3. H. W. Coover and M. A. McCall, U.S. Pat. 3,043,821 (July 10, 1962).
4. *Soviet Plastics*, **1963**, No. 4.
5. E. Tornqvist and A. W. Langer, U.S. Pat. 3,032,510 (May 1, 1962).

### Résumé

La polymérisation du phosphonate du bis- $\beta$ -chloroéthyl-vinyle en un solide cristallin a été effectuée au moyen d'un catalyseur Ziegler-Natta. On a confirmé la nature cristalline des polymères au moyen de la diffraction aux rayons-X. Les polymères ne fondent même pas à des températures de 620°C. mais commencent à ce moment à charbonner. Toutefois, ils sont solubles dans le diméthylformamide et l'acrylonitrile.

### Zusammenfassung

Die Polymerisation von Bis-( $\beta$ -chloräthyl) vinylphosphonat zu einem kristallinen Festkörper wurde mit einem Ziegler-Natta-Katalysator durchgeführt. Die kristalline Natur der Polymeren wurde durch Röntgenbeugung bestätigt. Die Polymeren konnten bei Temperaturen bis zu 620°C nicht zum Schmelzen gebracht werden, sondern begannen zu verkohlen. Sie waren aber in Dimethylformamid und Acrylnitril löslich.

Received December 9, 1965

Prod. No. 5035A



## Kinetic Studies of Polymerization of Propylene with Active $\text{TiCl}_3\text{-Zn}(\text{C}_2\text{H}_5)_2$

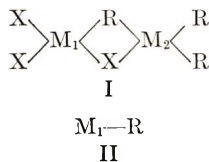
KAZUO SOGA and TOMINAGA KEII, *Department of Chemical Engineering, Tokyo Institute of Technology, Meguro, Tokyo, Japan*

### Synopsis

In order to elucidate the structure of the Ziegler-Natta polymerization center, we have carried out some kinetic studies on the polymerization of propylene with active  $\text{TiCl}_3\text{-Zn}(\text{C}_2\text{H}_5)_2$  in the temperature range of 25–56°C. and the  $\text{Zn}(\text{C}_2\text{H}_5)_2$  concentration range of  $4 \times 10^{-3}$ – $8 \times 10^{-2}$  mole/l., and compared the results with those obtained with active  $\text{TiCl}_3\text{-Al}(\text{C}_2\text{H}_5)_3$ . The following differences were found: (1) the activation energy of the stationary rate of polymerization is 6.5 kcal./mole with  $\text{Zn}(\text{C}_2\text{H}_5)_2$  and 13.8 kcal./mole with  $\text{Al}(\text{C}_2\text{H}_5)_3$ ; (2) the growth rate of the polymer chains with  $\text{Zn}(\text{C}_2\text{H}_5)_2$  is about three times slower at 43.5°C.; and (3) the polymerization centers formed with  $\text{Zn}(\text{C}_2\text{H}_5)_2$  are more unstable. It can be concluded that the structure of the polymerization center with  $\text{Zn}(\text{C}_2\text{H}_5)_2$  is different from that with  $\text{Al}(\text{C}_2\text{H}_5)_3$ .

### INTRODUCTION

Many investigations have been carried out to elucidate the mechanism of a Ziegler-Natta polymerization, especially to determine the nature of the polymerization centers. The proposed structures for the polymerization centers may be divided into the types I and II,



where  $\text{M}_1$  is a transition metal,  $\text{M}_2$  a metal such as Al, Be, or Zn, X is a halide, and R an alkyl group. The structure I has been proposed by Natta et al.<sup>1</sup> and structure II by Cossee et al.<sup>2</sup>

It is well known that some organometallic compounds such as  $\text{Al}(\text{C}_2\text{H}_5)_3$  have a polymeric tendency whereas others, such as  $\text{Zn}(\text{C}_2\text{H}_5)_2$  have not.<sup>1</sup> Accordingly, it may be considered that the latter cannot participate in forming structure I. However, the kinetic behavior of the polymerization with  $\text{Zn}(\text{C}_2\text{H}_5)_2$  may give some information to clear the structure of the polymerization center.

Some detailed studies on the polymerization of propylene with  $\alpha$  and  $\beta$   $\text{TiCl}_3\text{-Zn}(\text{C}_2\text{H}_5)_2$  have been reported by Boor,<sup>3</sup> who did not, however, discuss this problem.

In this paper, we have carried out some kinetic studies on the polymerization of propylene with active  $\text{TiCl}_3\text{-Zn}(\text{C}_2\text{H}_5)_2$  to compare the results with the kinetics of the polymerization of propylene with active  $\text{TiCl}_3\text{-Al}(\text{C}_2\text{H}_5)_3$ .<sup>4</sup>

## EXPERIMENTAL

Polymerizations were carried out with the same apparatus and procedures as reported in the previous paper.<sup>5</sup> Polymerization was quenched usually after 90 min. with a methanol-1*N* hydrochloric acid solution. After adequate washing with methanol and water, the polymers were dried overnight at room temperature in a vacuum oven.

Intrinsic viscosity was measured at 135°C. in Decalin containing 0.1% phenyl- $\beta$ -naphthylamine under a nitrogen atmosphere. Molecular weight was calculated by Kinsinger's equation:

$$\eta = 1.07 \times 10^{-4} \bar{M}^{0.8} \quad (1)$$

For the determination of the tacticity of the polymer, we used the method of extraction with boiling *n*-heptane and infrared spectroscopy<sup>6</sup> with a Shimadzu IR-27-A infrared spectrometer at 36°C.

Propylene was from Mitsubishi Petrochemical Co., purity 99.5%. *n*-Heptane (Enjay Co.) was purified by refluxing over sodium metal after distillation.  $\text{TiCl}_3$  was from Stauffer, AA-grade, and its surface area was measured as 15.4 m.<sup>2</sup>/g. by BET method with nitrogen adsorption.  $\text{Zn}(\text{C}_2\text{H}_5)_2$  (Nippon Tokushu Kagaku Co.) was used without any further purification. Decalin and xylene (Wako Pure Chemical Industries Co.) were purified by distillation.

## RESULTS

### Time Dependence of the Polymerization Rate

Typical results obtained are shown in Figure 1. In the previous paper,<sup>4</sup> we reported that the relation between the polymerization rate and the polymerization time is well expressed by (2) and (3):

$$r = BP (1 + fe^{-kt}) \quad (2)$$

or

$$\ln (r - BP) = \ln (BPf) - kt \quad (3)$$

where *r* is the polymerization rate at time *t*, *P* the propylene pressure and *B*, *f*, and *k* are constants.

The applicability of eqs. (2) and (3) for the present results (Fig. 1) is apparent from Figure 2.

### Temperature and Concentration Dependencies of the Rate

To investigate the dependence of the polymerization rate on the concentration of  $\text{Zn}(\text{C}_2\text{H}_5)_2$ , we carried out the polymerization at 43.5°C.

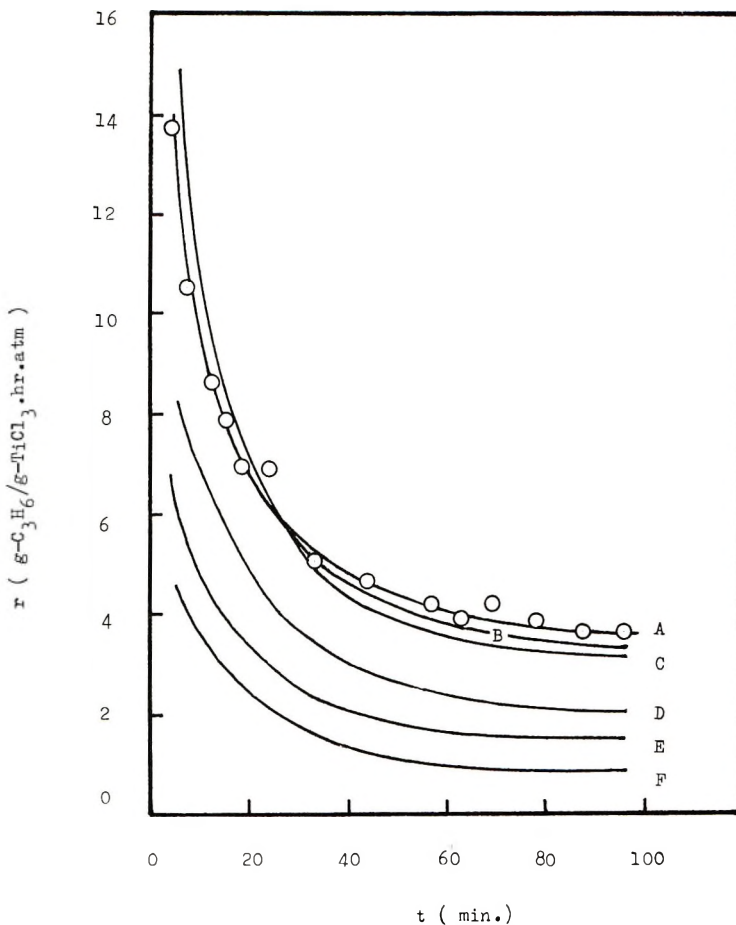


Fig. 1. Dependence of the polymerization rate on time at various  $\text{Zn}(\text{C}_2\text{H}_5)_2$  concentrations in *n*-heptane: (A) 80 mmole/l.; (B) 40 mmole/l.; (C) 28 mmole/l.; D 16 mmole/l.; (E) 8 mmole/l.; (F) 4 mmole/l.  $\text{TiCl}_3 = 1 \text{ g}$ ,  $P = 70 \text{ cm. Hg}$ , *n*-heptane = 250 ml.,  $T = 43.5^\circ\text{C}$ .

in the  $\text{Zn}(\text{C}_2\text{H}_5)_2$  concentration range of  $4 \times 10^{-3}$ – $8 \times 10^{-2}$  mole/l. *n*-heptane. The results are shown in Fig. 1, from which it is clear that the rate is almost independent of the concentration of  $\text{Zn}(\text{C}_2\text{H}_5)_2$  at its higher range ( $> 4 \times 10^{-2}$  mole/l. *n*-heptane).

The temperature dependence of the rate was examined in the temperature range of 25–56°C. at various concentrations of  $\text{Zn}(\text{C}_2\text{H}_5)_2$ .

The  $B$  values obtained on the basis of eq. (3) are shown in Figure 3 as a function of temperature. The temperature dependence (at  $< 43^\circ\text{C}$ .) of  $B$  in the case with the highest concentration of  $\text{Zn}(\text{C}_2\text{H}_5)_2$  ( $8 \times 10^{-2}$  mole/l. *n*-heptane) is given by eq. (4).

$$B = B_0 e^{-2.7 \text{ kcal./RT}} \quad (4)$$

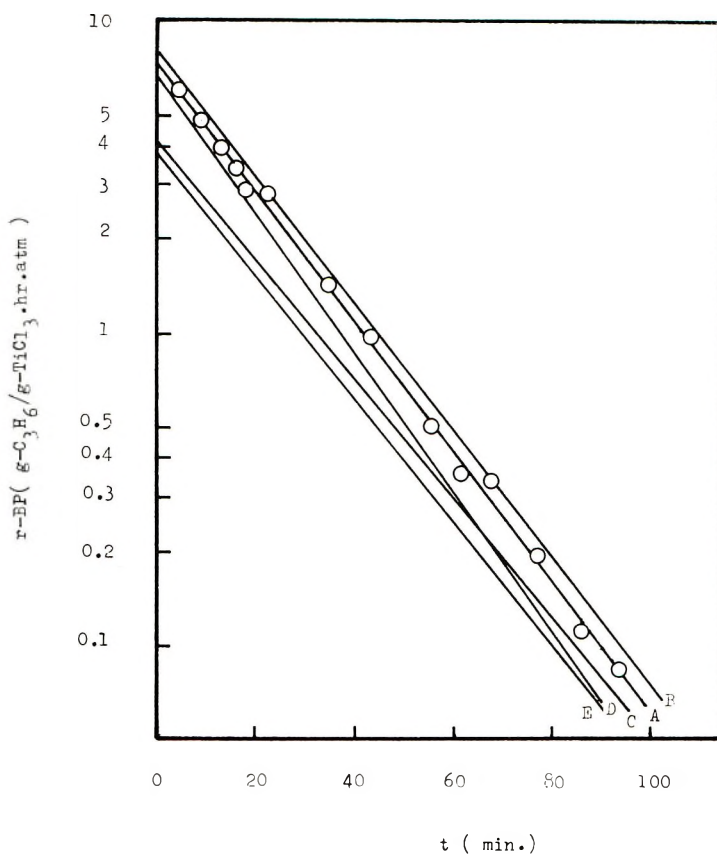


Fig. 2. Plots of  $\ln(r - BP)$  against  $t$  at various  $\text{Zn}(\text{C}_2\text{H}_5)_2$  concentrations in  $n$ -heptane: (A) 80 mmole/l.; (B) 28 mmole/l.; (C) 16 mmole/l.; (D) 8 mmole/l.; (E) 4 mmole/l.

The  $B_0$  values in Figure 3 calculated from eqs. (2)–(4) are shown in Table I. The Langmuir type dependence between the  $B_0$  values and the concentration of  $\text{Zn}(\text{C}_2\text{H}_5)_2$  was examined and confirmed by the eqs. (5) and (6) (Fig. 4).

TABLE I  
 $B_0$  Values Calculated from Equation (4)

Zn(C <sub>2</sub> H <sub>5</sub> ) <sub>2</sub> concn., mmole/l.	$B_0$ , g. C <sub>3</sub> H <sub>6</sub> /g. TiCl <sub>3</sub> -hr.-atm.			
	48.5°C.	43.5°C.	37.5°C.	30.5°C.
80	200	286	298	300
40	—	261	—	—
28	—	214	—	—
16	133	142	157	171
8	110	118	118	—
4	37	53	43	—

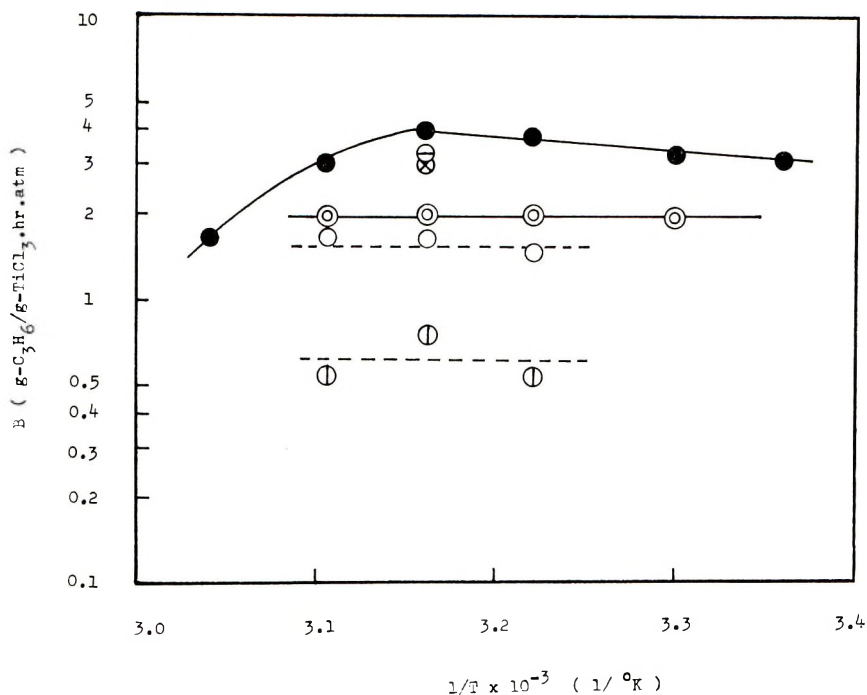


Fig. 3. Dependence of  $B$  on the polymerization temperature at various concentrations of  $\text{Zn}(\text{C}_2\text{H}_5)_2$  in  $n$ -heptane: (●) 80 mmole/l.; (⊗) 40 mmole/l.; (⊙) 28 mmole/l.; (⊖) 16 mmole/l.; (○) 8 mmole/l.; (⊕) 4 mmole/l.

$$B_0 = abC/(1 + aC) \quad (5)$$

$$C/B_0 = (1/ab) + (C/b) \quad (6)$$

where  $a$  and  $b$  are constants and  $C$  is the initial concentration of  $\text{Zn}(\text{C}_2\text{H}_5)_2$ . The  $a$  values calculated from the slopes and the intersections in Figure 4 are shown in Figure 5, from which we have eq. (7):

$$a = a_0 e^{3 \text{ kcal./}RT} \quad (7)$$

#### Temperature and Concentration Dependencies of the Deactivation Parameter $k$

The  $k$  values determined are shown in Figure 6, which shows that  $k$  is almost independent of the concentration of  $\text{Zn}(\text{C}_2\text{H}_5)_2$  and that the temperature dependence of  $k$  can be expressed by eq. (8):

$$k = k_0 e^{-3.8 \text{ kcal./}RT} \quad (8)$$

#### Molecular Weight and Tacticity

Both the molecular weights and the tacticities of polymers obtained at 43.5°C. are shown in Figure 7 as a function of the concentration of  $\text{Zn}(\text{C}_2\text{H}_5)_2$ . We have the following equation between the molecular

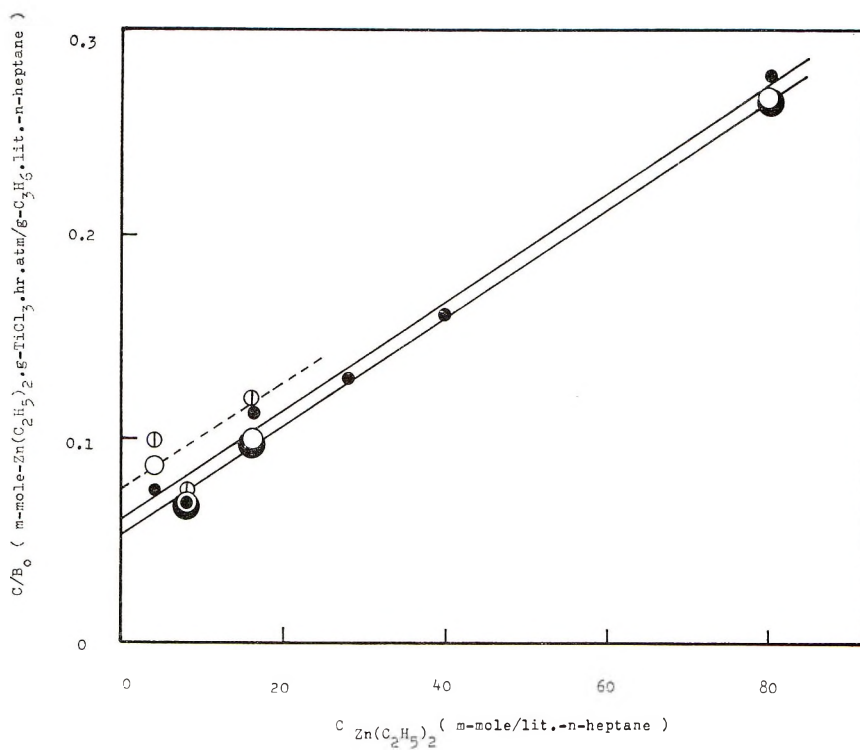


Fig. 4. Plots of  $C/B_0$  against  $C$ : ( $\odot$ ) 48.5°C.; ( $\bullet$ ) 43.5°C.; ( $\circ$ ) 37.5°C.; ( $\bullet$ ) 30.5°C.

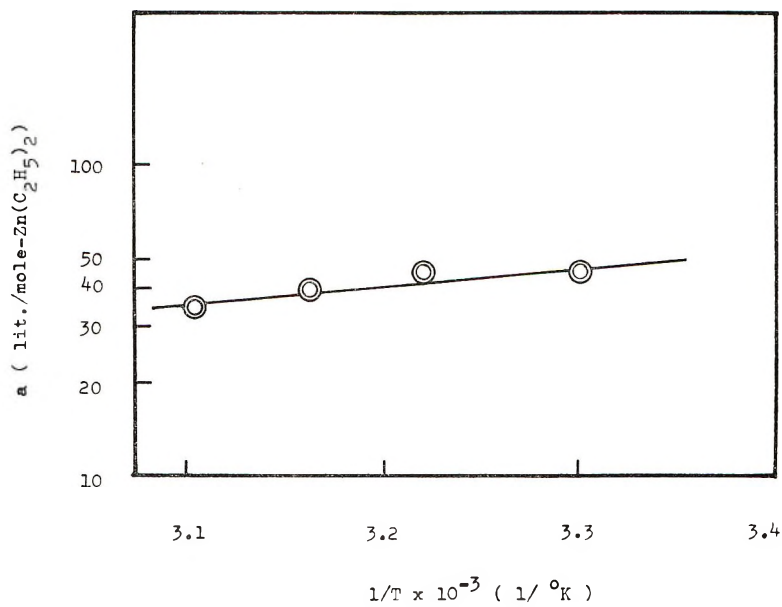


Fig. 5. Dependence of  $a$  on the polymerization temperature at 80 mmole  $Zn(C_2H_5)_2$ /l.  $n$ -heptane.

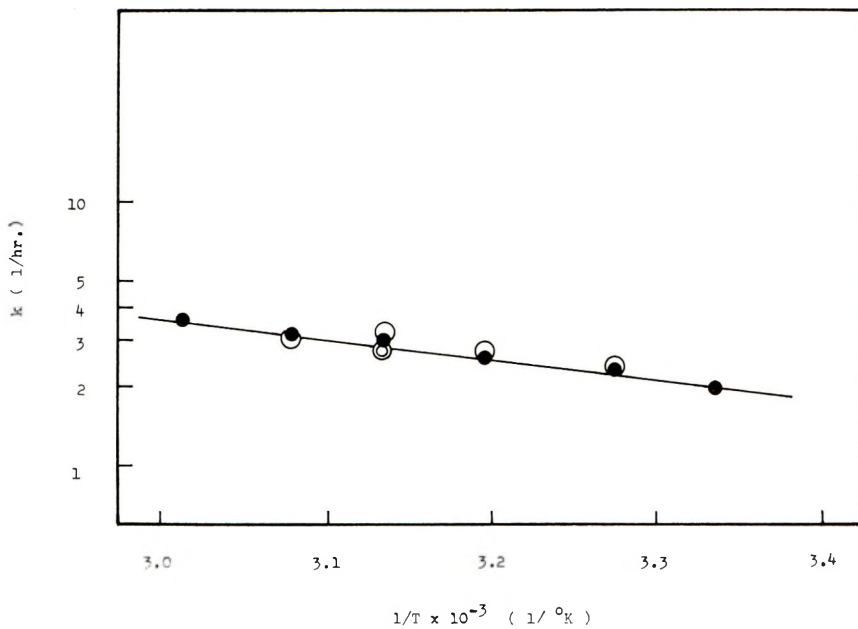


Fig. 6. Plots of  $k$  against  $1/T$  at various concentrations of  $Zn(C_2H_5)_2$  in  $n$ -heptane: (●) 80 mmole/l.; (⊙) 28 mmole/l.; (○) 16 mmole/l.

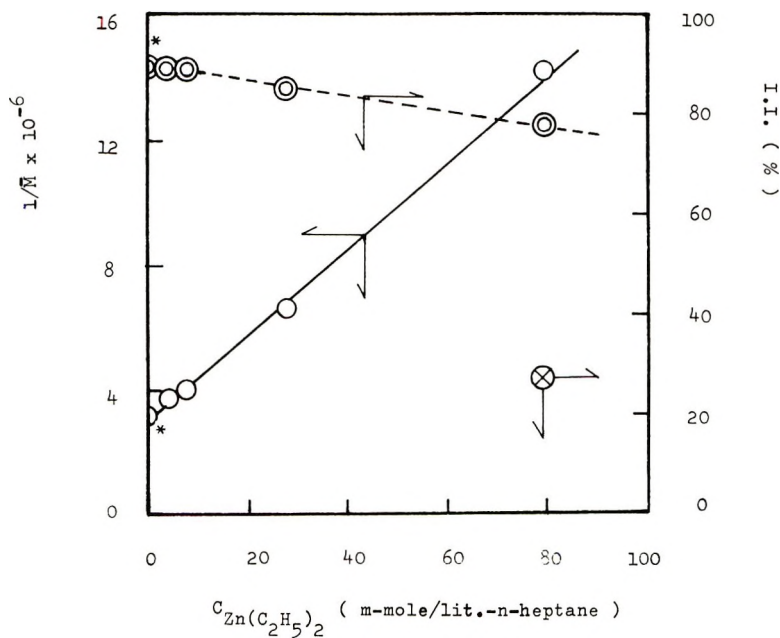


Fig. 7. Molecular weights and tacticities of polymers obtained at  $43.5^\circ\text{C}$ .: (⊙) determined by infrared method, (●) by extraction; (\*) experiment carried out in the absence of solute  $Zn(C_2H_5)_2$ .

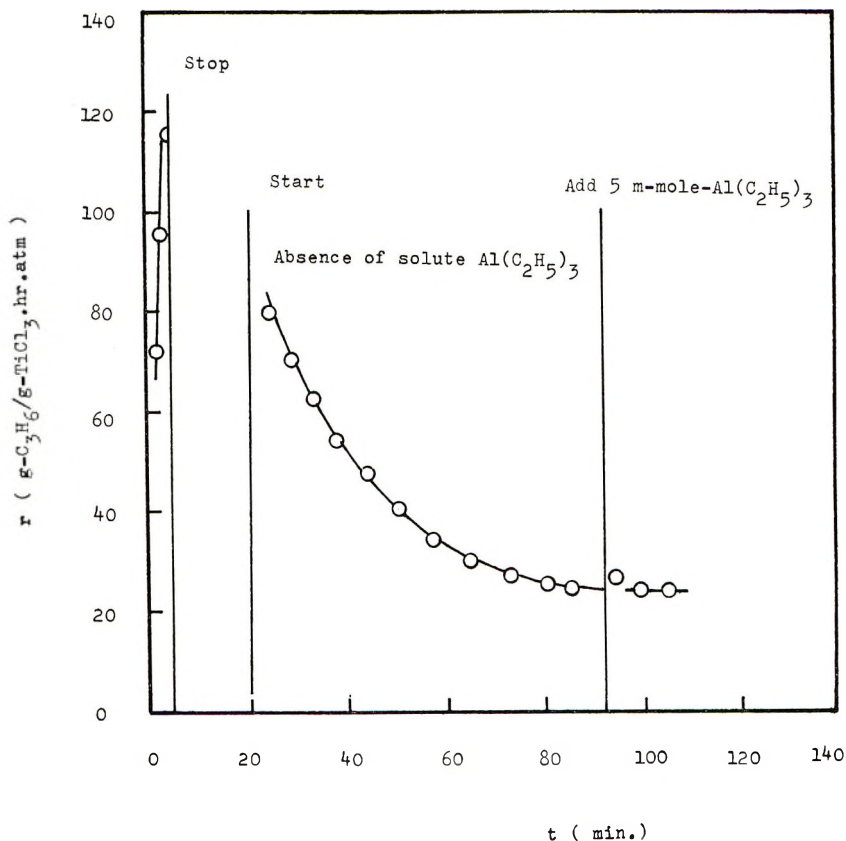


Fig. 8. Polymerization rate in the absence of solute  $\text{Al}(\text{C}_2\text{H}_5)_3$ .  $\text{TiCl}_3 = 0.7$  g., *n*-heptane = 250 ml., initial concentration of  $\text{Al}(\text{C}_2\text{H}_5)_3 = 20$  mmole/l.,  $\text{Al}/\text{Ti} = 1$ ,  $50^\circ\text{C}$ .

weights and the concentration of  $\text{Zn}(\text{C}_2\text{H}_5)_2$ , which proves the monomeric property of  $\text{Zn}(\text{C}_2\text{H}_5)_2$ .

$$1/\bar{M} = \alpha + \beta C \quad (9)$$

where  $\bar{M}$  is the viscosity-average molecular weight,  $C$  the concentration of  $\text{Zn}(\text{C}_2\text{H}_5)_2$ , and  $\alpha$  and  $\beta$  are constants.

#### Polymerization in the Absence of Solute $\text{Zn}(\text{C}_2\text{H}_5)_2$

It has been pointed out<sup>4</sup> that propylene is polymerized almost independently of the concentration of  $\text{Al}(\text{C}_2\text{H}_5)_3$  after the polymerization centers have been established in the presence of propylene monomer at a higher concentration of  $\text{Al}(\text{C}_2\text{H}_5)_3$  ( $\text{Al}/\text{Ti} \geq 1$ ), as shown in Figure 8.

Similar experiments were carried out here with active  $\text{TiCl}_3\text{-Zn}(\text{C}_2\text{H}_5)_2$  as follows. The usual polymerization was carried out for about 10 min. and then the propylene in the reaction vessel was replaced with nitrogen.



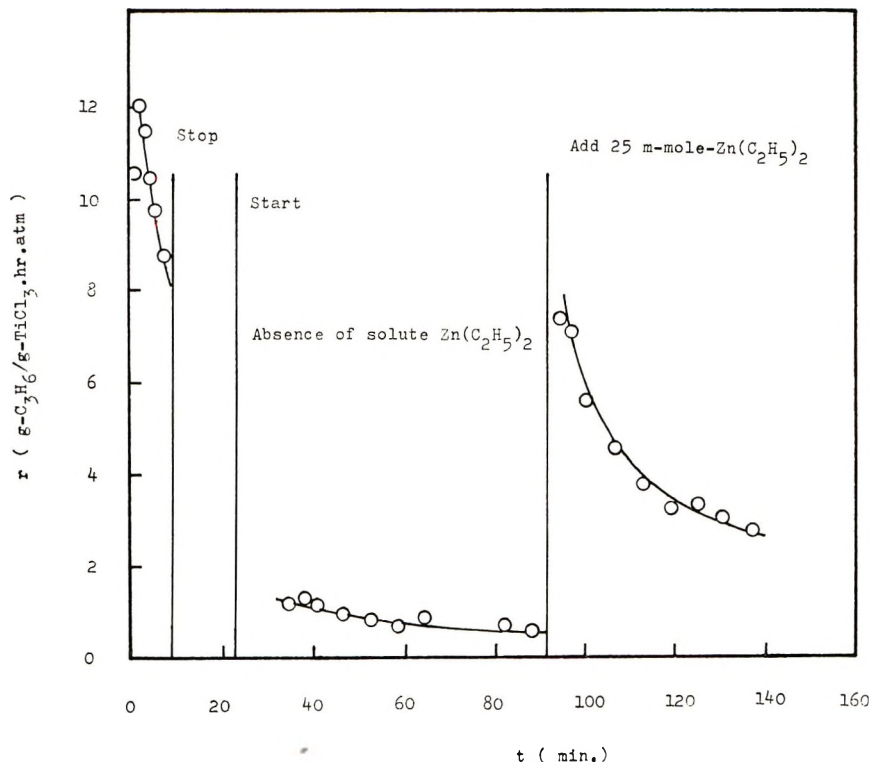


Fig. 9. Polymerization rate in the absence of solute  $\text{Zn}(\text{C}_2\text{H}_5)_2$ .  $\text{TiCl}_3 = 1 \text{ g.}$ ,  $n$ -heptane = 250 ml., initial concentration of  $\text{Zn}(\text{C}_2\text{H}_5)_2 = 80 \text{ mmole/l.}$ ,  $\text{Zn/Ti} = 2.5$ ,  $43.5^\circ\text{C.}$

After the solution was filtered completely, an equal amount of solvent was again added under nitrogen atmosphere and then polymerization was started by replacing the nitrogen with propylene, without adding any further  $\text{Zn}(\text{C}_2\text{H}_5)_2$ .

The results obtained are shown in Figure 9, the reproducibility of which was very good. The molecular weight and the tacticity of the polymer obtained after 80 min. (the same total polymerization period as in the usual polymerization) are shown in Figure 7.

## DISCUSSION

As stated in the introduction, the results are discussed here mainly in comparison with those obtained with active  $\text{TiCl}_3\text{-Al}(\text{C}_2\text{H}_5)_3$ . Generally speaking, the kinetic behaviors are similar to each other. Figure 4 indicates that adsorption of  $\text{Zn}(\text{C}_2\text{H}_5)_2$  on the surface of  $\text{TiCl}_3$  is of the Langmuir type with a heat of adsorption of 3 kcal./mole.\*

\* The authors have used the word "adsorption" for the sake of convenience, but it is uncertain just what reactions actually are involved.

This value is close to the one (1.8 kcal./mole) which was obtained calorimetrically by Boor.<sup>7</sup> The values of the adsorption constant  $a$  at 43.5°C. are 140 l./mole  $\text{Al}(\text{C}_2\text{H}_5)_3$  and 40 l./mole  $\text{Zn}(\text{C}_2\text{H}_5)_2$ . It is very interesting that a remarkable difference can be seen between the activation energy of  $B$  (2.7 kcal./mole) with  $\text{Zn}(\text{C}_2\text{H}_5)_2$  and that (10 kcal./mole) with  $\text{Al}(\text{C}_2\text{H}_5)_3$ . Taking into account the heat of solution of propylene in  $n$ -heptane (3.8 kcal./mole), we have 6.5 and 13.8 kcal./mole as the activation energy for propylene in the solution. The value (6.5 kcal./mole) is close to the one (8.2 kcal./mole) obtained by Firsov and Chirkov.<sup>8</sup>

It is well known that  $\text{Zn}(\text{C}_2\text{H}_5)_2$  is a good chain-transfer agent.<sup>1</sup> Accordingly, it is natural that molecular weight should be less if  $\text{Zn}(\text{C}_2\text{H}_5)_2$  is employed instead of  $\text{Al}(\text{C}_2\text{H}_5)_3$ .

But we think it significant to compare the molecular weight (about 280,000) of the polymer obtained in the absence of  $\text{Zn}(\text{C}_2\text{H}_5)_2$  solute (polymerization period 90 min. at 43.5°C.) with that (about 800,000) obtained in the absence of  $\text{Al}(\text{C}_2\text{H}_5)_3$  solute (90 min. at 43.5°C.). In these cases it may be considered that the rate of chain transfer becomes very small and that the mean lifetime of the "living" polymer becomes long, perhaps longer than 90 min. Accordingly, the ratio of these molecular weights (280,000/800,000) may be considered nearly to correspond to the ratio of propagation rates. Thus we have found that the growth rate of the polymer chains with  $\text{Al}(\text{C}_2\text{H}_5)_3$  is about three times that with  $\text{Zn}(\text{C}_2\text{H}_5)_2$  at 43.5°C.

The difference between Figures 8 and 9 shows that the polymerization centers formed with  $\text{Zn}(\text{C}_2\text{H}_5)_2$  are much more unstable than those with  $\text{Al}(\text{C}_2\text{H}_5)_3$ .

From above, we may conclude that the structure of the polymerization centers formed with  $\text{Al}(\text{C}_2\text{H}_5)_3$  is different from that with  $\text{Zn}(\text{C}_2\text{H}_5)_2$  and that the former corresponds to the structure I while the latter corresponds to structure II.

In order to confirm this suggestion, further more studies must be done.

On the other hand, Figure 7 shows that the isotacticity with  $\text{Zn}(\text{C}_2\text{H}_5)_2$  measured by the infrared method is at least as great as that with  $\text{Al}(\text{C}_2\text{H}_5)_3$ , while that measured by extraction is very small, which can be understood on the basis of the molecular weight.<sup>9</sup>

### References

1. G. Natta and I. Pasquon, *Adv. Catalysis*, **11**, 1 (1959).
2. E. J. Arlman and P. Cossee, *J. Polymer Sci.*, **3**, 99 (1964).
3. J. Boor, Jr., in *First Biannual American Chemistry Society Polymer Symposium (J. Polymer Sci. C, 1)*, H. W. Starkweather, Jr., Ed., Interscience, New York, 1963, p. 237.
4. T. Keii, K. Soga, and N. Saiki, paper presented at International Symposium on Macromolecular Chemistry, Prague 1965.
5. T. Keii, M. Taira, and T. Takagi, *Can. J. Chem.*, **41**, 206 (1963).
6. J. P. Luongo, *J. Appl. Polymer Sci.*, **3**, 302 (1960).
7. J. Boor, Jr. and E. A. Youngman, *J. Polymer Sci. B*, **2**, 265 (1965).
8. A. P. Firsov and N. M. Chirkov, *Izv. Akad. Nauk SSSR, Ser. Khim.*, **11**, 741 (1964).
9. G. Natta, P. Pino, and G. Mazzanti, *J. Polymer Sci. B*, **2**, 443 (1964).

### Résumé

En vue d'élucider la structure des centres de polymérisation de Ziegler-Matta, nous avons effectué certaines études cinétiques sur la polymérisation du propylène avec un catalyseur actif à base de  $\text{TiCl}_3\text{-Zn}(\text{C}_2\text{H}_5)_2$ , dans un domaine de température allant de 25 à 56°C et dans un domaine de concentration en  $\text{Zn}(\text{C}_2\text{H}_5)_2$  variant de  $4 \times 10^{-3}$  mole/l à  $8 \times 10^{-2}$  et nous avons comparé ces résultats avec ceux obtenus avec le système  $\text{TiCl}_3\text{-Al}(\text{C}_2\text{H}_5)_3$ . Des différences ont été trouvées entre elles: (1) l'énergie d'activation de la vitesse de polymérisation stationnaire est de 6,5 kcal/mole pour le zinc-diéthylé et 13,8 kcal/mole pour l'aluminium-triéthylé. (2) La vitesse de propagation des chaînes polymériques avec le zinc-diéthylé est environ 3 fois plus lente à 43,5°C. (3) Les centres de polymérisation formés avec le zinc-diéthylé sont beaucoup plus instables. On en conclut que la structure des centres de polymérisation avec le zinc-diéthylé est différente de celle avec l'aluminium triéthylé.

### Zusammenfassung

Um die Struktur der Ziegler-Natta-Polymerisationszentren aufzuklären, wurde eine kinetische Untersuchung der Propylenpolymerisation mit aktivem  $\text{TiCl}_3\text{-Zn}(\text{C}_2\text{H}_5)_2$  im Temperaturbereich von 25 bis 56°C und im Konzentrationsbereich von  $\text{Zn}(\text{C}_2\text{H}_5)_2$  von  $4 \cdot 10^{-3}$  bis  $8 \cdot 10^{-2}$  Mol/l ausgeführt. Die Ergebnisse wurden mit den mit aktivem  $\text{TiCl}_3\text{-Al}(\text{C}_2\text{H}_5)_3$  erhaltenen verglichen. Folgende Unterschiede wurden festgestellt: (1) Die Aktivierungsenergie der stationären Polymerisationsgeschwindigkeit ist für  $\text{Zn}(\text{C}_2\text{H}_5)_2$  6,5 kcal/Mol und für  $\text{Al}(\text{C}_2\text{H}_5)_3$  13,8 kcal/Mol; (2) Die Wachstumsgeschwindigkeit ist mit  $\text{Zn}(\text{C}_2\text{H}_5)_2$  bei 43,5°C etwa dreimal langsamer und (3) die mit  $\text{Zn}(\text{C}_2\text{H}_5)_2$  gebildeten Polymerisationszentren sind weniger stabil. Es kann geschlossen werden, dass die Struktur der Polymerisationszentren mit  $\text{Zn}(\text{C}_2\text{H}_5)_2$  von derjenigen mit  $\text{Al}(\text{C}_2\text{H}_5)_3$  verschieden ist.

Received December 2, 1965

Revised February 4, 1966

Prod. No. 5084A

## Electron Spin Resonance Studies on Ziegler-Natta Type Catalyst Systems

YOSHIO ONO and TOMINAGA KEII,  
*Department of Chemical Engineering,  
Tokyo Institute of Technology, Meguro, Tokyo, Japan*

### Synopsis

Electron spin resonance spectra of Ziegler-Natta type catalyst systems (titanium trichloride and alkyl aluminums) have been studied. When triethylaluminum was added to titanium trichloride, an absorption with a  $g$  value of 1.96 was observed from the solid phase of the system. The number of spins of this signal is equal to that of the active centers for propylene polymerization. The solid phase from the mixture of titanium trichloride and diethylaluminum chloride also gives the same signal, which suggests the identity of the action of two alkyl aluminums on titanium trichloride surface. The signals obtained from the liquid phase of the both systems are all ascribed to the reaction products of the reaction of alkyl aluminum with titanium tetrachloride occluded in solid.

### INTRODUCTION

Ziegler-Natta type catalyst systems, i.e., titanium tetra- or trichloride and alkyl aluminums, are well known as catalysts for the stereospecific polymerization of  $\alpha$ -olefins. Although many studies have been carried out, the nature of the polymerization center is not yet completely established. The electron spin resonance (ESR) technique is very useful for catalyst systems which involve a transition metal such as Ti. ESR studies on Ziegler-Natta catalyst systems have been carried out by many authors.<sup>1-4</sup> However, the systems investigated are rather limited to some homogeneous systems, such as biscyclopentadienyltitanium dichloride-alkyl aluminum systems. The purpose of the present study is to obtain some information on heterogeneous systems such as titanium trichloride and alkyl aluminums.

### EXPERIMENTAL

The titanium trichloride used was from Stauffer Co. (AA Grade) and its specific surface area, measured by nitrogen adsorption method, was 21 m.<sup>2</sup>/g. Triethylaluminum and diethylaluminum chloride (Ethyl Corp.) was purified by distillation.

Titanium trichloride and a 10% heptane solution of alkyl aluminum were mixed in an ESR sample tube (4 mm. in diameter) under a nitrogen atmosphere. In cases in which it was necessary to take the spectra of the

solid phase and the liquid phase of the mixture separately, ca. 5 ml. of alkyl aluminum and 1 g. of titanium trichloride were well mixed in a precipitation tube, and the two phases were separated by a centrifuge and then transferred to sample tubes.

The ESR measurements were carried out at room temperature with a JES-3110-X spectrometer with 100 kc./sec. field modulation.

## RESULTS AND DISCUSSION

### Titanium Trichloride-Triethylaluminum System

Titanium trichloride itself showed two absorptions. One is sharp ( $\Delta H_{msl} = 15$  gauss) with a  $g$  value of 1.94 and the other is very broad. The number of unpaired electrons of the former was measured as  $2 \times 10^{16}/g$ .

When triethylaluminum solution was added to titanium trichloride, a spectrum with two new absorptions was obtained as shown in Figure 1*a*. Intensity of the narrower signal gradually increased with time, while the other remained unchanged with time. To determine in which phase the species giving these absorptions is located, the spectra of the solid and the liquid phases were measured separately. An asymmetric absorption

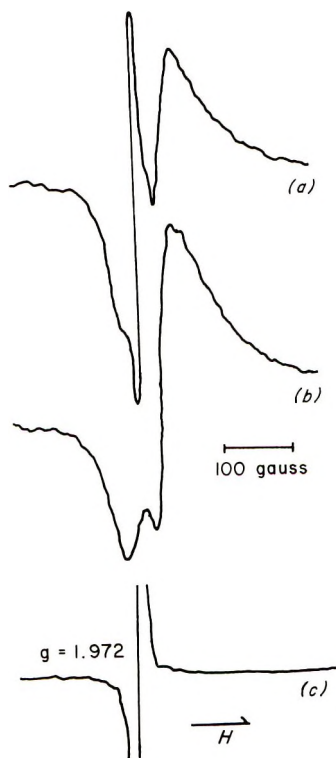


Fig. 1. ESR spectra from  $TiCl_3-Al(C_2H_5)_3$  system: (a)  $TiCl_3-Al(C_2H_5)_3$  mixture; (b) solid phase; (c) liquid phase.

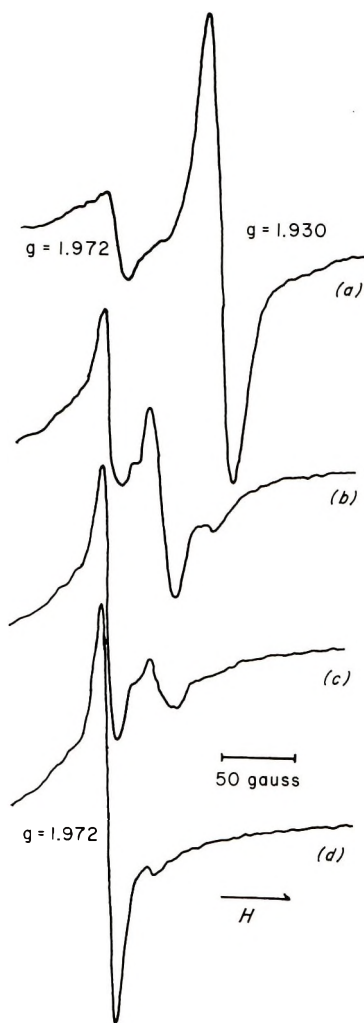


Fig. 2. Change in ESR spectrum from  $\text{TiCl}_4\text{-Al}(\text{C}_2\text{H}_5)_3$  mixture with time. Reaction time increases from (a) to (d).

with a  $g$  value of 1.96 was found from the solid phase (Fig. 1b). Its number of spins was  $1 \times 10^{20}/\text{g}$ . If the number is calculated from the surface area of titanium trichloride, we have spin numbers ( $5 \times 10^{14}/\text{cm}^2$ ) which correspond to the number of surface-active centers for propylene polymerization.<sup>5-7</sup> The liquid phase showed a sharp absorption with a  $g$  value of 1.972 and  $\Delta H_{\text{msl}}$  of 19 gauss, which has the hyperfine structure due to  $^{47}\text{Ti}$  and  $^{49}\text{Ti}$  nuclei (Fig. 1c). On comparing Figure 1a with Figure 1b, it is clear that the narrower signal in Figure 1a is due to the liquid phase and the other to the solid phase.

Triethylaluminum and titanium tetrachloride were mixed in a sample tube and the change in the ESR spectrum was followed with time. As

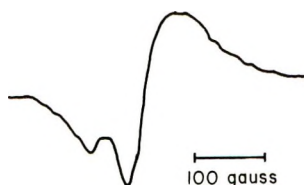


Fig. 3. ESR spectrum of the precipitate from  $\text{TiCl}_4\text{-Al}(\text{C}_2\text{H}_5)_3$  mixture.

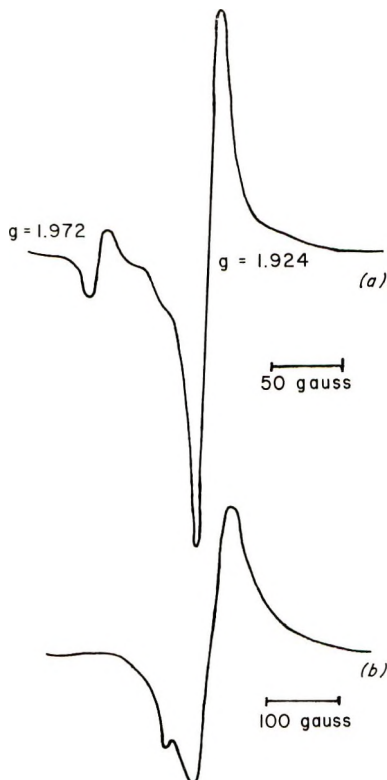


Fig. 4. ESR spectra of (a)  $\text{TiCl}_3\text{-Al}(\text{C}_2\text{H}_5)_2\text{Cl}$  mixture and (b) solid phase separated from the mixture.

shown in Figure 2, the spectrum changed with time and finally a spectrum with an absorption with a  $g$  value of 1.972, of which the intensity was remained unchanged, was obtained. The precipitate separated from the mixture showed an asymmetric absorption (Fig. 3). It is identical with the absorption shown in Figure 1*b*; that obtained from the solid phase of titanium trichloride-triethylaluminum mixture. The absorption with a  $g$  value of 1.972 may be assigned to one of the reaction products between triethylaluminum and titanium tetrachloride which is occluded in titanium trichloride.

The ESR measurement was carried out on a sample of titanium trichloride which had been evacuated at  $150^\circ\text{C}$ . for 2 hr. In this case, an

asymmetric absorption with a  $g$  value of 1.96 appeared immediately after mixing of the titanium trichloride and triethylaluminum, while the absorption with a  $g$  value of 1.972 appeared later. Thus, it may be concluded that the absorption with a  $g$  value of 1.96 is attributed to a surface of trivalent titanium on which triethylaluminum is adsorbed, and the other absorption with a  $g$  value of 1.972 is attributed to one of the reaction products between occluded tetrachloride and triethylaluminum.

### Titanium Trichloride-Diethylaluminum Chloride System

The spectrum shown in Figure 4a was obtained when 10% *n*-heptane solution of diethylaluminum chloride was added to titanium trichloride. The liquid phase of this system showed the same spectrum as the mixture, whereas the solid phase showed a different spectrum, which is similar to that of the solid phase from the titanium trichloride-triethylaluminum system (Fig. 4b). This strongly suggests that the action of diethylaluminum chloride on titanium trichloride is essentially the same as that of triethylaluminum. The weak absorption from the solid phase might be masked by the strong absorption from the liquid. Here should be noted the contradictory results reported by Adema et al.<sup>3,4</sup> who found no unpaired electrons in the ESR spectrum of the part of the precipitate from the titanium tetrachloride-diethylaluminum chloride system.

The liquid phase of this system gave an absorption with a  $g$  value of 1.924 ( $\Delta H_{msl} = 19$  gauss) as well as the one with a  $g$  value of 1.972 (Fig. 4a). The former absorption has been also recognized in the spectrum of the reaction mixture from titanium tetrachloride and diethylaluminum chloride.<sup>3,4</sup> Therefore, this absorption can be ascribed to one of the reaction products from these two compounds.

### SUMMARY AND CONCLUSIONS

(1) When triethylaluminum was added to titanium trichloride, an ESR absorption signal with a  $g$  value of 1.96 was observed in the solid phase of the reaction mixture.

(2) The number of the species giving this signal is equal to the number of the active centers of titanium trichloride for propylene polymerization.

(3) The action of diethylaluminum chloride on titanium trichloride is essentially the same as that of triethylaluminum.

Further experiments concerned with the nature of interaction between alkyl aluminum and the titanium trichloride surface are in progress.

### References

1. A. K. Zefirova, N. N. Tikhomirova, and A. E. Shilov, *Dokl. Akad. Nauk SSSR*, **132**, 1082 (1960).
2. A. U. Maki and E. W. Randall, *J. Am. Chem. Soc.*, **82**, 4109 (1960).
3. E. H. Adema, H. J. M. Bartelink, and J. Smidt, *Rec. Trav. Chim.*, **80**, 173 (1961).
4. E. H. Adema et al., *Rec. Trav. Chim.*, **81**, 73, 223 (1962).



5. E. Arlman, *J. Catalysis*, **3**, 89 (1964).
6. E. Arlman and P. Cossee, *J. Catalysis*, **3**, 99 (1964).
7. T. Keii, K. Soga, and N. Saiki, paper presented to International Congress on High Polymers, Prague, 1965.

### Résumé

Les spectres de résonance de spin électronique de systèmes catalyseurs du type Ziegler-Natta contenant du chlorure de titane et de l'alkyl-aluminium ont été étudiés. Lorsque le triéthylaluminium est additionné au trichlorure de titane, une absorption avec une valeur  $g$  de 1.96 a été observée au départ de la phase solide du système. Le nombre de spins de ce signal est égal à celui des centres actifs en cours de polymérisation du propylène. La phase solide au départ des mélanges de trichlorure de titane et de chlorure d'aluminium-diéthyle donne également le même signal, ce qui suggère la nature de l'action de deux aluminium-dialkyle sur la surface du trichlorure de titane. Les signaux obtenus au départ de la phase liquide des deux systèmes sont tous attribués au produit de réaction de la réaction de l'alkyl-aluminium avec le tétrachlorure de titane occlu au sein du solide.

### Zusammenfassung

Elektronenspinresonanzspektren von Katalysatorsystemen aus Titantrichlorid und Aluminiumalkylen wurden untersucht. Bei Zusatz von Triäthylaluminium zu Titantrichlorid wurde an der festen Phase des Systems eine Absorption mit einem  $g$ -Wert von 1,96 beobachtet. Die Zahl der Spins dieses Signals ist der Zahl der aktiven Zentren für die Propylenpolymerisation gleich. Die feste Phase bei der Mischung von Titantrichlorid und Diäthylaluminiumchlorid liefert das gleiche Signal, was für eine gleichartige Wirkung der beiden Aluminiumverbindungen auf die Titanchloridoberfläche spricht. Die an der flüssigen Phase beider Systeme erhaltenen Signale werden alle den Reaktionsprodukten der Reaktion zwischen Aluminiumalkyl und dem im Festkörper okkludierten Titan-tetrachlorid zugeschrieben.

Received December 9, 1965

Revised March 2, 1966

Prod. No. 5116A

## Rates of Copolymerization of Acrylonitrile and Ethylenesulfonic Acid

TURNER ALFREY, JR. and CHARLES R. PFEIFER,  
*The Dow Chemical Company, Williamsburg, Virginia*

### Synopsis

Use was made of differential absorption in the near-infrared region to follow the rates of copolymerization of acrylonitrile (AN,  $M_1$ ) with ethylenesulfonic acid (ESA,  $M_2$ ) in aqueous zinc chloride solution. The concentrations of the monomers were followed separately and simultaneously. It was found experimentally that the ratios  $d \log [M_1]/dt$  and  $d \log [M_2]/dt$  were each constant. This was interpreted to mean that the product of the reactivity ratios of the two monomers ( $r_1 r_2$ ) is unity and that the ratio of termination rate constants is equal to the propagation reactivity ratio. It was found that  $d \log [M_1]/d \log [M_2] = r_1 = 4.52$ . This value is in fair agreement with polymer composition data obtained independently. In the  $Q-e$  system the equality  $r_1 r_2 = 1$  is equivalent to the monomers having equal  $e$  values. Thus, in the AN-ESA system,  $P_1/P_2 = k_{11}/k_{21} = k_{12}/k_{22} = k_{1T}/k_{2T}$ , where  $P_1$  is the resonance constant of polymer radicals ending in units of  $M_1$ ; and  $k_{11}$ ,  $k_{12}$ , and  $k_{1T}$  are the rate constants involving the reaction of this radical with  $M_1$ ,  $M_2$ , and T (terminating agent), respectively. A gel effect was not observed even at  $M_1$  conversions as high as 88%.

### INTRODUCTION

There is a lack of complete agreement in the literature concerning the order dependence on monomer concentration in polymerization of AN. The recent review of this subject by Thomas is helpful.<sup>1</sup> In systems involving precipitation of polymer from the polymerization medium the situation appears to be complicated by adsorption of monomer on polymer with a resulting monomer order dependency of 1.5–2.0.<sup>2–4</sup>

Polymerization of AN in homogenous solution has been shown to be first-order in monomer by Bamford<sup>5</sup> in kinetic analyses in dimethylformamide (DMF) and in DMF containing added lithium salts. Higher orders (up to 1.5) have been reported at low monomer concentration.<sup>6</sup> First-order monomer dependence was also found in bulk polymerization.<sup>7</sup>

Work done in this laboratory has been in agreement with that of Bamford, although we did not perform a thorough rate analysis. The first-order AN disappearance found here was always within a given batch polymerization, and it cannot be stated categorically that all other factors affecting reaction rate were constant during polymerization.

In our observations of copolymerizations of AN with other monomers, we discovered that the near-infrared absorption spectra, which had previ-

ously been found useful in following rate of AN disappearance in this laboratory, could also be used to follow the simultaneous disappearance of ESA.

## EXPERIMENTAL

### Polymerizations

Polymerizations were carried out in the following manner. The desired amounts of monomers (12–14 wt.-%) and solvent (86–88%) were shaken together in the presence of air. Mole fraction of ethylenesulfonic acid (ESA) in the AN–ESA mix ranged from 0.081 to 0.315. Catalyst solution was added and the solution shaken quickly but thoroughly.

A portion of this solution was transferred immediately to the optical cell which was then placed in a jacketed cell-holder maintained at 60°C. in the instrument. After allowing the few minutes found necessary for the sample to reach jacket temperature, the spectrum was scanned from 2150 to 2350  $m\mu$ . The reference cell had previously been filled with solvent and inserted in its proper position also at 60°C.

### Materials

The monomers were used within 2 weeks after distillation. Acrylonitrile (AN) from Monomer-Polymer Laboratories was distilled through a 2-ft., glass helice-packed column. A narrow fraction, b.p. 77.3°C., was collected and stored at approximately –15°C. prior to use. Ethylenesulfonic acid (ESA) from The Dow Chemical Company, prepared in a manner similar to that reported by Breslow et al., was treated with charcoal (Norite A) and distilled at reduced pressure in a rotating evaporator apparatus to give a colorless liquid (b.p.  $\sim$ 110°C./0.5 mm.). The solvent used was a 60-wt.-% solution of zinc chloride. Catalysts used were either azobisisobutyronitrile (0.8–2.9% based on monomers) or hydrogen peroxide (0.2% based on monomers). The chain-terminating agent used was either thio-glycolic acid (with the AIBN catalyst) or copper ion (with the peroxide catalyst).

### Spectra

Spectra were recorded on a Beckman Model DK-2 spectrophotometer equipped with a special jacketed cell-holder through which oil at 60°C. was circulated. This apparatus was shown to permit the warming of cell contents to 60°C. in approximately 5 min. Less time was anticipated in actual use due to liberated heat of polymerization. The matched rectangular Vycor-type cells (10  $\times$  10 mm. with 9  $\times$  9 mm. spacers) used were obtained from Pyrocell Corporation.

## RESULTS AND DISCUSSION

### Analysis of Spectra

Some illustrative spectra obtained in the 2150–2350  $m\mu$  region are given in Figure 1. During the course of copolymerization of AN and ESA, the

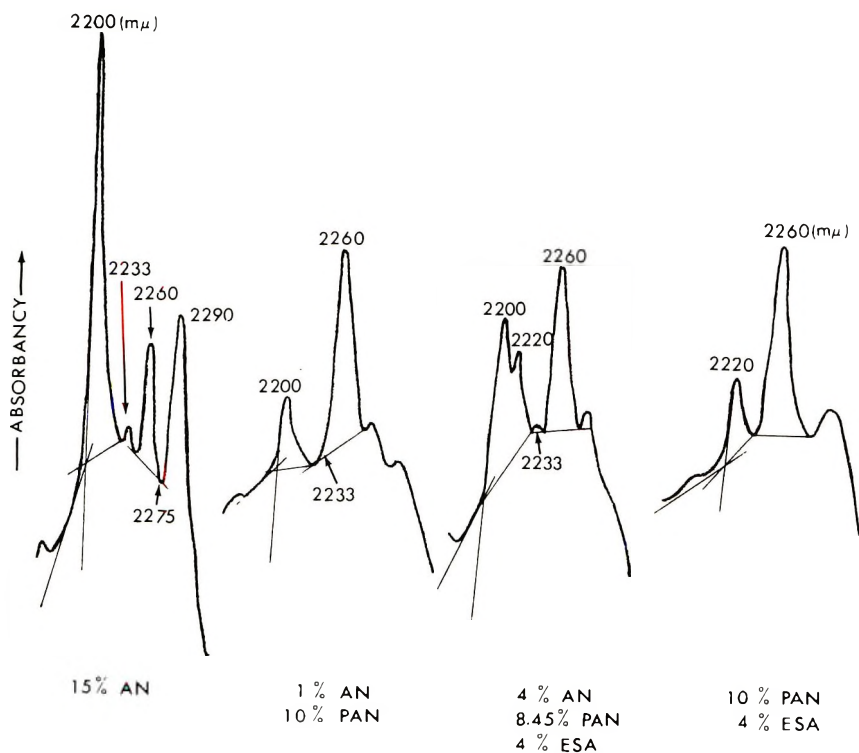


Fig. 1. Typical near-infrared spectra.

absorptions at 2200, 2220, and 2290  $m\mu$  diminish as the absorption at 2260  $m\mu$  increases. Although the latter is definitely associated with the formation of polyacrylonitrile we have never been able to eliminate it entirely from the AN monomer spectrum by purification.

A series of standard solutions was prepared simulating several stages of polymerization (increasing in polymer concentration with decreasing monomer concentrations). Another series was prepared without ESA. Analysis of the spectra of these standards led to the conclusion the AN concentration was correlated directly with absorbance at 2200  $m\mu$  (Fig. 2). Interference from neighboring absorption by ESA was negligible up to the 4% ESA level (percentage based on total solution weight) used in these solutions.

Correlation of ESA concentration with absorption data was complicated by strong interference or overlap of the AN peak at 2200  $m\mu$  with the ESA absorption at 2220  $m\mu$ . At high AN concentrations the ESA absorption was merely a shoulder on the 2200  $m\mu$  peak. This difficulty was overcome satisfactorily, however, by comparing the AN absorbancies at 2200 and 2220  $m\mu$  in the series without ESA. A linear relation was found (Fig. 3):

$$A_{2220 \text{ } m\mu} = 0.222A_{2200 \text{ } m\mu}$$

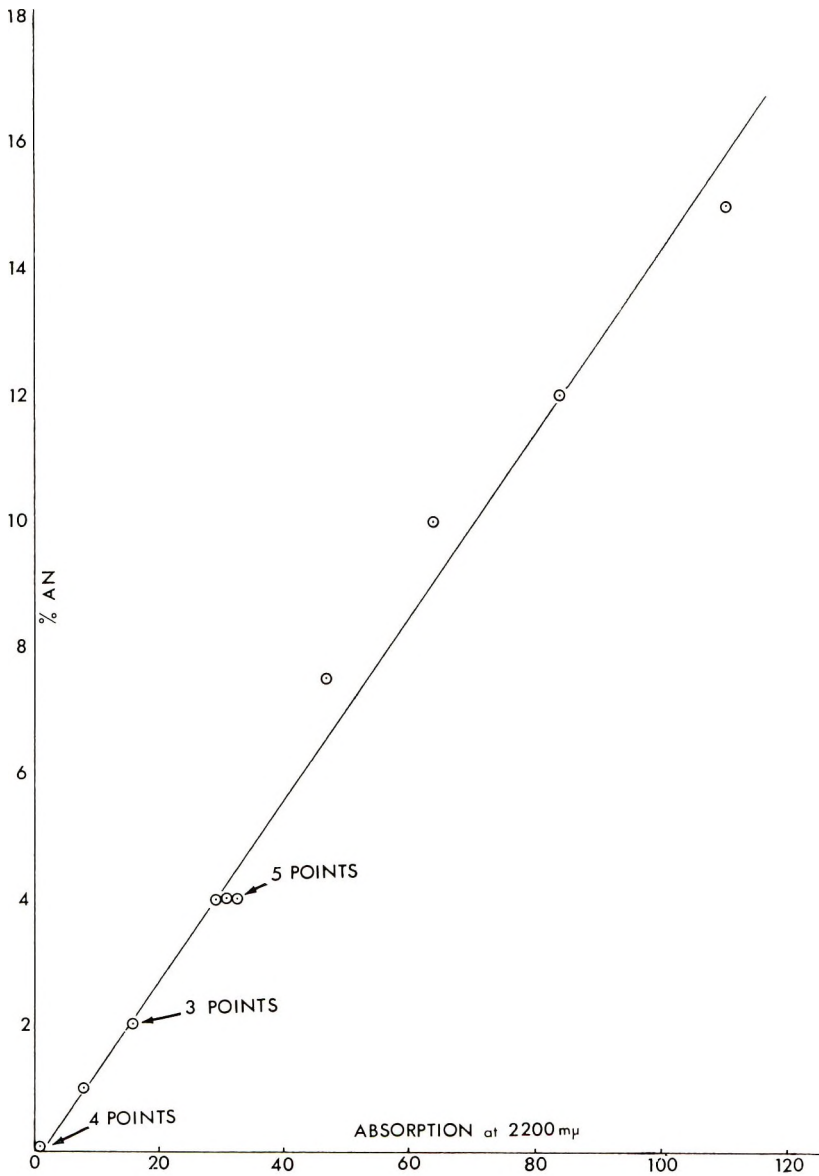


Fig. 2.  $A_{2200\text{m}\mu}$  vs. % AN.

Deduction of the AN absorbancy at 2220  $\text{m}\mu$  from the total 2220  $\text{m}\mu$  absorbancy gave a residual absorbancy at this frequency directly related to ESA concentration (Fig. 4).

#### Reaction Order

In view of the strict first-order dependency on monomer found within a given homopolymerization of AN, it was somewhat surprising to find that

during copolymerization of AN and ESA the disappearance of each monomer gave linear first-order rate plots (Figs. 5 and 6). Polymerization rates were obtained in the usual way from the slopes of these plots:

$$k = -d \log C/dt$$

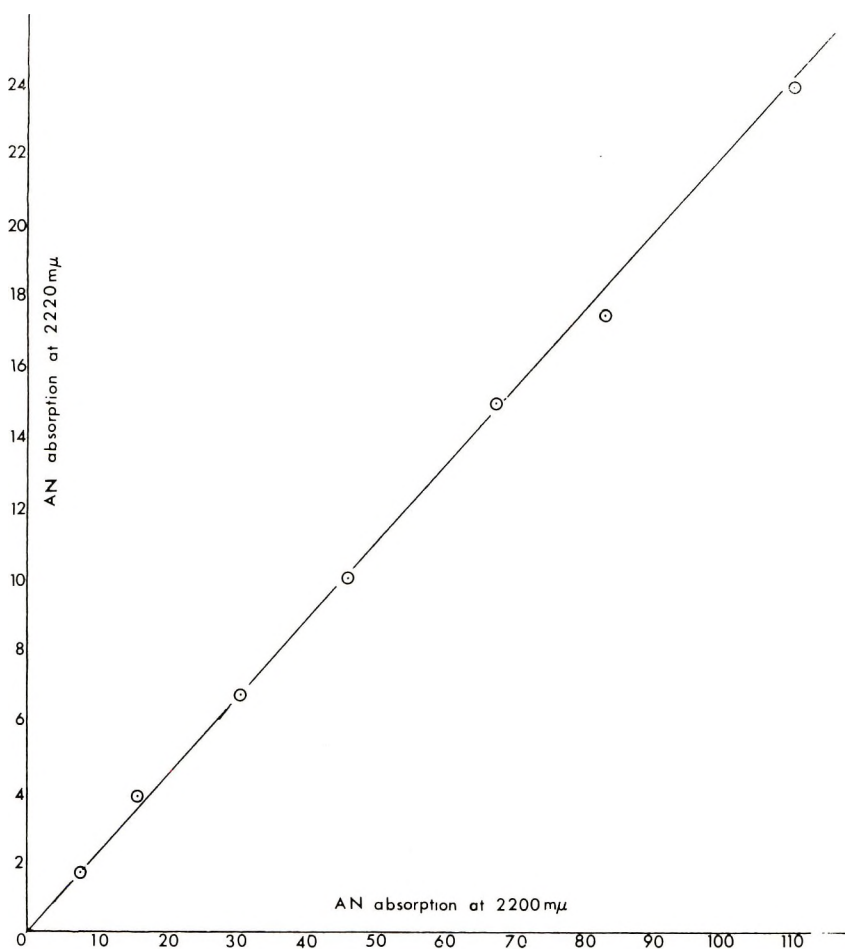


Fig. 3. AN absorption at 2220 mμ vs. AN absorption at 2200 mμ.

As can be seen from Figure 5, the near-infrared spectroscopic method was suitable for following polymerizations to high conversion.

A 1.7-order dependency on AN in aqueous zinc chloride with either AIBN or persulfate catalyst has been reported by Miyamichi et al.<sup>9</sup> We are not in agreement with their findings, however, as our AN disappearance data within a given run result in marked curvature when treated for 1.7-order kinetics (Fig. 7).

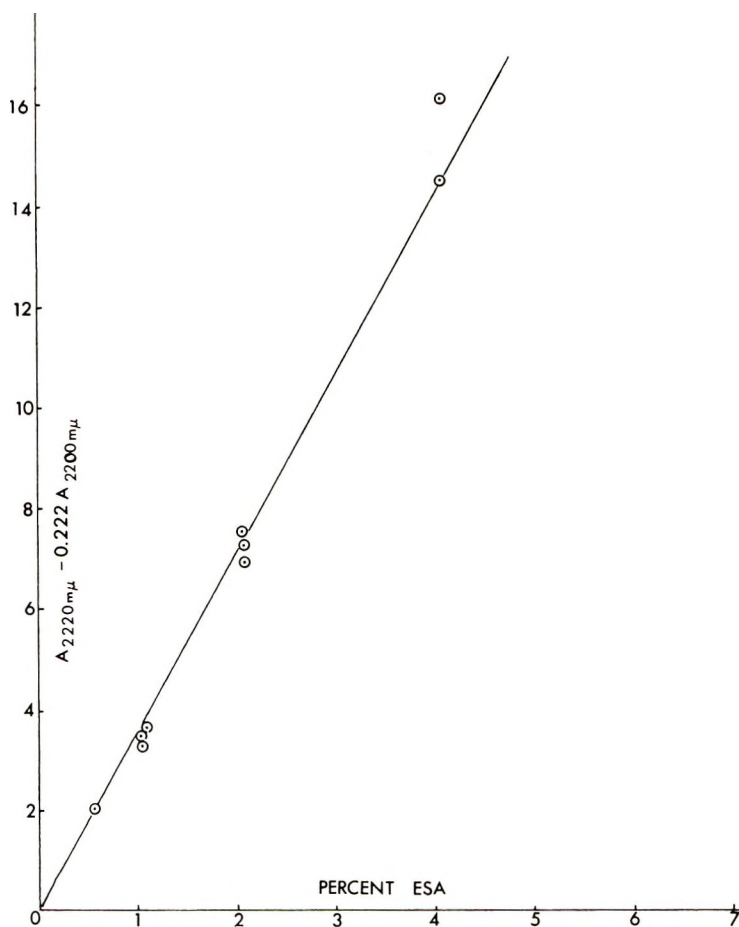


Fig. 4.  $A_{2220 m\mu} - 0.222 A_{2200 m\mu}$  vs. % ESA.

### Theoretical Model for Copolymerization

In the experimental study, it was observed that during the copolymerization of these two monomers the concentration of each monomer decreased exponentially with time. This apparent first-order disappearance of the individual monomers, even while a pronounced drift in monomer composition was taking place, was observed over an eightfold range of initial compositions. Such a simple kinetic pattern is not unusual in free-radical copolymerization, and calls for some mechanistic explanation.

The observed features of the aqueous acrylonitrile/ethylenesulfonic acid copolymerization can be generated theoretically from a reaction model encompassing the following plausible assumptions: (1) the rate of (catalyzed) initiation is constant throughout the reaction: (2) termination is by reaction of growing radicals with a chain terminator T, the concentration of which remains essentially constant throughout the reaction, i.e.,

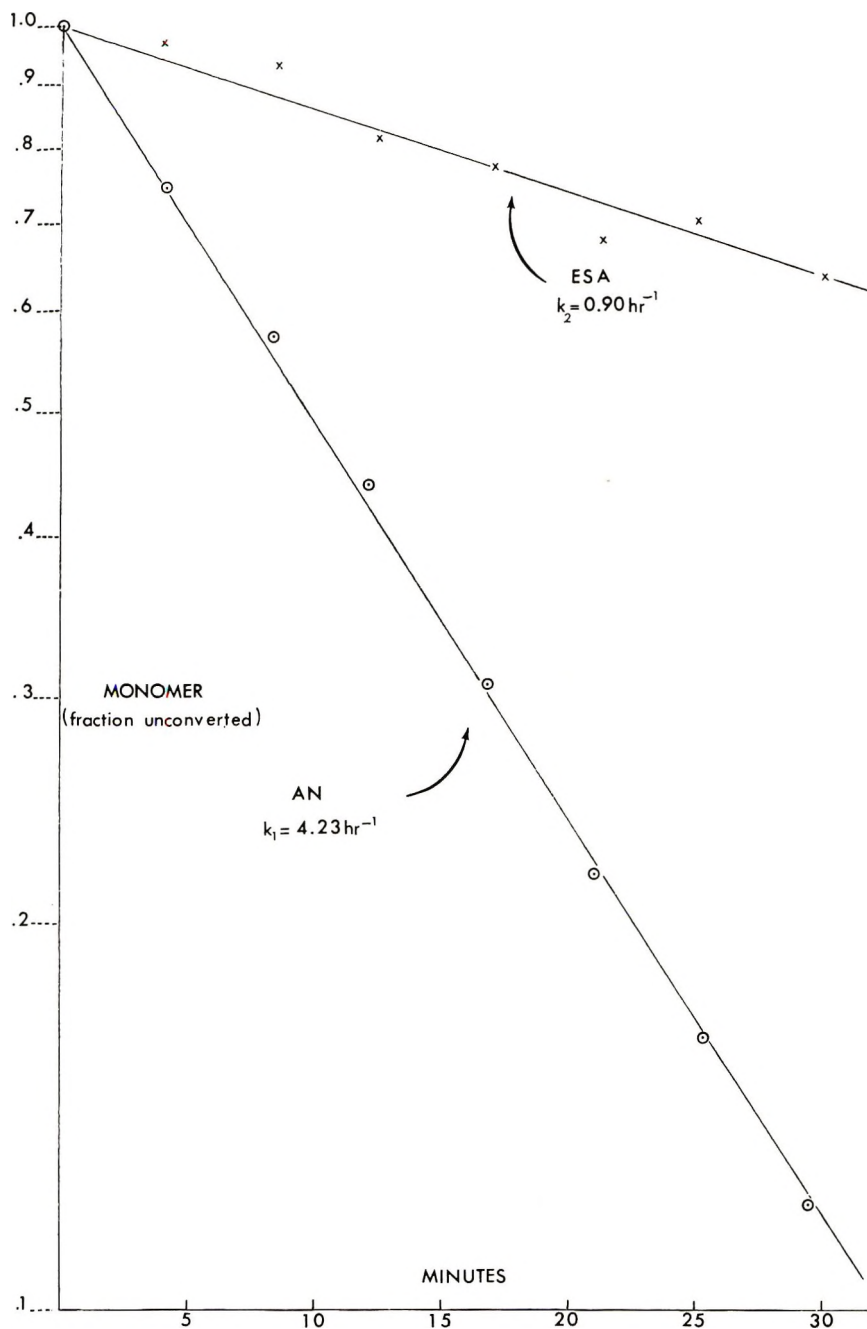
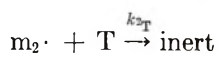
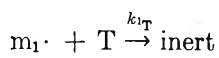


Figure 5.



(3) the reactivity ratio product,  $r_1r_2$ , is unity; (4) the ratio of termination rate constants is equal to a propagation reactivity ratio:

$$k_{1T}/k_{2T} = k_{11}/k_{21} \quad (1)$$

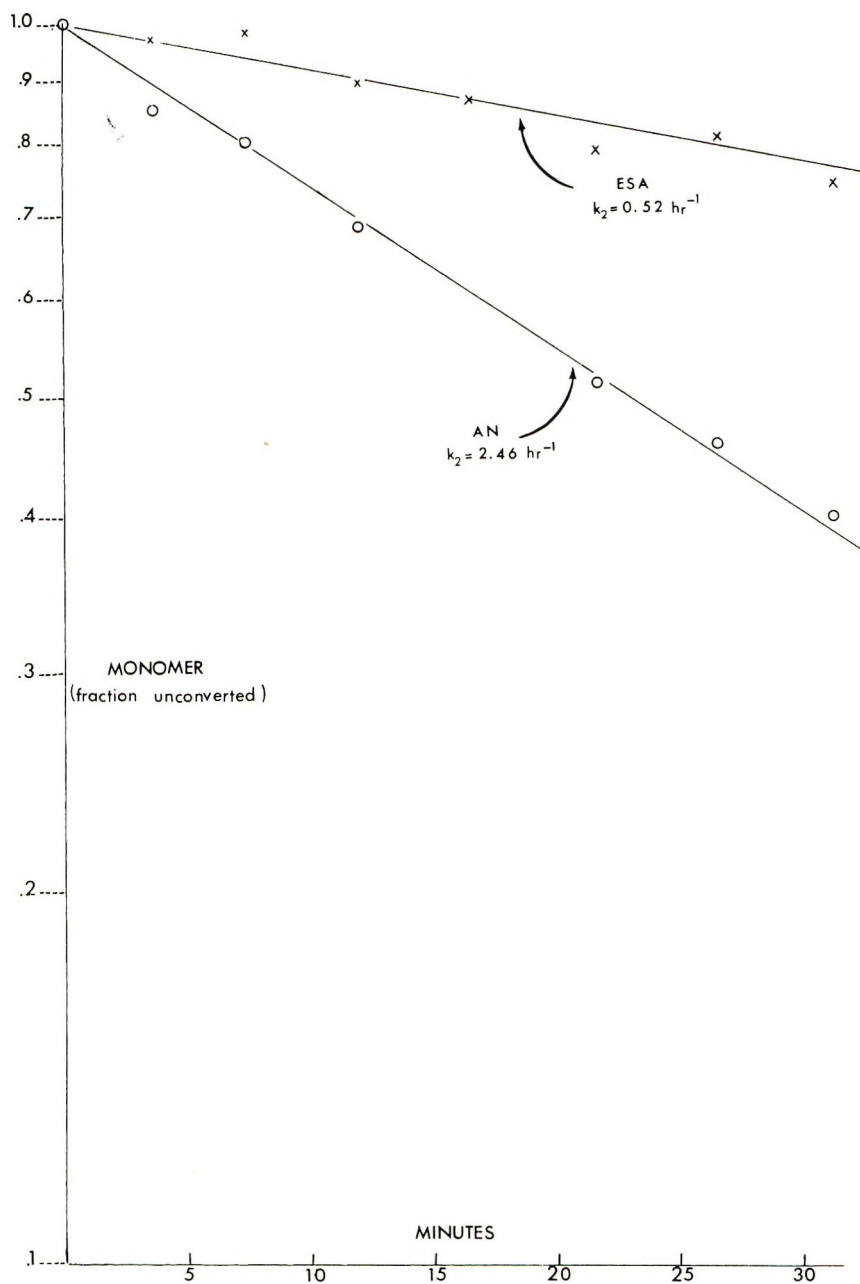


Figure 6.

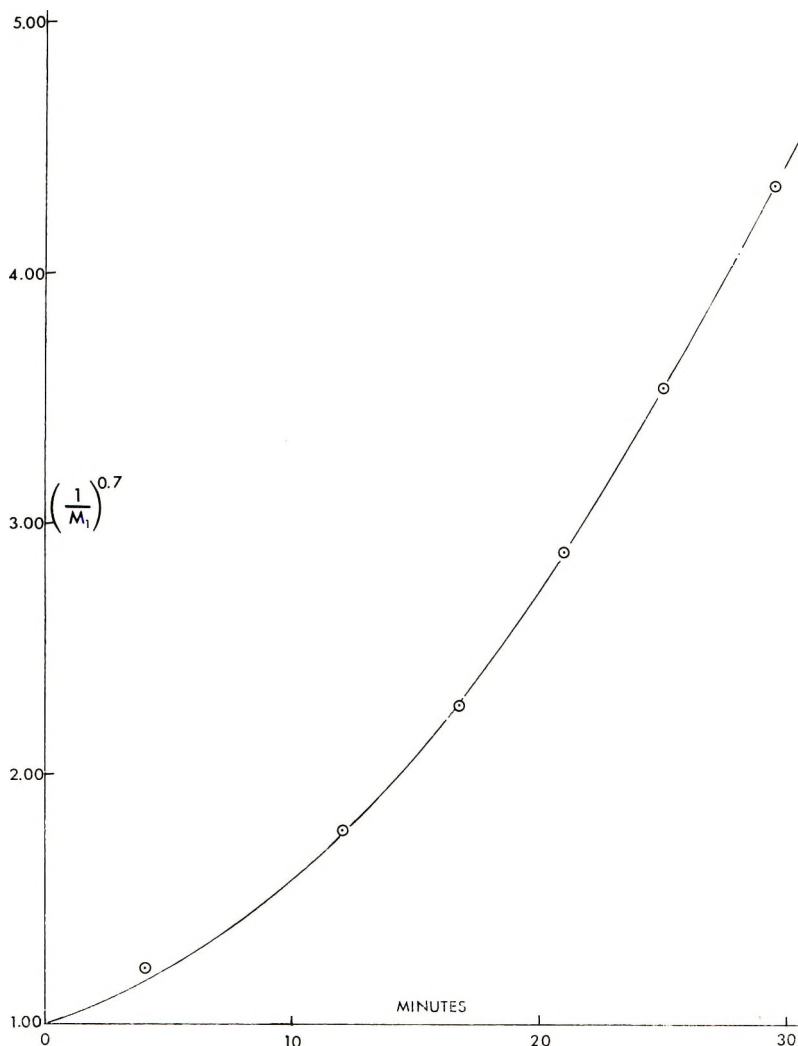


Fig. 7. Attempted fit of 1.7-order kinetics to copolymerization rate data.

Assumption (4) is somewhat unusual in form, since it relates reactivity ratios for two radicals competing for a common substrate rather than the more usual situation of two monomers competing for a common radical. However, if one is willing to invoke the  $Q-e$  scheme (for the termination reactions, as well as the propagation reactions), both assumptions (3) and (4) can be shown to follow from the single assumption that  $e_1 = e_2$  for these two monomers.\*

Let  $R_i$  be rate of initiation;  $k_{11}$ ,  $k_{12}$ ,  $k_{21}$ ,  $k_{22}$  are propagation rate constants;  $k_{1T}$ ,  $k_{2T}$  are termination rate constants;  $[M_1]$ ,  $[M_2]$  are the concentrations

\* For over 50 pairs of monomers having nearly identical values of  $e$  (closely related to  $e$ ) see Schwan and Price.<sup>10</sup>

of AN and ESA, respectively;  $[T]$  is the concentration of terminator;  $[m_1\cdot]$ ,  $[m_2\cdot]$  are concentrations of propagating radicals ending in units of AN and ESA, respectively; and

$$r_1 = k_{11}/k_{12}$$

$$r_2 = k_{22}/k_{21}$$

In the steady state,  $k_{12}[m_1\cdot][M_2] = k_{21}[m_2\cdot][M_1]$ , and hence:

$$[m_2\cdot] = (k_{12}/k_{21})([M_2]/[M_1]) m_1\cdot \quad (2)$$

Furthermore, application of the steady-state assumption to the initiation and termination steps yields:

$$R_i = k_{1T}[m_1\cdot][T] + k_{2T}[m_2\cdot][T] \quad (3)$$

Combining eqs. (2) and (3), and solving for  $[m_1\cdot]$  and  $[m_2\cdot]$  we obtain:

$$[m_1\cdot] = \frac{(R_i/[T])}{k_{1T} + k_{2T}(k_{12}/k_{21})([M_2]/[M_1])} \quad (4)$$

$$[m_2\cdot] = \frac{(R_i/[T])(k_{12}/k_{21})([M_2]/[M_1])}{k_{1T} + k_{2T}(k_{12}/k_{21})([M_2]/[M_1])} \quad (5)$$

The rates of disappearance of monomers  $M_1$  and  $M_2$  are given by:

$$\begin{aligned} -d[M_1]/dt &= k_{11}[m_1\cdot][M_1] + k_{21}[m_2\cdot][M_1] \\ &= [M_1] \left\{ \frac{k_{11}(R_i/[T]) + k_{21}(R_i/[T])(k_{12}/k_{21})([M_2]/[M_1])}{k_{1T} + k_{2T}(k_{12}/k_{21})([M_2]/[M_1])} \right\} \\ &= \left( \frac{k_{11}R_i}{k_{1T}[T]} \right) [M_1] \left\{ \frac{1 + (k_{12}/k_{11})([M_2]/[M_1])}{1 + (k_{2T}/k_{1T})(k_{12}/k_{21})([M_2]/[M_1])} \right\} \quad (6) \end{aligned}$$

$$\begin{aligned} -d[M_2]/dt &= k_{12}[m_1\cdot][M_2] + k_{22}[m_2\cdot][M_2] \quad (M_2) \\ &= [M_2] \left\{ \frac{k_{12}(R_i/[T]) + k_{22}(R_i/[T])(k_{12}/k_{21})([M_2]/[M_1])}{k_{1T} + k_{2T}(k_{12}/k_{21})([M_2]/[M_1])} \right\} \\ &= \frac{k_{22}R_i}{k_{2T}[T]} [M_2] \left\{ \frac{\frac{k_{12}k_{2T}}{k_{22}k_{1T}} + \left( \frac{k_{2T}}{k_{1T}} \right) \left( \frac{k_{12}}{k_{21}} \right) \left( \frac{[M_2]}{[M_1]} \right)}{1 + \left( \frac{k_{2T}}{k_{1T}} \right) \left( \frac{k_{12}}{k_{21}} \right) \left( \frac{[M_2]}{[M_1]} \right)} \right\} \quad (7) \end{aligned}$$

But if  $r_1 r_2 = 1$  and  $k_{1T}/k_{2T} = k_{11}/k_{21}$ , then the factors in braces become equal to unity, and the rate equations take the form:

$$-d[M_1]/dt = (k_{11}R_i/k_{1T}[T]) [M_1] \quad (8)$$

$$-d[M_2]/dt = (k_{22}R_i/k_{2T}[T]) [M_2] \quad (9)$$

If  $R_i$  and  $[T]$  remain constant during the copolymerization reaction—indeed, as long as their ratio remains constant—the two monomers will each disappear by individual, independent, first-order expressions.

By application of the  $Q-e$  scheme (with  $e_1 = e_2$ ) to the radical-terminator reactions as well as the propagation steps, the condition  $k_{1T}/k_{2T} = k_{11}/k_{21}$  can be given some measure of justification as a reasonable accompaniment to the relation ( $r_1 r_2 = 1$ ).<sup>11</sup> From the central assumption of the  $Q-e$  scheme

$$k_{ij} = P_i Q_j \exp \{ -e_i e_j \}$$

(where  $k_{ij}$  is the rate constant for the attack of radical  $i$  on monomer  $j$ ,  $P_i$  is a constant characteristic of radical  $i$ ,  $Q_j$  is the mean reactivity of monomer  $j$ , and  $e_i$  and  $e_j$  are the polarity factors of  $i$  and  $j$ , respectively), it follows that

$$k_{1T} = P_1 Q_T e^{-e_1 e_T} \quad (10)$$

$$k_{2T} = P_2 Q_T e^{-e_2 e_T} \quad (11)$$

$$k_{11} = P_1 Q_1 e^{-e_1^2} \quad (12)$$

$$k_{21} = P_2 Q_1 e^{-e_2 e_1} \quad (13)$$

Then, if  $e_1 = e_2$  (which follows from  $r_1 r_2 = 1$ )

$$k_{1T}/k_{2T} = P_1/P_2 = k_{11}/k_{22} = k_{12}/k_{22} \quad (14)$$

### Reactivity Ratios

It can readily be shown that when  $r_1 r_2 = 1$ , the slopes of the first-order rate plots can be used to give the reactivity ratios directly. Dividing eq. (6) by eq. (7) and making appropriate substitution for  $[m_1]$  from eq. (2) leads to the expression

$$\frac{d[M_1]}{d[M_2]} = \frac{[M_1]}{[M_2]} \left\{ \frac{r_1([M_1]/[M_2]) + 1}{([M_1]/[M_2]) + r_2} \right\} \quad (15)$$

Since  $r_2 = 1/r_1$ ,

$$\frac{d[M_1]}{d[M_2]} = ([M_1]/[M_2]) r_1 \quad (16)$$

or

$$\frac{d[M_1]/[M_1]}{d[M_2]/[M_2]} = \frac{d \ln [M_1]}{d \ln [M_2]} = r_1 \quad (17)$$

It is interesting to note that by varying polymerization conditions (e.g., pH, catalyst concentration, catalyst nature, terminator) the polymerization rates could be altered substantially, but the ratio of the two monomer conversion rates was relatively constant in the 4.4-4.7 range. The results of fourteen polymerizations are presented in Table I. Only occasionally did we observe indications of drastic departures from this range in rate ratios which, if real, suggested selective poisoning of one of the monomers. As a method of determining  $r_1$ , precision is somewhat poor. Based on the

TABLE I

Expt. no.	$k_{AN}$	$k_{ESA}$	$\frac{k_1}{k_3}$	ESA mole fraction in monomer	Remarks <sup>a</sup>
	$= \frac{d \log [M_1]}{dt}$	$= \frac{d \log [M_2]}{dt}$	$= \frac{d \log [M_1]}{d \log [M_2]}$		
1	4.23	0.90	4.7 <sub>1</sub>	0.081	
2	2.46	0.525	4.7 <sub>2</sub>	0.081	ESA stored 2 weeks in glass
3	2.16	0.40	5.4	0.081	ESA stored 2 weeks in poly- ethylene
4	1.78	0.35	5.1	0.081	AIBN catalyst (2.86%) <sup>b</sup>
5	1.32	0.35	3.8	0.0405	AIBN (0.8%) <sup>b</sup>
6	2.98	0.649	4.5 <sub>9</sub>	0.0405	AIBN catalyst (1.5%) <sup>b</sup>
7	1.98	0.625	3.2	0.081	
8	2.48	0.561	4.4 <sub>2</sub>	0.315	
9	2.58	0.55	4.6 <sub>9</sub>	0.229	
10	3.07	0.69	4.4 <sub>5</sub>	0.081	
11	2.54	0.795	3.2	0.081	
12	1.65	0.60	2.7 <sub>5</sub>	0.081	AIBN (1%) <sup>b</sup>
13	2.22	0.483	4.6	0.081	
14	2.73	0.358	7.6	0.081	

<sup>a</sup> Catalyst is 0.2% H<sub>2</sub>O<sub>2</sub> based on monomers unless otherwise noted. All percentages based on total monomer weight.

<sup>b</sup> Azobisisobutyronitrile catalyst; thioglycolic acid used as terminator.

data in Table I,  $\bar{r}_1 = 4.5_2$ ,  $s = 1.17$ . This is in fair agreement with low-conversion polymer composition data obtained by Hill.<sup>12</sup> From his study Hill estimated  $r_1 = 4.5-4.7$  and  $r_2 \sim 0.12$ .

These data are in poor agreement with Kunichika and Katagiri,<sup>13</sup> however, who reported  $r_1 = 1.5$ ,  $r_2 = 0.15$ . We believe they introduced a serious error, particularly in their value of  $r_1$ , by going to high conversions (55-67%) in their preparations of AN-rich copolymers.

## SUMMARY

In summary, the AN-ESA copolymerization system is a simplified one in which the reactivity ratios can be related to the individual monomer reaction rates in copolymerization.

$$r_1 = \frac{d \ln [M_1]}{d \ln [M_2]}$$

Concerning the monomers, it can be said

$$Q_1/Q_2 = k_{11}/k_{12} = k_{21}/k_{22} = r_1 = 1/r_2$$

and, concerning the radicals,

$$P_1/P_2 = k_{11}/k_{21} = k_{12}/k_{22} = K_1/K_2$$

This is consistent with  $e_1 = e_2$ , a not extremely uncommon circumstance. The AN-ESA system is unusual, however, in that the reactivity ratios were obtained from copolymerization rate data alone without recourse to polymer composition data other than for comparison.

We wish to extend our thanks to Dr. J. F. Voeks and Dr. R. L. Hill of The Dow Chemical Company for their interest in and contributions to this work and to R. C. Medford and L. P. Cahoon for conducting the numerous rate measurements involved.

### References

1. W. M. Thomas, *Fortschr. Hochpolymer.-Forsch.*, **2**, 401 (1961).
2. Katayama and Ogoshi, *Kobunshi Kagaku*, **13**, (1956); SLA Translation No. 60-18458.
3. Aybar, *Makromol. Chem.*, **58**, 130 (1962).
4. F. S. Dainton et al., *J. Polymer Sci.*, **34**, 209 (1959).
5. C. H. Bamford, A. D. Jenkins, and R. Johnston, *J. Polymer Sci.*, **29**, 355 (1958); *Trans. Faraday Soc.*, **55**, 168 (1959).
6. W. M. Thomas, E. H. Gleason, and J. J. Pellon, *J. Polymer Sci.*, **17**, 275 (1955).
7. P. F. Onyon, *J. Polymer Sci.*, **22**, 19 (1956).
8. Breslow et al., *J. Am. Chem. Soc.*, **76**, 5361 (1934).
9. K. Miyamichi, T. Senoo, and M. Katayama, *Kogyo Kagaku Zasshi*, **66**, 95 (1963).
10. T. C. Schwan and C. C. Price, *J. Polymer Sci.*, **40**, 460 (1959).
11. T. Alfrey and L. J. Young, in *Copolymerization*, G. Ham, Ed., Interscience, New York, 1964, 2nd Ed., pp. 67-88.
12. R. L. Hill, The Dow Chemical Company, private communication.
13. S. Kunichika and T. Katagiri, *Kogyo Kagaku Zasshi*, **64**, 929 (1961).

### Résumé

On a utilisé l'absorption différentielle dans l'infrarouge proche pour suivre les vitesses de copolymérisation de l'acrylonitrile (AN,  $M_1$ ) et l'acide éthylène-sulfonique (ESA,  $M_2$ ) en solution dans le chlorure de zinc aqueux. Les concentrations des monomères étaient suivies séparément et simultanément. On a trouvé expérimentalement que le rapport de  $d \log [M_1]/dt$  et  $d \log [M_2]/dt$  sont chacun constants. Ceci est interprété en admettant que le produit des rapport de réactivité des monomères  $r_1$  et  $r_2$  était égal à l'unité et que le rapport des vitesses de terminaison est égal au rapport des réactivités de propagation. On a trouvé que le  $d \log [M_1]/d \log [M_2] = r_1 = 4.5_2$ . Cette valeur est en accord avec la donnée de composition de polymère obtenue indépendamment. Dans un système  $Q-e$  l'égalité  $r_1 r_2 = 1$  est équivalente pour des monomères ayant une même valeur  $e$ . Ceci pour le système acrylonitrile et acide éthylène-sulfonique,  $P_1/P_2 = k_{11}/k_{21} = k_{12}/k_{22} = k_{1T}/k_{2T}$  ou  $P_1$  est la constante de résonance du radical polymérique finissant en unités de  $M_1$ ; et  $k_{11}$ ,  $k_{12}$  sont les constantes de vitesses correspondant aux réactions de ce radical avec  $M_1$ ,  $M_2$  et T (agent de terminaison) respectivement. Un effet de gel n'a pas été observé même à des degrés de conversion de  $M_1$  aussi élevé que 88%.

### Zusammenfassung

Die Copolymerisationsgeschwindigkeit von Acrylnitril (AN,  $M_1$ ) mit Äthylensulfonsäure (ESA,  $M_2$ ) in wässriger Zinkchloridlösung wurde durch Differentialabsorptionsmessungen im nahen Infrarot bestimmt. Die Monomerkonzentrationen wurden ge-

trennt und gleichzeitig gemessen. Die Quotienten  $d \log [M_1]/dt$  und  $d \log [M_2]/dt$  erwiesen sich jeder experimentell als konstant. Daraus wurde erschlossen, dass das Produkt der Reaktivitätsverhältnisse der beiden Monomeren ( $r_1, r_2$ ) 1 ist und dass das Verhältnis der Abbruchgeschwindigkeitskonstanten dem Reaktionsfähigkeitsverhältnis beim Wachstum gleich ist. Es ergab sich  $d \log [M_1]/d \log [M_2] = r_1 = 4,5$ . Dieser Wert stimmt gut mit den unabhängig erhaltenen Zusammensetzungsdaten für das Polymere überein. Im  $Q-e$ -Schema bedeutet  $r_1 r_2 = 1$ , dass die Monomeren gleiche  $e$ -Werte besitzen. Es ist daher im AN-ESA-System  $P_1/P_2 = k_{11}/k_{21} = k_{12}/k_{22} = k_{1T}/k_{2T}$ , wo  $P_1$  die Resonanzkonstante eines Polymerradikals mit  $M_1$ -Ende und  $k_{11}$ ,  $k_{12}$  und  $k_{1T}$  die Geschwindigkeitskonstanten für die Reaktionen dieses Radikals mit  $M_1, M_2$  und (kettenabbruchender Stoff) sind. Es wurde kein Geleffekt, auch nicht bei einem  $M_1$ -Umsatz von 88% beobachtet.

Received January 26, 1966

Prod. No. 5093A

## Effects of Metal Salts on Polymerization. Part II. Polymerization of Vinylpyridine Complexed with the Group IIb Metal Salts

SHIGEO TAZUKE, NORITAKA SATO, and SEIZO OKAMURA,  
*Department of Polymer Chemistry, Kyoto University, Kyoto, Japan*

### Synopsis

The following stoichiometric vinylpyridine complexes have been prepared:  $(4\text{-VP})_2\text{-Zn}(\text{SCN})_2$ ,  $(2\text{-VP})_2\text{-Zn}(\text{SCN})_2$ ,  $(\text{MVP})_2\text{-Zn}(\text{SCN})_2$ ,  $(\text{MVP})_2\text{-ZnCl}_2$ ,  $(\text{MVP})_2\text{-ZnBr}_2$ ,  $(\text{MVP})_2\text{-ZnI}_2$ , and  $(\text{MVP})_2\text{-HgCl}_2$ , where 4-VP, 2-VP, and MVP denote 4-vinylpyridine, 2-vinylpyridine, and 2-methyl-5-vinylpyridine, respectively. Results of radical polymerization initiated by azobisisobutyronitrile indicate that the effect of complex formation between the monomers and the metal salts is to enhance the rate of polymerization with the exception of the 2-VP complex. The  $R_p$  for the solution polymerization in dimethylformamide increases in the following order: (1)  $(\text{MVP})_2\text{-Zn}(\text{SCN})_2 > (\text{MVP})_2\text{-ZnCl}_2 > (\text{MVP})_2\text{-ZnBr}_2 > (\text{MVP})_2\text{-ZnI}_2 > \text{free MVP}$ ; (2)  $(4\text{-VP})_2\text{-Zn}(\text{SCN})_2 > (\text{MVP})_2\text{-Zn}(\text{SCN})_2 > \text{free MVP} > (2\text{-VP})_2\text{-Zn}(\text{SCN})_2$ ; and (3)  $\text{MVP} + \text{Zn}(\text{CH}_3\text{COO})_2 < \text{MVP} + \text{Cd}(\text{CH}_3\text{COO})_2$ . When ethanol, acetone, or tetrahydrofuran is used as solvent, the change in  $R_p$  is more marked, partly due to insolubility of the PMVP complexed with the metal salts. The increase in  $R_p$  would be attributed to the change in  $k_p$  since the molecular weights of PMVP are nearly proportional to  $R_p$  when  $(\text{MVP})_2\text{-ZnX}_2$  where X is  $\text{Cl}^-$ ,  $\text{Br}^-$ ,  $\text{I}^-$ , or  $\text{SCN}^-$  is polymerized in DMF under fixed conditions. Copolymerizations of  $\text{MVP-ZnX}_2$  complexes (where X is  $\text{Cl}^-$ ,  $\text{Br}^-$ ,  $\text{I}^-$ , or  $\text{CH}_3\text{COO}^-$ ) with styrene indicate that the  $e$  values of complexed MVP are more positive than that of free vinylpyridine, and the amounts of the positive shift in  $e$  values increase with decreasing polarizability of the halide anions. These results are discussed in terms of the charge-transfer properties of anions, the nature of coordination bonds, and the structures of vinylpyridines. The complexed monomers are hardly polymerized by a cationic or an anionic mechanism. Radiation-induced solid-state polymerization gives polymers in low yields.

### INTRODUCTION

There seems to be increasing interest in the effects of salts on radical reactions. When radical reactions are conducted in the presence of metal salts, modification of the feature of the reaction has been demonstrated in several cases. One is the interaction of metal salts with radicals. This will either bring about a redox reaction between a metal salt and a radical or affect the reactivity of radical. Many results have been published for ion-radical reactions which may proceed either by ligand transfer or by electron transfer mechanisms.<sup>1-3</sup> When the radical-ion interaction does not proceed to total charge transfer, the reactivity of the radical may be modified.<sup>4-6</sup>



Radical polymerization of acrylonitrile is accelerated in the presence of lithium chloride; this effect has been attributed to the increase in  $k_p$  due to formation of a complex of the salt with the growing polyacrylonitrile radical.<sup>5</sup> Similarly, the presence of aluminum chloride and other Lewis acids has been reported to modify radical polymerizations.<sup>6,7</sup> However it is not clear as to whether the metal salts or the Lewis acids interact with the growing radical, with the monomer, or with the initiator.

Another set of examples is the complex formation of reactants with metal salts. Imoto and his co-workers<sup>8-11</sup> studied the effects of zinc chloride on the polymerization of acrylonitrile and methyl methacrylate. Complexes are possibly formed between the monomers and zinc chloride. The enhancement of homopolymerizabilities and the positive shift of  $e$  values of these monomers by addition of zinc chloride were reported.

The present authors feel that the problem of salt effect must be treated from the viewpoint of coordination chemistry. Thus, the problem may be reduced to a study of the chemical reactivities of coordinated ligands towards radical reactions. Although various coordinated ligands have been studied for their chemical reactivities,<sup>12</sup> systematic information on the correlation between the nature of coordination bonds and the chemical reactivities is surprisingly scanty. This is in part due to the difficulties of establishing a suitable reaction system. Several conditions must be satisfied to obtain clear, systematic results. Firstly, the nature of the complexes must be well understood. Secondly, a series of stable complexes is required. Lastly, the complexing metal salts should not interfere with the reaction itself but merely modify the chemical reactivity of the ligands. The ideal system is difficult to achieve, and we must make concessions in some aspects.

Among various vinyl compounds, vinylpyridines seem to meet best the requirements mentioned above. For the combination of vinylpyridines with group IIb metal salts, the properties of complexes may be estimated from published data on the complexes of pyridine and its derivatives. A series of vinylpyridine complexes can easily be prepared by changing both metal salts and vinylpyridine isomers. In addition, polymerization of free vinylpyridine has already been investigated.<sup>13</sup>

For the above reasons, the polymerization of vinylpyridine complexes seems to be one of the most suitable reaction systems for the investigation of the effect of complex formation on polymerization.

## EXPERIMENTAL

### Materials

2-Methyl-5-vinylpyridine (MVP) (Tokyo Kasei Kogyo Co.), 4-vinylpyridine (4-VP) (Yuki Gosei Kogyo Co.) and 2-vinylpyridine (2-VP) (Yuki Gosei Kogyo Co.) were refluxed over potassium hydroxide and distilled in a stream of dry nitrogen under reduced pressure (5-10 mm. Hg).

TABLE I  
Preparation of Vinylpyridine Complexes

Complex	Metal salt		Type	Wt., g.	Monomer		Vol. solvent (ethanol), ml.	Yield after one recrystallization	
	Type	Wt., g.			Type	Vol., ml.		Wt., g.	%
(MVP) <sub>2</sub> -Zn(SCN) <sub>2</sub>	Zn(SCN) <sub>2</sub>	29.8	MVP	40	100	47.3	69.9		
(MVP) <sub>2</sub> -ZnCl <sub>2</sub>	ZnCl <sub>2</sub>	13.7	MVP	25	50	30.9	81.9		
(MVP) <sub>2</sub> -ZnBr <sub>2</sub>	ZnBr <sub>2</sub>	25.0	MVP	27.6	50	17.8	54.7		
(MVP) <sub>2</sub> -ZnI <sub>2</sub>	ZnI <sub>2</sub>	25.0	MVP	19.5	50	21.2	48.5		
(MVP) <sub>2</sub> -HgCl <sub>2</sub>	HgCl <sub>2</sub>	21.6	MVP	20	50	19.2	47.1		
(4-VP) <sub>2</sub> -Zn(SCN) <sub>2</sub>	Zn(SCN) <sub>2</sub>	33.7	4-VP	40	100	39.9	54.9		
(2-VP) <sub>2</sub> -Zn(SCN) <sub>2</sub>	Zn(SCN) <sub>2</sub>	33.7	2-VP	40	100	41.9	57.6		

Metal salts used for complexing the vinylpyridines were the Guaranteed Reagent grade reagents and were used without further purification.

Solvents used for the polymerization were purified from the G.R. grade reagents by fractional distillation after drying.

Azobisisobutyronitrile (AIBN) as a radical initiator was recrystallized twice from methanol. *n*-Butyllithium as an anionic initiator was prepared from *n*-butyl bromide and lithium metal in benzene *in vacuo*. Boron trifluoride etherate and stannic chloride were distilled and stored in ampules sealed in an atmosphere of dry nitrogen.

### Preparation of the Monomer Complexes

An example of the preparation of the monomer complexes is given as follows.

Zinc thiocyanate (29.8 g., 0.165 mole) was dissolved in 100 ml. of hot ethanol. MVP (40 ml., 0.328 mole) was then added to the ethanol solution. White crystals precipitated immediately and were collected after standing overnight in a refrigerator. After recrystallizing once from hot ethanol, 47.3 g. of MVP-Zn(SCN)<sub>2</sub> complex was obtained. The yield was 69.9% based on MVP added. The complex was kept in a desiccator saturated with the vapor of the monomer over potassium hydroxide.

Other complexes were prepared by similar procedures. The yields of complexes and the analytical data by chelate titration are tabulated in Tables I and II.

When the anion is acetate, solid complexes are not isolated. MVP-Zn(CH<sub>3</sub>COO)<sub>2</sub>, MVP-Cd(CH<sub>3</sub>COO)<sub>2</sub>, and MVP-Hg(CH<sub>3</sub>COO)<sub>2</sub> complexes were prepared in the polymerization mixtures by mixing MVP and the metal acetates ([MVP]/[metal acetate] = 2/1 by mole ratio).

TABLE II  
Analysis of Vinylpyridine Complexes

Complex	Metal, %		Melting point, °C.
	Calcd.	Found	
(MVP) <sub>2</sub> -Zn(SCN) <sub>2</sub>	15.56	15.7	134-136
(MVP) <sub>2</sub> -ZnCl <sub>2</sub>	17.45	17.2	114-120
(MVP) <sub>2</sub> -ZnBr <sub>2</sub>	14.10	13.7	132-134
(MVP) <sub>2</sub> -ZnI <sub>2</sub>	11.73	11.5	150-158
(MVP) <sub>2</sub> -HgCl <sub>2</sub>	39.34	39.4	>250
(4-VP) <sub>2</sub> -Zn(SCN) <sub>2</sub>	16.69	16.6	148-152
(2-VP) <sub>2</sub> -Zn(SCN) <sub>2</sub>	16.69	16.7	113-123

### Polymerization

Radical polymerizations were all conducted *in vacuo*. The rate of polymerization in DMF was measured either by dilatometry or by weighing the polymer. The shrinkage factors of MVP, 2-VP, and 4-VP were reported in the preceding paper<sup>14</sup> and assumed to be the same for the com-

plexed monomers. The polymer complexes formed during polymerization are insoluble in most of organic solvents and in these cases the yields of polymer were measured by weighing. After the polymerization was quenched by cooling, the polymerization mixture was poured into a large excess of 5% ammonia containing 10 g./500 ml. of ammonium chloride. Since the complexed monomers (except mercuric complexes) and the metal salts are soluble in the solution, the polymer thus precipitated is almost free from metal salts. The mercuric complexes are quite insoluble in any solvents, and complete separation of the polymer from mercuric ion was found to be difficult.

Radiation-induced solid-state polymerization was conducted by  $\gamma$ -ray irradiation at room temperature. The irradiated sample was dissolved in the precipitant mentioned above, and the undissolved polymer was collected.

Cationic and anionic polymerizations were carried out in semi-open systems with the use of a rubber-capped flask into which the reaction mixture and the initiator were injected. Treatments of the polymerization mixture were the same as for the radical polymerization.

### Copolymerization

Radical copolymerization of the complexed MVP with styrene was carried out in *N,N*-dimethylformamide (DMF) at 60°C.

The compositions of the copolymers were analyzed by infrared absorption spectroscopy by using absorptions at 906  $\text{cm.}^{-1}$  for styrene and at 1300  $\text{cm.}^{-1}$  for MVP.

## RESULTS AND DISCUSSION

### Vinylpyridine Complexes

Analytical data for all complexes agree with the formula  $(\text{VP})_2\text{-MX}_2$ . Corresponding pyridine complexes are also known to have the same chemical compositions. Crystallographic study of the corresponding pyridine complexes<sup>15</sup> indicates that  $\text{Py}_2\text{-ZnCl}_2$  has a tetrahedral structure, whereas  $\text{Py}_2\text{-CdCl}_2$  and  $\text{Py}_2\text{-HgCl}_2$  are of *trans* configuration in solid. Although no data are available for vinylpyridine-metal salt complexes, the structure might be expected to be the same as the pyridine complexes by analogy.

TABLE IIIA  
Stability Constants for Complexes of Pyridine with  $\text{Zn}^{+2}$ ,  $\text{Cd}^{+2}$ , and  $\text{Hg}^{+2}$  in Aqueous Media at 25°C.

Metal ion	Anion	$\log \beta_2^a$
$\text{Zn}^{+2}$	$\text{Cl}^-$ or $\text{NO}_3^-$	1.1-1.45
$\text{Cd}^{+2}$	$\text{NO}_3^-$	1.95-2.14
$\text{Hg}^{+2}$	$\text{NO}_3^-$	10.0

<sup>a</sup>  $\beta_2 = [\text{M}\cdot\text{Py}_2]/[\text{M}][\text{Py}]^2$ .

TABLE IIIB  
Stability Constants for Picoline-Ag<sup>+</sup> Complexes in Various Solvents

Ligand	log $\beta_2$		
	Ethanol (20°C.)	Acetonitrile (20°C.)	0.5 <i>N</i> KNO <sub>3</sub> (25°C.)
$\alpha$ -Picoline	4.68	4.45	4.68
$\beta$ -Picoline	5.23	4.99	4.35 <sup>a</sup>
$\gamma$ -Picoline	5.05	4.78	4.70
Pyridine			4.39 <sup>a</sup>
			4.22

<sup>a</sup>  $\mu \rightarrow 0$ .

The difficult problem of estimating the degree of dissociation of the complexes arises when the reactions of vinylpyridine complexes in solution are discussed. Stability constants of the vinylpyridine complexes may be estimated from those of pyridine complexes.<sup>16</sup> A number of consistent data have been reported on the complex formation of pyridine and its alkyl derivatives in aqueous solution and in organic media as shown in Table III.

As may be seen from Table IIIB, the stability of the silver complex of pyridine seems to be rather insensitive to change of solvent and also to alkyl substitution on the ligand.

We may therefore assume the stability constants for pyridine complexes in aqueous media to be fairly close to those for vinylpyridine. However, the effect of solvents on the stability constant may be stronger for zinc complexes than for silver complexes, since the weaker zinc complexes would be more readily influenced by solvents, particularly by coordinating solvents such as acetonitrile or dimethylformamide.

The coordinating anion might also influence the stability constants. Little attention has been paid to this aspect, and some of the data in Table IIIA would indicate there is no appreciable difference between chloride and nitrate at least. However, strong effects of the anion on the tetrahedral-octahedral equilibria of pyridine-cobalt complexes are known.<sup>17</sup> Tentatively we neglect the influence of anion on the stability constants.

The approximate calculations of the degree of dissociation based on the stability constants in Table IIIA give the following values: Zn complex, ~20%; Cd complex, ~13%; Hg complex, <0.1%.

### Radical Polymerization in Various Solvents

Results of radical polymerization of (MVP)<sub>2</sub>-Zn(SCN)<sub>2</sub> initiated by azobisisobutyronitrile in acetone, tetrahydrofuran, and ethanol are shown in Figures 1, 2, and 3, respectively.

Although the monomer complex is soluble in these solvents, the system becomes heterogeneous at an early stage of polymerization due to insolubility of the polymer complex. The autoacceleration found generally

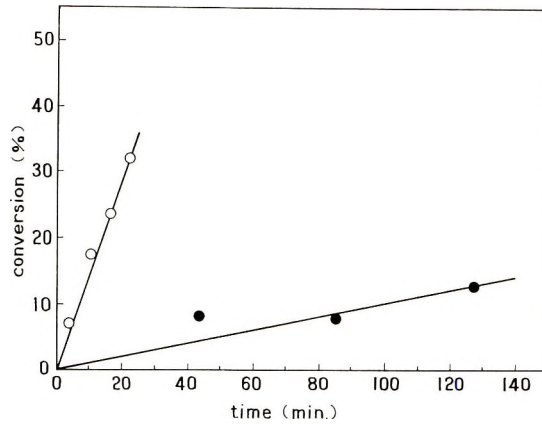


Fig. 1. Polymerization of  $(MVP)_2-Zn(SCN)_2$  in acetone at  $70^\circ C$ .: (O)  $(MVP)_2-Zn(SCN)_2$ ; (●) MVP.  $[AIBN] = 2.50 \times 10^{-3}$  mole/l.,  $[MVP] = 0.342$  mole/l.

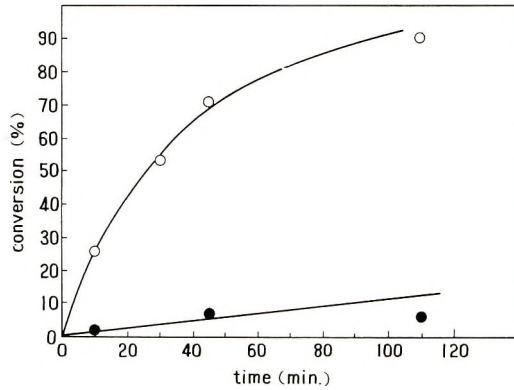


Fig. 2. Polymerization of  $(MVP)_2-Zn(SCN)_2$  in tetrahydrofuran at  $50^\circ C$ .: (O)  $(MVP)_2-Zn(SCN)_2$ ; (●) MVP.  $[AIBN] = 0.101$  mole/l.,  $[MVP] = 0.595$  mole/l.

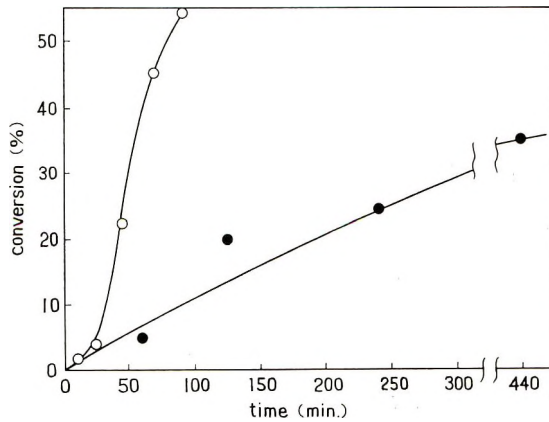


Fig. 3. Polymerization of  $(MVP)_2-Zn(SCN)_2$  in ethanol at  $70^\circ C$ .: (O)  $(MVP)_2-Zn(SCN)_2$ ; (●) MVP.  $[AIBN] = 2.50 \times 10^{-3}$  mole/l.,  $[MVP] = 0.357$  mole/l.

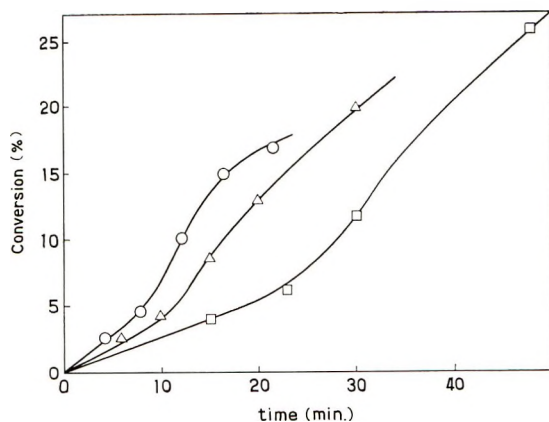


Fig. 4. Effect of anion of the polymerization of  $(\text{MVP})_2\text{-ZnX}_2$  in ethanol at  $70^\circ\text{C}$ .: (O)  $(\text{MVP})_2\text{-ZnCl}_2$ ; ( $\Delta$ )  $(\text{MVP})_2\text{-ZnBr}_2$ ; ( $\square$ )  $(\text{MVP})_2\text{-ZnI}_2$ .  $[\text{AIBN}] = 3.04 \times 10^{-3}$  mole/l.,  $[\text{MVP}] = 0.357$  mole/l.

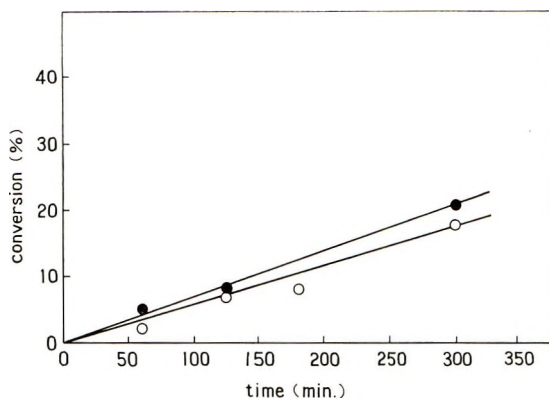


Fig. 5. Polymerization of  $(\text{MVP})_2\text{-Zn(SCN)}_2$  in pyridine at  $70^\circ\text{C}$ .: (O)  $(\text{MVP})_2\text{-Zn(SCN)}_2$ ; ( $\bullet$ ) (MVP).  $[\text{AIBN}] = 2.50 \times 10^{-3}$  mole/l.,  $[\text{MVP}] = 0.357$  mole/l.

with heterogeneous polymerization is not observed in Figures 1 and 2. Under the present experimental conditions the monomer concentration is as low as  $0.3\text{--}0.6M$  and the degree of polymerization would be determined by chain transfer to solvent. It has been recognized for the heterogeneous bulk polymerization of acrylonitrile and vinyl chloride<sup>18</sup> that the presence of chain-transfer agents tends to diminish autoacceleration.

A change of the rate of polymerization at about 5% conversion is observed in Figures 3 and 4. The different shape of the time-conversion curves for the ethanol system and for the tetrahydrofuran or acetone systems may be due to higher solubility of the polymer complexes in the former solvent than for the latter two solvents. The autoaccelerating effect in Figures 3 and 4 could therefore be understood as a change of phase from homogeneous to heterogeneous with increasing polymer yield; this is not observed in Figures 1 and 2, since the systems are heterogeneous

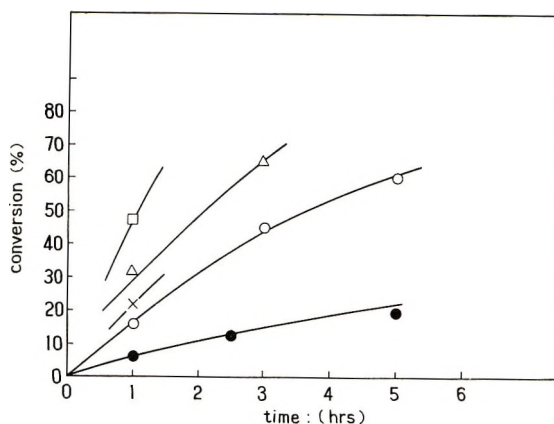


Fig. 6. Polymerization of  $(MVP)_2-Zn(SCN)_2$  in *N,N*-dimethylformamide at  $50^\circ C$ .: (●) MVP; (○)  $(MVP)_2-Zn(SCN)_2$ ; (×)  $(MVP)_2-Zn(SCN)_2 + Zn(SCN)_2$ , 0.0918 mole/l. (Δ)  $(MVP)_2-Zn(SCN)_2 + Zn(SCN)_2$ , 0.459 mole/l.; (□)  $(MVP)_2-Zn(SCN)_2 + Zn(SCN)_2$ , 0.918 mole/l.  $[AIBN] = 0.101$  mole/l.,  $[MVP] = 0.595$  mole/l.

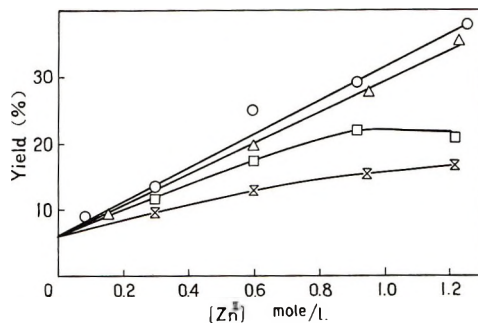


Fig. 7. Effect of zinc salts on the polymer yield in polymerization of MVP in DMF at  $70^\circ C$ .: (○)  $Zn(SCN)_2$ ; (Δ)  $ZnCl_2$ ; (□)  $ZnBr_2$ ; (×)  $ZnI_2$ .  $[AIBN] = 2.0 \times 10^{-2}$  mole/l.,  $[MVP] = 0.595$  mole/l.

at the very early stage of polymerization. The marked acceleration of polymerization rate in comparison with that of free MVP would therefore be partly due to heterogeneity of the system. Further addition of  $Zn(SCN)_2$  to the ethanol system has little effect on the rate.

Results of polymerizations of  $(MVP)_2-ZnX_2$ , where X is  $Cl^-$ ,  $Br^-$ , or  $I^-$ , in ethanol are shown in Figure 4. The effect of coordinated anions on the polymerizability is clearly seen from the time-conversion curves.

The requirements for good solubilities of both monomer and polymer in the presence of metal salts and for high stabilities of the complexes in solutions seem to conflict. Thorough examination of the solubility of the complexes led to the conclusion that homogeneous polymerization in a nondissociating solvent was impossible. DMF was eventually chosen as a solvent for homogeneous polymerization, although it allows partial



dissociation. The homogeneous polymerization can also be carried out in pyridine. However, the accelerating effect of metal salts is not observed for this strong coordinating solvent, as shown in Figure 5. This is an indication that the almost complete exchange of coordinated vinylpyridine with the solvent will occur. Consequently, it seems essential to form a coordination bond between the nitrogen of the monomer and the metal salt in order to obtain the acceleration effect.

The time-conversion curves for the polymerization in DMF are depicted in Figure 6. The yield of polymerization increases with increasing concentration of metal salts added to the system. The effects of adding metal salts on the polymerization of free MVP are shown in Figure 7.

The enhancement of the rate of polymerization with increasing metal salt concentration would indicate partial dissociation of the complexes.

The rates of polymerization of various vinylpyridine complexes in DMF are measured and tabulated in Tables IV-VI. In all cases the plots of volume contraction versus time fell on straight lines.

Since mercury complexes of polymer are sparingly soluble even in DMF, the polymerization system becomes turbid, and the measured rates are less precise for the complexes.

The molecular weights of polymers in Table IV determined by viscosity measurement<sup>19</sup> are plotted against the rates of polymerization in Figure 8. The plot falls on a straight line with the exception of  $(MVP)_2-Zn(SCN)_2$ . The problem of whether chain-transfer reactions or bimolecular terminations determine the molecular weight in the present systems was not stud-

TABLE IV  
Polymerization of  $(MVP)_2-ZnX_2^a$

	MVP	$(MVP)_2-Zn(SCN)_2$	$(MVP)_2-ZnCl_2$	$(MVP)_2-ZnBr_2$	$(MVP)_2-ZnI_2$
$R_p \times 10^5$ , mole/l.- sec.	1.22	5.22	4.69	3.85	2.00
$\frac{R_p \text{ Complex}}{R_p \text{ MVP}}$	1	4.26	3.84	3.16	1.59

<sup>a</sup>  $[MVP] = 0.595$  mole/l.,  $[AIBN] = 0.020$  mole/l.

TABLE V  
Effects of Central Metal Ions on  $R_p$  of Polymerization of MVP-Metal Salt Complexes<sup>a</sup>

	MVP + Zn- $(CH_3COO)_2$	MVP + Cd- $(CH_3COO)_2$	$(MVP)_2-ZnCl_2$	$(MVP)_2-HgCl_2$
$R_p \times 10^5$ , mole/l.- sec.	1.74	2.24	4.69	1.34 <sup>b</sup>

<sup>a</sup> Polymerization conditions same as for Table IV.

<sup>b</sup> Heterogeneous.

TABLE VI  
 Polymerizability of 2-VP, 4-VP, and MVP when the Vinylpyridines are Complexed with  $\text{Zn}(\text{SCN})_2^a$

Monomer	Free monomer, $R_{p0} \times 10^5$ , mole/l.-sec.	$(\text{VP})_2\text{-Zn}(\text{SCN})_2$ , $R_p \times 10^5$ , mole/l.-sec.	$R_p/R_{p0}$
2-VP	4.35	2.30	0.53
4-VP	5.02	24.4 <sup>b</sup>	4.86
MVP	1.22	5.20	4.26

<sup>a</sup> Polymerization at 70°C. in DMF.

<sup>b</sup> Heterogeneous.

ied. The change in  $R_p$  on addition of the metal salt may be attributed to a change in  $k_p/k_t^{1/2}$ , it being assumed that chain-transfer reactions, if any, are nondegradative; on the other hand, the molecular weight will be proportional to  $k_p/k_t$  if chain transfer is less important than bimolecular termination or to  $k_p/k_{tr}$  if chain transfer determines the molecular weight. The observed linear relationship between  $R_p$  and molecular weight would then require that  $k_p/k_t^{1/2}$  is proportional to either  $k_p/k_t$  or  $k_p/k_{tr}$ . The former case (i.e.,  $k_p/k_t^{1/2} \propto k_p/k_t$ ) requires that  $k_t$  be invariant with added metal salt and thus would imply the complexed monomer should have larger  $k_p$  than the free monomer, whereas the latter case (i.e.  $k_p/k_t^{1/2} \propto k_p/k_{tr}$ ) means either  $k_p$  alone is affected by the metal salts or the influence of complexing on  $k_{tr}$  is proportional to that on  $k_t^{1/2}$ . It seems, however, rather difficult to envision the proportionality of  $k_{tr}$  to  $k_t^{1/2}$  and the increase of  $k_p$  alone would therefore seem to be more probable.

The sequence of increasing  $R_p$  for different vinylpyridines by complexing is in the following order:  $R^{\text{complex}}/R^{\text{free monomer}}$  for 4-VP > for MVP > 1 > for 2-VP. The retardation of polymerization of 2 VP rather than acceleration may be explained by considering the steric interaction between

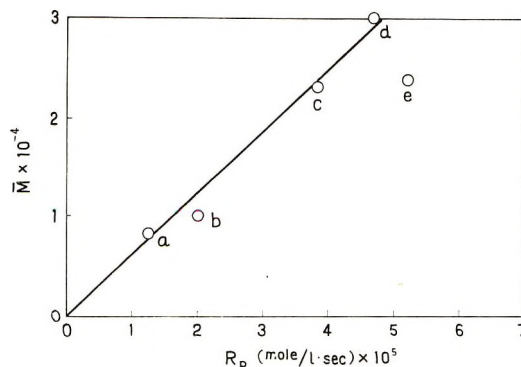


Fig. 8. Plot of  $R_p$  vs. molecular weight of polymer: (a) MVP; (b)  $(\text{MVP})_2\text{-ZnI}_2$ ; (c)  $(\text{MVP})_2\text{-ZnBr}_2$ ; (d)  $(\text{MVP})_2\text{-ZnCl}_2$ ; (e)  $(\text{MVP})_2\text{-Zn}(\text{SCN})_2$ .  $R_p$  taken from Table IV.

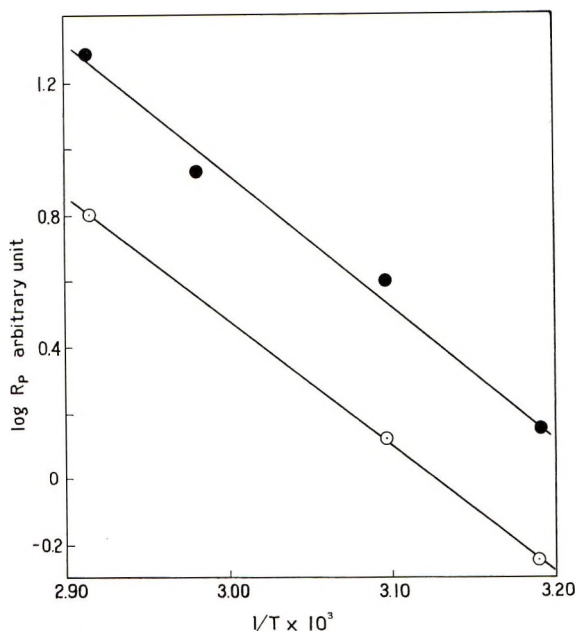


Fig. 9. Temperature dependence of  $R_p$ : (●) MVP; (○)  $(MVP)_2-Zn(SCN)_2$ .  $[MVP] = 0.595$  mole/l.,  $[AIBN] = 2.0 \times 10^{-2}$  mole/l., solvent DMF.

complex metal salt and vinyl group. In Part I<sup>14</sup> we discussed the possibility that the small initiating efficiency of cupric acetate on the polymerization of 2-VP might be due to the fact that the coordinating cupric salt with the nitrogen in the *ortho* position to the vinyl group would bring about steric interaction with the vinyl group and that the vinyl group could no longer stay in the same plane with the pyridine ring. The loss of resonance stabilization due to this steric effect would account for the small rate of polymerization of 2-VP complex. The finding that 4-VP is most strongly influenced by metal salt would indicate the importance of conjugation between the nitrogen atom of pyridine ring and the vinyl group, as discussed in the preceding paper.<sup>14</sup> If the interaction of vinylpyridine with the metal salt is confined to the  $\sigma$ -lone pair of the nitrogen atom, which is orthogonal to the  $\pi$ -system, and if the electric polarization is conducted only by induction effect, the sequence of the effect of metal salt should be 2-VP > MVP > 4-VP.

The effect of complexed anion on  $R_p$  will be discussed later.

The Arrhenius plots for the polymerizations of free MVP and complexed MVP are shown in Figure 9. A slightly lower activation energy (17.4 kcal./mole) is observed for complexed monomer than that (18.4 kcal./mole) for free MVP.

#### Copolymerization of Complexed MVP with Styrene

Since the electronic state of vinylpyridine would be modified by complex formation, copolymerization may be a suitable method to investigate the

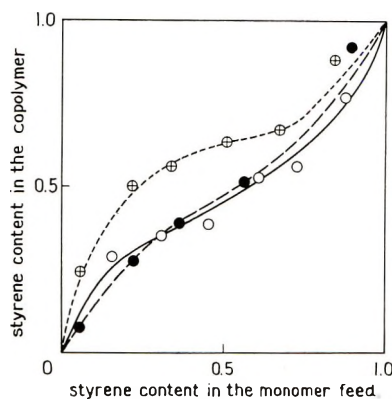


Fig. 10. Composition curves for the copolymerization of MVP and its zinc complexes with styrene at 60°C. in DMF: ( $\oplus$ )  $(\text{MVP})_2\text{-ZnCl}$ -styrene; (O)  $(\text{MVP})_2\text{-ZnBr}_2$ -styrene; ( $\bullet$ )  $(\text{MVP})_2\text{-ZnI}_2$ -styrene.  $[\text{AIBN}] = 2.0 \times 10^{-3}$  mole/l.,  $[\text{monomer}] = 0.98$  mole/l.

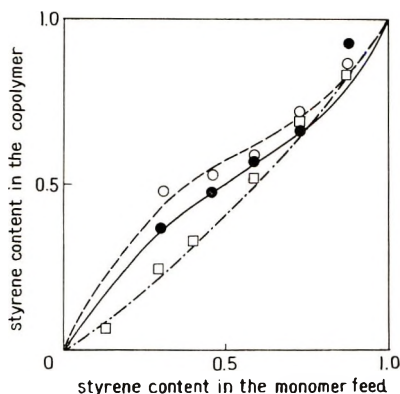


Fig. 11. Composition curves for the copolymerization of MVP and its complexes of the group IIb metal acetates with styrene at 60°C. in DMF: (O) MVP +  $\text{Zn}(\text{CH}_3\text{COO})_2$ ; ( $\bullet$ ) MVP +  $\text{Cd}(\text{CH}_3\text{COO})_2$ ; ( $\square$ ) MVP (free monomer).  $[\text{AIBN}] = 2.0 \times 10^{-2}$  mole/l.,  $[\text{monomer}] = 0.98$  mole/l.

effect of complexing. For this purpose, styrene was chosen as a comonomer so that the presence of these metal salts would not affect the polymerizability of the comonomer.

The copolymer composition curves are presented in Figures 10 and 11. The monomer reactivity ratios and the  $Q$ - $e$  values derived from them are tabulated in Table VII. The most distinct trend observed from the data in Table VII is the positive shift of  $e$  values in the case of the complexed monomer. The interaction of positively charged metal salts with the nitrogen atom of pyridine ring would decrease the electron density around the nitrogen and then the effect would be transferred to the vinyl group by induction or resonance effects.

The first half of Table VII shows the effect of anions. The  $e$  value becomes more positive when the anion is changed from  $I^-$  to  $Cl^-$ . Two modes of influence of coordinated anion on the pyridine-metal bond have been discussed by Nelson and his co-workers<sup>21</sup> for pyridine-cobalt complexes. The anions (halides or pseudohalides) transfer the charge to the metal in the cobalt-X bond to decrease the effective electron affinity of the metal. Two effects might then be expected: (1) a decrease in the attraction of the metal ion for the electrons in the cobalt-pyridine  $\sigma$ -bond (2) an enhancement of the overlap of the nonbonding metal  $\sigma$ -orbitals with pyridine  $\pi$ -orbitals. They presented following sequence of decreasing capacity of inducing dative  $\pi$ -bonding in the cobalt-pyridine complexes:  $I^- > Br^- > Cl^- \gg OCN^- \gg SCN^-$ . The double-bond nature of pyridine-metal coordination has been mentioned earlier by Sacconi and co-workers.<sup>22</sup>

TABLE VII  
Copolymerization of Complexed MVP ( $M_1$ ) with Styrene ( $M_2$ ) at 60°C.<sup>a</sup>

	$r_1$	$r_2$	$Q_1$	$e_1$
Free MVP	$1.20 \pm 0.13$	$0.72 \pm 0.23$	1.03 (0.99) <sup>b</sup>	-0.42 (-0.58) <sup>b</sup>
(MVP) <sub>2</sub> -ZnCl <sub>2</sub>	$0.08 \pm 0.015$	$0.93 \pm 0.075$	0.30	+0.81
(MVP) <sub>2</sub> -ZnBr <sub>2</sub>	$0.38 \pm 0.18$	$0.33 \pm 0.05$	0.97	+0.63
(MVP) <sub>2</sub> -ZnI <sub>2</sub>	$0.55 \pm 0.06$	$0.60 \pm 0.10$	0.70	+0.21
MVP + Zn(CH <sub>3</sub> COO) <sub>2</sub>	$0.32 \pm 0.03$	$0.75 \pm 0.045$	0.96	+0.40
MVP + Cd(CH <sub>3</sub> COO) <sub>2</sub>	$0.47 \pm 0.04$	$0.56 \pm 0.05$	0.71	+0.36
MVP + Hg(CH <sub>3</sub> COO) <sub>2</sub>	(0.4)	(0.5)		

<sup>a</sup> [Monomer] = 0.98 mole/l., [AIBN] =  $2.0 \times 10^{-3}$  mole/l., in DMF.

<sup>b</sup> Data of Ham.<sup>20</sup>

These discussions may be applied for the zinc complexes. Considering the zinc halide complexes, the polarizabilities of halides will follow the same sequence of the capacity to induce the back donation as presented above. The sequence of decreasing (or increasingly negative)  $e$  values of the three MVP complexes with zinc halides is the reversal of the order given above. Either releasing the  $\sigma$ -lone pair of MVP or increasing back donation via the dative  $\pi$ -bond between zinc and MVP or probably both would cause less positive  $e$  values.

The copolymerization behavior of MVP complexes does not change much when cadmium or mercury is used as a central metal ion. No general trend for the shift of  $Q$ - $e$  values can be found from the data in Table VII. The values for the mercury complex are a rough estimate, since the incorporation of mercury in the copolymer causes considerable fluctuations in the copolymer composition analysis.

Explanations for the change in reactivity index other than for the  $e$  value and correlation of the results of copolymerization with those of homopolymerization are difficult. The monomer reactivity index ( $1/r_2$ ) does not change regularly and cannot be correlated with the enhancement of the

rate of homopolymerization by complexing. The rate of homopolymerization is determined by the magnitude of  $k_p$  relative to  $k_t$ . The authors are not sure which of these rate constants is affected more by complexing. Another complicating feature is the dissociation of the complexes. As has been suggested by Bamford and co-workers,<sup>5</sup> the reactivity of the complexed radical with a positive  $e$  value towards the uncomplexed monomer which has a negative  $e$  value or vice-versa might be larger than for the propagation rate constant in the absence of metal salts. Clearly, more data on the equilibrium study of the vinylpyridine complexes in DMF are needed.

### Radiation-Induced Solid-State Polymerization of $(MVP)_2-ZnX_2$

Irradiation of  $(MVP)_2-ZnX_2$  complexes in the solid state produced polymer with a yield of less than 5% for the total dose of about 20 Mrad. The sequence of polymerizability in the solid state seems to be the same as for radical polymerization in solution. While the radical density of the irradiated sample by ESR spectroscopy<sup>23</sup> increases with the total dose, infrared spectroscopy measurements indicate that the vinyl groups of the complexes are kept almost unchanged during irradiation. Thus, there is a possibility that the polymerization may in fact proceed during dissolution of the irradiated complexes in precipitant.

For this reason, no further study was carried out.

### Attempts to Polymerize $(MVP)_2-ZnX_2$ by an Anionic and a Cationic Mechanism

Vinylpyridines are known to polymerize by an anionic mechanism. Upon the expectation that a positive  $e$  value for the complexed MVP would cause enhancement in anionic polymerizability,  $(MVP)_2-ZnX_2$  complexes were examined for anionic polymerization with the use of *n*-butyllithium as catalyst in THF at 25–60°C. Under such conditions that free MVP was nearly completely polymerized, the polymerization yields of  $(MVP)_2-ZnX_2$  were always less than 5%. The initiator activity of *n*-butyllithium may be lost in the presence of acidic  $ZnX_2$ .

Cationic polymerization of vinylpyridine is difficult because of the basic nitrogen in monomer. The cationic initiators form complexes with the basic nitrogen rather than initiate polymerization. We thought that cationic polymerization might be possible if the basic nitrogen is masked by metal salts prior to addition of the cationic initiator. However, polymerization scarcely proceeded when stannic chloride or boron trifluoride etherate were used as initiators in THF at temperatures between –78 and 40°C. All other solvents more favorable for cationic polymerization do not dissolve the monomer complexes to a concentration usable for polymerization. The large and positive  $e$  value would also make cationic polymerization difficult.

### Relation between Charge-Transfer Properties of Anions and Reactivities of Complexed Vinylpyridine

The preceding discussions lead to the conclusion that the charge distribution around the metal ion is the dominant factor deciding polymerizability and copolymerizability of MVP-ZnX<sub>2</sub> complexes. Thus, the electronics spectra due to the halide → metal charge transfer provide indices for the ability of anionic ligands to transfer negative charge to metal ions.

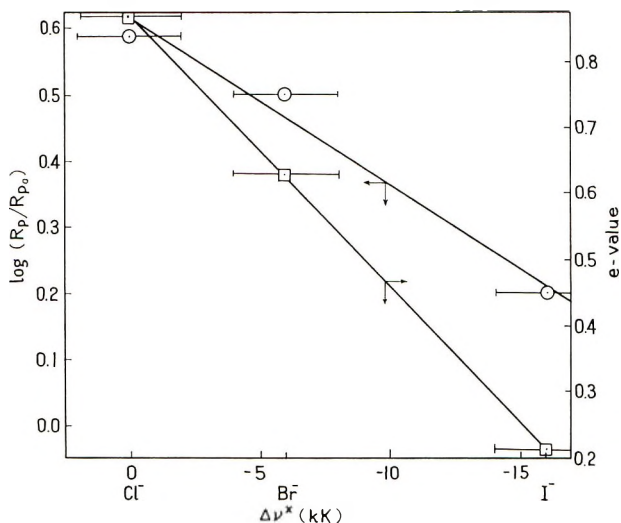


Fig. 12. Correlation of  $\Delta\nu^*$  of absorption maxima for various halide (X) → metal charge-transfer bands with the effects of the corresponding halide on  $R_p$  and the  $\epsilon$  value of the MVP-ZnX<sub>2</sub> complexes.  $E^z = E_{CT}(Cl^- - M^{n+}) - E_{CT}(X^- - M^{n+})$  in kK.

Several measurements of the charge-transfer bands for different combinations of metal ion and halides were made and the averaged energy differences between halides are presented in the literature.<sup>24</sup> Taking the absorption band of chloride complex as standard, differences of absorption bands (in kilokaiser units) for bromide and iodide complexes are plotted in Figure 12 against  $\log R_p/R_{p0}$  (from Table IV) and  $\epsilon$  values (from Table VII) of the corresponding complexes.

The fair linearity of the plots is good support for the concept that electronic effects are transferred to vinylpyridine through the metal-nitrogen coordination bond.

### References

1. E. Collinson, F. S. Dainton, B. Mile, S. Tazuke, and D. R. Smith, *Nature*, **198**, 26 (1963).
2. C. H. Bamford, A. D. Jenkins, and R. Johnston, *Proc. Roy. Soc. (London)*, **A239**, 214 (1957).

3. J. K. Kochi and D. M. Mog, *J. Am. Chem. Soc.*, **87**, 522 (1965), and references therein.
4. J. K. Kochi and F. P. Rust, *J. Am. Chem. Soc.*, **83**, 2017 (1961).
5. C. H. Bamford, A. D. Jenkins, and R. Johnston, *Proc. Roy. Soc. (London)*, **A241**, 364 (1957).
6. H. C. Haas and E. R. Karlin, *J. Polymer Sci.*, **9**, 588 (1952).
7. H. C. Haas, *Makromol. Chem.*, **80**, 232 (1964).
8. M. Imoto, T. Otsu, and S. Shimizu, *Makromol. Chem.*, **65**, 174 (1963).
9. M. Imoto, T. Otsu, and Y. Harada, *Makromol. Chem.*, **65**, 180 (1963).
10. M. Imoto, T. Otsu, and M. Nakabayashi, *Makromol. Chem.*, **65**, 194 (1963).
11. M. Imoto, T. Otsu, B. Yamada, and A. Shimizu, *Makromol. Chem.*, **82**, 277 (1965).
12. G. F. Gould, Ed., *Reactions of Coordinated Ligands*, Advances in Chemistry Series, No. 37, American Chemical Society, 1963.
13. P. F. Onyon, *Trans. Faraday Soc.*, **51**, 400 (1955).
14. S. Tazuke and S. Okamura, *J. Polymer Sci. A-1*, **4**, 141 (1966).
15. R. Zannetti and R. Serra, *Gazz. Chim. Ital.*, **90**, 328 (1960).
16. *Stability Constants*, Chemical Society Special Publication No. 7, Part 1, London, 1957; No. 17, London, 1964.
17. H. C. A. King, E. Körös, and S. M. Nelson, *J. Chem. Soc.*, **1963**, 5449.
18. C. H. Bamford, W. G. Barb, A. D. Jenkins, and P. F. Onyon, *The Kinetics of Vinyl Polymerization by Radical Mechanisms*, Academic Press, New York, 1958, p. 110, 119.
19. H. Sato and R. Yamamoto, *Nippon Kagaku Zasshi*, **80**, 1393 (1959).
20. G. E. Ham, *Copolymerization*, Interscience, New York, 1964, p. 848.
21. H. C. A. King, E. Körös, and S. M. Nelson, *Nature*, **196**, 572 (1962).
22. L. Sacconi, G. Lombardo, and P. Paoletti, *J. Chem. Soc.*, **1958**, 848.
23. K. Tsuji, unpublished data.
24. C. K. Jørgenson, *Absorption Spectra and Chemical Bonding in Complexes*, Pergamon Press, New York-London, 1962, p. 154.

### Résumé

On a préparé le complexe de vinylpyridine stœchiométrique suivant: A savoir,  $(4\text{-VP})_2\text{-Zn}(\text{SCN})_2$ ,  $(2\text{-VP})_2\text{-Zn}(\text{SCN})_2$ ,  $(\text{MVP})_2\text{-Zn}(\text{SCN})_2$ ,  $(\text{MVP})_2\text{-ZnCl}_2$ ,  $(\text{MVP})_2\text{-ZnBr}_2$ ,  $(\text{MVP})_2\text{-ZnI}_2$ , et  $(\text{MVP})_2\text{-gCl}_2$  où 4-VP, 2-VP et MVP ont les abréviations correspondantes à la 4-vinylpyridine, la 2-vinylpyridine et la 2-méthyl-5-vinyl-pyridine respectivement. Les résultats de polymérisation radicalaire initiée par l'azobisisobutyronitrile indiquent que l'effet de formation de complexes avec les monomères et les sels métalliques résident dans une augmentation de vitesse de polymérisation, sauf dans le cas du complexe de la 2-vinylpyridine. L'oxyde d'augmentation de vitesse de polymérisation  $R_p$  pour la polymérisation en solution dans le diméthyl formamide est dans l'ordre suivant: (1)  $(\text{MVP})_2\text{-Zn}(\text{SCN})_2 > (\text{MVP})_2\text{-ZnCl}_2 > (\text{MVP})_2\text{-ZnBr}_2 > (\text{MVP})_2\text{-ZnI}_2 > \text{MVP libre}$ ; (2)  $(4\text{-VP})_2\text{-Zn}(\text{SCN})_2 > (\text{MVP})_2\text{-Zn}(\text{SCN})_2 > \text{VP libre} > (2\text{-VP})_2\text{-Zn}(\text{SCN})_2$ ; (3)  $\text{MVP} + \text{Zn}(\text{CH}_3\text{COO})_2 < \text{MVP} + \text{Cd}(\text{CH}_3\text{COO})_2$ . Lorsque l'éthanol, l'acétone, le tétrahydrofurane sont utilisés comme solvant, le vitesse de polymérisation change de façon plus marquée, en partie par suite de l'insolubilité de la polyméthylevinylpyridine complexée avec les sels métalliques. L'augmentation de  $R_p$  pourrait être attribuée à une variation de  $k_p$ , étant donné que les poids moléculaire du PMVP sont environ proportionnel à  $R_p$  lorsque  $(\text{MVP})_2\text{-ZnX}_2$  sont polymérisées dans le diméthylformamide dans des conditions bien déterminées. Les copolymérisations de  $\text{MVP-ZnX}_2$  complexes (où  $X = \text{Cl}^-$ ,  $\text{Br}^-$ ,  $\text{I}^-$  ou  $\text{CH}_3\text{COO}^-$ ) avec le styrène montrent que les valeurs de  $e$  des MVP complexes sont plus fortement positives que la vinylpyridine libre, et l'importance du glissement positif des valeurs de  $e$  augmente avec une polarisabilité décroissante de l'anion halogénure. Les résultats sont discutés sur la base de propriétés



de transfert de charge des anions, de la nature des liens de coordination et de la structure des vinylpyridines intéressées. Les monomères complexés sont polymérisés difficilement par mécanisme cationique ou anionique. La polymérisation, l'état solide induite par irradiation fournit des polymères avec des rendements faibles.

### Zusammenfassung

Folgende Stöchiometrische Vinylpyridinkomplexe wurden dargestellt:  $(4\text{-VP})_2\text{Zn}(\text{SCN})_2$ ,  $(2\text{-VP})_2\text{Zn}(\text{SCN})_2$ ,  $(\text{MVP})_2\text{Zn}(\text{SCN})_2$ ,  $(\text{MVP})_2\text{ZnCl}_2$ ,  $(\text{MVP})_2\text{ZnBr}_2$ ,  $(\text{MVP})_2\text{ZnI}_2$  und  $(\text{MVP})_2\text{HgCl}_2$ , wo 4-VP, 2-VP und MVP die Abkürzungen für 4-Vinylpyridin, 2-Vinylpyridin und 2-Methyl-5-Vinylpyridin sind. Die Ergebnisse der mit Azobisisobutyronitril gestarteten radikalischen Polymerisation zeigen, dass der Einfluss der Komplexbildung zwischen den Monomeren und dem Metallsalz, mit Ausnahme des 2-VP-Komplexes in einer Erhöhung der Polymerisationsgeschwindigkeit besteht. Die Reihenfolge der Zunahme von  $R_p$  bei der Lösungspolymerisation in Dimethylformid ist die folgende:  $(\text{MVP})_2\text{Zn}(\text{SCN})_2 > (\text{MVP})_2\text{ZnCl}_2 > (\text{MVP})_2\text{ZnBr}_2 > (\text{MVP})_2\text{ZnI}_2 >$  freies MVP;  $(4\text{-VP})_2\text{Zn}(\text{SCN})_2 > (\text{MVP})_2\text{Zn}(\text{SCN})_2 >$  freies VP  $> (2\text{-VP})_2\text{Zn}(\text{SCN})_2$ ;  $\text{MVP} + \text{Zn}(\text{CH}_3\text{COO})_2 < \text{MVP} + \text{Cd}(\text{CH}_3\text{COO})_2$ . Bei Verwendung von Äthanol, Aceton oder Tetrahydrofuran als Lösungsmittel ist zum Teil wegen der Unlöslichkeit des mit den Metallsalzen komplexierten Polymethylvinylpyridins die Änderung von  $R_p$  deutlicher ausgeprägt. Die Zunahme von  $R_p$  kann der Änderung von  $k_p$  zugeschrieben werden, da die Molekulargewichte von PMVP bei der Polymerisation von  $(\text{MVP})_2\text{ZnX}_2$  (wo  $X = \text{Cl}^-$ ,  $\text{Br}^-$ ,  $\text{I}^-$  oder  $\text{SCN}^-$ ) unter bestimmten Bedingungen in DMF zu  $R_p$  nahezu proportional sind. Die Copolymerisation von MVP-ZnX<sub>2</sub>-Komplexen (wo  $X = \text{Cl}^-$ ,  $\text{Br}^-$ ,  $\text{I}^-$  oder  $\text{CH}_3\text{COO}^-$ ) mit Styrol zeigt, dass die  $e$ -Werte von komplexiertem MVP positiver sind als diejenigen von freiem Vinylpyridin und dass der Betrag der positiven Verschiebung der  $e$ -Werte mit abnehmender Polarisierbarkeit der Halogenidanionen zunimmt. Die Ergebnisse werden anhand der Ladungsübertragungseigenschaften der Anionen, der Natur der koordinativen Bindungen und der Struktur der Vinylpyridine diskutiert. Die komplexierten Monomeren werden nach einem kationischen oder anionischen Mechanismus fast nicht polymerisiert. Die strahlungsinduzierte Polymerisation in fester Phase liefert eine niedrige Ausbeute an Polymerem.

Received August 9, 1965

Revised February 15, 1966

Prod. No. 5094A

## Thermal Volatilization Analysis: A New Method for the Characterization of Polymers and the Study of Polymer Degradation

I. C. McNEILL, *Chemistry Department, University of Glasgow, Glasgow, Scotland*

### Synopsis

In a continuously evacuated system in which volatile products are passing from a heated sample to the cold surface of a trap some distance away, a small pressure will develop which varies with the rate of volatilization of the sample. If this pressure (measured by Pirani gage) is recorded as the sample temperature is increased in a linear manner, a TVA thermogram showing one or more peaks is obtained. TVA thermograms for a number of polymers and copolymers are presented and briefly discussed. The technique has some advantages over TGA for characterizing polymers or studying qualitative aspects of polymer degradation.

In recent years the techniques of differential thermal analysis (DTA) and thermogravimetric analysis (TGA) have been increasingly applied to problems of polymer characterization and degradation studies. Each involves the measurement of a convenient variable (in the former a temperature differential, and in the latter the loss in weight of the sample) during a gradual, linear increase in temperature.

Much useful information could in principle be obtained by combining linear temperature programming with the measurement of other variables. One of these is the pressure of volatile products during degradation. In a continuously evacuated system in which condensable volatile products are passing from a heated polymer sample to the cold surface of a trap, some distance away, a small pressure will develop due to the time taken by the products to travel from the hot to the cold surface. The magnitude of the pressure developed varies with the rate of volatilization of the sample. A system can be designed in which the pressure developed during the degradation of a convenient weight of polymer varies within the range  $10^{-4}$ – $10^{-1}$  torr and is therefore readily measured by means of a Pirani gage. This technique has been used by Grassie and co-workers<sup>1-3</sup> in isothermal degradation studies over a number of years. No previous attempt appears to have been made, however, to apply the method to temperature-programmed experiments.

When the variation in pressure of volatile products is recorded during a degradation in which the temperature of the polymer sample is increased

at a steady rate, the resulting thermogram is of considerable interest. It is proposed to refer subsequently to this technique as thermal volatilization analysis (TVA). The purpose of this communication is to illustrate the potential usefulness of the method by presenting and discussing very briefly a small selection of examples of TVA thermograms.

The apparatus required for TVA is simple, and since no moving parts are involved, it is sturdy. A flat-bottomed glass tube containing the polymer sample as a fine powder or film is inserted into the top of a small oven, the temperature of which is varied by means of a linear temperature programming unit. The glass tube is connected first to a trap surrounded with liquid nitrogen and then to a mercury diffusion pump and rotary oil pump. Between the tube and the trap is attached a Pirani gage head. The gage control unit provides an output for a 10-mv. potentiometric strip chart recorder so that a continuous trace of pressure versus time (temperature) may be obtained. Polymer samples from 10 to 250 mg. can conveniently be handled; in the case of materials which give only very small amounts of volatile products, increased sensitivity is readily obtained by using a 2.5-mv. recorder range. A fuller description of the apparatus and details of temperature calibration will be published later.

As with TGA and DTA, each polymer will, in general, give a characteristic thermogram, and detail differences may be observed for samples of a given polymer, depending on their history. TVA differs from TGA, however, in that the rate of volatilization is being measured, since the pressure at any temperature is related to the rate of volatilization at that temperature. Hence the TVA thermogram for a polymer sample shows one or more peaks, whereas in the case of TGA what is obtained is a trace with one or more points of inflection, which has to be differentiated to obtain a rate plot. For purposes of polymer characterization or qualitative investigation of the degradation of polymers, the technique of TVA therefore offers advantages in a convenient form of trace as well as in experimental simplicity. The possibilities for quantitative application of TVA are being examined.

### SELECTED EXAMPLES OF TVA THERMOGRAMS

The thermograms reproduced were all obtained with the use of 25-mg. samples, a linear heating rate of  $10^{\circ}\text{C./min.}$ , and a recorder sensitivity of 10 mv. The ordinate covers a nominal pressure range (based on the dry air calibration of the gage) from  $10^{-4}$  to  $3 \times 10^{-1}$  torr, the scale being non-linear and considerably compressed towards the high pressure end. The nonlinearity of the scale is useful, since smaller peaks, which may be of considerable interest when detail differences in similar polymer samples are being examined, are more readily detected.

As in the case of TGA, the trace obtained is somewhat dependent on the heating rate. In many cases the only difference observed with different heating rates is a slight shift in the positions of the rate maxima. With

some polymers, however, the changes can be more profound. A standard heating rate ( $10^{\circ}\text{C./min.}$ ) has therefore been adopted in the present work.

### Poly(methyl Methacrylate)

TVA thermograms are reproduced in Figure 1 for three samples prepared by bulk polymerization with azobisisobutyronitrile as initiator at  $60^{\circ}\text{C.}$  The number-average molecular weights were 820,000, 250,000, and approximately 20,000, respectively.

The two stages in the degradation are clearly distinguished. The first peak above  $200^{\circ}\text{C.}$  represents reaction initiated at unsaturated ends formed in the termination step of the polymerization.<sup>4,5</sup> The second, larger peak corresponds to reaction at higher temperatures, initiated by random scission of the main chain.<sup>6</sup> It is apparent that as the proportion of chain ends in the sample increases, the size of the first peak increases also. These TVA thermograms illustrate very clearly the conclusions recently drawn by MacCallum<sup>7</sup> in a general consideration of the mechanism of degradation of this polymer.

The peaks occurring below  $200^{\circ}\text{C.}$  can be attributed to trapped solvent, precipitant, etc. These show up very clearly, indicating the usefulness of TVA as a method of testing polymers for freedom from this type of impurity.

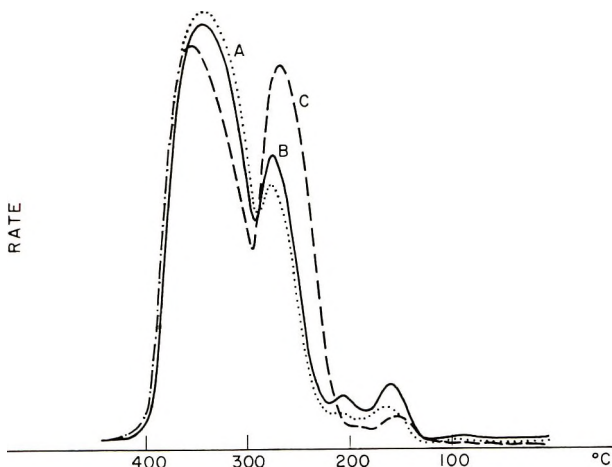


Fig. 1. TVA thermograms ( $10^{\circ}\text{C./min.}$ ) for samples of poly(methyl methacrylate) of various molecular weights: (a) 820,000; (b) 250,000; (c) approx. 20,000.

### Poly(vinyl Acetate) and Poly(vinyl Chloride)

The similarities in the degradation mechanisms of these two polymers make the TVA thermograms (Fig. 2) of great interest. The lower thermal stability of PVC shows up strikingly, but the second stage of the degradation of both polymers, corresponding to breakup of a  $(-\text{CH}=\text{CH}-)_n$  chain, is clearly similar in both polymers. The PVC sample was prepared by bulk polymerization with azobisisobutyronitrile as initiator; the PVA

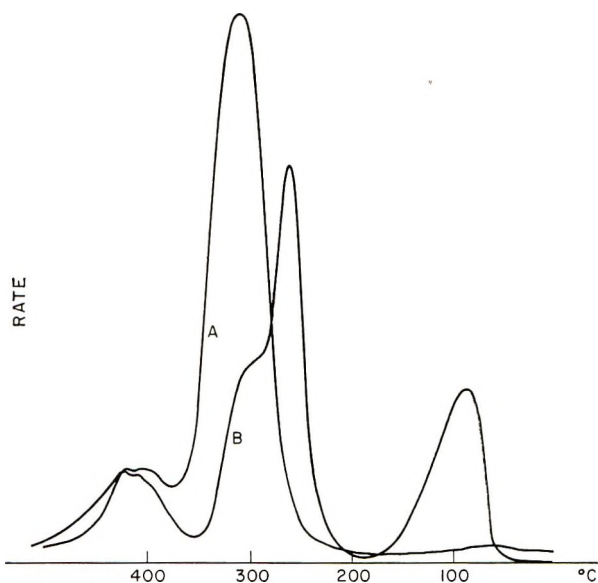


Fig. 2. TVA thermograms ( $10^{\circ}\text{C./min.}$ ) for (a) poly(vinyl acetate); (b) poly(vinyl chloride).

was a B.D.H. sample. The former shows a large solvent peak due to trapped solvent (cyclohexanone); the latter is almost free of trapped volatile material. A commercial PVC sample (Geon 101) gave a thermogram similar to Figure 2b, but without the solvent peak.

### Polyacrylonitrile and Polymethacrylonitrile

The degradation reactions of these polymers have been fully discussed.<sup>8,9</sup> The former gives only small amounts of volatile material, but the latter

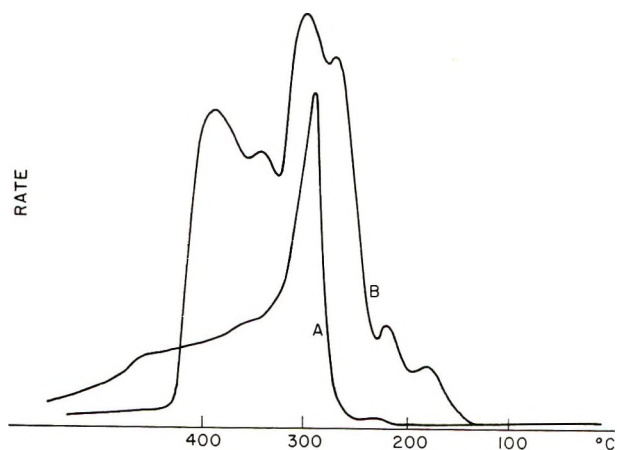


Fig. 3. TVA thermograms ( $10^{\circ}\text{C./min.}$ ) for (a) polyacrylonitrile; (b) polymethacrylonitrile.

undergoes a number of reactions, monomer being produced in large quantities (Fig. 3).

The PAN was a Chemstrand polymer. PMAN was prepared at 65°C. with azobisisobutyronitrile as initiator, and had a number-average molecular weight of approximately 12,000.

### Polystyrene, Poly- $\alpha$ -methylstyrene, and Poly- $\alpha$ -phenylacrylonitrile

Polystyrene and poly- $\alpha$ -methyl styrene both give thermograms consisting of single peaks (Fig. 4), that for the latter occurring at a very much lower temperature. Poly- $\alpha$ -phenylacrylonitrile is even less stable: degradation begins below 200°C., and in this case two or more reactions are clearly involved, because of the double peak.

The polystyrene sample was prepared by bulk polymerization at 60°C. with the use of azobisisobutyronitrile as initiator. Poly- $\alpha$ -methylstyrene was prepared at -78°C. in methylene chloride solution with stannic chloride as initiator. Poly- $\alpha$ -phenylacrylonitrile was a Chemstrand sample.

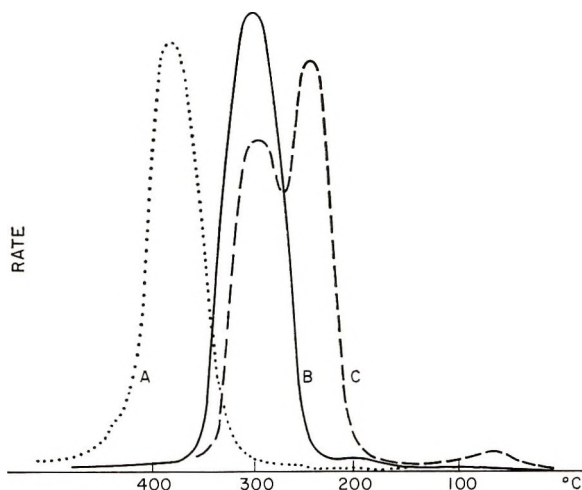


Fig. 4. TVA thermograms (10°C./min.) for (a) polystyrene; (b) poly- $\alpha$ -methylstyrene; (c) poly- $\alpha$ -phenylacrylonitrile.

### Polyisobutene, Butyl Rubber, and Chlorobutyl Rubber

The decrease in stability resulting from incorporation of small amounts of isoprene in a polyisobutene chain is apparent from a comparison of curves *a* and *b* in Figure 5. Conversion of butyl rubber to chlorobutyl rubber results in a further decrease in thermal stability (Fig. 5c).

Polyisobutene was prepared at -78°C. in methylene chloride solution with stannic chloride as initiator. Butyl (Enjay MD-501, 3.5 mole-% unsaturation) and chlorobutyl (Enjay HT 10-66, 1.5 mole-% unsaturation) were Esso samples.

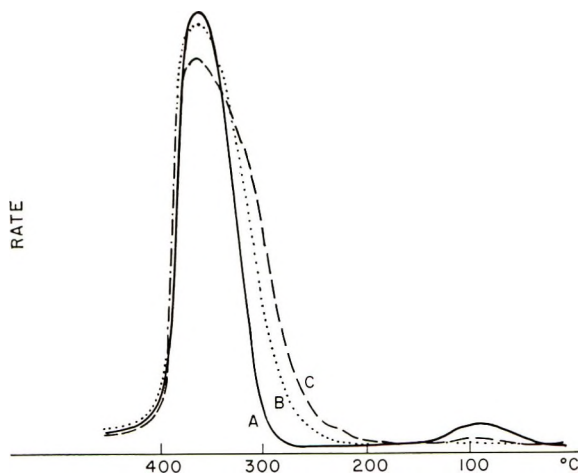


Fig. 5. TVA thermograms ( $10^{\circ}\text{C./min.}$ ) for (a) polyisobutene; (b) butyl rubber; (c) chlorobutyl rubber. See text for unsaturation data.

### Polystyrene and a Styrene-Butadiene Copolymer

Incorporation of large amounts of butadiene into the polystyrene chain does not result in lower thermal stability, but it is clear that less volatile degradation products are obtained in the case of the copolymer (Fig. 6). This is in agreement with the findings of Madorsky and co-workers.<sup>6</sup>

The polystyrene sample was the same as mentioned above (Fig. 4). The copolymer was an I.C.I. product (Butakon S 7001) containing 30% by weight of Butadiene.

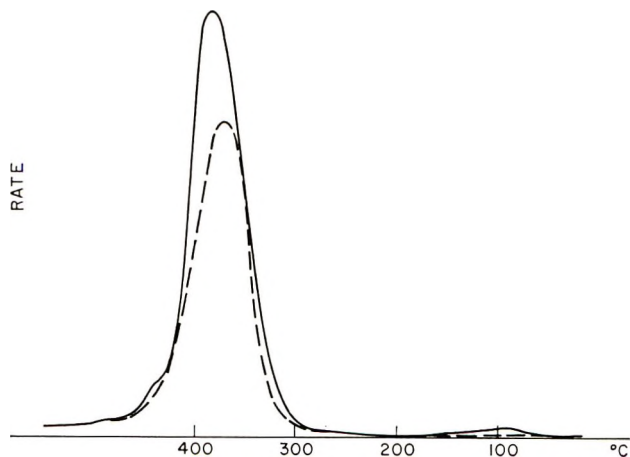


Fig. 6. TVA thermograms ( $10^{\circ}\text{C./min.}$ ) for (a) polystyrene; (b) a styrene-butadiene copolymer containing 30% butadiene.

### CONCLUSION

In conclusion, from a consideration of the examples of TVA given, the method would appear to have applications particularly in the following

fields: (1) characterization of polymer samples; (2) studies of the effect of structural details on polymer degradation behavior; (3) detection of volatile impurities in polymer samples; (4) studies of the effect of composition on copolymer stability.

The author is indebted to Dr. N. Grassie, Mr. I. F. McLaren, Mr. J. Pang, Mr. B. J. D. Torrance, and the firms mentioned in the text for kindly providing some of the samples used in this work.

### References

1. N. Grassie, *The Chemistry of High Polymer Degradation Processes*, Butterworths, London, 1956.
2. N. Grassie and I. C. McNeill, *J. Chem. Soc.*, **1956**, 3929.
3. D. H. Grant and N. Grassie, *Polymer*, **1**, 445 (1960).
4. N. Grassie and H. W. Melville, *Proc. Roy. Soc. (London)*, **A199**, 1 (1949).
5. N. Grassie and E. Vance, *Trans. Faraday Soc.*, **49**, 184 (1953).
6. A. Brockhaus and E. Jenckel, *Makromol. Chem.*, **18/19**, 262 (1956).
7. J. R. MacCallum, *Makromol. Chem.*, **83**, 137 (1965).
8. N. Grassie and I. C. McNeill, *J. Polymer Sci.*, **27**, 207 (1958); *ibid.*, **30**, 37 (1958); *ibid.*, **33**, 171 (1958); *ibid.*, **39**, 211 (1959).
9. S. L. Madorsky, *Thermal Degradation of Organic Polymers*, Interscience, New York, 1964.

### Résumé

Lorsqu'un produit volatil passe d'un échantillon chauffé à une surface refroidie d'une trappe située à une certaine distance de l'échantillon dans un système continuellement évacué, une faible pression se développera; elle variera avec la vitesse de volatilisation de l'échantillon. Si cette pression (mesurée au moyen d'une gauge de Pirani) est enregistrée, de même que la température de l'échantillon, et si elle augmente de façon linéaire, on obtiendra un thermogramme TVA manifestant un ou plusieurs pics. Les thermogrammes TVA obtenus pour un certain nombre de polymères et copolymères sont présentés et discutés brièvement. La technique présente certains avantages sur l'analyse thermogravimétrique pour caractériser les polymères ou pour étudier des aspects qualitatifs de la dégradation de polymères.

### Zusammenfassung

In einem kontinuierlich evakuierten System, in welchem flüchtige Produkte von einer erhitzten Probe zur kalten Oberfläche eines in einem gewissen Abstand befindlichen Abfängers übergehen, wird sich ein kleiner Druck einstellen, der von der Verflüchtigungsgeschwindigkeit der Probe abhängt. Bei Aufzeichnung dieses (mit einem Piranimanometer gemessenen) Druckes während der linearen Temperaturerhöhung der Probe wird ein TVA-Thermogramm mit einem oder mehreren Maxima erhalten. TVA-Thermogramme werden für eine Anzahl von Polymeren und Kopolymeren vorgelegt und kurz diskutiert. Das Verfahren besitzt einige Vorteile gegenüber der TGA zur Charakterisierung von Polymeren und zur Untersuchung der qualitativen Aspekte des Polymerabbaus.

Received July 27, 1965

Revised February 17, 1966

Prod. No. 5099A



## **Polymerization in the Crystalline State. IX. Relation between the Velocity of Radiation-Induced In-Source Polymerization and Post-Polymerization**

HERBERT MORAWETZ, *Department of Chemistry, Polytechnic Institute  
of Brooklyn, Brooklyn, New York 11201*

### **Synopsis**

A general relation is derived between the polymerization velocities to be expected for crystalline monomers during irradiation at a polymerization temperature and the post-polymerization observed in samples irradiated at very low temperatures and subsequently warmed outside the irradiation source. For acrylamide, the experimental data are in satisfactory agreement with the theoretical relationship. The possible reasons for a deviation from this relationship are discussed.

In studies of the polymerization of crystalline monomers initiated by ionizing radiation, two experimental techniques are commonly employed. In the first one, referred to as in-source polymerization, the monomer crystals are irradiated at a temperature at which polymerization can proceed. In the other technique, the crystals are exposed to irradiation at very low temperatures, which allow the formation of the initiating species but do not permit the growth of the polymer chain. The irradiated sample is then warmed outside the radiation source to a temperature at which post-polymerization may be observed. This procedure should yield data which are more easily interpretable, since effects resulting from chain propagation are not complicated by the superposition of a continuing chain initiation process. In addition, the post-polymerization technique has the advantage that polymer is not exposed to irradiation, which might lead to chain grafting, crosslinking, etc.

The question arises whether a general relationship between the kinetics of in-source polymerization and post-polymerization would be expected. This is, indeed, the case, provided we may assume that the two processes are characterized by similar efficiencies of the chain initiation step and that the kinetics of the propagation of any given polymer chain is unaffected by the irradiation of the crystal in which it is imbedded.

Post-polymerization has been studied in greatest detail on crystalline acrylamide.<sup>1</sup> Studies of the kinetics of the process and of the dependence of the molecular weight of the polymeric product on the post-polymerization time have established that the rate of propagation of the individual chains is independent of the concentration of growing chains. Bimolecular

chain termination appears to be negligible, but the rate of propagation decays rapidly with increasing chain length. The dependence of the fractional polymer yield  $Y$  on the post-polymerization time  $t$  has been shown, both in the case of acrylamide<sup>1</sup> and of acrylic acid salts,<sup>2</sup> to be of the form

$$Y = A \ln(1 + Bt) \quad (1)$$

Since the chain length of the polymer obtained at a given time is independent of the irradiation dose,  $A$  must be proportional to the dose  $R$  while  $B$  is independent of it:

$$Y = kR \ln(1 + Bt) \quad (2)$$

In an in-source polymerization experiment, the dose received in the time interval between  $t'$  and  $t' + dt'$  before the end of the irradiation is  $dR = Idt'$ , where  $I$  is the irradiation rate. The chains initiated in that interval are allowed to grow for a time  $t'$ . The total yield from chains initiated at any time during the irradiation is then

$$Y = kI \int_0^t \ln(1 + Bt') dt' = (kI/B)[(1 + Bt)\ln(1 + Bt) - Bt] \quad (3)$$

The polymerization rate obtained by differentiation of eq. (3) is

$$dY/dt = kI \ln(1 + Bt) \quad (4)$$

or, expressing the rate in terms of  $Y$ , we obtain by substitution of eq. (3) into eq. (4)

$$dY/dt = (BY + kIBt)/(1 + Bt) \quad (5)$$

Setting  $Bt = x$ ,  $BY/kI = y$ , eqs. (3) and (5) may be written as

$$\begin{aligned} y &= (1 + x)\ln(1 + x) - x \\ dY/dt &= kI(x + y)/(1 + x) \end{aligned} \quad (6)$$

### Comparison with Experimental Data

Acrylamide is the only crystalline monomer which has been studied extensively by both in-source polymerization and post-polymerization techniques. In studies by Baysal et al.<sup>3</sup> it was found that in-source polymerization leads to a polymer yield proportional to the square of the irradiation time, and this relationship was confirmed by Chapiro and Zumer<sup>4</sup> in more extensive recent investigations of in-source polymerization kinetics. We may note that eq. (3) leads to  $Y = kIBt^2/2$  in the limit of  $Bt \ll 1$ . The general relation between the dimensionless quantities  $YB/kI$  and  $Bt$  predicted from theory is represented on Figure 1, and we may see that for  $Bt > 1$  the yield is proportional to a significantly lower power of  $t$  (between  $Bt = 1$  and  $Bt = 10$ ,  $Y$  increases by a factor of 39, between  $Bt = 10$  and  $Bt = 100$  by a factor of 24). The post-polymerization data of Fadner and Morawetz<sup>1</sup> lead to  $B = 10^{-4} \text{ sec.}^{-1}$  and  $B = 2.5 \times 10^{-5} \text{ sec.}^{-1}$  at 35 and 25°C., respectively; we may then estimate  $B = 10^{-5} \text{ sec.}^{-1}$  at 20°C., the temperature

used by Chapiro and Zumer. The longest experiment for which they report data corresponds to  $t = 2 \times 10^5$  sec. or  $Bt = 2$ ; their observation of yields proportional to  $t^2$  is thus consistent with the theoretically predicted time dependence of the polymer yield as given in Figure 1. It may be predicted that in experiments with substantially lower radiation intensities (and correspondingly longer times) the polymer yield would depend on a substantially lower power of  $t$ .

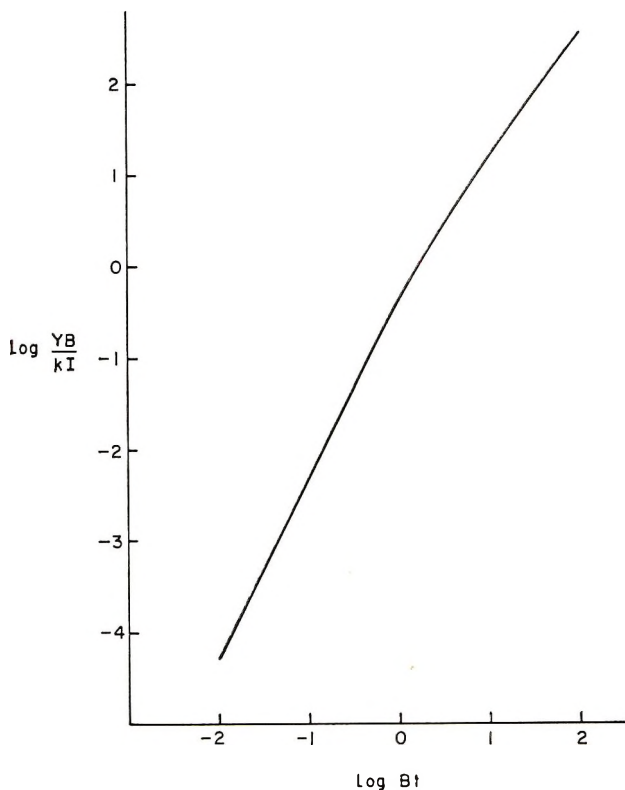


Fig. 1. Theoretically predicted time dependence of polymer yield for in-source polymerizations.

Figure 2 represents a plot of the polymerization rate  $dY/dt$  (where  $Y$  is the fractional conversion and  $t$  is in seconds) as a function of the irradiation intensity  $I$  at  $Y = 0.05$ . The solid curve represents the relation predicted by eq. (6) for  $B = 10^{-5}$  sec. $^{-1}$  and  $k = 2 \times 10^{-7}$  rad $^{-1}$ , estimated from the post-polymerization data.<sup>1</sup> The crosses represent the experimental data reported by Chapiro and Zumer; they lie somewhat above the theoretical curve with the discrepancy increasing with an increasing irradiation intensity from a factor of 2 at  $I = 1$  rad/sec. to a factor of 4 at  $I = 100$  rad/sec.

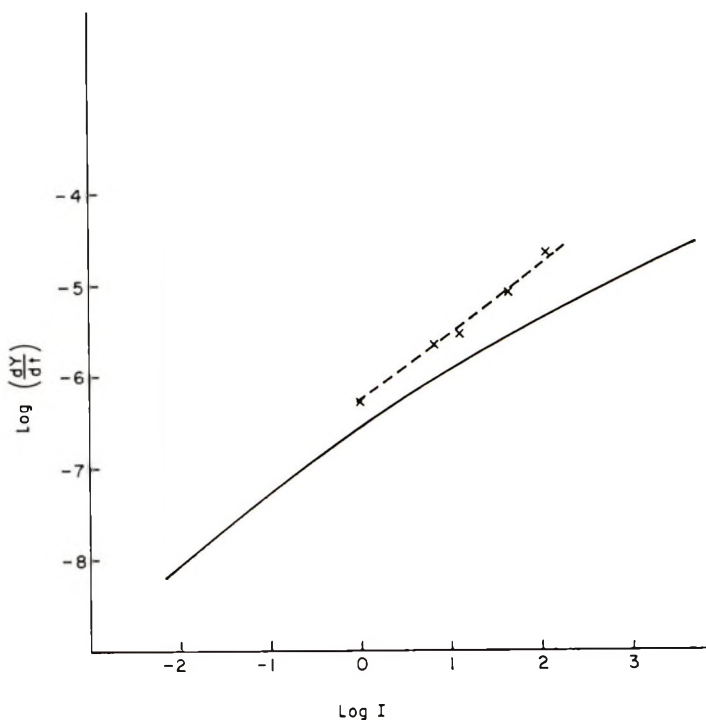
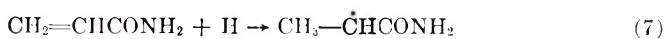


Fig. 2. Dependence of the in-source polymerization velocity of acrylamide at 20°C. and at a fractional conversion of 0.05 on the irradiation rate: (—) values predicted on the basis of constants obtained from post-polymerization data; (×) experimental results quoted by Chapiro and Zumer.<sup>4</sup>

### Discussion

In view of the uncertainty in the estimate of the constants  $B$  and  $k$ , the agreement between the observed in-source polymerization velocities with those predicted on the basis of post-polymerization data must be considered remarkably close. The tendency for the discrepancy to increase with increasing radiation intensities is hardly surprising. For  $I = 100$  rad/sec., the polymerization velocity at  $Y = 0.05$  is about 10%/hr.; this is a rate at which the dissipation of the heat of reaction presents problems even for liquid-phase polymerizations, and it may be doubted whether thermostatic conditions can be maintained in a polycrystalline sample, in which heat transfer is extremely inefficient.

In principle, there are several factors which might lead to deviations from the relations derived above. The initiation step in the radiation-induced polymerization of vinyl monomers seems to involve the addition of a hydrogen atom, detached from one monomer molecule, to the vinyl group of another monomer, e.g., for acrylamide



However, ESR data indicate generally the presence of one initiating radical only,<sup>5</sup> suggesting that only the radical formed by the addition of hydrogen atoms survives for an appreciable period of time, while the radicals formed by hydrogen atom abstraction presumably disappear by dimerization or some other process. We may then envisage at least two reasons why the chain initiation efficiency may be different in post-polymerization and in-source polymerization experiments. First, it is possible that irradiation at higher temperatures allows radicals formed by hydrogen atom abstraction to add a monomer unit before these relatively unstable species decay. Secondly, it is conceivable that the relative probability of hydrogen atom capture by a vinyl group, as compared with the combination of hydrogen atoms to form H<sub>2</sub> molecules, is different at different irradiation temperatures.

It is also necessary to consider the possibility that chain propagation might proceed at significantly different rates in the two types of processes. For instance, the mobility of monomer molecules may be highly sensitive to the presence of radiation-induced crystal dislocations, which might be partially annealed, in a post-polymerization experiment, before the sample attains the temperature at which polymerization is significant. Another possible cause for differences in results obtained by the two experimental techniques is the possibility that propagating chains might be terminated by hydrogen atoms in an in-source polymerization.

In view of all these possibilities, it is all the more remarkable that acrylamide should appear to behave in such a similar manner whether the post-polymerization or the in-source polymerization technique is employed. However, we should admit that the relationship between results obtained by these two techniques may be quite different for other monomers. Extreme cases of this type were described by Barkalov et al.,<sup>6</sup> who found that acrylonitrile and vinyl acetate polymerize in the solid state only during irradiation. They assumed that a short-lived excited state produced by the irradiation is essential for the chain propagation process. It would be desirable to obtain in-source and post-polymerization data for a larger number of crystalline monomers so as to assess the frequency with which such complicating factors become significant.

Finally, one point deserves special emphasis. Kargin et al.<sup>7</sup> have repeatedly claimed that kinetic data of the in-source polymerization of crystalline acrylamide gives evidence for an autocatalytic effect, as predicted from their theoretical treatment. Since post-polymerization of acrylamide irradiated at low temperatures shows a decay of the reaction rate from the outset of the process, and since the above calculations show that in-source polymerization kinetics may be predicted quantitatively from post-polymerization data, there is no possible basis for the assumption of an autocatalytic effect in this particular case.

This work was supported by the U. S. Atomic Energy Commission, contract AT(30-1)-1715.

### References

1. T. A. Fadner and H. Morawetz, *J. Polymer Sci.*, **45**, 475 (1960).
2. H. Morawetz and I. D. Rubin, *J. Polymer Sci.*, **57**, 669 (1962).
3. B. Baysal, G. Adler, D. Ballantine, and P. Colombo, *J. Polymer Sci.*, **44**, 117 (1960).
4. A. Chapiro and M. Zumer, *J. Chim. Phys.*, **1965**, 947.
5. G. Adler, D. Ballantine, and B. Baysal, *J. Polymer Sci.*, **48**, 195 (1960).
6. I. M. Barkalov, V. I. Goldanskii, N. S. Enikolopyan, S. F. Terekhova and G. M. Trofimova, *J. Polymer Sci. C*, **4**, 897, 909 (1964).
7. V. A. Kargin, V. A. Kabanov, and I. M. Papissov, *J. Polymer Sci. C*, **4**, 767 (1963); V. A. Kargin and V. A. Kabanov, *Zh. Vses. Khim. Obshchestva im. D. I. Mendeleeva*, **9**, [6], 602 (1964).

### Résumé

Une relation générale a été déduite entre les vitesses de polymérisation prévues pour des monomères cristallins en cours d'irradiation à une température de polymérisation, et les post-polymérisations observées sur des échantillons irradiés à très basses températures et ultérieurement chauffés en dehors de la source d'irradiation. Pour l'acrylamide, des données expérimentales sont en accord satisfaisant avec cette relation théorique. Les raisons possibles de déviation au départ de cette relation sont soumises à discussion.

### Zusammenfassung

Eine allgemeine Beziehung zwischen der für kristalline Monomere während der Bestrahlung bei einer bestimmten Polymerisationstemperatur zu erwartenden Polymerisationsgeschwindigkeit und der bei Proben, welche bei sehr tiefen Temperaturen bestrahlt und nachher aussergalb der Bestrahlungsquelle erwärmt wurden, beobachteten Nachpolymerisation wird abgeleitet. Bei Acrylamid stimmen die Versuchsdaten mit der theoretischen Beziehung befriedigend überein. Mögliche Gründe für eine Abweichung von dieser Beziehung werden diskutiert.

Received March 7, 1966

Prod. No. 5100A

## Cyclo- and Cyclized Diene Polymers. XII. Cationic Polymerization of Isoprene

N. G. GAYLORD and B. MATYSKA,  
*Gaylord Associates Inc., Newark, New Jersey* and  
K. MACH and J. VODEHNAL, *Institute of Physical Chemistry,  
Czechoslovak Academy of Sciences, Prague, Czechoslovakia*

### Synopsis

Polymerization of isoprene with Lewis acids in *n*-heptane is a process leading to a quasi-equilibrium which is characterized by very low conversions. Polymerization rates in aromatic solvents are much higher due to extensive chain transfer with solvent with regeneration of the original active centers. The rate of monomer disappearance in benzene or toluene when aluminum bromide is the catalyst is second order with respect to monomer concentration. The reaction order with respect to the catalyst depends on the reaction conditions; at constant monomer concentration it is approximately one. Polymerization rates in halogenated solvents with the use of syringe techniques are much higher than those in aromatic solvents. Polymers obtained with various cationic catalysts ranged from oils to white powders having molecular weights up to more than 100,000 depending on reaction conditions. All polymers exhibited infrared spectra characteristic of cyclopolydienes, and the content of linear structures usually did not exceed 20%, irrespective of the nature of the catalyst or solvent. In solvents of higher polarity, such as *o*-dichlorobenzene, more linear structures were detected. Among residual linear forms the *trans*-1,4 addition was found to prevail. Residual unsaturation in polymers did not exceed 30%.

### INTRODUCTION

Qualitative work on polymerization of conjugated dienes with protonic or Lewis acids as catalyst was carried out as early as the nineteenth century, and subsequently many patents and papers have appeared dealing with this subject.<sup>1,2</sup> It was found that isoprene as well as butadiene can be polymerized to powdery, tacky, or oily products, depending on the reaction conditions. Except for the early work there have been, however, only few data published concerning the polymerization kinetics or the microstructure of the polymers.

A review on cationic polymerization of isoprene appeared recently.<sup>3</sup> Martin and Farmer observed the formation of dimers of terpenic nature from dimethylbutadiene.<sup>4</sup> Ferington and Tobolsky<sup>5</sup> examined the influence of various cationic catalysts on the structure of polybutadienes obtained at  $-78^{\circ}\text{C}$ . They found that the ratio of 1,4-*trans*/1,2 units was in most cases nearly constant, irrespective of the nature of the catalyst,

over a wide range of concentrations and for different degrees of conversion. Some deviations were observed only in highly polar media such as nitrobenzene or nitroethane. Another investigation of the cationic polymerization of butadiene with the use of different catalysts was undertaken by Marvel and co-workers,<sup>6</sup> who found that the intrinsic viscosities of the polymers were in the range of 0.3 or less and the polymers contained approximately 50–60% of 1,4 addition units. More recently, Richardson<sup>7</sup> reexamined the structure of cationically polymerized polyisoprenes and polybutadienes by means of infrared spectroscopy and pointed out that the sum of linear addition forms never reached the theoretical 100% value but always remained far below. This phenomenon has also been observed by other authors.<sup>8,9</sup> Most investigators determined the structure by the method proposed by Binder,<sup>10</sup> relating the contents of each component to the so-called total found.

The possibility of the occurrence of cyclic structures in diene polymers obtained with Ziegler type catalysts containing an excess of the transition metal compound has been indicated by Gaylord and co-workers.<sup>11</sup> A comparative infrared study of the structure of cyclized natural polyisoprenes, synthetic polybutadienes, and polychloroprenes, and of cyclopolymers obtained directly by polymerization of each particular monomer under suitable conditions was published recently by Kössler and co-workers.<sup>12</sup> Preparation of cyclic polymers from different substituted butadienes has been claimed by Bell in a recent patent.<sup>13</sup> An investigation of the cyclopolymerization of isoprene with a mixed catalytic system ethylaluminum dichloride–titanium tetrachloride showed that the catalytic activity of the system in the formation of cyclic polymers increased with the increasing acid character of reaction products.<sup>14</sup>

The purpose of the present paper is to provide some more information concerning the microstructure of isoprene polymers obtained with different typical cationic catalysts under vigorous reaction conditions and to prove that the formation of cyclic structures in polyisoprenes always takes place when the polymerization is acid-catalyzed.

## EXPERIMENTAL

Polymerization experiments were performed by using two different experimental techniques, i.e., high-vacuum technique and the hypodermic-syringe technique.

### Experiments Performed by Using Vacuum Techniques

Isoprene was of analytical grade (Lachema). Before use it was rectified on a 35 TP column, then refluxed 4 hr. over sodium suspension and finally distilled through a small column filled with activated molecular sieves in vacuum, directly into ampules provided with a ground joint ending in a breakable tip, which were sealed off.

Hydrocarbon solvents were washed repeatedly with concentrated sulfuric acid until no discoloration occurred, then with water, caustic soda,



and repeatedly with distilled water and distilled on a 35 TP column. Thereafter they were refluxed over sodium suspension, distilled into a container connected with the vacuum manifold, frozen in liquid nitrogen, evacuated in the frozen state, and vacuum-distilled through a column packed with molecular sieves into ampules.

Aluminum alkyls were synthesized in the laboratory according to methods described in the literature and purified by repeated distillation in vacuum. Finally they were distilled into ampules containing a definite volume of pure dry *n*-heptane and the ampules were sealed off. Concentrations were determined from the aluminum and halide contents according to gravimetric analysis. Aluminum halides, titanium tetrachloride, tin tetrachloride, and antimony trichloride were from Lachema and were purified by repeated distillation or sublimation in vacuum. A similar procedure was used for the preparation of solutions as in the case of the aluminum alkyls.

Most polymerizations were performed in glass bottles attached to the vacuum line and provided with two ground joints through which the ampules with solvents and catalysts were attached. (More details are given in a previous paper.<sup>11</sup>) By means of a three-way stopcock the vacuum line could be separated from the polymerization vessel, and through the other opening gaseous isoprene from a thermostatted storage vessel could be introduced. After evacuation of the system to  $10^{-5}$  mm. Hg under simultaneous open-flame heating, the vacuum line was closed, and solvent and catalyst were charged into the polymerization vessel by turning the ampules in the joints and thus breaking their thin-wall tips. Polymerizations were started by introducing gaseous isoprene until the desired total pressure over the reaction mixture was reached. Then the inlet for isoprene was closed and the course of the polymerization was followed by recording the total pressure over the reaction mixture. It should be noted, however, that absolute concentrations of monomer can be calculated only when the system behaves ideally in the thermodynamic sense or when accurate vapor pressure data of corresponding binary systems are available, such as in the case of isoprene-*n*-heptane. Otherwise measurements are only of comparative value.

The amount of solvent used in most experiments was 30 ml. Temperature was kept constant by means of a Hoppler ultrathermostat at 21°C.

### Experiments Performed by Using Hypodermic-Syringe Techniques

The influence of the solvent nature on the structure of the polymers was studied by use of the common hypodermic-syringe technique. In that case solvents including *n*-heptane (Phillips Petroleum Co., Pure), cyclohexane (Fisher Scientific Co., Spectralanalyzed), and benzene were dried by storage over Drierite and calcium hydride, and before use they were distilled from calcium hydride. Halogenated solvents were stored over Drierite and distilled before use from activated molecular sieves, Linde 4A.

Aluminum alkyls (Texas Alkyls, Inc.) were used as 25% solutions in dry *n*-heptane without further purification.

Isoprene (Matheson, Coleman and Bell Co.) was dried and distilled in the same manner as hydrocarbon solvents. All polymerizations as well as any transfers of reagents were carried out under a stream of dry nitrogen.

Solid polymers were recovered by pouring the reaction mixture into methanol, filtering, and drying at 50°C. under reduced pressure. Oily products were isolated by vacuum distillation. Infrared spectra of CS<sub>2</sub> solutions and/or KBr pellets of polymers were taken on the UR-10 (Zeiss Jena) or Perkin-Elmer 21 spectrometers. Evaluation of spectra was carried out by the method described elsewhere.<sup>15</sup> In some cases molecular weights were determined by the light-scattering method or by mass spectrometry (in the case of oily products). The content of double bonds in some soluble polymers was determined by the usual iodine monochloride method. Intrinsic viscosities were measured in a Ubbelohde viscometer at 25°C. in benzene.

## RESULTS AND DISCUSSION

### Polymerization in *n*-Heptane

The course of the isoprene polymerization with Friedel-Crafts catalysts depends strongly on the type of solvent used as the polymerization medium. In carefully purified *n*-heptane at constant monomer concentration, with aluminum bromide, ethylaluminum dichloride, or stannic chloride as catalysts (Fig. 1), the reaction has an initial very fast stage followed by a period when the polymerization practically stops. The conversion at that stage is very low, as has similarly been observed in many other cationic polymerizations. Upon increasing stepwise the partial pressure of isoprene over the reaction mixture, i.e., the concentration of monomer in the reaction mixture, in each step further polymerization takes place until a new equilibrium is established (Fig. 2).

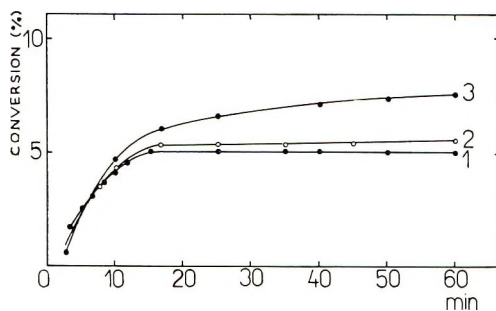


Fig. 1. Polymerization of isoprene in *n*-heptane at constant monomer concentration, 30 ml. of solvent, 21°C.: (1) 0.7 mmole C<sub>2</sub>H<sub>5</sub>AlCl<sub>2</sub>, monomer concentration 0.8 mole/l., (2) 0.8 mmole AlCl<sub>3</sub>, monomer concentration 0.8 mole/l., (3) 0.7 mmole AlBr<sub>3</sub>, monomer concentration 0.4 mole/l.

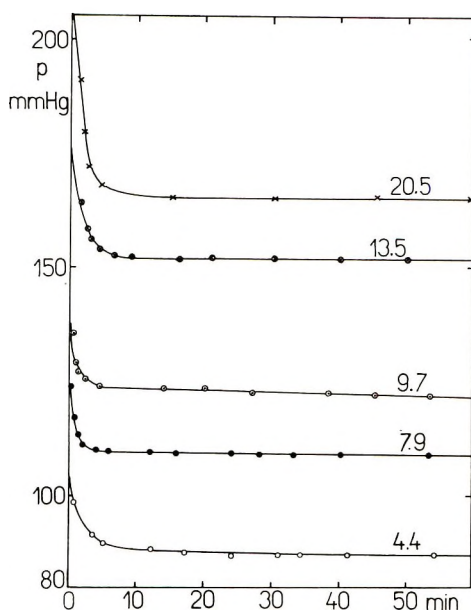


Fig. 2. Polymerization of isoprene in *n*-heptane, 30 ml. of solvent, 21°C., 0.7 mmole  $C_2H_5AlCl_2$ . Figures on curves indicate the per cent conversion at the equilibrium stage. At this point the isoprene pressure (concentration) was increased to the next highest level shown. Vapor pressure of pure *n*-heptane at 21°C. = 38 mm. Hg.

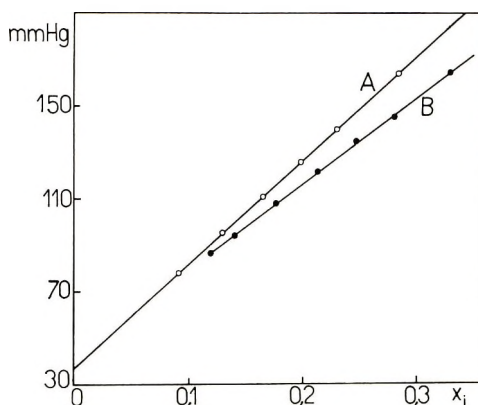


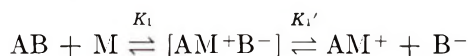
Fig. 3. Dependence of the vapor pressure over the binary mixture *n*-heptane-isoprene at 21°C. on the concentration of isoprene (expressed as the molar fraction  $X_i$ ): (A) in the absence of catalyst; (B) in the presence of 0.7 mmole  $C_2H_5AlCl_2$ .

The dependence of the total pressure over the reaction mixture in the presence and in the absence of catalyst versus the total amount of isoprene added is plotted in Figure 3. In the case B the concentration of isoprene which is expressed in the molar fraction  $X_i$  also includes the amount of monomer polymerized. It is seen that the difference between the vapor pressure over a binary mixture of isoprene and heptane and over the same

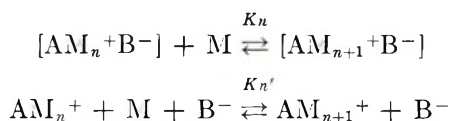
mixture which also contains a catalyst is very small and increases linearly with the concentration of isoprene. The pressure difference between curves *A* and *B* is directly proportional to the conversion. Based on the present results, unfortunately, it was not possible to calculate any equilibrium constants because an undefined portion of the monomer consumed had polymerized to dead polymer which did not contribute to the equilibrium, so that the amount of complexed monomer could not be determined.

A possible explanation for the quasi-equilibrium is the complete consumption of adventitious water acting as a cocatalyst. When an equilibrium mixture was sealed off under vacuum and stored at room temperature for several weeks, nearly 100% conversion was found at the end of that period. The clear solution over the precipitated polymer showed catalytic activity only slightly lower than that of the initial mixture. Although it is possible that cocatalytic water may have diffused back into the system during the storage period through joints, work with completely sealed systems has also shown that additional monomer is consumed on standing. These findings suggest the following qualitative explanation of the polymerization mechanism. The reaction of conjugated diene with metal halide results in the formation of a complex in which both double bonds of the monomer may be involved. This complex may exist as a coordination complex on a cation with a closely held undissociated gegenion. The ion-pair rapidly consumes monomer to regenerate ion-pair species.

If one considers the scheme



where *AB* is metal halide, dimeric, *M* is monomer, and  $[AM^+B^-]$  = intimate ion pair, propagation proceeds by monomer addition to the intimate ion pair or the dissociated ion pair:



(or addition of monomer can take place on both species). Then

$$K_1 = [AM^+B^-]/[AB][M]$$

$$K_1' = [AM^+][B^-]/[AM^+B^-] = [AM^+][B^-]/K_1[AB][M]$$

$$K_n = [AM_{n+1}^+B^-]/[AM_n^+][M][B^-]$$

$$K_n' = [AM_{n+1}^+][B^-]/[AM_n^+][M][B^-]$$

The apparent cessation of monomer consumption is related to the establishment of the indicated equilibria.<sup>16,17</sup> Addition of more monomer disturbs the equilibrium, and monomer consumption occurs until a new equilibrium is established. An alternative explanation may be that the growth of

polymeric species is terminated by proton transfer from polymer ion-pair to monomer, i.e., by chain transfer to monomer to produce a free carbonium ion, probably by interaction with only one double bond of the monomer. This carbonium ion may be relatively unreactive due to the partial neutralization of the cation by the electron density of the adjacent double bond, i.e., a relatively stable allylic cation is produced. However, over a long period of time, e.g., on standing several weeks, monomer consumption slowly continues.

The general course of the polymerization at constant monomer concentration in a medium of dry *n*-heptane is independent of the nature of the catalyst, although small differences in the equilibrium conversion have been observed with different Lewis acids (Table I). Titanium tetrachloride was found to be completely inactive unless moist *n*-heptane was added to the reaction mixture.

TABLE I  
Polymerization of Isoprene in *n*-Heptane Medium<sup>a</sup>

Catalyst Nature	Amount, mmole	Mono- mer concn., mole/l.	Time of reac- tion, min.	Con- version, %	Structure, % <sup>b</sup>			Note
					1,4	3,4	1,2	
AlEtCl <sub>2</sub>	0.7	0.8	180	5	12	2	1	
AlEtCl <sub>2</sub>	0.7	1.7	180	21	27	5	n.d.	
AlCl <sub>3</sub>	0.8	0.8	120	6	2	1	n.d.	Catalyst in sus- pension
AlBr <sub>3</sub>	0.7	0.4	120	8	n.d.	n.d.	n.d.	
TiCl <sub>4</sub>	0.8	0.8	180	0	—	—	—	
TiCl <sub>4</sub>	0.8	0.8	180	6	2	1	n.d.	5 ml. of moist <i>n</i> -hep- tane added
SnCl <sub>4</sub>	2.7	1.7	60	24	2	1	n.d.	
H <sub>2</sub> SO <sub>4</sub>	0.8	0.8	60	28	0	0	0	Oligomers, <i>n</i> = 1-5

<sup>a</sup> 30 ml. of solvent, 21°C.

<sup>b</sup> n.d. = not detectable.

All polymers prepared in *n*-heptane are powdery materials, insoluble in benzene at 25°C., the infrared spectra of which do not indicate the presence of any absorption bands characteristic of common linear addition forms (Fig. 8, below).

### Polymerizations in Aromatic Solvents

The use of aromatic solvents as polymerization medium has a marked influence on the polymerization rate as well as on the properties of polymers. In general, polymerizations in aromatic hydrocarbons are much faster, and the polymerization rate as well as the final conversion increase with increasing basic character of the solvent. Simultaneously, the molecular weight of polymers decreases very sharply. The influence of the solvent nature on the yield and light-scattering molecular weights of polymers

TABLE II  
 Polymerization of Isoprene in Aromatic Solvents Catalyzed by  $\text{AlBr}_3^a$

Amount $\text{AlBr}_3^b$ , mmole	Solvent	Conversion, %	Monomer, concn., mole/l.	Structure, % <sup>b</sup>		Unsatura- tion, %	Mol. weight	Appearance <sup>c</sup>
				cis-1,4	trans-1,4			
0.06	Toluene	19.5	1	—	5.5	15	—	TS + O
0.12	Toluene	60	1	—	4	16	—	TS + O
0.18	Toluene	79	1	n.d.	n.d.	—	—	TS + O
0.30	Toluene	86.5	1	n.d.	n.d.	20	—	O
0.30	Toluene	94	2	n.d.	n.d.	—	—	TS + O
0.19	Benzene	8	0.4	—	—	—	—	Powder
0.19	Benzene	33.5	0.8	<2	<1	—	—	Powder
0.19	Benzene	42	1.2	<2	<1	—	—	Powder
0.38	Benzene	50	0.4	(4.8)	9.6	—	—	Powder
0.25	Benzene	14	0.6	(3.5)	7	28	120,000	Powder
0.25	Benzene	14.5	0.6	(6)	12	26	110,000	Powder
0.75	Benzene	42.5	0.6	(7)	14	25	140,000	Powder
0.75	Benzene	41	0.6	(8)	15	25	—	Powder
1.0	Benzene	55	0.6	(7)	14	24	130,000	Powder
0.12	<i>p</i> -Xylene	92	1	2	10.5	—	—	O <sup>d</sup>

<sup>a</sup> 50 ml. of solvent,  $T = 21^\circ\text{C}$ ., 60 min. reaction time.

<sup>b</sup> n.d. = not detectable.

<sup>c</sup> TS = tacky solid, O = oil.

<sup>d</sup>  $[\eta] < 0.05$ .

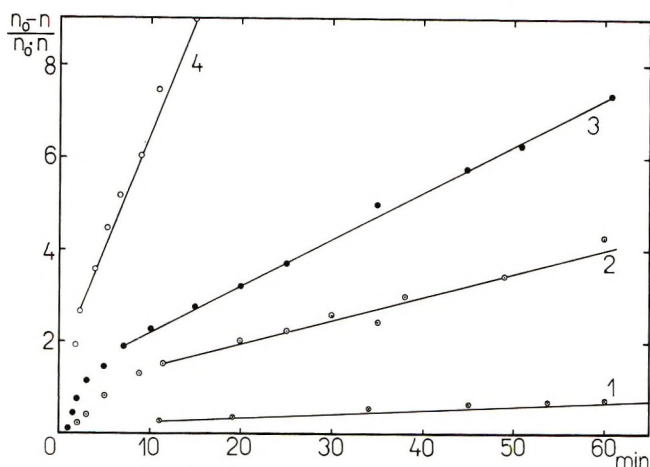


Fig. 4. Polymerization of isoprene in toluene catalyzed by  $\text{AlBr}_3$ , 30 ml. of solvent,  $21^\circ\text{C}$ .: (1) 0.06 mmole  $\text{AlBr}_3$ ; (2) 0.12 mmole  $\text{AlBr}_3$ ; (3) 0.18 mmole  $\text{AlBr}_3$ ; (4) 0.3 mmole  $\text{AlBr}_3$ ,  $n_0$  = initial amount of monomer (mmole),  $n$  = actual amount of monomer at time  $t$ .

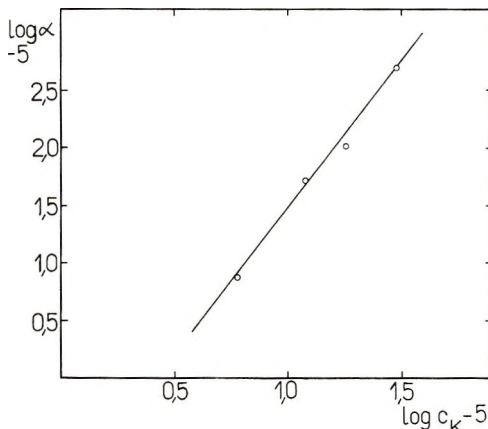


Fig. 5. Dependence of the slopes  $\alpha$  of curves from Fig. 4 upon the amount of catalyst ( $C_K$ ) used. All data are shown in Fig. 4.

obtained with aluminum bromide as catalyst is shown in Table II. Similar to the polymerization in *n*-heptane, the reaction in benzene also leads to an equilibrium characterized by a very low reaction rate. Equilibrium conversion in this case is much higher than that in *n*-heptane under similar conditions, however. When toluene or *p*-xylene was used, no such equilibrium stage was observed over a period of 3 hr. of polymerization. A set of conversion curves obtained in toluene with different concentrations of aluminum bromide as catalyst and with a constant initial monomer concentration is represented in Figure 4 in coordinates of a second-order reaction. It is seen that the overall kinetics of the monomer disappearance

TABLE III  
 Polymerization of Isoprene in Various Aromatic Solvents with Different Catalysts<sup>a</sup>

Catalyst	Mono- mer		Solvent	Reac- tion time, min.	Yield, g.	Structure, % <sup>b</sup>			Appear- ance <sup>c</sup>	Mol. weight	Un- sat- ura- tion, %	Note
	Amount, concn., mmole mole/l.					<i>cis</i> -1,4	<i>trans</i> -1,4	3,4				
$C_2H_5AlCl_2$	0.7	0.6	Benzene <sup>d</sup>	60	0.35	(5)	14	2	Powder	110,000	22	
$C_2H_5AlCl_2$	0.7	0.6	Toluene <sup>d</sup>	60	0.65	(7)	11	0.5	TS + O	—	—	
$C_2H_5AlCl_2$	0.7	0.6	<i>p</i> -Xylene <sup>d</sup>	60	0.90	n.d.	13	2	O	—	—	
$AlCl_3$	1	1	Benzene	60	2	(5)	9	2	Powder	80,000	17	Catalyst not completely dissolved
$AlBr_3$	1	1	Benzene	60	2.7	(7)	14	3	Powder	60,000	25	
$AlCl_3$	1	1	Toluene	60	2.5	n.d.	n.d.	1	TS + O	—	—	
$AlBr_3$	1	1	Toluene	60	3.1	(3.8)	8	0.5	O	—	26	
$CH_3TiCl_3$	1	1	Toluene	60	0.7	(7)	14.5	0.5	TS	—	—	
$C_2H_5AlCl_2 + TiCl_4$	2 } 10 }	0.8	Toluene	30	3.2	(5.4)	11	0.6	Powder	50,000	15	
$TiCl_4$	0.8	0.8	Toluene	180	0.1	—	—	—	TS	—	—	
$SnCl_4$	1.2	0.8	Benzene	60	0.9	8	<2	2	TS	—	—	
$SbCl_5$	5	0.8	Toluene	60	0.4	8	10	2	Powder	—	—	Catalyst not completely dissolved

<sup>a</sup> 50 ml. of solvent;  $T = 21^\circ C$ .

<sup>b</sup> n.d. = not detectable.

<sup>c</sup> TS = tacky solid, O = oil.

<sup>d</sup> 30 ml. of solvent.



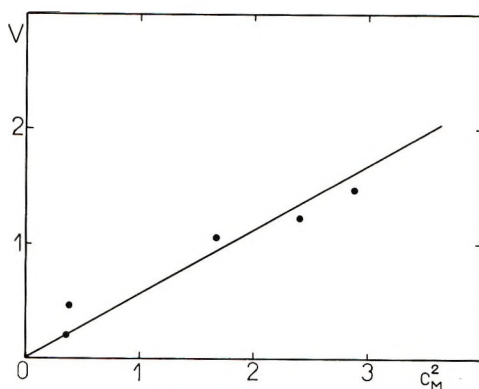


Fig. 6. Dependence of the polymerization rate in benzene on the square of the monomer concentration, 50 ml. of benzene, 21°C.  $C_M$  = concentration in mole/l.,  $V$  = polymerization rate expressed as the pressure change per minute, catalyst = 0.15 mmole of  $AlBr_3$ , concentration of monomer kept constant during each run. Polymerization rate measured 3 hr. after the start of the reaction.

over a certain reaction period corresponds to a second-order reaction, but in the initial stages serious deviations occur (similar deviations have been observed also at high conversions due to changes in the viscosity of the medium). Initial deviations from the linear plot are evidently due to a slow establishment of the equilibrium between all reaction components. The log-log plot of the slopes of the linear parts of the conversion curves from Figure 4 shows an approximately direct proportionality of the reaction rate to the square of the catalyst concentration (Fig. 5).

A qualitatively similar picture is obtained with the use of other catalysts such as aluminum chloride or ethylaluminum dichloride. Absolute reaction rates, however, characterized by the yield after 60 min. of polymerization, are in such cases usually much lower (Table III).

Polymerizations in benzene medium with aluminum tribromide as catalyst show similar kinetic features as those in toluene medium, but the reaction orders with respect to monomer as well as to catalyst concentration at constant volume are considerably lower than two. When the concentration of monomer was kept constant during the entire polymerization by continuous admission of the same amount of monomer which had polymerized, the reaction rate decreased continually from the start of the reaction to a practically constant value. This steady-state reaction rate was directly proportional to the square of the monomer concentration but to the first power of the catalyst concentration, which indicates clearly the participation of monomer in the reaction producing active centers (Figs. 6 and 7). It should, however, be pointed out that these results must be considered qualitative because the solvents, according to the coulometric analysis, contained about 5 ppm of water, and also the reaction rate is difficult to determine with precision since it changes over extended reaction times even at constant monomer concentration. It is clear that a compli-

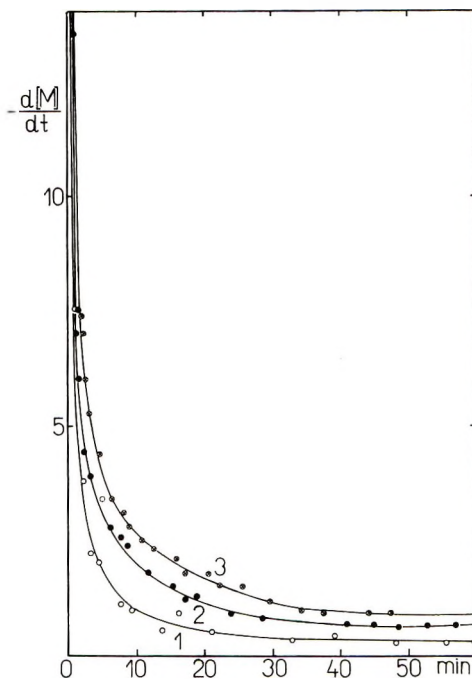


Fig. 7. Changes of the polymerization rate in mole/l. with time of reaction, 50 ml. benzene, 21°C. concentration of isoprene constant at 0.61 mole/l., at various concentrations of  $\text{AlBr}_3$ : (1)  $0.5 \times 10^{-2}$  mole/l.; (2)  $1.5 \times 10^{-2}$  mole/l.; (3)  $2 \times 10^{-2}$  mole/l.

cated reaction mechanism is operating which involves changes in the concentration of active particles. The driving force of the reaction may be the chain transfer with solvent with creation of the original active centers.

Polymers obtained with cationic catalysts in aromatic solvents are white powders, tacky solids, or oils (in *p*-xylene), very soluble in benzene at 25°C. Molecular weights of polymers from benzene medium have been found by light scattering to range between 50,000 and 100,000. Results of polymerization runs performed in different aromatic solvents and with different catalysts are presented in Table III.

### Polymerizations in Halogenated Solvents

The shape of the conversion curves in polymerizations performed in vacuum apparatus with the use of carbon tetrachloride or chloroform as solvents and aluminum tribromide as catalyst do not differ from those obtained in benzene medium. They show again an initial stage characterized by a high reaction rate which is followed by the stage in which the reaction rate is very low. The main difference from experiments performed in benzene is the limiting conversion. For example, in chloroform with aluminum bromide or aluminum trichloride as catalysts only low molecular oils were formed, but the final conversion was nearly 90%. Formation of oily products has also been observed in butyl bromide medium.

TABLE IV  
Polymerization of Isoprene in Halogenated Solvents<sup>a</sup>

Catalyst	Solvent	Yield, g.	Structure, %			Solubility, in benzene	[ $\eta$ ]	Dielectric constant $E$
			<i>cis</i> -1,4	<i>trans</i> -1,4	3,4			
$C_6H_5AlCl_2$	Benzene	4.2	—	13	2	Partly sol.	—	2.28
$C_2H_5AlCl_2$	Monochlorobenzene	4.6	(10)	21	1.8	Partly sol.	—	5.7
$C_2H_5AlCl_2$	<i>o</i> -Dichlorobenzene	3.6	(15)	37	1.6	Sol.	0.10	9.93
$C_6H_5AlCl_2$	1,2,4-Trichlorobenzene	2.9	5	9	1.1	Insoluble	—	—
$C_2H_5AlCl_2$	$CCl_4$	4.9	7	14	1.3	Partly sol.	—	2.38
$C_2H_5AlCl_2$	$C_2H_2Cl_4$	5.1	7	18	2	Partly sol.	—	7 (Br)
$C_6H_5AlCl_2$	$CH_2Cl_2$	4.8 <sup>c</sup>	11	20	2	Partly sol.	—	9.08
$C_2H_5AlCl_2$	1,2,4-Trichlorobenzene	5.3 <sup>b</sup>	(12)	24	1.5	Partly sol.	—	—
$(CH_3)_2Al_2Cl_3$	Monochlorobenzene	2.1	(12)	25	2.5	Partly sol.	—	5.7
$(CH_3)_2Al_2Cl_3$	<i>o</i> -Dichlorobenzene	1.8	(12,9)	37	1.6	Partly sol.	0.14	9.93
$(CH_3)_2Al_2Cl_3$	1,2,4-Trichlorobenzene	3.1	(11)	22	1.5	Sol.	0.03	—
$(CH_3)_2Al_2Cl_3$	1,2,4-Trichlorobenzene	3.5 <sup>b</sup>	(15)	28	2	Partly sol.	—	—
$(CH_3)_2Al_2Cl_3$	$CCl_4$	0.7	(11)	23	2	Partly sol.	—	2.38
$(CH_3)_2Al_2Cl_3$	$CH_2Cl_2$	3.8	10	24	2	Partly sol.	—	7 (Br)

<sup>a</sup> 50 ml. of solvent,  $T = 21^\circ C$ , 1 mmole of catalyst. Concentration of isoprene (initial) 2 moles/l.

<sup>b</sup> Initial concentration of isoprene 3 moles/l.

<sup>c</sup> Polymer contains 1.76% Cl.

A series of experiments with the use of different chlorinated solvents and ethylaluminum dichloride or methylaluminum sesquibromide as catalysts was carried out by the hypodermic-syringe technique. Under these conditions polymerization activity was always much higher than with identical experiments by the vacuum technique. Polymerization activity was characterized by conversion after 60 min. of the reaction, and the results are summarized in Table IV. From comparison of the conversions with  $\text{AlBr}_3$ ,  $\text{EtAlCl}_2$ ,  $(\text{CH}_3)_3\text{Al}_2\text{Br}_3$ , or  $\text{Et}_2\text{AlCl}$  in carbon tetrachloride medium it is seen that the polymerization activity decreases markedly with increasing acidic character of the catalyst. Reproducibility of yields, however, was not satisfactory under these conditions, so that no attempt has been made to elucidate the kinetics and the main attention has been focused on the structure of the polymers.

### Structure of Polymers

All polymers prepared under the conditions described above exhibited the same type of infrared spectra with only minor differences between various samples, i.e., the spectra were typical of polymers containing cyclic units as have already been described.<sup>11</sup> As can be seen from Figure 8, all spectra contain most of the absorption peaks characteristic of linear forms as minor extensions of the background, the only well-developed bands being those at  $1385\text{ cm.}^{-1}$  of the  $\text{CH}_3$  symmetrical deformation vibration, and at  $1460\text{ cm.}^{-1}$  of the  $\text{CH}_2$  bending together with  $\text{CH}_3$  antisymmetrical deformation vibration and the group of bands of C—H stretching vibrations in the region near  $3000\text{ cm.}^{-1}$ . The absorption due to the C=C stretching vibration near  $1640\text{ cm.}^{-1}$  is in all cases apparently broad, showing the presence of double bonds of different origin. In spite of the fact that most of the absorption bands of the linear forms were only slightly protuberant over the background they were analyzed by use of both the baseline and the extinction difference method.<sup>15</sup> Analysis of the content of the 1,4 addition was carried out by using the absorption band at  $840\text{ cm.}^{-1}$ . Because this absorption is due to the out-of-plane vibration of CH at the double bond of both *cis* and *trans* forms, the absorptivities of which are different, it was preferred to evaluate the absorption at that wavelength separately by using either the absorptivity for *cis* addition neglecting the content of *trans* configuration or vice versa. In some cases it was very difficult to decide whether the *cis* or *trans* form was prevalent. In these cases analyses for both forms are given, figures indicating the content of the form which (based on the general appearance of bands) might be present in minor amounts being given in parentheses. Absorptivities for KBr pellets were corrected according to the values for  $\text{CS}_2$  solutions, i.e., all extinctions obtained by using the pellet technique were multiplied by the factor representing the ratio of extinction coefficients of bands of balata in pellets and in solution. In some cases bands at  $600$  and  $1150\text{ cm.}^{-1}$  were used for control determinations of the *trans* form and bands at  $572$  and  $1130\text{ cm.}^{-1}$  for the determination of the *cis*-1,4 form. It should

be noted, however, that the application of calibration curves for *cis*-1,4 additions, obtained by means of natural rubber, to the analysis of polymers containing high amounts of cyclic units is not fully justified, and

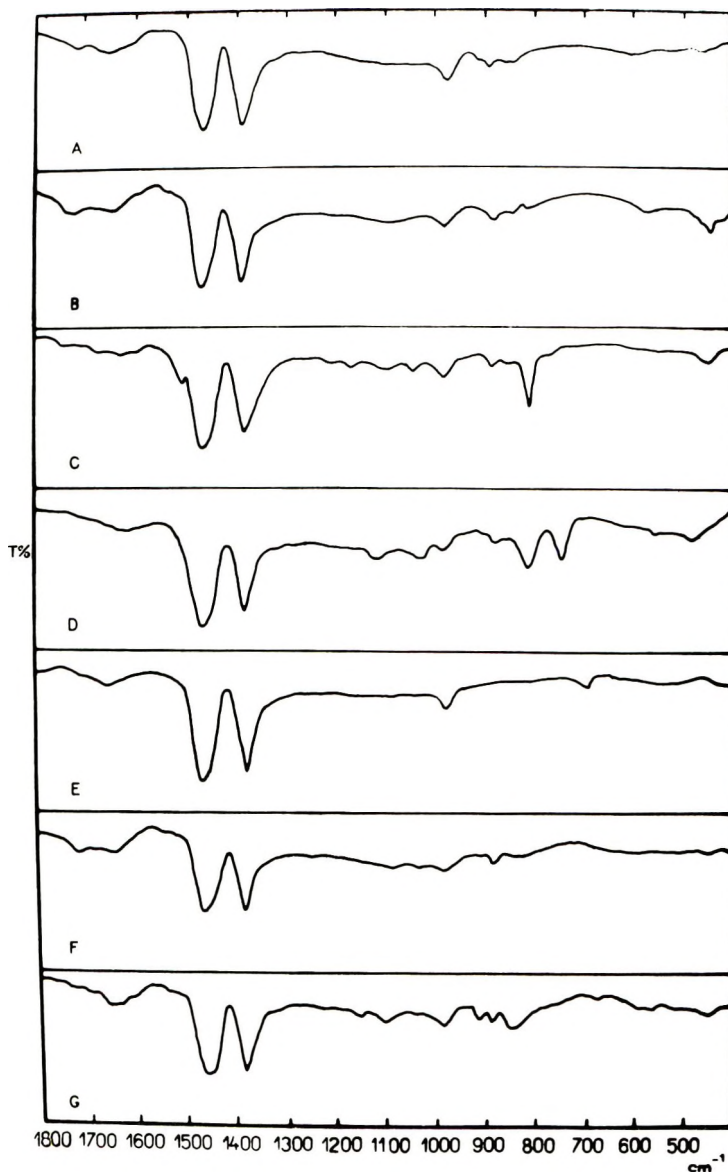


Fig. 8. Infrared spectra of cyclopolyisoprenes prepared under different conditions: (A) polymerization in *n*-heptane, catalyst  $C_2H_5AlCl_2$ ; (B) polymerization in  $CCl_4$ , catalyst  $AlCl_3$ ; (C) polymerization in *p*-xylene, catalyst  $C_2H_5AlCl_2$ ; (D) polymerization in toluene, catalyst  $C_2H_5AlCl_2$ ; (E) polymerization in benzene, catalyst  $C_2H_5AlCl_2$ ; (F) polymerization in 1,2,4-trichlorobenzene, catalyst  $C_2H_5AlCl_2$ ; (G) polymerization in *o*-dichlorobenzene, catalyst  $(CH_3)_3Al_2Br_3$ . KBr pellet technique.

analytical data based on this method are suitable mainly for comparative purposes. As is known from the infrared spectrum of balata, there are three bands in the region 800–900  $\text{cm}^{-1}$ , the band at 840  $\text{cm}^{-1}$  being the weakest. However, in the infrared spectrum of cyclopolymer, which according to the absorption at 1150 and 600  $\text{cm}^{-1}$  contain *trans*-1,4 addition units, both bands at 800 and 880  $\text{cm}^{-1}$  are absent, and the band at 840  $\text{cm}^{-1}$  is broad. It is also evident, as has already been shown for the absorption bands at 1130 and 1150  $\text{cm}^{-1}$ , that the incorporation of cyclic units into the chain very substantially influences vibrations of remaining linear forms. Also the data concerning the content of the 3,4 addition units are of comparative character because the absorption of the isopropenyl group is overlapped by the absorption due to the exomethylene group, the presence of which is very probable in cyclic segments.<sup>18</sup> Analyses of all polymers are included in the tables. Because the extinction coefficient of the absorption band at 840  $\text{cm}^{-1}$  of the 1,4-*trans* configuration is lower than that of the *cis* configuration, all data in samples where only the content of the *trans* configuration is given must be taken as the maximal possible content of the total 1,4 addition and in samples where only the content of *cis* form is indicated, this should be taken as the minimal content of 1,4 addition.

From the results of analyses presented in Tables I, II, and III it is seen that the content of linear addition forms in cationically polymerized isoprene in nonpolar media such as aliphatic or aromatic hydrocarbons is always less than 20% and remains almost unchanged, irrespective of the nature of the catalyst, over a wide range of conversions; it does not depend on molecular weight (provided that the product is not an oligomer). This finding is in accordance with the observations of Ferington and Tobolsky,<sup>5</sup> who found a similar invariance of the content of linear structures in polybutadienes prepared by cationic polymerization under various conditions.

Polymers obtained in chlorinated solvents (Table IV) contain, however, linear forms in substantially higher concentration. In all cases, in the 1,4 addition the *trans* form was prevailing, as was proved by the distinct appearance of the absorption at 1150  $\text{cm}^{-1}$ . From the relatively high 1,4 content in polymers prepared in *o*-dichlorobenzene and in methylene chloride it seems that the dielectric constant of the medium might be of some importance in favoring the formation of linear structures.

In aromatic solvents high amounts of higher substituted benzene rings were found to be incorporated in the polymer molecules, indicating that extensive chain transfer with solvent takes place (Fig. 8), as has been previously found in cationic polymerization.<sup>19</sup> In chlorinated benzenes no incorporation of solvent residues could be detected, but in methylene chloride or carbon tetrachloride the resulting polymers always contained some chlorine. The appearance of the polymers ranged from oils to tacky solids to powdery materials. The solubility in benzene at room temperature depended on the molecular weight of polymer. In general, polymers

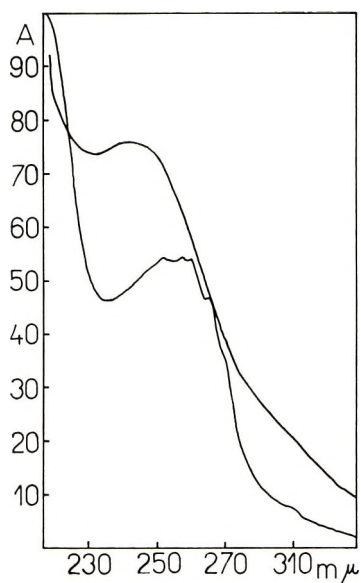


Fig. 9. Ultraviolet spectra of cyclopolymers in cyclohexane: (1) polymer prepared in  $\text{CCl}_4$ , catalyst  $\text{C}_2\text{H}_5\text{AlCl}_2$ ; (2) polymer prepared in benzene, catalyst  $\text{AlBr}_3$ .

prepared in aromatic solvents, chloroform, or butyl bromide were completely soluble, while those prepared in aliphatic solvents were almost completely insoluble under these conditions. There is the general implication in the literature that such powdery insoluble polymers are highly crosslinked. Although some formation of microgel occurred very frequently and became serious at very high conversion, it was found that many of the polymers which were insoluble in benzene dissolved readily in higher chlorinated benzenes such as trichlorobenzene, which indicates the minor importance of crosslinking in the general determination of the polymer structure.

In the case of some soluble polymers, the molecular weight and the total unsaturation of the polymers (after removing the microgel if present) were determined, the results being summarized in Tables II and III. When comparing both values, i.e., molecular weight and content of double bonds, it is evident that considerable amounts of double bonds have disappeared during the polymerization due to the formation of fused ring structures. Thus, for example, in the case of the polymer obtained in benzene using aluminum bromide as catalyst, the resulting polymer had a molecular weight of 110,000, the average degree of polymerization being thus roughly 1600, so that the contribution of terminal unsaturation could be neglected. According to the results of the infrared analysis, the polymer contained roughly 10% of linear forms. Thus, on the average, for each chain unit resulting from linear addition nine units should have been joined in cycles. However, the content of double bonds in high molecular weight products as determined by the  $\text{ICl}$  method exceeds the value which would correspond to

the sum of terminal groups together with the number of double bonds from linear addition forms determined by infrared spectroscopy. Thus, in the case mentioned above, the polymer contained 26 residual double bonds per each 100 linked monomer units. Taking this fact into account and assuming that each double bond corresponds to the end of one segment of the chain formed by fused rings the maximum number of fused units would be five or less.<sup>18</sup> It should be noted that precise calculations based on these results are not fully justified because the reliability of the ICI method is known to be limited and also the sensitivity of the infrared method in determining the linear units when the latter are linked between two cyclic units is unknown. Another complication arises from the fact that practically all soluble polymers exhibited absorption in the ultraviolet region with maxima in the range of 240–260 m $\mu$  (Fig. 9), which implies the presence of some conjugation. The appearance of absorption bands in the region near 1600 cm.<sup>-1</sup> in the infrared spectra supports the suspicion that only few double bonds are of the nature of isolated C=C bonds in a linear aliphatic chain.

Although these facts cloud somewhat the general picture, it can be qualitatively concluded that when isoprene is polymerized at room temperature with Lewis acids, the prevailing mode of addition of the monomer units is that leading to the formation of ring structures. This reaction is neither influenced by the nature of the original cation nor by the nature of the corresponding counter anion. Also, the solvation of cations or the solvent-catalyst complex formation with aromatics does not change the general course of the elementary reaction act of chain growth. Solvents of higher polarity seem to facilitate the formation of more linear structure.

### References

1. H. Barron, *Modern Synthetic Rubbers*, Chapman and Hall, London, 1943.
2. G. S. Whitby, *Synthetic Rubber*, Wiley, New York, 1954.
3. W. Cooper, in *The Chemistry of Cationic Polymerizations*, P. H. Plesch, Ed., Pergamon Press, Oxford, 1963, Chapt. 8.
4. E. H. Farmer and J. S. Martin, *J. Chem. Soc.*, **1940**, 1169.
5. T. E. Ferington and A. V. Tobolsky, *J. Polymer Sci.*, **31**, 25 (1958).
6. C. S. Marvel, R. Gilkey, C. R. Morgan, J. F. Noth, R. D. Rands, Jr., and C. H. Young, *J. Polymer Sci.*, **6**, 483 (1951).
7. W. S. Richardson, *J. Polymer Sci.*, **13**, 325 (1954).
8. B. A. Dolgoplosk et al., *J. Polymer Sci.*, **53**, 209 (1961).
9. M. Roha, *Fortschr. Hochpolymer.-Forsch.*, **1**, 512 (1960).
10. J. L. Binder, *J. Polymer Sci. A*, **1**, 37 (1963).
11. N. G. Gaylord, I. Kössler, M. Stolka, and J. Vodehnal, *J. Polymer Sci. A*, **2**, 3696 (1964).
12. I. Kössler, M. Stolka, and J. Vodehnal, *J. Polymer Sci. A*, **2**, 3987 (1964).
13. V. L. Bell, Jr. (to E. I. du Pont de Nemours and Co.), Belg. Pat. 623940 (Oct. 23, 1962).
14. B. Matyska, K. Mach, J. Vodehnal, and I. Kössler, *Collection Czechoslov. Chem. Commun.*, **30**, 2569 (1965).
15. J. Vodehnal and I. Kössler, *Collection Czechoslov. Chem. Commun.*, **29**, 2859 (1964).



16. A. V. Tobolsky, *J. Polymer Sci.*, **31**, 126 (1958).
17. I. Kössler, M. Stolka, and K. Mach, *J. Polymer Sci. C*, **4**, 977 (1963).
18. I. Kössler, M. Stolka, and J. Vodehnal, *J. Polymer Sci. A*, **3**, 2081 (1965).
19. P. E. M. Allen and P. H. Plesch, in *The Chemistry of Cationic Polymerizations*, P. H. Plesch, Ed., Pergamon Press, Oxford, 1963, Chapt. 3, p. 115.

### Résumé

La polymérisation de l'isoprène en présence d'acide de Lewis dans l'heptane-*n* est un processus qui mène à un quasi-équilibre, caractérisé par des conversions très basses. Les vitesses de polymérisation dans les solvants aromatiques sont beaucoup plus élevées par suite d'un transfert de chaînes très important avec les solvants avec régénération des centres actifs originaux. La vitesse de disparition du monomère dans le benzène ou le toluène en présence de bromure d'aluminium comme catalyseur est de second ordre par rapport à la concentration en monomère. L'ordre de réaction par rapport au catalyseur dépend des conditions de réactions; à concentration constante en monomère, il est environ approximativement unitaire. Des vitesses de polymérisations dans des solvants halogénés (utilisant les techniques aux seringues) sont beaucoup plus élevées que celles dans les solvants aromatiques. Les polymères obtenus avec différents catalyseurs cationiques variaient depuis des huiles jusqu'à des poudres blanches présentant des poids moléculaires pouvant aller jusqu'à 100.000 suivant les conditions de réaction. Tous ces polymères montrent des spectres infrarouges caractéristiques des cyclopolymères et la structure linéaire ne dépassait généralement pas 20%, indépendamment de la nature du catalyseur ou du solvant. Dans des solvants de polarité plus élevée tel que l'*o*-dichlorobenzène des structures plus fortement linéaires ont pu être obtenues. Parmi les formes linéaires résiduelles la *trans*-addition 1,4 est prépondérante. L'insaturation résiduelle dans les polymères ne dépassait pas 30%.

### Zusammenfassung

Die Polymerisation von Isopren mit Lewis-Säuren in *n*-Heptan führt zu einem durch sehr geringe Umsätze charakterisierten Quasi-Gleichgewicht. Die Polymerisationsgeschwindigkeit in aromatischen Lösungsmitteln ist wegen einer starken Kettenübertragung zum Lösungsmittel unter Rückbildung der ursprünglichen aktiven Zentren bedeutend höher. Die Geschwindigkeit des Monomerverbrauchs in Benzol oder Toluol mit  $AlBr_3$  als Katalysator ist von zweiter Ordnung in Bezug auf die Monomerkonzentration. Die Reaktionsordnung in Bezug auf den Katalysator hängt von den Reaktionsbedingungen ab und ist bei konstanter Monomerkonzentration ungefähr 1. Die Polymerisationsgeschwindigkeit in halogenierten Lösungsmitteln ist bei Anwendung einer Injektionsspritzenmethode viel höher als in aromatischen Lösungsmitteln. Die mit verschiedenen kationischen Katalysatoren erhaltenen Polymeren lagen je nach den Reaktionsbedingungen im Bereich von Ölen bis zu weissen Pulvern mit einem Molekulargewicht bis zu mehr als 100000. Alle Polymeren zeigten die für Zyklopolydiene charakteristischen IR-Spektren und der Gehalt an linearen Strukturen überschritt, unabhängig von der Natur des Katalysators oder Lösungsmittels gewöhnlich nicht 20%. In Lösungsmitteln von höherer Polarität wie *o*-Dichlorbenzol, wurde ein grösserer Anteil an linearen Strukturen gefunden. Unter den linearen Resten herrschte die *trans*-1,4-Addition vor. Die Ungesättigtheit des Polymeren überschritt nicht 30%.

Received November 3, 1965

Revised February 18, 1966

Prod No. 5106A

## Kinetic Study of Heterogeneous Polymerizations of Styrene and/or $\beta,\beta$ - $d_2$ -Styrene by Ziegler-Natta Catalysis

A. SIMON,\* P. A. JAROVITZKY,† and C. G. OVERBERGER,  
*Department of Chemistry, Polytechnic Institute of Brooklyn, Brooklyn,  
New York, 11201*

### Synopsis

Substantial concentrations of tetravalent titanium have been shown to exist in a  $\text{TiCl}_4\text{-Al}(\text{C}_2\text{H}_5)_3$ -benzene catalytic system for catalyst aging times  $\geq 20$  min. at  $60^\circ\text{C}$ . Substitution of  $\beta,\beta$ - $d_2$ -styrene for styrene with the above catalytic system appears to have no effect on either rate of polymerization or product intrinsic viscosities. These phenomena support a mechanism of chain propagation and termination as suggested earlier.

### INTRODUCTION

In an earlier publication,<sup>1</sup> in a discussion of probable polymerization mechanisms of styrene and/or  $\alpha$ - $d$ -styrene by  $\text{TiCl}_4\text{-Al}(\text{C}_2\text{H}_5)_3$  catalysis it became necessary to assume that a  $\text{TiCl}_4\text{-Al}(\text{C}_2\text{H}_5)_3$ -benzene system, upon catalyst aging, still maintains significant concentrations of tetravalent titanium species and to invoke a bimolecular termination mechanism as the primary mode of termination of active centers ( $\text{C}^*$ ), i.e., involving tetravalent titanium species adsorbed on a di- and/or trivalent titanium surface.

Based on the polymerization scheme evolved for styrene and/or  $\alpha$ - $d$ -styrene,<sup>1</sup> it became of interest to put these hypotheses to a test by: proving the existence of tetravalent titanium species under these polymerization conditions and by determining rates of polymerization and product viscosities for styrene and/or  $\beta,\beta$ - $d_2$ -styrene- $\text{TiCl}_4\text{-Al}(\text{C}_2\text{H}_5)_3$ -benzene systems.

It could then be hypothesized that dideuteration of styrene at the  $\beta$  position should produce rates of polymerization equal to those found for styrene itself and probably would only slightly (if at all) affect product viscosities, since the bimolecular termination was assumed to be primarily controlled by "free surface" available for adsorption and adsorption-desorption equilibria.

\* A. Simon, Post-Doctoral Fellow at the Polytechnic Institute of Brooklyn, 1964-1965. Present address: Research Institute for Plastics, Budapest, Hungary.

† Present address: American Cyanamid Co., Stamford Research Laboratories, Fibers Division, Stamford, Connecticut.

## EXPERIMENTAL

## Polymerizations

Procedures as outlined previously<sup>2</sup> were employed for the purification of benzene, styrene,  $\text{TiCl}_4$ , and  $\text{Al}(\text{C}_2\text{H}_5)_3$  for the catalyst solution preparation and its delivery to the polymerization equipment, and for polymerization equipment pretreatment to insure an inert atmosphere.

The  $\beta,\beta\text{-}d_2$ -styrene monomer (with an isotopic purity of 98%) was obtained from Merck and Dohme and was extracted with dilute KOH solution, washed with excess water, dried over molecular sieves, and finally vacuum-distilled. The purity of the monomer at this point was  $\sim 100\%$  by infrared analysis. The purified monomer was stored in a freezer until used.

The originally employed equipment to measure rates of polymerizations dilatometrically was modified to reduce the possibility of stopcock leakage and silicon grease contamination.

This modified catalyst mixing chamber and dilatometer assembly is shown as Figure 1. The apparatus employed a two-arm dilatometer section. The entire apparatus was immersed in a silicon oil bath and brought

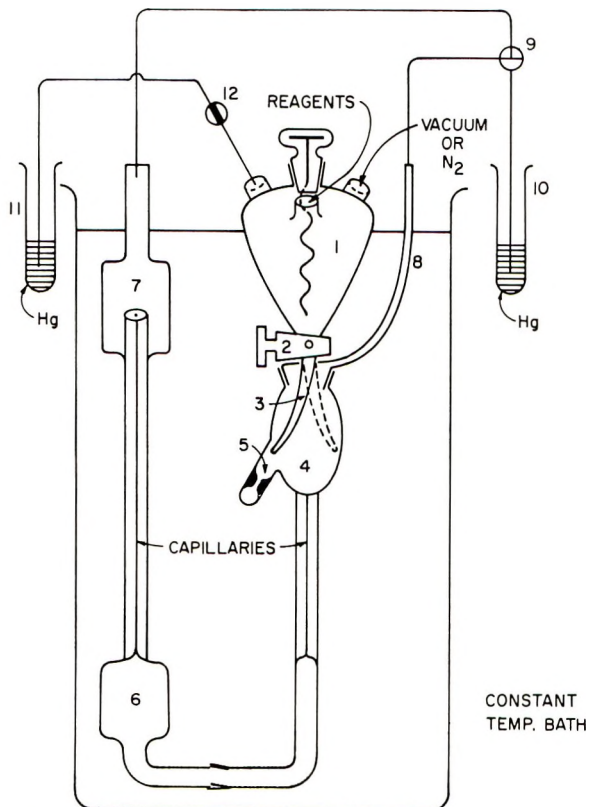


Fig. 1. Catalyst mixing chamber and dilatometer assembly.

to constant temperature; e.g.,  $60 \pm 0.05^\circ\text{C}$ . The catalyst was prepared in the absence of monomer and in a four-necked flask (1) fitted with a magnetic stirrer, a serum cap for adding reagents, inlet tubing for nitrogen purging, and an outlet for relieving pressure to a mercury valve (11) via stopcock (12). Fitted to stopcock (2) was a curved outlet (3) and a tube for equalizing pressure (8) between the two arms of the dilatometer. The entrance to the dilatometer section of the apparatus was a bulb (4) to which a trap (5) was sealed. By turning the flask (1), the curved catalyst delivery tubing (3) could be positioned above the capillary leading to the dilatometer bulb (6) for filling the system or above the trap (5) to eliminate dripping of reaction mixture from the delivery tip into the dilatometer section after completion of dilatometer filling. A third bulb (7) into which the dilatometer emptied was used as an emergency bulb in the event of overfilling. Bulb (7) was connected via a three-way stopcock (9) to a mercury valve (10) and to side-arm (8), thereby forming a closed system.

All polymerizations were carried out under the following conditions: total volume of reaction mixture delivered to the dilatometer assembly was  $20 \pm 0.5$  ml.;  $\text{Al}(\text{C}_2\text{H}_5)_3/\text{TiCl}_4$  ratio = 3.0;  $(\text{TiCl}_4) = 0.04$  mole/l.; temperature =  $60 \pm 0.05^\circ\text{C}$ .; catalyst "aging time" =  $20 \pm 1$  min.; dilatometer capillary inside diameter = 2 mm.; average total reaction time =  $65 \pm 5$  min.

The entire apparatus, immersed in the constant temperature bath and at  $60 \pm 0.05^\circ\text{C}$ ., was brought to an inert atmosphere ( $\text{N}_2$ ) by a series of alternating evacuations and nitrogen admissions by using the inlet tube of the flask (1) and by proper manipulation of stopcocks (9) and (12). Stopcock (2) was then closed, and the  $\text{TiCl}_4$ -benzene solution was injected via the serum cap covering one of the inlet tubes of the flask (1). Additional quantities of benzene were added similarly. The  $\text{Al}(\text{C}_2\text{H}_5)_3$ -benzene solution was next injected dropwise into the stirred  $\text{TiCl}_4$ -benzene solution over a ca. 5-min. interval. All pressure created on the system by the above deliveries was vented by the mercury valve (11). Stirring of the  $\text{TiCl}_4$ - $\text{Al}(\text{C}_2\text{H}_5)_3$ -benzene catalyst mixture was continued for an additional 15 min. to age the catalyst; yielding a total aging time of 20 min., counting from the beginning of the  $\text{Al}(\text{C}_2\text{H}_5)_3$  solution addition. After these 20 min. the monomer was injected into the catalyst mixture. The reaction mixture was transferred into the dilatometer, by turning the flask into a position so that the curved tubing (3) would be over the bulb (4) and opening stopcock (2). The amount of the transferred mixture was sufficient to fill the dilatometer up to the middle of the right-side capillary. If the dilatometer was overfilled, the excess was pushed into the bulb (7) by pressing the connecting rubber tubing over equalizing tubing (8). If there was a bubble in the mixture, it was driven out by moving the liquid in the same way.

After filling the dilatometer, the flask (1) was so turned that the curved tubing (3) would reach over the trap (5). In this way it was insured that, if some liquid remained in the tubing (3) or if there was a slow

flow through stopcock (2), the level in the capillaries would not be influenced. Pressure was equalized above the two arms of the dilatometer by stopcock (9).

Since all of the above manipulations required 3–4 min. after the addition of monomer, readings of the dilatometer level with time commenced about 5 min. after the addition of monomer. The dilatometer level was determined every 2–3 min. by using a cathetometer.

The reaction product was precipitated in a methanol-HCl solution. The polymer was washed with excess methanol and then dried in a vacuum oven at 60°C. (10–15 cm. Hg) for approximately 12 hr. Conversions were determined at this point. The polymer was reprecipitated once from a chlorobenzene solution, washed, and dried as described above prior to determining its intrinsic viscosity in a chlorobenzene solution at  $29.3 \pm 0.05^\circ\text{C}$ .

All experimental results are summarized in Table I.

TABLE I<sup>a</sup>

Run	$\beta,\beta\text{-d}_2$ - Styrene, wt.-%	Total monomer concn. [ $M_t$ ], mole/l.	Rate of polymerization, hr. <sup>-1</sup> ( $V_c/V_t$ ) $\times 10^{3b}$	Conversion, %	$[\eta]$ (29.3°C., C <sub>6</sub> H <sub>5</sub> Cl), dl./g.
A.S.-34 <sup>c</sup>	0	1.0	1.09	3.7	1.90
" -36 <sup>e</sup>	0	"	1.21	2.5	1.35
" -D8	8.8	"	1.17	2.0	2.20
" -D6	13.0	"	1.82	4.8	2.87
" -D2	47.5	1.3	1.19 <sup>d</sup>	5.2	2.50
" -D4	52.5	1.0	0.91	4.4	1.65
" -D3	56.6	"	0.99	4.0	1.80
" -D1	62.0	0.61	1.17 <sup>d</sup>	4.9	2.80
" -D5	100	1.0	1.27	4.6	1.95
" -D7	100	"	0.91	5.1	1.30

<sup>a</sup> Calculated average values: avg. conversion = 4.1 (R.M.D.) =  $\pm 21.0\%$ ; avg. initial rate of all runs = 1.17 (R.M.D.) =  $\pm 13.6\%$ ; avg. of all intrinsic viscosity = 2.03 (R.M.D.) =  $\pm 22.1\%$ ; avg. homopolystyrene ref. rate = 1.15 (R.M.D.) =  $\pm 5.2\%$ ; avg. initial rates for deuterium runs = 1.18 (R.M.D.) =  $\pm 15.8\%$ ; avg. homopolystyrene viscosities = 1.63 (R.M.D.) =  $\pm 16.9\%$ ; avg. deuterium run viscosities = 2.13 (R.M.D.) =  $\pm 21.5\%$ .

<sup>b</sup>  $V_c$  = initial rate of volume contraction (cm.<sup>3</sup>/hr.);  $V_t$  = experimental total volume = constant =  $20 \pm 0.5$  cm.<sup>3</sup>.

<sup>c</sup> 100% styrene reference.

<sup>d</sup> Initial rate corrected to  $[M_t] = 1$  mole/l., assuming rate  $\propto [M_t]^{1.5}$ .

### Determination of Tetravalent Titanium

**Description of Apparatus and Sample Preparation.** Apparatus used is shown as Figure 2. It consists of a two-necked catalyst mixing chamber (1), a filtration section using a medium porosity sintered glass filter (4), and a graduated liquid collection cylinder (6). Vacuum or nitrogen could be admitted by a side-arm (7). Reagents could be injected through a serum cap (3).

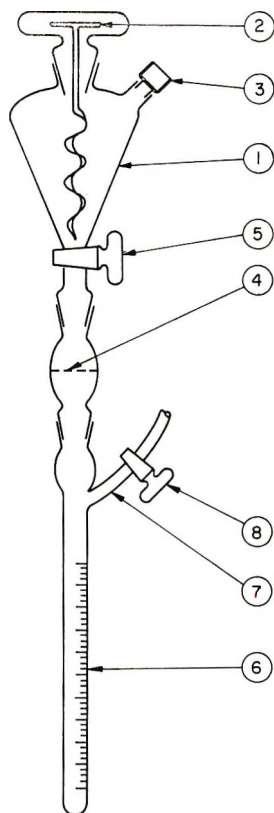


Fig. 2. Apparatus for the determination of titanium.

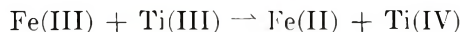
The system was brought to  $60.0 \pm .05^\circ\text{C}$ . in a thermostatted oil bath and then subjected to a series of alternating evacuations and nitrogen admissions so as to insure an inert atmosphere. The system was then brought to atmospheric pressure with nitrogen.

Catalyst was prepared in a manner identical to that described in the preceding section of this paper, i.e., identical procedure and quantities were used, thereby simulating polymerization conditions used here and in earlier publications.<sup>1,2</sup>

After allowing a catalyst aging time of 18–20 min., stopcocks (5) and (8) were opened, and nitrogen pressure was applied to the reaction mass by means of syringe needle in the serum cap (3), allowing the first liquid sample to be collected in the graduated receiver (6). Time necessary to collect this first liquid sample was 3–4 min.; therefore total catalyst aging time for this initial sample was  $\geq 20$  min. Pressure was then removed from the equipment, stopcocks (5) and (8) were closed, the equipment was removed from the constant temperature bath and the liquid sample of known volume emptied into an Erlenmeyer flask containing ca. 50 ml. of water. The collection cylinder (6) was rinsed two times, each time with ca. 3 ml. benzene, and these rinsings were added to the original sample now contained in the Erlenmeyer flask.

While the reaction flask was now cooling from the initial reaction temperature of  $60 \pm 0.05^\circ\text{C}$ . to a lower temperature, a second liquid sample was collected in a manner similar to the first and within 5–10 min. of the first sample. This second sample then represents a catalyst aging time of  $\geq 25$  min., but over a temperature range  $60\text{--}45^\circ\text{C}$ .

**Analytical Method for Tetravalent Titanium Determination.** Each liquid sample in ca. 50 ml. of water was allowed to age for ca. 2 min. to allow divalent titanium (if any) to be converted to trivalent titanium prior to adding 4 ml. of a nearly saturated aqueous solution of ferric chloride and 5 ml. of a 20% aqueous solution of sulfuric acid. After a waiting period of ca. 5 min., all of the trivalent titanium is expected to be converted to tetravalent titanium and an equivalent amount of ferric ion converted to ferrous ions; i.e.,



The amount of ferrous ion was determined by titration with a 0.001*N* aqueous potassium dichromate solution to a sodium diphenylamine sulfonate endpoint. After correcting for a blank titration, the amount of Ti(III) in the original liquid catalyst sample could be calculated. The final total liquid sample after completion of the dichromate titration was bottled and saved for a determination of total titanium, performed for us by the Analytical Department of the American Cyanamid Co., Stamford, Connecticut, Research Laboratories, by a spectrophotometric technique.<sup>3</sup>

Based on the determined total titanium, the amount of tetravalent titanium which must have been present in the original liquid catalyst sample could then be obtained by difference, i.e.,

$$\text{Ti (total)} - \text{Ti(III)} = \text{Ti(IV)}$$

It should be pointed out here that the use of a permanganate solution instead of a dichromate solution for the determination of ferrous ion is not satisfactory; the former results in a substantial error due to oxidation of chloride in addition to ferrous ion.

A summary of these results is shown in Table II.

## DISCUSSION AND CONCLUSIONS

As shown in Table II, substantial concentrations of Ti(IV) species exist under these experimental conditions and at catalyst aging times  $T_c \geq 20$  min. However, within the errors of these determinations it was not possible to demonstrate clearly a decrease of Ti(IV) species with increasing  $T_c$  for  $T_c \geq 20$  min., i.e., a decrease of Ti(IV) with  $T_c$  would be expected. It is concluded herewith that the previously invoked hypothesis regarding the existence of tetravalent titanium species,<sup>1,2</sup> under these experimental conditions, is substantiated.

As shown in Table I, and within the errors of these determinations,  $\beta,\beta\text{-}d_2\text{-styrene}$  appears to produce rates of polymerization and product intrinsic viscosities identical to those found for styrene, as anticipated

TABLE II  
Determination of Ti(IV) Concentration as a Function of Catalyst Aging Time  $T_e^a$

Run	$T_e$ , min.		Approx. total	Ti(III) $\times 10^5$ , g./ml. sample	Total Ti $\times 10^5$ , g./ml. sample	Ti(IV) $\times 10^5$ , g./ml. sample	Ti(IV), g./g. Ti(III)
	At $60 \pm 0.05^\circ\text{C}$ .	At $<60^\circ\text{C}$ .					
A.S.-7a	$\leq 25$	None	22	2.7	10.0	7.3	2.7
" -7b	"	$\leq 12$	31	1.9	7.1	5.2	2.7
" -8a	$\leq 22$	None	20	3.9	8.9	5.0	1.3
" -8b	"	$\leq 10$	25	3.0	8.0	5.0	1.6
" -9a	$\leq 21$	None	20	4.2	8.1	3.9	0.9
" -9b	"	$\leq 8$	29	5.0	8.2	3.2	0.6
" -10a	$\leq 29$	None	24	2.4	7.4	5.0	2.1
" -10b	"	$\leq 16$	32	1.9	8.6	6.7	1.6

<sup>a</sup> Reaction conditions: total volume = 17.5 ml.;  $[\text{TiCl}_4] = 4.4 \times 10^{-2}$  mole/l.;  $[\text{Al}(\text{C}_2\text{H}_5)_3] = 1.4 \times 10^{-1}$  mole/l.;  $\text{Al/Ti} = 3.1$ ; temp. =  $60.00 \pm 0.05^\circ\text{C}$ .; solvent, benzene.



based on earlier reported work.<sup>1,2</sup> If the homopolystyrene rates of Table I are recalculated in terms of the equipment used earlier,<sup>1,2</sup> excellent agreement can be demonstrated with those data reported earlier.

Earlier reported<sup>1,2</sup> intrinsic viscosity values were generally much higher ( $[\eta] = 3.0\text{--}3.5$  dl./g.) than those shown in Table I. No good explanation can be offered for this discrepancy at this time. However, based upon the earlier suggested mechanisms<sup>1,2</sup> for propagation and termination, intrinsic viscosities were believed to be complicated by low molecular weight contaminants, i.e., oligomers which may or may not be retained in the final purified polymer sample prior to the determination of intrinsic viscosities.

The apparent inability to produce substantially higher product intrinsic viscosities via  $\beta,\beta\text{-}d_2$ -styrene, compared to styrene, suggests strongly that the primary mode of polymer termination does not involve the beta hydrogens of styrene and/or abstraction of  $\beta$ -hydrogen is not rate-determining. Based on previously reported data,<sup>1,2</sup> the latter is probably true; propagating species are believed to be primarily adsorbed and/or chemisorbed Ti(IV)-containing sites, whose termination rate is governed by adsorption and desorption equilibria and/or available "free" surface. Termination probably occurs by a bimolecular mechanism; as per Table I, these data confirm the earlier reported<sup>1,2</sup> overall monomer dependence of  $v_p\alpha[M]^{1.5}$ .

The authors wish to thank the American Cyanamid Company's Stamford Research Laboratories, and in particular Mr. E. McEvoy for the determination of total titanium.

### References

1. C. G. Overberger and P. A. Jarovitzky, paper presented at 149th Meeting, American Chemical Society, Detroit, April 1965; *Polymer Preprints*, **6**, 234 (1965).
2. C. G. Overberger and P. A. Jarovitzky, in *Macromolecular Chemistry (J. Polymer Sci. C, 4)*, M. Magat, Ed., Interscience, New York, 1964, p. 37.
3. E. B. Sandell, *Colorimetric Determination of Traces of Metals*, 3rd Ed., Interscience, New York, 1959, p. 874.

### Résumé

Il existe des concentrations appréciables de titane tétravalent dans les systèmes catalytiques  $\text{TiCl}_4\text{-Al}(\text{C}_2\text{H}_5)_3$ -benzène pour des durées de vieillissement de catalyseurs supérieures à 20 min à 60°C. La substitution deutérée du styrène en  $\beta,\beta\text{-}d_2$ -styrène utilisant le système catalytique susmentionné n'exerce aucun effet, ni sur la vitesse de polymérisation, ni sur la viscosité intrinsèque du produit. Ces phénomènes confirment le mécanisme de propagation de chaînes et de terminaison tel qu'il a été suggéré antérieurement.

### Zusammenfassung

Es wurde gezeigt, dass in einem  $\text{TiCl}_4\text{-Al}(\text{C}_2\text{H}_5)_3$ -Benzol-Katalysatorsystem bei Alterungsdauern  $\geq 20$  Min wesentliche Konzentrationen an vierwertigem Titan vorhanden sind. Ein Ersatz von Styrol durch  $\beta,\beta\text{-}d_2$ -Styrol scheint bei obigem Katalysatorsystem keinen Einfluss auf Polymerisationsgeschwindigkeit oder Viskositätszahl des Polymeren zu besitzen. Die Ergebnisse bestätigen den früher vorgeschlagenen Mechanismus für Kettenwachstum und Abbruch.

Received March 7, 1966

Prod. No. 5107A

## Theoretical Studies on the Degradation of Ladder Polymers

MARTIN M. TESSLER,\* *Polymer Branch, Air Force Materials Laboratory, Wright-Patterson Air Force Base, Ohio*

### Synopsis

The random degradation of four- and six-membered ring ladder polymers was simulated on a digital computer by utilizing a Monte Carlo model. The degradation was compared with that of a single-chain linear polymer undergoing an identical degradation reaction. Significant differences in the change in molecular weight as a function of time were noted between the ladder polymer and the single chain polymer. Similar studies were conducted with imperfect ladder polymers which had occasional missing bonds in the ladder structure. These imperfections produced a marked drop in molecular weight at a given time compared with the perfect ladder polymer.

### Introduction

Interest in the development of thermally stable materials has produced much research into new and novel types of polymers. One area of investigation is the preparation of a ladder or double-strand polymer. Brown and co-workers<sup>1</sup> prepared the double-chain polyphenylsilesquioxane in which the polymer backbone is completely inorganic. Attempts to synthesize a ladder polymer with an organic backbone from vinyl isocyanate,<sup>2</sup> poly-3,4-isoprene,<sup>3</sup> and conjugated dienes<sup>4</sup> have recently been reported. These polymers have segments of fused rings, but they are not completely fused into the desired ladder structure.

This paper compares the thermal stability of a ladder polymer undergoing random degradation with that of a single chain polymer. A digital computer is used to set up a statistical (Monte Carlo)<sup>5</sup> model of the degrading system. The following assumptions for random degradation are made in defining the degrading system.

(1) The polymer sample is initially homogeneous; that is, only chains of one length are present. It is possible to assume almost any molecular weight distribution in the initial polymer sample. For a given number-average molecular weight, the change in number-average molecular weight during degradation is independent of whether the molecule being broken is small or large or if the break occurs in the middle of the molecule or near an end. The results should not vary too much due to

\* Present address: Esso Research and Engineering Co., Enjay Chemical Laboratories, Linden, New Jersey 07036.

a change in the initial molecular weight distribution. Since it is very convenient to use a homogeneous initial sample, this assumption was built into the program.

(2) All bonds in the polymer chain are of equal strength and equal accessibility, regardless of their positions in the molecule and the length of the chain. There are many possible mechanisms of degradation. One of the most thoroughly explored is random degradation,<sup>6</sup> where all bonds have an equal probability of breaking. There is no experimental evidence available on the degradation of ladder polymers, but this paper will study some of the theoretical aspects of random degradation. The computer program is flexible enough so that many other types of degradation can be investigated. In a ladder polymer, there are two types of bonds; side-chain bonds and crosslinks. To make the random degradation of the ladder polymer analogous to that of the single-chain polymer, it was assumed that these two types of bonds have the same strength and degrade at the same rate.

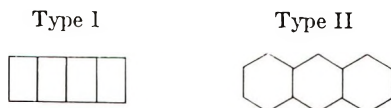
(3) The rate of breaking bonds is proportional to the number of bonds present in the degrading system. This assumption has been made by other workers<sup>6</sup> studying random degradation of polymers. The number of unbroken bonds can readily be calculated at any time during the degradation, and therefore the rate of breaking of the bonds can readily be obtained.

(4) The system is closed; that is, no fragments can leave the system. The case of an open system, where vaporization can occur, will be considered in future work.

The ratio of the number-average molecular weight (at time  $kt$ ) to the initial number-average molecular weight is obtained directly from the computer, where  $k$  is the proportionality constant between the rate of breaking bonds and the number of bonds present in the system at time  $t$ .

### Model Ladder Structures

Two types of ladder polymers were studied. Type I is a fused four-membered ring and type II is a fused six-membered ring. All the conclusions reached for a four-membered ring are equally applicable to an eight-membered ring.



Initially, a simplified scheme of degradation was considered. In this simple case, a broken bond can break a molecule only if the bond opposite it is broken. The fact that a broken crosslink will increase the probability of a molecule breaking is ignored. This type of degradation is shown in Figure 1. The complex case of degradation is shown in Figure 2, where breaks in the crosslinks will result in increased molecule breaks. This is a much more realistic picture of random degradation than the simple case.



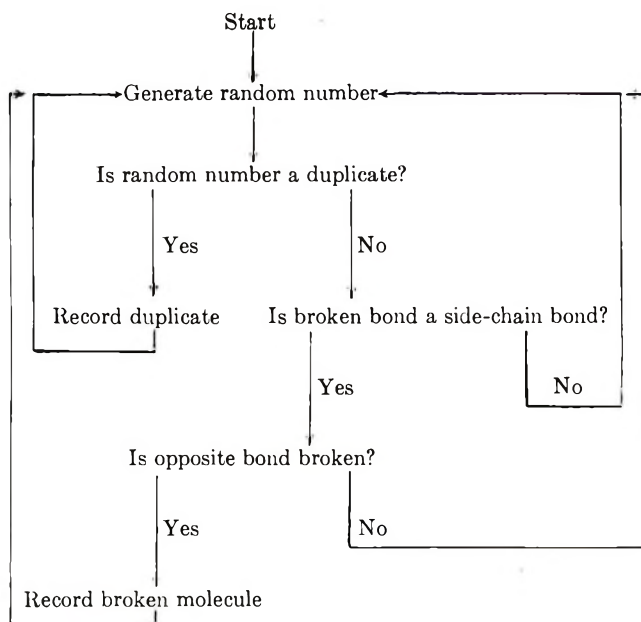


Fig. 3. Flow diagram of computer program for simple case ladder polymer degradation.

When a random number is generated, the bond which it represents is checked to see if it is broken or not. If it is already broken, a duplicate is recorded and a new random number generated. If it is not broken, the bond is set equal to one and, if the bond is a side-chain bond, the opposite bond checked. If the opposite bond is broken, a broken molecule is recorded and a new random number is then generated. If the opposite bond is not broken, no further work is done in the simple case and a new random number is generated. In the complex case, the computer checks all the crosslinks to the left and right until it either comes to an unbroken crosslink or the last crosslink at the end of the molecule. If the last crosslink is broken, a broken molecule is recorded and a new random number generated. If the computer finds an unbroken crosslink, it then scans all of the side-chain bonds on both sides of the ladder polymer from the broken bond produced by the random number generation to the last side chain bond before the unbroken crosslink. If any of the side-chain bonds are broken, a broken molecule is recorded and a new random number is then generated. If none of the side-chain bonds are broken, a new random number is generated. The computer keeps track at all times of the number of duplicates recorded. The number of bonds which are broken is equal to the number of random numbers generated minus the number of duplicates.

If the initial broken bond is a crosslink, no additional calculations are done in the simple case except that the number of unbroken bonds is re-

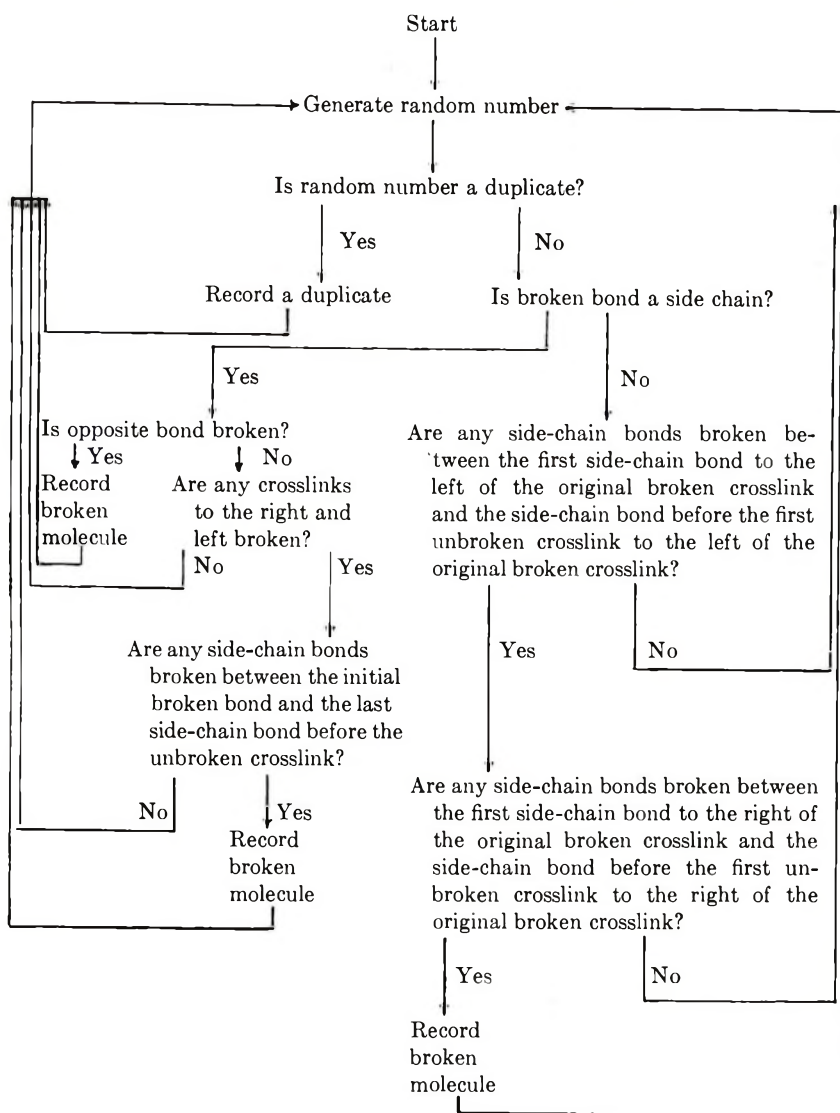


Fig. 4. Flow diagram of computer program for complex case ladder polymer degradation.

duced by one. In the complex case, the computer checks all of the crosslinks to the left of the initial broken crosslink until it either comes to an unbroken crosslink or the last crosslink at the end of the molecule. If the computer finds an unbroken crosslink, it scans all of the side-chain bonds on both sides of the ladder polymer from the first side-chain bond to the left of the initial broken crosslink to the side-chain bond before the first unbroken crosslink. If none of the side-chain bonds are broken, a new random number is generated. If one of the side-chain bonds is broken or if all of the crosslinks to the end of the molecule had been broken,

the computer scans all of the crosslinks to the right of the initial broken crosslink. If the computer finds an unbroken crosslink, it then scans all of the side-chain bonds from the first side-chain bond to the right of the initial broken crosslink to the side-chain bond before the first unbroken crosslink. If none of the side-chain bonds are broken, a new random number is generated. If one of the side-chain bonds is broken or if all of the crosslinks to the end of the molecule are broken, a broken molecule is recorded and a new random number generated. A slightly simplified flow diagram of the computer program for the simple case is shown in Figure 3 and the complex case in Figure 4.

$$-dB/dt = kB \quad (1)$$

The rate of breaking bonds is proportional to the number of unbroken bonds present in the degrading system. On solving eq. (1),  $kt$  is equal to  $\ln(B_0/B)$ , where  $B_0$  is the number of bonds present initially,  $B$  is the number of bonds present at time  $t$ , and  $k$  is the proportionality constant between the rate of breaking bonds and the number of bonds present in the system. The number of molecules present in the system is equal to the number of molecules present initially plus the number of broken molecules since each broken molecule produces one more fragment. The ratio of the number-average molecular weight at time  $kt$  to the initial number-average molecular weight is equal to  $A/(A + \text{number broken molecules})$ , where  $A$  is the number of molecules present initially. All of these quantities are readily calculated during the course of the degradation and the computer prints out the desired data at any convenient interval of  $kt$ . The proportionality constant  $k$  must be determined experimentally for a given polymer. The computer, therefore, calculates  $kt$  and not  $t$ .

The subprogram by which the computer generates a random number makes use of an equation in which multiplication and division are used, the output being the remainder after division. Several different sets of random numbers were used to check the accuracy of the method. The random number generator appears to be very reliable.

### Results for Perfect Ladder Polymers

The curve for the ratio of the number-average molecular weight at time  $kt$  to the initial number-average molecular weight versus  $kt$  is shown for ladder polymer type I in Figure 5 and for ladder polymer type II in Figure 6. Both the simple case and the complex case are shown as well as the analogous single chain polymer. The proportionality constant  $k$  is not known and it probably will have different values for different polymers. This will shift the curves, but the significant fact is the shapes of the curves. The single-chain polymer shows a very sharp drop in molecular weight as soon as degradation begins. The ladder polymer has an induction period where the molecular weight hardly changes and then it drops much more slowly than the corresponding single chain polymer. As degradation proceeds, both curves merge together. These results indicate that the ladder

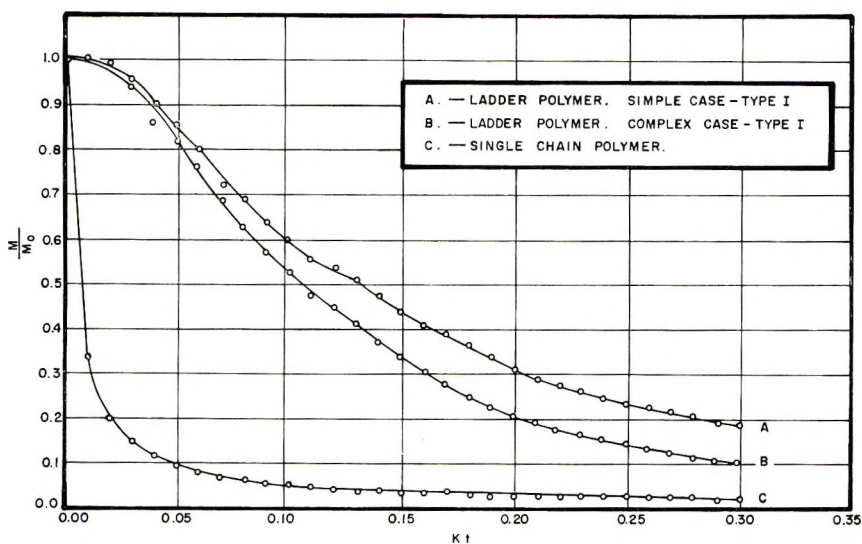


Fig. 5. Plot of the ratio of molecular weight to initial molecular weight vs. time for type I ladder polymers undergoing random degradation.

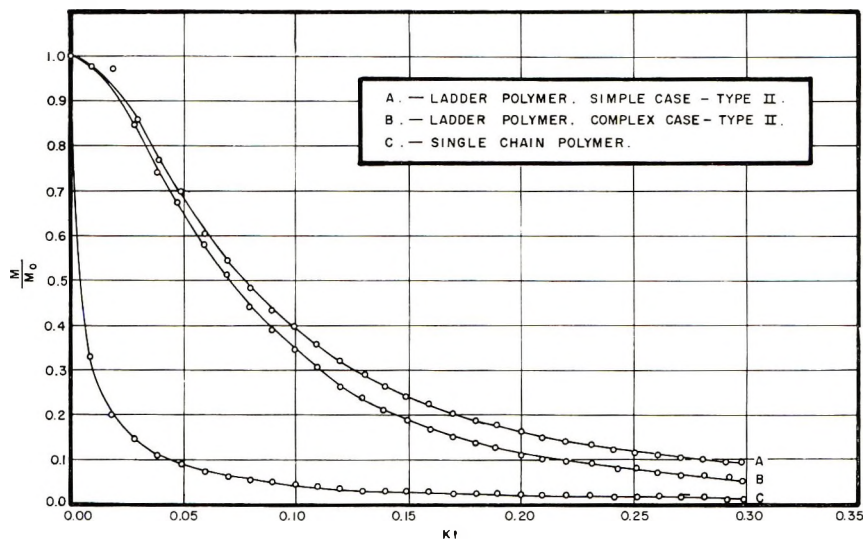


Fig. 6. Plot of the ratio of molecular weight to initial molecular weight vs. time for type II ladder polymers undergoing random degradation.

polymers should have increased thermal stability over a single-chain polymer, but the extent of this stability can only be determined by studying the chemistry of these compounds.

### Imperfect Ladder Polymers

Ladder polymers are of interest because of their potential stability at high temperatures. The double-chain polyphenylsilsesquioxane syn-



thesized by Brown and co-workers<sup>1</sup> has an inorganic ladder structure, and the silicon-oxygen bonds rearrange at elevated temperatures. The reported attempts to synthesize ladder polymers with an organic ladder structure<sup>2-4</sup> have all used the same general approach. A polymer is first prepared which has pendant nonconjugated 1,6 unsaturation along the chain of the molecule. Overberger and co-workers<sup>2</sup> polymerized vinyl isocyanate through the vinyl group or the isocyanate group to get the starting polymer. Angelo<sup>3</sup> prepared poly-3,4-isoprene and Gaylord and co-workers<sup>4</sup> used butadiene, isoprene, and chloroprene to obtain the desired polymer. Cyclization of the pendant nonconjugated 1,6 unsaturated polymer with suitable catalysts produces a ladder structure.

The problems in preparing a completely perfect ladder polymer are enormous. Imperfect ladder polymers can result from isolated unreactive groups, from alternative cyclizations or isomerizations, from cross-linking, and from chain-scission reactions. Another problem is that as the ladder polymer is being synthesized, its solubility is decreasing rapidly and it may precipitate out of solution before ring closure is complete. If the polymer with the pendant nonconjugated 1,6 unsaturation is not structurally perfect, complications will arise in the cyclization step. For example, the poly-3,4-isoprene used by Angelo contained up to 10% of 1,4 structural units.

The difficulty in preparing perfect double-chain polymers raises the question as to how the thermal stability of an imperfect ladder polymer compares with that of a single chain polymer. A partial solution to this problem can be obtained by setting up in the storage of a digital computer, an imperfect ladder polymer. Each storage location will correspond to a different bond and a random number generator will be used to locate the bond which is being broken during degradation. An unbroken bond will be represented by a zero and a broken bond by a one. If all the bonds are initially set equal to zero, we will have a perfect ladder polymer. If we initially set a bond equal to one at prescribed intervals along the chain we will have an imperfect ladder polymer with the "broken bonds" corresponding to missing bonds in an imperfectly synthesized ladder polymer. If the random number generator should produce a number corresponding to one of these missing bonds, a duplicate will be recorded and a new random number will be generated without any further calculations. It is assumed that the polymer sample is homogeneous, all bonds in the polymer have an equal probability of being broken, the rate of breaking bonds is proportional to the number of bonds present in the degrading system and no fragments can leave the system.

The Monte Carlo calculations are identical to those described previously.

Four- (type I) and six- (type II) membered ring ladder polymers were studied and both the simple and complex cases of degradation examined. A single-chain polymer with the same number of bonds per molecule was degraded simultaneously in the computer for comparison purposes.

Type I ladder polymers were studied with single bonds first at every sixth

and then at every twelfth bond along the chain. Type II ladder polymers were studied with single bonds first at every twelfth and then at every twenty-fourth bond along the chain.

### Results for Imperfect Ladder Polymers

The introduction of single bonds along the chain of the ladder polymer results in a sharp decrease in molecular weight, as degradation occurs, compared to a perfect ladder polymer. The stability of the imperfect ladder polymer is still much greater than that of an analogous single-chained polymer. The shape of the curves when the ratio of the number-average molecular weight at time  $kt$  to the initial number-average molecular weight is plotted against  $kt$  is very interesting (Figs. 7-10). With a small number of single bonds within the ladder chain, the curves still have an induction period where the change of molecular weight is relatively small. It then drops very rapidly, although not as fast as a single chain polymer. As the number of single bonds is increased, the induction period disappears, and the shape of the curve is the same as that of the single chain polymer, although the molecular weight still does not decrease as fast. With a suitable value of  $k$ , it is possible that the curves will become superimposable and that the imperfect ladder polymer will have no increased advantage in thermal stability over a single chain polymer. The answer to this problem must await the synthesis and characterization of imperfect ladder polymers

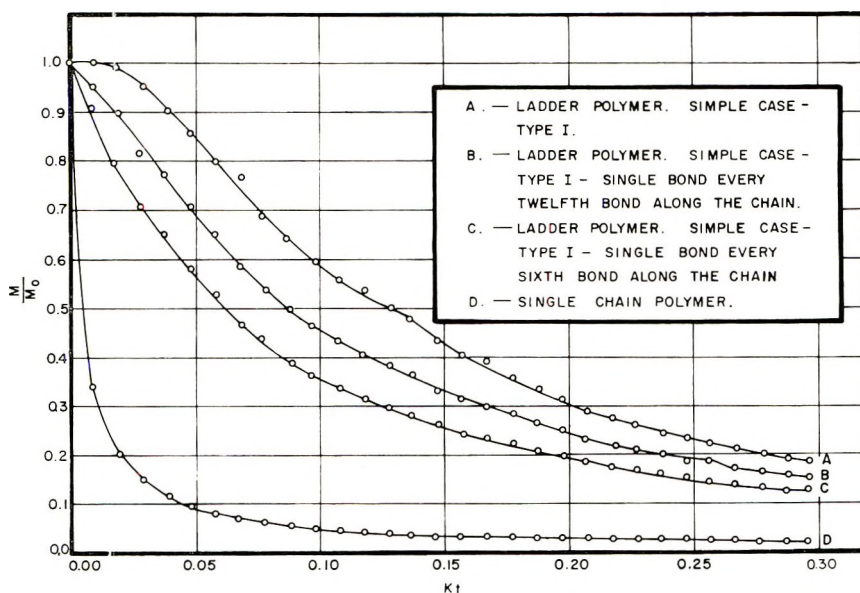


Fig. 7. Plot of the ratio of molecular weight to initial molecular weight vs. time for type I imperfect ladder polymers undergoing random degradation by simple mechanism.

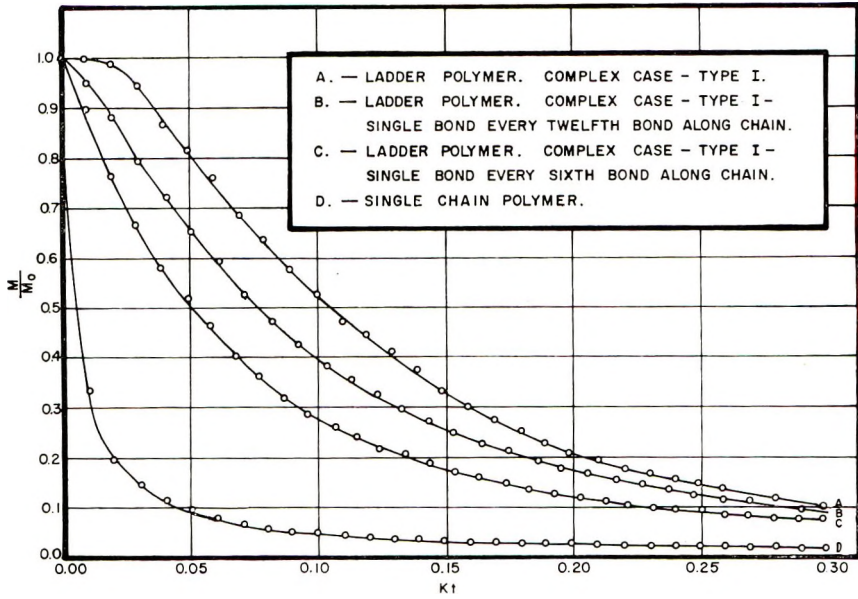


Fig. 8. Plot of the ratio of molecular weight to initial molecular weight vs. time for type I imperfect ladder polymers undergoing random degradation by complex mechanism.

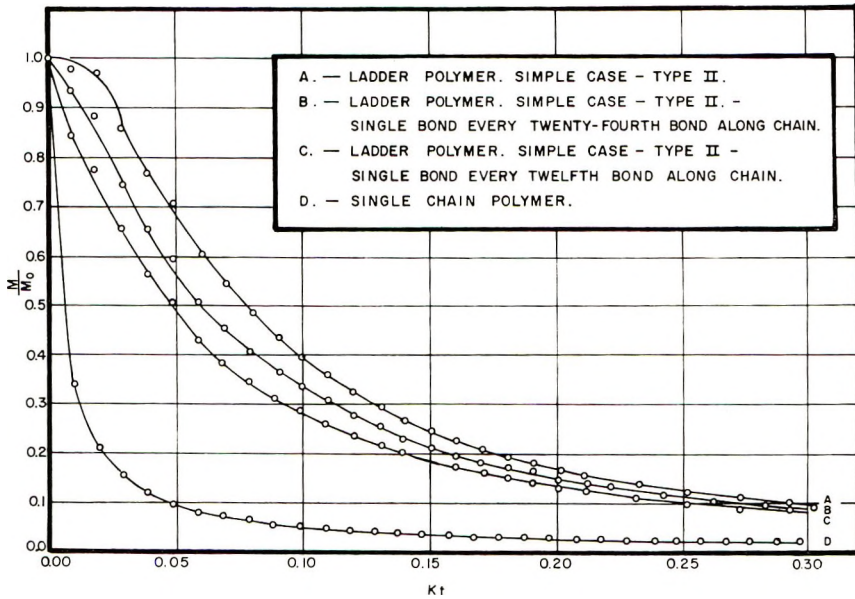


Fig. 9. Plot of the ratio of molecular weight to initial molecular weight vs. time for type II ladder polymers undergoing random degradation by simple mechanism.

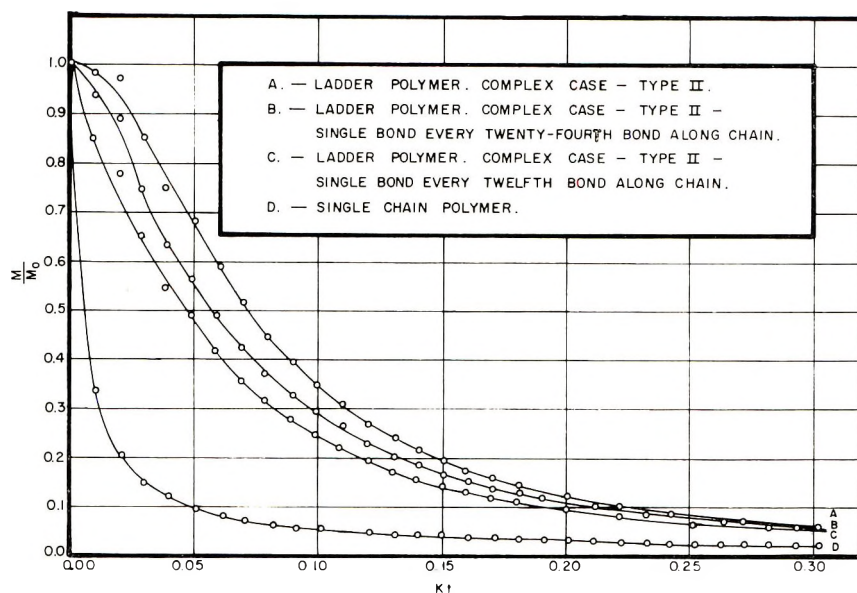


Fig. 10. Plot of the ratio of molecular weight to initial molecular weight vs. time for type II ladder polymers undergoing random degradation by complex mechanism.

and a study of their chemical behavior when undergoing thermal degradation.

The author wishes to thank Elwin C. Penski for many helpful discussions.

### References

1. J. F. Brown, Jr., L. H. Vogt, Jr., A. Katchman, J. W. Eustance, K. M. Kiser, K. W. Krantz, *J. Am. Chem. Soc.*, **82**, 6194 (1960).
2. C. G. Overberger, S. Ozaki, and H. Mukamol, *Proceedings of the Battelle Symposium on Thermal Stability of Polymers*, Battelle Memorial Institute, Columbus, Ohio, Dec. 5-6, 1963.
3. R. J. Angelo, paper presented at symposium honoring the late Dr. W. H. Carothers, Institute of Rubber Research, Univ. of Akron, 1963.
4. N. G. Gaylord, I. Kössler, M. Stolka, and J. Vodehnal, *J. Am. Chem. Soc.*, **85**, 641 (1963).
5. A. S. Householder, G. E. Forsythe, and H. H. Germond, *Monte Carlo Method*, Applied Mathematics Series 12, National Bureau of Standards, Washington, D. C., 1951.
6. H. H. G. Jellinek, *Degradation of Vinyl Polymers*, Academic Press, New York, 1955.

### Résumé

La dégradation statistique de polymères en échelle à anneaux hexa- et tétraatomiques a été représentée sur un ordinateur digitale utilisant le modèle Monte-Carlo. La dégradation a été comparée avec celle de la réaction de dégradation d'un polymère linéaire simple subissant une même réaction. Des différences significatives de variations de poids moléculaires en fonction du temps ont été notées entre le polymère en échelle et la chaîne polymérique linéaire. Des études similaires ont été conduites avec des poly-

mères en échelle imparfaite, qui présentaient ci- de là des liaisons manquantes dans la structure en échelle. Ces imperfections produisaient une diminution notable du poids moléculaire à un temps déterminé comparé à un polymère en échelle de structure parfaite.

### **Zusammenfassung**

Der statistische Abbau von Leiterpolymeren mit vier- und sechsgliedrigen Ringen wurde mit einem Digitalcomputer an einem Monte-Carlo-Modell simuliert. Der Abbau wurde mit demjenigen eines einfachen linearen Kettenpolymeren bei identischer Abbaureaktion verglichen. Zwischen dem Leiterpolymeren und dem Polymeren mit einfacher Kette wurden signifikante Unterschiede in der Molekulargewichtsänderung als Funktion der Zeit festgestellt. Ähnliche Untersuchungen wurden an fehlerhaften Leiterpolymeren ausgeführt, bei welchen stellenweise Bindungen in der Leiterstruktur fehlen. Diese Fehlstellen führten in Vergleich zu dem fehlerfreien Leiterpolymeren zu einem merklichen Abfall des Molekulargewichts bei einer bestimmten Zeit.

Received April 26, 1965

Revised March 14, 1966

Prod. No. 5108A

## Graft Copolymers of Phenolic Novolacs on Polyamide Backbones

A. RAVVE and C. W. FITKO, *Corporate R&D, Continental Can Company, Chicago, Illinois 60620*

### Synopsis

The formation of graft copolymers of novolacs on polyamide backbones was carried out under conditions which permitted product isolation and investigation. Grafting was performed on nylons 11, 610, 66, and 6 with the use of the condensates of formaldehyde with either phenol, *p*-cresol, or *p*-nonyl phenol. Physical properties of the reaction products were studied, and the proof of grafting was established by means of chemical, infrared, and NMR investigations.

### INTRODUCTION

Grafting reactions of phenolic novolacs to polyamides have been reported.<sup>1,2</sup> No information is available in the literature, however, on the nature or properties of these graft copolymers because they were not isolated and studied.

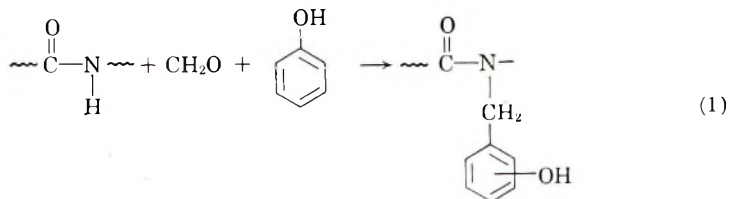
This paper reports preparation of such graft copolymers by a method which enables product isolation. Subsequent study of the resultant materials shows proof of grafting.

### RESULTS AND DISCUSSION

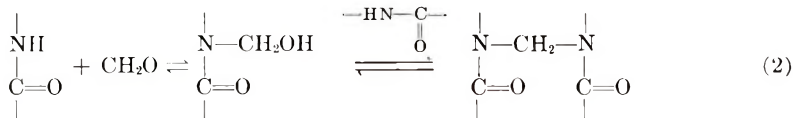
Four different polyamides were employed in these grafting reactions: nylons 6, 66, 610, and 11. These reactions were carried out with the use of phenol, *p*-cresol, and *p*-nonyl phenol with formaldehyde as the condensing agent.

Generally, when the condensation reactions with formaldehyde are being carried out simultaneously on both phenols and amides, competing reactions take place. Thus, whether the methylol groups will form preferentially on the phenol or on the amide groups is very much a function of experimental conditions.<sup>3</sup> Furthermore, the ability of the subsequently formed methylol groups to react further with molecules of another amide or a phenol is also a function of the reaction medium.<sup>4</sup> As a result, one can speculate on the following reactions. (1) Formaldehyde reacts preferentially with an amide group to form *N*-methylol derivatives. These then react with other amides and crosslink the nylons by forming methylene bridges. The phenols do not enter these reactions. (2) The phenols

may condense with formaldehyde to form resinous reaction products which are not grafted to the polyamide. (3) A trimolecular condensation will take place involving all three, the amide, formaldehyde, and the phenol, simultaneously or in sequence, as shown in eq. (1).



Only the last step will lead to successful grafting reaction. The picture is further complicated by the reversibility of many of these reactions. Cairns and co-workers<sup>5</sup> have shown the reversibility of *N*-methylolation and of polyamide methylene bridges [eq. (2)].

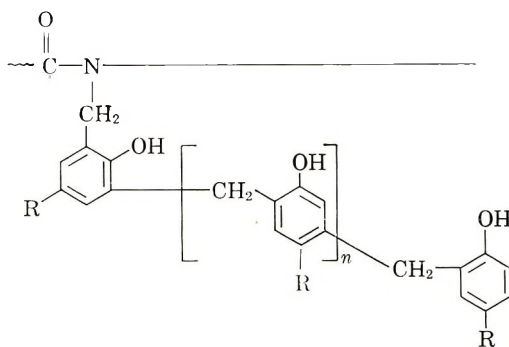


In this investigation, in the presence of moderately strong acids like formic, the rates of formaldehyde condensation with amides were found by us to be apparently more rapid than with phenols, leading to results described in case (1). In weaker acids, like acetic acid, reaction could be controlled through the introduction of small quantities of water, but the amount of phenol in the product was found to be small.

Advantage was then taken of the fact that phenols will condense with formaldehyde at 140°C. or higher without the aid of a catalyst.<sup>6</sup> These reactions were carried out in the presence of excess phenols which thus served, not only as correctants, but as solvents as well. Xylene was a useful diluent. Thus, the reaction of the phenols and formaldehyde was accomplished first, and then, upon addition of catalytic quantities of a strong acid such as toluenesulfonic acid, attachment was accomplished to the polyamide backbone. It appears likely that at that temperature, only a small fraction of the phenol alcohols dehydrated to the quinone methides.<sup>7</sup> When the reaction was repeated at 180°C. to evaluate the grafting efficiency with greater amount of quinone methides present,<sup>8</sup> less grafting actually took place.

By using one mole of amide for three moles of phenol with one mole of formaldehyde, it was possible to achieve weight increases from the starting material which ranged from 20 to 25%. The formaldehyde was conveniently added in three or more increments to prevent the viscosity build-up of the reaction medium. This was done usually over a period of 3 hr., followed by addition of a small quantity of toluenesulfonic acid (0.05 mole) to achieve the grafting of the phenol alcohols to the backbone. On occasions, the additions of this strong acid caused immediate thickening

of the reaction mediums and almost gelation, but apparent reversibility<sup>9</sup> of these semigels caused gradual restoration of the original reaction viscosities. The infrared spectra of the resultant graft copolymers are shown in Figures 1-5 together with those of their parent compounds. New twin peaks appeared at 9.65 and 9.8  $\mu$ . This corresponds to the 1,4 and 1,2,4 aromatic substitutions.<sup>10</sup> By watching the development of these peaks in the spectra on reaction aliquots, it is possible to follow the progress of grafting and also to observe when the reaction reaches its maximum. Another peak at 12.1-12.25  $\mu$ , corresponding to the carbon-hydrogen out-of-plane deformation with two adjacent hydrogens on the aromatic ring,<sup>10</sup> yields additional evidence of grafting and suggests that at least some of the benzene rings are trisubstituted. This absorption band shows up stronger in some graft copolymers than in others, particularly in the case of alkyl phenols which should end up as being trisubstituted and even tetrasubstituted in cases of side chain growth (I).



I

Further evidence of grafting was obtained from nuclear magnetic resonance data obtained on the product of graft copolymerization of phenol-formaldehyde on nylon 11, as shown in Figure 6. A chemical shift can be observed at 6.95 ppm, signifying aromatic hydrogen.<sup>11</sup>

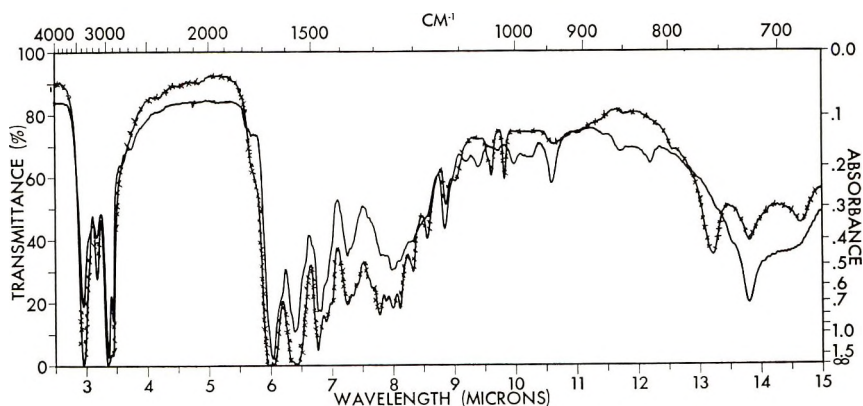


Fig. 1. Infrared spectra of: (—) nylon 11; (---) polymer I.



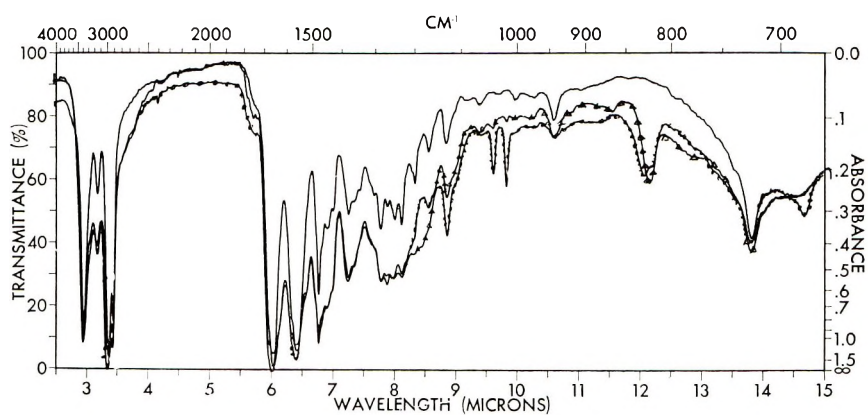


Fig. 2. Infrared spectra of: (—) nylon 11; (—△—△—) polymer II; (—●—●—) polymer III.

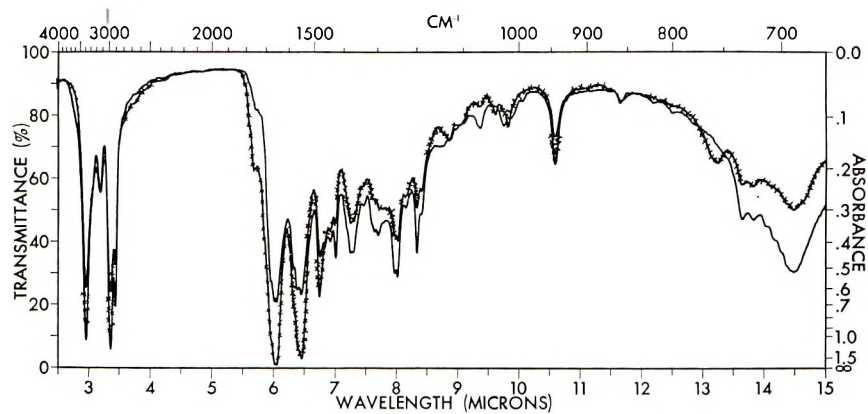


Fig. 3. Infrared spectra of: (—) nylon 610; (—X—X—) polymer IV.

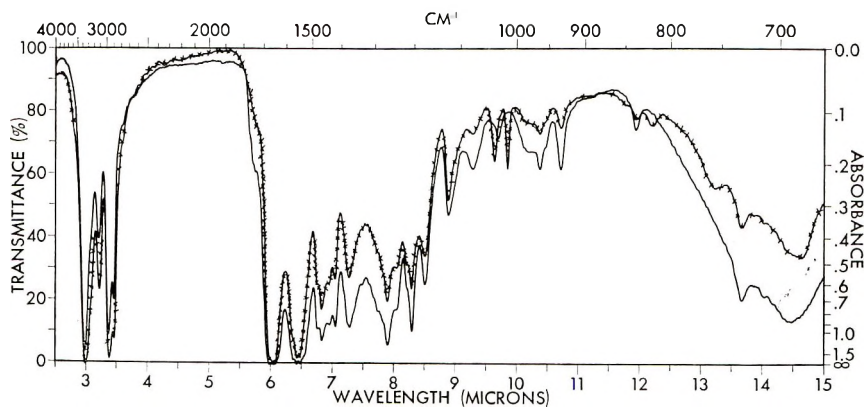


Fig. 4. Infrared spectra of: (—) nylon 66; (—X—X—) polymer V.

TABLE I  
Composition, Melting Points, and Solubilities

Polymer	Composition, Found			M.p., °C.	Solubilities (5% solution) <sup>a</sup>					
	C, %	H, %	N, %		BuOH	Anyl alcohol	DMF	DMSO	Cyclohexanone	
Nylon 11	72.08	11.55	7.64	190-192	I	I	SH	SH	SH	
Polymer I	72.72	10.65	6.32	154-161	SH	SH	SH	S <sup>b</sup>	SH	
Polymer II	72.48	10.71	6.33	170-173	PSH	SH	SH	SH	SH	
Polymer III	73.99	11.27	5.41	159-161	I	SH	SH	SH	SH	
Nylon 610	68.04	10.71	9.92	215	I	I	PSH	SH	I	
Polymer IV	68.35	10.43	8.98	214-216	I	I	SH	SH	I	
Nylon 66	63.68	9.80	12.30	262-270	I	I	I	SH	I	
Polymer V	64.27	9.24	11.77	255-267	I	I	PSH	SH	I	
Nylon 6	63.68	9.80	12.30	215-220	I	I	PSH	SH	I	
Polymer VI	63.71	9.30	10.94	216-220	PSH	I	SH	S <sup>b</sup>	I	

<sup>a</sup> S = soluble; I = insoluble; SH = soluble hot; PSH = partly soluble hot.

<sup>b</sup> Hazy solution on cooling.

The shift at 4.60 ppm signifies the  $\text{CH}_2$  group<sup>11</sup> between phenyl and oxygen, suggesting the possibility of either phenol alcohols or diphenyl ethers. The shift at 3.20 ppm represents an amide  $\text{CH}_2$  attached to nitrogen; that at 2.20 ppm an amide  $\text{CH}_2$  attached to a CO group, and the shift at 1.28 ppm a straight chain  $\text{CH}_2$ .<sup>11</sup> The shift at 5.30 ppm may signify a phenolic OH group in the *ortho* position.<sup>11</sup>

The NMR spectrum also indicates that there are about fourteen  $\text{CH}_2$  groups to one phenol.<sup>11</sup>

The phenols can potentially attach themselves through the OH groups, thereby forming ethers as well as through the aromatic nucleus leaving free phenolic hydroxyls. In order to determine the quantity of the aromatic OH groups, therefore, the graft copolymer from phenol-formaldehyde condensation on nylon 11 was dissolved in an alcoholic solution of

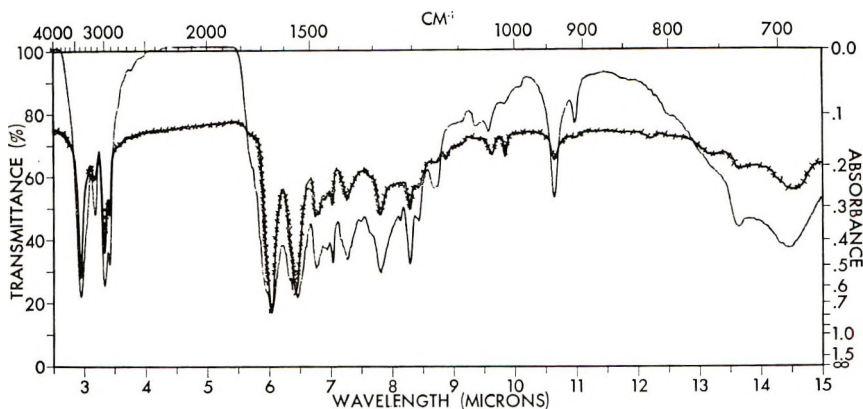


Fig. 5. Infrared spectra of: (—) nylon 6; (-X-X-) polymer VI.

sodium methylate to form sodium phenolates. Ash determination on these products revealed 2.25–2.30% sodium pickup by the resin, as calculated from the sodium carbonate ash. This matches well the calculated 20–25% weight pick-up in grafting and corresponds to a hydroxylbenzyl group attached to every fifth amide. The aromatic to aliphatic hydrogen shift from the NMR data coincides well with this ratio. We can conclude, therefore, that all the phenolic groups are attached through the aromatic nucleus.

The melting points and solubility data on the graft copolymers as well as the backbones, are shown in Table I.

Three different graft copolymers were prepared from nylon 11: polymer I is the product of grafting phenol-formaldehyde condensate; polymer II, the product from grafting *p*-cresol-formaldehyde; polymer III, the product from grafting *p*-nonyl phenol-formaldehyde. Phenol-formaldehyde condensate was also grafted by this procedure to nylon 610, yielding polymer IV; to nylon 66, yielding polymer V; and to nylon 6, yielding polymer VI.

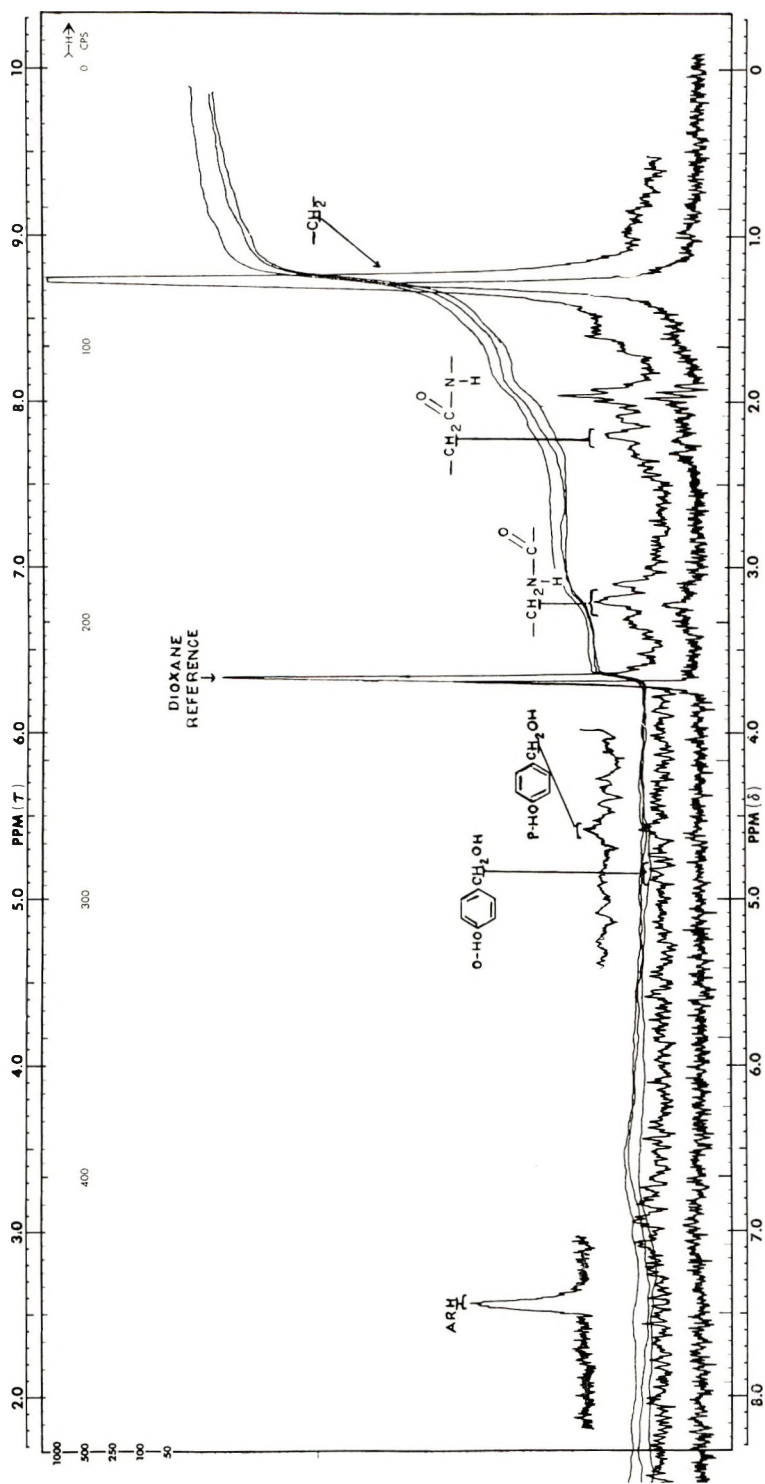


Fig. 6. NMR spectrum of polymer I.

As no significant differences were observed during the experimental conditions, Table I shows that lower melting points were obtained for the grafts on nylon 11 compared to the parent backbone. It also is interesting to note that the phenol-formaldehyde graft to nylon 11, polymer I, shows a lower melting range than a similar graft of *p*-cresol, polymer II. On the other hand, the other graft copolymers melted within the range of the parent backbones.

As expected, the solubilities of the graft copolymers differed from those of their backbone materials. Dimethyl sulfoxide (DMSO) turned out to be the most effective solvent tried, permitting complete solutions of all the macromolecules when hot. Polymers I and VI remained in solution upon cooling, though these two solutions became hazy in appearance.

## EXPERIMENTAL

### Materials

Nylon 11, grade BCL nylon 1107, was obtained from Belding Chemical Industries, New York, New York.

Nylon 6 was Zytel 211; nylon 66 was Zytel 101, and nylon 610 was Zytel 31. These materials were obtained from the Plastic Department of E. I. du Pont de Nemours & Company, Wilmington, Delaware.

### Preparation

A typical grafting reaction is illustrated by the preparation of phenol-formaldehyde-nylon 11 graft copolymer.

Into a 1-liter three-necked round-bottomed flask fitted with a stirrer, reflux condenser, and thermometer were placed 36.6 g. (0.2 mole of repeating unit) nylon 11, 56.4 g. (0.6 mole) phenol, and 109.8 g. xylene. The mixture was heated to 130–140°C. and stirred until the nylon dissolved in the phenol-xylene solution. Then 2.2 g. (0.067 mole) of paraformaldehyde in flake form was added and allowed to react for 1 hr. at 140°C. This step was repeated twice upon two more consecutive hours. After the final addition the formed water of condensation was allowed to distil off. One hour after the final addition of paraformaldehyde, 1.9 g. (0.01 mole) of *p*-toluene-sulfonic acid dissolved in 6 g. of phenol was added slowly. The reaction at 140°C. was continued for an additional hour. The batch was cooled and the graft copolymer was precipitated by slowly adding 500 ml. of acetone to the reaction solution. The precipitate was filtered off and purified by extracting the precipitate overnight in a Soxhlet extractor with acetone. The graft copolymer was dried under vacuum at 80°C.

### References

1. Y. Muira, Y. Haruhara, and T. Kondo, Jap. Pat. 2184 (1962); *Chem. Abstr.*, **58**, 14240 (1963).
2. K. Oshima, S. Ogaki, and K. Hashimoto, Jap. Pat. 23,473 (1963); *Chem. Abstr.*, **60**, 4309 (1964).

3. D. M. McQueen, U. S. Pat. 2,423,460 (July 8, 1947).
4. T. L. Cairns, U. S. Pat. 2,430,860 (November 18, 1947).
5. T. L. Cairns, H. D. Foster, A. W. Larchar, A. K. Schneider, and R. S. Schreiber, *J. Am. Chem. Soc.*, **71**, 651 (1949).
6. H. Dostal and R. Raft, *Z. Physik. Chem.*, **B36**, 117 (1936).
7. H. von Euler, E. Adler, and S. Tingstam, *Arkiv Kemi Min. Geol.*, **A15**, No. 10, 1 (1941).
8. N. J. L. Megson, *Phenolic Resin Chemistry*, Academic Press, New York, 1958, pp. 77, 78.
9. H. D. Foster and A. W. Larchar, U. S. Pat. 2,430,923 (1947).
10. L. J. Bellamy, *The Infra-Red Spectra of Complex Molecules*, Wiley, New York, 1959, pp. 64-91.
11. L. M. Jackman, *Application of Nuclear Magnetic Resonance Spectroscopy in Organic Chemistry*, Pergamon Press, London, 1959, pp. 66-81.

### Résumé

La formation de copolymères greffés de novolacs sur des troncs de polyamide a été effectuée dans des conditions qui permettaient l'isolement du produit en son étude. Des greffages ont été réalisés sur des nylons 11, 610, 66, et 6 utilisant la condensation du formaldéhyde avec soit le phénol, le *p*-crésol ou le *p*-nonylphénol. Les propriétés physiques des produits de réaction ont été étudiées et la preuve des greffages a été donnée grâce à des études chimiques infra-rouges et par résonance nucléaire magnétique.

### Zusammenfassung

Die Bildung von Pfropfcopolymeren von Novolaken auf Polyamidketten wurde unter Bedingungen ausgeführt, welche eine Isolierung und Untersuchung der Produkte gestatteten. Die Aufpfropfung wurde auf Nylon 11, 610, 66 und 6 mit den Kondensaten von Formaldehyd mit Phenol, *p*-Kresol oder *p*-Nonylphenol ausgeführt. Die physikalischen Eigenschaften der Reaktionsprodukte wurden untersucht und die Aufpfropfung durch chemische, Infrarot- und NMR-Messungen nachgewiesen.

Received February 3, 1966  
Prod. No. 5123A

## Study of Crosslink Formation by Partial Conversion Properties. IV. Copolymerization of Styrene with Poly(ethylene Fumarate)

G. M. BURNETT, J. M. PEARSON, and J. D. B. SMITH, *Department of Chemistry, University of Aberdeen, Aberdeen, Scotland*

### Synopsis

The mechanism of the crosslinking reaction in the copolymerization of poly(ethylene fumarate) and styrene has been studied by using partial conversion number-average molecular weights and viscosities. In dilute solution the reaction is mainly the formation of intramolecular crosslinks, illustrated by a reduced dependence of  $\bar{M}_n$  and  $[\eta]$  on conversion. Increasing the monomer concentrations increases the contribution from intermolecular reactions and gives a much greater dependence of  $\bar{M}_n$  and  $[\eta]$  on conversion.

### INTRODUCTION

The application of partial conversion properties in the study of crosslinking reactions between butadiene and a number of vinyl monomers was developed by Wall.<sup>1</sup> The crosslinking reactions of the unsaturated polyester, poly(ethylene fumarate) (PEF), with styrene and methyl methacrylate in dilute solution in dioxane have been similarly characterized.<sup>2-4</sup> It was shown that the kinetics of the crosslinking reaction were different for the two vinyl monomer systems. In the PEF-styrene copolymerization the main step was one of the formation of intramolecular crosslinks with little or no development of intermolecular processes at the concentrations used. In contrast to this, the intermolecular reaction was the predominant one in the PEF-methyl methacrylate system.

The partial conversion number-average molecular weight,  $\bar{M}_n$ , is given by eq. (1):

$$\bar{M}_n = \bar{M}_n^2 / [\bar{M}_n - W(d\bar{M}_n/dW)] \quad (1)$$

where  $W$  is the weight conversion of polymer,  $N$  the corresponding number of molecules, and  $\bar{M}_n (= W/N)$  is the number-average molecular weight. When crosslinking takes place the quantity  $(dN/dW)$ , i.e.,  $1/\bar{M}_n$  will become negative, since the number of molecules is decreasing with conversion. Any change in the mechanism of the crosslinking reaction (i.e., in the relative contribution of inter- and intramolecular reactions to the overall process) will be reflected in the variation of  $\bar{M}_n$  with conversion.

In the PEF-styrene system the crosslinking reaction was intramolecular at the reactant concentrations studied. Variation of the reactant concentrations should alter the crosslinking reaction and hence the partial conversion properties. Increasing the monomer concentrations, in particular the PEF concentration, should increase the probability of intermolecular crosslinking.

This change in the crosslinking mechanism should also be shown by a variation in the partial conversion viscosity,  $[\bar{\eta}]$ , which is given by eq. (2):

$$[\bar{\eta}] = [\eta] + W(d[\eta]/dW) \quad (2)$$

where  $W$  is the weight conversion of polymer and  $[\eta]$  is the intrinsic viscosity. Since  $\bar{M}_n < \bar{M}_v < \bar{M}_w$ , then the partial conversion viscosity should be a more sensitive guide to the synthesis of large polymeric networks than the partial conversion number-average molecular weight, since this latter quantity is biased in favor of the smaller molecules.

In this present paper we have studied the effect of varying the monomer concentrations in the PEF-styrene copolymerization in order to determine, using partial conversion parameters, the changes in the crosslinking mechanism.

## EXPERIMENTAL

The experimental techniques and the preparation and purification of reagents are described in previous publications.<sup>2,3</sup> The course of reaction was followed by sample analysis during the polymerization. Conversions were measured by copolymer analysis (chemical and infrared). Molecular weights were measured in dioxane solution by using osmometry,<sup>4</sup> ebulliometry,<sup>5</sup> and viscometry. Viscosity measurements were conducted at 25°C. in a suspended-level Ubbelohde viscometer.

## RESULTS

Copolymerization reactions were carried out under nitrogen at 60°C. in dioxane with benzoyl peroxide as initiator ( $1.4 \times 10^{-6}$  g.-mole/l.). Since the transfer constant to solvent is very small for the radicals present,<sup>6</sup> transfer effects are negligible. The monomer feed ratios and PEF concentrations for the polymerization runs are listed in Table I. The number-average molecular weight of the initial polyester used in these experiments was 1940, as measured in dioxane.

### Partial Conversion Number-Average Molecular Weights

The plots of number-average molecular weight as a function of conversion are given in Figure 1 and in Figure 2, the corresponding plots of the partial conversion parameter. The data for the graphs are shown in Table I.



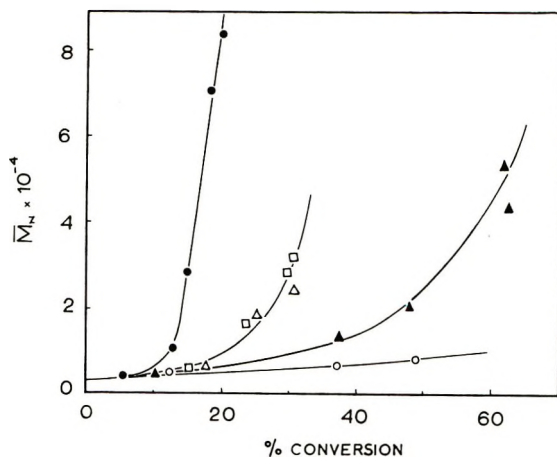


Fig. 1. Effect of monomer concentration on the number-average molecular weight ( $\bar{M}_n$ )-total monomer conversion plot: (O) run 11; ( $\blacktriangle$ ) run 26; ( $\square$ ) run 29, ( $\triangle$ ) run 27, ( $\bullet$ ) run 28.

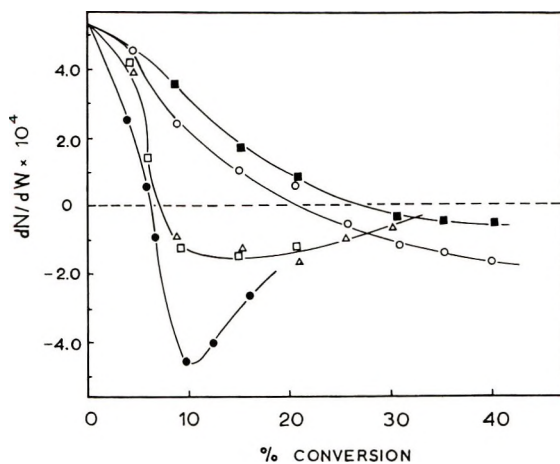


Fig. 2. Partial conversion number-average molecular weight ( $dN/dW = 1/\bar{M}_n$ ) as a function of total monomer conversion: ( $\blacksquare$ ) run 11; (O) run 26; ( $\triangle$ ) run 27; ( $\square$ ) run 29; ( $\bullet$ ) run 28.

### Partial Conversion Viscosities

The variations of the intrinsic viscosity with conversion are shown in Figure 3, and the corresponding partial conversion viscosities calculated from eq. (2) are shown in Figure 4. The relevant results are in Table I.

### DISCUSSION

The results in Figure 1 illustrate the effect of initial monomer concentration on the  $\bar{M}_n$  of the polymer produced at a given conversion. These would suggest that as the initial monomer concentration increases larger

TABLE I  
 Partial Conversion Results for the Copolymerization of Styrene with PEF<sup>a</sup>

Run no.	[PEF], mole/l.	[S], mole/l.	W, %	$\bar{M}_n$	$[\eta]$	$d\bar{M}_n/dW$	$d[\eta]/dW$	$\bar{M}_n \times 10^{-4}$	$[\eta]$
11	0.1231	0.1164	10	2,000	0.080	50	0.0002	0.27	0.082
			20	2,500		110		2.08	
			30	4,200	0.088	160	0.0008	-2.13	0.112
			40	6,000	0.100	200	0.0016	-1.79	0.164
			50		0.120		0.0025		0.245
26	0.2450	0.0750	10	2,200	0.080	110	0.0002	0.44	0.082
			15	2,800		130		0.93	
			20	3,500		150		2.44	
			25	4,500	0.093	240	0.0011	-1.35	0.121
			35	8,000	0.106	500	0.0016	-0.67	0.162
			40	11,000		700		-0.71	
			45		0.126		0.0026		0.243
65		0.206		0.0056		0.570			
70		0.235		0.0064		0.683			

27	0.2880	0.4580	5	2,000	0.085	100	0.0013	0.28	0.098
			10	2,500	0.105	300	0.0035	-1.23	0.175
			20	8,000	0.125	1,000	0.0060	-0.53	0.275
			25	14,000	0.165	1,500	0.0240	-0.83	0.885
			30	23,000	0.102	2,400	0.0050	-1.08	0.127
28	0.3741	0.5945	5	2,200	0.130	200	0.0065	0.41	0.195
			7	2,800	0.166	350	0.0094	2.28	0.307
			10	4,400	0.270	1,300		-0.25	
			15						
			16	24,000		10,500		-0.40	
			22				0.0290		0.974
			5	2,000		100		0.28	
29	0.3750	0.1455	7	2,300	0.095	250	0.0028	0.96	0.123
			10	3,000	0.110	400	0.0030	-0.90	0.155
			15	6,000	0.125	750	0.0040	-0.69	0.205
			20	10,500	0.150	1,200	0.0065	-0.78	0.313
			25		0.190		0.0140		0.610
			30						

\* Solvent, dioxane; temperature, 60°C.; benzoyl peroxide,  $1.4 \times 10^{-6}$  g.-mole/l.

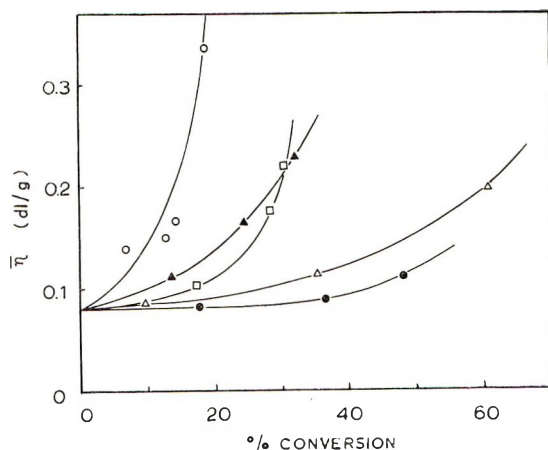


Fig. 3. Effect of monomer concentration on the intrinsic viscosity  $[\eta]$ -total monomer conversion plot: (●) run 11; (△) run 26; (□) run 29; (▲) run 27; (○) run 28.

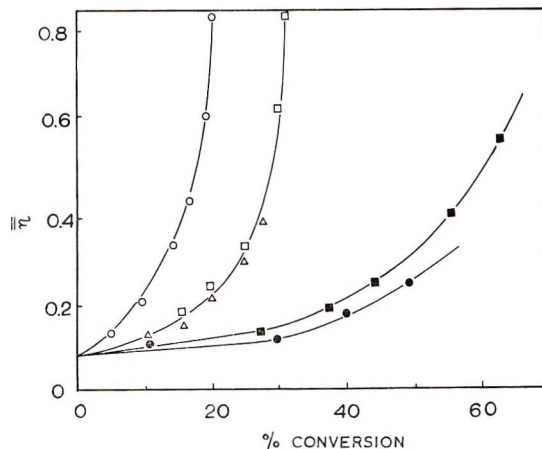


Fig. 4. Partial conversion intrinsic viscosity  $[\bar{\eta}]$  as a function of total monomer conversion: (●) run 11; (■) run 26; (△) run 27; (□) run 29; (○) run 28.

molecular species are being formed. This is particularly true for an increase in the PEF concentration, e.g., compare runs 27, 28, and 29. The partial conversion plots in Figure 2 indicate that the  $dN/dW$  values are also lowest for those systems in which the PEF concentration is the highest. Also, the rate of decrease of  $dN/dW$  with conversion is greatest for these runs. These results are indicative of an increase in the intermolecular crosslinking reaction as the monomer concentration increases. Gelation occurred in run 28 after approximately 25% conversion, accounting for the very rapid increase in  $\bar{M}_n$  in Figure 1. The crosslinked molecules formed in the other runs remained soluble up to much higher conversions and in the most dilute runs (runs 11 and 26) no gelation took place. A comparison of the results for run 27 and run 28, where the initial monomer feed

ratios are the same, reveals that the  $\bar{M}_n$ -conversion plots are affected by solvent dilution. The difference is probably due to increased intramolecular crosslinking in run 27 where the overall monomer concentration is less. Figures 3 and 4 show the intrinsic viscosity and partial conversion viscosity results as a function of conversion for the same systems given in Figures 1 and 2. The two sets of results are closely parallel and give the same conclusions. In run 28 in which gelation occurred at very low conversion there is a very rapid rise in the value of  $[\eta]$  prior to gelation. This indicates the formation of very large polymeric species and substantiates the rapid decrease observed in the  $dN/dW$ -conversion curve for the same run. In run 11 the partial conversion viscosity shows little change with conversion, indicative of intra- rather than intermolecular crosslinking. A similar conclusion can be drawn from the corresponding curve in Figure 2. Again, runs 27 and 28, with the same monomer feed ratio, display different conversion dependence on molecular weight (in this case the viscosity-average molecular weight). The decreased intrinsic viscosities in run 27 reflect the increased intramolecular reaction. The similar conclusions drawn from the partial conversion viscosity and number-average molecular weight data demonstrate clearly the effect of dilution on the reaction kinetics. Intramolecular reactions are favored at higher dilution, as shown by a reduced dependence of  $\bar{M}_n$  and  $[\eta]$  on conversion. Increasing the monomer concentration, and in particular the PEF concentration, increases the importance of intermolecular processes and produces a much greater dependence of  $\bar{M}_n$  and  $[\eta]$  on conversion. This increase in the intermolecular reaction at higher monomer concentrations is in agreement with the data from a previous publication.<sup>4</sup> The reactivity ratios for the PEF-styrene copolymerization were found to be dependent on the PEF concentration, and this dependence was attributed to the relative importance of intramolecular or cyclization reactions as the system is diluted. On increasing the monomer concentrations the measured reactivity ratios approached the values found for the diethyl fumarate-styrene copolymerization which may be considered as an intermolecular reaction. In conclusion, it should be pointed out that the variation of the partial conversion parameters with solvent dilution for the PEF-styrene system may be somewhat fortuitous. The intramolecular crosslinking reaction is favored by the alternating tendency in this copolymerization, i.e., the radicals produced will attack the opposite monomer species. Since this is the case, the magnitude of the differences in this particular system may not be observed in other crosslinking copolymerizations.

### References

1. F. T. Wall, *J. Am. Chem. Soc.*, **67**, 1929 (1945), and the following papers in this series.
2. G. M. Burnett, J. N. Hay, and J. D. B. Smith, *J. Polymer Sci. A*, **2**, 5111 (1964).
3. G. M. Burnett, J. N. Hay, and J. D. B. Smith, paper presented at Symposium on Chemistry of Polymerization Processes, Society of Chemical Industry, London, April 1965.

4. G. M. Burnett, J. M. Pearson, and J. D. B. Smith, paper presented at I.U.P.A.C. Symposium on Macromolecular Chemistry, Prague, 1965; *J. Polymer Sci. C*, in press.

5. R. S. Lehrle and T. G. Majury, *J. Polymer Sci.*, **29**, 219 (1958).

6. R. A. Gregg and F. R. Mayo, *J. Am. Chem. Soc.*, **75**, 3530 (1953).

### Résumé

Le mécanisme de la réaction de pontage en cours de copolymérisation du fumarate de polyéthylène et du styrène a été étudié, utilisant des poids moléculaires moyens en nombre et des viscosités à des degrés de conversion partiels. En solution diluée, la réaction consiste principalement dans la formation de ponts intramoléculaires ce qui est illustré par une dépendance réduite de  $\bar{M}_n$  et de  $[\eta]$  en fonction du degré de conversion. Un accroissement de concentration en monomère augmente la contribution de réactions intermoléculaires et fournit une dépendance plus grande de  $\bar{M}_n$  et de  $[\eta]$  en fonction du degré de conversion.

### Zusammenfassung

Der Mechanismus der Vernetzungsreaktion bei der Kopolymerisation von Poly(äthylenfumarat) und Styrol wurde mittels der Zahlenmittelwerte der Molekulargewichte und der Viskositäten bei partiellem Umsatz untersucht. In verdünnter Lösung besteht die Hauptreaktion in einer Bildung intramolekularer Vernetzungen, was sich in einer schwächeren Abhängigkeit von  $\bar{M}_n$  und  $[\eta]$  vom Umsatz widerspiegelt. Eine Erhöhung der Monomerkonzentrationen steigert den Beitrag der intermolekularen Reaktionen und liefert eine viel stärkere Abhängigkeit von  $\bar{M}_n$  und  $[\eta]$  vom Umsatz.

Received March 16, 1966

Prod. No. 5125A

## Kinetics of Urethane Cleavage in Crosslinked Polyurethanes

AJAIB SINGH and LEONARD WEISSBEIN, *Research Laboratories, American Cyanamid Company, Bound Brook, New Jersey 08805*

### Synopsis

A series of clean, well-defined polyurethane networks was synthesized from polyester glycols, 2,4-tolylene diisocyanate, and 1,1,1"-trimethylolpropane by means that afforded precise control over the content of urethane groups per network chain. The thermal cleavage of these networks was studied using the technique of stress relaxation. Analysis of the stress-relaxation data on each network structure revealed two exponential decay processes differing in rate by about an order of magnitude. The rate of the slower process, which dominates the overall stress decay, was shown to be directly dependent on the content of urethane groups per network chain. Positive identification of this process with urethane cleavage was thereby established. The kinetic and thermodynamic constants associated with urethane cleavage were then calculated from data on this process at different temperatures. The more transient stress-decay process was not uniquely definable, but probably originated from the cleavage of one or more types of weak linkages found in small but variable proportions in the different polyurethane networks. The nature and origin of these weak linkages was discussed.

### INTRODUCTION

Various attempts<sup>1-8</sup> have been made to study the kinetics of thermal degradation of polyurethane elastomers from measurements of stress relaxation rates. Those measurements were made on chemically cross-linked elastomers in the temperature range of 100-180°C. The data obtained were originally interpreted on the basis of a simple Maxwell model<sup>1-5</sup> expressed as

$$E_r(t) = E_r(0) \exp \left\{ - t/\tau \right\} \quad (1)$$

where  $E_r(0)$  and  $E_r(t)$  are, respectively, the initial relaxation modulus and that measured after relaxation time  $t$  at constant sample extension and temperature, and  $\tau$  is the measured relaxation time constant. An attempt was then made to calculate the specific rate constant  $k$  for urethane cleavage by using the relationship<sup>3</sup>

$$1/\tau = km \quad (2)$$

where  $m$  is the number of urethane linkages per network chain.

However, because of synthesis difficulties, the network structure of the polyurethane elastomers used in those studies was not sufficiently defined

to yield a precise knowledge of  $m$ . Furthermore, it was later pointed out that the chemical stress decay data obtained thus far on polyurethane elastomers are more closely approximated by a multi-Maxwell model<sup>6-8</sup>

$$E_r(t) = \sum_{i=1,2,\dots} E_{r_i}(0) \exp \{ -t/\tau_i \} \quad (3)$$

involving two and sometimes three exponential terms. Convincing evidence that the processes represented by these exponential terms are all chemical in origin<sup>6</sup> led to the present concept of the stress-decay behavior of polyurethanes as a manifestation of simultaneous network cleavage processes involving different types of linkages. A theoretical treatment of this concept was presented by Tobolsky et al.<sup>7,8</sup> It was speculated that the slower network cleavage process involves the urethane linkage, whereas the faster one (or ones) is associated with weaker type linkages, e.g., allophanate, biuret, mixed anhydrides, etc., that are inadvertently formed when the elastomers are fabricated.

Further elucidation of the kinetics of urethane cleavage through stress relaxation awaited the synthesis of clean, well-defined polyurethane networks for which the number  $m$  of urethane linkages per network chain would be known precisely and could be varied uniquely.

The objectives of this study were (1) to synthesize such networks, (2) to identify their chemical stress-relaxation rates with urethane cleavage, and (3) to determine the kinetic and thermodynamic parameters associated with this process.

## DISCUSSION OF RESULTS

To achieve the aforementioned objectives, a technique for synthesizing model NCO-terminated urethane prepolymers from diisocyanates and polyester glycols was developed. Model prepolymers made by this technique are devoid of allophanate branching and free diisocyanate and have a structure consisting of one polyester glycol molecule capped on either end by a diisocyanate molecule.

This technique was used to synthesize a series of model prepolymers P-1, P-2, and P-3 from 2,4-tolylene diisocyanate (2,4-TDI) and polyethyleneadipate glycols (PEAG) with  $\bar{M}_n$  values ranging from 1250 to 3620. A prepolymer P-4 was prepared from the same ingredients that were used in making P-1. However, in preparing P-4, the mole ratio of 2,4-TDI to PEAG was modified to promote its chain extension. Pertinent descriptive data on the prepolymers P-1 through P-4 are listed in Table I. Also included in Table I are data on a model prepolymer P-5 made with poly(butyleneadipate glycol) (PBAG) with  $\bar{M}_n = 1010$ .

Reaction of the prepolymers with an equivalent of 1,4-butanediol (BDO) produced elastomers that were linear, as indicated by their chloroform solubility and complete thermoplasticity when heated to 100°C. These results showed that the prepolymers were essentially free from allophanate branching, and that allophanate formation did not occur to any appreciable



TABLE I  
Model Prepolymers Based on 2,4-TDI and Polyester Glycols

Pre-polymer	PEG	$\bar{M}_n$ of PEG <sup>a</sup>	Acid no. of PEG	Charge ratio PEG/TDI	Viscosity of prepolymer, cp <sup>b</sup>	Isocyanate equivalent of prepolymer	
						Theoretical <sup>c</sup>	Observed
P-1	PEAG <sup>d</sup>	1250	0.20	0.33	1404	799	785
P-2	PEAG	2060	0.99	0.33	2649	1155	1195
P-3	PEAG	3620	0.69	0.33	7523	1984	2050
P-4	PEAG	1250	0.20	0.57	5245	799	1160
P-5	PBAG <sup>e</sup>	1010	0.60	0.33	1390	679	680

<sup>a</sup> As measured on dehydrated polymer.

<sup>b</sup> Viscosity measured at 70°C.

<sup>c</sup> Calculated on basis of one polyester glycol molecule condensed with two TDI molecules.

<sup>d</sup> Polyethyleneadipate glycol.

<sup>e</sup> Polybutyleneadipate glycol.

extent under the conditions used in reacting the prepolymers with diol. Similar observations were reported for certain polyurethanes prepared by Colodny and Tobolsky.<sup>2</sup> These results also suggested that reaction of the prepolymers with a triol under the same conditions would yield crosslinked elastomers similarly free of allophanate branch points.

The excellent agreement between the measured NCO equivalents of P-1, P-2, P-3, and P-5 and the values expected from theory (see Table I) confirmed that these prepolymers were the desired capped polyesters with structures generally represented by I. The isocyanate equivalent, i.e., the equivalent weight of prepolymer based on its isocyanate content, was determined by following the general method for isocyanate analysis described in the literature.<sup>9</sup>



The high viscosity and high NCO equivalent of prepolymer P-4 relative to P-1 were indications that some chain extension had occurred during the preparation of P-4.

Prepolymers P-1, P-2, P-3, and P-5 were reacted with the equivalent of 1,1',1''-trimethylolpropane (TMP) to form crosslinked elastomers E-1, E-2, E-3, and E-5 consisting of well-defined and highly uniform networks containing exactly four urethane linkages per network chain. Reaction of P-4 with an equivalent of TMP produced elastomer E-4 composed of network chains containing more than four urethane linkages on the average.

If the elastomer networks were free from extraneous weak linkages and if then the urethane linkages were the only thermally cleavable ones, the

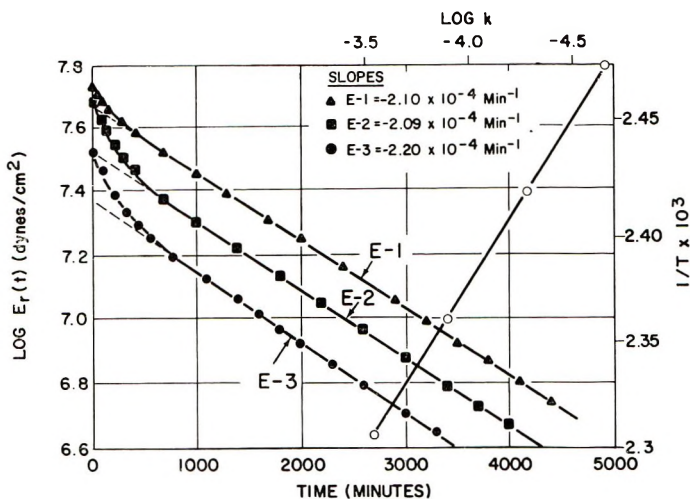


Fig. 1. Stress-relaxation plots of elastomers E-1, E-2, and E-3 at 150°C.

chemical stress-decay behavior of these elastomers should be governed by the simple exponential rate expression:

$$E_r(t) = E_r(0) \exp \{ -kmt \} \quad (4)$$

In that case, semilogarithmic plots,  $\log E_r(t)$  versus  $t$ , of the stress-decay rate data for these elastomers should be linear with slopes equal to  $-km/2.3$ . According to the theoretical considerations of Tobolsky and Peterson,<sup>3</sup> one would expect the slopes of the stress-decay plots of elastomers E-1, E-2, E-3 to be equivalent, since their network structures are all chemically similar and their network chains all contain exactly four urethane groups ( $m = 4$ ). One would further expect the slope of the plot for elastomer E-4 to be steeper than the others, for the average number of urethane groups per network chain in this elastomer is greater than four.

Consistency of the experimental results with these predictions would unequivocally identify the stress-decay behavior of these elastomers with urethane cleavage. In that event, the specific rate constant  $k$  and thermodynamic constants associated with the urethane cleavage process could be determined from stress-decay rate data obtained with elastomers E-1, E-2, E-3, or E-5 at different temperatures in the range of interest. It should be mentioned in this connection that two of the four urethane groups contained in each network chain of these elastomers were joined to the 2-position of the TDI ring, the other two being joined to the 4-position. The cleavage rates of these two types of urethane linkages are probably different but of similar magnitude, in which case the  $k$  values obtained would be the average of the specific rate constants for both types of linkages.

Stress relaxation data on elastomers E-1 through E-5 were taken at various temperatures in the range of 130–160°C. and plotted as  $\log E_r(t)$  versus  $t$ . Plots of the data taken at 150°C. are presented in Figures 1 and

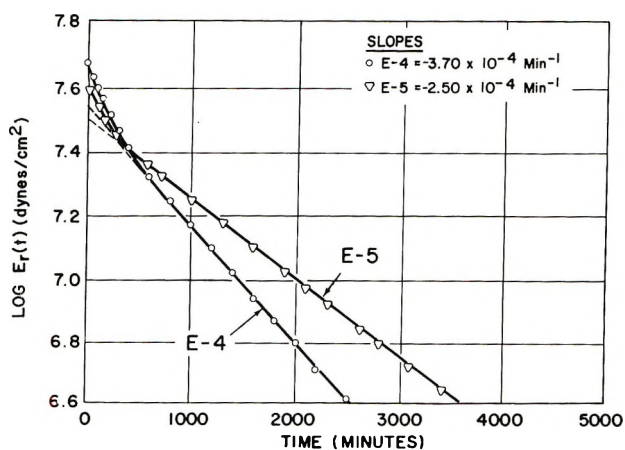


Fig. 2. Stress-relaxation plots of elastomers E-4 and E-5 at 150°C.

2. The curves shown are typical in form of those drawn from data taken at the other temperatures. They are essentially linear, although some initial deviation from linearity is evident in all cases.

Graphic analysis by a procedure described previously<sup>6-8</sup> showed that the data taken at the various temperatures conformed extremely well to the two-component Maxwell model:

$$E_r(t) = E_{r_1}(0) \exp \left\{ -t/\tau_1 \right\} + E_{r_2}(0) \exp \left\{ -t/\tau_2 \right\} \quad (5)$$

with  $E_{r_1}(0) + E_{r_2}(0) = E_r(0)$  at  $t = 0$  and  $\tau_1 > \tau_2$ .

The linear part of the  $\log E_r(t)$  versus  $t$  curves (extrapolated to zero time) is represented by the first exponential term of this model with the second exponential term accounting for the initial nonlinearity. The nature and origin of the transient stress-decay process responsible for this nonlinearity will be discussed later.

It is apparent from Figures 1 and 2 that the slopes of the linear parts of the stress-decay curves of elastomers E-1, E-2, and E-3 for which  $m = 4$  are all equivalent, whereas that of elastomer E-4 for which  $m > 4$  is steeper than others. The consistency of these experimental results with earlier predictions unequivocally establishes the identity of the linear part of these stress-decay curves with urethane cleavage, thereby enabling one to equate  $1/\tau_1$  of eq. (5) with  $km$  of eq. (4).

Whereas elastomers E-1, E-2, and E-3 were made to contain the same number of urethane linkages per network chain, the concentration of urethane linkages per unit network volume was varied in this series by almost three-fold through the use of polyester glycols of different chain lengths in the prepolymer preparation step. It is evident from the data of Figure 1 that the stress-decay rate associated with urethane cleavage is independent of the concentration of urethane linkages per unit network volume. This observation, together with the apparent linearity of the part of the stress-

TABLE II  
Kinetic and Thermodynamic Constants for Thermal Cleavage of Urethanes Based on 2,4-TDI

Elastomer	$k \times 10^6, \text{min.}^{-1}$				$\Delta E^\ddagger,$ kcal./mole	$\Delta S^\ddagger,$ e.u./mole
	130°C.	140°C.	150°C.	160°C.		
E-1	2.14	5.17	12.10	28.10	$29.60 \pm 1$	$-17.10 \pm 2$
E-2	2.08	4.50	12.10	28.40		
E-3	2.05	4.50	12.70	29.30		
Mean values	2.09	4.73	12.30	28.60		
E-5			14.40			

decay curves associated with urethane cleavage, suggests that the urethane cleavage reaction follows an apparent first-order rate law.

Values of  $k$  at various temperatures were calculated from the slopes of the rate curves of elastomers E-1, E-2, and E-3 for which  $m = 4$ . The individual  $k$  values and their mean value at each temperature are listed in Table II. An Arrhenius plot of these data, from which the energy and entropy of activation associated with the urethane cleavage process were calculated, is shown in Figure 1. The energy and entropy of activation are given in Table II.

Also given in Table II is the  $k$  value (at 150°C.) for elastomer E-5, which was made with PBAG in place of PEAG. The similarity of this rate constant to that of elastomers E-1, E-2, or E-3 at the same temperature indicates that the thermal stability of the urethane linkage is not strongly dependent on the polyester glycol moiety from which it is derived.

According to eq. (5), the transient process  $E_{r2}(0) \exp \{-t/\tau_2\}$ , which is responsible for the initial nonlinearity of the polyurethane stress-decay curves, can be isolated from these curves by plotting  $\log [E_r(t) - E_{r1}(0) \exp \{-t/\tau_1\}]$  versus relaxation time. Those plots would be linear with

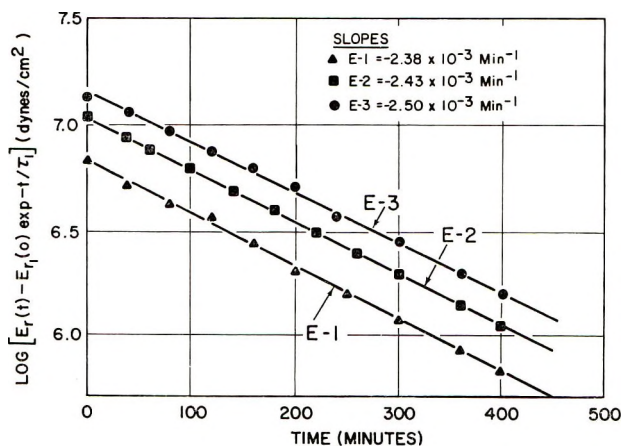


Fig. 3. Plots of transient stress decay at 150°C.

slopes equal to  $-1/(2.3\tau_2)$  and intercepts equal to  $\log E_{\tau_2}(0)$ . Such plots of data taken from the curves of Figure 1 are presented in Figure 3. A comparison of the slopes of these lines with the slopes of the lines in Figure 1 shows that  $\tau_1 = 11\tau_2$  at  $150^\circ\text{C}$ .

The similarity in slope of the lines in Figure 3 was fortuitous, since this similarity was not observed with data taken at other temperatures. In fact, the activation energies associated with  $\tau_2$  for elastomers E-1, E-2, and E-3 in the  $130\text{--}160^\circ\text{C}$ . temperature range varied from 19 to 28 kcal./mole. It would appear, then, that this transient stress-decay process is not uniquely definable, but probably originates from the cleavage of one or more types of weak linkages formed in small but variable proportions in the different polyurethane networks.

The most probable sources of weak linkages would be the free acid endgroups of the polyester glycols (see Table I for their acid numbers) and traces of moisture. The former would react with free NCO groups to form substituted urea and mixed anhydride linkages, whereas the latter would react to form substituted urea and biuret linkages.<sup>10</sup> Other possibilities that cannot be overlooked are allophanate branch points that might have been formed in small quantities upon reaction of the prepolymers with triol and occasional weak links of an unknown nature that might have been present in the polyester glycol chains themselves.

### Model Prepolymers

The formation of NCO-terminated urethane prepolymers via the condensation of polyester glycols with excess diisocyanate is usually attended by allophanate branching. In synthesizing suitable model prepolymers, it was found that allophanate branching, through the reaction of free NCO with urethane groups, can be prevented by maintaining the reaction temperature at or below  $50^\circ\text{C}$ .

The prepolymer formation is also complicated by the tendency of the prepolymer to undergo chain extension by condensing with unreacted polyester glycol. The species of larger molecular size thus formed can further react to form species of still larger molecular size. At complete reaction, the reaction mixture would, therefore, contain a distribution of NCO . . . terminated species of different molecular sizes, including the free diisocyanate, which is in excess.

Flory<sup>11</sup> derived an expression that shows how the molecular size distribution at completion of a linear condensation reaction would vary with changes in the mole ratio of the two reactant monomers involved. Taking the polyester glycol to be one of the reactant monomers and the diisocyanate to be the other (which is present in excess) Flory's expression becomes

$$P_x(\text{NCO}) = r^{(x-1)/2}(1-r) \quad \begin{array}{l} x = 1,3,5, \dots \\ r < 1 \end{array} \quad (6)$$

where  $P_x(\text{NCO})$  is the mole fraction of each (NCO terminated)  $x$ -mer species present at complete reaction, with  $x$  (an odd integer) representing the total number of polyester glycol and diisocyanate molecules combined in the polymer species. The parameter  $r$  is the mole ratio of polyester glycol to diisocyanate charged in the reactor. According to eq. (6), the mole fraction of any  $x$ -mer species present at complete reaction is  $1/r$  times greater than that of the next higher  $x$ -mer specie. This relationship suggests that chain extension of the prepolymer (trimer) tends to be suppressed as  $r$  is minimized. It also suggests that complete suppression of chain extension would require an impractically large (virtually infinite) excess of diisocyanate.

Fortunately, however, this equation was derived on the assumption of equal reactivity of all functional groups of each kind, irrespective of the size of the molecule to which they are joined. With an asymmetric, aromatic diisocyanate such as 2,4-TDI the two NCO groups are of unequal reactivity. Moreover, the reactivity of either NCO group is decreased upon reaction of the other. In an involved theoretical treatment, Di Giacomo<sup>12</sup> predicted that the molecular size distribution resulting from the complete condensation of a glycol with excess, 2,4-TDI would be skewed toward the desired prepolymer (trimer) species for all values of  $r < 1$ . In that case, a relatively small excess of the diisocyanate would be required to suppress chain extension to the desired extent. Because of the unequal reactivity of the NCO groups, the dropwise addition of polyester glycol to the 2,4-TDI would further tend to favor the formation of the trimer over higher  $x$ -mer species.

These predictions were substantiated by experimental results of this study, where it was found that the dropwise addition of one mole of polyester glycol to three moles of 2,4-TDI gave, at complete reaction, a mixture composed essentially of the trimer and free 2,4-TDI. As a consequence of the estimated five- to sixfold difference in reactivity between the free NCO groups of this diisocyanate,<sup>12</sup> the predominant structure of the trimer would be that shown above as I.

Complete removal of free diisocyanate from the prepolymer was accomplished by means of continuous liquid/liquid extraction with the use of  $n$ -hexane as the extraction solvent. The procedure used is a modification of one that had been disclosed previously.<sup>13</sup> The polymerization reactors were so designed that they could be readily converted into continuous liquid/liquid extractors without danger of exposing the reaction mixture to atmospheric moisture. Details of the prepolymer preparation and other experimental procedures follow.

## EXPERIMENTAL

### Materials

The poly(ethyleneadipate glycols) of  $\bar{M}_n$  1250 and 2060 and the poly(butyleneadipate glycol) ( $\bar{M}_n$  1010) were purchased from the Witco Chem-

ical Company and were dehydrated for 4 hr. at 135°C./1 mm. before being used. The poly(ethyleneadipate glycol) ( $\bar{M}_n$  3620) was prepared by transesterification of the polyester glycol of  $\bar{M}_n$  2060. The 2,4-tolylenediisocyanate was purchased from E. I. du Pont de Nemours and contained over 94% 2,4-isomer. It was used as received without further purification. The 1,1',1''-trimethylolpropane (Celanese Chemical Company) was vacuum-dried overnight at 50°C./1 mm. before it was used.

### Prepolymer Preparation

Prepolymers P-1, P-2, P-3, and P-5 were all prepared under identical conditions. In each preparation, 1 mole of polyester glycol was added dropwise to 3 moles of 2,4-TDI over a period of 5-6 hr. The resulting reaction was allowed to proceed, under a dry nitrogen blanket, until the isocyanate content of the reaction mixture decreased to a precalculated value, which was based upon the complete capping of the polyester glycol. During the reagent addition and reaction periods, the reaction mixture was maintained at 50°C. and stirred continuously. Upon completion of the capping reaction, the resulting prepolymer was quantitatively stripped of excess 2,4-TDI by continuous liquid/liquid extraction with dry *n*-hexane as the extraction solvent. After stripping, the prepolymer was placed in a vacuum oven at 50°C. to flash off the hexane.

In preparing prepolymer P-4, 1 mole of the polyester glycol was added to 1.75 mole of 2,4-TDI. In all other respects, the preparation procedure was the same as that described above.

### Polyurethane Sample Preparation

Equivalent amounts (based on the isocyanate content of the prepolymer) 1,1',1''-trimethylolpropane and 0.5% (based on the weight of the prepolymer) of *N*-ethylmorpholine were blended into the prepolymers, which had been preheated to 100°C. The resulting mixtures were fabricated into 75-mil sheets by pressure-molding at 100°C. for 16 hr.

The polyurethane sheets were die-cut into 2 × 0.25 in. strips for stress-relaxation measurement.

These strip samples were Soxhlet-extracted for 24 hr. in hot tetrahydrofuran (THF) to remove the *N*-ethylmorpholine catalyst and any other THF-extractable impurities that might have been present. (Further THF extraction was found previously to have no measurable effect on the stress-relaxation rates.) The extracted samples were then deswelled and freed of THF in a warm vacuum oven.

### Stress-Relaxation Measurements

The stress-relaxation experiments were performed on a six-channel autographic relaxometer described previously.<sup>6</sup> The stress-relaxation measurements were made at a constant sample extension of  $10 \pm 0.05\%$ . The

experimental temperatures were 130, 140, 150, and 160°C., and they were maintained to within  $\pm 0.2^\circ\text{C}$ . during each experimental run.

The authors are grateful to Drs. G. Mino and S. Kaizerman for helpful discussions. Special thanks are due Mr. J. C. Mollica for his valuable experimental assistance in carrying out the measurements and in developing suitable experimental procedures.

### References

1. J. A. Offenbach and A. V. Tobolsky, *J. Colloid Sci.*, **11**, 39 (1956).
2. P. C. Colodny and A. V. Tobolsky, *J. Am. Chem. Soc.*, **79**, 4320 (1957).
3. A. V. Tobolsky and E. Peterson, *J. Phys. Chem.*, **67**, 930 (1963).
4. A. V. Tobolsky, H. Yu, and R. Thach, *J. Appl. Polymer Sci.*, **6**, 544 (1962).
5. A. V. Tobolsky, *Properties and Structure of Polymers*, Wiley, New York, 1960, Chap. 5.
6. A. Singh and L. Weissbein, *J. Polymer Sci. A*, **3**, 1675 (1965).
7. A. V. Tobolsky, V. Johnson, and W. J. MacKnight, *J. Phys. Chem.*, **69**, 476 (1965).
8. A. V. Tobolsky, *J. Polymer Sci. B*, **2**, 823 (1964).
9. B. A. Dombrow, *Polyurethanes*, Reinhold, New York, pp. 216-218.
10. J. H. Saunders and K. C. Frisch, *Polyurethane Chemistry and Technology*, Part I, Interscience, New York, 1962, pp. 69-71.
11. P. J. Flory, *J. Am. Chem. Soc.*, **58**, 1877 (1936).
12. A. Di Giacomo, *J. Polymer Sci.*, **47**, 435 (1960).
13. W. R. McElory, U. S. Pat. 2,969,386 (1961).

### Résumé

Une série de réseaux polyuréthaniques bien définis, a été synthétisée au départ de 2,4-diisocyanate de tolylène et de 1,1',1"-triméthylolpropane de telle sorte que l'on ait un contrôle précis de la teneur des groupes uréthaniques par chaîne réticulaire. La scission thermique de ces réseaux a été étudiée avec la technique de relaxation sous tension. L'analyse des résultats de relaxation tension de structures réticulées a montré l'existence de deux processus exponentiels de disparition, différents de vitesse d'environ un ordre de grandeur. La vitesse du processus plus lent qui domine le processus global de disparition de tension était directement fonction de la teneur en groupes uréthaniques par chaîne du réseau. Une identification de ce processus par rupture du lien uréthanique a été ainsi établie. Les constantes cinétiques et thermodynamiques associées à la rupture du lien uréthanique ont été calculées au départ des résultats de ce processus à différentes températures. Le processus plus rapide de disparition de la tension n'était pas aussi facile à définir, mais probablement trouve son origine dans la rupture d'un ou plusieurs types de liaisons faibles trouvées en petites, mais proportions variables, dans les réseaux polyuréthaniques. La nature et l'origine de ces liens faibles sont soumises à discussion.

### Zusammenfassung

Eine Reihe sauberer, gut definierter Polyurethannetzwerke wurde aus Polyester glykolen, 2,4-Tolylendiisocyanat und 1,1',1"-Trimethylolpropan derartig synthetisiert, dass eine genaue Kontrolle des Gehalts an Urethangruppen pro Netzketten möglich war. Die thermische Spaltung dieser Netzwerke wurde mittels der Spannungsrelaxationsmethode untersucht. Die Analyse der Spannungsrelaxationsdaten für jede der Netzwerkstrukturen liess zwei exponentielle Abklingprozesse erkennen, deren Geschwindigkeit sich etwa um eine Grössenordnung unterschied. Die Geschwindigkeit des langsameren, für den gesamten Spannungsabfall ausschlaggebenden Prozesses zeigt eine direkte Abhängigkeit von Gehalt an Urethangruppen pro Netzketten. Dadurch konnte dieser Prozess mit einer



Urethanspaltung identifiziert werden. Die kinetischen und thermodynamischen Konstanten für die Urethanspaltung wurden aus den auf diesen Prozess bezüglichen Daten bei verschiedenen Temperaturen berechnet. Der rascher verlaufende Spannungsabklingvorgang konnte nicht eindeutig definiert werden, kam aber wahrscheinlich durch die Spaltung von schwachen, in kleiner, aber variabler Menge in den verschiedenen Polyurethannetzwerken auftretenden Bindungen zu Stande. Die Natur und der Ursprung dieser schwachen Bindungen wurden diskutiert.

Received January 26, 1966

Revised March 28, 1966

Prod. No. 5126A

## Costereosymmetric $\alpha$ -Olefin Copolymers\*

H. W. COOVER, JR., RICHARD L. McCONNELL, F. B. JOYNER,  
D. F. SLONAKER, and R. L. COMBS, *Research Laboratories,  
Tennessee Eastman Company, Division of Eastman Kodak Company,  
Kingsport, Tennessee*

### Synopsis

Copolymerization of propylene and 1-butene with highly stereospecific three-component coordination catalysts produced multiblock crystalline copolymers having stereoregular sequences of both propylene and 1-butene. Copolymers containing from 3 to about 80% 1-butene had two DTA melting points which were attributable to polypropylene and poly-1-butene crystallinity. Those containing from 18 to about 70% 1-butene had x-ray diffraction patterns showing peaks characteristic of polypropylene and form I poly-1-butene, but form II poly-1-butene crystallinity was never observed. The multiblock copolymer structure observed is also supported by the fact that the product of the reactivity ratios is greater than unity. The composition distributions of low-conversion and continuously prepared copolymers were similar and relatively broad. For example, copolymers containing an average of 12% 1-butene had species containing from 5-30% 1-butene. High-conversion copolymers had an even broader composition distribution due to the gradual increase of the 1-butene concentration in the comonomer mixture as the copolymerization proceeded. The absence of homopolymers was demonstrated by fractionation. The ability to detect homopolymers was proved by the fact that a mixture of stereoregular polypropylene and poly-1-butene were readily separated. Increasing the amount of 1-butene tended to decrease those properties dependent upon crystallinity such as hardness, tensile strength, stiffness, density, and melting point, but tended to improve significantly the impact strength, low temperature properties, and clarity of molded objects. These duocrystalline copolymers retained a much higher level of properties than that observed for random copolymers prepared with less stereospecific coordination catalysts.

Three-component coordination catalysts containing alkylaluminum halides such as ethylaluminum dichloride or ethylaluminum sesquichloride in combination with hexamethylphosphoric triamide (HPT) and violet titanium(III) chloride are highly stereospecific for the homopolymerization of  $\alpha$ -olefins.<sup>1-3</sup> It was of interest, therefore, to determine the influence of these catalysts on the copolymerization behavior of  $\alpha$ -olefins and to determine the effects of the nature and concentration of each comonomer on the structure and properties of the copolymers made with these highly stereospecific catalysts.

\* Presented in part at a seminar held at the Polytechnic Institute of Brooklyn, April 24, 1965, and at the National American Chemical Society Meeting at Phoenix, Arizona, January 16-21, 1966.

Random copolymers of ethylene and propylene were obtained by Natta and co-workers with catalysts containing a trialkylaluminum in combination with vanadium or titanium chlorides.<sup>4-9</sup> Random copolymers were also obtained with  $(C_6H_{13})_3Al/VCl_3$  or  $(C_6H_{13})_3Al/VCl_4$  catalysts for the copolymerization of ethylene with 1-butene and propylene with 1-butene.<sup>10,11</sup> As a general rule, the addition of a comonomer to ethylene in a polymerization system results in a polymer of reduced crystallinity. If only a small amount of the comonomer (propylene for example) is included in the polymer, the polymer will show the characteristic crystal structure of polyethylene, but the degree of crystallinity will be reduced. As the amount of comonomer is increased, the polymer will tend to become amorphous. For example, Natta and co-workers have reported that ethylene-propylene copolymers containing more than 20% propylene show virtually no crystallinity.<sup>9</sup>

In an "ideal" copolymerization leading to a random copolymer, the product of the reactivity ratios for the two monomers is equal to unity. The product of the reactivity ratios determined by Natta and co-workers for ethylene-propylene, ethylene-1-butene, and propylene-1-butene was usually equal to or less than one.

Karol and Carrick found that when ethylene and propylene were copolymerized with various metal alkyls in combination with a common transition metal compound such as  $VCl_4$ , the same reactivity ratios were obtained, but when a common metal alkyl such as triisobutylaluminum was used in combination with different transition metal compounds, different reactivity ratios were obtained in every case.<sup>12</sup> These results differ from those observed for typical vinyl copolymerizations, since the reactivity ratios for a given pair of vinyl monomers are constant regardless of the initiator used.

Copolymers of 3-methyl-1-butene and 4-methyl-1-pentene were reported by Reding and Walter to show x-ray crystallinity characteristic of poly-3-methyl-1-butene for compositions which were predominantly 3-methyl-1-butene and crystallinity characteristic of poly-4-methyl-1-pentene for those which were predominantly 4-methyl-1-pentene. While the crystal structure of these copolymers changed continuously with composition, no composition contained crystallinity characteristic of both homopolymers.<sup>13</sup> The authors suggested that either type of monomer unit should fit into the crystal lattice structure of the homopolymer of the other (i.e., cocrystallize) with very little change in unit cell dimensions, since the pendant isopropyl and isobutyl groups are structurally similar and since the two homopolymers have very similar crystal structures.

In the copolymerization of styrene with 4-methyl-1-pentene and with 5-methyl-1-hexene, Burnett and co-workers obtained broad composition distributions with fractions rich in styrene showing crystallinity characteristic of polystyrene and those rich in 4-methyl-1-pentene (or 5-methyl-1-hexene) having crystallinity characteristic of the homopolymer of that monomer.<sup>14-16</sup> As the comonomer concentration increased, the crystallinity of the copolymer was reported to decrease rapidly and no fraction had crystallinity characteristic of both homopolymers.

Bier and co-workers described block copolymers prepared by introducing ethylene and propylene alternately into the reaction mixture and by using a catalyst consisting of an organoaluminum compound in combination with  $\beta$ - $\text{TiCl}_3$ .<sup>17,18</sup> Such compositions are known to contain homopolymers of both monomers as well as block copolymer.

In the present work, it was discovered that mixtures of propylene and 1-butene, when polymerized with the highly stereospecific catalysts  $\text{C}_2\text{H}_5\text{-AlCl}_2/0.6 \text{ HPT/TiCl}_3$  and  $2(\text{C}_2\text{H}_5)_3\text{Al}_2\text{Cl}_3/\text{HPT}/3\text{TiCl}_3$ , produced copolymers in which the monomer units were not randomly arranged as in conventional copolymers of vinyl monomers or in the random  $\alpha$ -olefin copolymers prepared by Natta and co-workers, but were arranged in long sequences or blocks as suggested by the following structure:



These blocks were highly stereoregular, and the copolymers demonstrated crystallinity characteristic of the two stereosymmetric homopolymers—hence, the name “costereosymmetric” copolymers.

## EXPERIMENTAL WORK

### Equipment

Polymerizations were conducted in 300-ml. stainless steel microautoclaves.

### Materials

All solvents for polymerizations were dried over sodium wire for at least 24 hr. prior to use. The solvents used were Eastman-grade heptane from Distillation Products Industries, odorless mineral spirits from Texas Eastman Co., Reagent-grade benzene from Fisher Scientific Co., and Bayol D (a mixture of saturated hydrocarbons; b.p. 190–210°C.) from Esso Standard Oil Co.

Tetralin used as the fractionation solvent was obtained from Baird Chemical Industries, Inc. and acetone used to precipitate the fractions was obtained from Tennessee Eastman Co.

Monomers were dried by passing them through a bed of Molecular Sieve 4A supplied by the Linde Co. Those monomers used were propylene, 98.7% (propane, 1.2%; ethylene and carbon dioxide, <0.1%; oxygen, trace) from Sun Oil Co., and 1-butene, 98.2% [2-butene, 0.8%; isobutylene (2-methylpropene), 0.6%; butane, 0.4%] from Petro-Tex Chemical Corp.

Other chemicals used were titanium (III) chloride (HA grade) from Stauffer Chemical Co., ethylaluminum dichloride from Ethyl Corp., hexamethylphosphoric triamide from Tennessee Eastman Co., and isobutyl alcohol from Texas Eastman Co.

The Santonox R used for fraction stabilization was obtained from Monsanto Co.

### Typical Preparation of Propylene-1-Butene Copolymer

In a nitrogen-filled dry box, 100 ml. of pure, sodium-dried solvent (benzene, heptane, or a mixture of the two) was added to clean, dry 300-ml. stainless steel microautoclave. The total catalyst charge was usually 1.0 g. When a catalyst consisting of 1/0.6/1 mole proportions of  $C_2H_5AlCl_2$ /HPT/ $TiCl_3$  was used, the  $C_2H_5AlCl_2$ -HPT adduct (0.6 g.) was always added first, followed by the violet  $TiCl_3$  (0.4 g.).

The autoclave was sealed with a neoprene stopper, removed from the dry box, and then capped with a clean, dry autoclave head assembly while being purged with dry nitrogen.

The desired amounts of liquid 1-butene and liquid propylene were charged to the autoclave with a calibrated sight glass. In some cases, propylene and 1-butene were premixed in a separate vessel and the desired amount of this monomer mixture was charged to the autoclave. The total amount of monomer mixture was 100 ml. when 100 ml. of inert solvent was used and 200 ml. when no solvent was used. The reaction was conducted at a specified temperature with rocking, and the mixture was then cooled and vented. Isobutyl alcohol was added to deactivate the catalyst, and the reaction mixture was digested in isobutyl alcohol on a steam bath to remove catalyst residues. The polymer slurry was cooled to 25°C., filtered, washed with methanol, and then the polymer was dried in air. Final drying was conducted in a circulating-air oven at 50°C.

In addition to these batch-prepared materials, propylene-1-butene copolymers were also prepared in liquid monomer mixture by a continuous process.

### Analysis of Polymers

**Inherent Viscosity.** Inherent viscosities were determined on 0.25% (w/v) solutions of polymer in tetralin at 145°C.<sup>19</sup> High-viscosity polymers (> 3.5) sometimes caused gel formation in tetralin. In these cases, the viscosities were determined on 0.1% (w/v) solutions.

**X-Ray Diffraction Patterns.** The x-ray diffractometric curves were obtained on pressed-powder buttons or pressed films with a General Electric XRD-5 Diffractometer.

**Melting Points.** Melting points were obtained by the differential thermal analysis (DTA) technique. The normal heating rate was 2.35°C./min. and sand was used in the reference tube.

Melting points of fractions were determined on a hot-stage polarized light microscope where the heating rate was 1°C./min. Some fractions were also examined in a differential scanning calorimeter (DSC) made by Perkin-Elmer Corp.

**Density Measurements.** Densities were obtained on film samples in density-gradient tubes. Crystalline samples were conditioned by heating at 155°C. for 1 hr., followed by gradual cooling to 25°C., before the density was measured.

**Infrared Spectra.** Infrared spectra were determined on a Beckman IR-5 spectrophotometer. Spectra were generally obtained on films of 1–10 mil thickness.

#### Analysis for 1-Butene

The amount of 1-butene in the copolymer was determined from the infrared spectrum obtained on the molten polymer to eliminate the effects of crystallinity bands. The ratio of per cent transmission of the poly-1-butene peak at  $13.1 \mu$  to per cent transmission of the polypropylene peak at  $12.4 \mu$  for 5-mil-thick samples was used to determine the amount of 1-butene (weight per cent) in copolymers containing less than 30% 1-butene. When the copolymers contained more than 30% 1-butene, the sample thickness was 2 mils and the polypropylene peak at  $8.7 \mu$  was used instead of the one at  $12.4 \mu$ . Calibration curves for these analyses were established with radioactive propylene-1-butene copolymers containing propylene-1- $^{14}\text{C}$ .

#### Crystallinity Fractionation Procedure

The polymer (2.0000 g.) was dissolved in 160 ml. of nitrogen-saturated tetralin which had been stabilized with 0.1% Santonox R at  $170 \pm 10^\circ\text{C}$ . The Pyrex fractionation column was 41 mm. o.d. by 950 mm. long. It was filled to within 6.5 in. of the top with 100- $\mu$  glass beads (Superbrite No. 130, Minnesota Mining and Manufacturing Co.) with tetralin present to occupy the free volume. The column was heated to  $150^\circ\text{C}$ ., and the polymer solution was added to the 6.5-in.-deep free space at the top. After the solution was digested onto the column, the dissolving flask was rinsed with 40 ml. of tetralin at approximately  $170^\circ\text{C}$ . The rinse solution was added to the column. The flow was stopped at the bottom of the column, and the column was cooled to room temperature with cold water. The temperature and time programs were established on the master control unit, and the fractionation was started by connecting the top of the column to a tetralin reservoir and allowing the tetralin to flow through the column continuously. A heated capillary was used at the bottom of the column for flow control. Fifteen fractions were collected stepwise at increasing temperatures in 1-liter beakers. Approximately 600 ml. of solvent was collected at each temperature when the fractionation was complete, and 1.5 volumes of acetone were added to each fraction to precipitate the polymer. After standing overnight, each fraction was filtered in a sintered glass funnel. The residual polymer was washed at least twice with acetone and was then stabilized with a 0.1% solution of Santonox R. The anti-oxidant solvent was allowed to evaporate, and the polymer fractions were dried at  $50^\circ\text{C}$ . for at least 6 hr. at less than 3 mm. Hg pressure. The fractions were then weighed and removed from the funnels.

#### DISCUSSION

Propylene-1-butene copolymers were prepared in a continuous manner with liquid monomer mixtures and in batch preparations with both un-

TABLE I  
Preparation and Characterization of Costereosymmetric Propylene-1-Butene Copolymers

No.	Polymer- ization temp., °C.	Conver- sion, %	1-Butene in mono- mer, %	1-Butene in poly- mer, %	Inherent viscosity	Melt flow, <sup>a</sup> dg./min.	Density, g./ml.	Crystallinity by x-ray analysis	M.p., °C.	DTA	
										Crystal- lization temp., °C.	Crystal- lization temp., °C.
1	85	40	0	0	2.0 <sup>b</sup>	1.9	0.913	Polypropylene	162	119	
2	85	40	4	1.5	1.8 <sup>b</sup>	1.6	0.915	Polypropylene	160	123	
3	85	40	8	3	2.0 <sup>b</sup>	1.2	0.910	Polypropylene	53; 158	123	
4	85	40	14	5	2.3 <sup>b</sup>	0.7	0.905	Polypropylene	152	—	
5	75	40	21	8.5	1.9 <sup>b</sup>	1.6	0.903	Polypropylene	51; 146	107	
6	70	40	28	12	2.1 <sup>b</sup>	0.7	0.897	Polypropylene	50; 146	107	
7	75	97	20	18	3.3	—	—	Polypropylene and form I	—	—	
8	70	95	20	19	2.7	—	0.905	poly-1-butene Polypropylene and form I	103; 146	99	
9	90	60	50	38	2.0	—	0.886	poly-1-butene Polypropylene and form I poly-1-butene	68; 136	95	

10	90	80	65	39	1.8	5.0	0.883	Polypropylene and form I	45; 67; 149	73; 41
11	90	21	60	47	—	—	—	Polypropylene and form I	—	—
12	85	35	59	54	2.6	—	0.881	Polypropylene and form I	—	—
13	25	60	60	58	4.7	—	0.891	Polypropylene and form I	—	—
14	90	72	80	78	1.3	—	0.896	Polypropylene and form I	61; 113	—
15	70	80	100	100	2.2	1.2	0.917	Polypropylene and form I	122	76
16	—	—	—	50/50 blend	2.1	1.3	0.914	Polypropylene and form I	126; 170	130; 80

<sup>a</sup> Melt flow measured at 230°C. with a 2.16-kg. weight.

<sup>b</sup> Polymerization conducted in presence of H<sub>2</sub> to control the molecular weight of the copolymer.

<sup>c</sup> In powder form, form I as well as trace of form III was observed.



TABLE II  
Preparation and Characterization of Low-Conversion Costereosymmetric Propylene-1-Butene Copolymers

No.	Polymer-ization temp., °C.	Conversion, %	1-Butene		Inherent viscosity	Density, g./ml.	Crystallinity by x-ray analysis	M.p., °C.	Crystallization temp., °C.
			in mono-mer, %	in poly-mer, %					
17	32	4	28	10	1.6	0.908	Polypropylene <sup>a</sup>	147	109
18	32	5	28	13	4.9	0.899	Polypropylene	—	—
19	50	4	39	15	3.6	—	Polypropylene	140	110
20	50	4	39	15	3.6	—	Polypropylene	65-96; 142	110
21	50	4	39	18	3.1	—	Polypropylene	—	—
22	90	6	40	18	—	—	Polypropylene	121; 138	102
23	32	5	41	21	4.5	0.899	Polypropylene <sup>a</sup>	140	103
24	30	2	67	38	gel	—	Polypropylene and form I poly-1-butene	—	—
25	30	3	67	36	gel	—	Polypropylene and form I poly-1-butene	—	—
26	70	6	86	45	1.6	—	Polypropylene and form I poly-1-butene	—	—
27	32	2	79	61	3.2	0.891	Form I poly-1-butene and polypropylene <sup>b</sup>	70; 115	90
28	50	1	85	74	—	—	Form I poly-1-butene	78; 109	54
29	50	2	85	77	—	—	Form I poly-1-butene	77; 110	52

<sup>a</sup> High  $\alpha$ -polypropylene crystallinity as well as a low concentration of  $\gamma$ -polypropylene crystallinity was observed.

<sup>b</sup> Poly-1-butene crystallinity predominates.

TABLE III  
 Physical Properties of Propylene-1-Butene Costereosymmetric Copolymers<sup>a</sup>

Property	No. 30	No. 31	No. 32	No. 33	No. 34	No. 35	No. 36	No. 37	No. 38	No. 39	No. 40	No. 41	No. 42	No. 43	No. 44	No. 45
Melt flow rate, dg./min.	6	3.6	10.3	1.2	3.0	13.8	0.66	3.1	1.6	4.3	14.0	0.69	2.8	3.0	13.4	1.9
Density, g./ml.	0.9145	0.915	0.917	0.9098	0.9100	0.9102	0.9054	0.9056	0.9034	0.9051	0.9034	0.8974	0.8991	0.9023	0.9032	0.9103
Inherent viscosity (melters) extractables, % (MIBK) at reflux <sup>b</sup>	1.8	1.66	1.37	2.04	1.74	1.46	2.3	1.66	1.87	1.54	1.16	2.09	1.81	1.65	1.24	2.0
Softening point, Vicat, °C.	14	147	156	137	146	149	3	4	4	132	124	8	116	124	9	13
Brittleness temperature, °C.	150	7	156	49	49	46	139	135	126	13	124	115	116	124	122	150
Tensile yield strength, psi	4840	4880	4970	4950	4930	4860	4526	23	15	13	8	21	20	91	8	10
Tensile break strength, psi	3260	3280	3080	3390	3260	2950	3290	3870	3890	4040	3540	3120	3240	3680	3610	5170
Elongation at break, %	560	570	640	220	430	470	230	>630	401	—	—	—	—	—	—	4730
Stiffness in flexure, psi	140,000	140,000	140,000	130,000	130,000	140,000	100,000	80,000	105,000	105,000	70,000	70,000	70,000	90,000	80,000	165,000
Hardness Rockwell R scale	95	97	99	91	95	99	82	81	84	87	79	56	66	78	82	99
1/2-in. impact strength at 23°C., ft.-lb./in. of notch	0.7	0.6	0.3	1.5	0.9	0.7	2.3	1.5	1.6	1.0	1.0	12.4	8.3	1.9	1.0	0.7
Unnotched 1/2-in. impact strength at -10°C., ft.-lb./in. of width	5.3	5.3	4.3	5.3	5.1	4.5	7-12	5.7-13.4	29.1	20.8	23.3	>80	>80	>80	23.3	6.4
Tensile impact strength, ft.-lb./in. <sup>2</sup>	205	152	89	263	151	90	263	253	266	233	253	412	392	326	221	143
Heat distortion temp., °C.	149	159	161	149	156	158	141	126	126	149	147	136	147	150	148	165
Melting point, °C.	161	159	161	136	156	158	152	153	143	149	147	136	147	150	148	165
1-Butene, %	1	1	1	3	3	3	5	5	8	8	8	12	12	12	12	0

<sup>a</sup> Properties were determined on injection-molded specimens which were aged at 23°C. for 7 days.

<sup>b</sup> MIBK is 4-methyl-2-pentanone.

diluted liquid monomer mixtures and mixtures containing inert hydrocarbon diluents. The reaction conditions and properties of the copolymers made to both high and low conversions are summarized in Tables I and II, respectively. These copolymers were characterized by x-ray diffraction, melting point (DTA, DSC, and Vicat softening point), density, molecular weight (solution viscosity), infrared spectroscopy, and fractionation. Physical properties measured on injection-molded specimens of polypropylene and copolymers containing up to 12% 1-butene are listed in Table III.

### X-Ray Diffraction and Differential Thermal Analysis Studies

The high degree of crystallinity of a propylene-1-butene copolymer prepared with the  $C_2H_5AlCl_2/0.6HPT/TiCl_3$  or  $2(C_2H_5)_3Al_2Cl_3/HPT/3TiCl_3$  catalyst is indicated by its relatively high density, its low amorphous content (by extraction), and its relatively high melting point. Surprisingly, copolymers containing 3 to about 80% 1-butene had two distinct crystalline

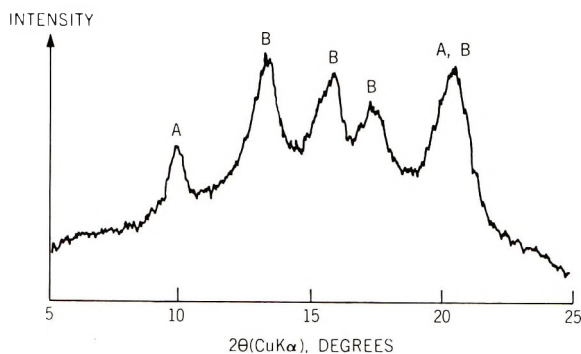


Fig. 1. X-ray diffraction curve of a 60/40 propylene-1-butene copolymer having both polypropylene and poly-1-butene crystallinity: (A) poly-1-butene, (B) polypropylene.

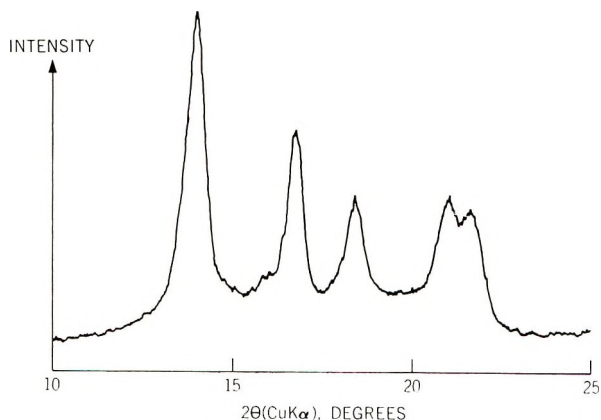


Fig. 2. X-ray diffraction curve of polypropylene.

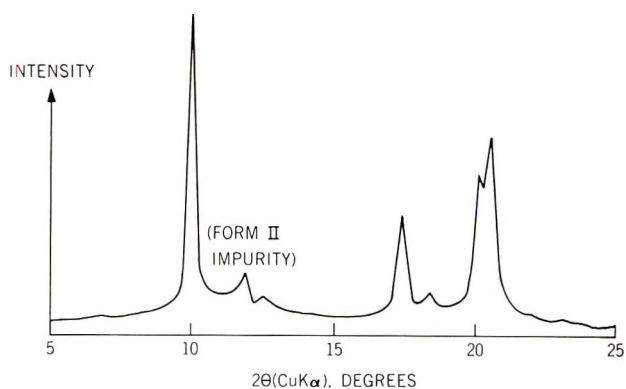


Fig. 3. X-ray diffraction curve of form I poly-1-butene.

melting points, and copolymers containing 18 to about 70% 1-butene had x-ray crystallinity characteristic of the two stereosymmetric homopolymers. For example, slowly cooled films of copolymers containing 18% 1-butene prepared with the highly stereospecific three-component catalysts exhibited x-ray diffraction peaks characteristic of both polypropylene and poly-1-butene crystallinity.

An x-ray diffraction curve for a 60/40 propylene-1-butene copolymer is shown in Figure 1. The x-ray diffraction curves for the homopolymers of propylene and 1-butene prepared with the same catalyst are included for comparison (Figs. 2 and 3, respectively).

Polypropylene was observed to have sharp characteristic peaks at  $14.0^\circ$ ,  $16.7^\circ$ , and  $18.4^\circ$ , with a doublet appearing at  $21.0^\circ$  and  $21.6^\circ$ . X-ray diffraction peaks for form I poly-1-butene were observed at  $10.0^\circ$ ,  $17.4^\circ$ ,  $20.1^\circ$ , and  $20.5^\circ$ . In a typical diffraction curve (Fig. 1) for a 60/40 propylene-1-butene copolymer, a peak at  $10.0^\circ$  (characteristic of form I poly-1-butene), peaks at  $13.5^\circ$ ,  $16.1^\circ$ , and  $17.6^\circ$  (due to the presence of polypropylene crystallinity), and a peak at  $20.3^\circ$  (due to both polypropylene and poly-1-butene crystallinity) were observed. It should be noted that the diffraction peaks for the polypropylene crystalline phase in the copolymer are shifted from their normal homopolymer positions.

As expected, the amount of poly-1-butene crystallinity evident in the x-ray pattern increased with increasing 1-butene content with a concomitant decrease in the degree of polypropylene crystallinity. At a concentration of about 70% 1-butene, polypropylene crystallinity was no longer detectable by x-ray diffraction, and only form I poly-1-butene crystallinity was present in pressed-film samples. In powder form, however, a very small amount of form III poly-1-butene crystallinity was also evident. Form II poly-1-butene crystallinity was not observed in the costereosymmetric propylene-1-butene copolymers. The typical form I crystallinity was always observed regardless of whether the molded objects or films were quenched or allowed to cool slowly. At any given concentration, the presence of the poly-1-butene crystallinity was easier to detect in a

high-conversion copolymer than in a low-conversion one. This is readily explained by the fact that the high-conversion copolymer has a much broader composition distribution than a low-conversion copolymer containing the same average amount of comonomer. The presence of both monomers is also readily evident in the infrared curves obtained on slowly cooled films of these copolymers. Even copolymers containing as little as 2–3% 1-butene provide spectra which have a band at about  $13\ \mu$  characteristic of poly-1-butene.

The crystallite size must be at least about 50 Å. in order for crystallinity to be detected by x-ray analysis. This indicates that some of the monomer sequences contain at least 20 monomer units. The length of the segments in the costereosymmetric copolymers appears to depend on both the polymerization temperature and the composition of the starting monomer mixture. For example, polymerizations at low temperatures (25°C.) produce copolymers having higher densities as well as sharper x-ray diffraction peaks and DTA melting peaks than those made at higher temperatures (70°–90°C.). Increasing the 1-butene concentration decreases the length of the propylene blocks. It is significant to note that a 50/50 copolymer still has appreciable crystallinity as evidenced by two crystalline melting points, two types of x-ray crystallinity, and a density of 0.88–0.89 instead of 0.85 expected for an essentially amorphous, random copolymer.

The two DTA melting points observed for a propylene–1-butene costereosymmetric copolymer are depressed from the melting points observed for the homopolymers of propylene and 1-butene. In general, compositions rich in propylene have a melting peak attributable to the polypropylene segments very near that observed for the propylene homopolymer, while the melting point of the poly-1-butene segments is considerably depressed. In a similar manner, copolymers rich in 1-butene have a melting point near that observed for poly-1-butene homopolymer while showing an appreciable depression in the melting point of the polypropylene segments. In high-conversion copolymer containing 39% 1-butene, three distinct melting peaks were observed: a major poly-1-butene peak at 67°C., a smaller polypropylene melting peak at 149°C., and a minor peak at 45°C.

The factors responsible for the crystallization of the 1-butene chain segments of the copolymer directly in the form I structure have not been investigated in detail. It is an interesting coincidence, however, that the crystal structures of both polypropylene and form I poly-1-butene involve 3:1 helical chain conformations and have identical fiber, or chain, axes. It is thought that the 1-butene chain segments rejected by the polypropylene lamellae during the crystallization process are restricted in their spatial arrangements by the crystallized propylene segments and this may impose upon the butene segments a bias toward the 3:1 helical conformation. This bias may then lower the activation energy for the subsequent crystallization of the 1-butene segments into the form I structure.

It is also believed that during the crystallization process an occasional propylene monomer unit is incorporated into the lattice of the crystallized 1-butene segments. Since the pendant methyl group in propylene could easily fit into the physical space normally occupied by the pendant ethyl group of a 1-butene unit, no significant change in the lattice dimensions would be anticipated. Such an imperfection in the poly-1-butene crystal lattice, however, could account in part for the lowered melting point of the poly-1-butene crystalline phase. The mere presence of polypropylene would not account for the depression of the melting point, however, since a physical blend of polypropylene and poly-1-butene shows undepressed DTA melting points for both homopolymers. The depressed melting point for the polypropylene crystalline phase in the copolymer suggests that 1-butene units might also be incorporated into the crystal lattice for polypropylene. However, since the pendant ethyl group of 1-butene is too large to fit into the space normally occupied by a methyl group of propylene, this would necessitate an expansion of the polypropylene crystal lattice, probably in a manner similar to that observed for branched polyethylene.<sup>20,21</sup> This expanded lattice would also account for the shifts observed in the x-ray diffraction peaks for the polypropylene crystalline phase of the copolymers. These data, therefore, further confirm the presence of costereosymmetric copolymers as opposed to homopolymer mixtures, since the latter exhibit x-ray diffraction patterns with peaks at their characteristic locations.

The multiblock structure of the costereosymmetric copolymers is also supported by the fact that the densities and melting points are lower than those observed for comparable two-period block copolymers.

### Reactivity Ratio Studies

The rate of propagation of propylene is faster than that of 1-butene in homopolymerization, as well as in copolymerizations involving these two monomers. The reactivity ratios for the copolymerization of propylene and 1-butene at 30°C. with the  $C_2H_5AlCl_2/0.6$  HPT/ $TiCl_3$  catalyst in the presence of  $H_2$  as a chain-transfer agent have been determined to be  $r_1$  (propylene) = 4.3 and  $r_2$  (1-butene) = 0.8.<sup>22</sup> The fact that the product of  $r_1$  and  $r_2$  (3.44) is greater than unity adds further support to the multiblock copolymer structure, since in random copolymerizations the products of  $r_1$  and  $r_2$  are approximately one. In the absence of  $H_2$ , the reactivity ratio values were observed to be drastically different ( $r_1 = 3.3$  and  $r_2 = 0.45$ ). The fact that  $r_2$  is less than one for 1-butene suggests that only in monomer mixtures rich 1-butene would one expect to obtain segments of 1-butene long enough to crystallize. This is supported by the low-conversion runs in which poly-1-butene crystallinity was observed by x-ray analysis only on copolymers made from monomer mixtures rich in 1-butene. However, since poly-1-butene crystallinity was observed from a rather broad range of comonomer compositions and since the copolymers obtained from all comonomer compositions had broad composition distributions, the

observed reactivity ratio values probably represent the average situation and may not be indicative of the true relative reactivities of the monomers.

A possible explanation for the formation of the multiblock structure is that chain propagation is determined by the nature of the preceding segments which constitute the growing helix. For example, if at least three propylene monomer units enter the polymer chain in a stereoregular sequence at a given catalyst site, the polypropylene helix will be formed and will, in general, tend to continue growing by addition of propylene with only occasional addition of a 1-butene molecule. The addition of at least three 1-butene monomer units in a row would change the nature of the growing end of the helix to that characteristic of poly-1-butene, and then 1-butene would be preferentially added at that site.

### Fractionation Studies

Additional confirmation of a true duocrystalline multiblock copolymer, as opposed to a physical blend containing homopolymers, was obtained by fractionation studies. Thus, blends of polypropylene and poly-1-butene, as well as the costereosymmetric copolymers were fractionated by the fractionation technique outlined in the experimental section. Both crystallinity (melting point under polarized light) and monomer distributions were obtained.

When physical blends were fractionated, only a small amount of poorly crystalline polypropylene was eluted at the temperature at which the bulk of the poly-1-butene was eluted. The melting point distribution of a physical blend comprised of equal weights of the two homopolymers is shown in Figure 4. The first sudden increase in  $S(\Sigma \text{ wt.-%})$  corresponds to the point at which poly-1-butene was heavily eluted from the column.

The plateau region of the curve represents a temperature range within which very little polymer melted. The second break in the curve represents the melting of the bulk of the propylene homopolymer. The integral melting point distribution of a 40% 1-butene costereosymmetric copolymer is also given in Figure 4. This curve is continuous, however, with no sudden breaks comparable to those shown by the blend distribu-

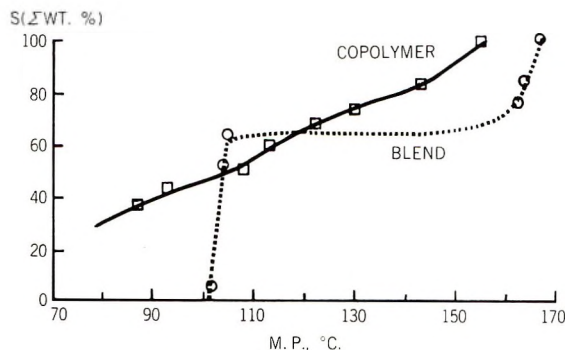


Fig. 4. Melting point distributions of blend and costereosymmetric copolymer.

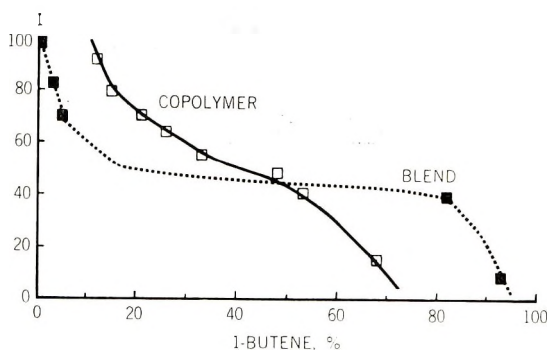


Fig. 5. Monomer distributions of blend and costereosymmetric copolymer.

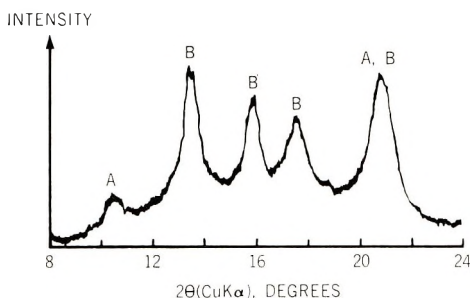


Fig. 6. X-ray diffraction curve of a costereosymmetric copolymer fraction: (A) poly-1-butene; (B) polypropylene.

tion included for comparison. Several fractions have melting points lower than poly-1-butene, while the remainder have melting points intermediate between that of poly-1-butene and polypropylene. As predicted, the monomer distributions of the fractions from the copolymer and from the blend shown in Figure 5 were quite different. Monomer distribution is shown here as a function of  $I$ , the sum of the weight per cent to the mid-point of the measured fraction. These data indicate that almost complete separation of the blend was achieved, and that the different species of the copolymer were separated according to their respective solubilities also. The copolymer molecules richer in 1-butene were more soluble; however, all fractions from the copolymer contained significant amounts of both 1-butene and propylene. Since the monomers in the copolymer could not be separated by fractionation as they were in the blend and since a smooth, unbroken melting curve was obtained, it is evident that a true copolymer free of homopolymer has been confirmed. In view of this, films of selected fractions were examined by x-ray diffraction analysis for crystallinity. The x-ray diffractometric curve for a propylene-1-butene copolymer fraction illustrated in Figure 6 shows the characteristic patterns of both polypropylene and form I poly-1-butene crystallinity. Only the first several fractions which were rich in 1-butene showed both types of crystallinity by x-ray diffraction. When the 1-butene concentration of the frac-



TABLE IV  
Costereosymmetric Copolymer Fractionation Data

No.	M.p., °C.	Inherent viscosity	1-Bu-tene, %	X-ray diffraction type	Extraction temp., °C.
46	79-87	0.92	68	Polypropylene and form I poly-1-butene <sup>a</sup>	<18
47	82-93	0.49	53	Polypropylene and form I poly-1-butene	33
48	100-108	0.64	48	Polypropylene and form I poly-1-butene	47
49	102-113	0.80	33	Polypropylene	53
50	115-122	0.81	26	Polypropylene	64
51	122-130	1.07	21	Polypropylene	72
52	133-143	0.96	15	Polypropylene	98
53	149-155	1.48	12	Polypropylene	130

<sup>a</sup> Poly-1-butene crystallinity predominates.

tions reached about 33%, only polypropylene crystallinity could be detected by x-ray diffraction analysis. This is evident from the data given in Table IV for fractions of a 60/40 propylene-1-butene costereosymmetric copolymer. A differential scanning calorimeter curve for one of these copolymer fractions is shown in Figure 7. There are four endothermic peaks in this thermogram which are associated with melting. The peaks at 61 and 100°C. are thought to be the premelting peaks, respectively, for the 74 and 111°C. peaks. The latter are thought to be the ultimate melting peaks of the poly-1-butene and polypropylene crystallinities in this copolymer fraction.

Figure 8 illustrates the effect of conversion upon the ultimate monomer distribution in the polymer. The monomer distribution of a low-conversion (5.7%) 55/45 propylene-1-butene copolymer was unusually narrow, while that of a high-conversion copolymer (75%) having similar average butene composition was observed to be rather broad. All fractions of the low-conversion copolymer showed both polypropylene and

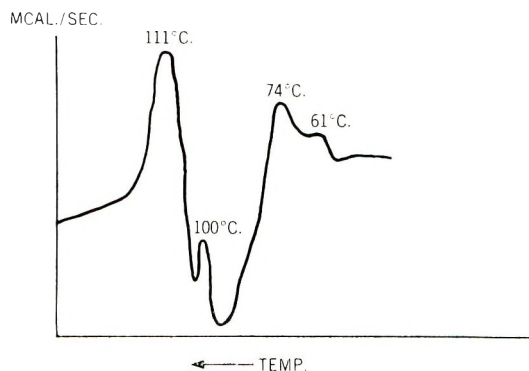


Fig. 7. DSC thermogram of a costereosymmetric copolymer fraction.

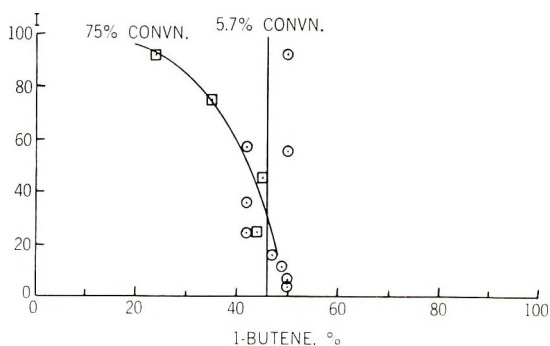


Fig. 8. Costereosymmetric copolymer with very narrow monomer distribution.

poly-1-butene crystallinity by x-ray diffraction analysis. These data provide strong support for the multiblock structure postulated for the costereosymmetric propylene-1-butene copolymers.

The composition distributions of some low-conversion copolymers and continuously prepared copolymers were similar and relatively broad. For example, low-conversion and continuously prepared copolymers which contained an average of 12% 1-butene had fractions containing 4-30% and 7-30% 1-butene, respectively. Due to the gradual increase of the 1-butene concentration in the comonomer mixture as the copolymerization proceeded, a high-conversion (58%) copolymer had a slightly broader composition distribution (the fractions containing 4-33% 1-butene). Again no homopolymers were detected.

### Physical Properties of Injection-Molded Specimens

The physical properties obtained on injection-molded propylene-1-butene costereosymmetric copolymers are included in Table III. Properties of a highly stereoregular polypropylene are given for comparison. Increasing the 1-butene content of the costereosymmetric copolymers decreases those properties which are dependent on crystallinity (hardness, tensile strength, stiffness, and melting point) and improves significantly the impact strength, low-temperature properties, and clarity. For example, only 3-5% 1-butene in a high molecular weight copolymer reduces the brittleness temperature to the range of  $-23$  to  $-26^{\circ}\text{C}$ . This is about as low as the brittleness temperature of the copolymer can be lowered with 1-butene, since the glass transition temperature of poly-1-butene is only about  $-25^{\circ}\text{C}$ . Data in this laboratory have indicated that the brittleness temperature of a polyolefin cannot be lower than its glass transition temperature. The brittleness temperature increases with increasing melt flow as expected.

The improved clarity of the crystallized costereosymmetric copolymers is attributed to the presence of smaller spherulites as compared with the large spherulites observed in mixtures of the two homopolymers. Thus,

the clarity is further evidence in favor of the segmented copolymer structure rather than homopolymer mixtures.

The excellent impact strength of the copolymers was demonstrated by the fact that the copolymer containing 12% 1-butene has a notched Izod impact strength several times greater than that of polypropylene having a similar inherent viscosity. The copolymer also has a tensile impact strength three times greater than that of polypropylene at 23°C. This improvement in impact strength and low-temperature properties was achieved with a minimum loss in other important properties. For example, tensile strength, hardness, stiffness, and melting point remained at a relatively high level. Those polymers containing 12% 1-butene had melting points in the 140–150°C. range, which is only 15–25°C. lower than the melting point of highly stereoregular polypropylene and is substantially higher than that observed for linear polyethylene.

### SUMMARY

It has been demonstrated that the copolymerization of propylene-1-butene mixtures with highly stereospecific three-component catalysts produces multiblock copolymers which generally show crystallinity characteristic of both polypropylene and form I poly-1-butene. Fractionation showed that no homopolymers were present in these copolymers and, therefore, that the duocrystallinity must be due to the presence of crystallizable stereoregular segments of at least 20 monomer units in the copolymer molecular chains. The multiblock copolymer structure is also supported by the fact that the product of the reactivity ratios is greater than unity.

A possible explanation for the multiblock structure of these copolymers is that the instant probability of the enchainment of one comonomer relative to the other is determined principally by the nature of the preceding triad of monomer units in the growing polymer chain.

Increasing the amount of 1-butene decreases the hardness, tensile strength, stiffness, and melting point of the copolymers and improves significantly the impact strength, low-temperature properties, and clarity of molded objects.

### References

1. H. W. Coover, Jr. and F. B. Joyner, *J. Polymer Sci. A*, **3**, 2407 (1965).
2. H. W. Coover, Jr. and F. B. Joyner (to Eastman Kodak Co.), U. S. Pat. 2,956,991 (1960).
3. H. W. Coover, Jr. and F. B. Joyner (to Eastman Kodak Co.), U. S. Pat. 2,969,345 (1961).
4. G. Natta, G. Mazzanti, A. Valvassori, and G. Pajaro, *Chim. Ind. (Milan)*, **39**, 733 (1957).
5. G. Mazzanti, A. Valvassori, and G. Pajaro, *Chim. Ind. (Milan)*, **39**, 743 (1957).
6. G. Mazzanti, A. Valvassori, and G. Pajaro, *Chim. Ind. (Milan)*, **39**, 825 (1957).
7. G. Natta, G. Mazzanti, A. Valvassori, and G. Sartori, *Chim. Ind. (Milan)*, **40**, 717 (1958).
8. G. Natta, A. Valvassori, G. Mazzanti, and G. Sartori, *Chim. Ind. (Milan)*, **40**, 896 (1958).

9. G. Natta, G. Mazzanti, A. Valvassori, G. Sartori, and D. Morero, *Chim. Ind. (Milan)*, **42**, 125 (1960).
10. G. Natta, G. Mazzanti, A. Valvassori, and G. Pajaro, *Chim. Ind. (Milan)*, **41**, 764 (1959).
11. G. Mazzanti, A. Valvassori, G. Sartori, and G. Pajaro, *Chim. Ind. (Milan)*, **42**, 468 (1960).
12. F. J. Karol and W. L. Carrick, *J. Am. Chem. Soc.*, **83**, 2654 (1961).
13. F. P. Reding and E. R. Walter, *J. Polymer Sci.*, **37**, 555 (1959).
14. I. H. Anderson, G. M. Burnett, and P. J. T. Tait, *Proc. Chem. Soc.*, **1960**, 225.
15. G. M. Burnett, paper presented at the 54th annual meeting of the American Institute of Chemical Engineers, New York, December 1961.
16. I. H. Anderson, G. M. Burnett, and P. J. T. Tait, *J. Polymer Sci.*, **56**, 391 (1962).
17. G. Bier, *Angew. Chem.*, **73**, 186 (1961).
18. G. Bier, A. Gumboldt, and G. Lehman, *Plastics Inst. (London) Trans. J.*, **28**, 98 (1960).
19. R. M. Schulken, Jr. and M. L. Sparks, *J. Polymer Sci.*, **26**, 227 (1957).
20. E. A. Cole and D. R. Holmes, *J. Polymer Sci.*, **46**, 245 (1958).
21. P. R. Swan, *J. Polymer Sci.*, **56**, 409 (1962).
22. Tennessee Eastman Company, unpublished data.

### Résumé

La copolymérisation du propylène et du 1-butène avec des catalyseurs à trois composants hautement stéréospécifiques produit des copolymères cristallins à plusieurs blocs ayant des séquences stéréorégulières à la fois de propylène et 1-butène. Des copolymères contenant de 3 à 80% de butène-1, ont deux points de fusion DTA qui peuvent être attribués à la cristallinité du polypropylène et du poly-butène-1. Ceux-ci contenant de 18 à 70% de butène-1 présentent des diagrammes de diffraction aux rayons-X manifestant des pics caractéristiques du polypropylène et du poly-1-butène sous sa variété I; la forme II du poly-1-butène n'a jamais été observée. La structure copolymérique à plusieurs blocs observée est également confirmée par le fait que le produit des rapports de réactivités est plus grand que l'unité. Les distributions de composition des copolymères préparés en continu et à basse conversion, sont semblables et relativement larges, par exemple le copolymère contenant en moyenne 12% de butène-1 contenant de 5 à 30% de butène-1. Les copolymères de haute conversion ont une distribution de composition encore plus large par suite de l'augmentation progressive de la concentration en butène-1 dans le mélange du comonomère à mesure que la copolymérisation progresse. L'absence d'homopolymères a été démontrée par fractionnement. La possibilité de détecter des homopolymères a été prouvée par le fait que des mélanges de polypropylène stéréorégulier et de poly-1-butène ont été facilement séparés les uns des autres. En augmentant la quantité du butène-1 on diminue les propriétés liées à la cristallinité, telle que la dureté, la résistance à la tension, la rigidité, la densité, le point de fusion, mais on améliore de façon significative la résistance aux chocs, les propriétés de basses températures et la translucidité des objets moulés. Ces copolymères à deux composants cristallins gardent un niveau beaucoup plus élevé de propriétés, que les copolymères statistiques préparés avec les catalyseurs de coordination moins stéréospécifique que ceux cités ici.

### Zusammenfassung

Die Kopolymerisation von Propylen und Buten-1 mit hochgradig stereospezifischen Drei-Komponenten-Koordinationskatalysatoren lieferte kristalline Multiblockkopolymere mit stereoregulären Sequenzen von Propylen und Buten-1. Kopolymere von 3 bis etwa 80% Buten-1 besaßen zwei DTA-Schmelzpunkte, welche der Kristallinität von Polypropylen und Polybuten-1 zugeordnet werden konnten. Diejenigen mit 18

bis etwa 70% Buten-1 zeigten Röntgenbeugungsdiagramme mit den charakteristischen Maxima für Polypropylen und Polybuten-1 der Form I, hingegen wurde niemals die Kristallinität von Polybuten-1 der Form II beobachtet. Die beobachtete Multiblockkopolymerstruktur wird weiter durch die Tatsache gestützt, dass das Produkt der Reaktivitätsverhältnisse grösser als 1 ist. Die Zusammensetzung des Kopolymeren bei niedrigem Umsatz und bei kontinuierlicher Darstellung war ähnlich und verhältnismässig breit. Zum Beispiel enthielten Kopolymere mit einem mittleren Buten-1-Gehalt von 12% Individuen mit 5 bis 30% Buten-1. Bei hohem Umsatz besaßen die Kopolymere wegen der kontinuierlichen Zunahme der Buten-1-Konzentration in der Monomermischung beim Fortschreiten der Kopolymerisation eine noch breitere Zusammensetzungsverteilung. Das Fehlen von Homopolymeren wurde durch Fraktionierung nachgewiesen. Die Möglichkeit, Homopolymere nachzuweisen, wurde dadurch erhärtet, dass eine Mischung von stereoregulärem Polypropylen und Polybuten-1 leicht getrennt werden konnte. Eine Steigerung des Anteil an Buten-1 bewirkt einen Abfall der von der Kristallinität abhängigen Eigenschaften wie Härte, Zugfestigkeit, Steifigkeit, Dichte und Schmelzpunkt, verbessert jedoch merklich die Stossfestigkeit, die Tieftemperatureigenschaften sowie die Klarheit geformter Gegenstände. Diese zweifach kristallinen Kopolymere bewahren einen viel höheren Eigenschaftsstandard als er bei mit weniger stereospezifischen Katalysatoren dargestellten statistischen Kopolymeren beobachtet wurde.

Received December 28, 1965

Revised March 24, 1966

Prod. No. 5127A

## Active Site Measurements in the Coordinated Anionic Polymerization of Propylene\*

H. W. COOVER, JR., J. E. GUILLET,†

R. L. COMBS,‡ and F. B. JOYNER,

*Research Laboratories, Tennessee Eastman Company,*

*Division of Eastman Kodak Company, Kingsport, Tennessee 37662*

### Synopsis

The active-site concentration was determined by using tritium labeling on three coordinate anionic catalysts containing violet titanium(III) chloride [hereafter referred to as titanium(III) chloride or  $TiCl_3$ ]. These catalysts were used in the polymerization of propylene. Three-component catalysts, as well as two-component catalysts, were investigated. Previous estimates of active-site concentrations for  $(C_2H_5)_2AlCl-TiCl_3$  catalysts appear to be too high by at least a factor of 10. The reason for the previous high estimates can be attributed to the marked reduction in chain-transfer rate which occurs when the amount of polymer formed exceeds about 2 g./g.  $TiCl_3$ . The chain-transfer process appears to involve both alkylaluminum and monomer, but the effective monomer concentration is apparently not reduced until a later stage in the polymerization. The propagation rate is, therefore, unaffected; but the transfer rate is reduced, leading to the formation of polymer with much higher molecular weight. Extension of this process could lead to the observed broad distribution of molecular weights in polypropylene. As a result of the low value of active-site concentrations [about  $10^{-3}$  mole/mole titanium(III) chloride], the absolute value calculated for the propagation rate constant for propylene polymerization is in the range of 50 l./mole sec., and the average lifetime of a growing polymer molecule during the early stages of the polymerization is about 1 min.

### INTRODUCTION

The kinetics of propylene polymerization with two-component catalysts made from titanium(III) chloride and various metal alkyls have been studied by a number of authors. The earliest work was that of Natta and co-workers,<sup>1</sup> who studied catalysts made from titanium(III) chloride and triethylaluminum (system I) and catalysts made from titanium(III) chloride and diethylaluminum chloride (system II). The general features of the polymerization were thoroughly discussed in these papers, and proposals were made for values of the rate constants and activation energies

\* Presented at the 145th National Meeting of the American Chemical Society, New York, N. Y., September 1963.

† Present address: Department of Chemistry, University of Toronto, Toronto, Canada.

‡ To whom inquiries should be sent.

for propagation and chain-transfer reactions. Estimates of the active site concentrations were made by using alkylaluminum compounds labeled with  $^{14}\text{C}$ . More recent information regarding active site concentrations and rate constants has been published by Chien,<sup>2</sup> who also used  $^{14}\text{C}$ -labeled diethylaluminum chloride, and by Kohn and co-workers,<sup>3</sup> who used tritiated methanol to quench the reaction and who estimated the active sites from the observed amount of tritium included in the polymer.

The present study was initiated to determine the kinetics of a typical three-component system consisting of a catalytic mixture of titanium(III) chloride, ethylaluminum dichloride, and hexamethylphosphoric triamide (HPT) (system III). When studies were made of the active site concentrations for this catalyst at low conversions, the results were different from those predicted from the data of Natta, Chien, and Kohn.<sup>1-3</sup> Consequently, additional studies were made of the kinetics of the two-component catalysts.

## EXPERIMENTAL

### Materials

Propylene (Texas Eastman Co.) was found to contain  $\text{C}_3\text{H}_6$ , 98.8%;  $\text{C}_3\text{H}_8$ , 1.0%;  $\text{C}_2\text{H}_4$  and/or  $\text{CO}_2$ , 0.1%;  $\text{C}_2\text{H}_6$ , 0.1%; and  $\text{O}_2$ ,  $\text{N}_2$ ,  $\text{CH}_4$ , and/or  $\text{CO}$ , trace.

Nitrogen (Southern Oxygen Co., prepurified grade) was 99.998% pure, with a trace of argon present.

Heptane (Distillation Products Industries), b.p. 96–97°C., was dried twice over sodium.

Benzene (Baker and Adamson, reagent grade, Code 1442) was dried twice over sodium.

Titanium(III) chloride (Stauffer Chemical Co., HA grade) was used as received.

Triethylaluminum (Texas Alkyls, Inc.) was redistilled twice.

ANAL. Calcd. for  $(\text{C}_2\text{H}_5)_3\text{Al}$ : Al, 23.63%; ethane evolution, 76.37%. Found: Al, 24.45%; ethane evolution, 75.22%.

Diethylaluminum chloride (Texas Alkyls, Inc.) was used as received.

ANAL. Calcd. for  $(\text{C}_2\text{H}_5)_2\text{AlCl}$ : Al, 22.41%; Cl, 29.44%; ethane evolution, 48.15%. Found: Al, 21.35%; Cl, 28.87%; ethane evolution, 46.70%.

Ethylaluminum dichloride (Ethyl Corp.) was recrystallized.

ANAL. Calcd. for  $\text{C}_2\text{H}_5\text{AlCl}_2$ : Al, 21.25%; Cl, 55.85%; ethane evolution, 22.89%. Found: Al, 21.14%; Cl, 59.26%; ethane evolution, 21.81%.

Hexamethylphosphoric triamide (Dow Chemical Co.) was distilled, and no impurities were detected by gas chromatography,  $n_D^{20} = 1.4590$ .

Tritium-labeled water (New England Nuclear Corp., Lot 81-200, specific activity 1.0 mc./mg.) was used as received.

Methanol was fractionally distilled over magnesium turnings by using an iodine catalyst to give less than 20 ppm water.

Methanol-*t* was made by exchange with small amounts of tritium-labeled water and had a specific activity of 410–1900 mc./mmole.

### Apparatus

The apparatus used for this study is shown schematically in Figure 1. The reaction vessel was a 230-ml. Pyrex pressure bottle with indented sides to improve the mixing. The stirring bar was a Teflon-covered magnet. The reaction bottle was closed with a rubber-stopper assembly that allowed loading it in a dry box under a nitrogen atmosphere and transferring it to an oil bath. The stopper was made so that an injection tube with a rubber cap could be inserted. Temperature was controlled by a circulating oil system (Cole-Parmer temperature bath, Cat. No. 1700). The reservoirs were so arranged that one or all could be used to furnish the monomer feed. The pressure drop on the reservoir was measured and recorded as a function of time by a Taylor Transair and Transet instrument. For extremely slow rates, all reservoirs could be cut off from the feed system to allow only the monomer in the lines (approximately 75 ml.) to be fed into the reactor bottle.

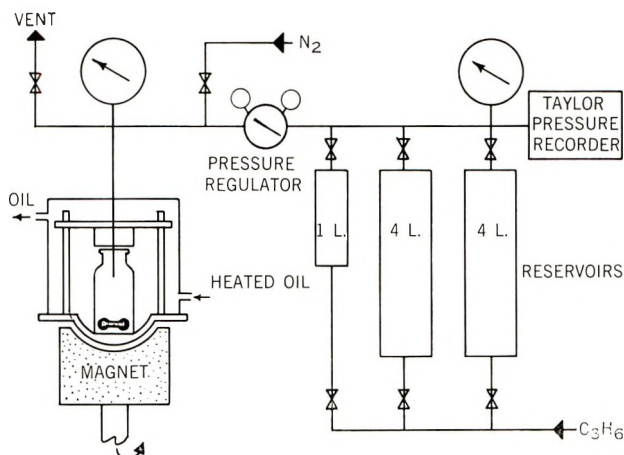


Fig. 1. Magnetically stirred kinetic apparatus.

### Procedures

**Kinetic Experiments.** The solvent and catalyst components were placed in the reaction bottle in a dry box under a nitrogen atmosphere, and the bottle was then attached to the kinetic apparatus. The total volume of solution was 100 ml. at room temperature, and the composition of the solvent was 40% (v/v) benzene in heptane. The reaction bottle was flushed six times with the monomer after it had been placed on the apparatus. The magnetic stirrer was then turned on, and the rate was re-



corded as a function of time. The run was terminated by quenching with isobutyl alcohol. The polymer was washed several times with hot isobutyl alcohol and finally with methanol. The polymer was dried in air at room temperature and then in a circulating air oven at 50°C. The crystallinity (crystallinity index) was determined by extracting approximately 5 g. of polymer with 4-methyl-2-pentanone at refluxing temperatures. The inherent viscosity was determined by using a 0.25% (w/v) solution in Tetralin at 145°C.

**Tritium-Labeling Experiments.** The reaction bottle for these experiments was equipped with an injection tube with a self-sealing gasket. This allowed the liquid components of the catalyst to be added after equilibrium with respect to temperature and monomer concentration had been reached. By this method, rates could be measured at extremely low conversions. After the desired time had elapsed, the run was terminated by injection of methanol-*t*.

The amount of methanol required to stop the polymerization completely varied with the type of alkylaluminum; 0.5 mole of labeled methanol per mole of ethylaluminum dichloride deactivated the  $C_2H_5AlCl_2/HPT/TiCl_3$  (1/0.6/1) catalyst; but to ensure complete reaction, a twofold amount was used. The following amounts of labeled methanol were used with the different catalysts: with  $(C_2H_5)_3Al/TiCl_3$  (1/1), 4 moles methanol/mole alkyl; with  $(C_2H_5)_2AlCl/TiCl_3$  (1/1), 2 moles methanol/mole alkyl; with  $C_2H_5-AlCl_2/HPT/TiCl_3$  (1/0.6/1), 1 mole methanol/mole alkyl.

In order to assay the polymer, it was first oxidized by the conventional Pregl method, and the labeled water was collected in a Dry Ice trap. The water was then reacted stoichiometrically with diethylaluminum chloride to produce labeled ethane which contained all the tritium in the original sample. The ethane was swept into a Cary ionization chamber with carbon dioxide, and the drift rate was determined with a Cary Model 31 vibrating reed electrometer. A standard sample of tritium-labeled polymer (Nuclear Chicago Co.) was used to calibrate the entire method.<sup>4</sup>

A correction for the isotope effect was made by using the data published by Kohn and co-workers<sup>3</sup> for similar systems (factor = 1.3). A preliminary check on the isotope effect in our work gave a factor of 1.56. This difference is most likely due to the fact that only a twofold excess of methanol was used in our experiments. If we had used the factor 1.56 for the isotope effect in our calculations, our values for the number of metal-polymer bonds would have been consistently higher by 20%.

## RESULTS AND DISCUSSION

With the apparatus used in our studies, the rate of polymerization can be followed continuously through the reaction by recording the pressure drop on the propylene reservoir. Rates obtained in this way correlate well with those obtained by direct methods, such as weighing the amount of polymer formed after a given time.

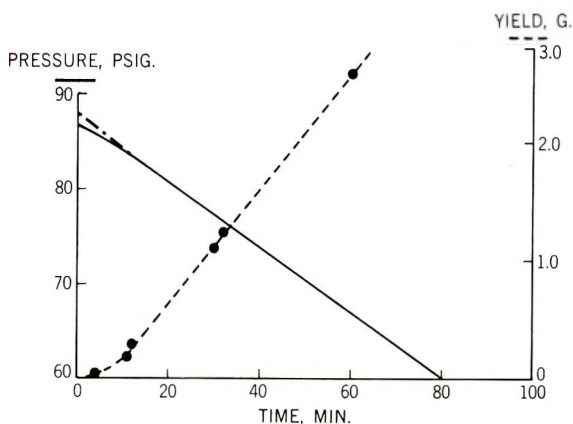


Fig. 2. Rate curves for system III.

With the three catalyst systems studied, polymerization started as soon as the catalyst was contacted with monomer. However, with titanium(III) chloride-diethylaluminum chloride (system II) and titanium(III) chloride-diethylaluminum dichloride-HPT (system III), there was an initial period of approximately 10 min. during which the rate accelerated continuously after addition of the metal alkyl. After this, the rate remained virtually constant for an hour or more. Typical rate curves obtained from pressure-drop measurements and by gravimetric measurements are shown in Figure 2. The pressure drop and yield curves both indicate that the rate increases within the first 10 min. A single batch of titanium(III) chloride was used; it was divided among many small containers so that the activity remained constant over the period of the experiments. The rates recorded in most of this work were calculated from the straight-line portion of the curve. All experiments were run in duplicate, and the rates recorded are averages. If the duplicates disagreed by more than 20%, additional runs were made and averaged. Generally, the difference between duplicate experiments was less than 5%. For system II, the overall polymerization rates per gram of titanium(III) chloride agree within a factor of 2 with those obtained by other workers,<sup>1-3</sup> even though we used different solvents and different catalyst concentrations.

The kinetics for catalyst system III have been described by Coover and Joyner.<sup>5</sup> The standard catalyst proportions used were 1/0.6/1 of  $C_2H_5-AlCl_2/HPT/TiCl_3$ . With this system at 70°C., the overall rate of polymerization  $R_p$  was a linear function of the pressure and, hence, of the monomer concentration. This first-order dependence on monomer concentration has been shown for systems I and II by Natta and others.<sup>1</sup>

The rate was also first-order in titanium concentration, as was also found for other titanium(III) chloride systems. Changing the amount of HPT, however, caused the rate to reach a maximum when the mole proportion of HPT was about 0.7. No appreciable polymerization was obtained in the

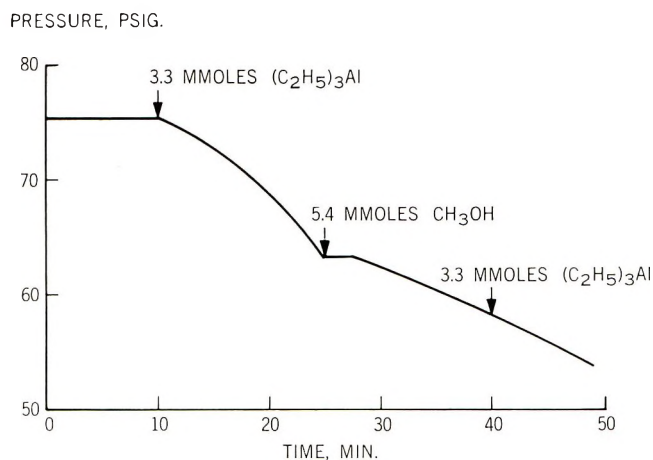


Fig. 3. Rate curves during catalyst deactivation of system I.

absence of HPT or with more than 1.0 mole HPT/mole of ethylaluminum dichloride.<sup>5</sup> The rate of polymerization increased with temperature up to 80°C., with an apparent activation energy of 8.7 kcal./mole.

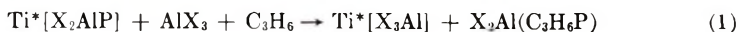
These results were consistent with those published on other catalyst systems containing titanium(III) chloride. However, the key to understanding the mechanism of polymerization lies in obtaining a better knowledge of the nature of the active sites. In the present study, tritiated methanol was used to destroy the active sites, and an estimate of the number of metal-carbon bonds was made by counting the tritium chemically united with the polymer. The techniques used were similar to those of Feldman and Perry<sup>6</sup> and Kohn and co-workers.<sup>3</sup> It was shown experimentally that 0.5 mole methanol/mole ethylaluminum dichloride was required to stop the polymerization completely. Smaller amounts would stop the polymerization temporarily; but after a few minutes it would start again, usually at a reduced rate. A typical rate curve for deactivation of the triethylaluminum-titanium(III) chloride catalyst (system I) is shown in Figure 3. This is strong evidence that the active sites are deactivated first, but that some are regenerated if excess alkylaluminum remains in solution. The addition of more triethylaluminum at a later stage did not alter the rate. This indicates that the metal alkyl is acting as a chain-transfer agent.

In agreement with the work of Kohn and co-workers,<sup>3</sup> our work indicates that the number of metal-polymer bonds increases rapidly with time, even when the rate of polymerization is constant. This indicates a relatively high rate of chain transfer resulting in the formation of a metal-polymer bond unattached to an active site. Measurements of the effect of propylene concentration on the rate of chain transfer (Table I) indicate that the rate is directly proportional to the monomer concentration during the initial stages of the polymerization. These results agree with those of Natta.<sup>1</sup>

TABLE I  
Effect of Monomer Concentration on Chain-Transfer Rate  
of  $(C_2H_5)_2AlCl-TiCl_3$  System

Pressure, psi	[M], mole/l.	$R_{tr} \times 10^7$ , mole/l.-sec.	$R_{tr}/[M] \times 10^7$ , sec. <sup>-1</sup>
10.0	0.47	3.24	6.9
40.0	1.39	9.25	6.7

Thus, the chain-transfer process involves both monomer and alkylaluminum and may be written as follows:



where X may be alkyl or halogen and P is the polymer chain. The rate of chain transfer  $R_{tr}$  is given by eq. (2)

$$R_{tr} = k_{tr}[M][A]^\alpha[C^*] \quad (2)$$

where  $k_{tr}$  is the chain-transfer rate constant, [M] is the monomer concentration, [A] is the concentration of absorbed alkyl, and [C\*] is the concentration of active sites. The exponent  $\alpha$  is placed in the equation since Natta found  $\alpha = 1/2$ , but for our calculation,  $\alpha$  can be any value. Our studies indicate that the rate of chain transfer during the very early stages of the polymerization is very much higher than during the later stages. This is shown in Table II and Figure 4 for system III and in Table III and Figure 5 for system II. This is in contrast to studies of Natta,<sup>1</sup> Kohn and co-workers,<sup>3</sup> and Chien,<sup>2</sup> who measured the rate of transfer at considerably higher conversions and found much lower values. Data abstracted from these papers are shown in Figure 6, along with our data plotted on a comparable scale. These results at low conversions indicate that the extrapolations to zero time used by previous workers to estimate the number of active sites are open to question. In Figure 6, note that our experimental

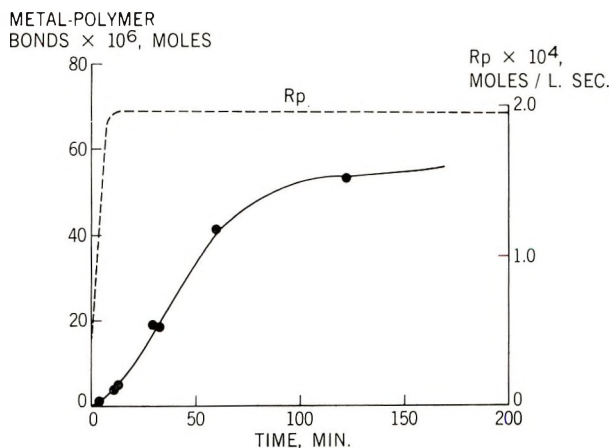


Fig. 4. Rate of formation of metal-polymer bonds in system III.

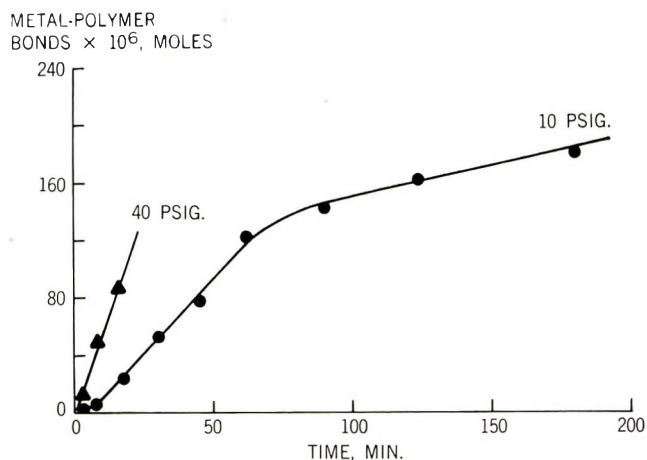


Fig. 5. Rate of formation of metal-polymer bonds in system II.

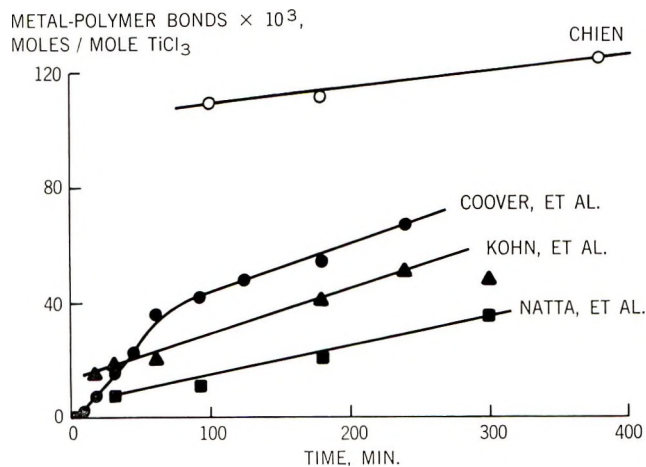


Fig. 6. Rate of formation of metal-polymer bonds for system II reported by various investigators.

data at high conversion agree with those of the previous literature and could be used to give a similar level of active site concentrations. Because of our experimental results at low conversions, however, we could not make the assumptions necessary for this extrapolation to zero time.

From our data for the  $\text{TiCl}_3$ -monochloride catalyst (system II), we concluded that the rate of formation of metal-polymer bonds is not constant throughout the polymerization. A plot of this rate as a function of time is shown in Figure 7. It can be seen that there are four distinct regions in the curve. In the first region, A, the rate of formation of metal-polymer bonds increases. Since this period coincides with the period when the rate of polymerization also increases, it seems reasonable to ascribe this acceleration to an increase in the number of active sites  $[\text{C}^*]$ . The rate is then

TABLE II  
Kinetics of  $C_2H_5AlCl_2$ -HPT- $TiCl_3$  System<sup>a</sup>

Time, min.	Yield, g.	Specific activity $\times 10^2$ , $\mu c./mg.$	No. metal- polymer bonds	
			$N \times 10^6$ , mole	$N \times 10^3$ , mole/mole $TiCl_3$
4	0.0426	2.71	0.79	0.24
11	0.1716	2.97	3.48	1.05
12	0.2747	0.50	3.78	1.15
30	1.104	2.46	18.6	5.60
32	1.237	2.10	17.8	5.32
60	2.573	2.3	40.4	12.1
121	4.524	1.7	52.6	15.8

<sup>a</sup> Reaction conditions: 106 ml. solvent; temp. = 70°C.; pressure = 10 psig.; [Ti] = 31.4 mmole/l.; [Al] = 31.4 mmole/l.

TABLE III  
Kinetics of  $(C_2H_5)_2AlCl$ - $TiCl_3$  System<sup>a</sup>

Pres- sure, psig	Time, min.	Yield, g.	Specific activity $\times 10^3$ , $\mu c./mg.$	$N \times 10^6$ , mole	$N \times 10^3$ , mole/mole $TiCl_3$
10	3	0.0457	13.8	2.01	0.61
10	8	0.239	8.75	6.61	2.0
10	18	1.66	21	24	7.2
10	30	3.09	5.13	51.8	15.7
10	45	5.45	4.45	76.7	23.2
10	62	8.44	4.56	122	37.0
10	90	9.12	4.86	142	42.5
10	124	11.99	4.24	161	48.8
10	180	14.65	4.03	177	53.7
10	240	17.46	3.98	220	67.0
40	2.6	0.600	5.49	9.6	2.9
40	8	2.64	6.47	49.9	15.1
40	17	6.08	4.84	85.6	25.9

<sup>a</sup> Reaction conditions: 106 ml. solvent; temp. = 70°C.; [Ti] = 31.4 mmoles/l.; [Al] = 31.4 mmoles/l.

nearly constant for about an hour (region B); then, it decreases to a considerably lower value (region C) and remains constant (region D) for a period of at least 4 hr. Since the rate of polymerization remains unaltered during the entire region covered by B, C, and D, it is unlikely that these changes can be due to a reduction in the active site or monomer concentrations. We suggest that the observed decrease in rate of metal-polymer bond formation occurs after depletion of absorbed alkylaluminum adjacent to the catalyst site, when the equilibrium concentration of alkyl is reduced because of the necessity for diffusion through a relatively thick layer of polymer surrounding the site.

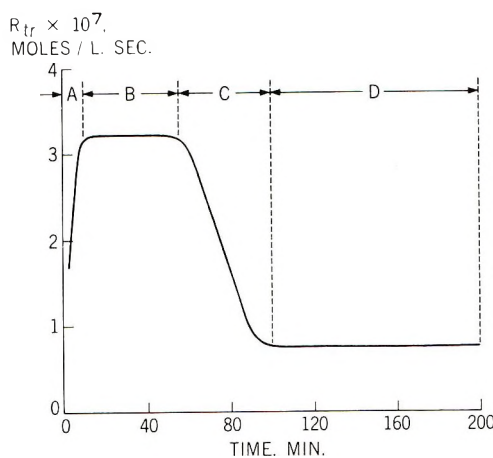


Fig. 7. Rate of formation of metal-polymer bonds for system II as function of time of polymerization.

An estimate of the number of active sites present during the early stages of the polymerization can be made if one makes the reasonable assumption that the rate of chain transfer is proportional to the number of active sites as described in eq. (2). The total number of metal-polymer bonds  $N'$  formed by chain transfer in time  $t$  is as given in eq. (3).

$$N' = \int_0^t R_{tr} dt = \int_0^t k_{tr} [M] [A]^\alpha [C^*] dt \quad (3)$$

The monomer concentration is constant under the experimental conditions, and  $[A]$  appears to be constant during the first 10–60 min. We can, therefore, write:

$$N' = k_{tr} [M] [A]^\alpha \int_0^t [C^*] dt \quad (4)$$

The amount of polymer,  $w$ , formed in time  $t$  is given by eq. (5):

$$w = \int_0^t R_p dt = k_p [M] \int_0^t [C^*] dt \quad (5)$$

and

$$N' = w k_{tr} [A]^\alpha / k_p \quad (6)$$

where  $R_p$  is the rate of propagation and  $k_p$  is the propagation rate constant. The value of  $k_{tr} [A]^\alpha / k_p$  can be determined from the ratio of the chain-transfer rate  $R_{tr}$  to the propagation rate  $R_p$ , which is the polymerization rate after steady-state conditions have been reached; at which time, the concentration of active centers is constant. Thus, at steady-state conditions

$$N' = w R_{tr} / R_p \quad (7)$$

The measured number of metal-polymer bonds  $N$  at any time  $t$  will be equal to

$$N = [C^*] + N' \quad (8)$$

TABLE IV  
Calculation of Active Site Concentrations for  $(C_2H_5)_2AlCl-TiCl_3$  System

Time, min.	Yield, g.	Propylene poly- merized, mmole	$k_p[A]^0/k_p$ $\times 10^4$	$N' \times 10^6$ , mole	$N \times 10^6$ , mole	$[C^*]$ $\times 10^6$ , mole
3	0.0457	1.09	5.94	0.65	2.01	1.4
8	0.239	5.68	5.94	3.37	6.61	3.2
18	1.66	39.4	5.94	23.4	24	0.6
30	3.09	73.4	5.94	43.7	51.8	8.1

which allows the calculation of  $[C^*]$  from the experimental data. If, as in the present case, the actual rate of polymerization at the time of deactivation is determined, it is then possible to estimate the absolute value of the propagation rate constant  $k_p$  from eq. (5). Examples of such calculations are shown in Table IV for system II.

The difficulty in these calculations is that the chain-transfer rate is so much greater than was estimated from earlier work that it is necessary to stop the reaction at very low conversions (less than 0.2 g. polymer/g.  $TiCl_3$ ); otherwise, the correction for chain transfer is very much larger than  $[C^*]$ , which must be determined by difference. This is shown in Table IV where after 18 min. the correction is too large to allow an estimate of  $[C^*]$ . Estimates of  $[C^*]$  for the three catalyst systems are shown in Table V, along with values for the propagation rate constant at 70°C. The important factor to note is that the number of active sites per mole of titanium, estimated in this way, is far lower than estimated previously. This suggests that the active sites may be present only at dislocations of the crystal surface and are not available at virtually every part of the titanium(III) chloride surface as was indicated by earlier results.<sup>2</sup> Further, the absolute propagation rate appears to be greater, at least ten times, than that of earlier estimates. This means that the lifetime  $\tau$  of a growing polymer chain is very short at low conversions. The propagation rate is of the same magnitude as that for the free-radical polymerization of styrene ( $k_p = 145$  l./mole-sec. at 60°C.). Our data for active site concentrations obtained with system II are compared with data reported by Natta, Chien, and Kohn and co-workers in Table VI. These data were obtained with catalysts at similar temperatures and monomer concentrations, and the measured polymerization rates were similar. We attribute the discrepancies to the measurement of transfer rates at relatively high conversions by the other authors. If our data at high conversions are extrapolated to zero time, the active site concentrations are similar to those calculated by other authors (Fig. 6).

It should also be noted that in our work, after about 60 min. in the case of system II, the rate of formation of metal-polymer bonds decreased markedly to about the value determined by previous work (Figs. 6 and 7). This occurs when the yield of polymer exceeds 2 g./g.  $TiCl_3$ . At this point,



TABLE V  
 Active Site Measurements

Catalyst system	Catalyst	$R_p \times 10^4$ , mole/l.-sec.	$R_{tr} \times 10^7$ , mole/l.-sec.	$[C^*] \times 10^5$ , mole/l.	$\bar{W}k_{tp}$ , l./mole-sec.	$\tau$ , sec.	$[C^*] \times 10^3$ , mole/mole TiCl <sub>3</sub>
I	(C <sub>2</sub> H <sub>5</sub> ) <sub>3</sub> Al/TiCl <sub>3</sub> (1/1) <sup>a</sup>	22.6	26	~10	48	38	3
II	(C <sub>2</sub> H <sub>5</sub> ) <sub>2</sub> AlCl/TiCl <sub>3</sub> (1/1) <sup>a</sup>	5.45	3.2	3	40	94	1
III	C <sub>2</sub> H <sub>5</sub> AlCl <sub>2</sub> /HPT/TiCl <sub>3</sub> (1/0.6/1) <sup>a</sup>	1.86	1.3	0.8	50	62	0.2

<sup>a</sup> Mole proportions of components.

 TABLE VI  
 Summary of Active Site Data for (C<sub>2</sub>H<sub>5</sub>)<sub>2</sub>AlCl-TiCl<sub>3</sub> System

Reference	Solvent	Temp., °C.	Propylene, psia	TiCl <sub>3</sub> concn., mmole/l.	Method	$[C^*] \times 10^3$ , mole/mole TiCl <sub>3</sub>
Chien <sup>2</sup>	Heptane	50	19.3	1.25	C <sup>14</sup>	80-120
Kohn et al. <sup>3</sup>	Hexane	50	27.0	6.0	H <sup>3</sup>	28
Natta et al. <sup>1</sup>	Heptane	70	8.7	19.5	C <sup>14</sup>	6
Coover et al.	40/60 Benzene-heptane	70	24.7	31.4	H <sup>3</sup>	1

the inherent viscosity of the polymer begins to increase. This effect can be explained by the occlusion of the active site with relatively large amounts of polymer. This would reduce the rate at which the metal alkyl can reach the site and, hence, the effective rate of chain transfer. To explain the invariance of the polymerization rate, it must be assumed that the monomer is not prevented from reaching the site by the presence of polymer, at least not until considerably higher conversions are reached.

### CONCLUSION

Our studies indicate that previous estimates of active site concentrations for  $(C_2H_5)_2AlCl-TiCl_3$  catalysts are probably too high by at least a factor of 10. The reason for the previous high estimates is the marked reduction in chain-transfer rate which occurs when the amount of polymer formed exceeds about 2 g./g.  $TiCl_3$ . It is probable that this lower chain-transfer rate can be attributed to the exhaustion of chemisorbed metal alkyl adjacent to the site and to the necessity for diffusion of free metal alkyl through a relatively thick layer of polymer to reach the site during the later stages of the polymerization. The chain-transfer process appears to involve both alkylaluminum and monomer, but the effective monomer concentration is apparently not reduced by the diffusion process until a later stage in the polymerization. The propagation rate is, therefore, unaffected; but the chain-transfer rate is reduced. This leads to the formation of polymer with a much higher molecular weight. Extension of this process leads to the observed broad distribution of molecular weights in polypropylene.

As a result of the low value of active site concentrations (about  $10^{-3}$  mole/mole  $TiCl_3$ ) determined in this work for the  $C_2H_5AlCl_2-HPT-TiCl_3$  catalyst, the absolute value calculated for the propagation rate constant for propylene polymerization is in the range of 50 l./mole-sec.; and the average lifetime of a growing polymer molecule during the early stages of the polymerization is very short (minutes). These are of the same order as those for the free-radical polymerization of styrene.

These results, particularly the active site studies, suggest that a reevaluation of previous kinetic work should be undertaken. In particular, more data should be obtained on the kinetics of the very early stages of the polymerization, and more attention should be directed to the role of the solid polymer layer which surrounds the active site.

The authors thank C. M. Shelton, for his very capable work on the kinetic runs and tritium-labeling experiments; M. A. McCall, for purification and preparation of many of the compounds used; and T. R. Booher and K. J. Fraley for radioactive counting of the labeled polymers.

### References

1. G. Natta and I. Pasquon, *Advan. Catal.*, **9**, 1 (1959).
2. J. C. W. Chien, *J. Polymer Sci. A*, **1**, 425 (1963).
3. E. Kohn, H. J. L. Schuurmans, J. V. Cavender, and R. A. Mendelson, *J. Polymer Sci.*, **58**, 681 (1962).

4. T. R. Booher, Tennessee Eastman Co., unpublished work.
5. H. W. Coover, Jr. and F. B. Joyner, *J. Polymer Sci. A*, **3**, 2407 (1965).<sup>†</sup>
6. C. F. Feldman and E. Perry, *J. Polymer Sci.*, **46**, 217 (1960).

### Résumé

La concentration en site actif a été déterminée en utilisant des catalyseurs anioniques coordonnés marqués au tritium contenant du chlorure de titane III violet (dénommé dans cette communication comme chlorure de titane III ou  $\text{TiCl}_3$ ). Ces catalyseurs ont été utilisés pour la polymérisation du propylène. Des catalyseurs à trois composants, aussi bien que des catalyseurs à deux composants ont été utilisés. Des estimations antérieures de la concentration en site actif pour  $(\text{C}_2\text{H}_5)_2\text{AlCl-TiCl}_3$  semblent être trop élevées d'au moins un facteur de 10. La raison de ces estimations antérieures élevées peut être attribuée à la réduction appréciable de vitesse de transfert de chaîne qui se passe lorsque la quantité de polymères formées dépasse 2 g./g. de  $\text{TiCl}_3$ . Le processus de transfert de chaîne apparaît impliquer à la fois l'alcoylaluminium et le monomère; mais la concentration de monomère effective est apparemment non réduite jusqu'à une étape ultérieure de la polymérisation. La vitesse de propagation est, de ce fait, non affectée; mais la vitesse de transfert est réduite, amenant à la formation d'un polymère de poids moléculaire beaucoup plus élevé. Par extension de ce processus on pourrait expliquer la distribution plus large des poids moléculaires du polypropylène. Comme résultat de la faible valeur des concentrations en site actif (environ  $10^{-3}$  mole/mole de chlorure de titane III), la valeur absolue calculée pour la constante de vitesse de propagation de la polymérisation de propylène se situe vers 50 l. mole<sup>-1</sup> sec<sup>-1</sup>, et la durée de vie moyenne d'une molécule de polymère croissante au cours des premières étapes de polymérisation est d'environ 1 minute.

### Zusammenfassung

Die Konzentration der aktiven Stellen an drei anionischen Koordinationskatalysatoren mit violetter Titan(III)chlorid (Später als Titan(III)chlorid oder  $\text{TiCl}_3$  bezeichnet) wurde durch Markierung mit Tritium bestimmt. Diese Katalysatoren wurden bei der Propylenpolymerisation verwendet. Es wurden 3-Komponenten und 2-Komponenten-Katalysatoren untersucht. Frühere Berechnungen der Konzentration der aktiven Stellen für  $(\text{C}_2\text{H}_5)_2\text{AlCl-TiCl}_3$ -Katalysatoren scheinen um mindestens einen Faktor 10 zu hoch zu sein. Der Grund für diese früheren hohen Werte kann in der bei einer Bildung einer Polymermenge von mehr als etwa 2 g/g  $\text{TiCl}_3$  auftretenden Herabsetzung der Kettenübertragungsgeschwindigkeit liegen. Der Kettenübertragungsvorgang scheint sowohl über Aluminiumalkyl als auch über Monomeres zu verlaufen, jedoch wird die effektive Monomerkonzentration erst in einem späteren Stadium der Polymerisation reduziert. Die Wachstumsgeschwindigkeit bleibt daher unbeeinflusst. Die Übertragungsgeschwindigkeit jedoch wird reduziert, was zur Bildung von Polymeren mit viel höherem Molekulargewicht führt. Eine Vergrößerung dieses Prozesses konnte zur beobachteten breiten Molekulargewichtsverteilung bei Polypropylen führen. Als Folge des niedrigen Wertes der Konzentration aktiver Stellen [etwa  $10^{-3}$  Mol/Mol Titan(III)chlorid] liegt der für die Wachstumsgeschwindigkeitskonstante bei der Propylenpolymerisation berechnete Absolutwert im Bereich von 50 l.-Mol<sup>-1</sup> sec<sup>-1</sup> und die Mittlere Lebensdauer eines wachsenden Polymermoleküls ist während des Frühstadiums der Polymerisation etwa 1 min.

Received April 27, 1966

Prod. No. 5144A

## ESR Study of Free Radicals Formed by $\gamma$ -Irradiation of Poly(ethylene Terephthalate)\*

D. CAMPBELL, K. ARAKI, and D. T. TURNER, *Camille Dreyfus Laboratory, Research Triangle Institute, Durham, North Carolina 27709*

### Synopsis

Free radicals formed by  $\gamma$ -irradiation of oriented samples of poly(ethylene terephthalate) (PET) were studied at 25°C. by ESR spectroscopy. The  $G$  value for trapped free radicals is 0.02. The predominant radical is identified as  $-\text{O}-\dot{\text{C}}\text{H}-\text{CH}_2-\text{O}-$ , and a minor component of the spectrum is tentatively assigned to the radical  $-\text{CO}-\dot{\text{C}}_6\text{H}_3-\text{CO}-$ . The absence of cyclohexadienyl type radicals is discussed. Previously reported dose rate effects in PET are explained by reference to a chain reaction involving  $\beta$ -bond scission of the radical  $-\text{O}-\dot{\text{C}}\text{H}-\text{CH}_2-\text{O}-$ .

### INTRODUCTION

Previously, samples of polyethylene terephthalate (PET) were reported to give ESR spectra of width up to 100 gauss after exposure to various high energy radiations but these had too little fine structure to allow identification of free radicals.<sup>1-4</sup> Recently, a better-resolved signal was obtained by  $\gamma$ -irradiation of an oriented sample of PET and eight lines assigned to the free radical  $-\text{O}-\dot{\text{C}}\text{H}-\text{CH}_2-\text{O}-$ .<sup>5</sup> Actually, such a radical would be expected to give either eight- or six-line spectra depending on orientation in the magnetic field.<sup>6</sup> The present paper describes attempts to find such spectra by varying the orientation of PET exposed to  $\gamma$ -radiation *in vacuo* and reports evidence for the presence of a further radical. This information is used to interpret the mode of formation of carboxyl groups and its dependence on dose rate.<sup>7</sup>

### EXPERIMENTAL

The PET was a biaxially oriented film of about 50% crystallinity, as judged by x-ray studies<sup>8</sup> (Mylar C film, duPont, of thicknesses 0.0025 and 0.00125 cm.). Samples were cut from a roll of film and either rolled up or arranged in stacks (Fig. 1). After thorough degassing, samples were sealed *in vacuo* in Suprasil tubes and exposed, either in liquid nitrogen or at room temperature, to  $\gamma$ -radiation from a <sup>60</sup>Co source; dose rate 0.2 Mrad/hr. After irradiation, tubes were annealed and first or second

\* Presented in part, at the 150th National Meeting, American Chemical Society, Atlantic City, N. J., September 1965.

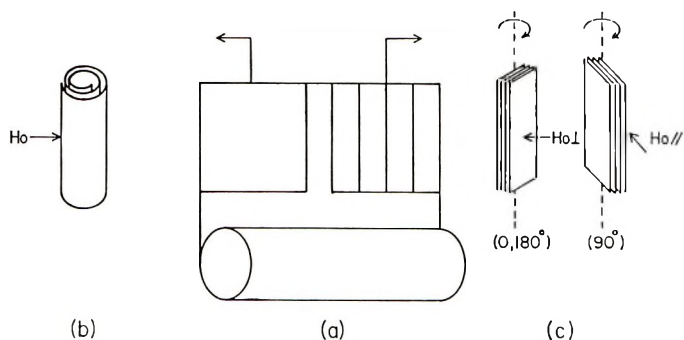


Fig. 1. Sampling of roll, and orientation of stacks with respect to magnetic field  $H_0$ .

derivatives of absorption intensity recorded as a function of magnetic field intensity with a Varian V.4502-10 spectrometer. The orientation of samples in the magnetic field, and in particular the designation used for stacks of films rotated through  $180^\circ$ , is indicated in Figure 1.

The number of free radicals was determined by numerical integration of a first derivative curve and by comparison with  $\alpha, \alpha'$ -diphenyl- $\beta$ -picryl-hydrazyl.

## RESULTS AND DISCUSSION

### Irradiation at $-196^\circ\text{C}$ .

PET became violet on irradiation at  $-196^\circ\text{C}$ . and when examined at this temperature, after a dose of 2 Mrad, gave the signal shown in Figure 2*a*. When this sample was removed from liquid nitrogen it became colorless and the signal decayed within a few minutes to a scarcely detectable level. A more pronounced room temperature spectrum was eventually obtained by reirradiation of the same sample, to make a total dose of 5 Mrad at  $-196^\circ\text{C}$ ., and by increasing the signal amplification to 20 times that used in obtaining Figure 2*a*. The new signal was distinctly different (Fig. 2*b*).

Previously, it was reported that after a dose of 50 Mrad at  $-196^\circ\text{C}$ . PET became reddish-brown and gave a singlet spectrum. On warming, this color gradually faded and the singlet decayed without any distinct change in shape such as reported here in Figure 2. It was suggested that the  $-196^\circ\text{C}$ . signal was due to two paramagnetic species which disappear at different rates on warming.<sup>4</sup>

The more explicit interpretation offered here for the rather different observations made in the present work is as follows. The signal observed at  $-196^\circ\text{C}$ . and the intense coloration of the sample is due to a relatively large concentration of trapped electrons and positive ions. On warming, these charged species combine and the new signal is due to a smaller concentration of trapped free radicals. Previously, electron trapping at  $-196^\circ\text{C}$ . has been suggested in ESR studies of a number of compounds including succinic acid.<sup>9</sup>

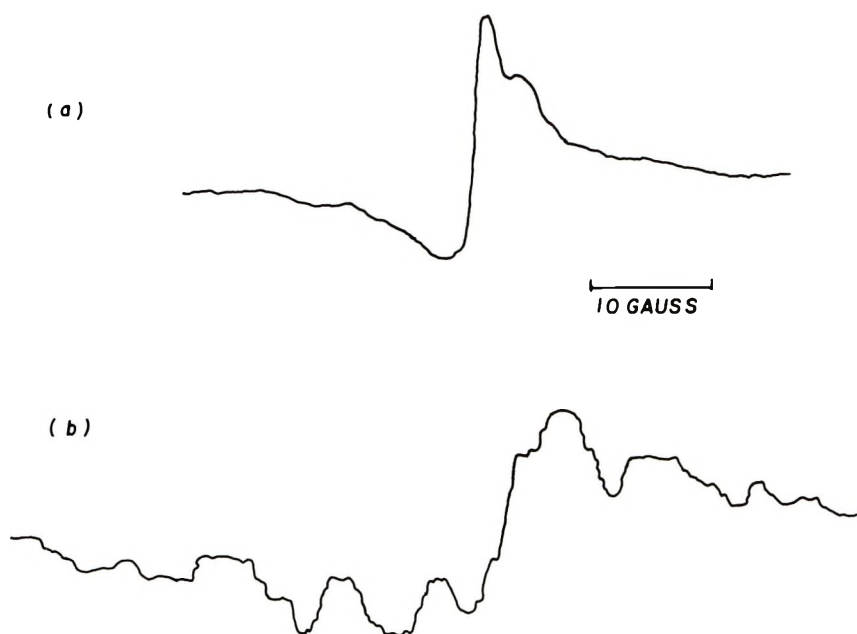
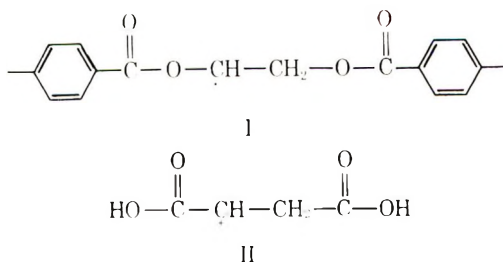


Fig. 2. ESR spectra of roll of Mylar film: (a) at  $-196^{\circ}\text{C}$ . (2 Mrad at  $-196^{\circ}\text{C}$ .); (b) at  $25^{\circ}\text{C}$ . (5 Mrad at  $-196^{\circ}\text{C}$ .). Amplification (b) is 20 times (a).

Spectra obtained after irradiation at  $-196$  or  $25^{\circ}\text{C}$ . were similar when examined at room temperature. Subsequent discussion will be limited to the paramagnetic species which remain trapped in  $\gamma$ -irradiated PET after heating to room temperature or above.

### Irradiation of Oriented Stacks of Film

It was shown previously that when  $\gamma$ -irradiated rolls of PET were examined with the magnetic field as shown in Figure 1b a nine-line spectrum resulted. By neglecting the central line, on the assumption that it was a contribution from some other unidentified radical, the remaining eight lines could be assigned to the free radical I.<sup>5</sup> An important feature of this assignment was an analogy with similar eight-line spectra which had been reported for  $\gamma$ -irradiated single crystals of succinic acid and which had been assigned to the free radical II.<sup>6</sup> Actually, the succinic acid work included



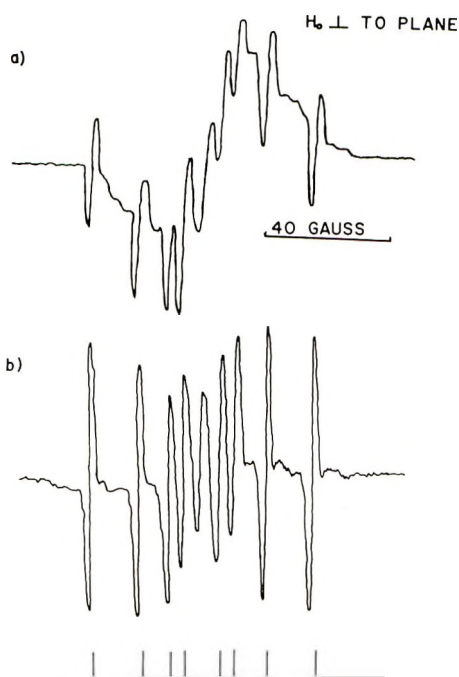


Fig. 3. ESR spectra of stack of films ( $H_0$  perpendicular to film c.f. Fig. 1c), dose, 10 Mrad at 25°C.: (a) examined *in vacuo*; (b) examined *in vacuo* after post-irradiation exposure to air for several minutes.

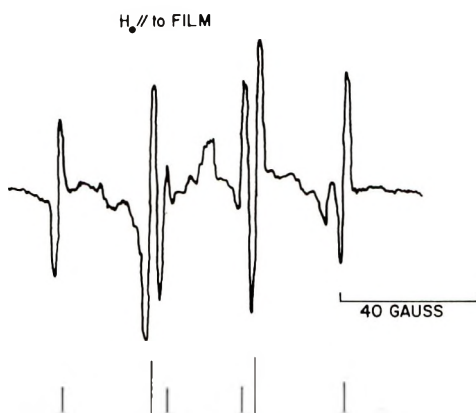


Fig. 4. ESR spectrum of stack of films after post-irradiation exposure to air ( $H_0$  parallel to film), dose, 10 Mrad at 25°C.

a detailed study of the variation of the spectrum with orientation of the  $\gamma$ -irradiated crystals in the magnetic field and showed that in addition, six-line hyperfine spectra occurred when the coupling of the anisotropic  $\alpha$ -proton became equal to that of one of the two nonequivalent  $\beta$ -protons. Attempts to simulate the behavior reported for  $\gamma$ -irradiated succinic acid were

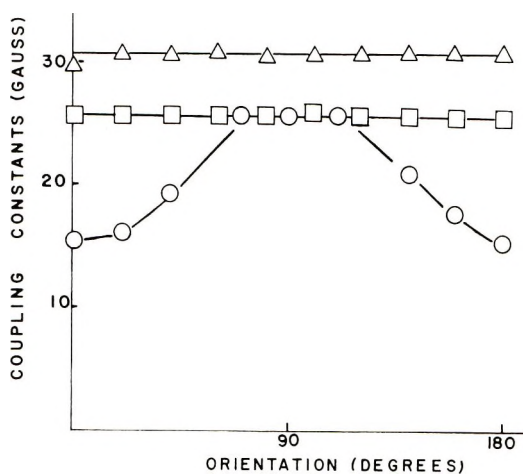


Fig. 5. Variation of proton coupling constants with orientation of stacks of films.

successful with the arrangements of film shown in Figure 1c. Examples of eight- and six-line spectra for PET are given in Figures 3 and 4, respectively. (Again, the central line is attributed to an unassigned radical.) The orientation dependence of the three coupling constants is shown in Figure 5; these results are similar to those reported for  $\gamma$ -irradiated succinic acid.<sup>6</sup>

A useful technique for improving the definition of the eight-line component at the expense of the diffuse background, which is evident in Figure 3a, is to allow access of air for a short time, and then to reexamine the sample *in vacuo*. The efficiency of such treatment may be judged by comparison of Figures 3a and 3b. The rationale for this procedure was that oxygen might be expected to destroy free radicals in the amorphous regions more rapidly, leaving a population of oriented radicals in the crystalline regions. This experiment was tried with the thinner films and consideration of the diffusion constant for oxygen in amorphous PET suggests that this explanation is reasonable.<sup>10</sup> This technique seems worth stressing as it may prove helpful in other cases where an amorphous component has to be tolerated in an otherwise oriented sample available for ESR studies.

The above data are offered as compelling evidence that the radical I is present in  $\gamma$ -irradiated PET. The data are of additional interest in relation to molecular orientation in the crystalline regions of such samples, but this aspect will not be pursued here.

#### Radicals Stable at 160°C.

Irradiated samples were heated in the unopened tubes between the glass transition and melting temperatures of the polymer, 80–260°C., to find whether any especially stable radical could be isolated from the population stable at room temperature. It was found that after heating for 20 min. at 160°C. the initial signal had largely decayed, leaving a doublet; resolution was best when stacks of films were examined with the orientation  $H_0 \perp$



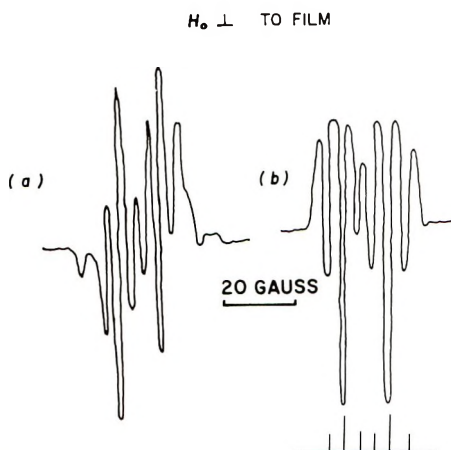
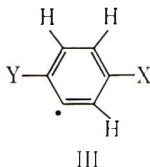


Fig. 6. Residual ESR spectrum after heating to 160°C. ( $H_0$  perpendicular to film): (a) first derivative; (b) second derivative.

(c.f. Fig. 1c). The spectrum comprises two triplets with intensity ratios of about 1:2:1 (Fig. 6). It is assigned to a radical in which the unpaired electron interacts with three protons; one has a coupling constant of 15 gauss and the other two are equivalent, having a coupling constant of about 4.5 gauss. This spectrum might be assigned to a radical of type III, in which neither X nor Y is a proton, on the assumption



that the coupling constants of the protons are in the order *ortho* (15 gauss) > *meta* (4.5 gauss) = *para*. These values may be compared with those reported previously for phenyl radicals, viz., *ortho* ( $18.1 \pm 1$  gauss) > *meta* ( $6.4 \pm 0.5$  gauss) > *para* (negligible).<sup>11</sup> Differences between the two sets of coupling constants may be due to differences in chemical structure, but more detailed information on the influence of substituents and orientation on the spectrum of a phenyl radical is required to justify more than a provisional assignment.

Evidence that the radical responsible for the spectrum shown in Figure 6 was present prior to heating was obtained by examination of a sample, which had not been heated, at sufficiently high microwave power to saturate the signal from radical I. The residual spectrum had phenyl characteristics, in the sense mentioned above, but could not be resolved as clearly as the spectrum shown in Figure 6.

#### Absence of Cyclohexadienyl Radicals

In earlier work ethylene glycol dibenzoate was studied as a single crystal model compound for PET. In addition to the  $-\text{O}-\dot{\text{C}}\text{H}-\text{CH}_2-\text{O}-$

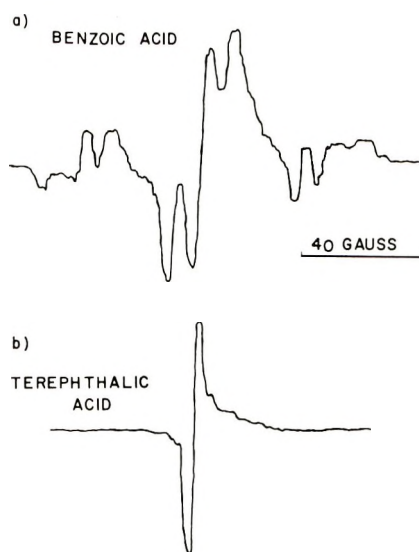
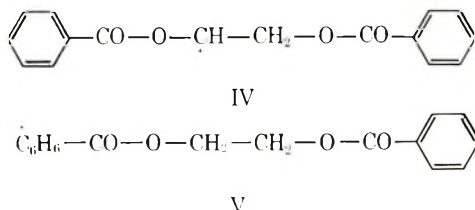


Fig. 7. ESR spectra of (a) polycrystalline benzoic acid; (b) polycrystalline terephthalic acid. Dose, 10 Mrad at 25°C.

radical (IV), convincing evidence was obtained for the presence of a cyclohexadienyl radical (V) after  $\gamma$ -irradiation at 25°C.; the latter radical was not evident in



samples irradiated at  $-196^\circ\text{C}$ .<sup>5</sup> In the present work, samples of PET were  $\gamma$ -irradiated at temperatures of up to  $160^\circ\text{C}$ . but no evidence for cyclohexadienyl radicals could be found. It was conjectured that the addition of a hydrogen atom to a substituted benzene ring might be sufficiently sensitive to the number and nature of the substituents to account for the difference between ethylene glycol dibenzoate (monosubstituted) and PET (*para*-disubstituted). Examination of a range of substituted benzenes lent weight to this point of view as may be illustrated by comparison of ESR spectra obtained after  $\gamma$ -irradiation of polycrystalline samples of benzoic acid and terephthalic acid. Benzoic acid gives a main triplet with a large coupling constant, about 45 gauss, which is characteristic of the methylene group in a cyclohexadienyl radical, along with secondary triplets which may be explained by coupling with other protons in the benzene ring (Fig. 7a; c.f. earlier spectrum for benzoic acid and comments on cyclohex-

adienyl radical<sup>12</sup>). By contrast, there is no indication of the presence of such a radical in the spectrum from terephthalic acid (Fig. 7b).

### Yield of Trapped Radicals

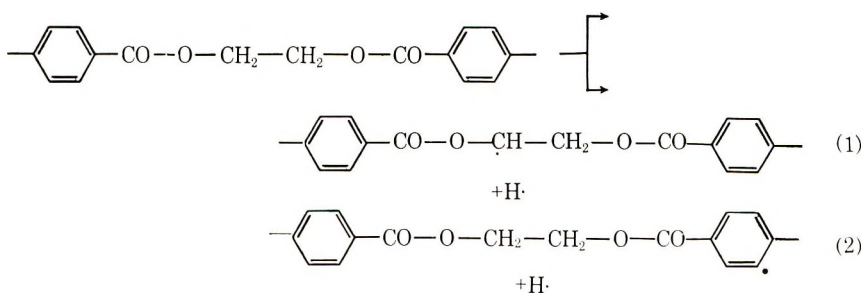
The concentration of free radicals which remained trapped in the polymers at 25°C. was proportional to the radiation dose in the range 0–20 Mrad and was similar for samples irradiated at –196 and at 25°C.:  $G$  (trapped radicals) = 0.02.

From a comparison of peak heights it is estimated that 90–95% of all the trapped radicals have the structure I.

### Comparison of Free Radicals and End Products

The following initial  $G$  values have been reported on  $\gamma$ -irradiation of PET *in vacuo* at 47°C. and at a dose rate of 0.12 Mrad/hr.: —COOH = 0.77, CO<sub>2</sub> = 0.17, CO = 0.11, H<sub>2</sub> = 0.015, and CH<sub>4</sub> = 0.003. Crosslinking and fracture of the macromolecules occurs. The ratio of fractures to crosslinks is too low for the polymer to reach the gel point, even after doses of up to 5000 Mrad.<sup>13</sup> For a given total dose the yield of carboxyl groups was found to decrease with increasing dose rate while, conversely, the limiting viscosity number of the polymer increased.<sup>7</sup>

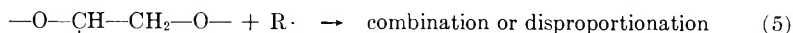
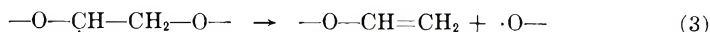
The closeness of the initial  $G$  values for trapped radicals and hydrogen suggests that reactions (1) and (2) are primary reactions resulting in radical formation on  $\gamma$ -irradiation of PET. In the absence of detectable amounts of radicals other than I and III it may be concluded that, at low doses, hydrogen atoms either combine or abstract hydrogen atoms from molecules. The result is the generation of isolated polymer radicals or pairs which are sufficiently separated in the crystalline or glassy regions for the partners to remain uncombined.



No radicals have been detected which could be associated directly with the copious evolution of CO and CO<sub>2</sub>. Presumably, such radicals would be formed in pairs with a separation of only one or two atomic diameters and are able to combine at 25°C. It is not clear whether radicals of this type contribute to the –196°C. signal.

The most striking feature of the radiation chemistry of PET is the dose rate effect. Previously, it was explained by a general free-radical mechan-

ism which did not specify either the concentration or chemical structure of the free-radicals involved. The present results allow a more explicit discussion of dose rate dependence. Free radicals of type I may suffer  $\beta$ -bond scission and provide a free-radical fragment [eq. (3)] which, in a further reaction [eq. (4)], provides another radical of type I along with a carboxyl endgroup.



This chain reaction continues until the type I radical encounters a second polymer radical or a hydrogen atom [eq. (5)]. The probability of termination of the chain would be expected to increase with dose rate and result in a lower yield of carboxyl groups for a given total dose. Also, it would result in a higher limiting viscosity number because of the earlier suppression of the chain of scission reactions.

Comparison of the low  $G$  (radical) value with the high value for  $G(-\text{CO}-\text{OH})$ , 0.77, suggests that reactions (2) and (3) involve fairly long chains. This observation would seem to provide a reasonable basis for understanding how a bimolecular reaction, such as reaction (5) might occur in a rigid medium. Previously, a "radical hopping" mechanism was proposed to account for certain features of the radiation chemistry of crystalline polyethylene.<sup>14</sup>

We thank Dr. Ichiro Miyagawa of the University of Alabama for valuable discussions.

This work was supported by the Langley Research Center of the National Aeronautics and Space Administration under NASA Contract NAS1-3183.

### References

1. S. Ohnishi, Y. Ikeda, M. Kashiwagi, and I. Nitta, *Polymer*, **2**, 119 (1961).
2. Z. Kuri and H. Ueda, *J. Polymer Sci.*, **50**, 349 (1961).
3. J. Sobue, Y. Tabata, and M. Hiraoka, *Kogyo Kagaku Zasshi*, **64**, 372 (1961).
4. Y. Hama, S. Okamoto, and N. Tamura, *Repts. Progr. Polymer Phys. Japan*, **7**, 351 (1964).
5. K. Araki, D. Campbell, and D. T. Turner, *J. Polymer Sci. B*, **3**, 993 (1965).
6. C. Heller and H. M. McConnell, *J. Chem. Phys.*, **32**, 1535 (1960).
7. G. F. Pezdirtz, G. D. Sands, and D. T. Turner, *J. Polymer Sci. A*, **4**, 252 (1966).
8. J. B. Lando, private communication.
9. H. C. Box, H. G. Freund, and K. T. Liga, *J. Chem. Phys.*, **42**, 1471 (1965).
10. V. T. Stannett, private communication.
11. J. E. Bennett, B. Mile, and A. Thomas, *Chem. Commun.*, **12**, 265 (1965).
12. S. Ohnishi, T. Tanei, and I. Nitta, *J. Chem. Phys.*, **37**, 2402 (1962).
13. S. D. Burow, G. F. Pezdirtz, G. D. Sands, and D. T. Turner, *J. Polymer Sci. A-1*, **4**, 613 (1966).
14. M. Dole and C. D. Keeling, *J. Am. Chem. Soc.*, **75**, 6082 (1953).

### Résumé

Des radicaux libres formés par irradiation  $\gamma$  d'échantillons orientés de téréphthalate de polyéthylène (PET) ont été étudiés à 25°C par spectroscopie électronique paramagnétique. La valeur  $G$  des radicaux libres piégés est 0.02. Le radical prédominant a été

identifié comme  $-\text{O}-\dot{\text{C}}\text{H}-\text{CH}_2-\text{O}-$  et un composant moins important du spectre est un radical de structure probable  $-\text{CO}-\dot{\text{C}}_6\text{H}_3-\text{CO}-$ . L'absence de radicaux du type cyclohexadiényle est discuté. Les effets précédemment rapportés concernant la vitesse de dose au sein du PET sont expliqués par comparaison avec la réaction en chaîne qui inclut une scission du lien  $\beta$  du radical  $-\text{O}-\dot{\text{C}}\text{H}-\text{CH}_2-\text{O}-$ .

### Zusammenfassung

Durch  $\gamma$ -Bestrahlung orientierter Polyäthylenterphthalatproben (PET) gebildete freie Radikale wurden bei 25°C ESR-spektroskopisch untersucht. Der  $G$ -Wert für eingefangene freie Radikale ist 0,02. Das vorherrschende Radikal wird als  $-\text{O}\dot{\text{C}}\text{H}-\text{CH}_2-\text{O}-$  identifiziert und eine Nebenkomponente im Spektrum wird vorläufig dem Radikal  $-\text{CO}-\dot{\text{C}}_6\text{H}_3-\text{CO}-$  zugeordnet. Die Abwesenheit von Radikalen vom Zyklohexadienyltyp wird diskutiert. Früher festgestellte Dosisleistungseffekte beim PET werden durch Annahme einer Kettenreaktion über  $\beta$ -Bindungsspaltung des Radikals  $-\text{O}-\dot{\text{C}}\text{H}-\text{CH}_2-\text{O}-$  erklärt.

Received March 31, 1966

Prod. No. 5128A

## Studies of Thermal Cyclizations of Polyamic Acids and Tertiary Amine Salts

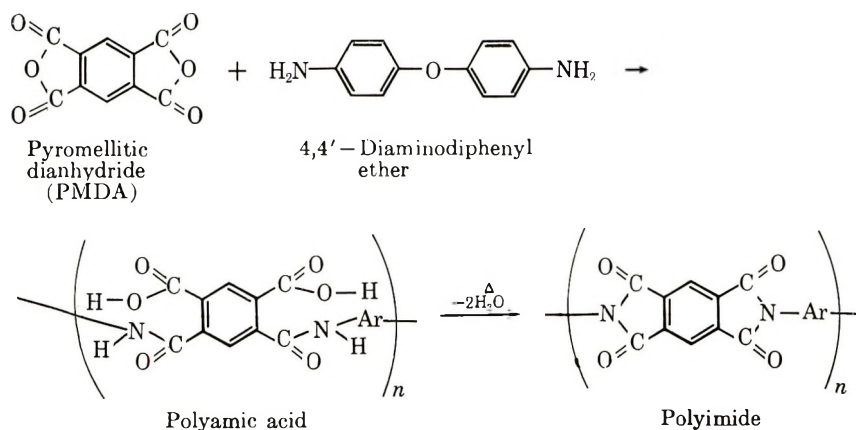
JOHN A. KREUZ, A. L. ENDREY, F. P. GAY, and C. E. SROOG,  
*Film Department, E. I. du Pont de Nemours and Company, Inc.,  
 Buffalo, New York 14207*

### Synopsis

Thermal conversion rates of the polyamic acid derived from pyromellitic dianhydride and 4,4'-diaminodiphenyl ether are presented. Formation of the imide ring proceeds by fast and slow first-order processes. Tertiary amines give ring closures faster by a factor of 10 than the free acid. The enhancement is an activation entropy rather than an activation energy effect.

### INTRODUCTION

A general method of preparation of cyclic imides from amic acids is thermal dehydration. Variations of this technique include heating above the melting point,<sup>1</sup> azeotroping the water of cyclization,<sup>2</sup> boiling in glacial acetic acid,<sup>3</sup> and heating in the presence of triethylamine.<sup>4</sup> Until recently, these syntheses were restricted to small molecules, but the discovery<sup>5,6</sup> of polyamic acids has extended thermal cyclization as a convenient route to polyimides.<sup>5-8</sup> Accordingly, rate data on thermal ring closures of polyamic acids and polyamic acid tertiary amine salts become of interest. Data for the system derived from pyromellitic dianhydride (PMDA) and 4,4'-diaminodiphenyl ether are presented.



The symmetrical and asymmetrical polyamic acid structures are intended, since both are possible.

## RESULTS AND DISCUSSION

The polyamic acid was prepared by the technique described previously,<sup>5-8</sup> and the thermal ring closure rate studies were made with films of this polymer cast from dimethylacetamide (DMAc). After attaining constant weight at room temperature under vacuum, the polyamic acid films contain about 28% DMAc. Thermogravimetric analyses of polyamic acid films show weight losses of 29% to 32% in the region of 170–200°C. (Fig. 1). Infrared analysis indicates about 80% conversion to polyimide after these treatments, so the weight losses include both solvent and water of cyclization, which alone would amount to only a 7% weight loss. These data suggest one mole of DMAc is associated with each carboxyl function. The theoretical value of DMAc on this basis is 29.4%, and such a solvate would lose 35.9% of its initial weight after 100% conversion. Solvate formation is reasonable in view of identification of complexes between DMAc and aromatic carboxylic acids<sup>8,9</sup> and makes simple weight loss measurements unsatisfactory for cyclization measurements.

The infrared spectra of polyamic acids differ significantly from those of the corresponding polyimides, so spectrophotometry is a convenient way to follow thermal imidization. Absorption of *n*-imide at 725 cm.<sup>-1</sup> was

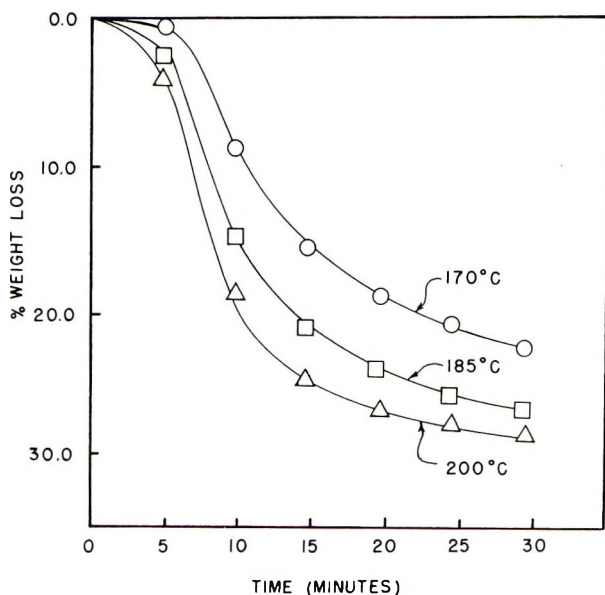


Fig. 1. Weight losses of polyamic acid films: ( $\Delta$ ) 28.5% after 100 min.; ( $\square$ ) 30.5% after 100 min.; ( $\circ$ ) 31.5% after 50 min. Film samples were 100 mg. each and 0.20 mil thick. Weight losses were produced isothermally in helium at the temperature specified. The arrows refer to the times at which the temperature reached the desired maximum.

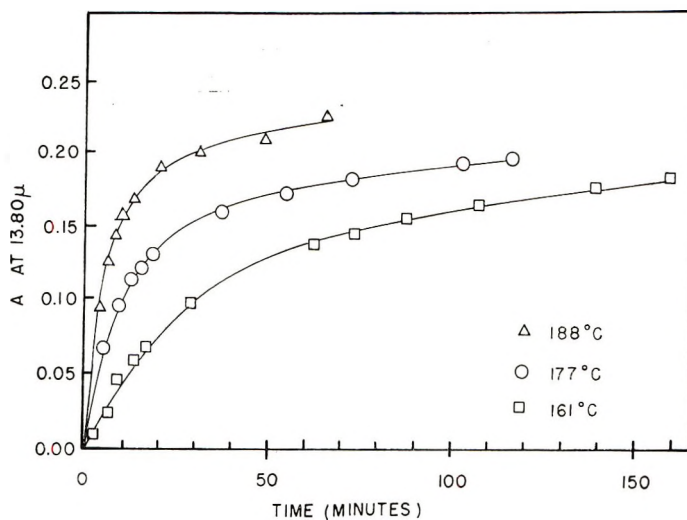


Fig. 2. Conversion rates of polyamic acid at various temperatures.

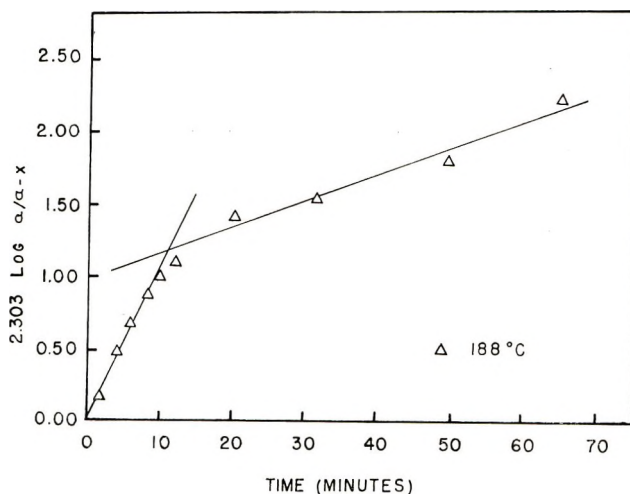


Fig. 3. Logarithmic plot of conversion of polyamic acid.

monitored with film samples placed in a heated cell which surrounded the sample beam of a spectrophotometer. Beer's law was followed by DMAc solutions of *N-p*-phenoxyphenylphthalimide at  $725\text{ cm}^{-1}$  between 0.1 and 1.0M. The molar absorbance  $\epsilon$  is 315, and this value was close to that of our insoluble polyimide.

With the polyamic acid investigated, cyclization is very slow below  $150^\circ\text{C}$ . Beyond this point, imidization rate increases rapidly with temperature and is characterized by an initial rapid cyclization which changes into a slower cyclization process (Fig. 2). The data do not allow an unequivocal determination of the order of the reaction. Logarithmic plots



TABLE I  
Cyclizations of Poly(amic Acid)  
(4,4'-Diaminodiphenyl Ether with Pyromellitic Dianhydride)

Temp., °C.	$k$ , min. <sup>-1</sup> (1st step)	$k$ , min. <sup>-1</sup> (2nd step)	Conversion, % (1st step)
161	$1.95 \times 10^{-2}$	$4.5 \times 10^{-3}$	45 (in 38.0 min.)
177	$4.85 \times 10^{-2}$	$7.80 \times 10^{-3}$	55 (in 20.0 min.)
188	$1.12 \times 10^{-1}$	$1.94 \times 10^{-2}$	66 (in 11.5 min.)

of these data can be interpreted to mean that these imidizations can be divided into rapid and slow first-order ring closure steps. Figure 3 gives an example of this behavior at 188°C. As seen below, first-order behavior is observed in the thermal cyclization of model compounds. Diffusion control is believed to be unimportant during the first rapid cyclization, since a fivefold variation of film thickness does not influence this rate. Rate constants calculated on the basis of two first-order reactions are summarized in Table I together with the amount of conversion accomplished in the fast cyclization.

Analysis of these data gives an activation energy for the fast cyclization of  $26 \pm 3$  kcal./mole. The activation energy for the slow cyclization is  $23 \pm 7$  kcal./mole. The difference in the two values is not significant. The difference in the entropy of activation,  $-10$  e.u. for the fast reaction and  $-24$  e.u. for the slow, is significant and indicative that control of the rates resides in the frequency factor.

The reason for the larger loss of entropy of activation during the latter portion of conversion is not known at present. Possibly the role of diffusion is large, and the reaction should not be interpreted as first order. Increasing chain stiffness as cyclization proceeds may also decrease the ability of the amide groups of the chain to arrange themselves for cyclization, although the freedom of the carboxyl groups would not be expected to change appreciably. Another possible explanation, qualitatively agreeing with thermogravimetric analyses, is that DMAc assists in favorable orientation for ring closure and its loss before conversion retards imidization rates. A review of Figure 1 shows the largest percentages of total weight losses occur within 30 min. over the temperature range 170–200°C. These weight losses consist largely of DMAc, and comparison of rates of weight loss to rates of cyclization reveals that only temperatures above 177°C. give ring closure rates which are faster than weight loss rates.

For comparison with the polymeric system, rates of imidizations of two model compounds, *N*-phenylphthalamic acid and *N*-*p*-methoxyphenylphthalamic acid, were followed in DMAc at 150°C. Under these conditions these amic acids and their corresponding imides are soluble over the entire range of conversion. Both compounds cyclize without deviation from the first-order rate law to greater than 75% of the total cyclization, and rate constants are  $4.60 \times 10^{-2}$  and  $5.37 \times 10^{-2}$  min.<sup>-1</sup> for *N*-phenylphthalamic acid and *N*-*p*-methoxyphenylphthalamic acid, respectively. Although

TABLE II  
Rates of Cyclization of Tertiary Amine Salts of the Polyamic Acid of  
PMDA and 4,4'-Diaminodiphenyl Ether

Tertiary amine added <sup>a</sup>	$k$ , min. <sup>-1</sup> (1st step)	$k$ , min. <sup>-1</sup> (2nd step)	Relative rates <sup>b</sup>	Conversion, % (1st step)
Dimethyldodecylamine	$2.06 \times 10^{-1}$	$1.85 \times 10^{-2}$	10.6	83 (in 8 min.)
Tri- <i>n</i> -butylamine	$1.05 \times 10^{-1}$	$4.09 \times 10^{-3}$	5.4	73 (in 15 min.)
Tri- <i>n</i> -butylamine (140°C.)	$3.03 \times 10^{-2}$	—	—	—
Tri- <i>n</i> -butylamine (123°C.)	$4.80 \times 10^{-3}$	—	—	—
Triethylamine	$7.57 \times 10^{-2}$	$1.33 \times 10^{-2}$	3.9	69 (in 18 min.)
No amine	$1.95 \times 10^{-2}$	$4.52 \times 10^{-3}$	1.0	45 (in 38 min.)

<sup>a</sup> Temperatures at 161°C. unless otherwise specified.

<sup>b</sup> Relative rates are comparisons of the rate of the first fast cyclizations at 161°C. to that of the free polyamic acid.

these model amic acids bear out the first-order rate dependence of this cyclization, kinetic similarities to the thermal conversions of polyamic acids are limited. The primary difference of polymeric films is their sudden rate decrease during cyclization, but this as suggested above may be mainly a reflection of the loss of DMAc during conversion. In this regard, it is significant that cyclizations of these model compounds are facile in solutions of DMAc even at 150°C., whereas the polyamic acid in the presence of little DMAc requires a slightly higher temperature. Also, cyclization of *N*-phenylphthalamic acid in the solid phase at 150°C. is 42% complete at 80 min., but in DMAc at the same temperature 42% conversion occurs in 12 min.

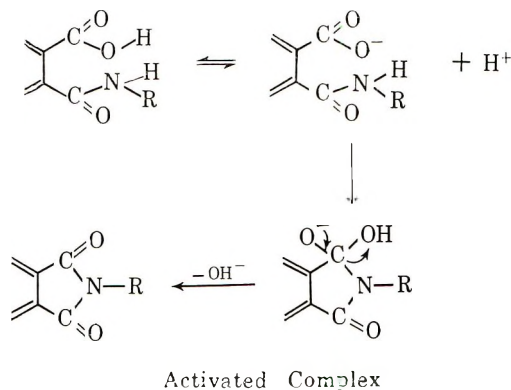
Addition of strong tertiary amines to polyamic acid solutions greatly increases the solution viscosity, and plots of intrinsic viscosity versus concentration show a steep rise similar to that previously reported.<sup>8</sup> For cyclization rate studies, the polymer of PMDA and 4,4'-diaminodiphenyl ether in combination with stoichiometric quantities of dimethyldodecylamine, tri-*n*-butylamine, and triethylamine were cast into films. After removal of excess solvent in vacuum, the presence of these tertiary amines is qualitatively detected in the infrared spectra by strong absorption in the aliphatic C-H stretching region at 2900 cm.<sup>-1</sup> Films of this polyamic acid contain 30 wt.-% of tri-*n*-butylamine and 6 wt.-% of triethylamine.

Thermal ring closures of salt films were amenable to infrared analysis. Rates are much faster than those of the corresponding free polyamic acid. Qualitatively, the rate curves are similar to those of untreated polyamic acid; initially there is a fast first-order conversion, which is followed by a slower first-order conversion. These data are summarized in Table II. Depending on the tertiary amine used, rates up to ten times that of the free

polyamic acid are observed. The tri-*n*-butylamine salt of *N*-*p*-methoxyphenylphthalamic acid in DMAc also cyclizes by a first-order process up to 80% conversion with a rate constant (150°C.) of  $1.42 \times 10^{-1} \text{ min.}^{-1}$ . This is faster by a factor of 2.6 than that of the free amic acid under the same conditions.

The fast conversion step of the tri-*n*-butylamine/polyamic acid salt (Table II) gives an activation energy of  $26 \pm 3 \text{ kcal./mole}$  and an activation entropy of  $-5.3 \text{ e.u.}$  Again, the effect seems to reside primarily in the activation entropy.

A reaction path consistent with our data involves the ionized form of the polyamic acid as the preferred precursor to the activated complex. Equilibration of the *ortho* carboxylate anion with the amide hydrogen could afford an easy route to ring closure. We believe the free polyamic acid also cyclizes by the same path through ionization of polyamic acid but cannot exclude "neutral" ring closure through undissociated acid on the basis of the present data.



## EXPERIMENTAL

### Materials

Dimethylacetamide was distilled in dry equipment under an atmosphere of nitrogen at reduced pressure, and it was stored under nitrogen over Molecular Sieve 5A. Pyromellitic dianhydride was sublimed at 200°C./0.05 mm. just before use. Sublimation of 4,4'-diaminodiphenyl ether was carried out at 190°C./0.05 mm. The tertiary amines were distilled under nitrogen before use. Boiling temperatures of middle fractions were: dimethyldodecylamine, 94°C./1 mm.; tri-*n*-butylamine, 88°C./11 mm.; triethylamine, 38°C./126 mm.

### Preparation of Polyamic Acid Films

The polyamic acids were prepared by adding solid PMDA to a DMAc solution of a stoichiometric equivalent of diamine at room temperature under dry conditions.<sup>5,6</sup> The polymer of 4,4'-diaminodiphenyl ether

always constituted 10% solids in DMAc and ranged in inherent viscosity from 2.5 to 2.8 (0.5% in DMAc at 30°C.). Films of the polymer were cast onto dry glass plates with a 1.5-mil Bird applicator; the films were dried under nitrogen and vacuum at room temperature. Thermogravimetric analyses in He and measurements of ring closure rate were carried out with films prepared in this way. The instrument used was an Aminco Thermograv, American Instrument Co., Silver Spring, Md.

### Preparation of Tertiary Amine Salt Films

Solutions of tertiary amine salts of the polyamic acid of 4,4'-diaminodiphenyl ether were prepared by mixing the stoichiometric amount of the respective amine with a known weight of the polymer.<sup>10</sup> Occasionally, a local precipitation of polymer was observed at the point of addition of the tertiary amine, but a homogeneous solution resulted with continued stirring. Large increases in solution viscosity were noted on the addition of the tertiary amines. Films were prepared in the same manner as that described for the free polyamic acids, and measurements of ring closure rate were carried out.

### Determination of DMAc in Films

Determination of DMAc in the polyamic acid films were carried out by refluxing known weights of the films with aqueous sodium hydroxide (1*N*) for 1 hr., distilling the dimethylamine, and titrating the distillate as dimethylamine.<sup>5,6</sup> Controls showed this was efficient for total hydrolysis of DMAc. Determination of DMAc in the effluent gases of thermogravimetric studies were done by the Kjeldahl method, and up to 0.17 meq. of nitrogen was detected in 100 mg. of film sample.

### Analysis of Tertiary Salt Films

Estimations of tertiary amines present in polyamic acid salt films were carried out by nonaqueous titrations with perchloric acid with glacial acetic acid as solvent. Stirring the film samples for 2 hr. with the acetic acid effectively extracted the tertiary amines. A control titration of free polyamic acid films of 4,4'-diaminodiphenyl ether gave a blank showing 0.0058 meq. of amine per 46 mg. of film sample.

### Measurements of Temperature

A Perkin-Elmer 21 spectrophotometer was equipped with a hot cell which surrounded the sample beam of the spectrophotometer. Control of temperatures of the hot cell used to study the thermal conversions of polyamic acids consisted of a ballast heater-Variac combination on the bottom of the cell, and control heaters on opposite sides which were regulated with a Thermotrol. By adjusting the Variac and Thermotrol, narrow temperature variations were achieved with the hot cell. To prevent flow of heat from the hot cell to the Perkin-Elmer 21 spectro-

photometer, the plate attaching it to the spectrophotometer was water cooled. For monitoring temperatures, an iron-constantan thermocouple connected to a potentiometer was inserted into the brass block of the hot cell close to where the film holder and sample were located. If the thermocouple was placed in the well of the hot cell where the film sample resided, a constant but different temperature from that which was observed in the brass block itself was noted. Reported temperatures of conversions are based on averages of these measurements.

The time required for a film sample to reach the temperature of the hot cell or experimental conversion temperature was also determined by following the rate of increase of temperature of the brass film sample holder on insertion into the well of the hot cell. Repeated experiments showed that 3-5 min. was required for the brass film holder to attain the desired temperature.

### Measurements of Rates

Primary rate data based on absorbance at  $725\text{ cm.}^{-1}$  consisted of the differences in peak heights and base lines after each scan between  $754$  and  $690\text{ cm.}^{-1}$ . The base line was redrawn after every scan, since the background absorbance appeared to change continuously through the course of conversion. Data for the appearance of *n*-imide were subsequently fitted into the first-order rate expression:

$$2.303 \log[a/(a - x)] = kt$$

where  $a$  is the maximum absorption at  $725\text{ cm.}^{-1}$  for the film sample at experimental temperature when fully converted,  $x$  is the absorption of the peak at  $725\text{ cm.}^{-1}$  at experimental temperature, and  $t$  is time in minutes.

Complete conversion was assumed after treatment of a given polyamic acid film for 1 hr. at  $300^\circ\text{C.}$ , and it was noted that absorption at  $725\text{ cm.}^{-1}$  did not increase with time. When the diamine was 4,4'-diaminodiphenyl ether, the  $a$  value of a film 0.20 mil thick (dial gage) was 0.310 at room temperature. In addition, it was also determined on the basis of absorbance measurements at different temperatures that the band at  $725\text{ cm.}^{-1}$  at  $150$ - $200^\circ\text{C.}$  absorbed about 80% as intensely as at room temperature. This provided an  $a$  value of 0.250 between  $150^\circ\text{C.}$  and  $200^\circ\text{C.}$  for 0.20-mil films, and this value was varied proportionately for films of different thicknesses.

### Percentages of Conversion

Estimates of percentage conversion of the polyamic acid film samples were made after establishing the *n*-imide maximum absorptions or  $a$  values as described above. Assuming Beer's law was obeyed by absorption at  $725\text{ cm.}^{-1}$ , the percentage of conversion of any film sample was measured by a direct relationship of absorbance at  $725\text{ cm.}^{-1}$  to the  $a$  value.

### Activation Parameters

Activation energies were calculated in the normal way.

### Ring Closure Rates of Model Systems

The method of adding a chloroform solution of the amine to a stoichiometric equivalent of phthalic anhydride dissolved in chloroform was used to prepare *N*-phenylphthalamic acid and *N-p*-methoxyphenylphthalamic acid.<sup>11</sup> Precipitation of each amic acid continued as addition of amine proceeded. Each white product was filtered 30 min. after all amine was added, it was washed with chloroform, and dried under nitrogen and vacuum. A 96% yield of *N*-phenylphthalamic acid was obtained; it melted at 170.0–171.5°C.; analysis showed 5.80% N (calculated 5.80% N for C<sub>14</sub>H<sub>11</sub>NO<sub>3</sub>).

A 97% yield of *N-p*-methoxyphenylphthalamic acid was obtained, and it melted at 159.0–160°C. Analysis showed 5.15% N (calculated 5.16% N for C<sub>15</sub>H<sub>13</sub>NO<sub>4</sub>).

Solution rate studies in DMAc were carried out by heating aliquots of the amic acids in DMAc in an oil bath at 150°C. for varying lengths of time. Samples were removed at different time intervals and isolated in 50 ml. of distilled water to precipitate the amic acid and imide product. The products were washed with distilled water, dried under nitrogen and vacuum and weighed. After trituration with 50 ml. of methylene chloride, the products were filtered and after evaporation of solvent from the residue and methylene chloride soluble portion, the samples were reweighed. The weight of methylene chloride-soluble product was taken as *n*-imide, and this was checked by infrared analysis. Weights of methylene chloride-insoluble fractions were taken as amic acid and these also were confirmed by infrared analysis. For *N*-phenylphthalamic acid, the concentration of the DMAc solution was 0.83*M* and each aliquot was 10 ml. The *N-p*-methoxyphenylphthalamic acid solution was 0.5*M*, and 5 ml. aliquots were used per sample.

A similar procedure was followed with the tri-*n*-butylamine salt of *N-p*-methoxyphenylphthalamic acid in DMAc. In this case, the precipitates in water were totally soluble in methylene chloride and their infrared spectra showed the product to be *n*-imide. The tri-*n*-butylamine salt of *N-p*-methoxyphenylphthalamic acid did not precipitate in water.

The solid-phase thermal conversion of *N*-phenylphthalamic acid was carried out with 2.0-g. samples which were heated in test tubes for various lengths of time. Weighing, extraction, and analyses proceeded as described above.

The authors are grateful to Dr. J. E. Dickens, who designed the hot cell for the spectrophotometer, and to Dr. G. D. Patterson, Jr. for analytical assistance.

### References

1. B. A. Porai Koshitz, *Aniline Krasochnaya Prom.*, **4**, 295 (1934).
2. G. B. Hoey and C. T. Lester, *J. Am. Chem. Soc.*, **73**, 4473 (1951).
3. G. Vanags and A. Veinsbergs, *Ber.*, **75B**, 1558 (1942).
4. A. K. Bose, F. Greer, and C. C. Price, *J. Org. Chem.*, **23**, 1335 (1958).

5. C. E. Sroog, A. L. Endrey, S. V. Abramo, C. E. Berr, W. M. Edwards, and K. L. Olivier, *J. Polymer Sci. A*, **3**, 1373 (1965).
6. W. M. Edwards, U. S. Pat. 3,179,614 (1965).
7. J. I. Jones, F. W. Ochynski, and F. A. Rackley, *Chem. Ind. (London)*, **1962**, 1686.
8. G. M. Bower and L. W. Frost, *J. Polymer Sci. A*, **1**, 3135 (1963).
9. G. E. Ham and A. B. Beindorff, U. S. Pat. 2,811,548 (1957).
10. A. L. Endrey, U. S. Pat. 3,179,631 (1965).
11. M. L. Sherrill, F. L. Schaeffer, and E. P. Shoyer, *J. Am. Chem. Soc.*, **50**, 474, (1928).

### Résumé

Les vitesses de conversion thermique de l'acide polyamique dérivé du dianhydride pyromellitique et de l'éther 4,4'-diaminodiphénylé sont présentées. La formation d'un cycle imide progresse par des processus rapides et lents de premier ordre. Les amines tertiaires fournissent des fermetures de cycle avec un facteur d'environ 10 fois rapide que l'acide libre. Ceci est dû à un effet d'entropie d'activation plutôt qu'un effet d'énergie d'activation.

### Zusammenfassung

Die thermische Umwandlungsgeschwindigkeit der von Pyromellitsäuredianhydrid und 4,4'-Diaminodiphenyläther abgeleiteten Polyamidsäure wird bestimmt. Die Bildung des Imidringes erfolgt durch rasche und langsame Reaktionen erster Ordnung. Tertiäre Amine liefern einen um einen Faktor 10 rascheren Ringschluss als die freie Säure. Die Beschleunigung ist ein Effekt der Aktivierungsentropie und nicht der Aktivierungsenergie.

Received April 15, 1966  
Prod. No. 5133A

## Fluorothiocarbonyl Compounds. VI. Free-Radical Polymerization of Thiocarbonyl Fluoride\*

A. L. BARNEY, J. M. BRUCE, JR., J. N. COKER, H. W. JACOBSON, and W. H. SHARKEY, *Central Research Department, E. I. du Pont de Nemours and Company, Inc., Wilmington, Delaware 19898*†

### Synopsis

Thiocarbonyl fluoride,  $\text{CF}_2=\text{S}$ , and thiocarbonyl chlorofluoride,  $\text{CFCl}=\text{S}$ , undergo addition polymerization in free radical-initiated systems. In addition, both compounds copolymerize with various unsaturated compounds, including typical vinyl and vinylidene monomers. The chlorofluoride, because of its rapid polymerization rate, copolymerizes best with very active monomers, of which 2,3-dichloro-1,3-butadiene is an example. Thiocarbonyl fluoride polymerizes best at low temperatures. The trialkylborane-oxygen redox couple has been adapted to free-radical polymerizations and copolymerizations from  $-60$  to  $-120^\circ\text{C}$ . With such initiation  $\text{CF}_2=\text{S}$  has been copolymerized with terminal and internal olefins, vinyl compounds, allyl compounds, and acrylic esters. Copolymerization with propylene is unusual, in that it proceeds in a manner that strongly favors a product composed of two molecules of  $\text{CF}_2=\text{S}$  for each propylene. In other cases, product compositions are more responsive to the ratio of monomers charged.

### RESULTS AND DISCUSSION

Early in our studies on polymers from thiocarbonyl fluoride,  $\text{CF}_2=\text{S}$ , we obtained evidence that polymerization can be brought about by initiation with benzoyl peroxide under pressure at  $80^\circ\text{C}$ . However, it was not until we turned our attention to thiocarbonyl chlorofluoride,  $\text{CFCl}=\text{S}$ ,<sup>2</sup> that the effectiveness of free-radical polymerization of fluorine-containing thiocarbonyl compounds became fully appreciated. Free-radical polymerization of  $\text{CFCl}=\text{S}$  is easily demonstrated by exposing monomer at  $25^\circ\text{C}$ . to a sunlamp. A small amount of polymer is obtained that is greatly increased by irradiation in the presence of benzoyl peroxide and enormously increased in the presence of benzoin methyl ether. Most importantly, it was discovered that free-radical polymerization proceeds best at low temperatures. Thus,  $\text{CFCl}=\text{S}$  cooled with solid carbon dioxide is converted to polymer almost quantitatively by irradiation with high-energy electrons.

Examination of polymerization by free radicals generated chemically also indicated that polymer formation is favored at low temperatures.

\* Paper V in this series is by W. J. Middleton et al.<sup>1</sup>

† Contribution No. 1177.



TABLE I  
 Copolymerization of Thiocarbonyl Chlorofluoride with Vinyl Monomers

Monomers	Vol. monomer, ml.	Polymerization conditions <sup>a</sup>		Copolymer yield, g.	Analysis		Product
		Temp., °C.	Time, hr.		Element, %	CFCIS, %	
CFCIS	1	0	4	0.5	Cl, 32.4	90	Soft, tough polymer
Ethyl acrylate	1	0	4	0.5	Cl, 32.4	90	Soft, tough polymer
CFCIS	1	0	4	1.0	Cl, 34.9	97	Soft polymer
Vinyl acetate	1	0	4	1.0	Cl, 34.9	97	Soft polymer
CFCIS	1	0	4	1.1	Cl, 31.4	87	Elastomer
Styrene	1	0	4	1.1	Cl, 31.4	87	Elastomer
CFCIS	1	0	4	1.8	S, 30.5	94	Elastomer
CF <sub>2</sub> =CFC	1	0	4	1.8	S, 30.5	94	Elastomer
CFCIS	1	0	4	1.5	N, 0.18	98	Elastomer
Acrylonitrile	1	0	4	1.5	N, 0.18	98	Elastomer
CFCIS	1	-80	16	1.5	N, 0.9	96	Tough, opaque elastomer
Acrylonitrile	1.5	-80	16	1.5	N, 0.9	96	Tough, opaque elastomer

CFCIS	2.5									
Vinyl acetate	1	-80	16	4.0	Cl, 34.2	95				Tough polymer
CFCIS	1.5									
Vinyl acetate	2.5	-80	16	1.5	Cl, 33.9	95				Fairly tough polymer
CFCIS	2.5									
Methyl acrylate	1	-80	18	4.0	Cl, 33.6	94				Tough polymer
CFCIS	1.5									
Methyl acrylate	2	-80	18	3.0	Cl, 25.9	70				Soft elastomer
CFCIS	2									
Allyl chloride	2	0	16	1.5	S, 28.42	87				Soft polymer, $\eta_{inh} = 0.40$
CFCIS	2									
Allyl chloride	2	-80	16	2.0	S, 31.85	98				Tough polymer, $\eta_{inh} = 0.72$

<sup>a</sup> The initiator was 0.05 ml. of tri-*n*-butylborane used with adventitious oxygen.

The critical feature here was how to generate free radicals at low temperatures. This was done by employing the reaction of trialkylboranes with oxygen. Initiation of polymerization with trialkylboranes was reported in 1957 by Kolesnikov and Klimentova,<sup>3</sup> who described use of tributylborane to promote the polymerization of styrene and methyl methacrylate. Shortly thereafter, Furukawa and Tsuruta<sup>4</sup> showed that a mixture of oxygen and a trialkylborane is a very effective polymerization initiator. Evidence that these are free-radical polymerizations has been supplied by the work of Fordham and Sturm<sup>5</sup> and further supported by Zutty and Welch.<sup>6</sup> Both groups found that copolymers prepared by using either trialkylboranes or trialkylboranes to which oxygen had been added have compositions similar to those obtained from conventional radical systems. We have found that the tributylborane-oxygen couple initiates polymerization of  $\text{CFCl}=\text{S}$  at  $0^\circ\text{C}$ . and also leads to rapid formation of high molecular weight polymer in quantitative conversions at the very low temperature of  $-80^\circ\text{C}$ .

Polymers of  $\text{CFCl}=\text{S}$  formed in this way are tough elastomers that do not crystallize when stretched at  $0^\circ\text{C}$ . nor when cooled in the relaxed state to  $-80^\circ\text{C}$ . This is in marked contrast to poly(thiocarbonyl fluoride), which crystallizes rapidly when stretched and cooled at temperatures below  $35^\circ\text{C}$ .<sup>1</sup>

Thiocarbonyl chlorofluoride readily polymerizes in free-radical systems in the presence of other vinyl monomers, but because it reacts so rapidly the products in most cases are composed mostly of the chlorofluoride. This is illustrated in Table I.

2,3-Dichloro-1,3-butadiene (DCD), like  $\text{CFCl}=\text{S}$ , polymerizes rapidly under free-radical initiation. As shown in Table II, copolymerization of DCD with  $\text{CFCl}=\text{S}$  leads to products having compositions more closely approximating those of the monomer mixtures.

The trialkylborane-oxygen redox couple also promotes the polymerization of  $\text{CF}_2=\text{S}$  to high molecular weight polymer. This compound polymerizes more slowly than  $\text{CFCl}=\text{S}$ , and copolymerization of it with usual

TABLE II  
Copolymerization of Thiocarbonyl Chlorofluoride with 2,3-Dichloro-1,3-Butadiene (DCD)

Monomer mixture	Polymerization conditions <sup>a</sup>		CFCIS in product, %	Polymer appearance
	Temp., °C.	Time, hr.		
90/10 CFCIS/DCD	0	16	81	Soft elastomer
80/20 CFCIS/DCD	0	16	75	Soft elastomer
65/35 CFCIS/DCD	0	16	64	Tough elastomer
20/80 CFCIS/DCD	10	16	17	Plastic
10/90 CFCIS/DCD	0	16	ca. 1	Hard plastic

<sup>a</sup> The initiator was 0.05 ml. tri-*n*-butylborane used with adventitious oxygen.

vinyl monomers gives products containing substantial quantities of the comonomer. The products formed appear to be random copolymers. Fractionation of a  $\text{CF}_2=\text{S}$ /vinyl acetate copolymer indicated very little variation of  $\text{CF}_2=\text{S}$  content with molecular weight (see Table III).

TABLE III  
Fractionation of a  $\text{CF}_2=\text{S}$ /Vinyl Acetate Copolymer (16 g.)

Fraction	Weight, g.	S, %	$\text{CF}_2=\text{S}$ , %	$\eta_{inh}$
I	2.8	34.16	87.5	1.36
II	4.0	33.64	86.3	1.00
III	4.0	33.78	86.6	0.44, 1.02 <sup>a</sup>
IV	1.4	32.76	84.0	0.74, 0.44 <sup>a</sup>
V	1.0	31.70	81.3	0.37
VI	0.5 (grease)			

<sup>a</sup> Repeat determinations.

### Copolymerization of Thiocarbonyl Fluoride with Vinyl Compounds

To determine the scope of the copolymerizability of  $\text{CF}_2=\text{S}$  with vinyl compounds, a series of bulk copolymerizations was made with the use of either tri-*n*-butylborane or triethylborane with oxygen. These experiments demonstrated that a large variety of unsaturated compounds readily copolymerizes with  $\text{CF}_2=\text{S}$ . This is illustrated in Table IV in which copolymerizations with such hydrocarbons as propylene, isobutylene, 2-butene, cyclohexene, and tetramethylethylene, such halocarbons as vinyl chloride, vinyl fluoride, 2-chloropropene, allyl chloride, and allylchloroform, such esters as vinyl acetate, ethyl acrylate, and allyl acetate, such ethers as ethyl vinyl ether, allyl vinyl ether, and diallyl ether, and such other compounds as allyl chloroformate, allyltrichlorosilane, and vinyltrichlorosilane are described.

It is remarkable that propylene, ethylene, and isobutylene copolymerize so readily with  $\text{CF}_2=\text{S}$ . What is more astonishing is that olefins with sterically hindered double bonds, which are generally unreactive in polymerizations, also copolymerize with  $\text{CF}_2=\text{S}$ . Examples of such compounds are 2-butene, cyclohexene, and tetramethylethylene. Nonconjugated diolefins gave crosslinked products. Conjugated dienes inhibited the polymerization of  $\text{CF}_2=\text{S}$  under these conditions.

### Initiator System

In the course of these studies many apparent anomalies were encountered. For example, in some cases adventitious oxygen filled the requirement for oxidant, while in others considerable oxygen had to be added. As a consequence, it appeared desirable to study the initiator system in some detail. To keep the experiments as uncomplicated as possible, homopolymerization of  $\text{CF}_2=\text{S}$  was used as the model.

It was quickly established that in the complete absence of oxygen trialkylboranes do not initiate polymerization of bulk monomer or solutions

TABLE IV  
 Copolymerizations of  $CF_2=CF-S$ 

Monomer charge, ml. $CF_2=CF-S$ /ml. comonomer	Comonomer	Yield, g.	Analysis		Product
			S, %	Comonomer, mole-%	
3.2/1.0	Propylene <sup>a</sup>	1.2	31.16	33	Tough, elastic
2.10/0.6	Ethylene	2.5	31.07	43	Elastomeric
1.0/1.8	Isobutylene	1.4	26.89	40	Tough, elastic
1.0/4.7	<i>cis</i> -2-Butene <sup>b</sup>	1.2	28.51	35	Soft, elastic
2.0/1.2	1-Butene <sup>b</sup>	1	30.16	30	Elastic and slightly tacky
1.1/1.8	1-Hexene	1	27.74	28	Elastic and slightly tacky
1.5/2.0	Cyclohexene <sup>b</sup>	1	30.73	21	Elastic, tacky
1.0/4.0	Tetramethylethylene <sup>b</sup>	1	25.58	34	Elastic and slightly tacky
1.3/2.8	Vinylcyclohexene	2	24.15	24	Tough, crosslinked
2.1/2.6	Vinylcyclohexane	4.4	24.33	31	Elastic and slightly tacky
2.5/2.0	5-Methylenebicyclo[2.2.1]- heptene	1.9	19.84	43	Elastomeric
1.5/3.0	1,5-Hexadiene	2.2	27.33	30	Crosslinked
3.0/7.0	Vinyl chloride	1.7	27.82	34	Slightly tacky
1.5/6.0	Vinyl fluoride	2.9	34.59	19	Tough
1.0/1.5	2-Chloropropene	1	24.63	38	Soft and tacky

0.9/2.3	Allyl chloride	1.7	25.83	35	Tough, elastic
1.9/2.9	Allyl chloroform	1.4	27.81	17	Tacky elastomer
3.0/4.0	Vinyl acetate	5.4	27.36	29	Tacky
1.9/0.4	Ethyl acrylate	1	22.07	39	Tough elastomer
2.0/3.0	Allyl acetate	1		21	Weak and tacky
1.3/3.0	Allyl butyrate	2.8	24.59	27	Slightly tacky elastomer
2.0/3.1	Isopropenyl acetate	3.9	25.44	28	Weak and tacky
1.1/3.0	Ethyl vinyl ether	1.4	20.81	22	Crosslinked
1.5/2.0	Allyl vinyl ether	2.2	26.50	32	Crosslinked
2.0/3.0	Allyl $\beta$ -allyloxypropionate	3.9	21.94	27	Crosslinked
2.0/3.1	Allyl tetrafluoroethyl ether	2.7	24.89	23	Tough elastomer
1.5/2.0	Cyclohexyl vinyl ether	1	18.44	42	Weak and tacky
2.5/3.0	Diallyl ether	2.2	26.78	28	Crosslinked
1.0/0.83	Allyl chloroformate	2.2	21.19	41	Soft and tacky
1.9/2.9	Allyl chloroformate	2.2	25.58	26	Tough elastomer
6.7/1.6	Allyl chloroformate	6.0	35.27	5	Very tough elastomer
1.7/3.0	Allyltrichlorosilane	3.3	22.28	26	Water-sensitive elastomer
2.3/2.5	Vinyltrimethylsilane	1.4	27.24	26	Granular
2.2/3.2	Vinyltriethoxysilane	1.9	21.94	25	Crosslinked
2.2/2.8	Vinyltrichlorosilane	3.0	23.26	20	Crosslinked
11.0/2.2	Allylidene diacetate	9.5	35.14	5	Tough, slightly tacky elastomer
2.0/0.3	Dimethylvinylcarbinyl isocyanate	1	29.30	20	Tacky elastomer

<sup>a</sup> Run at -25 to -35°C. in 30 ml. heptane.

<sup>b</sup> Reverse addition.

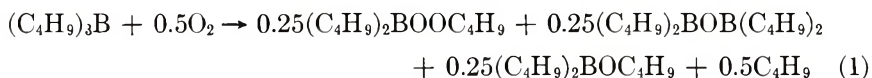
thereof in inert media. However, upon addition of oxygen to these systems, a very rapid and exothermic reaction takes place. Very small amounts of oxygen suffice, 1/20th the amount of borane being effective, but for good reproducibility an oxygen/trialkylborane ratio of 0.5 appears to be near the optimum. Excess oxygen inhibits the reaction as was shown by the very small amount of polymer formed with oxygen/trialkylborane ratios of 2 or greater.

Further insight into the initiating system was obtained by investigation of the reaction of trialkylboranes with excess oxygen. It was found that these materials react on a mole-for-mole basis at  $-78^{\circ}\text{C}$ . to form a peroxyborane of the formula  $\text{R}_3\text{BOOR}$ . No further reaction takes place at this low temperature. This was shown by the correspondence of moles of oxygen consumed with moles of peroxide formed in the reaction of oxygen with either tri-*n*-butylborane or triethylborane.

The peroxyboranes are not themselves polymerization initiators at  $-78^{\circ}\text{C}$ ., but they react with trialkylboranes to generate initiating radicals. Stoichiometric studies have shown the reaction involves one molecule of peroxyborane for each two molecules of trialkylborane. This result was confirmed by the reaction of 0.5 mole of oxygen with 1 mole of tri-*n*-butylborane to give 0.25 mole of peroxyborane (see Table V).

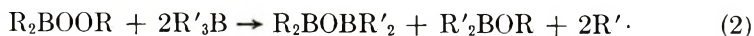
TABLE V  
Peroxide Formation for the Reaction of  $\text{R}_3\text{B}$  with  $\text{O}_2$

Time after $\text{O}_2$ added, min.	Peroxide content (by titration) $\times 10^4$ , mole	$\text{R}_3\text{B}$ converted to $\text{R}_2\text{BOOR}$ , %
5	11.04	20
20	13.35	24
60	14.00	25
90	12.60	23



Evidence that alkyl radicals are formed and that their genesis is in the trialkylborane was obtained by examination of gases formed by typical initiating couples. Products from the reaction of diethyl(ethylperoxy)borane and triethylborane in heptane included a  $\text{C}_2$ - $\text{C}_4$  gas mixture, the composition of which was 25% ethylene, 65% ethane, and 10% *n*-butane. The formation of these gases indicates that ethyl free radicals had been present, as such radicals characteristically disproportionate to give ethylene and ethane and combine to give *n*-butane. The larger amount of ethane relative to ethylene probably was the result of hydrogen abstraction by ethyl free radicals. Use of di-*n*-butyl(*n*-butylperoxy)borane with triethylborane also indicated that ethyl free radicals are generated. The  $\text{C}_2$ - $\text{C}_4$  gas mixture from such a reaction contained 28% ethylene, 53% ethane, 15% *n*-butane, and 3% 1-butene. The presence of the 1-butene

may mean that a small number of radicals come from the peroxyborane. It is concluded that the major reaction responsible for generation of the polymerization initiator is



This reaction of eq. (2) is written to indicate wide generality, and such is believed to be the case. Several combinations involving boranes not usually encountered are given in Table VI. In all of these cases, respect-

TABLE VI  
Polymerization of  $CF_2=S$  with Trialkylboranes

Oxidant	Trialkylborane	Polymer yield, %
$(C_2H_5)_2BO_2C_2H_5$	$(CH_2=CHCH_2)_3B^a$	46
$(C_{12}H_{25})_2BO_2C_{12}H_{25}$	$(C_{12}H_{25})_3B^a$	85
$O_2$	$(C_{12}H_{25})_3B^b$	46
$O_2$	$\left( \text{C}_8\text{H}_{15} \right)_3\text{B}^a$	85
$O_2$	$\left( \text{CH}_2 \right)_3\text{B}-\text{CH}_2-\text{CH}^a$	90

<sup>a</sup> 0.63 mole-% of the trialkylborane was used with approximately half as much oxidant. These polymerizations were run in either  $CF_2Cl_2$  or heptane at  $-78^\circ C.$  for 10 min. to 1 hr.

<sup>b</sup> 0.22 mole-% tridodecylborane was used with 0.11 mole-% oxygen. The polymerization was carried out in dichlorodifluoromethane at  $-78^\circ C.$  for 2 hr.

able yields of poly(thiocarbonyl fluoride) were obtained in relatively short reaction periods.

Solutions of peroxyboranes are as effective as oxygen as the oxidizing part of the initiator and are advantageous because they allow the formulation of homogeneous systems. Though many of our polymerizations were done in bulk, solution polymerizations were smoother because they allowed better control of reaction temperature. Such solvents as dichlorodifluoromethane and hexafluoropropylene were satisfactory media for polymerizations initiated with a trialkylborane and either a peroxyborane or oxygen.

### Copolymerization of Thiocarbonyl Fluoride with Propylene

A more careful study was made of the bulk copolymerization of  $CF_2=S$  with excess propylene by using the diethyl(ethylperoxy)borane-triethylborane combination. As shown in Table VII,  $-78^\circ C.$  appears to be near the optimum polymerization temperature for forming copolymer in high



TABLE VII  
 CF<sub>2</sub>=S/Propylene Copolymers

Polymerization conditions		Yield, % <sup>a</sup>	CF <sub>2</sub> =S/C <sub>3</sub> H <sub>6</sub> <sup>b</sup>	$\bar{M}_n$ <sup>c</sup>	$\eta_{inh}$ <sup>d</sup>
Temp., °C.	Time, hr.				
-65 <sup>e</sup>	2.5	55	2.2	108,000	0.30
-78	2.5	80	2.2	645,000	2.38
-100	2.5	75	2.2	267,000	1.98
-120	5	20	2.3	389,000	2.96

<sup>a</sup> Based on CF<sub>2</sub>=S and corrected for polymer composition.

<sup>b</sup> Determined by sulfur analysis.

<sup>c</sup> By osmometry using benzene solutions.

<sup>d</sup> Determined using 0.1% solutions in benzene.

<sup>e</sup> 15 ml. of CCl<sub>2</sub>F<sub>2</sub> used to moderate the reaction.

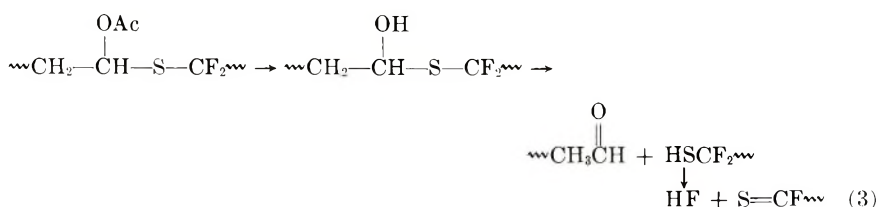
yields and with high molecular weight. It appears that there is a strong tendency for two molecules of CF<sub>2</sub>=S to combine with one of propylene in these copolymerizations. That this ratio is characteristic of the entire polymer was demonstrated by fractionation of a 2.2:1 CF<sub>2</sub>=S/propylene copolymer into eight fractions all of which contained approximately two molecules of CF<sub>2</sub>=S for each molecule of propylene. Solution polymerizations in dichlorodifluoromethane proceeded similarly. Use of mole ratios of 1:2.5 to 1:1 CF<sub>2</sub>=S/propylene in the monomer charge gave 2.2:1 to 2.3:1 CF<sub>2</sub>=S/propylene copolymers. Even a 6:1 CF<sub>2</sub>=S/propylene monomer ratio gave only a 3.4:1 CF<sub>2</sub>=S/propylene copolymer.

The best propylene copolymers were prepared in dichlorodifluoromethane solutions and had CF<sub>2</sub>=S/propylene mole ratios between 2.3 and 2.1. They had molecular weights as high as 820,000, as determined by osmometry in benzene solutions. The corresponding inherent viscosity as measured on 0.1% benzene solutions for the highest molecular weight copolymer was 4.45. This product is a soft, pliable elastomer that retains flexibility at very low temperatures. Its crystalline melting point is in the -55 to -60°C. range.

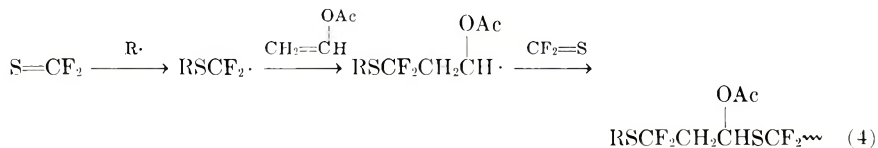
Other comonomers do not behave in the same way as propylene. *tert*-Butylethylene, for example, copolymerizes well with CF<sub>2</sub>=S to give high molecular weight copolymers, but the composition of the products closely approximates the monomer mixture used. Similarly, vinyl acetate copolymers led to products whose composition was near that of the monomer charge.

### Copolymers of Thiocarbonyl Fluoride with Acetates

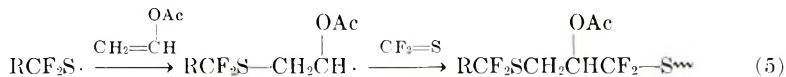
The acetate groups of the vinyl acetate copolymers could be removed by methanolysis. However, this was accompanied by extensive degradation to low molecular weight products. It is thought that this degradation comes about because of proximity of acetate groups to the sulfide link.



The structure shown in eq. (3) would not be expected as it would appear to be the result of free-radical addition to the sulfur atom.



An energetically more favorable product from the first step is  $\text{RCF}_2\text{S}\cdot$ , which would be expected to add to the  $\text{CH}_2$  of vinyl acetate.



Perhaps  $\text{RCF}_2\text{S}\cdot$  is formed and adds abnormally to vinyl acetate to give  $\text{RCF}_2\text{SCH}(\text{OAc})\text{CH}_2\cdot$ .

Further insight into the above phenomenon was obtained by insulating the acetate group from the chain, which should lead to hydrolytically stable copolymers. Interposing one methylene group was accomplished by copolymerization of  $\text{CF}_2=\text{S}$  with allyl acetate. These copolymers, though readily formed, were all insoluble. This result is presumed to be related to the ease with which the activated allylic hydrogens of allyl acetate are removed by free radicals. This presumption led us to try 3-butenyl acetate in which the acetate group is two carbons away from the chain backbone. This compound copolymerized readily with  $\text{CF}_2=\text{S}$  to give products that had molecular weights as high as 800,000, as determined by osmometry. The  $\text{CF}_2=\text{S}$ /3-butenyl acetate copolymers could be methanolized to hydroxyl-containing polymers without degradation. Such hydroxyl-containing polymers are tough elastomers that can be readily crosslinked by reaction with diisocyanates.

### Copolymerization of Thiocarbonyl Fluoride with Allyl Chloroformate

Allyl chloroformate copolymers were studied at some length because it was found they could be crosslinked by reaction of the acid chloride groups with zinc oxide. This crosslinking will be discussed in a subsequent paper. The copolymerization takes place readily in solution to give homogeneous products of high molecular weight. Incorporation of as little as 2-3 mole-% of the comonomer is sufficient to give good crosslinkable compositions and to reduce the crystalline melting point, which is  $35^\circ\text{C}$ . for  $\text{CF}_2=\text{S}$  homopolymer, to below  $0^\circ\text{C}$ .

## EXPERIMENTAL DETAILS

### Thiocarbonyl Chlorofluoride

2-Chloro-2,4,4-trifluoro-1,3-dithietane was pyrolyzed by passage through a platinum tube heated to 600°C. Thiocarbonyl chlorofluoride was isolated from the pyrolysate by fractional distillation. It is a bright yellow liquid, b.p. 8–10°C. Material used for polymerization was further purified by gas chromatography by using a silicone oil-on-firebrick column. The monomer was stored in glass at –78°C. under nitrogen and showed no evidence of degradation or polymerization under these conditions for periods as long as several weeks.

### Polymerization of Thiocarbonyl Chlorofluoride

Three small Pyrex tubes were each charged with 0.5 ml. of  $\text{CFCl}=\text{S}$ . Benzoyl peroxide (2 mg.) was added to one and benzoin methyl ether (2 mg.) was added to another. The third was kept as a control. All were sealed and placed 6 in. from an RS sunlamp. The tubes were irradiated 3 hr. at 25°C. The liquid in the tube containing benzoyl peroxide became viscous. Polymer isolated by pouring the contents of the tube into methanol, followed by filtration and drying of the precipitate amounted to about 100 mg. The liquid in the tube containing benzoin methyl ether was very viscous. The amount of polymer recovered from it by methanol precipitation was about 300 mg. The liquid in the control tube was not viscous and yielded only a trace of polymer. A film was pressed from the product formed in the presence of benzoin methyl ether. It was flexible and moderately tough.

ANAL. Calcd. for  $\text{CClFS}$ : Cl, 35.9%; S, 32.5%; Found: Cl, 34.7%; S, 32.14%.

$\text{CFCl}=\text{S}$  (0.5 ml.) was sealed in a Pyrex tube, the tube was cooled with solid carbon dioxide, and then exposed to 2 M.e.v. electrons (62.5 watt-sec./cm.<sup>2</sup>). The thiocarbonyl chlorofluoride was essentially completely converted to a tough polymer.

$\text{CFCl}=\text{S}$  (0.5 ml.) was placed in a small flask and cooled to 0°C. Tri-*n*-butylborane (0.02 ml.) was then added, followed by addition of 2 ml. of air. After 2 hr., the reaction mixture was poured into methanol to give 0.2 g. polymer. It had a high molecular weight as shown by hot-pressing, which gave a tough, flexible film.

Polymerization of 2 ml. of  $\text{CFCl}=\text{S}$  in 5 ml. of diethyl ether at –78°C. with the use of 0.05 ml. of tri-*n*-butylborane gave 2 g. of polymer after 2 hr. Hot-pressing of this polymer at 100°C. gave a tough, logy film that did not crystallize at –78°C. in relaxed form nor at 0°C. when stretched.

### Copolymerization of Thiocarbonyl Chlorofluoride with Unsaturated Compounds

Copolymerization of thiocarbonyl chlorofluoride with acrylic esters, vinyl acetate, styrene, chlorotrifluoroethylene, acrylonitrile, and 2,3-

dichloro-1,3-butadiene was done as described above. As shown in Tables I and II, temperatures were varied from  $-78$  to  $+10^{\circ}\text{C}$ ., and the time allowed for polymerization was varied from 4 to 18 hr. In all cases, oxygen dissolved in the monomer or present in the polymerization tube or flask was used along with 0.02 ml. of tri-*n*-butylborane as the redox initiation couple. Inherent viscosities of the allyl chloride copolymers were determined on 0.1% solutions in chloroform at  $25^{\circ}\text{C}$ .

#### Fractionation of a Thiocarbonyl Fluoride/Vinyl Acetate Copolymer

Vinyl acetate (5 ml.) and 20 ml. of  $\text{CF}_2=\text{S}$ , which was prepared by pyrolysis of 2,2,4,4-tetrafluoro-1,3-dithietane,<sup>2</sup> were placed in a nitrogen-filled flask at  $-78^{\circ}\text{C}$ . and mixed thoroughly. Then 0.4 ml. of a 10% solution of tributylborane in petroleum ether was added to the flask. In the first 30 min., the mixture thickened appreciably, and after 18 hr. at  $-78^{\circ}\text{C}$ . the contents of the reactor had solidified. This product was broken up in methanol and dried. Pressed films of this product were weak at  $25^{\circ}\text{C}$ . but retained elasticity at  $0^{\circ}\text{C}$ . The yield of polymer was 16 g.

This polymer (16 g.) was dissolved in 250 ml. of chloroform for fractionation (Table III). To the viscous chloroform solution was added 300 ml. of petroleum ether followed by 160 ml. of absolute alcohol. Material that precipitated was taken as fraction I. Fraction II was obtained by adding an additional 30-ml. portion of alcohol. Successive fractions were precipitated by further addition of 50-ml. portions of alcohol. The last fraction was recovered by evaporation of the solvents. Inherent viscosities ( $\eta_{\text{inh}}$ ) were determined on 0.1% solutions in chloroform at room temperature. Recovery was 13.7 g. or 85%.

#### Bulk Copolymerizations of Thiocarbonyl Fluoride

The comonomer was placed in a graduated reaction tube and thoroughly degassed at  $-78^{\circ}\text{C}$ . by bubbling helium through it. The tube was cooled in liquid nitrogen, and  $\text{CF}_2=\text{S}$  that had been degassed with helium was condensed in it. Then the monomers were warmed to  $-78^{\circ}\text{C}$ . and thoroughly mixed. A heptane solution of 8–25% tri-*n*-butylborane or triethylborane was added in an amount sufficient to give a concentration of 0.3–0.8 mole-%. This was followed by injection of 0.5 mole of oxygen for each mole of borane. The reaction mixture was shaken vigorously at  $-78^{\circ}\text{C}$ . for several minutes and was then stored in a solid carbon dioxide-acetone bath for 2–24 hr. Methanol or petroleum ether was then added, and the precipitated polymer was dried and pressed into a film at  $50$ – $150^{\circ}\text{C}$ . in a Carver press. Results are given in Table IV.

Some candidate comonomers were sufficiently basic to initiate polymerization of  $\text{CF}_2=\text{S}$  anionically. In these cases, the trialkylborane was mixed with  $\text{CF}_2=\text{S}$  before admission of the comonomer. The boron compounds are sufficiently good Lewis acids to counteract slightly basic comonomers. This is referred to as reverse addition in Table IV.

### Effect of Oxygen Concentration on Thiocarbonyl Fluoride Polymerization

A dry reaction flask was thoroughly purged of air with nitrogen, cooled to  $-78^{\circ}\text{C}$ ., and charged with 5 ml. of  $\text{CF}_2=\text{S}$ . A 0.5-ml. portion of a heptane solution containing  $5 \times 10^{-4}$  mole of tri-*n*-butylborane was added. There was no evidence of polymer formation in 1.5 hr. Oxygen (6 ml., approximately  $2.5 \times 10^{-4}$  mole) gas was then added. After  $1/2$  hr., the flask contained only white solid. After an additional hour, methanol was added, and the insoluble polymer was washed with methanol in a Waring Blendor. The polymer (6.24 g.) was isolated by filtration and dried.

In a similar run in which 24 ml. of oxygen (approximately  $10^{-3}$  mole) was used, only traces of polymer were formed in 1 hr. However, after injection of an additional  $10^{-3}$  mole of tri-*n*-butylborane, rapid polymerization ensued to give almost complete conversion of monomer to polymer in 15 min. After 1 hr., the polymer was isolated by washing in methanol, filtering, and drying. It weighed 6.43 g. and was of low molecular weight as shown by poor strength.

A dry reactor fitted with a neck closed by a rubber serum cap, and a neck for attachment to a manifold was charged with 9 ml. of  $\text{CF}_2=\text{S}$  and 0.5 ml. of heptane containing  $5 \times 10^{-4}$  mole of tri-*n*-butylborane. The reactor was purged by cooling in liquid nitrogen, evacuation, and admission of nitrogen. It was then warmed to  $-78^{\circ}\text{C}$ . A syringe fitted to deliver 0.2 ml. of oxygen/5 minutes was inserted through the serum cap. Oxygen was added slowly. After 0.4 ml. of oxygen (approximately  $0.16 \times 10^{-4}$  moles) had been added, an exothermic reaction occurred and complete conversion of monomer to polymer took place in about 15 minutes. Yield of polymer after washing with methanol and drying was 11.37 g.

### Reaction of Trialkylboranes with Excess Oxygen

A glass, cylindrical vessel  $1\frac{1}{4} \times 4$  in., containing a Teflon fluorocarbon-coated magnetic stirring bar and having a neck at the top covered by a rubber serum cap was connected by means of a second neck, in which a stopcock had been inserted, to a manifold. The manifold was attached to a mercury-filled manometer, a gas buret, and a source of oxygen. The apparatus was thoroughly purged with oxygen and filled with oxygen at atmospheric pressure. After the reaction vessel was cooled to  $-78^{\circ}\text{C}$ ., 17 ml. of *n*-heptane was added by syringe through the serum cap. Then 3 ml. of a heptane solution of tri-*n*-butylborane (approximately 26.6% by weight or about 0.00312 mole) was added with stirring. In 27 min., 74 ml. of oxygen had been consumed, after which time no further reaction took place.

The reaction mixture was assayed by withdrawing 5 ml. and injecting it into a solution of 1 ml. saturated potassium iodide,<sup>7</sup> 1 ml. acetic acid, and 50 ml. isopropyl alcohol. The iodine released was titrated with thio-sulfate. Results were as follows:

$$\begin{aligned}(\text{C}_4\text{H}_9)_3\text{B} &= 3.12 \times 10^{-3} \text{ mole (as prepared)} \\ &= 3.02 \times 10^{-3} \text{ mole (by O}_2 \text{ consumption)} \\ &= 3.32 \times 10^{-3} \text{ mole (by titration)}\end{aligned}$$

Reaction of triethylborane with oxygen was carried out similarly. A heptane solution (20 ml.) containing  $2.43 \times 10^{-3}$  mole of triethylborane and cooled to  $-78^\circ\text{C}$ . was exposed to oxygen. In 26 min., 66 ml. of  $\text{O}_2$  was taken up, after which no further reaction occurred. Titration indicated the presence of  $2.54 \times 10^{-3}$  mole of a diethyl(ethylperoxy)borane as opposed to  $2.70 \times 10^{-3}$  mole by oxygen consumption.

#### Reaction of Tri-*n*-butylborane with 0.5 Mole Oxygen

To 10 ml. of heptane containing  $55.5 \times 10^{-4}$  mole of tri-*n*-butylborane cooled to  $-78^\circ\text{C}$ ., there was added 63 ml. (approximately  $28 \times 10^{-4}$  mole) of oxygen at  $-78^\circ\text{C}$ .. Peroxide content was determined at intervals by iodide titration. Results are given in Table V.

#### Reaction of Di-*n*-butyl(*n*-butylperoxy)borane and Tri-*n*-butylborane

In a reaction vessel of the type described above, tri-*n*-butylborane was oxidized at  $-78^\circ\text{C}$ . in heptane to give a solution containing  $3.1 \times 10^{-3}$  mole of di-*n*-butyl(*n*-butylperoxy)borane. The solution was blanketed with nitrogen and  $4.2 \times 10^{-3}$  mole of tri-*n*-butylborane was added. After 20 min. at  $-78^\circ\text{C}$ ., the reaction was complete. The peroxide content of the reaction mixture was found by iodimetry to be  $0.9 \times 10^{-3}$  mole. The theoretical amount of peroxide, assuming it reacts with two molecules of borane, would be  $1 \times 10^{-3}$  mole.

#### Gases Formed by Reaction of a Peroxyborane and a Trialkylborane

Diethyl(ethylperoxy)borane ( $4.2 \times 10^{-3}$  mole) in 6 ml. of heptane was prepared in the reaction vessel previously described by reaction of oxygen at  $-78^\circ\text{C}$ . with an appropriate amount of triethylborane. The reaction vessel was evacuated, blanketed with nitrogen, evacuated again, and connected to a stainless steel cylinder cooled with liquid nitrogen. Heptane (5.5 ml.) containing  $11.0 \times 10^{-3}$  mole of triethylborane was then added, and off gases were collected in the cylinder. The pressure was then increased to about 50 mm. by admission of nitrogen, and the solution stirred as it was allowed to warm to room temperature. At the end of the reaction, about 10% of the peroxide remained as determined by iodimetry. Weight of off-gases in the cylinder was 0.2565 g. (the theoretical amount was 0.22 g.). Mass spectrographic analysis of the off-gases indicated the presence of *n*-butane, ethane, and ethylene along with considerable amounts of air and small amounts of heptane and a hexane. Distribution of the  $\text{C}_2$ - $\text{C}_4$  gases as determined by gas chromatography was 24.8% ethylene, 65.0% ethane, and 10.2% *n*-butane.

Di-*n*-butyl(*n*-butylperoxy)borane ( $3.645 \times 10^{-3}$  mole) was reacted with  $8.0 \times 10^{-3}$  mole of triethylborane as described above. The weight of

off-gas obtained was 0.1508 g. Composition of the C<sub>2</sub>-C<sub>4</sub> fraction of the off-gas, as determined by gas chromatography, was 28.3% ethylene, 53.3% ethane, 15.2% *n*-butane, and 3.2% 1-butene.

### Rate of Thermal Decomposition of Dialkyl(alkylperoxy)boranes

The half-lives of diethyl(ethylperoxy)borane and di-*n*-butyl(*n*-butylperoxy)borane were determined at various temperatures by titration of peroxide remaining. Results are shown in Table VIII.

TABLE VIII

Temperature, °C.	Half-life, min.	
	(C <sub>2</sub> H <sub>5</sub> ) <sub>2</sub> BOOC <sub>2</sub> H <sub>5</sub>	(C <sub>4</sub> H <sub>9</sub> ) <sub>2</sub> BOOC <sub>4</sub> H <sub>9</sub>
15	190	110
35	35	20
50	10	5

By extrapolation, it is estimated that half-lives of these peroxides is in excess of one week at -40°C.

### Solution Polymerization of Thiocarbonyl Fluoride

A. A glass trap containing CF<sub>2</sub>=S (15 ml. at -78°C., ca. 20 g.) was connected to a polymerization vessel containing 150 ml. of oxygen-free dichlorodifluoromethane. The CF<sub>2</sub>=S was transferred under vacuum to the polymerization vessel cooled with liquid nitrogen. The CF<sub>2</sub>=S and dichlorodifluoromethane were degassed by melting under vacuum to remove any trace of oxygen. The solution of monomer was stirred in a solid carbon dioxide bath, and the initiator [1.6 × 10<sup>-4</sup> mole of diethyl(ethylperoxy)borane followed by 9.7 × 10<sup>-4</sup> mole of triethylborane] was added by hypodermic syringe. Polymerization proceeded slowly. After 18 hr., the polymer (ca. 20 g.) was isolated by adding cold methanol, allowing the dichlorodifluoromethane to evaporate, and drying. Homopolymer prepared in this medium appeared to be of lower molecular weight, as judged by toughness, than that obtained by anionic initiation.<sup>1</sup>

B. CF<sub>2</sub>=S (9 ml., ca. 12 g.) was distilled into a polymerization vessel containing 15 ml. of hexafluoropropylene as polymerization medium. The solution was stirred at -78°C., and the initiator (1 × 10<sup>-4</sup> mole triethylborane followed by 1.2 cc. O<sub>2</sub>) was added by hypodermic syringe. After 6 hr., methanol was added, and the vessel was warmed to distil hexafluoropropylene. The poly(thiocarbonyl fluoride) (ca. 12 g.) was treated with boiling water and air-dried. Films pressed at 150°C. appeared to be equivalent in toughness to polymer prepared by anionic initiation.

### Copolymerization of Thiocarbonyl Fluoride and Propylene

A reactor of the type described earlier was charged with 10 ml. of propylene and 5 ml. of CF<sub>2</sub>=S at temperatures of -65 to -120°C.

Then,  $1 \times 10^{-4}$  mole of diethyl(ethylperoxy)borane and  $2 \times 10^{-4}$  mole triethylborane were added with stirring. After 2.5–5 hr., methanol was added to the reaction mixture and the precipitated product washed in methanol and dried. Yields, analysis, and molecular weights are shown in Table VII.

A glass trap containing  $\text{CF}_2=\text{S}$  (35 ml. at  $-78^\circ\text{C}$ ., ca. 47 g.) was connected to a polymerization vessel containing dichlorodifluoromethane (300 ml.) and propylene (70 ml., ca. 43 g.). Both vessels were immersed in liquid nitrogen, and, after the contents had frozen, the system was evacuated and the  $\text{CF}_2=\text{S}$  was distilled into the polymerization vessel. The solid contents of the polymerization vessel were then allowed to melt under vacuum to remove any dissolved oxygen. The solution was stirred at  $-78^\circ\text{C}$ ., and the initiator [ $7.5 \times 10^{-4}$  mole diethyl(ethylperoxy)borane followed by  $13.4 \times 10^{-4}$  mole triethylborane] was added by hypodermic syringe. Polymer formed, and at the end of 2.5 hr. cold methanol was added, and the vessel was allowed to warm to room temperature. Dichlorodifluoromethane and excess propylene were evaporated. The polymer was dissolved in 300 ml. of chloroform and was precipitated by pouring this solution into methanol. The dried elastic polymer weighed 51 g. and had a sulfur content of 32.02%, corresponding to a mole ratio of  $\text{CF}_2=\text{S}$ /propylene of 2.34/1.

A 12-g. portion of a 2.26:1  $\text{CF}_2=\text{S}$ /propylene copolymer ( $\eta_{\text{inh}}$  for 0.1% chloroform solution = 3.21) prepared as described above was dissolved in 1200 ml. of benzene. A 500-ml. portion of 20 vol.-% of methanol in benzene was then added followed by slow addition of 700 ml. methanol to develop a cloudy solution. Material that separated on overnight standing was taken as fraction 1. Successive fractions obtained by further additions of methanol are described in Table IX.

TABLE IX

Fraction no.	Vol. methanol added, ml.	Weight, g.	$\eta_{\text{inh}}$	Mole ratio $\text{CF}_2=\text{S}$ /propylene
1	—	0.78	1.68	1.89
2	25	2.94	4.83	2.01
3	25	2.60	3.67	2.14
4	50	2.23	4.64	2.26
5	50	0.56	—	2.36
6	100	0.57	—	2.53
7	200	0.43	—	2.13
8	1000	0.04	—	2.26
Residue	—	0.39	—	1.59

### Thiocarbonyl Fluoride/*tert*-Butylethylene Copolymers

Mixtures of  $\text{CF}_2=\text{S}$  and *tert*-butylethylene were copolymerized in dichlorodifluoromethane at  $-78^\circ\text{C}$ . following the procedure used with the



TABLE X

Monomer mole ratio $\text{CF}_2=\text{S}/\text{C}_6\text{H}_{12}$	Yield, %	Polymer mole ratio $\text{CF}_2=\text{S}/\text{C}_6\text{H}_{12}$
7.8:1	85	7.8:1
8.4:1	97	8.9:1 <sup>b</sup>
15.7:1	98	18.2:1
21:1	86	21:1

<sup>a</sup> Based on  $\text{CF}_2=\text{S}$  and corrected for polymer composition.

<sup>b</sup> Molecular weight by osmometry = 320,000;  $\eta_{inh}$  (0.1% in benzene) = 1.68.

propylene copolymers. Results from runs with various mole ratios of reactants are shown in Table X.

### Thiocarbonyl Fluoride/Vinyl Acetate Copolymers

Copolymerization of thiocarbonyl fluoride with vinyl acetate was done in dichlorodifluoromethane solution with the use of the diethyl(ethylperoxy)borane and triethylborane initiator combination as described above for the propylene copolymers. Yields and polymer compositions were as shown in Table XI.

TABLE XI

Monomer mole ratio $\text{CF}_2=\text{S}/\text{vinyl acetate}$	Polymer yield, % <sup>a</sup>	Polymer mole ratio $\text{CF}_2=\text{S}/\text{vinyl acetate}$
4:1	73%	4.3:1
13:1	84%	14:1

<sup>a</sup> Based on  $\text{CF}_2=\text{S}$  and corrected for polymer composition.

Molecular weight of the 14:1 copolymer by osmometry (benzene solutions) was 64,000;  $\eta_{inh}$  (0.1% in benzene) was 0.95.

A 5-g. portion of a  $\text{CF}_2=\text{S}/\text{vinyl acetate}$  copolymer prepared from a 10:1 monomer ratio was dissolved in 10 ml. tetrahydrofuran containing 5 g. anhydrous hydrogen chloride. Methanol (10 ml.) was added, and the solution was heated under reflux for 6 hr. The viscosity of the solution gradually decreased. Addition of water precipitated hydrolyzed polymer, which was washed with methanol and dried. A sticky material of apparently low molecular weight was obtained.

### Thiocarbonyl Fluoride/Allyl Acetate Copolymers

These copolymers were prepared by the method described for copolymers of propylene. Polymer yields varied from 60 to 95%. The products were insoluble in chloroform and benzene.

### Thiocarbonyl Fluoride/3-Butenyl Acetate Copolymers

The procedure described for copolymerization of  $\text{CF}_2=\text{S}$  and propylene was employed, with the use of 100 ml. of dichlorodifluoromethane, 15 ml. (20 g.) of  $\text{CF}_2=\text{S}$  at  $-78^\circ\text{C}$ ., and 2 ml. of 3-butenyl acetate (mole ratio of starting monomers = 13.4:1). The initiator was  $5.64 \times 10^{-4}$  mole of triethylborane in 0.5 ml. of heptane and 6 ml. of oxygen gas. The polymerization was allowed 16 hr. at  $-78^\circ\text{C}$ ., and the product was isolated in the usual way. High molecular weight copolymer (12 g.) was obtained. Analysis showed the presence of 35.36% S, which corresponds to a 13:1 mole ratio of  $\text{CF}_2=\text{S}$ /3-butenyl acetate.

A second copolymerization was carried out as described above with the use of 37 ml. (49.5 g.) of  $\text{CF}_2=\text{S}$  and 2 ml. of 3-butenyl acetate (mole ratio of starting monomers = 33.2:1). The product (44 g.) contained 37.38% S, which corresponds to a 30.5:1 mole ratio of  $\text{CF}_2=\text{S}$ /3-butenyl acetate. Molecular weight by osmometry (chloroform solutions) was 802,000 and  $\eta_{\text{inh}}$  (0.1% in  $\text{CHCl}_3$ ) was 1.43.

A 5-g. portion of a  $\text{CF}_2=\text{S}$ /3-butenyl acetate copolymer was dissolved in 100 ml. of tetrahydrofuran containing 5% anhydrous hydrogen chloride. The mixture was heated to  $60^\circ\text{C}$ . and 10 ml. of methanol slowly added. Heating was continued for 5 hr., after which polymer was precipitated by pouring the reaction solution into water. The polymer was dried and pressed into a film that was elastic. Polymer dipped in toluene diisocyanate, blotted dry, and then pressed into a film at  $115^\circ\text{C}$ . gave a clear, colorless film that was tightly crosslinked.

### Copolymerization of Thiocarbonyl Fluoride with Allyl Chloroformate

Into a 1-liter polymerization flask was distilled dichlorodifluoromethane (750 ml.) and  $\text{CF}_2=\text{S}$  (78 ml. at  $-78^\circ\text{C}$ ., ca. 103 g.). The solution was degassed once, and allyl chloroformate (4.7 ml., ca. 5.9 g.) was added. To the stirred solution at  $-78^\circ\text{C}$ . was added the initiator comprising  $15.3 \times 10^{-4}$  mole triethylborane and  $7.7 \times 10^{-4}$  mole  $\text{O}_2$  (17.5 ml.). Polymerization proceeded, and after 4 hr. the dichlorodifluoromethane was allowed to evaporate. The polymer was stirred successively with two 1-lb. portions of petroleum ether. It was then filtered under nitrogen and dried in a vacuum desiccator. Copolymers prepared from the above monomer ratio (ca. 3.6 mole-% allyl chloroformate) were found to contain 0.9–1.4% Cl, corresponding to 2.15–3.28 mole-% allyl chloroformate.

The authors gratefully acknowledge the assistance of Dr. W. J. Middleton, with whom many conversations were held.

### References

1. W. J. Middleton, H. W. Jacobson, R. E. Putnam, H. C. Walters, D. G. Pye, and W. H. Sharkey, *J. Polymer Sci. A*, **3**, 4115 (1965).
2. W. J. Middleton, E. G. Howard, and W. H. Sharkey, *J. Org. Chem.*, **30**, 1375 (1965).
3. G. S. Kolesnikov and N. V. Klimentova, *Izvest. Akad. Nauk SSSR, Otdel. Khim. Nauk*, **1957**, 652.

4. J. Furukawa and T. Tsuruta, *J. Polymer Sci.*, **28**, 227 (1958).
5. J. W. L. Fordham and C. S. Sturm, *J. Polymer Sci.*, **33**, 503 (1958).
6. N. L. Zutty and F. J. Welch, *J. Polymer Sci.*, **43**, 445 (1960).
7. R. C. Petry and F. H. Verhoek, *J. Am. Chem. Soc.*, **78**, 6416 (1956).

### Résumé

Le fluorure de thiocarbonyle,  $\text{CF}_2=\text{S}$ , et le chlorofluorure de thiocarbonyle  $\text{CFCl}=\text{S}$ , subissent une polymérisation par addition, en présence de systèmes initiateurs à base de radicaux libres. En outre, les deux composés copolymérisent avec des dérivées variées et insaturés y compris des monomères vinyliques et vinyliidéniques. Le chlorofluorure, par suite de sa vitesse de polymérisation, élevée, copolymérise le mieux avec des monomères très réactionnels dont le 2,3-dichloro-1,3-butadiène est un exemple. Le fluorure de thiocarbonyle polymérise le mieux à basse température. Les couples oxydo-réducteurs trialkylborane-oxygène ont été adaptés à la polymérisation radicalaire et copolymérisation à  $-60^\circ$  jusque  $-120^\circ\text{C}$ . Avec une telle initiation,  $\text{CF}_2=\text{S}$  a été copolymérisé avec des oléfines terminales et internes, des dérivés vinyliques, des dérivés allyliques, des esters acryliques. Avec le propylène, la copolymérisation est inhabituelle en ce sens qu'elle procède de façon à former un produit composé de deux molécules de  $\text{CF}_2=\text{S}$  par molécule de propylène. Dans les autres cas, la composition du produit répond mieux aux rapports des monomères engagés.

### Zusammenfassung

Thiocarbonylfluorid  $\text{CF}_2=\text{S}$  und Thiocarbonylchlorfluorid  $\text{CFCl}=\text{S}$  liefern in radikalisch gestarteten Systemen Additionspolymere. Ausserdem kopolymerisieren beide Verbindungen mit verschiedenen ungesättigten Verbindungen wie typischen Vinyl- und Vinylidenmonomeren. Das Chlorfluorid kopolymerisiert wegen seiner grossen Polymerisationsgeschwindigkeit am besten mit sehr aktiven Monomeren, wofür 2,3-Dichlor-1,3-butadien ein Beispiel ist. Thiocarbonylfluorid polymerisiert bei tiefen Temperaturen am besten. Das Redoxpaar Trialkylbor-Sauerstoff wurde für radikalische Polymerisationen und Kopolymerisationen bei  $-60$  bis  $-120^\circ\text{C}$  herangezogen. Mit diesem Starter wurde  $\text{CF}_2=\text{S}$  mit endständigen und inneren Olefinen, Vinylverbindungen, Allylverbindungen und Acrylsäureestern kopolymerisiert. Die Kopolymerisation mit Propylen ist dadurch ausgezeichnet, dass vornehmlich ein Produkt mit zwei Molekülen  $\text{CF}_2=\text{S}$  auf jedes Propylen geliefert wird. In anderen Fällen ist die Zusammensetzung der Produkte mehr von der Zusammensetzung der Monomerenmischung abhängig.

Received December 28, 1965

Revised March 22, 1966

Prod. No. 5134A

# Polymers Derived from Fluoroketones. I. Preparation of Fluoroalkyl Acrylates and Methacrylates\*

A. G. PITTMAN, D. L. SHARP, and R. E. LUNDIN,  
*Western Regional Research Laboratory,  
Agricultural Research Service, U. S. Department of Agriculture,  
Albany, California 94710*

## Synopsis

The preparation and physical properties of some perhaloalkyl acrylate and methacrylate esters are discussed. In the synthetic route to the perhaloalkyl esters, acryloyl or methacryloyl chloride is made to react with a metal fluoride-perhaloketone adduct. A side reaction which accompanies esterification is the formation of acryloyl or methacryloyl fluoride. Possible mechanisms for the formation of acyl fluoride and ester are considered. Evidence is presented which suggests that acyl fluoride formation may occur by a breakdown of the fluoroalkyl esters through an intramolecular fluorine shift.

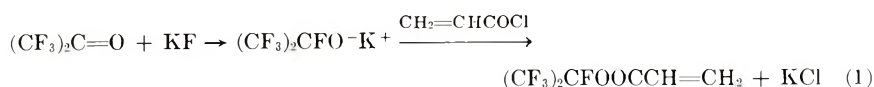
## INTRODUCTION

A variety of acrylates prepared from acrylic acid or acryloyl chloride and fluorinated alcohols has been reported.<sup>1</sup> Polymers of these fluoroalkyl acrylates have interesting surface properties and have been found to be useful in conferring oleophobic properties to a variety of surfaces.<sup>2-4</sup> In addition, one of these polymers has been suggested for use as a solvent-resistant rubber which has flexibility at low temperatures.<sup>5</sup>

## DISCUSSION

Since completely fluorinated alcohols are generally unstable,<sup>6</sup> the 1,1-dihydroperfluoroalcohols have been employed in esterification reactions with the acyl halide. We have found that it is possible to convert fluorinated ketones into fluoroalkyl acrylates and methacrylates without a preliminary reduction step to a secondary alcohol. The reaction scheme circumvents the instability of the  $\alpha$ -fluoroalcohols by acylating the alkali fluoride-fluoroketone 1:1 addition product which forms readily in polar solvents.<sup>7,8</sup> The overall reaction is illustrated for hexafluoroacetone, potassium fluoride, and acryloyl chloride [eq. (1)]. In this manner a wide

\* Presented in part at the 3rd International Symposium on Fluorine Chemistry, Munich, Germany, Sept. 1, 1965.



variety of perhaloalkyl esters can be prepared in good yields. We have used potassium and cesium fluoride interchangeably in this reaction and such solvents as *N,N*-dimethylformamide (DMF), acetone, bis(2-methoxyethyl)ether (diglyme), and acetonitrile. Acylation has been carried out at from  $-10^\circ\text{C}$ . to room temperature, and the work-up procedures have varied with the boiling point differential between product and solvent. In general, the simplest work-up procedure, with the solvents mentioned above, involved pouring the crude product-solvent mixture into water and washing the resulting fluorocarbon layer several times with additional water. After these washings, the esters contained small amounts of impurities, generally less than 10%, which could be removed by distillation. This procedure usually resulted in lower yields, presumably as a result of ester hydrolysis, than when the product was distilled directly from the solvent.

The only side reaction of any consequence noted during the acylation reaction was the formation of acryloyl or methacryloyl fluoride. These compounds did not form to an appreciable extent in diglyme or DMF but became more serious in acetonitrile and acetone (Table I). In acetone, acyl fluoride formation was minimized by conducting the esterification at  $-10$  to  $+10^\circ\text{C}$ .

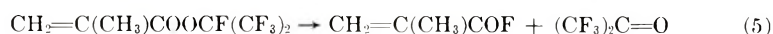
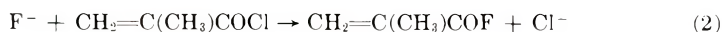
TABLE I  
Solvent Effects in the Preparation of Heptafluoroisopropyl  
Methacrylate (HM)

Solvent	Ester yield, % <sup>a</sup>	Ratio HM/MF <sup>b</sup>
DMF	73	49/1
Diglyme	60	9.5/1
Acetone	38	1.4/1
Acetonitrile	43	1.5/1

<sup>a</sup> Based on gas chromatographic analyses of material recovered water washing.

<sup>b</sup> MF is methacryloyl fluoride.

We have considered four possible reaction paths for the formation of acid fluoride. Two of these routes to acid fluoride involve the attack of free fluoride ion on either the acid chloride [eq. (2)] or the ester [eq. (3)]. The third route would result from attack of the acid chloride by the fluorine atom of the fluoroketone-potassium fluoride addition product [eq. (4)], and a fourth path would involve a breakdown of the ester into acid fluoride and hexafluoroacetone [eq. (5)].



The attacking fluoride ion in eqs. (2) and (3) would presumably arise by the breakdown of the fluoroketone-potassium fluoride addition product [eq. (6)].



In order to examine the ease of fluoroalkoxide displacement by fluoride [eq. (3)] we treated heptafluoroisopropyl methacrylate with a 10 mole-% quantity of potassium fluoride in acetonitrile and examined the product ratio of unreacted ester to methacryloyl fluoride at intervals (Table II). At room temperature acid fluoride formed slowly. The rate of acid fluoride formation increased with increasing temperature. In contrast, when methacryloyl chloride was added directly to the hexafluoroacetone-potassium fluoride adduct in acetonitrile at room temperature, heptafluoroisopropyl methacrylate and methacryloyl fluoride were formed immediately in the ratio of 1.5/1 (see Table I).

TABLE II  
Preparation of Methacryloyl Fluoride (MF) by the Reaction  
of Fluoride Ion with Heptafluoroisopropyl Methacrylate (HM)

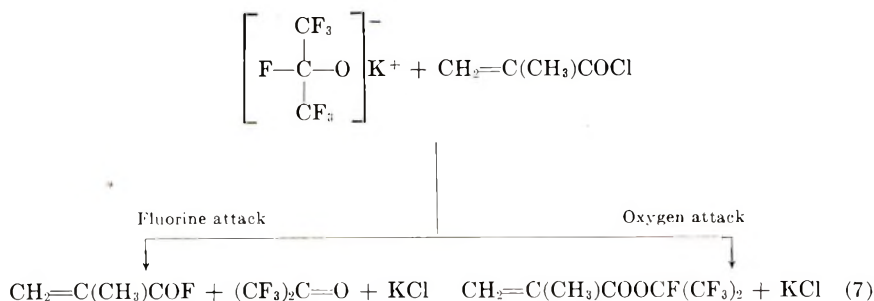
Reaction time, hr.	Temperature, °C.	Ratio HM/MF
0	23	14.4/1 <sup>a</sup>
0.5	23	14.4/1
1.0	23	12.6/1
1.5	65	6.4/1
2.0	65	2.5/1
2.5	65	1.8/1
3.0	65	1.5/1

<sup>a</sup> The starting ester contained methacryloyl fluoride as an impurity in this ratio.

The formation of methacryloyl fluoride by the direct displacement of chloride by fluoride in acetonitrile [eq. (2)] was also found to be a sluggish reaction (see Experimental) in comparison with the direct addition of methacryloyl chloride to the hexafluoroacetone-potassium fluoride adduct. In addition, the formation of free fluoride ion through the equilibration of fluoroketone with fluoride ion [eq. (6)] does not seem to have significance at room temperature. We attempted to demonstrate the presence of free hexafluoroacetone by shifting the equilibrium to the right by removing hexafluoroacetone under vacuum. Solutions containing the hexafluoroacetone-potassium fluoride adduct in diglyme and DMF were maintained at 24°C. and placed under a 6-mm. vacuum for 7 hr. At the end of this time, no hexafluoroacetone had collected in attached Dry Ice traps.

It would seem therefore, that acid fluoride formation does not occur by the reaction of free fluoride ion with either the ester or acid chloride.

The reaction suggested in eq. (4) would involve a fluoroalkoxide anion which could attack at the carbonyl carbon of the acyl halide either through oxygen or fluorine [eqs. (7)].



Bradley et al.<sup>9</sup> have proposed that although the negative charge in the trifluoromethoxide ion  $(\text{OCF}_3)^-$  formally rests on oxygen, the greater electronegativity of fluorine would lead to a more even distribution of charge over the ion, enhancing its stability. Similarly, with the fluoroketone-potassium fluoride adduct, the negative charge, although formally resting on oxygen, may be distributed between oxygen and fluorine giving the anion ambident character.

Kornblum et al.<sup>10</sup> have shown that with ambident anions such as nitrite and cyanide, as a substitution reaction acquires an increasing degree of  $S_N1$  character, the incoming nucleophile tends to attack with its most electronegative atom, but as the reaction acquires more  $S_N2$  character the incoming group tends to attack with the less electronegative atom. If the fluoroketone-potassium fluoride adduct resembles an ambident anion in its reaction with acid chlorides, an increase in attack by the more electronegative fluorine atom in more polar solvents such as acetonitrile and acetone would be expected. The role of DMF as a solvent in this reaction becomes difficult to assess, since DMF is known to form addition products with acyl halides.<sup>11</sup>

Although we cannot eliminate as a possibility the reaction path given by eq. (4), we have evidence which suggests that the breakdown of the fluoroalkyl esters into an acyl fluoride and a fluoroketone [eq. (5)] is the most plausible explanation for the formation of acid fluoride. During the preparation of the saturated ester, heptafluoroisopropyl propionate, we found that this ester exhibited a pronounced tendency to break down into propionyl fluoride and hexafluoroacetone on standing at room temperature. This type of instability had not been observed with either the fluoroalkyl acrylate or methacrylate esters. Breakdown of the saturated propionate

TABLE III  
Room Temperature Decomposition of Crude Heptafluoroisopropyl Propionate (HP) into Propionyl Fluoride (PF) and Hexafluoroacetone

Time elapsed, hr.	Ratio PF/HP
0	1/99
12	1/21
30	1/3.1
80	1/1.6

TABLE IV  
Acrylate Properties and Analyses ( $R_f-O-C(=O)CH=CH_2$ )

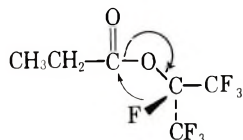
$R_f$	B.p., °C./mm. Hg	$n_D^{25}$	$d_4^{25}$ , g./ml.	Infrared, cm. <sup>-1</sup> (carbonyl)	Analyses			
					Carbon, %		Fluorine, %	
					Calcd.	Found	Calcd.	Found
$(CF_3)_2CF-$	86-87/760	1.3116	1.42	1795	30.01	29.42	55.3	56.2
$(CF_3)(CF_2Cl)CF-$	118-19/760	1.3464	1.47	1794	28.09	30.30	44.4	43.9
$(CF_2Cl)_2CF-$	148/760	1.3794	1.51	1792	26.40	26.38	34.8	34.9

TABLE V  
Methacrylate Properties and Analyses ( $R_f-O-C(=O)C(CH_3)=CH_2$ )

$R_f$	B.p., °C./mm. Hg	$n_D^{25}$	$d_4^{25}$ , g./ml.	Analyses			
				Carbon, %		Fluorine, %	
				Calcd.	Found	Calcd.	Found
$(CF_3)_2CF-$	102/760	1.3240 <sup>23</sup>	1.37 <sup>23</sup>	33.08	33.14	52.3	51.5
$(CF_3)(CF_2Cl)CF-$	132/760	1.3574 <sup>22</sup>	1.41 <sup>22</sup>	31.07	30.47	42.1	42.6
$(CF_2Cl)_2CF-$	162/760	1.3895 <sup>24</sup>	1.45 <sup>24</sup>	29.29	29.80	33.1	32.5



ester was catalyzed by some impurity or impurities in the freshly prepared unpurified material (Table III). After purification of the ester by either preparative gas chromatography or distillation, the stability of the ester was increased. An examination of Fisher-Hirschfelder models revealed an interesting difference which might explain the difference in stability between the acrylate-methacrylate esters and the saturated propionate ester. There appears to be considerable hindrance to free rotation of the heptafluoroisopropyl group in the saturated propionate ester due to the steric requirements of the  $\text{CH}_3\text{CH}_2-$  group. On the other hand, the unsaturated ethylenic group of the acrylate and methacrylate esters does not substantially interfere with the free rotation of the heptafluoroisopropyl group. It was also noted that in the less hindered conformations of the propionate ester, the fluorine atom on the secondary carbon atom of the perfluoroisopropyl group is in an excellent position for the required backside attack on the carbonyl carbon.



Traces of hydrogen fluoride, arising from hydrolysis of acyl fluoride, are believed to be the catalyst in the decomposition of the crude propionate ester. Protonation of the carbonyl oxygen should enhance the electrophilicity of the carbonyl carbon and assist in the type of intramolecular fluorine shift we are proposing.

We are continuing to investigate the instability of certain fluoroalkyl esters in order to further elucidate this reaction mechanism.

A tabulation of the physical properties for several fluoroalkyl acrylates and methacrylates is given in Tables IV and V.

The fluoroalkyl acrylates and methacrylates have been homopolymerized and copolymerized by free-radical catalysts in bulk, in solution, and emulsions. Physical properties of the polymeric acrylates and methacrylates and details of polymerization will be published in a forthcoming article.

## EXPERIMENTAL

Boiling points are uncorrected. Infrared spectra were obtained on a Perkin-Elmer 137 spectrophotometer and a Beckman Model IR7 spectrophotometer. Proton NMR spectra were taken on a Varian Associates 60 Mcycle high resolution NMR spectrometer. Fluorine NMR spectra were taken on a Varian HR-56. Gas chromatographic studies were carried out with an Aerograph Autoprep Model A-700 having a 20-ft. column ( $\frac{3}{8}$  in. o.d.) packed with 30% silicone gum rubber on Chromasorb P of 60/80 mesh, which had been acid washed and pretreated with dimethyldichlorosilane. In some cases, yields were calculated from the peak areas of gas chromatograms.

The materials used and their sources of supply follow: halogenated ketones from Allied Chemical Corp. and Du Pont; acryloyl and methacryloyl chlorides, from Borden Monomer-Polymer Laboratories; potassium fluoride (anhydrous), from Allied Chemical Corp., General Chemical Division, and redried as indicated; cesium fluoride (anhydrous), from American Potash and Chemical Corp., redried as indicated; acetone, Baker analyzed (99.5%), dried over CaSO<sub>4</sub>; diglyme [bis(2-methoxyethyl)ether], from Eastman Organic Chemicals, distilled from fresh sodium before use; acetonitrile, distilled from P<sub>2</sub>O<sub>5</sub>, *N,N*-dimethylformamide, from Eastman Organic Chemicals, distilled from BaO before use.

### Preparation of Heptafluoroisopropyl Methacrylate in Acetone

A 500-ml. three-necked round-bottomed flask was equipped with a dropping funnel, Dry Ice condenser, gas inlet tube, and magnetic stirring bar. The assembled apparatus was heated under vacuum with a burner to remove moisture and then allowed to cool to room temperature while a stream of dry nitrogen was bled through the system. Anhydrous KF (14.5 g., 0.25 mole) was introduced into the flask, and the apparatus and KF were placed under vacuum and heated again with a burner to remove moisture which might have been adsorbed during the introduction of the fluoride. After the flask had again cooled to room temperature, 200 ml. of anhydrous acetone was quickly introduced and the condenser filled with Dry Ice. Hexafluoroacetone (42 g., 0.25 mole) was added to the KF-acetone dispersion at such a rate that gas condensed and dripped rapidly from the Dry Ice condenser. The formation of potassium heptafluoroisopropylate was complete after about 20 min., as evidenced by the disappearance of dispersed KF and the lack of condensed hexafluoroacetone on the Dry Ice condenser even when the solution was warmed to ca. 50°C. The solution was then stirred and cooled to -45°C. Methacryloyl chloride (26 g., 0.25 mole) was added through the dropping funnel over a 5-min. period. The cooling bath was removed and the solution allowed to warm. The reaction began at about -15°C. when the solution became slightly turbid from KCl precipitation. A water-ice bath was then placed around the flask and the reaction mixture maintained at 5-10°C. for 1.5 hr. The resulting slurry was poured into 300 ml. of an ice-water mixture. The lower fluorocarbon layer was recovered and washed once with 100 ml. cold (5°C.) water and twice with tap water (23°C.). A 38-g. yield of crude product (56%) was obtained. Gas chromatographic analysis of the crude product revealed, in addition to the methacrylate ester, ca. 10% residual solvent acetone and ca. 4% methacryloyl fluoride. The identity of methacryloyl fluoride was confirmed by infrared and NMR spectroscopy and by several of its physical properties (b.p. 55.3°C./760 mm.;  $n_D^{25}$  1.3664; reported<sup>12</sup> b.p. 56.5-58°C./760 mm.;  $n_D^{25}$  1.3703).

The methacrylate ester was further purified by distillation, b.p. 102°C./760 mm. The proton NMR spectrum of a 20% solution of the purified product was taken. The vinyl proton signals occurred at  $\tau = 3.75$  (1.0 H)

and 4.16 (1.0 H) with multiple incompletely resolved splittings of 0.8 cps. The lower field signal had a linewidth of 2.8 cps and the higher, 4.4 cps. The signal from the allylic methyl protons occurred at  $\tau = 8.00$  (3.0 H) with incompletely resolved splittings of 0.6, 0.8, and 1.0 cps and a linewidth of 3.4 cps. The  $F^{19}$  spectrum of this solution was taken with fluorotrichloromethane added as the fluorine internal standard. Positions were determined by the standard interpolation technique using modulation sidebands. The perfluoromethyl signal (6.0 F) occurred as a doublet ( $J = 2.1$  cps) at 78.67 ppm (in field) above the reference. The fluorine on the secondary carbon (1.0 F) occurred as a presumed septet ( $J = 2.1$  cps, first and last peaks obscured by noise) at 141.52 ppm above the reference.

### Preparation of Heptafluoroisopropyl Acrylate in Diglyme

A 250-ml. three-necked round-bottomed flask equipped with a stirring bar, gas-inlet tube, and Dry Ice reflux condenser was dried under vacuum as in the preceding example. Anhydrous potassium fluoride (9.6 g., 0.16 mole) was introduced and then 150 ml. of dry diglyme added. The mixture was stirred and cooled in a Dry Ice-acetone bath. After Dry Ice was placed in the reflux condenser and the diglyme-KF slurry had cooled to ca.  $-20^{\circ}\text{C}$ ., 27 g. of hexafluoroacetone was added through the gas-inlet tube. It was found advantageous to cool the diglyme-KF slurry because the KF addition occurred more slowly in this solvent than in acetone. After about 15 min., the gas addition was complete and the cooling bath was removed. After about 30 minutes more, alcoholate formation was assumed to be complete since the solution had come to room temperature and there no dispersed KF was visible. Acryloyl chloride (12.9 ml., 0.16 mole) was then added dropwise with a syringe through an inlet equipped with a rubber septum. The mixture was maintained at  $23-25^{\circ}\text{C}$ . during this addition by cooling in a water bath. A precipitate of KCl formed during the acyl halide addition. After the addition, the flask was equipped with a Claisen head and the product was removed from the slurry by distilling under a slight vacuum (20 mm.). The product was collected in a Dry Ice trap. When the temperature of the Claisen head rose sharply and diglyme began to distill, the distillation was discontinued. The distillate was poured into 150 ml. of an ice-water mixture, and the lower fluorocarbon layer was washed twice with 50 ml. portions of tap water. This yielded 28 g. (71%) of product, b.p.  $86-88^{\circ}\text{C}/760$  mm. Gas chromatographic analysis of the product revealed less than 1% acryloyl fluoride and no residual diglyme or acryloyl chloride.

The acylation reaction was repeated, but instead of removing product from the diglyme by distillation, the slurry was poured directly into cold water ( $5^{\circ}\text{C}$ .). The fluorocarbon layer was collected and washed twice as in the preceding example. In this manner, a 47% yield of acrylate ( $\sim 99\%$  purity) was obtained.

### Preparation of $\beta,\beta'$ -Dichloropentafluoroisopropyl Acrylate with CsF in Diglyme

A 250-ml. three-necked round-bottomed flask was equipped with a condenser, stirring bar, and rubber septum-sealed inlet and dried under vacuum as in the preceding examples. Anhydrous CsF (16.8 g., 0.126 mole) was introduced, and the flask and CsF were placed under vacuum and heated again to remove adsorbed moisture. After the flask had again cooled to room temperature, 100 ml. of dry diglyme was quickly introduced. The flask was cooled in a water bath and 1,3-dichlorotetrafluoroacetone (25 g., 0.126 mole) was added over a 10-min. period. Acryloyl chloride (11.7 g., 0.126 mole) was then added dropwise with a syringe to the stirred solution.

After the addition, the mixture was stirred at room temperature an additional 0.5 hr. The slurry was then poured into 200 ml. ice-water mixture and washed twice with 50-ml. portions of tap water. The crude product was dried over  $\text{CaSO}_4$  and then distilled under reduced pressure (50°C./15–20 mm.). A 51% yield of purified acrylate (17.5 g.) was obtained.

#### Solvent Effects in Ester Preparation

Addition of methacryloyl chloride to the hexafluoroacetone-KF adduct was carried out at room temperature (23°C.) in diglyme, DMF, acetone, and acetonitrile. In each case 4 ml. of anhydrous solvent was used per gram of hexafluoroacetone. The addition was carried out at room temperature. Both the acetonitrile and acetone solutions cooled slightly during addition of the acid chloride to the adduct as a result of the evolution of gaseous hexafluoroacetone. After the acid chloride had been added, the reaction medium was stirred an additional  $\frac{1}{2}$  hr. at room temperature, then poured into two volumes of cold (5°C.) water. The fluorocarbon layer was collected and washed twice with cold water and analyzed by gas chromatography. The results are given in Table I.

#### Reaction of Fluoride Ion with Heptafluoroisopropyl Methacrylate

In a three-necked 250-ml. flask were placed 20 g. (0.08 mole) heptafluoroisopropyl methacrylate, 80 ml. anhydrous acetonitrile, and 0.46 g. (0.008 mole) anhydrous KF. At  $\frac{1}{2}$ -hr. intervals a 2-ml. sample was withdrawn from the mixture and poured into 5 ml. cold water. The fluorocarbon layer was washed twice with 1 ml. water. The product was then analyzed by gas chromatography to determine the ratio of methacrylate/acid fluoride (Table II).

#### Reaction of Fluoride Ion with Methacryloyl Chloride

In a three-necked 250-ml. flask were placed 20 ml. acetonitrile, 5 g. (0.05 mole) methacryloyl chloride, and 2.9 g. (0.05 mole) KF. The reaction mixture was stirred at 65°C. for 2 hr. A 4-ml. sample was withdrawn and poured into a centrifuge tube containing 4 ml. cold water. The

water layer was discarded and the organic layer washed twice with 1 ml. portions of cold water. Gas chromatographic analysis revealed the presence of methacryloyl chloride and methacryloyl fluoride in the ratio 5/1.

### Instability of Heptafluoroisopropyl Propionate

The 1:1 addition product of hexafluoroacetone and potassium fluoride was prepared as described in the previous examples with the use of 46 g. (0.27 mole) hexafluoroacetone, 15.6 g. (0.27 mole) anhydrous KF, 24.4 g. (0.27 mole) propionyl chloride, and 200 ml. anhydrous diglyme. The reaction mixture was poured into 300 ml. cold water, the lower layer removed and washed three times with water. The yield was 51 g. (77%) of crude product. Gas chromatographic analysis of the crude product revealed the presence of heptafluoroisopropyl propionate and propionyl fluoride in the ratio 99/1. There was no indication of other impurities in the crude product by gas chromatographic analysis.

The crude product was divided into three equal portions and examined in the following manner: One portion was placed over anhydrous  $\text{CaSO}_4$  in a small vial sealed with a rubber septum. At various intervals, a sample of liquid was withdrawn and examined by gas chromatography. The results of these analyses are given in Table III. The identity of hexafluoroacetone gas as one of the decomposition products was confirmed by infrared spectroscopy. The hexafluoroacetone gas was vented from the vial at intervals in order to reduce the pressure build-up. The identity of propionyl fluoride and heptafluoroisopropyl propionate was confirmed by trapping samples from the preparative gas chromatographic unit and examining the samples by infrared and NMR spectroscopy.

A second portion of the original 51-g. crude sample was distilled slowly at atmospheric pressure using a small Vigreux column. During distillation of this crude sample, breakdown of the propionate ester occurred. Gas chromatographic analysis of the distilled product revealed the presence of heptafluoroisopropyl propionate and propionyl fluoride in the ratio 1/4.5.

A third and final portion of the original 51-g. crude sample was allowed to stand over anhydrous  $\text{CaSO}_4$  and sodium fluoride for about 1 hr. Sodium fluoride was added in order to absorb any hydrogen fluoride present in the liquid. The liquid was then transferred from the solid by flash distillation under 0.5 mm. pressure. The product was collected in a Dry Ice trap. The propionate ester was now distilled at atmospheric pressure without any noticeable decomposition, b.p. 89–90°C./768 mm.;  $n_D^{23}$  1.3009. The infrared spectrum of the ester revealed carbonyl stretching at 1825  $\text{cm.}^{-1}$

ANAL. Calcd. for  $\text{C}_6\text{F}_7\text{H}_3\text{O}_2$ : C, 29.71%; H, 2.05%. Found: C, 29.53%; H, 2.0%.

Reference to a company or product name does not imply approval or recommendation of the product by the U. S. Department of Agriculture to the exclusion of others that may be suitable.

### References

1. D. W. Codding, T. S. Reid, A. H. Ahlbrecht, G. H. Smith, Jr., and D. R. Husted, *J. Polymer Sci.*, **15**, 515 (1955).
2. M. K. Bennett and W. A. Zisman, *J. Phys. Chem.*, **66**, 1207 (1962).
3. E. J. Grajeck and W. H. Petersen, *Textile Res. J.*, **32**, 320 (1962).
4. W. A. Zisman, *Record Chem. Progr.*, **26**, No. 1, 13 (1965).
5. H. G. Bryce, in *Fluorine Chemistry*, J. H. Simons, Ed., Academic Press, New York, 1964, Vol. 5, pp. 477-479.
6. A. M. Lovelace, D. A. Rausch, and W. Postelnek, *Aliphatic Fluorine Compounds*, Reinhold, New York, 1958, p. 137.
7. A. G. Pittman and D. L. Sharp, *Textile Res. J.*, **35**, 190 (1965).
8. A. G. Pittman and D. L. Sharp, *J. Polymer Sci. B*, **3**, 379 (1965).
9. D. C. Bradley, M. E. Redwood, and C. J. Willis, *Proc. Chem. Soc.*, **1964**, 416.
10. N. Kornblum, R. A. Smiley, R. K. Blackwood, and D. C. Iffland, *J. Am. Chem. Soc.*, **77**, 6269 (1955).
11. H. K. Hall, Jr., *J. Am. Chem. Soc.*, **78**, 2717 (1956).
12. Brit. Pat. 591,383 (to Du Pont), August 15, 1947.

### Résumé

La préparation et les propriétés physiques de certains esters perhaloalcoylés acryliques et méthacryliques est discutée. Du point de vue de la synthèse des esters perhaloalcoylés, on fait réagir du chlorure d'acryloyle ou de méthacryloyle avec le produit d'addition d'un fluorure métallique à une cétone perhalogénée. Une réaction secondaire qui accompagne l'estérification réside dans la formation de fluorure d'acryloyle et de méthacryloyle. Les mécanismes possibles de formation de fluorures d'acyle et d'esters sont considérés. On suggère que la formation de fluorure d'acyle résulte de la cassure des esters fluoroalcoylés par suite d'un réarrangement intramoléculaire du fluor.

### Zusammenfassung

Die Darstellung und die physikalischen Eigenschaften einiger perhalogenierter Alkylacrylat- und Methacrylatester werden diskutiert. Die Synthese der perhalogenierten Alkyester erfolgt durch Reaktion von Acryloyl- oder Methacryloylchlorid mit einem Metallfluorid-perhalogenoketonaddukt. Die Veresterung wird von der Bildung von Acryloyl- oder Methacryloylfluorid als Nebenreaktion begleitet. Mögliche Mechanismen für die Bildung von Acylfluorid und Ester werden in Betracht gezogen. Die Acylfluoridbildung scheint durch eine intramolekulare Fluorverschiebung in den Fluoroalkylestern zustande zu kommen.

Received March 17, 1966

Prod. No. 5146A

## Copolymerization of Isopropenyl and Isopropylidene Oxazolones with Styrene

YOSHIO IWAKURA, FUJIO TODA, and YOSHINORI TORII,

*Department of Synthetic Chemistry, Faculty of Engineering,*

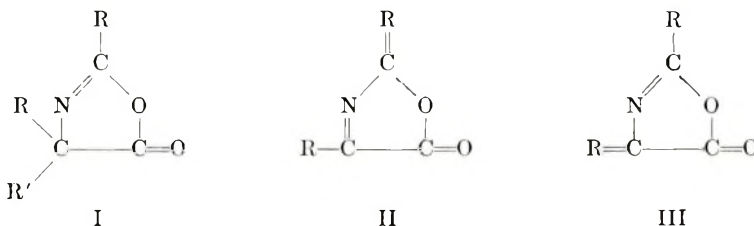
*The University of Tokyo, Tokyo, Japan*

### Synopsis

2-Isopropenyl-4-isopropyl-2-oxazolin-5-one ( $M_2$ ), was copolymerized with styrene ( $M_1$ ), and the monomer reactivity ratios were determined to be  $r_1 = 0.31 \pm 0.03$ ,  $r_2 = 1.12 \pm 0.10$ . New isomerized oxazolones ( $M_2$ ), 2-isopropylidene-4-methyl-3-oxazolin-5-one, 2-isopropylidene-4-isopropyl-3-oxazolin-5-one, and 2-isopropylidene-4-isobutyl-3-oxazolin-5-one were prepared and copolymerized with styrene. The monomer reactivity ratios were:  $r_1 = 0.36 \pm 0.07$ ,  $r_2 = 0.0$ ;  $r_1 = 0.39 \pm 0.06$ ,  $r_2 = 0.00 \pm 0.10$ ;  $r_1 = 0.39 \pm 0.10$ ,  $r_2 = 0.0$ , respectively. The isomerized oxazolones showed no tendency towards homopolymerization by radical initiator. From the results of infrared and NMR spectra and hydrolysis of the copolymer, it was indicated that the isomerized oxazolones participated in copolymerization in the form of 1-4 polymerization of the conjugated dienes (exo double bond at  $C_2$  and the  $C=N$  in the ring). Copolymers reacted with nucleophilic reagents such as amines and alcohols.

### INTRODUCTION

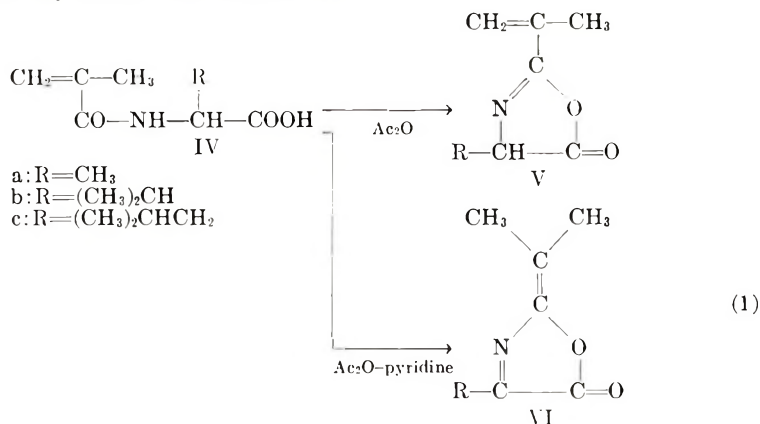
Much work has been done in recent years on the preparation of polymers having chemically reactive groups. The present study was undertaken to investigate the synthesis of vinyl and isopropenyl derivatives<sup>1</sup> of oxazolones which have great reactivity towards nucleophilic reagents,<sup>2,3</sup> and to prepare the so-called reactive polymers.<sup>4,5</sup> Oxazolones<sup>6</sup> are conveniently classified into two groups; saturated (I) and unsaturated ones (II and III).



Types II and III differ in the position of double bonds. There have been few reports on the preparation of II.<sup>7,8</sup>

It has been shown in this laboratory<sup>9</sup> that *N*-methacryloyl- $\alpha$ -amino acids (IV) are converted into 2-isopropenyl-2-oxazolin-5-ones (V) by the technique of Lynn<sup>1</sup> and that, when IV is treated with an equimolar amount of

acetic anhydride in pyridine at 100°C., isomerized oxazolones, i.e., 2-isopropylidene-3-oxazolin-5-ones (VI), are obtained as a result of migration of double bonds. In order to investigate the relationship between the structures of the monomers and the sites of polymerization of oxazolones, V and VI were copolymerized with styrene by radical initiators, and monomer reactivity ratios were determined.



From infrared and NMR spectra, and the hydrolysis of the copolymer, and further, from the monomer reactivity ratios, it was concluded that V participated in the copolymerization by the opening of isopropenyl double bond, while VI was involved in 1-4 polymerization of the conjugated double bonds (exo C=C at C<sub>2</sub> and C=N in the ring). Such a 1-4 polymerization is considered to be quite unusual, because the conjugated diene is very sterically crowded at the 1 and 4 positions and it contains a nitrogen atom in the diene system.

## EXPERIMENTAL

### Materials

*N*-Methacryloyl-*DL*- $\alpha$ -amino acids were prepared by the reaction of *DL*-alanine, *DL*-valine, and *DL*-leucine with methacryloyl chloride with the use of twice the equimolar amount of sodium hydroxide as an acid acceptor. Melting points and yields of the products are as follows: *N*-methacryloyl-alanine<sup>10</sup> (IVa), 117–118°C. (73%), *N*-methacryloylvaline<sup>1</sup> (IVb) 101–102°C. (86%), *N*-methacryloylleucine (IVc), 105–106°C. (71%).

ANAL. Calcd. for C<sub>7</sub>H<sub>11</sub>NO<sub>3</sub> (IVa): C, 53.49%; H, 7.05%; N, 8.91%. Found: C, 53.93%; H, 6.96%; N, 9.14%.

Calcd. for C<sub>10</sub>H<sub>17</sub>NO<sub>3</sub> (IVc): C, 60.28%; H, 8.60%; N, 7.03%. Found: C, 60.60%; H, 8.34%; N, 7.16%.

2-Isopropenyl-4-isopropyl-2-oxazolin-5-one (Vb) was prepared by the following procedure.<sup>1</sup> A solution of *N*-methacryloylvaline in acetic anhydride was added to acetic anhydride heated previously to 100°C. and the mixture was kept for 5 min. at the same temperature. After removal



of excess acetic anhydride and acetic acid under reduced pressure, the product was obtained by vacuum distillation at 100°C./20 mm. Hg.

2-Isopropylidene-3-oxazolin-5-ones were synthesized by the following method. Acetic anhydride was added to a solution of IV in pyridine, then the mixture was heated to 100°C. for 2 hr.<sup>11</sup> After pyridine was removed under reduced pressure, the residue was submitted to fractional distillation *in vacuo*. Boiling points of the products obtained are as follows: 2-isopropylidene-4-methyl-3-oxazolin-5-one (VIa), 54–56°C./1.5 mm. Hg; 2-isopropylidene-4-isopropyl-3-oxazolin-5-one (VIb), 74–76°C./1 mm. Hg.; 2-isopropylidene-4-isobutyl-3-oxazolin-5-one (VIc), 84–86°C./1 mm. Hg.

ANAL. Calcd. for C<sub>7</sub>H<sub>9</sub>NO<sub>2</sub> (VIa): C, 60.42%; H, 6.52%; N, 10.07%. Found: C, 60.28%; H, 6.30%; N, 10.01%.

Calcd. for C<sub>9</sub>H<sub>13</sub>NO<sub>2</sub> (VIb): C, 64.65%; H, 7.78%; N, 8.38%. Found: C, 64.16%; H, 7.93%; N, 8.88%.

Calcd. for C<sub>10</sub>H<sub>15</sub>NO<sub>2</sub> (VIc): C, 66.27%; H, 8.34%; N, 7.73%. Found: C, 66.07%, H, 8.10%; N, 7.91%.

It was found necessary for VI to be stored in a sealed tube in order to avoid the formation of polyperoxide with oxygen in the air.<sup>11</sup>

### Copolymerization Procedure

About 5 g. of a mixture of styrene (M<sub>1</sub>) and an oxazolone (M<sub>2</sub>) was kept at 60°C. for 24–48 hr. in a sealed tube with the use of 0.02 g. of  $\alpha,\alpha'$ -azobisisobutyronitrile. Polymerization was stopped by cooling the ampule to room temperature at 5–10% conversion. The resulting viscous solution was poured into a large amount of methanol, and the precipitate was collected by filtration and washed with methanol several times. The polymer was further purified by reprecipitation in benzene to methanol. After drying, the polymer was submitted to elemental analyses for determination of  $r_1, r_2$  values.

### Hydrolysis of Copolymers

A sample (100 mg.) of copolymer (VIIIa) of VIa with styrene (content of VIa = 36.4 mole-%,  $[\eta] = 0.42$  at 30°C. in dioxane) was dissolved in 5 ml. of dioxane. To this solution, 1 ml. of concentrated HCl was added, and the mixture was kept at 80°C. for 5 hr. After neutralization with dilute NaOH, the product (68 mg.) obtained was not soluble in toluene. Reduced specific viscosity determined in dioxane was 0.04 at  $C = 1.00$  g./dl.

The copolymer (VII) of Vb with styrene (1 g., content of Vb = 22.9 mole-%,  $[\eta] = 0.16$  in dioxane) was treated by the same procedure. The intrinsic viscosity of the hydrolyzed product (958 mg.) was 0.16 in dioxane. Valine was also detected by paper chromatography of neutralized filtrate with *n*-butanol-acetic acid-water mixture (4:2:1) at  $R_f = 0.58$ .<sup>12</sup>

### Reaction of Copolymers with Amine

A sample of copolymer (1 g.) was dissolved in 10 ml. of toluene and after addition of five times the equimolar amount of *n*-butylamine, the polymer



TABLE I  
 Reactivity Ratios of Monomers

Monomer	$r_1$	$r_2$
2-Isopropenyl-4-isopropyl-2-oxazolin-5-one (Vb)	$0.31 \pm 0.03$	$1.12 \pm 0.10$
2-Isopropylidene-4-methyl-3-oxazolin-5-one (VIa)	$0.36 \pm 0.07$	0.0
2-Isopropylidene-4-isopropyl-3-oxazolin-5-one (VIb)	$0.39 \pm 0.06$	$0.00 \pm 0.10$
2-Isopropylidene-4-isobutyl-3-oxazolin-5-one (VIc)	$0.39 \pm 0.10$	0.0
2-Vinylpyridine <sup>a</sup>	$1.14 \pm 0.08$	$0.55 \pm 0.025$
3-Vinyl-5-phenylisoxazole <sup>b</sup>	0.72	$0.48 \pm 0.04$
2-Isopropenyl-4,5-dimethyloxazole <sup>c</sup>	0.15	2.20

<sup>a</sup> Data of Walling et al. (at 60°C.).<sup>16</sup>

<sup>b</sup> Data of Sumitomo et al. (at 60°C.).<sup>17</sup>

<sup>c</sup> Data of Toda (60°C.).<sup>17</sup>

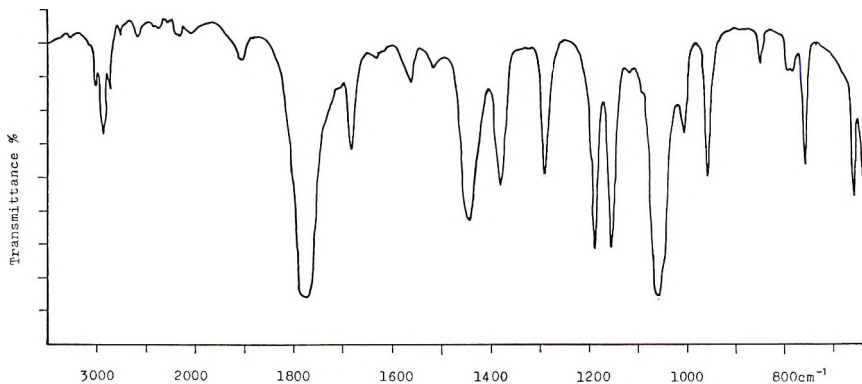
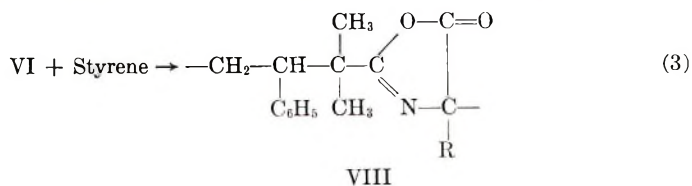


Fig. 1. Infrared spectrum of VIa (capillary).

other hand, the wave number of the C=N bond decreased to  $1665 \text{ cm.}^{-1}$  in the polymer. This indicates disappearance or migration of C=N bond in VIa as the result of polymerization. The NMR spectra of monomer VIa and its copolymer are shown in Figures 4 and 5. Absorptions at  $\tau$  7.96, 7.90, and 7.71 (assigned to methyl group at 4 position of the ring) shown in the spectrum of VIa are not found in that of VIIIa at all. In view of the fact that all methyl proton resonances shifted to higher field on polymerization, it was thought that the double bond of isopropylidene group was concerned to the copolymerization with styrene as shown in eq. (3).



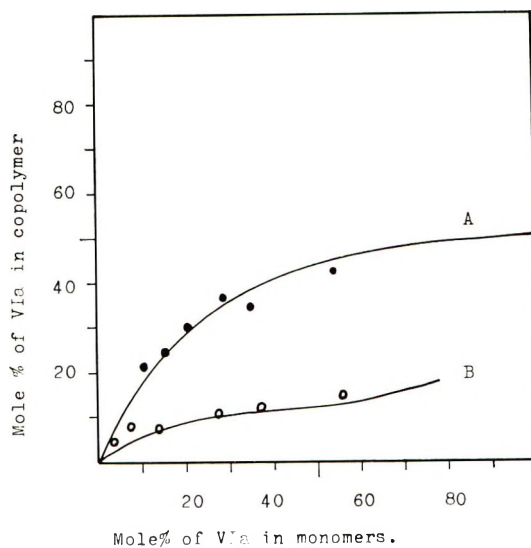


Fig. 2. Copolymer composition vs. composition of monomer feed: (A) copolymerization of VIa with styrene; (B) copolymerization of VIa with MMA.

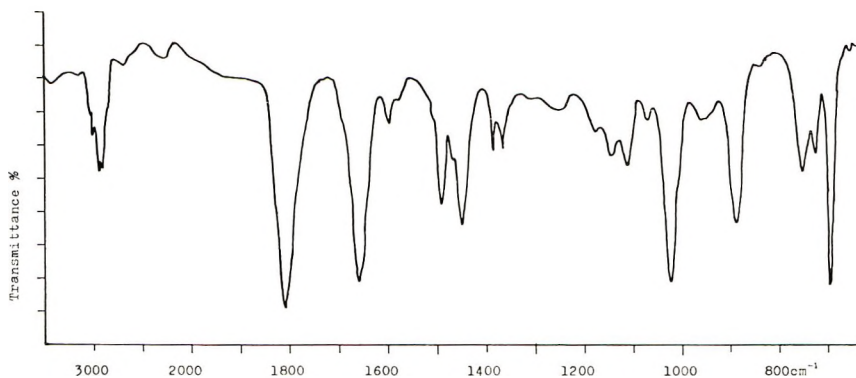


Fig. 3. Infrared spectrum of the copolymer of VIa with styrene (36.4 mole-% VIa, film).

In VII, oxazolone rings are pendant from the polymer chain, while in VIII, they are contained in the polymer chain itself. Infrared spectra of both VII and VIIIb were substantially identical; therefore, it was rather difficult to distinguish between the copolymers on the basis of these spectra.

VII and VIIIa, however, differed with respect to behavior on acid hydrolysis due to the difference of polymer structure. It was found that the films could not be hydrolyzed by either 5% aqueous NaOH or 5% aqueous HCl. In order to bring the copolymers into sufficiently close contact with the reagents, hydrolysis was carried out with the copolymers in a solution or swollen state. VIIIa was hydrolyzed from high polymer ( $[\eta] = 0.42$  in dioxane) to low molecular weight substances ( $\eta_{sp}/c = 0.04$  in dioxane), while VII withstood degradation by hydrolysis. The infrared

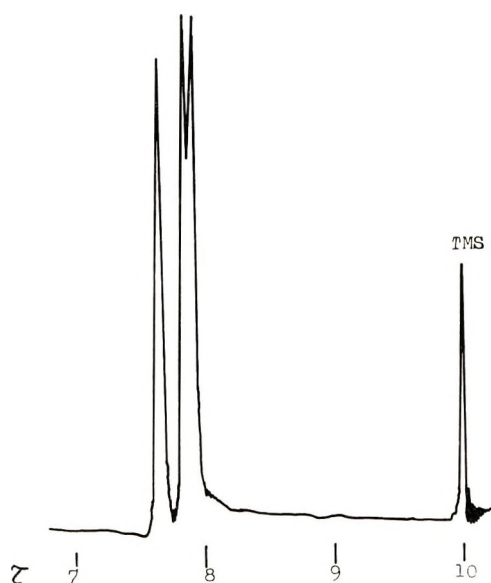
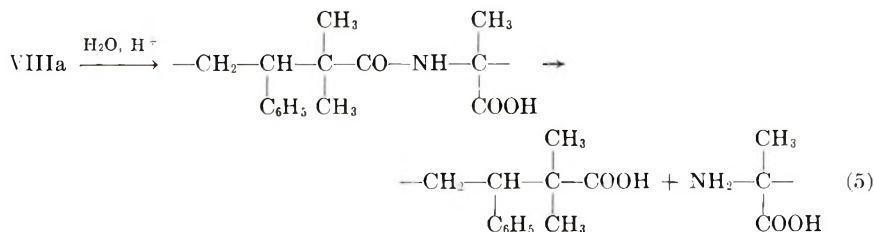
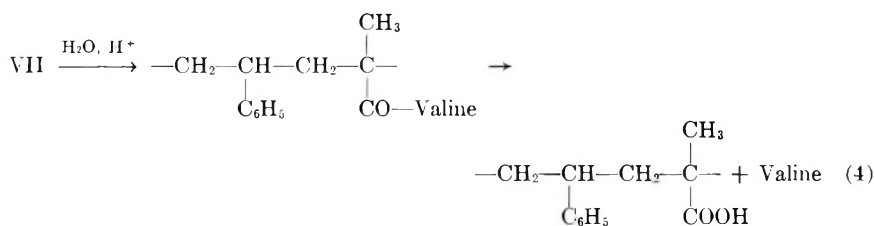


Fig. 4. NMR spectrum of VIa (10% in  $\text{CCl}_4$ ,  $20^\circ\text{C}$ ., 60 Mc. Model DP-60, Varian Associates).

spectra of hydrolyzed polymer from VII resembled that of styrene-methacrylic acid copolymer. From these facts, the reaction scheme shown in eqs. (4) and (5) is postulated.



It may also be concluded from the results that copolymerization of VI proceeded through 1-4 polymerization of the conjugated diene as mentioned above.

VII and VIII were thought to be converted to polyamides<sup>5</sup> with amines as the result of ring opening reaction of oxazolone. The results of polymer reaction with *n*-butylamine are shown in Table II.

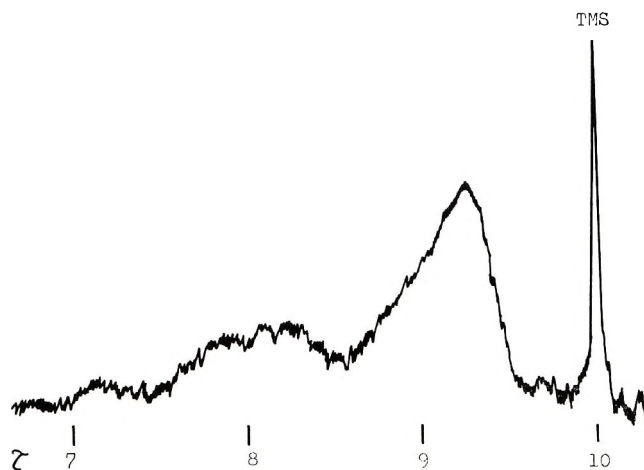
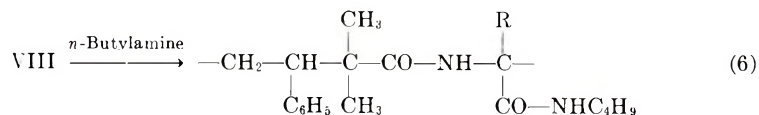


Fig. 5. NMR spectrum of VIIIa (5% in  $\text{CHCl}_3$ , 50°C., 60 Mc., Model C-60, JEOL).

TABLE II  
Reaction of Copolymers with *n*-Butylamine

Copolymer	Before reaction			After reaction		
	N, %	Oxazo- lone, mole-%	Viscosity [ $\eta$ ] (30°C., in dioxane)	N, %	Viscosity [ $\eta$ ] (30°C., in dioxane)	Ring opening, %
Vb-styrene	2.70	22.9	0.16	5.13	0.16	100
VIb-styrene	2.23	19.1	0.25	2.60	0.24	55
VIIb-styrene	4.02	36.5	0.27	4.76	0.18	24.5

VII, the pendant polymer, reacted with *n*-butylamine readily, while in VIII the percentages of ring opening by the amine were low under the same reaction conditions because of increased steric hindrance to the attacking agents. The increase in absorption intensities of the infrared spectra of VIII at 1660  $\text{cm}^{-1}$  (amide I) and the decrease of  $\nu_{\text{C=O}}$  at 1815  $\text{cm}^{-1}$  arising from the oxazolone ring, would indicate the change of copolymer structure in the course of reaction as shown in eq. (6).



We thank the Ajinomoto Co. Inc. for supplying amino acids.

### References

1. J. W. Lynn, *J. Org. Chem.*, **24**, 1030 (1959).
2. M. T. Leplawy, D. S. Jones, G. W. Kenner, and R. C. Sheppard, *Tetrahedron*, **11**, 39 (1960).
3. F. Weygand, W. Steglich, and H. Tanner, *Ann.*, **658**, 128 (1962).
4. W. Kern and R. C. Schulz, *Angew. Chem.*, **69**, 153 (1957).

5. C. S. Cleaver and B. C. Pratt, *J. Am. Chem. Soc.*, **77**, 1541, 1544 (1955).
6. H. E. Carter, *Organic Reactions*, Vol. III, Wiley, New York, 1962, p. 199.
7. R. C. Elderfield, *Heterocyclic Compounds*, Vol. V, Wiley, New York, 1957, p. 298.
8. R. Filler and E. J. Piasek, *J. Org. Chem.*, **29**, 2205 (1964).
9. F. Toda, *Bull. Tokyo Inst. Technol.*, **57**, 93 (1964).
10. R. K. Kulkarni and H. Morawetz, *J. Polymer Sci.*, **54**, 491 (1961).
11. Y. Iwakura et al., *Tetrahedron Letters*, in press.
12. S. Akabori, *Chemistry of Proteins*, Vol. I, Kyoritsu, Tokyo, 1954, p. 144.
13. Y. Shimodoi, K. Masuda, and N. Murata, *Kogyo Kagaku Zasshi*, **65**, 1664 (1962).
14. F. Weygand, W. Steglich, D. Mayer, and W. von Philipsborn, *Chem. Ber.*, **97**, 2023 (1964).
15. M. Fineman and S. D. Ross, *J. Polymer Sci.*, **5**, 269 (1950).
16. C. Walling, E. R. Briggs, and K. B. Wolfstirn, *J. Am. Chem. Soc.*, **70**, 1543 (1948).
17. S. Sumitomo, N. Ueda, and M. Imoto, *Kogyo Kagaku Zasshi*, **66**, 1505 (1963).
18. F. Toda, unpublished data.
19. M. Kobayashi, *Bull. Chem. Soc. Japan*, **33**, 1416 (1960).

### Résumé

Une oxazolone vinylique polymérisable, la 2-isopropényl-4-isopropyl-2-oxazoline-5-one ( $M_2$ ) a été copolymérisée avec le styrène ( $M_1$ ) et les rapports de réactivité des monomères ont été déterminés et trouvés égaux à  $r_1 = 0.31 \pm 0.03$ ,  $r_2 = 1.12 \pm 0.010$  respectivement. Des nouvelles oxazolones isomérisées ( $M_2$ ), 2-isopropylidène-4-méthyl-3-oxazoline-5-one, le 2-isopropylidène-4-isopropyl-3-oxazoline-5-one et le 2-isopropylidène-4-isobutyl-3-oxazoline-5-one ont été préparées et copolymérisées avec le styrène  $M_1$ . Les rapports de réactivité monomérique sont  $r_1 = 0.36 \pm 0.07$ ,  $r_2 = 0.0$ ;  $r_1 = 0.39 \pm 0.06$ ,  $r_2 = 0.00 \pm 0.10$ ;  $r_1 = 0.39 \pm 0.10$ ,  $r_2 = 0.0$  respectivement. Les oxazolones isomérisées ne montraient pas de tendance à homopolymériser sous l'influence d'initiateurs radicalaires. Au départ des résultats de spectres infra-rouges et de résonance nucléaire et d'hydrolyse de copolymères, on a trouvé que les oxazolones isomérisées participent à la copolymérisation sous la forme de polymérisation 1-4 des diènes conjuguées (la double liaison exo au carbone-2 et le groupe C=N dans le noyau). Les copolymères réagissent avec les réactifs nucléophiles tels que les amines et les alcools.

### Zusammenfassung

Ein als Vinylverbindung polymerisierbares Oxazolon, 2-Isopropenyl-4-isopropyl-2-oxazolin-5-on ( $M_2$ ) wurde mit Styrol ( $M_1$ ) copolymerisiert und das Monomerreaktivitätsverhältnis zu  $r_1 = 0,31 \pm 0,03$  und  $r_2 = 1,12 \pm 0,10$  bestimmt. Neu isomerisierte Oxazolone ( $M_2$ ), 2-Isopropyliden-4-methyl-3-oxazolin-5-on, 2-Isopropyliden-4-isopropyl-3-oxazolin-5-on und 2-Isopropyliden-4-isobutyl-3-oxazolin-5-on wurden dargestellt und mit Styrol copolymerisiert. Die Monomerreaktivitätsverhältnisse waren:  $r_1 = 0,36 \pm 0,07$ ,  $r_2 = 0,0$ ; bzw.  $r_1 = 0,39 \pm 0,06$ ,  $r_2 = 0,00 \pm 0,10$ ; bzw.  $r_1 = 0,39 \pm 0,10$ ,  $r_2 = 0,0$ . Die isomerisierten Oxazolone zeigten keine Neigung zur radikalischen Homopolymerisation. Die Ergebnisse der Infrarot- und NMR-Spektroskopie sowie der Hydrolyse des Copolymeren zeigten, dass die Isomerisierten Oxazolone an der Copolymerisation in Form einer 1,4-Polymerisation als konjugierte Diene (Exodoppelbindung am Kohlenstoff 2 und C=N im Ring) teilnahmen. Die Copolymeren reagierten mit nukleophilen Reagentien wie Aminen und Alkoholen.

Received February 3, 1966

Revised April 5, 1966

Prod. No. 5148A

## Polymerization and Crosslinking Characteristics of a 3-Methoxybutyl Acrylate

JOHN R. COSTANZA and JOSEPH A. VONA, *Celanese Research  
Company, Summit, New Jersey*

### Synopsis

Polymers of 3-methoxybutyl acrylate (3-MBA) were prepared by mass, solution, and emulsion polymerization techniques. The 3-MBA polymers could be converted from soft, rubbery, soluble, thermoplastic films to hard, glossy, flexible, crosslinked films when exposed to air and/or transition metal catalysts at elevated temperatures. The crosslinked polymers are resistant to common organic solvents and to mineral acids. Strong alkalis degraded the crosslinked polymers. The second-order transition temperature of poly-3-MBA is  $-56^{\circ}\text{C}$ . as determined by volume dilatometry. A comparison of the crosslinking properties of poly-3-MBA and other alkyl and alkoxyalkyl polymers is discussed. An autoxidative mechanism is proposed for the crosslinking of 3-MBA polymers.

### INTRODUCTION

The preparation and properties of several monomeric and polymeric acrylic esters of ether-alcohols have been reported.<sup>1-3</sup> It was found that the poly(alkoxyalkyl acrylates) could be converted from soft thermoplastic resins to hard, thermoset resins by the use of transition metal catalysts at elevated temperatures in air. The preparation and polymerization of several fluoroalkoxyalkyl acrylates has also been reported.<sup>4</sup> The poly-(fluoroalkoxyalkyl acrylates) could be cured to thermoset resins with metal oxide catalysts. In addition, they could be compounded with standard vulcanization materials and cured to form elastomers.<sup>5</sup>

The polymerization of 3-methoxybutyl acrylate (3-MBA) and its curing or crosslinking characteristics are described in this paper.

### RESULTS AND DISCUSSION

#### Polymerization of 3-MBA

3-MBA can be mass-polymerized at room temperature with peroxides as initiators to yield clear, colorless, soft, elastic tacky masses. Polymerization of 3-MBA in aromatic hydrocarbons, esters, or chlorinated hydrocarbons yields clear, colorless, solution polymers. Polymers isolated from these solutions are soft, elastic, and tacky. Emulsion polymerization of 3-MBA proceeds readily by using standard emulsion polymerization techniques to yield soft, elastic, tacky polymers.



### Crosslinking of Poly-3-MBA and Other Acrylate Polymers

The crosslinking ability of 3-MBA polymers was compared with that of other acrylate polymers. It was observed that films cast from solution polymers of 3-MBA with metallic driers (0.01% cobalt) crosslink to a tack-free state when placed in an air-circulating oven at 150°C. for 90 min. Corresponding films of poly(methoxyethyl acrylate) and poly(ethoxyethyl acrylate) reached a tack-free state within 60 min. at 150°C. Films of poly(*n*-butyl acrylate) and poly(isobutyl acrylate) do not crosslink to a tack-free state when heated for several hours under the same conditions. The tackiness of these various films was measured with a Zapon tack tester (Atlas Powder Company) with the use of a 500-g. weight for 5 sec.

It was also observed that films of a 2-ethylhexyl acrylate solution polymer crosslink to a tack-free state with the aid of a cobalt catalyst after several hours exposure at 130–150°C. in an air-circulating oven. However, though tack-free, the crosslinked poly(2-ethylhexyl acrylate) films are softer than the films of crosslinked poly-3-MBA obtained under the same conditions.

Tin and zinc driers were compared with cobalt driers as crosslinking catalysts for 3-MBA polymer films, and their effect on the crosslinking rate and discoloration of the films was determined. Films of 3-MBA emulsion and solution polymers containing these catalysts (0.01%) were exposed to air at 150°C., and their change in properties was noted. It was found that 3-MBA films containing tin or zinc catalysts required two to three times the exposure time at 150°C. to crosslink to a tack-free state than did the cobalt-containing films. However, the crosslinked cobalt-catalyzed films were significantly more discolored than the tin- or zinc-catalyzed films.

### Properties of Crosslinked 3-MBA Polymer Films

The crosslinked 3-MBA polymer films exhibited excellent resistance to common organic solvents such as hexane, toluene, acetone, or ethyl acetate. Good adhesion of the crosslinked 3-MBA polymers to glass, wood, and metal was observed.

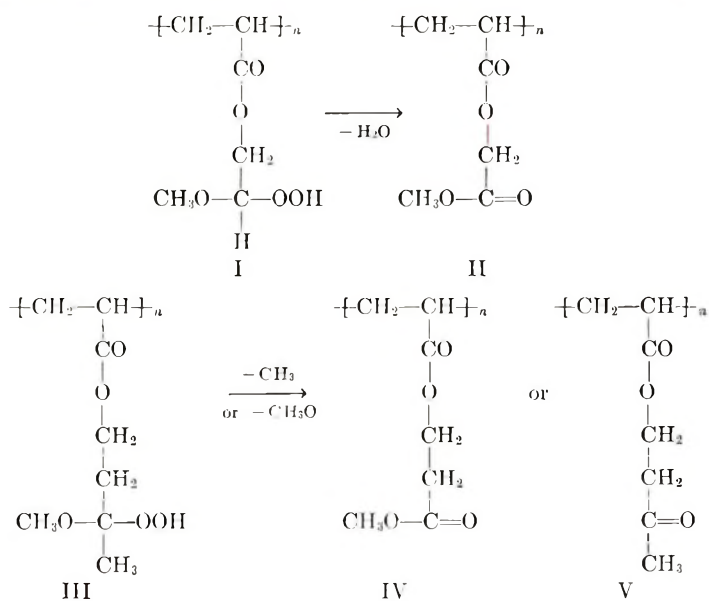
The discoloration of the colorless, uncrosslinked poly-3-MBA films to yellowish crosslinked films increased with the concentration of metal catalyst and with the time and temperature of the crosslinking reaction.

The acid and alkaline resistance of 3-MBA polymer films was measured. A film of a 3-MBA solution polymer containing cobalt (0.010%) was crosslinked by suspending it in an air-circulating oven at 150°C. for several hours. Sections of the cured film were then immersed in a 4% sodium hydroxide solution, a 1% sodium carbonate solution, and a 10% sulfuric acid solution. It was found that the 4% sodium hydroxide solution completely disintegrated the crosslinked 3-MBA polymer film within several hours of immersion, whereas the 1% sodium carbonate and the 10% sulfuric acid did not disintegrate the cured 3-MBA film after an immersion period of several weeks.

However, it has been reported in the literature<sup>2</sup> that crosslinked poly-(alkoxyalkyl acrylates) are vigorously attacked by 1% sodium carbonate

solutions. Therefore the alkaline resistance of crosslinked 3-MBA polymer films was compared with that of other poly(alkoxyalkyl acrylates). Films of solution polymers of 3-MBA, methoxyethyl acrylate and ethoxyethyl acrylate, prepared under identical conditions and containing equivalent amounts of cobalt naphthenate (0.01%) catalyst, were cast on glass plates and heated in an air-circulating oven at 150°C. for 16 hr. These cross-linked films were immersed in 1% sodium carbonate solutions and were left standing at room temperature for several weeks. A gradual attack of the alkaline solution on the poly(methoxyethyl acrylate) and the poly(ethoxyethyl acrylate) films occurred, whereas the poly-3-MBA film remained unchanged. After an immersion period of 7 weeks, the poly(ethoxyethyl acrylate) film was almost completely dissolved, the poly(methoxymethyl acrylate) film had dissolved to a large extent, but the 3-MBA polymer film appeared unchanged.

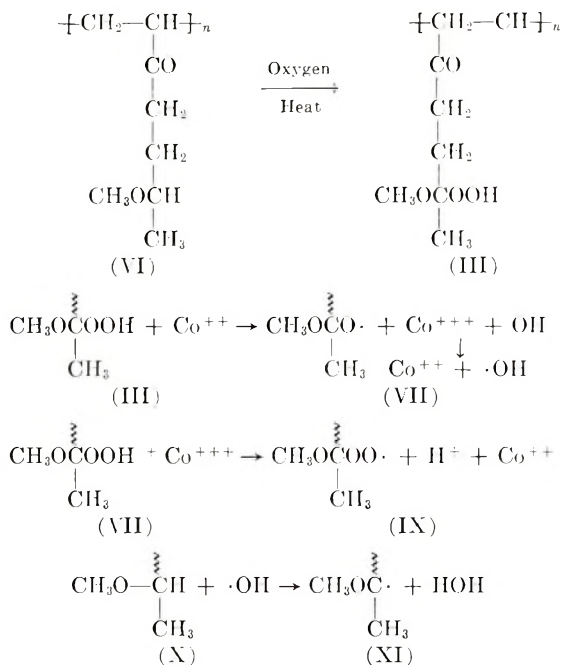
Several possibilities for an explanation of these results can be discussed. First, since it has been reported that the sensitivity to alkali of cured poly(alkoxyalkyl acrylate) films appears proportional to the degree of cure, it is possible that the poly-3-MBA film was not as highly cured as were the poly(alkoxyalkyl acrylate) films.<sup>2</sup> Secondly, the alkali solubility of cobalt-cured poly(vinyl ether) films has been reported to be attributed to hydrolysis of the ester groups formed by the oxidation of the ether side chains.<sup>6</sup> In addition, previous work has indicated that alkali degradation of cured poly(alkoxyalkyl acrylates) involves formation of carboxyl groups.<sup>2</sup> Based on this work, it is possible to assume that in the oxidative curing of the poly(alkoxyalkyl acrylates) a greater concentration of ester groups is formed than in the corresponding oxidative curing of poly-3-MBA. This might in part be due to a lower energy decomposition of the polyalkoxyalkyl acrylate side chain hydroperoxide (I) to form an ester group (II) than occurs



with the poly-3-MBA side-chain hydroperoxide (III). In the former, water would be eliminated to form an ester (II), while in the latter an alkyl or an alkoxy group would be lost to form an ester (IV) or a ketone (V), respectively.

### Mechanism of Crosslinking

The reaction occurring in the crosslinking of poly-3-MBA(VI) probably follows an autoxidation mechanism.<sup>7,8</sup> The initial stages of such a mechanism involve formation of the hydroperoxide (III) on the methoxy-substituted carbon of the poly-3-MBA side chain. Catalytic decomposition of the hydroperoxide (III) by cobalt ion would result in a variety of polymer free radicals (VII), (IX), and (XI). Termination of the reaction mechanism by recombination of these free radicals would lead to polymer crosslinking.



### Second-Order Transition Temperature of Poly-3-MBA

The second-order transition temperature  $T_g$  of 3-MBA was determined in order to characterize its low temperature flexibility. Volume dilatometry (the measurement of specific volume versus temperature using a silicone oil as a confining liquid) was used to determine  $T_g$ .<sup>9</sup> The polymers used were prepared by emulsion polymerization techniques and were isolated by coagulation, extensive washing, and drying. The second-order transition temperature was taken as the intersection of the extrapolated straight-line portions of a plot (Fig. 1) of specific volume versus temperature. The results of these experiments are reported in Table I. It can be seen that the method used to determine the second-order transition

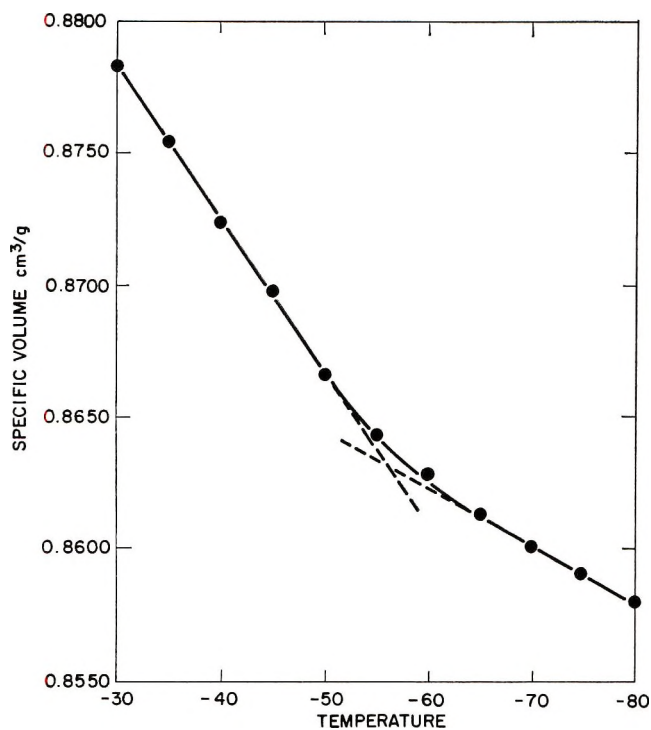


Fig. 1. Second-order transition temperature of 3-MBA.

temperature of 3-MBA gave reasonable correlation between observed and reported values when poly(ethyl acrylate) and poly(*n*-butyl acrylate) were used as controls. Table II contains the reported second-order transition

TABLE I  
Comparison of Observed and Reported Second-Order Transitions  
of Several Polyacrylates

Polyacrylate	$T_g$ , °C.	
	Observed value	Reported value <sup>a</sup>
3-MBA	-56	—
<i>n</i> -Butyl	-64	-70
Ethyl	-27	-28

<sup>a</sup> Data of Bovey et al.<sup>10</sup>

TABLE II  
Reported Second-Order Transition Temperature for  
Poly(alkoxyalkyl Acrylates)<sup>a</sup>

Poly(alkoxyalkyl Acrylate)	$T_g$ , °C.
Methoxyethyl	-50
Ethoxyethyl	-50
Methoxypropyl	-75
Ethoxypropyl	-68

<sup>a</sup> Data of Bovey and Abere.<sup>4</sup>

temperature for various poly(alkoxyalkyl acrylates) and is included for comparison purposes.

## EXPERIMENTAL

### Preparation and Properties of 3-MBA

The synthesis of 3-MBA is readily accomplished by the transesterification of ethyl acrylate and 3-methoxybutanol according to published procedures.<sup>2</sup> 3-MBA is a colorless liquid having a mild sweet odor. It has a boiling point of 79–80°C./15 mm./Hg, an index of refraction  $n_D^{25}$  of 1.4252, and a specific gravity 25°C./20°C. of 0.9607.

ANAL. Calcd.: C, 60.74%; H, 8.92%; molar refraction, 41.97; saponification equivalent, 158.2. Found: C, 60.50%; H, 8.66%; molar refraction, 42.13; saponification equivalent, 156.9.

### Mass Polymerization of 3-MBA

The mass polymerization of 3-MBA could be conveniently initiated at 70–80°C. by using benzoyl peroxide as the catalyst. An example of such a polymerization and the properties of the polymer obtained follows:

To 150 g. of uninhibited 3-MBA was added 0.3 g. of benzoyl peroxide. This solution was poured into the lower half of a Petri dish up to a point approximately  $\frac{5}{8}$  in. from the bottom, and then the dish was placed on a hot plate set at  $70 \pm 3^\circ\text{C}$ . The 3-MBA acrylate polymerized (exothermic reaction) within 15 min., and the polymer was kept on the hot plate for an additional 2 hr. at  $70 \pm 3^\circ\text{C}$ .

The Petri dish containing the polymer was placed in an air-circulating oven at 100–110°C. for 24 hr. and then left in a constant temperature room (73°F., 50% R.H.) overnight. The following day it was observed that the polymer had shrunk to approximately  $\frac{1}{4}$  in. The surface of the polymer was tough and nontacky, whereas underneath this top layer, the polymer was soft and tacky. The tough polymer surface was not attacked by organic solvent indicating that crosslinking had occurred. The subsurface was still soluble or swollen by organic solvents, indicating little or no crosslinking had taken place.

### Solution Polymerization of 3-MBA

The following formulation was used in the preparation of solution polymers of 3-MBA: 3-MBA (uninhibited), 75.0 g.; ethyl acetate, 142.0 g.; benzoyl peroxide, 0.50 g.

The apparatus used was a 500-ml., three-necked, ground glass flask equipped with a thermometer, stirrer, and condenser. This apparatus was immersed in a water bath used for heating and cooling. The reagents were then charged into the reaction flask and the stirring speed was set at 50–150 rpm. The batch temperature was then raised to 75–85°C., whereupon a moderately vigorous reaction started. After the initial exotherm, the solution was kept at a mild reflux for 1–2 hr. and then cooled to room temperature. A clear, fluid solution was obtained, and the per cent solids

found for this solution indicated a complete conversion to polymer. This polymer had an inherent viscosity of 0.62 in toluene (0.1%) at 25.0°C. A polymer of butyl acrylate prepared in the same manner had an inherent viscosity of 0.64.

### Emulsion Polymerization of 3-MBA

The emulsion polymerization of 3-MBA was carried out by using ammonium persulfate as the catalyst and anionic surfactants as emulsifiers. The formulation used was the following: 3-MBA (uninhibited), 80.0 g.; Tergitol #4, 6.0 g.; Triton X-200 (28%), 5.0 g.; water (distilled), 96.0 g.; ammonium persulfate, 0.02 g.

The apparatus consisted of a 500-ml., three-necked, ground glass flask equipped with a stirrer, thermometer, and condenser. A water bath was used for heating. All the reagents were charged into the flask, and the bath was raised to 60–80°C. to initiate the reaction. After the polymerization was complete, the reaction was heated to 95°C. and held there for 30 min. The reaction was cooled to room temperature. A stable polymer emulsion was obtained with complete conversion to polymer. Coagulation of the polymer was accomplished by addition of acetone. The coagulated polymer was shredded into small pieces and placed in a beaker which was covered with a screen. Continuous washing of the shredded polymer with hot water was carried out for one hour to remove emulsifiers. After drying the isolated polymer had an inherent viscosity of 2.0 in toluene (0.1%) at 25°C.

This polymer was found soluble to the extent of 1 wt.-% in ethyl acetate, xylene, chloroform, cyclohexanone, and tetrahydrofuran at room temperature without apparent formation of gels.

### Crosslinking of Polymer Films

To evaluate the crosslinking properties of 3-MBA polymers, films from emulsion and solution polymers were cast on glass plates and the volatiles were allowed to evaporate at room temperature. In most cases, the films were approximately 0.002 in. in thickness when dry. If curing catalysts were to be incorporated in the polymer films, then 0.005–0.010% of the metallic ion (based on polymer solids) was added to polymer solution or emulsion prior to casting of the film. The cobalt, tin, and zinc driers used were obtained from Nuodex Products, Inc., Elizabeth, New Jersey. The films were crosslinked by exposure to a temperature of 150°C. in an air-circulating oven.

### Second-Order Transition Temperature Determination

The method of volume dilatometry was chosen to determine the second-order transition temperature of 3-MBA because it offered a convenient means of measuring changes in specific volume versus temperature at very low temperatures. The literature<sup>7</sup> describes various methods of studying volume-temperature relationships by using volume dilatometry. One of the best published descriptions of the technique of volume dilatometry

is that reported by the National Bureau of Standards.<sup>9</sup> The polymers to be investigated were prepared by emulsion polymerization procedures previously described. They were isolated and purified by coagulation, extensive washing and drying. The second-order transition temperature of these polymers was taken as the intersection of the extrapolated straight-line portions of a plot of specific volume versus temperature (Fig. 1). The results of these experiments are reported in Table I.

### References

1. M. L. Fein, W. P. Ratchford, and C. H. Fischer, *J. Am. Chem. Soc.*, **66**, 1201 (1944).
2. C. E. Rehberg and W. A. Fancette, *J. Org. Chem.*, **14**, 1094 (1949).
3. C. E. Rehberg and C. H. Fischer, U. S. Pat. 2,458,888 (Jan. 11, 1949).
4. F. A. Bovey and J. F. Abere, *J. Polymer Sci.*, **15**, 537 (1955).
5. P. J. Stedry, J. F. Abere, and A. M. Borders, *J. Polymer Sci.*, **15**, 558 (1955).
6. W. J. Schneider, L. E. Gast, E. H. Melvin, C. A. Glass, and H. M. Teeter, *J. Am. Chemists' Soc.*, **34**, 244 (1957).
7. D. W. Swern, H. B. Knight, J. T. Scanlon, and W. C. Ault, *J. Am. Chem. Soc.*, **67**, 1134 (1945).
8. L. A. O'Neill, *Chem. Ind. (London)*, **1954**, 384 (April 3, 1954).
9. N. Bekkedahl, *J. Res. Natl. Bur. Std.*, **43**, 145 (1949).
10. F. A. Bovey, J. F. Abere, G. B. Rathmann, and C. L. Sandburg, *J. Polymer Sci.*, **15**, 525 (1955).

### Résumé

Les polymères de 3-méthoxybutylacrylate (3-MBA) ont été préparés en bloc, en solution et par polymérisation en émulsion. Les polymères de 3-MBA peuvent être transformés en films souples caoutchouteux solubles, thermoplastiques et en films durs, vitreux, flexibles et ponté lorsqu'on les expose à l'air et/ou à des catalyseurs à base de métaux de transition à températures élevées. Les polymères pontés sont résistants à la plupart des solvants organiques usuels et aux acides minéraux. Les bases fortes dégradent les polymères pontés. La température de transition vitreuse du poly-3-MBA est de  $-56^{\circ}\text{C}$  ainsi qu'on a pu le déterminer par dilatométrie. La comparaison des propriétés de pontage du 3-MBA et d'autres polymères alcoylés et alcoxyalkylés est discutée. Un mécanisme d'autooxydation est proposé pour le pontage des polymères de 3-MBA.

### Zusammenfassung

Polymere von 3-Methoxybutylacrylat (3-MBA) wurden durch Polymerisation in Substanz, in Lösung und in Emulsion hergestellt. Die 3-MBA-Polymeren konnten durch Einwirkung von Luft und von Übergangsmetallkatalysatoren bei erhöhter Temperatur von weichen kautschukartigen thermoplastischen Filmen in harte glänzende vernetzte Filme umgewandelt werden. Die vernetzten Polymeren waren gegen normale organische Lösungsmittel und Mineralsäuren beständig. Durch starke Alkalien wurden die vernetzten Polymeren abgebaut. Die Umwandlungstemperatur zweiter Ordnung von Poly-3-MBA liegt nach dilatometrischen Messungen bei  $-56^{\circ}\text{C}$ . Ein Vergleich der Vernetzungsfähigkeit von Kohlen-3-MBA und anderen Alkyl- und Alkoxyalkylpolymeren wird durchgeführt. Für die Vernetzung von 3-MBA-Polymeren wird ein Autoxydationsmechanismus angenommen.

Received December 22, 1965

Revised April 7, 1966

Prod. No. 5149A

## Poly(vinyl Fluoride) Solution Characteristics\*

M. L. WALLACH and M. A. KABAYAMA,†

*Film Department, E. I. du Pont de Nemours and Company, Inc.,  
Wilmington, Delaware 19898*

### Synopsis

Nine unfractionated poly(vinyl fluoride) samples were characterized for molecular weight and polydispersity by means of sedimentation velocity, osmometry, and viscosity measurements. Molecular weights were in the range of 143,000–654,000 and  $\bar{M}_w/\bar{M}_n = 2.5$ –5.6. The Mark-Houwink (M-H) relation was established as  $[\eta] = 6.52 \times 10^{-5} M^{0.80}$ . The M-H exponent is at the Flory-Fox upper limit (0.80), as is characteristic of extended, polar polymers, in good solvents. The unperturbed chain dimensions, characteristic ratio and steric factor were derived by the methods of Stockmayer and Fixman and Kurata and Stockmayer. The steric factor is 1.7, which agrees with data reported for other poly(vinyl halides).

### INTRODUCTION

A number of studies have been reported on poly(vinyl fluoride) (PVF), including investigations of high resolution nuclear magnetic resonance spectroscopy,<sup>2</sup> crystal structure,<sup>3</sup> telomer chemistry,<sup>4</sup> and the effect of polymerization variables on polymer<sup>5</sup> and film properties.<sup>6</sup> However, no systematic studies of the solution properties of this polymer have been reported. It was, therefore, of interest to characterize selected samples of poly(vinyl fluoride) in order to establish the Mark-Houwink relation and derive chain conformational parameters for this material. Inasmuch as these parameters are available for other poly(vinyl halides), it was also of interest to compare them with these results for poly(vinyl fluoride).

### EXPERIMENTAL

Polymers were prepared by Dr. M. J. Eitel<sup>7</sup> via radical initiation with azobisisobutyramidine hydrochloride (0.003–0.2 wt.-%), with the use of isopropanol as modifier (0.1%), at monomer pressures of 1–5 Kpsi and temperatures of 67–97°C. The polymers were not fractionated.

Sedimentation velocity, osmometry, and viscometry techniques were employed. Measurements were made in dimethylformamide (DMF,

\* Paper presented at the Winter Meeting of the American Chemical Society, Phoenix, Arizona, January 16–21, 1966.<sup>1</sup>

† Present address: Ethicon Inc., Research Div., Somerville, N. J.



du Pont technical grade) which was distilled prior to use and made 0.1*N* in anhydrous lithium bromide (Lithium Corp. of America).\*

### Viscometry

Intrinsic viscosities  $[\eta]$  were measured at 90°C. in Cannon-Fenske viscometers. Flow times were kept above 100 sec. to minimize corrections. The precision of the data is estimated to be  $\pm 0.3\%$ .

### Osmometry

Number-average molecular weights were determined with Zimm-Meyerson osmometers at 90°C. with the use of gauge 116 gel cellophane membranes. Osmotic height readings were taken with a Gaertner M908 cathetometer over a 2-day period. They ranged from 1 to 6 cm. Equilibrium heights were extrapolated back to zero time to correct for diffusion. Small capillary ( $\sim 0.1$  cm.) and asymmetry ( $\sim 0.5$  cm.) corrections were also applied. The uncertainty in the derived molecular weights due to cathetometer, temperature, and concentration errors was estimated to be less than 10%.

### Ultracentrifugation

The sedimentation velocity technique was used to arrive at the weight-average molecular weights, rather than direct thermodynamic methods such as light scattering or sedimentation equilibrium, because no solvent could be found with a high enough specific refractive index increment for PVF. In DMF,  $dn/dc \cong 0.02$  cc./g. Sedimentation velocity measurements were run at 100°C., at a speed of 42,040 rpm with the Spinco Model E ultracentrifuge equipped with phase-plate Schlieren optics and a rotor temperature control unit. Long (18 mm.) centerpieces were employed because of the low  $dn/dc$ . Runs were generally about 50 min. in duration. Typical sedimentation diagrams for a PVF sample (4) are shown in Figure 1. The ordinate is proportional to the concentration (or refractive index) gradient, and the abscissa is a measure of the distance from the center of rotation. We note the presence of some low molecular weight material—as indicated by the flat portion of the curves near the meniscus—and a high molecular weight tail in the distribution. The plates were read with a Nikon Shadowgraph to 0.002 mm. Sedimentation coefficients  $S$  were obtained from the rate of movement of the boundary peak, extrapolating to infinite time ( $S$  versus  $1/t$ ) to reduce the effects of diffusion. The pressure dependence of  $S$  was not taken into account, but it is probably small due to the short duration of the experiment. The  $S$  values are estimated to be accurate to about 5%.

\* Salt was added to suppress an apparent polyelectrolyte effect which appeared in some determinations.

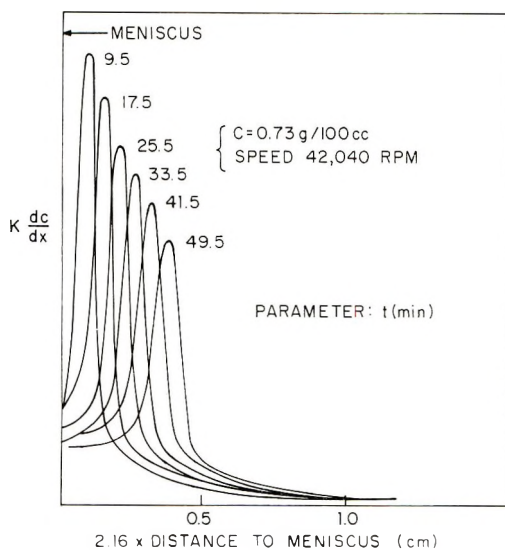


Fig. 1. Schlieren diagrams for a typical poly(vinyl fluoride), sample 4.

## RESULTS AND DISCUSSION

The results are given in Table I. The intrinsic viscosities range from 0.88 to 3.20 dl./g., the sedimentation constants from 10.4 to 19.7 S. and the number-average molecular weights from 76,400 to 234,000.

### Sedimentation Constants and Molecular Weights

Sedimentation constants were measured at a single concentration for each polymer and extrapolated to zero concentration using the relation:

$$S_0 = S(1 + 1.66[\eta]C) \quad (1)$$

The factor  $1.66[\eta]$  has been found to hold for many vinyl polymers in good solvents.<sup>8</sup> Molecular weights were calculated from the  $S_0$  values by using the Mandelkern-Flory equation:<sup>9</sup>

$$S_0[\eta]^{1/3}/M^{2/3} = \bar{\beta}(1 - \bar{V}\rho)/\eta N \quad (2)$$

where  $\bar{\beta}$  is a hydrodynamic constant ( $2.5 \times 10^6$ ) which is practically independent of the solvent power and coil draining,  $\bar{V}$  is the partial specific volume of the polymer (0.720 cc./g.) which we approximate by the reciprocal of the amorphous density,  $\rho$  is the solvent density (0.875 g./cc.),  $\eta$  is the solvent viscosity ( $4.22 \times 10^{-3}$  poise), and  $N$  is Avogadro's number. In a polydisperse system the molecular weights calculated from this equation are a characteristic average lying between the number-average  $\bar{M}_n$  and the weight-average  $\bar{M}_w$  but being closer to  $\bar{M}_w$ . It has been shown<sup>10</sup> that if the distribution is not too broad, then  $M_s \sim 0.9 \bar{M}_w$  for a variety of

TABLE I  
Summary of Characterization Parameters

Sample	$[\eta]_{\text{DMF}}$ , dl./g.	$S_0$ , S.	$M_s$	$\bar{M}_n$	$M_s/\bar{M}_n$	$\sim \bar{M}_w/\bar{M}_n$
1	0.88	10.4	143,000	—	—	—
2	1.59	14.3	311,000	140,000	2.22	2.47
3	1.80	15.4	369,000	76,400	4.83	5.37
4	2.02	15.9	411,000	159,000	2.58	2.87
5	2.06	18.6	526,000	234,000	2.25	2.50
6	2.54	19.7	634,000	196,000	3.23	3.59
7	2.76	16.5	506,000	153,000	3.31	3.68
8	2.88	17.2	553,000	218,000	2.54	2.82
9	3.20	18.6	654,000	130,000	5.03	5.59

distributions. Molecular weights calculated from eq. (2) are listed in Table I. These molecular weights,  $M_s$ , range from 143,000 to 654,000.\*

The sedimentation constant is plotted against the molecular weight in Figure 2. The data can be expressed by the equation:

$$S_0 = 0.0929 M_s^{0.40} \quad (3)$$

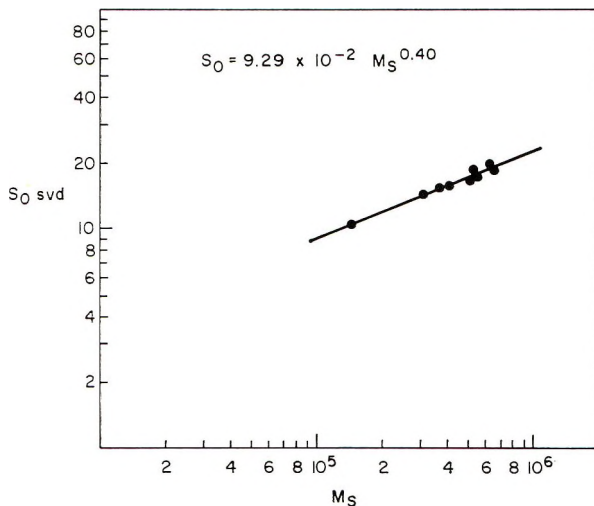


Fig. 2. Sedimentation constant in dimethylformamide at 100°C. vs. molecular weight derived from the Flory-Mandelkern equation.

Thus, one can obtain the molecular weight from a measured sedimentation constant and calculate molecular weight distributions from the sedimentation boundary curves.<sup>11,12†</sup>

\* These molecular weights are higher than those reported previously<sup>1</sup> due to a better choice of parameters in eq. (2). However, the conformational parameters are hardly affected since in eq. (5) the value of  $K$  only varies as  $M^{-1/2}$  and  $A \sim K^{1/3}$ .

† Of course, in order to derive distributions by this technique one would need Schlieren diagrams at a series of concentrations as well as for various times of centrifugation.

### Correlation with Intrinsic Viscosities

The intrinsic viscosities are plotted against the ultracentrifuge molecular weights in Figure 3. The data can be described by the relation:

$$[\eta] = 6.42 \times 10^{-5} M_s^{0.80} \quad (4)$$

which can be derived from eqs. (2) and (3). The exponent is at the Flory-Fox upper limit. Such moderately high exponents are generally found with extended, polar polymers in good solvents.

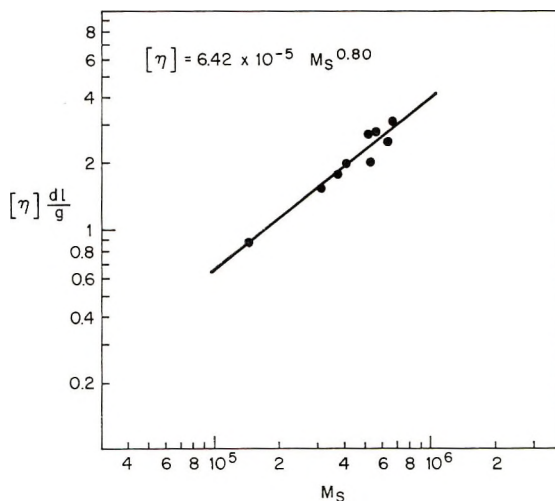


Fig. 3. Intrinsic viscosity in dimethylformamide at 90°C. vs. molecular weight derived from the Flory-Mandelkern equation.

### Degree of Polydispersity

One can obtain information about the degree of polydispersity by comparing the weight-average molecular weight obtained from the sedimentation constants [ $\bar{M}_w \cong (M_s/0.90)$ ] to number averages obtained from osmometry. The values of  $\bar{M}_w/\bar{M}_n$  are listed in Table I. They range from 2.47 to 5.59. Deviations from a normal distribution where  $\bar{M}_w/\bar{M}_n = 2.0$  can be attributed to effects of chain branching.<sup>13</sup>

### Unperturbed Dimensions

**Case of Free Rotation.** The intrinsic viscosity of a polymer in a theta solvent is related to the molecular weight  $M$  by the well-known equation:

$$[\eta]_\theta = KM^{1/2} \quad (5)$$

where

$$K = \Phi A^3$$

and

$$A = \sqrt{\overline{r_0^2}/M}$$

$\Phi$  is a universal constant which has the limiting value  $2.87 \times 10^{21}$  in a mono-disperse system and  $\overline{r_0^2}$  is the mean-square end-to-end distance in the absence of coil swelling due to solvent-polymer interaction. If there is complete freedom of rotation about all of the valence bonds in the polymer chain,  $A^2$  becomes  $A_f^2$ , which can be expressed by the equation:

$$A_f^2 = \overline{r_0^2}/M = 2nl^2/m \quad (6)$$

where  $n$  is the number of in-chain valence bonds,  $l$  is the carbon-carbon bond length, and  $m$  is the molar monomer weight. For poly(vinyl fluoride) ( $n = 2$ ,  $l = 1.54 \times 10^{-8}$  cm., and  $m = 46$ ), the quantity  $2nl^2/m$  is  $0.209 \times 10^{-16}$  cm.<sup>2</sup>, and  $A_f = 0.457$  a.u.

**Actual Case.** Due to the volume occupied by side groups and electrostatic repulsions, actual polymer dimensions  $A$  are generally larger than expected in the case of free rotation. The value of the steric factor  $\sigma = A/A_f$  is a measure of chain extension due to these so-called volume effects. For poly(vinyl fluoride),  $K$ ,  $A$ , and  $\sigma$  were derived from these data by the

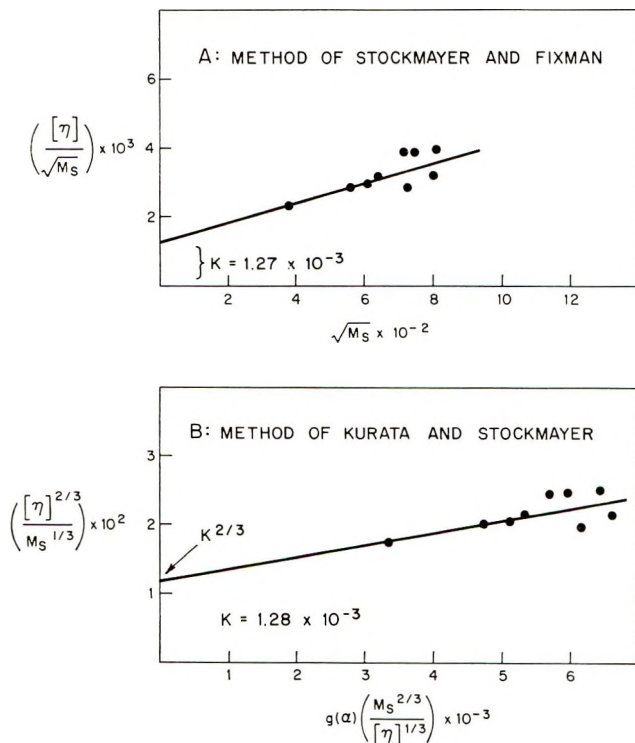


Fig. 4. Derivation of unperturbed chain dimensions  $A$ , where  $A = (K/\Phi)^{1/3}$  and  $\Phi$  as corrected for polydispersity is  $2.63 \times 10^{21}$ .

methods of Stockmayer and Fixman<sup>14</sup> and Kurata and Stockmayer<sup>15</sup> (Fig. 4). The values of these conformational parameters are given in Table II.\* There is good agreement between respective data obtained by each of the two techniques. We note also that the steric factor (1.72) is similar to that found for other poly(vinyl halides), which means that the degree of steric hindrance to free rotation about the C—C—X bond is about the same for these polymers. Finally, we note in Table III that—apart

TABLE II  
Conformational Parameters for Poly(vinyl Fluoride)<sup>a</sup>

	Kurata- Stockmayer	Stockmayer- Fixman
Unperturbed dimensions $\sqrt{r_0^2/M}$ , Å	0.787	0.785
Characteristic ratio $r_0^2/nl^2$	6.01	5.98
Steric factor $\sigma$	1.72	1.72

<sup>a</sup> These data have been corrected for polydispersity using the average  $\bar{M}_w/\bar{M}_n$  value from Table I (3.52) and assuming a Schultz distribution function which leads to a corrected  $\Phi$  value of  $2.63 \times 10^{21}$ .

TABLE III  
Comparison of Steric Factors

	Poly(vinyl fluoride)	Poly(vinyl chloride)	Poly(vinyl bromide)
Steric factor $\sigma$	1.72	1.83, <sup>a</sup> 2.08 <sup>b,c</sup>	1.82 <sup>a,c</sup>
Molar volume of substituent, cc.	12	28	35
Electronegativity difference of C—X bond atoms	1.5	0.5	0.3

<sup>a</sup> Data of Kurata and Stockmayer.<sup>15</sup>

<sup>b</sup> Data of Sato et al.<sup>17</sup>

<sup>c</sup> Data for theta solvent.

from the recent  $\theta$ -solvent data of Sato<sup>17</sup>—the similarity of the steric factors for the poly(vinyl halides) can be explained by a compensation between two opposing effects; an increase in molar volume of the halide substituent which should increase the unperturbed dimensions and a corresponding decrease in electronegativity difference<sup>18</sup> between the C—X bond atoms which should decrease the unperturbed chain dimensions.

The authors would like to thank Prof. W. H. Stockmayer of Dartmouth College, Prof. W. R. Krigbaum of Duke University, and Drs. W. J. Pangonis and J. B. Nichols of the Du Pont Company for many helpful suggestions.

\* It is noteworthy that branching corrections are not needed for the intercepts in Figure 4 if the distribution of branch points is random<sup>16</sup> and that the unperturbed dimensions as expressed by the quantity  $A$  are proportional to only  $K^{1/2}$ . Therefore, a reasonable estimate of chain dimensions can be obtained even though there is some scatter of the data. Specifically a 25% uncertainty in the intercept of Figure 4 leads to an uncertainty in  $A$  and  $\sigma$  of only 3%.

## References

1. M. L. Wallach and M. A. Kabayama, *Polymer Preprints*, **7**, No. 1, 237 (1966).
2. R. E. Naylor, Jr. and S. W. Lasoski, Jr., *J. Polymer Sci.*, **44**, 1 (1960).
3. R. C. Golike, *J. Polymer Sci.*, **42**, 583 (1960).
4. T. Dougherty, *J. Am. Chem. Soc.*, **86**, 460 (1964).
5. G. H. Kalb, D. D. Coffman, T. A. Ford, and F. J. Johnson, *J. Appl. Polymer Sci.*, **4**, 55 (1960).
6. V. L. Simril and B. A. Curry, *J. Appl. Polymer Sci.*, **4**, 62 (1960).
7. M. J. Eitel, unpublished work.
8. R. L. Baldwin and K. E. VanHolde, *Fortschr. Hochpolymer. Forsch.*, **1**, 451 (1960).
9. L. Mandelkern and P. J. Flory, *J. Chem. Phys.*, **20**, 121 (1952).
10. K. E. VanHolde, unpublished work.
11. R. Signer and H. Gross, *Helv. Chim. Acta*, **17**, 726 (1934).
12. J. W. Williams, *J. Polymer Sci.*, **12**, 351 (1954).
13. P. J. Flory, *Principles of Polymer Chemistry*, Cornell Univ. Press, Ithaca, N. Y., 1953.
14. W. H. Stockmayer and M. Fixman, in *First Biannual American Chemical Society Polymer Symposium*, *J. Polymer Sci. C*, **1**, H. W. Starkweather, Ed., Interscience, New York, 1963, p. 137.
15. M. Kurata and W. H. Stockmayer, *Fortschr. Hochpolymer. Forsch.*, **3**, 196 (1963).
16. M. Wales, P. A. Marshall, S. Rothman, and S. G. Weissberg, *Ann. N. Y. Acad. Sci.*, **57**, 353 (1953).
17. M. Sato, Y. Koshiishi, and M. Asahina, *J. Polymer Sci. B*, **1**, 233 (1963).
18. L. Pauling, *The Nature of the Chemical Bond*, Cornell Univ. Press, Ithaca, N. Y., 3rd Ed., 1960.

## Résumé

Une série de 9 échantillons non-fractionnés de fluorure de polyvinyle (PVF) a été caractérisée du point de vue de leurs poids moléculaires et de leur polydispersité au moyen de mesures de vitesse de sédimentation, de pression osmotique et de viscosité. Les poids moléculaires variaient de 143.000 à 654.000 et le rapport  $\bar{M}_w/\bar{M}_n = 2.5-5.3$ . La relation de Mark-Houwink a été établie et trouvée  $[\eta] = 6.52 \times 10^{-6} M^{0.80}$ . L'exposant de M-H est la limite supérieure pour la théorie de Flory-Fox et caractéristique de polymères étendus et polaires dans de bons solvants. Les dimensions de la chaîne non-perturbée, le rapport caractéristique, et le facteur stérique sont dérivés par les méthodes de Stockmayer-Fixman et Kurata-Stockmayer. Le facteur stérique est de 1.7, ce qui est en accord avec les données rapportées pour d'autres halogénures de polyvinyle.

## Zusammenfassung

Eine Reihe von neun unfraktionierten Polyvinylfluoridproben (PVF) wurde in bezug auf Molekulargewicht und Polydispersität durch Sedimentationsgeschwindigkeit, Osmometrie und Viskositätsmessungen charakterisiert. Die Molekulargewichte lagen im Bereich von 143.000-654.000, und  $\bar{M}_w/\bar{M}_n$  variierte von 2,5 bis 3,5. Folgende Mark-Houwink-Beziehung (M-H) wurde aufgestellt:  $[\eta] = 6,52 \cdot 10^{-5} M^{0,80}$ . Der M-H-Exponent liegt an der oberen Flory-Fox-Grenze, wie es für ausgeweitete, polare Polymere in guten Lösungsmitteln charakteristisch ist. Die ungestörten Kettendimensionen, das charakteristische Verhältnis, und der sterische Faktor wurden nach der Methode von Stockmayer-Fixman und Kurata-Stockmayer abgeleitet. Der sterische Faktor beträgt 1,7 und stimmt mit den für andere Polyvinylhalogenide mitgeteilten Werten überein.

Received April 11, 1966

Prod. No. 5154A

## Studies on Addition Polymerization in Mixed Solvent System. Part I. Chain Transfer of Water in Polymerization of Methyl Methacrylate

BHUPATI RANJAN BHATTACHARYYA  
and UMASANKAR NANDI, *Indian Association for the  
Cultivation of Science, Jadavpur, Calcutta, India*

### Synopsis

The role of water as a chain-transfer agent in addition polymerization of methyl methacrylate and acrylamide in a mixed solvent system was studied. Water does not have any transfer with the growing polymer radical. The degree of polymerization is found to increase with increasing water concentration. This is probably due to a reduced termination rate resulting from coiling of the polymer chain in the presence of a nonsolvent like water.

### INTRODUCTION

Since the introduction of the concept by Flory,<sup>1</sup> chain transfer has been studied extensively. However, the studies have generally been restricted to the homogeneous phase. Investigations of substances which are insoluble in the monomer have hardly been attempted because of difficulties involved, i.e., phase separation at the very beginning of the reaction. Recently Nandi et al.<sup>2,3</sup> suggested a method for determining the chain-transfer constants of such substances. Their work on methyl methacrylate polymerization with the use of water as a chain-transfer agent has produced highly interesting results. Jenkins and Johnston's<sup>4</sup> work was limited to polymerization of acrylonitrile in dimethylformamide in the presence of water. The purpose of the present work is to study in some detail the role of water as a chain-transfer agent as well as its effect on the transferring capacity of the cosolvent employed to keep the system homogeneous. *tert*-Butyl alcohol was selected as the cosolvent to keep the mixture of water and methyl methacrylate in homogeneous phase.

### EXPERIMENTAL

#### Processing of the Monomer

Stabilized methyl methacrylate was washed free of stabilizer with 5% caustic soda solution followed by repeated washing with water. It was then dried over calcium chloride and distilled twice in an all-glass apparatus,



just before use. The distillation was carried out under reduced pressure. Acrylamide was recrystallized twice from warm chloroform.

### Purification of Solvents

The solvents used were AR quality samples. They were purified by the usual methods,<sup>5</sup> dried, and fractionally distilled before use.

### Purification of Initiators

2,2-Azobisisobutyronitrile and 2,2-azobisisobutyroamidine were twice crystallized from methanol and water, respectively.

### Polymerization Experiments

Pyrex glass ampules were used in the polymerization experiments. They were thoroughly cleaned with chromic acid, washed successively with water and sulfurous acid solution, and finally washed with water and dried. Weighed amounts of water were taken in 4 ml. of a stock mixture of methyl methacrylate and *tert*-butyl alcohol (1:1 ratio by volume) in these ampules, frozen in liquid oxygen, and sealed under vacuum. In the case of the catalyzed experiments, the initiator (2,2-azobisisobutyronitrile;  $C_I \simeq 0$ ) was dissolved in the stock mixture of the monomer and *tert*-butyl alcohol; the rest of the process was the same as that for the uncatalyzed reaction. The tubes were then kept at the required temperature within an accuracy of  $\pm 0.05^\circ\text{C}$ ., in an oil thermostat maintained by means of a thermoregulator. After about 10% conversion, the tubes were taken out, chilled, and broken open. The polymer was then precipitated with petroleum ether (b.p. 40–60°C.) followed by reprecipitation from benzene solution and finally dried in vacuum at 50°C. to constant weight.

### Determination of the Degree of Polymerization

The degree of polymerization was determined from viscosity measurement at  $30 \pm 0.05^\circ\text{C}$ . in benzene solution from the relation  $DP = K[\eta]^\alpha$ , where  $[\eta]$  is the intrinsic viscosity of the solution and  $K$  and  $\alpha$  are constants for each polymer system in benzene. The values used in the calculation in the present work are  $K = 2.035$  and  $\alpha = 1.320$  as reported by Fox.<sup>6</sup>

## RESULTS

### Determination of Chain Transfer for Water

The general equation for the degree of polymerization  $\bar{P}$  can be easily deduced and is

$$1/\bar{P} = C_M + C_S([S]/[M]) + C_I([I]/[M]) + R_p(\delta^2/[M]^2) \quad (1)$$

where  $C_M$ ,  $C_S$ , and  $C_I$  are the chain-transfer constants for monomer, solvent, and initiator, respectively;  $[S]$ ,  $[M]$ , and  $[I]$  are solvent, monomer, and initiator concentration, respectively;  $R_p$  is the rate of polymerization,

and  $\delta$  ( $= k_t^{1/2}/k_p$ ) is the ratio of rate constants for propagation ( $k_p$ ) and termination ( $k_t$ ).

In case of mixed solvent system, where two solvents,  $S_1$  and  $S_2$ , are employed, the eq. (1) can be written

$$1/\bar{P} = C_M + C_{S_1}([S_1]/[M]) + C_{S_2}([S_2]/[M]) + R_p(\delta^2/[M]^2) \quad (2)$$

for thermal polymerization or for the catalyzed system, where  $C_1 \simeq 0$ . Keeping the ratio  $[S_1]/[M]$  constant (1:1 in the present case) and varying the concentration of  $S_2$  we can write

$$\begin{aligned} \left( \frac{1}{\bar{P}} - R_p \frac{\delta^2}{[M]^2} \right) &= C_M + C_{S_1} \frac{[S_1]}{[M]} + C_{S_2} \frac{[S_2]}{[M]} \\ &= \text{constant} + C_{S_2} \frac{[S_2]}{[M]} \end{aligned} \quad (3)$$

In the present case *tert*-butyl alcohol was selected as the cosolvent ( $S_1$ ) to keep the mixture of methyl methacrylate or its polymer and water ( $S_2$ ) homogeneous. Under these conditions the slope of the plot of  $\{ (1/\bar{P}) - R_p(\delta^2/[M]^2) \}$  against  $[H_2O]/[M]$  would give the value of  $C_{H_2O}$ .

TABLE I  
Polymerization of Methyl Methacrylate in the Presence of Water (pH = 7) at 80.5°C

$\frac{[H_2O]}{[M]} \times 10^2$	$\frac{1}{\bar{P}} \times 10^5$	$R_p \times 10^5$ , mole/l.-sec.	$\left( \frac{1}{\bar{P}} - \frac{R_p \delta^2}{[M]^2} \right) \times 10^{5a}$
[ <i>tert</i> -Butyl alcohol]/[Monomer] = 0 <sup>b</sup> ; [AIBN] = 0			
0.00	4.30	1.70	3.77
0.52	4.17	1.83	3.59
1.65	3.69	1.90	3.09
5.34	3.61	2.01	2.99
13.50	3.78	2.37	3.04
[AIBN] = 0			
0.00	5.67	0.64	4.90
1.24	5.42	1.22	4.20
5.25	5.28	1.37	3.92
11.11	5.11	1.40	3.72
23.11	5.20	1.44	3.76
46.00	5.41	1.53	3.69
[AIBN] = $3.05 \times 10^{-4}$ mole/l.			
0.00	23.42	11.50	8.95
0.65	21.69	11.62	7.06
3.87	20.85	11.73	6.09
18.54	20.09	11.80	5.24
24.46	19.84	11.92	4.84
32.65	20.43	12.21	5.06

<sup>a</sup>  $\delta = 5.23^{.10}$

<sup>b</sup> All other sets of experiments in Tables I and II have [*tert*-butyl alcohol]/[monomer] in the ratio of 1:1.

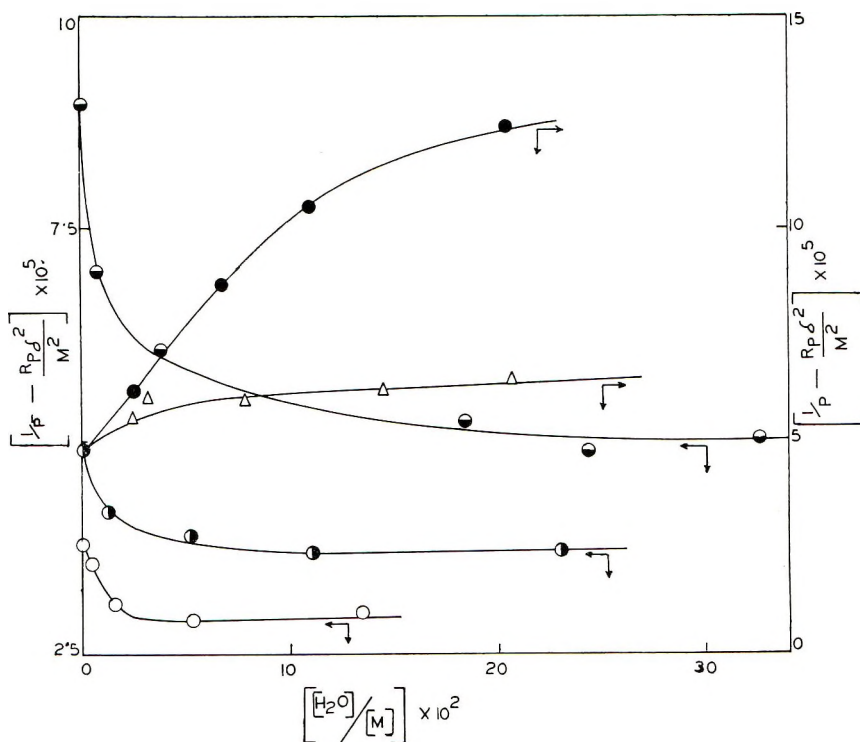


Fig. 1. Effect of water on degree of polymerization of methyl methacrylate at 80.5°C.: (○) pH 7 bulk, thermal; (●) pH 7 *tert*-butyl alcohol, thermal; (◐) pH 7 *tert*-butyl alcohol, catalyzed; (●) pH 3, *tert*-butyl alcohol, thermal; (Δ) pH 11, *tert*-butyl alcohol, thermal.

Polymerization experiments with varying amounts of water were carried out at  $80.5 \pm 0.05^\circ\text{C}$ .; the results are given in Table I and Figure 1.

Variation of the pH of water employed markedly changes the nature of the above plot and can be seen in Figure 1 and Table II.

Polymerization was carried out with varying amounts of water and dimethylformamide at a constant total volume of the mixture; results are given Table III, and the plots of  $1/\bar{P}$  against  $[\text{H}_2\text{O}]/[\text{M}]$  and  $[(1/\bar{P}) - (1/\bar{P}_0)]$  against  $[\text{DMF}]/[\text{M}]$  are shown in Figure 2.

## DISCUSSION

The most remarkable feature of the result is that addition of water even in small quantity brings about an almost monotonous increase in molecular weight instead of the expected decrease due to chain transfer and dilution. A plot of the results (Fig. 1), i.e., of  $\{(1/\bar{P}) - R_p(\delta^2/[\text{M}]^2)\}$  against  $[\text{H}_2\text{O}]/[\text{M}]$ , shows the peculiar nature of the curve. Instead of the usual straight line with a positive slope, the curve takes a reverse course finally becoming almost parallel with the  $[\text{H}_2\text{O}]/[\text{M}]$  axis. This indicates that in all probability water has no chain-transfer capacity.<sup>3</sup> In addition, end-group analysis by the dye-partition technique<sup>7</sup> did not show the presence

TABLE II  
 Polymerization of Methyl Methacrylate in Presence of Water (at Various pHs) at 80.5°C.

$\frac{[\text{H}_2\text{O}]}{[\text{M}]} \times 10^2$	$\frac{1}{\bar{P}} \times 10^5$	$R_p \times 10^5$ , mole/l.-sec.	$\left(\frac{1}{\bar{P}} - \frac{R_p \delta^2}{[\text{M}]^2}\right) \times 10^{5a}$
pH = 3, [AIBN] = 0			
0.00	5.67	0.64	4.88
2.78	7.41	1.04	6.10
4.40	7.53	1.54	5.60
7.15	11.09	1.67	9.01
11.03	12.70	1.74	10.50
20.75	14.69	1.76	12.70
23.32	14.93	1.80	12.42
37.53	15.21	1.97	12.73
pH = 11, [AIBN] = 0			
0.00	5.67	0.64	4.89
2.72	6.63	0.92	5.47
3.02	6.89	0.72	6.01
9.08	5.86	0.74	5.94
14.78	7.15	0.87	6.06
19.63	7.28	0.73	6.46
20.99	7.23	0.66	6.40
39.01	7.33	0.72	5.90

<sup>a</sup>  $\delta = 5.23 \cdot 10$

 TABLE III  
 Polymerization of Methyl Methacrylate in Dimethylformamide-Water System (pH = 7),  
 $1/\bar{P}_0 = 6.10$ 

$\frac{[\text{DMF}]}{[\text{M}]}$	$\frac{1}{\bar{P}} \times 10^4$	$\frac{[\text{H}_2\text{O}]}{[\text{M}]}$	$\left(\frac{1}{\bar{P}} - \frac{1}{\bar{P}_0}\right) \times 10^4$
0.00	6.10	0.00	0.00
2.75	8.48	0.00	2.38
2.68	7.81	0.30	1.72
2.60	7.40	0.59	1.31
2.54	7.23	0.89	1.14
2.47	7.04	1.18	0.95
2.40	6.41	1.48	0.32
2.34	6.17	1.72	0.07
2.19	6.09	2.36	-0.01
2.06	6.01	2.95	-0.10

of OH endgroups in the poly(methyl methacrylate) samples. This further supports the view that in case of water the  $C_{\text{H}_2\text{O}}$  value is approximately zero. Jenkins and Johnston<sup>4</sup> also report that water reduces the reactivity of solvent as a transfer agent. This is not surprising, in view of the fact that alkyl radicals,  $\text{X}-\text{CH}_2-\text{CHR}$  do not react with water<sup>8</sup> and as shown by Merz and Waters<sup>9</sup> that even the highly reactive phenyl radical can persist in aqueous solution until it collides with a suitable solute radical or molecule. The unexpected increase in the degree of polymerization as well as the negative slope of the plot of  $\left\{ \frac{1}{\bar{P}} - R_p(\delta^2/[\text{M}]^2) \right\}$  against  $[\text{H}_2\text{O}]/[\text{M}]$  may

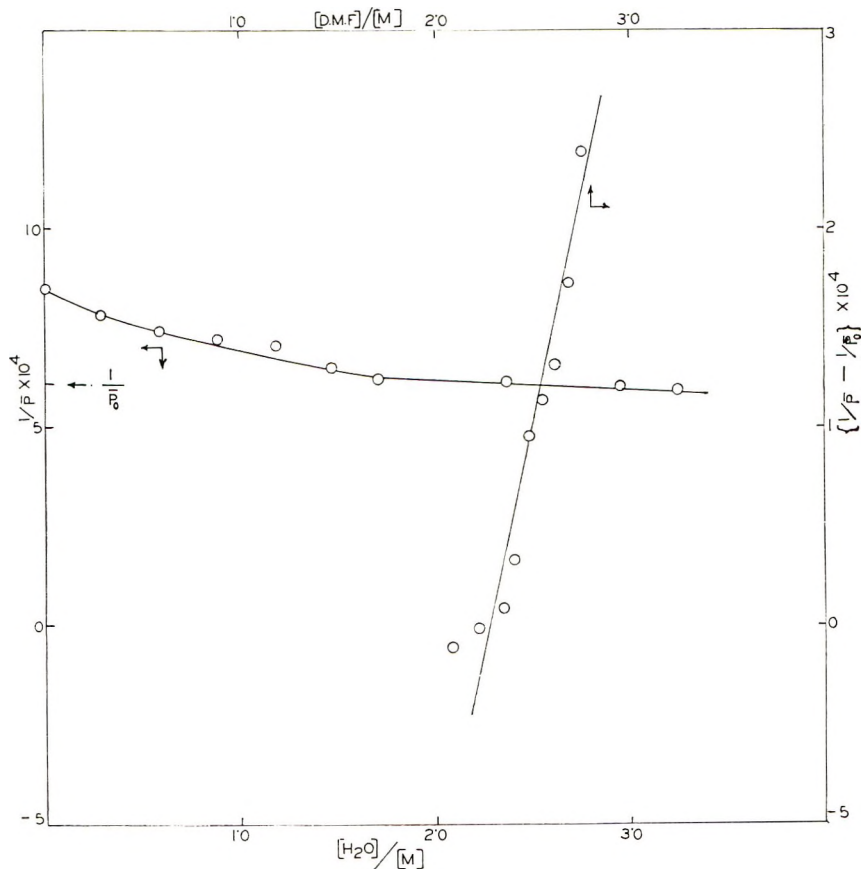


Fig. 2. Effect of water on degree of polymerization of methyl methacrylate in DMF at 80.5°C.

be attributed to tighter coiling of the polymer chain in the presence of a nonsolvent like water, leading to a reduced termination rate, as suggested in our previous work.<sup>3</sup>

Jenkins and Johnston<sup>4</sup> in their work on acrylonitrile in the dimethylformamide-water system proposed that water forms a 1:1 complex with dimethylformamide and that this complex has a lower chain-transfer capacity than dimethylformamide itself. They further predicted that at a ratio dimethylformamide/water of 1:1 there would be no chain transfer with the growing polymer radical and the value of  $1/\bar{P}$  would be equal to  $1/\bar{P}_0$ , i.e., the reciprocal degree of polymerization for bulk polymerization. We have carried out a similar experiment with methyl methacrylate, and the results are reported in Table III and Figure 2. It may be seen that the value of  $1/\bar{P}$  gradually decreases on addition of water, and even at the predicted 1:1 dimethylformamide/water ratio,  $1/\bar{P}$  still decreases to a value even below that for  $1/\bar{P}_0$ . This is not expected, according to the viewpoint of Jenkins and Johnston that  $1/\bar{P}$  should attain a minimum value of  $1/\bar{P}_0$  at the 1:1 ratio. In addition to our work in mixed solvents,

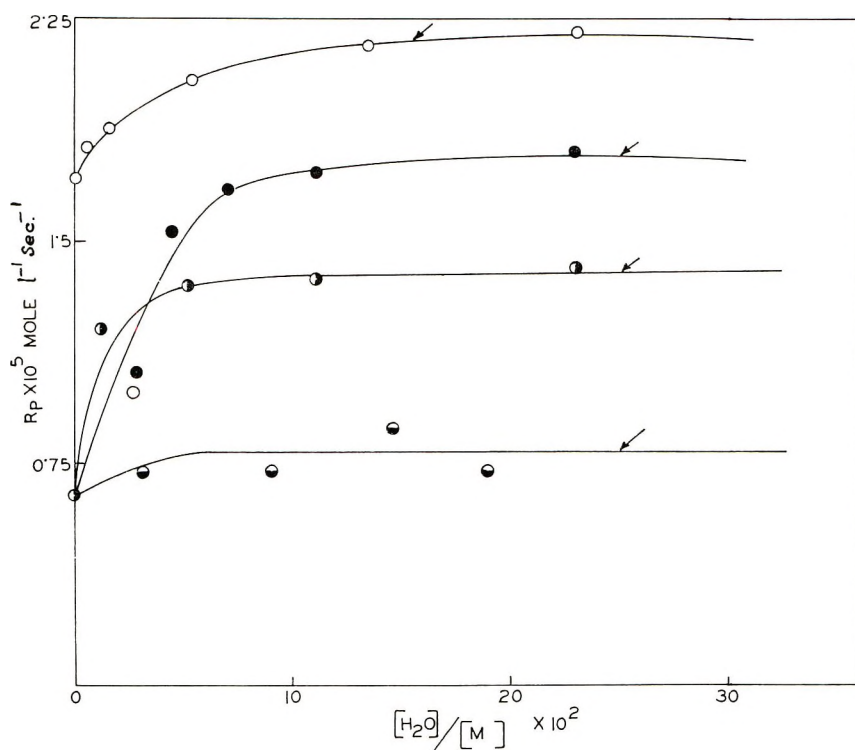


Fig. 3. Effect of water on  $R_p$  in the polymerization of methyl methacrylate at 80.5°C.: (○) pH 7, bulk, thermal; (●) pH 7, *tert*-butyl alcohol, thermal; (●) pH 3, *tert*-butyl alcohol, thermal; (◐) pH 11, *tert*-butyl alcohol, thermal.

work has been carried out with bulk methyl methacrylate with small amounts of added water; the results are reported in Table I and Figure 1. It may be noticed that the trend of  $1/\bar{P}$  is the same as that for the dimethylformamide–water or *tert*-butyl alcohol–water systems, and  $1/\bar{P}$  decreases monotonously, finally attaining a steady value. Considering all these facts the only conclusion we are led to is that the increase in the value of the degree of polymerization ( $\bar{P}$ ) is in all probability due to a reduced termination rate and may not be due to reduction of the solvent-transfer capacity.

Experiments carried out in water at acid or alkaline pH shows altogether a different trend. Instead of gradually decreasing,  $1/\bar{P}$  increases with addition of water, finally reaching a plateau. This is not surprising, since the added acid or alkali has a high transfer capacity and the rise of  $1/\bar{P}$  is the result of this. The overall increase is the net result of transfer with added acid or alkali and the coiling property of the polymer radical in the presence of water. With sufficient amount of water this attains steady value without any further increase.

Since water is a nonsolvent for poly(methyl methacrylate) we have chosen acrylamide for our work, polyacrylamide being soluble in water. In the acrylamide–water system polymerization was carried out at differ-

ent concentrations of water with 2,2-azobisisobutyroamidine as initiator. The degree of polymerization was found to be independent of the water concentration, and the plot of  $1/\bar{P}$  against  $[\text{H}_2\text{O}]/[\text{M}]$  gave a straight line parallel to the  $[\text{H}_2\text{O}]/[\text{M}]$  axis, indicating that in this system also there is no chain transfer to water.

A somewhat similar, though reversed, trend is noticeable in the rate of polymerization as a function of water concentration and is represented in Figure 3. As expected, the rate increases continuously, finally reaches an almost constant value. The points marked with an arrow represent the concentrations of water where phase separation was noticeable; beyond these concentrations both the rate and the degree of polymerization attain a somewhat constant value.

The authors are grateful to Prof. Santi R. Palit for constant encouragement and helpful discussion during the course of work.

### References

1. P. J. Flory, *J. Am. Chem. Soc.*, **59**, 241 (1937).
2. U. S. Nandi and S. R. Palit, *Nature*, **185**, 235 (1960).
3. U. S. Nandi, P. Ghosh, and S. R. Palit, *Nature*, **195**, 1197 (1962).
4. A. D. Jenkins and R. Johnston, *J. Polymer Sci.*, **39**, 81 (1959).
5. A. Weissberger and E. S. Proskauer, Eds., *Organic Solvents, Technique of Organic Chemistry*, Vol. VII, Interscience, New York, 1955.
6. T. G. Fox, J. B. Kinsinger, H. F. Mason, and E. M. Schuele, *Polymer*, **3**, 71 (1962).
7. P. Ghosh, P. K. Sengupta, and A. K. Pramanik, *J. Polymer Sci. A*, **3**, 1725 (1965).
8. W. A. Waters, *Vistas in Free Radical Chemistry*, Pergamon Press, London, 1959, p. 157.
9. J. Merz and W. A. Waters, *J. Chem. Soc.*, **1949**, 2427.
10. F. E. Ferigton and A. V. Tobolsky, *J. Colloid Sci.*, **10**, 536 (1955).

### Résumé

Le rôle de l'eau comme agent de transfert de chaîne dans la polymérisation par addition a été étudié dans le cas du méthacrylate de méthyle et de l'acrylamide dans des solvants mixtes. On a observé que l'eau n'a aucune action de transfert avec la chaîne polymérique en croissance. Le degré de polymérisation a été trouvé croître avec une augmentation de la concentration en eau et ceci est probablement dû à une vitesse de terminaison réduite résultant de l'empelotonnement de la chaîne polymérique en présence d'un non-solvant tel que l'eau.

### Zusammenfassung

Die Rolle des Wassers als Kettenüberträger bei der Additionspolymerisation wurde an Methylmethacrylat und Acrylamid in einem Mischlösungsmittelsystem untersucht. Wasser zeigt keine Übertragungsreaktion mit dem wachsenden Polymerradikal. Der Polymerisationsgrad nahm mit steigender Wasserkonzentration zu, was wahrscheinlich auf die Herabsetzung der Abbruchgeschwindigkeit durch eine Verknäuelung der Polymerkette in Gegenwart eines Fällungsmittels wie Wasser zurückzuführen ist.

Received April 18, 1966

Prod. No. 5155A

## Mechanism of Ozone Attack on $\alpha$ -Methyl Glucoside and Cellulosic Materials

ANDREW A. KATAI\* and CONRAD SCHUERCH, *Department of Chemistry, State University College of Forestry, Syracuse, New York 13210*

### Synopsis

Ozone attack on cellulose and related substances was investigated and appears to involve a twofold mechanism. One is a free-radical chain mechanism involving oxygen in the propagating step. This slow reaction is highly indiscriminate, showing very little, if any, specificity as to the site of attack and resulting in the formation of peroxide, carbonyl, carboxyl, and presumably lactone groups. In the presence of oxygen, kinetic chain lengths of over 100 were measured, but in nitrogen atmosphere the total oxidation of substrate was equivalent to the amount of ozone consumed. The second process appears to be an electrophilic attack which liberates the anomeric carbon of glycosides via an ozone-catalyzed hydrolysis of glycosidic linkages. This reaction, analogous to a nitronium or chloronium ion- or proton-catalyzed hydrolysis, is postulated since chain degradation of polysaccharides is equally severe in the presence or absence of oxygen, and occurs in buffered solutions or suspensions even in the neutral pH range, and because the main product of ozone attack on  $\alpha$ -methyl glucoside is glucose. Brightness improvement in cellulose involves an electrophilic attack on double bonds and therefore is a direct function of the quantity of ozone used, like chain degradation. It is therefore not surprising that we have found no method of enhancing the specificity of ozone attack on the colored material relative to chain degradation. Because of the topochemical and diffusion-controlled character of the reaction on cellulose, the use of a different temperature range will cause only a trivial difference in the relative rates of attack.

The reaction of ozone with olefinic compounds is well understood, and the Criegee mechanism,<sup>1</sup> which comprises electrophilic attack and zwitterion formation, has been receiving broad confirmation and essentially universal acceptance. The much slower processes that occur when saturated compounds are allowed to react with ozone are much more complex and difficult to define. Nevertheless, the fact that ozone is an industrial bulk chemical and has been applied repeatedly to carbohydrate materials—such as starch,<sup>2</sup> cellulose, wood, and pulp—for various purposes, including bleaching<sup>3</sup> and grafting,<sup>4-7</sup> encouraged us to investigate the chemical processes which occur in these systems.

Because of the low rates and extents of oxidation and the low concentrations of ozone possible, analytical methods in many cases had to be modified to obtain even adequate precision and accuracy. However, we believe

\* National Science Foundation Cooperative Graduate Fellow 1963-65; present address: Esso Chemical Company, Inc., New York, N. Y. 10019.



that valid trends have been found and correct qualitative conclusions can be drawn. In the following discussion attention will be called to the limitations of our analytical methods as is necessary.

Methyl  $\alpha$ -D-glucoside was used as an appropriate monomeric substrate, since it is available in high purity, has similar functional groups to starch and cellulose, and the low viscosity of its solutions permits a much wider range of experimental conditions than is possible with polymers. The physical problems of accessibility and ozone transport have been studied previously.<sup>3,8,9</sup>

Initially methyl  $\alpha$ -D-glucoside was ozonized in both oxygen and nitrogen atmosphere in a closed system in which the exact amount of ozone could be determined with good accuracy. The amount of ozone added per mole of substrate was varied by using different concentrations of solution and sizes of reaction vessel since the ozone concentration could only be altered within narrow limits (see Experimental). The oxidation levels in these experiments were extremely low, and the specific rotation after ozonization of the solutions was within one-half degree of the reported value<sup>10</sup> for methyl  $\alpha$ -D-glucoside,  $[\alpha]_D = 158.9$ – $159.0^\circ$ . It will be noted that in many experiments in oxygen several moles of carbonyl are produced for each mole of ozone added (Table I). This is in contrast to experiments run in a nitrogen atmosphere in which, within experimental error, only about one carbonyl is produced per mole of ozone. The amounts of carbonyl formed were clearly a function of substrate concentration and apparently also a function of the ratio of ozone to substrate (Table I). This can be seen most readily by placing the numerical values listed in Table I, column 6 (mole carbonyl per mole ozone) on a two-dimensional graph of solution concentration versus millimoles ozone/mole methyl glucoside. All

TABLE I  
Dependence of Carbonyl Formation on the Ratio of Ozone to Substrate  
for Methyl  $\alpha$ -D-Glucoside Ozonized in Oxygen Atmosphere

Concn. of methyl glucoside, g./l.	Initial concn. of O <sub>3</sub> in O <sub>2</sub> , mmole/l.	Vol. soln., ml. Vol. vessel, ml.	Ozone, mmole/ mole methyl glucoside	Carbonyl, mmole/mole methyl glucoside	Carbonyl, mole/ mole ozone
19	0.969	150/275	4.0	4.0	1.0
23	0.925	50/549	38.2	35.5	0.9
25	0.835	100/2098	64.8	66.5	1.0
40	0.380	100/549	8.1	6.9	0.9
54	0.500	150/549	4.8	11.0	2.0
85	0.873	50/549	12.5	10.1	0.8
103	0.814	150/275	0.64	1.5	2.3
123	0.600	50/549	8.5	10.1	1.2
208	1.025	50/549	4.8	10.4	2.5
236	0.303	195/549	0.45	3.0	6.6
320	0.925	100/2098	5.6	31.0	5.5
388	1.079	150/275	0.22	1.8	8.1
441	0.727	150/275	0.13	0.71	5.3

values of apparent kinetic chain length greater than 1 fall in a quadrant in which substrate concentration is above 45 g./l., and the ratio of millimoles of ozone per mole of methyl glucoside is less than 7. In a quadrant with higher ratios of ozone to substrate and lower substrate concentrations than 45 g./l., all values of chain length are 1.0 or less.

In spite of analytical difficulties, the trends appear clear and are entirely consistent with an ozone-initiated free-radical oxidation. Increased substrate concentration will favor propagation over termination, and will insure that spontaneous ozone decomposition will be at a minimum. A low ozone-to-substrate ratio will favor low concentrations of free radicals and, therefore, propagation over termination, as has been demonstrated by Briner<sup>11</sup> for the oxidation of aldehydes.

The oxidation of methyl  $\alpha$ -D-glucoside by ozone is by no means limited, even under these conditions, solely to the formation of carbonyl groups. Traces of acids were also found and lactone groups may have been present. An accurate measure of the true kinetic chain length can, therefore, in principle only be obtained by a measurement of total oxidation. This was achieved by oxidizing both the initial and the ozonized solutions by a wet combustion method.<sup>12,13</sup> The extent of oxidation by ozone-oxygen mixtures was determined by difference.

The data of Table II again show that there is, in fact, a chain oxidation reaction, the length of which is dependent on both the concentration of the substrate and the substrate/ozone ratio. In two series of four runs each, the initial concentration of the ozone in the gas phase was kept as constant as possible. For all reactions the total volume of the system was fixed (513 ml.). In both sets the concentration of the methyl glucoside solution was varied in exactly the same way, the only difference being in the volume

TABLE II  
Wet Combustion of Methyl  $\alpha$ -D-Glucoside Ozonized in Oxygen Atmosphere

Expt. no.	Concn. of methyl glucoside, g./l.	Initial concn. of ozone in oxygen, mmole/l.	Vol. soln., ml. Vol. vessel, ml.	O <sub>3</sub> , mmole/mole methyl glucoside	Kinetic chain length <sup>a</sup>
61	0.74	0.50	250/513	137	1.0/0.26 = 4.0
62	6.0	0.40	250/513	13.5	4.2/0.21 = 20
63	61	0.46	250/513	1.52	17/0.24 = 71
64	376	0.36	250/513	0.196	47/0.19 = 250
66	0.74	0.27	100/513	286	0.23/0.22 = 1.0
67	6.0	0.36	100/573	47.6	0.36/0.30 = 1.2
68	61	0.36	100/573	4.76	5.1/0.30 = 17
69	376	0.44	100/513	0.91	19/0.36 = 53
70	61	0.36 <sup>b</sup>	100/513	0.19	18/1.2 = 15

<sup>a</sup> Milliequivalents of oxidation/milliequivalents of ozone consumed = kinetic chain length, where 1 equivalent of ozone = O<sub>3</sub>/2.

<sup>b</sup> Average concentration measured over four separate runs repeated on the same substrate.

of the solution: 250 ml. for experiments 61, 62, 63, and 64, and 100 ml. for all the others.

The effect of substrate concentration on the kinetic chain length is obvious. Within each series (experiments 61-64 and 66-69), with increasing methyl glucoside concentration the kinetic chain length increases quite consistently. On comparing the results of runs in the first set with their counterparts in the second set (experiments 61 and 66, 62 and 67, etc.), we find that the kinetic chain length values calculated for the second series are consistently lower. This, we assume, is due to the fact that in the second case the solution volume is lower, resulting in a higher ozone/substrate ratio. The available ozone is depleted at a slower rate, allowing its partial pressure to remain higher. This results in both larger extent of spontaneous decomposition and also a higher concentration of ozone in the liquid phase. A higher ozone content in the liquid phase means higher free-radical concentration and shorter kinetic chain length.

The last entry (experiment 70) in Table II is the combined result of four consecutive ozonizations on the same substrate solution, and the kinetic chain length found was essentially the same as that obtained by a single ozonization under identical conditions (experiment 68). Had the 1.2 meq. of ozone been added in a single batch, the kinetic chain length would have been expected to decrease substantially, due to the decrease of substrate/ozone ratio; but, since each ozone addition was made only after the preceding one had reacted completely, the total amount of ozone at any one time did not exceed that of the comparable run in the second set. The agreement between the calculated values of kinetic chain lengths (15 vs. 17) for these two runs is excellent.

Although analytical errors in these oxidations were rather large (we estimate as much as 50% for the runs with the highest substrate concentration), in the fourfold experiment they were drastically reduced. The data show that the kinetic chain length is not a function of the extent of oxidation of the substrate (which is very low, to be sure) or of the total amount of ozone used.

In order to identify functional groups and products in more detail than was possible in the above experiments, 10-15% solutions of methyl glucoside were ozonized for 18-40 hr. by continuously bubbling through 3-3½% ozone in oxygen at a rate of 8.4 l./hr. The extent of ozonization even after 20 hr. of reaction was still quite low, as shown by the optical rotation  $[\alpha]_D$ , which in no case fell below 152°.

The end product of the reaction contained considerable amounts of active oxygen that decomposed slowly. After 20 hr. of ozonization, a 10% solution of methyl glucoside contained 22 mmole of active oxygen per mole of substrate, whereas comparable ozonization of pure water failed to yield even traces of active oxygen. These results are in agreement with those of Kargin et al.,<sup>5</sup> who found hydroperoxy groups by ozonizing starch under very similar conditions.

The solutions of methyl glucoside were found to be strongly acidic

TABLE III  
Carbon Dioxide Evolution and Acid Formation  
on Continuous Ozonization of Model Substrates

Substrate	Rate of CO <sub>2</sub> evolution mmole/ mole-hr. <sup>a</sup>	Induction period, hr.	Acid at completion of ozonization, mmole	Reaction time, hr.
Methyl glu- coside	0.52	2.0	8.6	10.1
Dihydroxy- acetone	0.58	1.6	12.2	17.0
Glucose	0.34	5.0	18.6	20.0
Glycerol	0.48	1.2	23.8	24.8
			14.4	24.8

<sup>a</sup> A constant rate of evolution after induction period.

(pH 2.2–2.7), and contained methanol, formaldehyde, and formic acid as volatile materials. The end gases contained carbon dioxide but no carbon monoxide or methane. The formation of carbon monoxide, although unlikely, is not entirely excluded, since it can slowly oxidize to carbon dioxide with excess ozone. This oxidation is slow enough, however, that if appreciable amounts of carbon monoxide were formed some would have remained.

The carbon dioxide did not originate solely from methanol but from the sugar skeleton as well for the rate of carbon dioxide evolution was nearly the same for four compounds tested under comparable conditions (methyl  $\alpha$ -D-glucoside, glucose, glycerol, and dihydroxyacetone). Although these compounds did not have the same number of reaction sites (all were ozonized in 2.0M solution), in this concentration range the substrate was in huge excess over ozone, and therefore the number of functional groups present had little influence on the rate. While glucose showed a somewhat slower rate of carbon dioxide evolution than the other three, it had the highest rate of acid formation (see Table III).

The conclusion can be made from the data above that ozone is a highly nonspecific oxidizing agent and attacks keto, aldehyde, and alcohol groups with similar ease. This result was confirmed by paper chromatography of the nonvolatile products of ozonization of methyl  $\alpha$ -D-glucoside. Ten bands were separated and most of these appeared to be somewhat impure or mixtures of closely related substances. Typical results obtained with a standard basic developing system are shown in Table IV. However, the identity of the products cannot be satisfactorily explained by postulating solely a nonspecific ozone-initiated radical oxidation chain. By far the largest single product is glucose, and others are products which were shown in comparable experiments to be derived from glucose. Most of the glucose formation is clearly the result of acid-catalyzed hydrolysis, for when the reaction was repeated in a solution buffered to pH 5.7, the amount of glucose and glucose transformation products formed was substantially less.

Nevertheless, glucose remained by far the largest single product of the reaction even in the buffered systems. Another process must therefore also lead to its formation. In part this process may involve the well-known peroxidation of ethers; however, it is inconceivable to us that the methyl group will be greatly preferred as a site of radical oxidation over all other positions (including the aldehydic hydrogen of C<sub>1</sub>) in the methyl glucoside molecule. We, therefore, propose that in this process as in that occurring on olefins, ozone attacks as an electrophilic reagent in the same

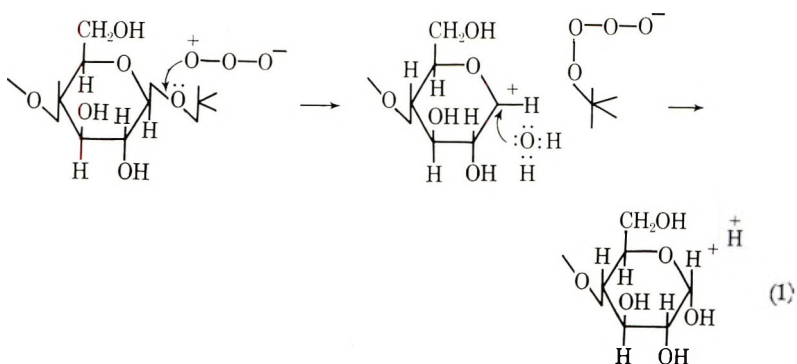
TABLE IV  
Nonvolatile Ozonization Products

Band	$R_f$	Derived from $\alpha$ -methyl glucoside <sup>a</sup>		Derived from glucose <sup>a</sup>	Remarks and identification	Meth- oxyl content, %
		Not buffered, mg./100 ml.	Buf- fered, mg./100 ml.			
A	<0.04	47	+	+	Probably mixed uronic acids	6.4
B	0.10	} 102	+	+		
C	0.22-0.27		+	+		
D	0.40	} 63	+	+	6.6	
E	0.46		+	-		
F	0.65	55	+	-		12.1
G	1.00	370	132	+	Largely glucose	2.1
H	1.22-1.27	158	++	+	Largely arabinose	4.8
I	1.82	-	-	+		-
J	1.70-2.00	+++	+++	-	Methyl $\alpha$ -D-glu- coside	15.0
K	2.25-2.35	178	76	-		15.2

<sup>a</sup> Plus signs (+) represent substances determined qualitatively; minus signs (-) represent compounds not observed to be present. "Derived from glucose" reports qualitative results obtained on a comparable ozonization of glucose in the absence of buffer. Numbers are glucose equivalents (mg./100 ml.).

<sup>b</sup> Determined on fractions obtained on products from ozonization of unbuffered  $\alpha$ -methyl glucoside solutions.

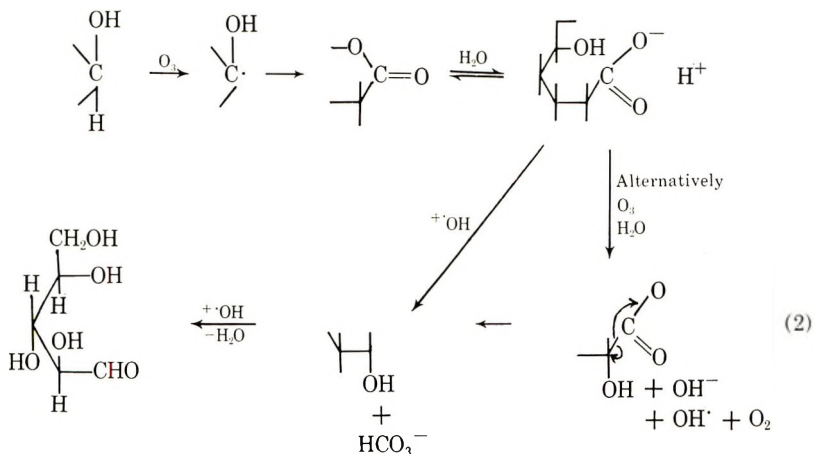
fashion as a proton cleaving the glucosidic linkage to form a carbonium ion on C<sub>1</sub>. The carbonium ion thereupon reacts with water molecule to form glucose. This mechanism is essentially analogous to the chlorine-,<sup>14-18</sup> chlorine dioxide,<sup>14</sup> and nitronium and nitrosonium ion-catalyzed<sup>19</sup> hydrolytic cleavage of aromatic ethers, and even more closely analogous to reactions of chlorine, chlorine dioxide, chlorite, and hypochlorite on methyl glycosides and cellulose, observed under conditions which eliminated the possibility of acid hydrolysis by Theander,<sup>20</sup> Purves,<sup>21,22</sup> and Henderson.<sup>23</sup> The fate of the attacking ozone molecule thereafter is not known.



We will use this speculation later to explain the fact that methyl cellulose is degraded nearly as severely by ozone in nitrogen as by ozone in oxygen.

Since the acid- and ozone-catalyzed glycosidic cleavages are the most significant reactions in the treatment of methyl  $\alpha$ -D-glycoside with ozone, it is certain that these reactions are of critical importance in limiting the use of ozone in bleaching, pulping, and grafting applications.

Arabinose is a second major product which was identified by rechromatography and color reactions. This undoubtedly is derived from glucose by radical oxidation and decarboxylation of C<sub>1</sub> that can be formulated as shown in eqs. (2).



This reaction is similar to the well-known Ruff degradation<sup>24</sup> and is analogous to the oxidative decarboxylation of  $\alpha$ -hydroxy acids as discussed by Stewart.<sup>25</sup> It is significant to note that deBelder et al.<sup>26</sup> found arabinose and glucose among a greater number of oxidation products upon treating methyl  $\beta$ -D-glucoside with hydrogen peroxide in the presence of ferrous sulfate. They suggest that arabinose is formed from glucose by an unspecified free-radical process.

The slowly moving products found in bands A and B probably consist largely of mixed uronic acids and lactones. The high methoxyl values of

bands F and K suggest that these products are derived directly from methyl  $\alpha$ -D-glucoside, and bands in this region are in fact not obtained by ozonization of glucose. If radical abstraction of a secondary hydrogen were followed by replacement by a second hydrogen in a chain-transfer process, it would be possible to obtain other sugars such as galactose or mannose. This process appears unlikely, since hydrogen abstraction from water involves homolytic cleavage of the hydrogen-oxygen bond, an energetically unfavorable process, and hydrogen abstraction from a second substrate molecule to form a conformationally less stable sugar is improbable. Although these unlikely products are not proven to be completely absent, evidence is that, if present, the quantities are minute. For the most part the remaining materials are reducing compounds which appear to be mixtures of complex oxidation products.

The ozonolysis of olefins has a low activation energy, and temperature has little influence on its rate.<sup>27</sup> However, this is not necessarily the case for carbohydrates as well. The formation of glucose during ozonization of methyl glucoside was followed at temperatures of 15, 25, and 40°C. in a buffered system (Fig. 1). The solubility of ozone is lowered at higher temperatures, while the rate of its simultaneous decomposition is increased. Since both of these properties decrease the effective concentration of ozone, a slower rate of glucose formation is expected at elevated temperatures.

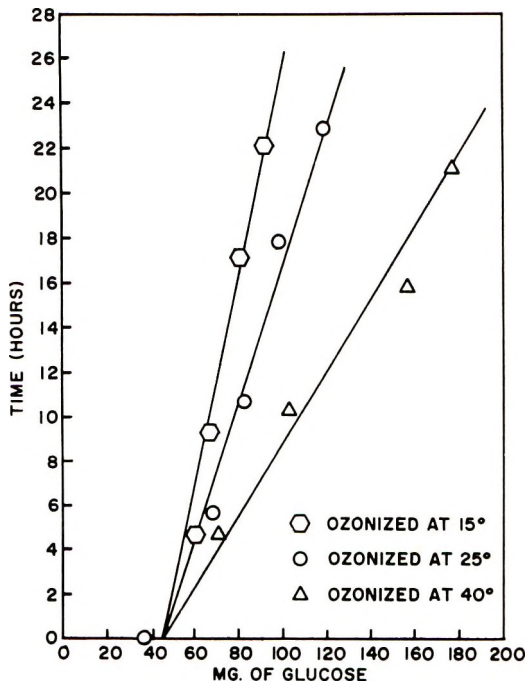


Fig. 1. Rate of glucose formation during ozonization of methyl  $\alpha$ -D-glucoside. Conditions: 100 ml. of 12% substrate solution in 2M phosphate buffer at pH 5.7, ozonized with 3-3 $\frac{1}{2}$  O<sub>3</sub> in O<sub>2</sub> at a rate of 8.4 l./hr.

Instead, under our conditions the rate increased threefold, from 2.1 mg./hr. at 15°C. to 6.2 mg./hr. at 40°C. Thus, the activity of ozone is sufficiently enhanced at higher temperatures to counteract substantially the loss of reactivity caused by lower ozone concentrations. Szymanski<sup>2</sup> similarly found that the highest reactivity of ozone in the formation of carbonyl groups on starch is obtained at around 50°C. As the temperature is raised above 50°C. the effective ozone concentration is decreased too much to result in further increase in reaction rate. Since glucose formation from methyl glucoside corresponds to chain breaking in a polysaccharide, low temperatures of reaction should result in lower rates of depolymerization.

The reaction of ozone with methyl cellulose was also investigated. The polymer was a typical, commercial, water-soluble derivative with approximate degree of substitution of 1.5 and a molecular weight by viscometry equal to  $1.0 \times 10^5$ . Carbonyl group formation was measured by the same method used on methyl  $\alpha$ -D-glucoside, a quantitative hydrogenation with sodium borohydride in a solution buffered to pH 9.5<sup>28-31</sup> in equipment modified from the design used by Lindberg and co-workers.<sup>29,30</sup> With the modifications described in the experimental section, errors in the determination of carbonyl were reduced to about 15% on glucose when amounts equivalent in carbonyl content to the range of our interest were analyzed. (0–0.015 g. glucose is equivalent in carbonyl content to 0–40 carbonyls per macromolecule of 0.20 g. of methyl cellulose with a degree of polymerization of 530 and molecular weight of  $= 1 \times 10^5$ .) When more manageable amounts were analyzed (such as 0.070 g. of glucose and up) the error was reduced to below 1%. Carboxyl group measurements were made by conductometric titration of methocel solutions after they had been passed through an ion

TABLE V  
Composition of Methyl Cellulose Ozonized in the Presence of Oxygen

Ozone, mole/mole methyl cellulose	DP	$k'$	Number of carbonyls/ mole methyl cellulose	Number of carboxyls/ mole methyl cellulose	(1/DP) $\times 10^3$
0.0	534	0.57	0.75	0.0	1.87
0.8	474	0.54	—	0.9	2.11
1.2	—	—	9.3	1.5	—
1.9	383	0.58	14.0	1.6	2.61
3.2	335	0.50	21.0	2.7	2.99
3.6	266	0.60	25.0	2.9	3.76
5.3	198	0.55	—	3.1	5.05
7.0	213	0.51	31.6	3.4	4.69
9.1	175	0.61	—	3.0	5.71
10.0	199	0.52	33.4	3.2	5.02
12.1	192	0.49	34.8	3.1	5.21
13.5	174	0.56	34.0	3.0	5.75
16.6	152	0.58	36.2	2.6	6.58
18.8	164	0.49	34.0	1.8	6.10



TABLE VI  
Composition of Methyl Cellulose Ozonized in Nitrogen Atmosphere

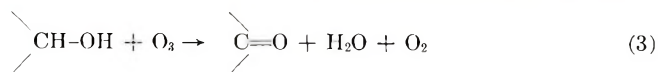
Ozone, mole/mole methyl cellulose	DP	$k'$	Number of carbonyls/ mole methyl cellulose	Number of carboxyls/ mole methyl cellulose	(1/DP) $\times 10^3$
0.0	530	—	2.8	0.2	1.89
3.9	473	0.51	2.7	0.0	2.11
9.6	302	0.50	13.6	0.2	3.31
11.2	276	0.46	13.8	0.0	3.62
19.4	186	0.54	18.1	0.6	5.38
27.5	152	0.56	26.0	1.0	6.58
31.9	115	0.58	33.9	1.1	7.52
45.3	123	0.64	40.2	2.4	8.13

exchange column. The method was believed to give values within 20% of the correct value. Two series of experiments were run to determine the amount of carbonyl and carboxyl groups produced by ozonization in an oxygen and a nitrogen atmosphere. The results, which are consistent with those obtained on  $\alpha$ -methyl glucoside, are listed in Tables V and VI.

Experiments were run in a closed system in the range of 0–45 moles of ozone per mole of methyl cellulose. The carboxyl formation was quite minor in this range, although there is a trend toward higher numbers at higher extents of ozonization. In oxygen atmosphere somewhat more carboxyl was formed than in nitrogen atmosphere.

The difference between the two series is much more pronounced in the formation of carbonyl groups. Within the experimental error the number of carbonyls produced in the nitrogen series was equal to the number of moles of ozone consumed, over the entire range of ozone to methyl cellulose ratios. In contrast, in oxygen atmosphere at low extents of ozonization, one mole of ozone produced about 8 moles of carbonyls. This ratio rapidly decreased at higher proportions of ozone, and the number of carbonyls did not increase beyond about 40, even though 20 moles of ozone was used per mole of methyl cellulose.

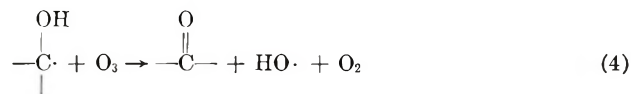
The data obtained for the nitrogen series are thus consistent with a reaction in which the ozone attack approximates the reaction shown in eq. (3).



The same process might occur in oxygen, but the possibility of a chain reaction with relatively short kinetic chain length and involving oxygen must be considered since the number of carbonyl groups is consistently higher than that accountable for by the simple stoichiometry of eq. (3). This chain reaction is presumably free radical in character and is initiated by ozone, since it does not occur appreciably in oxygen alone. Thus, after 18 hr. of reaction time (which is the same as the reaction time of ozone with

methyl cellulose) under comparable conditions, in pure oxygen only 4.8 moles of carbonyl and 1.3 moles of carboxyl were produced per mole of methyl cellulose. The degree of polymerization was found to be 525, only slightly less than the original 534 for untreated, freshly dissolved methyl cellulose.

One explanation for the relative decrease in the amount of oxidation at higher extents of ozonization is that the spontaneous decomposition of ozone is more pronounced. It was shown by Heidt and Forbes<sup>32-34</sup> that the rate of ozone decomposition is a function of its partial pressure. (In our case one means of obtaining higher ozone to methocel ratios was to increase the ozone concentration.) The decomposition is also via a chain mechanism, catalyzed by light, although intensity and wavelength are apparently of minor importance. Quantum yields of up to 130 have been obtained,<sup>32</sup> and dark rates were found to be as high as 20% of the total rates.<sup>33</sup> Other possible reasons for the shortening of the kinetic chain length at higher ozone concentrations are the faster recombination of free radicals in higher concentration and a possible reaction of an intermediate with residual ozone leading to induced decomposition of ozone [eq. (4)].



Several of the reaction mixtures were tested for the presence of methanol,<sup>35</sup> formaldehyde,<sup>36</sup> and formic acid. In all cases the presence of trace quantities of methanol and formaldehyde was established. Traces of formic acid were detected only in runs with the highest degree of ozonization.

The change in molecular weight of methyl cellulose with increase in extent of ozonization was also followed in these experiments (Fig. 2). Each point on this figure represents a single experiment with a fixed volume of 1.5-1.9% methyl cellulose solution (200 ml.) treated with a fixed volume (900 ml.) of gas containing a particular concentration of ozone. In the experiments shown in Figure 2, less than one chain break is produced per mole of ozone introduced into the system. In the unbuffered oxygen system, to cut the molecular weight in half requires about 4 mole of ozone. When the same experiments were carried out in a system buffered to pH 5.7, substantially less degradation occurred. Clearly, the difference in these two cases was the result of acid-catalyzed hydrolysis due to carboxyl functions introduced into the polymer chain. This result can be correlated with the acid-catalyzed hydrolysis of methyl glucoside to glucose described above. When the ozonization was performed in nitrogen atmosphere and without buffer, the results were comparable to those obtained with oxygen and a buffer. Apparently the radical chain oxidation, which one would expect at low ozone/methyl cellulose ratios and which must occur partly on C<sub>1</sub> and C<sub>4</sub> does not necessarily result in chain cleavage. The small differences in

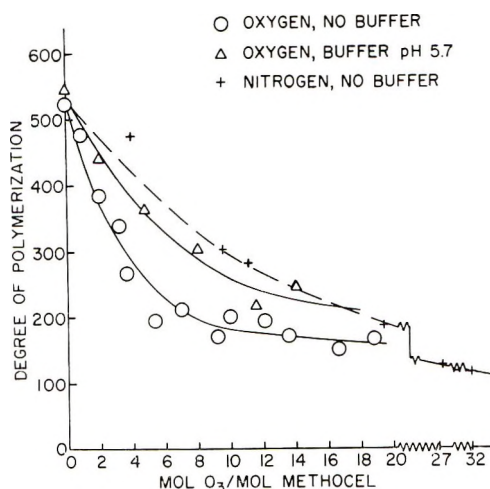


Fig. 2. Decrease in molecular weight of methyl cellulose with increase in ozonization.

degree of polymerization of the products from the nitrogen and buffered oxygen systems are scarcely beyond the range of experimental error.

Finally, it can be noted that at the higher ozone/methyl cellulose ratios, i.e., 18:1 and above, there is little difference between the results in the three systems. This probably reflects the shorter chain length in autoxidation at high ozone concentrations, the greater spontaneous ozone decomposition, and the greater relative importance of chain breakage by ozone-initiated hydrolysis.

The conclusions appear inescapable that radical chain oxidations occur on ozonization of methyl cellulose as they do with methyl glucoside, that their main result is the introduction of oxidized functions, but that the main chain-degrading processes are due to the direct attack of ozone presumably inducing hydrolysis and are also due to acid-catalyzed hydrolysis as an indirect effect of the formation of carboxyl functions.

To apply to cellulose itself the information obtained throughout the course of this research, unbleached kraft pulp was subjected to ozonization under conditions believed to result in the least possible amount of deterioration of the cellulose component of the pulp. Acidic hydrolysis was eliminated by buffering the suspension, and the reactions were carried out in nitrogen atmosphere to reduce or eliminate possible chain oxidation.

On plotting ozone consumption versus brightness or degree of polymerization, or the two pulp properties against each other, there was found to be no appreciable difference between data obtained in nitrogen or oxygen atmosphere (Table VII). This result, although disappointing, is consistent with that obtained on the ozonization of methyl cellulose. With methyl cellulose, the decrease in degree of polymerization was not a function of oxygen content in the gas phase but depended on the amount of ozone used. The gain in brightness is similarly due to the electrophilic degradation of colored bodies (lignin) by ozone and not due to oxygen. Therefore,

TABLE VII  
Effect of Ozone on Some Physical Properties of Unbleached Kraft Pulp<sup>a</sup>

Amount of ozone, meq.	Carrier gas	Brightness, %	DP	<i>k'</i>
0.00	—	27.6	1190	0.76
0.04	N <sub>2</sub>	28.1	1130	0.71
0.95	N <sub>2</sub>	28.2	1100	0.67
1.42	N <sub>2</sub>	29.3	1060	0.70
2.02	N <sub>2</sub>	34.0	910	0.70
3.48	O <sub>2</sub>	37.5	812	0.63
6.96	N <sub>2</sub>	48.2	594	0.60
10.47	O <sub>2</sub>	58.3	493	0.68
11.61	N <sub>2</sub>	69.7	414	0.61

<sup>a</sup> 1.35 g. of pulp in 800 ml. of 0.2*M* phosphate buffer in a 2100 ml. vessel. Thus, the volume of the gas is 1300 ml.

although elimination of oxygen will presumably decrease the number of cellulose functional groups oxidized, it does little to increase the degree of polymerization of a pulp at a given brightness.

No exactly comparable experiments were run in the absence of buffers, so the influence of buffers on the extent of degradation of pulp was not determined. Presumably under these conditions (ozonization for 22 hr. in a closed system until all ozone was used up), hydrolysis would cause further degradation than that observed in the buffered system. However, the relation between degree of polymerization and brightness of the pulp bleached in buffers was not greatly different from that observed in earlier work in these laboratories<sup>3,8,9</sup> on pulps bleached in water with a stream of ozone in oxygen for periods of 10–20 min. Presumably during the short periods of treatment which correspond more closely to a practical bleaching cycle, acid-catalyzed hydrolysis is not significant.

In conclusion, it appears worthwhile to summarize the kinds of reactions occurring on ozonization of carbohydrates and their probable relative importance.

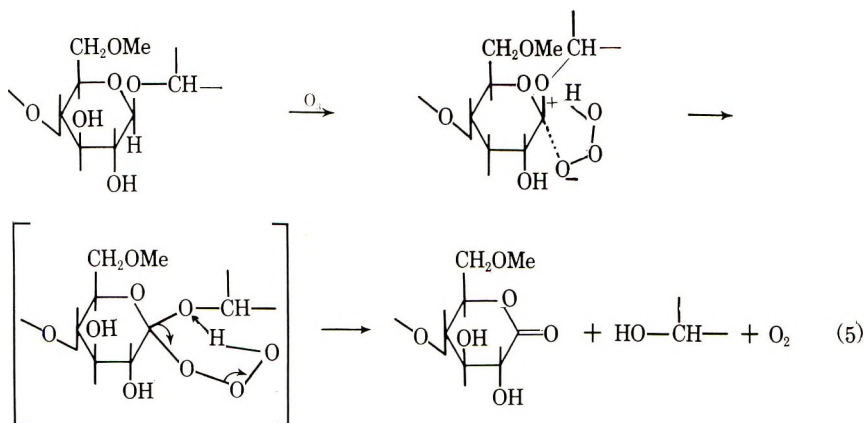
Acid-catalyzed hydrolysis of glycosidic linkages has been shown to occur during the ozonization of methyl glucoside and methyl cellulose in the absence of buffers, but probably is not of too much significance during brief periods of ozonization of cellulose. Presumably the process is slow and has been observed in this research primarily because reactions were run for over 20 hr. to complete the reaction with ozone. The mechanism of this process is well known and the ozone-catalyzed hydrolysis formulated above is based on it [eq. (1)].

Ozone-catalyzed hydrolysis [eq. (1)] is postulated to account for the fact that glucose is produced as the primary product of the ozonization of methyl  $\alpha$ -D-glucoside in the presence of buffers. It appears inconceivable that the major ozonization product could be the result of an oxidative attack on the methyl residue. Furthermore, the degradation of methyl cellulose

in buffers under our conditions is nearly independent of the presence of oxygen, and therefore cleavage of the glycosidic linkage in the polysaccharide must be by direct attack of ozone.

Price and Tumolo<sup>36</sup> have proposed a polar mechanism for the attack of ozone on ethers which accounts for the formation of esters and hydrogen peroxide without the involvement of oxygen. If a similar reaction occurs on C<sub>1</sub> or C<sub>4</sub> of starch or cellulose, oxidation might occur at this site with little degradation of the polysaccharide. Furthermore, an attack of the same general character on any hydroxyl-bearing compound would result in the stoichiometry observed in the ozonization of methyl cellulose in nitrogen [eq. (3)]. Equation (5) is reminiscent of the Price and Tumolo mechanism but results in lactone and 4-hydroxy endgroups. Such a process may contribute to chain cleavage but presumably would not result in the formation of glucose from a glucoside. An alternative course would be the abstraction of the hydride ion from the C<sub>4</sub>-position which would yield hemiacetal and 4-keto endgroups. Such electrophilic oxidations may be of considerable importance under conditions which disfavor radical chain mechanism.

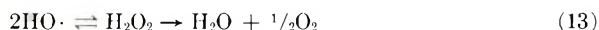
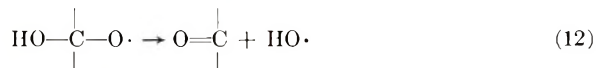
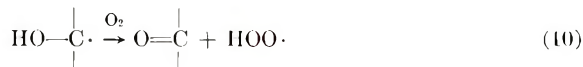
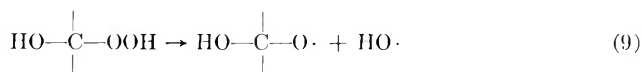
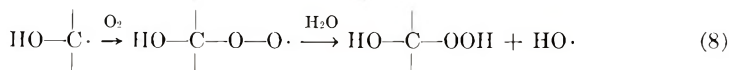
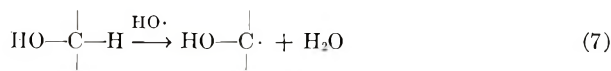
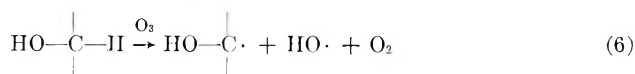
Chain degradation may also occur without oxidative attack at C<sub>1</sub> or C<sub>4</sub>. It is well known that introduction of electronegative groups such as carbonyls or carboxyls in glucose moieties of a polysaccharide labilize



glycosidic bonds to nucleophilic attack. This process does not seem to have contributed much to the chain degradation we measured, however, since if this were the case we should have observed more degradation in the presence than in the absence of oxygen. However, a gradual decrease in viscosity of cupriethylene diamine solutions of ozonized cellulose was observed, no doubt caused by the greater lability of oxidized units. Furthermore, cleavage of a polysaccharide chain by multiple attack on a single glucose unit (for example, breaking a ring C<sub>2</sub> and C<sub>3</sub> and between C<sub>4</sub> and C<sub>5</sub>) must be excluded under our conditions for the possible reaction sites

of the substrate vastly outnumber the moles of ozone available for the reaction.

Finally, it appears demonstrated that ozone initiates an autoxidation process such as is formulated in eqs. (2) and (6)–(13) which leads to the formation of oxidized functional groups, carbonyls, carboxyls, lactones, and hydroperoxides. The quantitative determination of these functional groups cannot be considered entirely satisfactory since the hydroperoxides



have a limited lifetime and their determination and that of lactones in the presence of carbonyls is not straightforward. In at least one case the total oxidation caused by autoxidation was far greater than the sum of carbonyl and carboxyl and it is not clear whether volatile products, hydroperoxides and lactones can account for the difference.

Nevertheless, the fact that long oxidation chain lengths are favored at low ozone and high substrate concentrations in the presence of oxygen points to the fact that in reactions on cellulosic fibers and solids such as starch granules, this process will presumably be of great importance. Since the reaction on solids will be topochemical, at some depth within the solid matrix the ozone concentration will be depleted and chain processes favored. Multiple oxidation of accessible units will be expected to occur along an advancing front within the solid. This drastic oxidation would be limited by the use of an inert carrier gas.

## EXPERIMENTAL

### Ozonization in a Closed System

Ozone was produced by means of a conventional laboratory generator described previously.<sup>8,9</sup> At 140 ml./min. flow rate of oxygen, the gas

leaving the reactor contained 3% ozone. Concentration was varied over a moderate range by changing the flow rate.

The ozonization system consisted of oxygen and nitrogen sources, ozone generator, manometer, a U-tube containing 80–100 mesh silica gel (which when chilled in Dry Ice adsorbed 6% ozone by weight), two flasks of approximately equal size, a connection to a vacuum line, and appropriate stopcocks. Flasks and U-tubes of various sizes were used to alter the amount of ozone collected and the ratio of ozone to substrate. In a typical reaction, the system was evacuated and ozone-containing gas was passed into the two flasks simultaneously, one of which served as control and the second as reaction vessel. The latter was closed off during the period of the reaction. By analyzing the ozone content in the control, it was found possible to estimate the amount of ozone in the reaction vessel within 3%. Spontaneous decomposition of ozone at an initial concentration of 2% was approximately 25–30% in 24 hr. Ozone-containing oxygen was passed into the flasks directly from the ozonizer. If nitrogen was desired as the carrier gas, ozone was adsorbed on the chilled silica gel to saturation, the oxygen eliminated from the system, and nitrogen allowed to sweep the ozone from the silica gel (as the Dry Ice trap was cautiously removed) into the evacuated flasks. The amount of ozone in nitrogen was metered by altering the amount of silica gel used.

Methyl cellulose (Dow Methocel DS = 1.5; DP = 540; 16 g./per 1000 ml. filtered) solution in aliquots of 200 ml. was allowed to react with ozone in the described system. The substrate/oxidant ratio was varied by changing the oxygen flow rate and also by changing the volume of gas above the liquid phase. In some experiments 0.2; phosphate buffer of pH 5.7 was used, and in these reactions there was no change in the pH of the system.

Molecular weights were determined by viscometry in water or buffer at  $25.0 \pm 0.1^\circ\text{C}$ . Solvent flow time was 124.2 sec. Staudinger's constant of 120 was used to calculate the degree of polymerization.<sup>37</sup> A modification of the method of Lindberg and co-workers<sup>28–31</sup> was used for the determination of carbonyl since the method, as reported, was unsatisfactory for the very low carbonyl concentration found in this work. Instead of a vessel of three chambers,<sup>29,30</sup> a simple 25-ml. flask was used which was fitted with two thin necks, one connected to a gas buret by a short piece of Tygon tubing, the other stoppered with a self-closing rubber septum (syringe cap). Exactly 10 ml. solution of methyl cellulose or methyl  $\alpha$ -D-glucoside was placed in the vessel together with 1 ml. of 0.1M boric acid. The vessel was attached to the gas buret and stoppered. Through the septum 1 ml. of 0.007M sodium borohydride in 0.1N sodium hydroxide was added with a Gilmont plunger type micropipet (M15401, Manostat Corp., New York, N. Y.) to which a hypodermic needle was attached. Two identical sets of apparatus were run simultaneously, one the actual analysis, the second a blank. In this manner errors due to changes in temperature, atmospheric pressure, and concentration of the sodium borohydride solution were elim-

inated. The reaction mixtures were shaken for 2 hr. On completion of the run 1 ml. of 0.5*M* sulfuric acid was added by a hypodermic syringe (or micropipet) to liberate the unreacted hydrogen. The difference in volume between the blank and the actual analysis was the amount of hydrogen consumed by the sample. Carboxyl determinations were made by conductometric titration of the solution after deionization with sulfonated polystyrene.

For the determination of volatile products the ozonized methyl cellulose solution was distilled and the distillate was tested for methanol, formaldehyde, and formic acid. Formaldehyde was determined colorimetrically according to the process developed by Bricker and Johnson,<sup>35</sup> chromotropic acid and sulfuric acid being used to form a colored complex. The procedure used for the measurement of methanol was essentially the modification of the standard method of oxidizing methanol to formaldehyde with potassium permanganate and determining the latter as described above.<sup>18</sup> Formic acid was measured by conductometric titration with 0.002*N* sodium hydroxide.

Methyl  $\alpha$ -D-glucoside (Eastman  $[\alpha]_D^{25} = 159.0^\circ$ ; m.p. 163–165°C.; glucose content = 0.30%) was ozonized at various concentrations according to the same procedure. Analytical methods were as above. To determine the total oxidation of the substrate the wet combustion method of Lang<sup>12,13</sup> was employed. An aliquot of ozonized methyl  $\alpha$ -D-glucoside, containing 30–40 mg. of substrate, was treated with 10 ml. of 1*N* potassium dichromate and 30 ml. of concentrated sulfuric acid, boiled for 3 min., and then cooled. The solution was diluted to 500 ml.; to a 50-ml. portion potassium iodide was added to reduce the excess chromic acid. The amount of iodine liberated was determined by titrating with 0.1*N* sodium thiosulfate. Unozonized methyl glucoside was used as blank. The accuracy of the method at low conversions and high concentrations of the substrate left much to be desired, since to measure the total oxidation a small difference of two large numbers had to be determined. All care was taken to assure maximum sensitivity but in extreme cases the value may have been in error by a factor of 2. The accuracy was considerably improved by measuring the amount of potassium dichromate with a micropipet.

### Continuous Ozonization of Methyl $\alpha$ -D-Glucoside

Methyl  $\alpha$ -D-glucoside was continuously ozonized by bubbling 3% ozone in oxygen through a 10–15% solution of the substrate at a rate of 140 ml./min. To insure that the concentration of methyl glucoside remained the same throughout the run the gases were saturated first by bubbling through distilled water. Reaction times were varied between 18–40 hr.

The end products were analyzed for active oxygen by first flushing the system with nitrogen for 3–5 hr. at a rate of 280 ml./min., or until no ozone was detected in the gases leaving the reaction vessel. About 1 g. of potassium iodide and 3 ml. of 2*M* sulfuric acid was added to 50 ml. of solution,



and the liberated iodine was titrated with standard sodium thiosulfate solution. Water, ozonized and flushed with nitrogen under the same conditions, failed to liberate measurable amounts of iodine.

The reaction mixture was distilled to near dryness under vacuum, and the methanol, formaldehyde, and acid contents were determined as described previously.

To establish the presence of carbon dioxide and possibly other gaseous products the end gases leaving the system were bubbled into a gas washing bottle containing saturated barium hydroxide solution. Periodically 5-ml. samples of the base were withdrawn and were added to 30 ml. of 0.1*M* hydrochloric acid which was back-titrated with 0.1*N* sodium hydroxide with the use of phenolphthalein as indicator. The difference between the sodium hydroxide titer of the actual run and the blank yielded the amount of carbon dioxide which reacted with the base to form barium carbonate.

The end gases leaving the first barium hydroxide bottle were passed through a glass tubing (~3 in. in length) containing a platinum coil heated by an electric current to a red glow. The gases then passed into another barium hydroxide gas washer. Although haziness and white precipitate (barium carbonate) appeared in the first gas washer soon after the flow of ozone began, the second washer remained clear even after 15 hr. of ozonization. It was concluded that no carbon monoxide or carbonaceous gases other than carbon dioxide were formed during ozonization of methyl glucoside.

The nonvolatile reaction products were separated by paper partition chromatography. About 0.16 ml. of the solution was applied linearly to a sheet of Whatman No. 1 chromatography paper 18<sup>1</sup>/<sub>4</sub> × 22<sup>1</sup>/<sub>2</sub> in., the apparatus of ASTM D1915-61T being used.<sup>38</sup> A mixture of butanol, pyridine, and water, in the ratio of 10:3:3, was used as irrigant. The time of elution was about 40 hr. at 25°C. The chromatograms were sprayed with aniline-phthalic acid and silver nitrate-alcoholic potassium hydroxide developers.<sup>39</sup>

For preparative-scale chromatography, essentially the same method was followed as described above,<sup>38</sup> the only difference being what Whatman No. 3MM paper was used, which was streaked four times. Guide strips were developed to establish the location of the separated products, which were eluted from the paper with distilled water at 60°C. All fractions were analyzed for methoxyl content by a modified Zeisel method<sup>40</sup> and by infrared and ultraviolet spectrophotometry.

Quantitative chromatography was performed on separable fractions using Whatman No. 1 chromatography paper according to the standard ASTM method.<sup>38</sup> Results were obtained as glucose equivalents and are reported as such in Table IV.

### Ozonization of Unbleached Kraft Pulp

Unbleached kraft pulp (1.35 g. containing 6% moisture) was dispersed in 800 ml. of 0.2*M* phosphate buffer, with the use of a high-speed Dumore

stirrer (Type KB-210, The Dumore Co., Racine, Wisconsin) until all the fibers were separated. The suspension was ozonized in a closed system for 18 hr. under 1300 ml. of gas phase. The fibers were filtered and thoroughly washed with distilled water. Brightness measurements were taken on small sheets with an Elrepho photoelectric reflection photometer (Model G50-660e, Carl Zeiss Co., Oberkochen, Wurttemberg, Germany) with the use of the No. 8 blue light TAPPI filter set to a brightness of 76.9% of the standard brightness MgO plate.<sup>41</sup> Triplicate samples were prepared and the average of three determinations is reported. Errors were of the order of 3%.

The remaining ozonized pulp was dried in a vacuum oven at 50°C., and its molecular weight was determined by viscometry in cupriethylenediamine.

The present report is abstracted from the Ph.D. thesis of A. A. Katai.

The authors gratefully acknowledge the support of the Herman Frasch Foundation and the National Science Foundation.

### References

1. R. Criegee, paper presented at the International Ozone Conference, Chicago, Ill., 1956; *Advan. Chem. Ser.*, **21**, 143 (1959).
2. C. D. Szymanski, *J. Appl. Polymer Sci.*, **8**, 1597 (1964).
3. C. Schuerch, in *Fourth Cellulose Conference, J. Polymer Sci. C*, **2**, R. H. Marchessault, Ed., Interscience, New York, 1963, p. 79, and references therein.
4. V. A. Kargin, Kh. U. Usmanov, and B. I. Aikhodzhaev, *Vysokomol. Soedin.*, **1**, 149 (1959).
5. V. A. Kargin, P. A. Kozlov, N. A. Plate, and I. I. Konoreva, *Vysokomol. Soedin.*, **1**, 114 (1959).
6. S. Suta, A. Pikler, and D. Sabikova, *Sb. Prac. Chem. Fak. Svst.*, **1962**, 119; *Chem. Abstr.*, **59**, 10333h (1963).
7. Kh. U. Usmanov, B. I. Aikhodzhaev, and U. Azizov, *J. Polymer Sci.*, **53**, 87 (1961).
8. Z. Osawa, W. A. Erby, K. V. Sarkanen, E. Carpenter, and C. Schuerch, *Tappi*, **46**, 84 (1963).
9. Z. Osawa and C. Schuerch, *Tappi*, **46**, 79 (1963).
10. G. N. Bollenback, *Methyl Glucoside*, Academic Press, New York, 1958.
11. E. Briner, paper presented at the International Ozone Conference, Chicago, Ill., 1956; *Advan. Chem. Ser.*, **21**, 184 (1959).
12. W. Lang, *Papier*, **10**, 41 (1956).
13. W. Lang, *Oesterr. Chem. Ztg.*, **57**, 98 (1956).
14. C. W. Dence, M. K. Gupta, and K. V. Sarkanen, *Tappi*, **45**, 29 (1962).
15. C. Dence and K. Sarkanen, *Tappi*, **43**, 87 (1960).
16. K. V. Sarkanen, *Pure Appl. Chem.*, **5**, 219 (1962).
17. K. V. Sarkanen and C. W. Dence, *J. Org. Chem.*, **25**, 715 (1960).
18. K. V. Sarkanen and R. W. Strauss, *Tappi*, **44**, 459 (1961).
19. C. A. Bunton, E. D. Hughes, C. K. Ingold, D. I. H. Jacobs, E. J. Minkoff, and R. I. Reed, *J. Chem. Soc.*, **1950**, 2628.
20. O. Theander, *Svensk Papperstid.*, **18**, 581 (1958).
21. R. H. Zienius and C. B. Purves, *Can. J. Chem.*, **37**, 1820 (1959).
22. R. H. Zienius and C. B. Purves, *Tappi*, **43**, 27 (1960).
23. J. T. Henderson, *J. Am. Chem. Soc.*, **79**, 5304 (1957).
24. W. Pigman, Ed., *The Carbohydrates*, Academic Press, New York, 1957.

25. R. Stewart, *Oxidation Mechanisms*, Benjamin, New York, 1964.
26. A. N. deBelder, B. Lindeberg, and O. Theander, *Acta Chem. Scand.*, **17**, 1012 (1963).
27. G. Wagner and A. Greiner, *Z. Physik. Chem.*, **215**, 92 (1960).
28. S. Lindman-Safvat and O. Theander, *Svensk Papperstid.*, **61**, 42 (1958).
29. B. Lindberg and A. Misiorny, *Svensk Papperstid.*, **55**, 13 (1952).
30. B. Lindberg and O. Theander, *Svensk Papperstid.*, **57**, 83 (1954).
31. J. C. Rankin and C. L. Mehlretter, *Anal. Chem.*, **28**, 1012 (1956).
32. G. S. Forbes and L. J. Heidt, *J. Am. Chem. Soc.*, **56**, 1671 (1934).
33. G. S. Forbes and L. J. Heidt, *J. Am. Chem. Soc.*, **56**, 2369 (1934).
34. L. J. Heidt, *J. Am. Chem. Soc.*, **57**, 1710 (1935).
35. C. E. Bricker and H. R. Johnson, *Ind. Eng. Chem. Anal. Ed.*, **17**, 400 (1945).
36. C. C. Price and A. L. Tumolo, *J. Am. Chem. Soc.*, **86**, 4691 (1964).
37. A. B. Savage, Cellulose Products Laboratory, The Dow Chemical Company, Midland, Mich., personal communication.
38. *Standard Methods*, D 1915-61T, American Society for Testing and Materials, Philadelphia, Pa., 1961.
39. R. Stock and C. B. F. Rice, *Chromatographic Methods*, Reinhold, New York, 1963.
40. *Methods in Carbohydrate Chemistry*, R. L. Whistler, Ed., Vol. III, Academic Press, New York, 1963, p. 277.
41. *Standard Testing Methods*, T 230sm-50, Technical Association of the Pulp and Paper Industry, New York.

### Résumé

L'ozone attaque la cellulose et les substances voisines suivant un mécanisme double. L'un est un mécanisme en chaîne par radicaux-libres comportant l'oxygène dans l'étape propagatrice. Cette réaction lente ne manifeste qu'une faible spécificité en ce qui concerne le site d'attaque et résulte de la formation de groupes peroxydes, carbonyles, carboxyles et probablement lactoniques. En présence d'oxygène, des longueurs de chaînes cinétiques supérieures à cent, ont été mesurées, mais sous atmosphère d'azote l'oxydation totale du substrat est équivalente à la quantité d'ozone consommé. Le second processus consiste en une attaque électrophile basée sur la libération de carbone des glucosides par une hydrolyse catalysée par l'ozone des liens glucosidiques. Cette réaction, analogue à celle d'un ion nitronium ou chloronium ou d'une hydrolyse catalysée par les protons est postulée parce que la dégradation en chaîne de polysaccharides est également prononcée, en présence ou absence d'oxygène et se passe dans des solutions tamponnées ou en suspension, même dans le domaine des pH neutres, et parce que le produit principal de l'attaque de l'ozone de l'-méthyl glucoside est le glucose. Le brillant de la cellulose est amélioré, car il comporte une attaque électrophile des doubles soudures et est une fonction directe de la quantité d'ozone utilisée, de même que la dégradation de la chaîne. Il n'est dès lors pas surprenant que nous n'avons pas trouvé de méthode permettant d'augmenter la spécificité de l'attaque à l'ozone sur le matériel coloré par apport à la dégradation. Par suite du caractère topochemique, contrôlé par diffusion de la réaction sur la cellulose, l'utilisation de températures différentes occasionnera uniquement une faible différence dans les vitesses relatives d'attaque.

### Zusammenfassung

Der Ozonangriff auf Zellulose und verwandte Substanzen wurde untersucht und scheint nach zwei Mechanismen abzuverlaufen. Der eine ist ein radikalischer Kettenmechanismus mit Beteiligung von Sauerstoff in der Kette. Diese langsame Reaktion ist wenig, wenn überhaupt, spezifisch in bezug auf die Angriffsstelle und führt zur Bildung von Peroxyd-, Carbonyl-, Carboxyl- und vermutlich Lactongruppen. In Anwesenheit

von Sauerstoff wurden kinetische Kettenlängen bis über 100 gemessen. In Stickstoffatmosphäre war aber die Gesamtoxydation des Substrats der verbrauchten Ozonmengen äquivalent. Der zweite Prozess scheint in einem elektrophilen Angriff zu bestehen, der über eine Ozon-katalysierte Hydrolyse der Glucosidbindungen den anomeren Kohlenstoff der Glucoside freisetzt. Diese Reaktion wird in Analogie zur Nitronium-, Chloronium- oder Proton-katalysierten angenommen, da der Kettenabbau der Polysaccharide in Gegenwart und Abwesenheit von Sauerstoff gleich bedeutungsvoll ist und in gepufferten Lösungen oder Suspensionen sogar bei neutralem pH stattfindet und weil das Reaktionsprodukt des Ozonangriffs auf  $\alpha$ -Methylglucosid Glucose ist. Die Helligkeitsverbesserung verläuft bei Zellulose über einen elektrophilen Angriff auf Doppelbindungen und ist daher, sowie der Kettenabbau, der verwendeten Ozonmenge direkt proportional. Es ist daher nicht überraschend, dass keine Methode zur Erhöhung der Spezifität des Ozonangriffs auf das gefärbte Material gegenüber dem Kettenabbau gefunden werden konnte. Wegen des topochemischen und diffusionskontrollierten Charakters der Reaktionen mit Zellulose würde die Verwendung eines anderen Temperaturbereiches nur zu trivialen Unterschieden der relativen Angriffsgeschwindigkeiten führen.

Received December 28, 1965

Revised March 25, 1966

Prod. No. 5157A

## NOTES

*Thermal Gradients in Degradation Reactions*

Data were presented in a recent publication<sup>1</sup> on the thermal degradation of poly(methyl methacrylate) carried out in closed quartz and steel reaction vessels. The predominant reaction is the formation of monomer. The reaction vessels were approximately of cylindrical shape with flat bottom walls which were coated with thin films of polymer. Small parts of the side walls were also covered by polymer. The vessels were completely submerged in a thermostated liquid metal bath. It was found that the rate constants determined in the steel vessel were consistently larger than those derived from the experiments in the quartz vessel for the same bath temperature. It is believed that this discrepancy is due to thermal gradients across the quartz reaction vessel wall and the polymer film. The film temperature will be lower than that of the bath, as depolymerization is an endothermic reaction. As far as the steel vessel is concerned, the thermal gradients will be quite small. The heat conductivity of steel is about fifty times larger than that of quartz. A heat-transfer analysis of the difference between the bath and film temperature is presented here, yielding results which compare quite favorably with those derived directly from experimental data.<sup>1,2</sup>

## HEAT TRANSFER CALCULATIONS OF TEMPERATURE DIFFERENCES

A reaction vessel of cylindrical shape, having plane-parallel end walls, is considered in the following discussion. This closed vessel is assumed to be completely submerged in an opaque liquid of constant temperature. The bottom wall of the vessel is taken to be coated by a thin polymer film, which degrades to monomer. The vessel is quickly plunged into the bath at  $t = 0$ . The endothermic reaction acts as a heat sink. Radiation, which rapidly decreases as the vessel heats up to the bath temperature, will take place between the parallel vessel walls. Also, heat transfer by gas convection will be operative; the gas will be heated quickly to the reaction-vessel temperature and will therefore be hotter than the film. Here again the term will eventually become quite small. Storage of heat will take place due to the heat capacities of the materials present. The following relationship for non-isothermal heat transfer will then hold at time  $t$  of the degradation process,

$$T_{B/W} - T_{F,t} = \left( \frac{l_{F,t}}{k_F} + \frac{l_W}{k_W} \right) \left\{ \left( \frac{dm_1}{dt} \right)_t (-\Delta H_p + \Delta H_v) - \frac{\rho}{1/\epsilon_W + 1/\epsilon_F - 1} (T_{B/W}^4 - T_{F,t}^4) - h(T_{B/W} - T_{F,t}) + s_F m_{F,t} \left( \frac{dT}{dt} \right)_{F,t} + s_W m_W \left( \frac{dT}{dt} \right)_{W,t} \right\} \quad (1)$$

Here, the symbols and numerical values chosen are as follows:  $T_{B/W}$  and  $T_{F,t}$  = temperature of outer reaction vessel wall (equal to that of the bath temperatures 673.16 and 648.16°K., respectively, used for the present calculations) and the unknown film temperature, respectively;  $l_{F,t}$  and  $l_W$  = film thickness at time  $t$  ( $5 \times 10^{-3}$  cm. at time  $t = 0$ ) and wall thickness ( $1.8 \times 10^{-1}$  cm.), respectively;<sup>2</sup>  $k_F$  and  $k_W$  = heat conductivity

coefficients of the polymer film ( $5 \times 10^{-4}$  cal.-cm. $^{-1}$  sec. $^{-1}$  °C. $^{-1}$ ) and the quartz wall ( $2.55 \times 10^{-3}$  cal.-cm. $^{-1}$  sec. $^{-1}$  °C. $^{-1}$ ), respectively;<sup>3</sup>  $(dm_1/dt)_t$  = rate of volatile (monomer) formation at time  $t$  in m.-sec. $^{-1}$  cm. $^{-2}$ , obtained from differentiating the experimental monomer versus time curves<sup>2</sup> (see also Table I below);  $-\Delta H_p$  = heat of depropagation (depolymerization);  $+\Delta H_p$  ( $-13.4 \pm 0.5$  Kcal.-m. $^{-1}$ ) is the heat of propagation (polymerization);<sup>4</sup>  $\Delta H_v$  = heat of monomer vaporization ( $8.6 \pm 0.4$  Kcal.-m. $^{-1}$ );<sup>5</sup>  $\rho$  = Stefan's radiation constant ( $1.3556 \times 10^{-12}$  cal.-cm. $^{-2}$  sec. $^{-1}$  °K. $^{-4}$ );<sup>6</sup>  $\epsilon_w$  and  $\epsilon_f$  = emissivity of wall and film, respectively, both taken as 1 (black body); calculation shows that  $\epsilon_w = \epsilon_f = 0.8$  yields a negligible difference in  $T_{B/W} - T_{F,t}$  at 60% conversion of polymer to monomer;  $h$  = convection heat transfer coefficient ( $8 \times 10^{-5}$  to  $5.6 \times 10^{-4}$  cal.-cm. $^{-2}$  sec. $^{-1}$ ); calculation shows that the difference in  $T_{B/W} - T_{F,t}$  at 60% conversion is practically the same for the whole range of  $h$  values; the maximum value gives the results given here);<sup>7</sup>  $s_f$  and  $s_w$  = specific heats of film ( $0.40$  cal.-g. $^{-1}$  °C. $^{-1}$ ) and quartz ( $0.25$  cal.-g. $^{-1}$  °C. $^{-1}$  at  $400^\circ\text{C}$ .), respectively;<sup>3</sup>  $m_{f,t}$  and  $m_w$  = mass of film at time  $t$  (at  $t = 0.5 \times 10^{-3}$  g.-cm. $^{-2}$ ) and wall ( $4.76 \times 10^{-1}$  g.-cm. $^{-2}$ );<sup>2</sup>  $(dT/dt)_{F,t}$  and  $(dT/dt)_{w,t}$  = rates of change with time of mean temperatures of film and wall in °K.-sec. $^{-1}$ , respectively.

The numerical evaluation of equation (1) was carried out by means of a computer. At time  $t = 0$ , the film and reaction vessel are at room temperature ( $298.16^\circ\text{K}$ ).  $(dT/dt)_{F,t}$  is replaced by  $(T_{F,t_2} - T_{F,t_1})/\Delta t$  where  $T_{F,t_2}$  and  $T_{F,t_1}$  are the mean film temperatures at time  $t_2$  and  $t_1$  respectively, ( $\Delta t = t_2 - t_1$ ). The film is so thin that its temperature is equal to the temperature at the interface  $T_{W/F}$ . The mean temperature of the wall is given by  $(T_{F,t_2} - T_{F,t_1})/2\Delta t$ . The radiation term can be evaluated by replacing  $T_{F,t_2}^4$  by  $T_{F,t_2}^4 - \Delta t$  if  $\Delta t$  is chosen small enough.<sup>8</sup>  $l_{F,t_2}$  and  $m_{F,t_2}$  are inserted as the proper fractions of their values at  $t = 0$ ;  $(dm_1/dt)_{t_2}$  is obtained by differentiating the experimental monomer ( $m_1$ ) versus time curves.<sup>2</sup> Density and specific heat changes with temperature have been neglected. The time intervals were  $\Delta t = 1$  sec. and  $\Delta t = 2$  sec. for experiments at  $400^\circ\text{C}$ . and  $375^\circ\text{C}$ .,<sup>1,2</sup> respectively.

Some typical ( $T_{B/W} - T_{F,t}$ ) values obtained from the calculations are given in Table I.

TABLE I  
Typical Temperature Differences between Bath (= Outer Reaction Vessel Wall) and Polymer Film (PMMA) Calculated by Computer for Various Stages of the Degradation Process from Eq. (1) (For Experimental Values see Ref. 1 and 2), Initial Amount of Polymer  $5 \times 10^{-6}$  monomeric unit-moles-cm. $^{-2}$

Bath temperature $T_{B/W}$ , °K.	Reaction time, sec.	Monomer m. $\times 10^6$ cm. $^{-2}$	% Con- version	$10^7(dm_1/dt)$ , m.-sec. $^{-1}$ cm. $^{-2}$	$T_{B/W} - T_{F,t}$ , °K.
648.16	8	4	20	7.34	78.95
	16	6	30	5.60	16.94
	26	8	40	4.30	2.83
	40	10	50	3.22	0.64
	57	12	60	2.44	0.39
	69	14	70	1.95	0.31
	83	16	80	1.82	0.24
673.16	8	4	20	12.22	74.69
	12	6	30	11.42	32.61
	17	8	40	10.40	11.93
	22	10	50	9.37	4.87
	28	12	60	7.32	2.12
	36	14	70	5.13	1.03
	48	16	80	3.12	0.54

TABLE II  
 Comparison of Temperature Differences between Batch and Polymer Film Calculated from Equations (1) and (2), Respectively, for 60% Conversion of Polymer to Monomer (See Also Ref. 1 and 2)

Bath temperature $T_{B/W}$ , °K.	Reaction time $t_r$ , sec.	Rate of monomer formation ( $dm_1/dt$ ) <sub>60%</sub> quartz vessel, m.-cm. <sup>-2</sup> sec. <sup>-1</sup>	Rate constants, sec. <sup>-1</sup>		$T_{B/W} - T_{F,60\%}$ °K.	
			$k_i(\text{Quartz, } 60\%)$	$k_i(\text{Steel, } 60\%)$	From eq. (1), °K.	From eq. (2), °K.
673.16	28	$7.32 \times 10^{-7}$	$4.13 \times 10^{-2}$	$6.21 \times 10^{-2}$	2.12	7.42
648.16	57	$2.44 \times 10^{-7}$	$1.49 \times 10^{-2}$	$1.58 \times 10^{-2}$	0.39	1.00

## CALCULATION OF EXPERIMENTAL TEMPERATURE DIFFERENCES

The calculated temperature differences at 60% conversion may be compared with values derived directly from experiment. It is assumed that the same Arrhenius equation holds for experiments carried out either in a quartz or stainless steel reaction vessel, which is only approximately the case (see Fig. 3, ref. 1). One has, then, for the same bath temperature, the following relationships,

$$\log k_{(\text{Steel}, 60\%)} = - \frac{E}{2.303RT_{(\text{Steel} \cong \text{Film} = \text{Bath})}} + \log A$$

and

$$\log k_{(\text{Quartz}, 60\%)} = \frac{-E}{2.303RT_{(\text{Film})}} + \log A$$

Hence,

$$\log \frac{k_{(\text{Steel}, 60\%)}}{k_{(\text{Quartz}, 60\%)}} = \frac{E}{2.303R} \left( \frac{1}{T_{(\text{Film})}} - \frac{1}{T_{(\text{Bath})}} \right) = \frac{E}{2.303R} \Delta \left( \frac{1}{T} \right) \quad (2)$$

The rate constants at 60% conversion were obtained from the slopes of  $dm_1/dt$  versus monomer plots, hence  $k_{(60\%)} = [d(dm_1/dt)/dm_1]_{(60\%)} \text{ sec.}^{-1}$ .

The results obtained in this way are given in Table II.

## Discussion

Table I shows that the temperature differences  $T_{B/W} - T_{F,60\%}$  calculated from eq. (1) change quite rapidly with percentage conversion, which makes the results quite sensitive with respect to small differences in conversion. Further,  $T_{B/W} - T_{F,60\%}$  obtained from eq. (2) is appreciably dependent on small changes in the ratio of the rate constants. The experimental values for the monomer formed at 60% have standard deviations of about  $\pm 5$  to  $\pm 7\%$  for the rate constants obtained in the steel vessel at 375°C. and 400°C.<sup>1</sup> The standard deviations for the quartz vessel are larger:  $\pm 20\%$  and  $\pm 10\%$  at 400°C. and 375°C.<sup>2</sup> Changing the rate constants by these percentages, maximum and minimum values can be calculated for the temperature difference. It is quite likely that the standard deviations for the rate constants are even larger than those for conversion, as the former have been obtained by two successive differentiations. The maximum and minimum temperature differences are calculated in this way from eq. (2) (see Table III).

TABLE III

	$k_{\text{Quartz}, 60\%}, \text{sec.}^{-1}$	$k_{\text{Steel}, 60\%}, \text{sec.}^{-1}$	$T_{B/W} - T_{F,60\%}$ from eq. (2), °K.
673.16°K.	$3.3 \times 10^{-2}$	$6.5 \times 10^{-2}$	14.16
	$4.9 \times 10^{-2}$	$5.7 \times 10^{-2}$	4.76
648.16°K.	$1.34 \times 10^{-2}$	$1.66 \times 10^{-2}$	2.46
	$1.50 \times 10^{-2}$	$1.64 \times 10^{-2}$	<0

A change of a few kilocalories in the energy of activation has less effect than a change in the ratio of the rate constants. At about 400°C., the activation energy starts to decrease due to diffusion-controlled monomer formation;<sup>1</sup> a smaller  $E$  in eq. (2) would result in a smaller  $\Delta T$ .

In order to obtain more accurate values of the temperature differences for bath and film from eq. (2), larger  $\Delta(1/T)$  values are required. This can, in principle, be achieved by making the quartz wall and the polymer film thicker and the reaction temperatures



higher. However, in the case of polymethylmethacrylate, the monomer formation becomes diffusion controlled beyond 400°C. and the energy of activation decreases from 49.5 to 16.1 kcal./mole for a film 50  $\mu$  thick.<sup>1</sup> The thicker the film, the lower the temperature will become for the onset of the diffusion-controlled monomer formation.

The radiation and heat convection terms and also the heat capacity terms for the film in eq. (1) become quite negligible when 60% conversion is reached, but they make some small contributions at the start of the reaction.

In view of the uncertainties pointed out above, it must be concluded that the values calculated for the temperature difference between bath and film from eq. (1) compare quite favorably with the experimental values derived from the Arrhenius equation (eq. 2).

### Summary

The difference in rate constants for identical reaction bath temperatures obtained from degradation of polymer films in a stainless steel and a quartz vessel, respectively, are due to thermal gradients caused by the endothermic depolymerization reaction. Heat-transfer calculations of the temperature differences between the outer quartz vessel wall, whose temperature is equal to the bath temperature, and the polymer film compare favorably with values derived from Arrhenius equations.

The author is indebted to Mr. Ming Dean Luh for computer and other numerical calculations and to Prof. H. Schenck, Jr. for helpful discussions. The work was made possible by a Grant from the Army Research Office, Durham.

### References

1. H. Kachi and H. H. G. Jellinek, *J. Polymer Sci. A*, **3**, 2714 (1965).
2. J. E. Clark and H. H. G. Jellinek, *J. Polymer Sci. A*, **3**, 1171 (1965); also H. H. G. Jellinek and J. E. Clark, *Can. J. Chem.*, **41**, 355 (1963).
3. *Handbook of Chemistry and Physics*, 44th ed., Chemical Rubber Publ. Co., Cleveland, 1963.
4. F. S. Dainton and K. J. Ivin, *Chem. Soc. Quart. Rev. (Long.)*, **12**, 61 (1958).
5. Rohm and Haas, *The Acrylic Library*, Compilation of Technical Literature.
6. G. W. Castellan, *Physical Chemistry*, Addison-Wesley, Reading, 1964, p. 391.
7. R. B. Bird, W. E. Stewart, and E. N. Lightfoot, *Transport Phenomena*, Wiley, New York, 1960, Table 13.1-1, p. 393.
8. H. Schenck, Jr., *Fortran Methods in Heat Flow*, Ronald Press, New York, 1963; see also H. Schenck, Jr., *Heat Transfer Engineering*, Prentice Hall, Englewood Cliffs, 1959.

H. H. G. JELLINEK

Department of Chemistry  
Clarkson College of Technology  
Potsdam, New York

Received September 20, 1965

Revised March 4, 1966

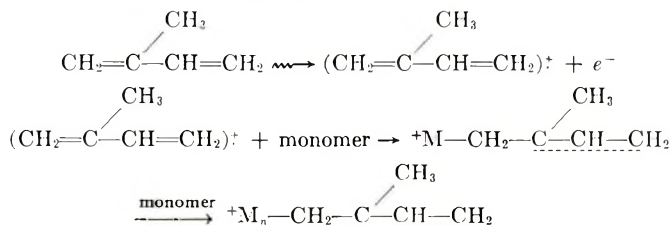
### Electron Spin Resonance Study of Radiation-Induced Solid-State Polymerization of Conjugated Dienes

Several electron spin resonance (ESR) studies have so far revealed that the radiation-induced solid-state polymerization of acrylic acid,<sup>1</sup> its amide<sup>2-6</sup> and its metal salts<sup>7-9</sup> proceeds by a free-radical mechanism, where propagating radicals are found. On the other hand, the polymerization of acrylonitrile<sup>10</sup> and isoprene<sup>11</sup> at low temperature was found to proceed by ionic mechanism, though free radicals were also observed in polymerizing systems. However, no definite conclusion was attained on the correlation between the observed free radicals and the active species responsible for the polymerization reaction. Present study is aimed to clarify this correlation in the solid-state polymerization of some conjugated dienes at  $-196^{\circ}\text{C}$ .

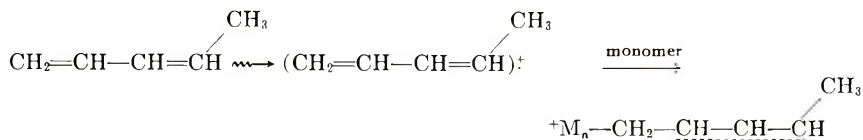
When isoprene, 1,3-pentadiene, and 2,3-dimethyl-1,3-butadiene were irradiated by electrons from a Van de Graaff accelerator at  $-196^{\circ}\text{C}$ ., free radicals were observed in solid monomers by ESR measurements. The structures of free radicals are assigned from their ESR spectra and summarized in Table I. They look like a propagating-type free radical, as if formed by addition of an alkyl radical,  $\text{R}\cdot$ , to the end carbon atom of diene monomers.

To elucidate the mechanism of the formation of trapped free radicals in irradiated solid monomers, free radicals were also produced in the solid monomers at  $-196^{\circ}\text{C}$ . by several methods of radical reaction, as follows; (a) by reaction with  $\text{HO}\cdot$  radicals (the frozen mixture of a small amount of *tert*-butyl hydroperoxide and monomer was photoirradiated with a high-pressure mercury arc), (b) by reaction with  $\text{CH}_3\cdot$  radicals (the frozen mixture of a small amount of methyl iodide and monomer was photoirradiated with the high-pressure mercury arc), and (c) by ultraviolet irradiation (mainly with 2537-Å. light from a medium-pressure mercury arc).

In Table I are summarized the structures of free radicals formed by the radical reactions and assigned from those ESR spectra. Evidently, the free radicals formed by the ionizing radiation are quite different from those produced by the radical reactions. Free radicals abstract a hydrogen atom from the methyl group of isoprene molecule and do not add to its conjugated double bond. Therefore, the free radicals found in the electron-irradiated monomer are not formed by actual addition of  $\text{R}\cdot$  radicals, but formed through another process. The process is probably an ion-molecule reaction involving an ion-radical as a reaction intermediate:



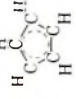
For pentadiene, radicals add to the 3-carbon atom. Therefore, the free radicals found in the electron-irradiated monomer are not formed by actual addition of  $\text{R}\cdot$  radicals to the 1-carbon atom of the monomer. The radical is probably formed through the following mechanism similar to that of isoprene:



For dimethylbutadiene, a similar mechanism is also possible, but not yet very conclusive.

In the above scheme, an ion-radical is primarily formed by loss of a  $\pi$ -electron from

TABLE I. Structure of Trapped Free Radicals and Types of Reactions of Conjugated Dienes (Assigned from Electron Spin Resonance Spectra)

Reaction method	Isoprene	Pentadiene	Dimethylbutadiene
	$\begin{array}{c} \text{CH}_3 \\   \\ \text{CH}_2=\text{C}-\text{CH}=\text{CH}_2 \\   \quad   \\ 1 \quad 2 \quad 3 \quad 4 \end{array}$	$\begin{array}{c} \text{CH}_3 \\   \\ \text{CH}_2=\text{CH}-\text{CH}=\text{CH} \\   \quad   \\ 1 \quad 2 \quad 3 \quad 4 \end{array}$	$\begin{array}{c} \text{CH}_3 \quad \text{CH}_3 \\   \quad   \\ \text{CH}_2=\text{C}-\text{C}=\text{CH}_2 \\   \quad   \\ 1 \quad 2 \end{array}$
Electron irradiation	<p>R-Addition type (1-carbon)</p> $\begin{array}{c} \text{CH}_3 \\   \\ \text{R}-\text{CH}_2-\text{C}-\text{CH}=\text{CH}_2 \\   \quad   \\ \text{CH}_2 \end{array}$	<p>R-Addition type (1-carbon)</p> $\begin{array}{c} \text{CH}_3 \\   \\ \text{R}-\text{CH}_2-\text{CH}-\text{CH}=\text{CH} \\   \quad   \\ \text{OH} \end{array}$	<p>R-Addition type (1-carbon)</p> $\begin{array}{c} \text{CH}_3 \quad \text{CH}_3 \\   \quad   \\ \text{R}-\text{CH}_2-\text{C}-\text{C}=\text{CH}_2 \\   \quad   \\ \text{CH}_3 \end{array}$
Reaction with HO·	<p>Abstraction of H·</p> $\begin{array}{c} \text{CH}_2 \\   \\ \text{CH}_2-\text{C}-\text{CH}=\text{CH}_2 \\   \\ \text{CH}_2 \end{array}$	<p>Addition of HO· to 3-carbon</p> $\begin{array}{c} \text{CH}_3 \\   \\ \text{CH}_2=\text{CH}-\text{CH}-\text{CH} \\   \quad   \\ \text{OH} \end{array}$	<p>No radical from the monomer</p>
Reaction with CH <sub>3</sub> ·	<p>Abstraction of H·</p> $\begin{array}{c} \text{CH}_3 \\   \\ \text{CH}_2-\text{C}-\text{CH}=\text{CH}_2 \\   \\ \text{CH}_3 \end{array}$	<p>Complicated spectra not to be assigned</p>	<p>Addition of CH<sub>3</sub>· to 1-carbon</p> $\begin{array}{c} \text{CH}_3 \quad \text{CH}_3 \\   \quad   \\ \text{CH}_3\text{CH}_2-\text{C}-\text{C}-\text{H} \\   \quad   \\ \text{CH}_3 \end{array}$
Ultraviolet irradiation	<p>Loss of H·</p> $\begin{array}{c} \text{CH}_2 \\   \\ \text{CH}_2-\text{C}-\text{CH}=\text{CH}_2 \\   \\ \text{CH}_2 \end{array}$	<p>(a) Addition of R· to 3-carbon</p> $\begin{array}{c} \text{CH}_3 \\   \\ \text{CH}_2=\text{CH}-\text{CH}-\text{CH} \\   \quad   \\ \text{R} \end{array}$ 	<p>Loss of H·</p> $\begin{array}{c} \text{CH}_2 \quad \text{CH}_2 \\   \quad   \\ \text{CH}_2-\text{C}-\text{C}=\text{CH}_2 \\   \quad   \\ \text{CH}_2 \end{array}$

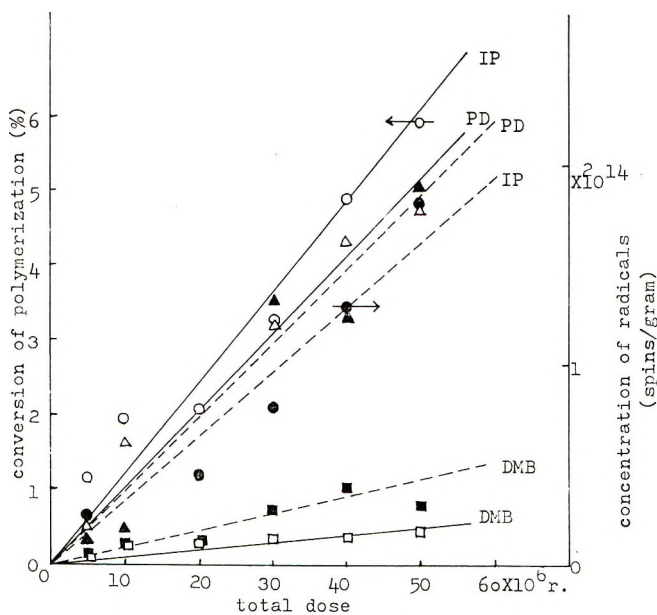


Fig. 1. Variation of conversion of polymerization and concentration of trapped free radicals of dienes with electron-irradiation dose at  $-196^{\circ}\text{C}$ . (dose rate is  $1.5 \times 10^6$  r/sec.). (O) isoprene (IP), ( $\Delta$ ) pentadiene (PD), ( $\square$ ) dimethylbutadiene (DMB); (—) conversion, (---) concentration of trapped free radicals.

a monomer molecule with ionizing radiation. This molecule-ion then adds to a monomer and so initiates the ionic polymerization from its ionic end. The radical end of the parent ion-radical, which is isolated from the ionic end by ionic propagation, is thought to be unreactive at  $-196^{\circ}\text{C}$ . and trapped in the solid monomer matrix. The observed radicals are inactive radical residues involved in the ionic propagation process, though their ESR spectra are the same as those expected for the propagating free-radical end in the radical polymerization. Primary ion-radicals were not observed by ESR measurement, presumably because the ion-radicals are unstable and reactive even at  $-196^{\circ}\text{C}$ .

The intimate correlation between the concentration of free radicals and the conversion of polymerization, shown in Fig. 1, may support the proposed scheme of reactions, where one free-radical end corresponds to one polymer chain.

(The full paper will be published in the *Memoirs of the Faculty of Engineering, Kyoto University*.)

#### References

1. Y. Shioji, S. Ohnishi, and I. Nitta, *J. Polymer Sci. A*, **1**, 3373 (1963).
2. T. A. Fadner, I. Rubin, and H. Morawetz, *J. Polymer Sci. A*, **37**, 549 (1963).
3. T. A. Fadner and H. Morawetz, *J. Polymer Sci. A*, **45**, 475 (1960).
4. B. Baysal, G. Adler, D. Ballantine, and P. Colombo, *J. Polymer Sci. A*, **44**, 117 (1960).
5. G. Adler, D. Ballantine, and B. Baysal, *J. Polymer Sci. A*, **48**, 195 (1960).
6. H. Ueda and Z. Kuri, *J. Polymer Sci. A*, **61**, 333 (1962).
7. H. Morawetz and I. D. Rubin, *J. Polymer Sci. A*, **57**, 669 (1962).
8. J. H. O'Donnell, B. McGarvey, and H. Morawetz, *J. Am. Chem. Soc.*, **86**, 2322 (1964).
9. J. B. Lando and H. Morawetz, *J. Polymer Sci. C*, **4**, 789 (1964).

10. I. M. Barkalov, V. I. Coldanskii, N. S. Enikolopyan, S. F. Terekhova, and G. M. Trofimova, *J. Polymer Sci. C*, **4**, 897 (1964).
11. A. Hirschberger and G. Marchal, *Compt. Rend.*, **358**, 2329 (1964).

KEIJI TAKEDA  
HIROSHI YOSHIDA\*  
KOICHIRO HAYASHI  
SEIZO OKAMURA

Department of Polymer Chemistry  
Kyoto University  
Kyoto, Japan

\* Research Reactor Institute,  
Kyoto University  
Kyoto, Japan

Received March 7, 1966  
Revised April 13, 1966

### ***Reactivity Ratios for the Copolymerization of Vinyl Acetate with Methyl Acrylate***

Although vinyl acetate and methyl acrylate are isomeric monomers, they have very different reactivities. This is shown in the data for copolymerization with styrene given in Table I which enable a ratio of 1:73 to be calculated for the relative reactivities of vinyl acetate and methyl acrylate to the polystyryl radical. Mayo et al.<sup>1</sup> obtained the reactivity ratios for the copolymerization of vinyl acetate with methyl acrylate by polymer analysis, and their data are given in Table I. They used a rather lengthy analysis based on hydrolysis and an estimation of the acetic acid produced. This, and the rather high conversion to polymer that was used, might have contributed to the deviation of  $\pm 0.1$  that they reported for  $r_{(\text{vinyl acetate})}$ . More recently, Witnauer et al.<sup>3</sup> have used elemental analysis to obtain the reactivity ratios in the system vinyl stearate-methyl acrylate and from this and similar work have concluded that the length of the acid side-chain in the vinyl ester has a negligible effect on the reactivities of either the monomer or the polymer radical. The values they obtained are given in the table, and although these are somewhat lower than the mean values given by Mayo et al. for the vinyl acetate system, they almost fall in the range of error reported. More accurate values for the reactivity ratios of the vinyl acetate-methyl acrylate system would be useful for this comparison. Since we required vinyl acetate-methyl acrylate copolymers of known composition for diffusion studies,<sup>4</sup> we have, at the same time, carried out a re-determination of the reactivity ratios for the system.

#### **Experimental**

Well outgassed, purified, dry monomers were polymerized in bulk at 50°C. using benzoyl peroxide (0.03%) as initiator. The conversion to polymer was restricted to between 2 and 3% to minimize changes in monomer composition during the polymerization. The polymer was isolated by precipitating twice into petroleum ether and was subsequently heated for several hours in vacuum to remove all traces of monomers and solvents. An infrared method was used for analyses of the polymers. In spite of the similarity of the two monomer units, the two ester groups have absorption bands for the C—O stretching vibration at different frequencies. The vinyl acetate, like other acetate esters,<sup>5</sup> has a band at 1240  $\text{cm.}^{-1}$  and the acrylate has one at 1160  $\text{cm.}^{-1}$  similar to the esters of long-chain acids,<sup>6</sup> and these can be used for analysis. Spectra were obtained using a 1% solution of the polymers in methylene chloride and the compositions of the copolymers were found to  $\pm 1\%$  by comparison of their spectra with the spectra of known mixtures of the homopolymers. A spectrum of one of the copolymers is given in Figure 1, together with the spectra of the two homopolymers for comparison.

The reactivity ratios were found by the intersecting-line method after making some allowance for the small change in monomer composition that occurred due to the finite conversion to polymer.

#### **Results and Discussion**

The values obtained for the reactivity ratios at 50°C. are  $r_1 = 6.7 \pm 2.2$  and  $r_2 = 0.029 \pm 0.011$  for methyl acrylate as monomer 1 and vinyl acetate as monomer 2. These ratios are given in Table I for comparison with other values. They fall within the range given by Mayo et al.<sup>1</sup> and will be seen to be very close indeed to the ratios given for the vinyl stearate system, thus giving extra support to the hypothesis of Witnauer et al.<sup>3</sup> that the long hydrocarbon chain has very little effect on the reactivity.

It is interesting to compare our experimental values with those predicted by the two schemes for summarizing monomer and radical reactivities. The Alfrey and Price  $Q$  and  $e$  values for vinyl acetate and methyl acrylate have been given by L. J. Young<sup>2</sup> and are included in Table I. These enable values of 0.054 and 9.9 to be obtained for the reactivity ratios, while the values given by Bamford and Jenkins<sup>7</sup> for the  $\alpha$ ,  $\beta$ , and  $\sigma$  pa-

TABLE I  
 Copolymerization Parameters for Various Monomers

	Source	Parameter	Vinyl Acetate	Vinyl Stearate	Methyl Acrylate
Reactivity ratios for copolymerization with styrene as monomer 1 and vinyl acetate or methyl acrylate as monomer 2		$r_1$	$5.5 \pm 10^1$	—	$0.76 \pm 0.03^a$
		$r_2$	$0.01 \pm 0.01^1$	—	$0.19 \pm 0.02^a$
	Alfrey and Price <sup>2</sup> parameters	$e$	$-0.22$	—	$0.60$
		$Q$	$0.026$	—	$0.42$
Parameters of Bamford et al. <sup>7</sup>		$\alpha$	$0$	—	$-3$
		$\beta$	$3.00$	—	$5.20$
		$\sigma$	$0$	—	$0.57$
Reactivity ratios for copolymerization with methyl acrylate as monomer 1 and vinyl acetate or vinyl stearate as monomer 2	Mayo et al. <sup>1</sup>	$r_1$	$9 \pm 2.5$	—	—
		$r_2$	$0.1 \pm 0.1$	—	—
	This work	$r_1$	$6.7 \pm 2.2$	—	—
		$r_2$	$0.029 \pm 0.011$	—	—
	Witauer et al. <sup>3</sup>	$r_1$	—	$5.8$	—
		$r_2$	—	$0.03$	—
	Calculated from $Q-e$	$r_1$	$9.9$	—	—
		$r_2$	$0.54$	—	—
	Calculated from $\alpha-\beta-\sigma$	$r_1$	$3.1$	—	—
		$r_2$	$0.016$	—	—

<sup>a</sup> A mean of the five values collected together in reference (2).

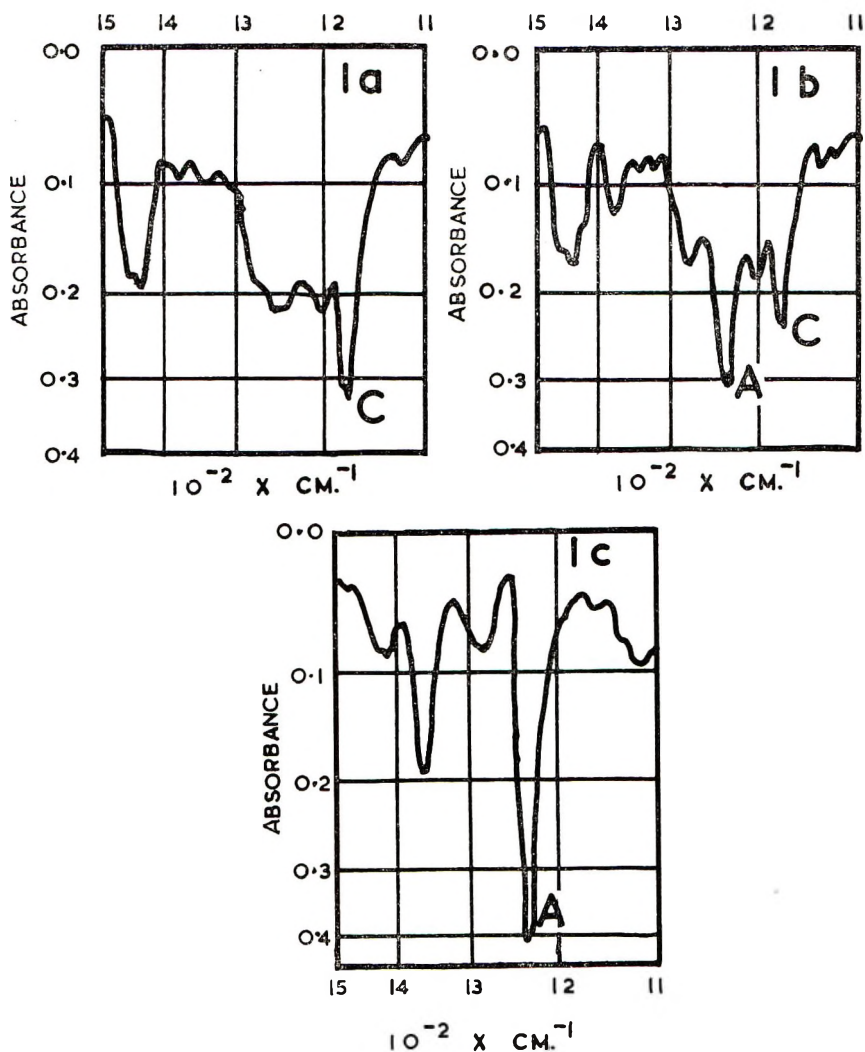


Fig. 1. Infrared spectra of methyl acrylate-vinyl acetate polymers: (a) polymethyl acrylate; (b) copolymer containing 67% methyl acrylate residues; (c) polyvinyl acetate. A = acetate band at  $1240\text{ cm.}^{-1}$ . C = acrylate band at  $1160\text{ cm.}^{-1}$ .

rameters enable the ratios of 0.016 and 3.1 to be calculated. The values calculated from the  $Q-e$  scheme are both higher than our values, while the ones calculated from the  $\alpha-\beta-\sigma$  scheme are too low. A geometric (or arithmetic) mean of these calculated values agrees very well with our measured values.

#### References

1. F. R. Mayo, C. Walling, F. M. Lewis, and W. F. Hulse, *J. Am. Chem. Soc.*, **70**, 1523 (1948).
2. L. J. Young, *J. Polymer Sci.*, **54**, 411 (1961).
3. L. R. Witnauer, N. Watkins, and W. S. Port, *J. Polymer Sci.*, **20**, 213 (1956).
4. T. A. Garrett and G. S. Park, *J. Polymer Sci. C*, in press.



5. H. W. Thompson and P. Torkington, *J. Chem. Soc.*, **1945**, 640.
6. D. N. Kendall, R. R. Hampton, H. Hausdorff, and F. Pristera, *Appl. Spectr.*, **7**, 179 (1953).
7. C. H. Bamford and A. D. Jenkins, *Trans. Faraday Soc.*, **59**, 530 (1963).

T. A. GARRETT

G. S. PARK

Department of Chemistry and Biology  
Welsh College of Advanced Technology  
Cathays Park, Cardiff, U. K.

Received April 13, 1966

Revised May 9, 1966

## ERRATA

### Polymers from Aryl Glycidyl Ethers

(article in *J. Polymer Sci. A-1*, 4, 917-922, 1966)

By T. B. GIBB, JR., R. A. CLENDINNING, and W. D. NIEGISCH

*Research and Development Department, Plastics Division,  
Union Carbide Corporation, Bound Brook, New Jersey*

On page 918, the first paragraph under Table I should read, in part, as follows:  
“ . . . lowers the melting point of the polyether compared to the parent compound. An exception to this generalization is the *p*-methyl group. . . ”

### Kinetics of Heterogeneous Cellulose Reactions. I. Cyanoethylation of Cotton Cellulose

(article in *J. Polymer Sci. A-1*, 4, 459-474, 1966)

By PRONoy K. CHATTERJEE and CARL M. CONRAD

*Plant Fibers Pioneering Research Laboratory, Southern Utilization Research and Development Division, Agricultural Research Service, U. S. Department of Agriculture, New Orleans, Louisiana*

On page 469, column 3 of Table I should read as follows:

Reaction rate constants

$$\left. \begin{aligned} k_{[\text{OH}]^{0.5}} &= 2.59 \times 10^{-3} \\ k_{[\text{OH}]^{0.6}} &= 4.27 \times 10^{-3} \\ k_{[\text{OH}]^{1.0}} &= 1.85 \times 10^{-3} \\ k_{[\text{OH}]^{1.0}} &= 2.82 \times 10^{-3} \\ k_{[\text{OH}]^{1.1}} &= 17.23 \times 10^{-3} \\ k_{[\text{OH}]^{1.5}} &= 25.0 \times 10^{-3} \end{aligned} \right\}$$